ISSN 1948-5204 (online)

World Journal of *Gastrointestinal Oncology*

World J Gastrointest Oncol 2023 May 15; 15(5): 700-910

Published by Baishideng Publishing Group Inc

World Journal of Gastrointestinal Oncology

Contents

Monthly Volume 15 Number 5 May 15, 2023

ABOUT COVER

Editorial Board Member of *World Journal of Gastrointestinal Oncology*, Claudio Luchini, MD, PhD, Associate Professor of Pathology, Department of Diagnostics and Public Health, University and Hospital Trust of Verona, Verona 37134, Italy. claudio.luchini@univr.it

AIMS AND SCOPE

The primary aim of *World Journal of Gastrointestinal Oncology* (*WJGO*, *World J Gastrointest Oncol*) is to provide scholars and readers from various fields of gastrointestinal oncology with a platform to publish high-quality basic and clinical research articles and communicate their research findings online.

WJGO mainly publishes articles reporting research results and findings obtained in the field of gastrointestinal oncology and covering a wide range of topics including liver cell adenoma, gastric neoplasms, appendiceal neoplasms, biliary tract neoplasms, hepatocellular carcinoma, pancreatic carcinoma, cecal neoplasms, colonic neoplasms, colorectal neoplasms, duodenal neoplasms, esophageal neoplasms, gallbladder neoplasms, *etc*.

INDEXING/ABSTRACTING

The *WJGO* is now abstracted and indexed in PubMed, PubMed Central, Science Citation Index Expanded (SCIE, also known as SciSearch®), Journal Citation Reports/Science Edition, Scopus, Reference Citation Analysis, China National Knowledge Infrastructure, China Science and Technology Journal Database, and Superstar Journals Database. The 2022 edition of Journal Citation Reports® cites the 2021 impact factor (IF) for *WJGO* as 3.404; IF without journal self cites: 3.357; 5-year IF: 3.250; Journal Citation Indicator: 0.53; Ranking: 162 among 245 journals in oncology; Quartile category: Q3; Ranking: 59 among 93 journals in gastroenterology and hepatology; and Quartile category: Q3. The *WJGO*'s CiteScore for 2021 is 3.6 and Scopus CiteScore rank 2021: Gastroenterology is 72/149; Oncology is 203/360.

RESPONSIBLE EDITORS FOR THIS ISSUE

Production Editor: *Xiang-Di Zhang*; **Production Department Director:** *Xiang Li*; **Editorial Office Director:** *Jia-Ru Fan*.

NAME OF JOURNAL
World Journal of Gastrointestinal Oncology

ISSN
ISSN 1948-5204 (online)

LAUNCH DATE
February 15, 2009

FREQUENCY
Monthly

EDITORS-IN-CHIEF
Monjur Ahmed, Florin Burada

EDITORIAL BOARD MEMBERS
https://www.wjgnet.com/1948-5204/editorialboard.htm

PUBLICATION DATE
May 15, 2023

INSTRUCTIONS TO AUTHORS
https://www.wjgnet.com/bpg/gerinfo/204

GUIDELINES FOR ETHICS DOCUMENTS
https://www.wjgnet.com/bpg/GerInfo/287

GUIDELINES FOR NON-NATIVE SPEAKERS OF ENGLISH
https://www.wjgnet.com/bpg/gerinfo/240

PUBLICATION ETHICS
https://www.wjgnet.com/bpg/GerInfo/288

PUBLICATION MISCONDUCT
https://www.wjgnet.com/bpg/gerinfo/208

ARTICLE PROCESSING CHARGE
https://www.wjgnet.com/bpg/gerinfo/242

STEPS FOR SUBMITTING MANUSCRIPTS
https://www.wjgnet.com/bpg/GerInfo/239

ONLINE SUBMISSION
https://www.f6publishing.com

World Journal of Gastrointestinal Oncology

Submit a Manuscript: https://www.f6publishing.com

World J Gastrointest Oncol 2023 May 15; 15(5): 700-712

DOI: 10.4251/wjgo.v15.i5.700

ISSN 1948-5204 (online)

OPINION REVIEW

Restaging rectal cancer following neoadjuvant chemoradiotherapy

Dajana Cuicchi, Giovanni Castagna, Stefano Cardelli, Cristina Larotonda, Benedetta Petrello, Gilberto Poggioli

Specialty type: Oncology

Provenance and peer review: Invited article; Externally peer reviewed.

Peer-review model: Single blind

Peer-review report's scientific quality classification

Grade A (Excellent): 0
Grade B (Very good): B
Grade C (Good): C, C
Grade D (Fair): 0
Grade E (Poor): 0

P-Reviewer: Gu GL, China; Sun J, China; Tsimogiannis K, Sweden

Received: December 22, 2022
Peer-review started: December 22, 2022
First decision: February 24, 2023
Revised: March 1, 2023
Accepted: March 29, 2023
Article in press: March 29, 2023
Published online: May 15, 2023

Dajana Cuicchi, Giovanni Castagna, Stefano Cardelli, Cristina Larotonda, Benedetta Petrello, Gilberto Poggioli, Department of Medical and Surgical Sciences, Surgery of the Alimentary Tract, IRCCS Azienda Ospedaliero-Universitaria di Bologna, Bologna 40138, Italy

Corresponding author: Dajana Cuicchi, MD, PhD, Surgeon, Department of Medical and Surgical Sciences, Surgery of the Alimentary Tract, IRCCS Azienda Ospedaliero-Universitaria di Bologna, Via Albertoni 15, Bologna 40138, Italy. dajana.cuicchi@aosp.bo.it

Abstract

Correct tumour restaging is pivotal for identifying the most personalised surgical treatment for patients with locally advanced rectal cancer undergoing neoadjuvant therapy, and works to avoid both poor oncological outcome and overtreatment. Digital rectal examination, endoscopy, and pelvic magnetic resonance imaging are the recommended modalities for local tumour restaging, while chest and abdominal computed tomography are utilised for the assessment of distant disease. The optimal length of time between neoadjuvant treatment and restaging, in terms of both oncological safety and clinical effectiveness of treatment, remains unclear, especially for patients receiving prolonged total neoadjuvant therapy. The timely identification of patients who are radioresistant and at risk of disease progression remains challenging.

Key Words: Locally advanced rectal cancer; Restaging; Pelvic magnetic resonance imaging; Endorectal ultrasound; Computed tomography scan; Colonoscopy

Core Tip: Correct tumour restaging is pivotal for identifying the most personalised surgical treatment for patients with locally advanced rectal cancer undergoing neoadjuvant therapy; it allows avoidance of both poor oncological outcomes and overtreatment. However, there are no guidelines regarding the definition, timing, and diagnostic techniques to be carried out. This study provides the most up-to-date evidence on this topic and the outstanding issues worthy of future research.

Citation: Cuicchi D, Castagna G, Cardelli S, Larotonda C, Petrello B, Poggioli G. Restaging rectal cancer following neoadjuvant chemoradiotherapy. *World J Gastrointest Oncol* 2023; 15(5): 700-712
URL: https://www.wjgnet.com/1948-5204/full/v15/i5/700.htm
DOI: https://dx.doi.org/10.4251/wjgo.v15.i5.700

INTRODUCTION

Treatment of locally advanced rectal cancer (LARC) requires a multidisciplinary approach. In recent decades, the widespread use and optimisation of total mesorectal excision (TME) and the constant use of neoadjuvant chemoradiotherapy (nCRT) have sharply decreased the rate of local recurrence after surgery[1,2]. Two randomised phase 3 trials investigating total neoadjuvant therapy (TNT) have recently resulted in a significant improvement in disease-free survival (DFS) and disease-related treatment failure as compared with standard nCRT, setting a new standard of care[3,4]. Nevertheless, the response to neoadjuvant therapy remains highly divergent. It is well established that, after neoadjuvant therapy, many patients with LARC respond very well to the treatment; indeed, pathological complete response (pCR), defined as the absence of residual tumour cells at the primary tumour site and the mesorectal lymph nodes, is achieved in approximately 20% of patients. This rate may be as high as 28%-38% with the implementation of TNT regimens; as a result, an even larger proportion may have a near-complete response[5-7]. Patients with pCR after TME resection demonstrate excellent survival, with fewer than 1% having local failure and 8% having systemic recurrence[8]. Therefore, the benefit of TME in patients achieving a complete response has been questioned. Organ-preservation strategies are becoming more popular to safely avoid the morbidities associated with radical surgery and to maintain anorectal function in those patients who achieved a clinical complete response (cCR) or a near-cCR (ncCR)[9]. On the other hand, approximately 40% of patients respond poorly or not at all to therapy[5]. This is likely attributable to more aggressive tumour biology. Poor responders and non-responders to neoadjuvant therapy are at risk of both local and distant relapse, which may be higher than that of the average LARC patient[10,11]. In these patients, the possibility of disease progression during neoadjuvant treatment or the waiting period should be taken into account. Its correct identification allows for modification of the treatment plan, intensifying the systemic treatment, or optimising surgical management by extending resection beyond the mesorectal plane or performing multiorgan resection.

Therefore, the ability to accurately assess the response to neoadjuvant therapy is the key to tailored treatment to avoid poor oncological outcomes or overtreatment. The aim of this review is to evaluate the current evidence regarding tumour response assessment in terms of definition, timing, and diagnostic techniques.

DEFINITION OF TUMOUR RESPONSE TO NEOADJUVANT THERAPY

There is no standardisation with respect to tumour response assessment criteria. Originally, Habr-Gama *et al*[12] dichotomised the categorisation into complete and incomplete. They considered patients to have cCR if there was an absence of any residual ulcer, mass, or stenosis of the rectum by digital rectal exam (DRE) and proctoscopy; whitening of the mucosa, teleangiectasias, and subtle loss of pliability of the rectum were also considered to be consistent with cCR. They did not routinely perform endoscopic biopsies and considered radiological imaging consistent with cCR in the absence of suspicious mesorectal enlarged, irregularly bordered, and heterogeneous nodes, and in the presence of fibrotic changes within the rectum (*i.e.* low signal intensity areas with or without submucosal hypertrophy)[13]. The guidelines suggested the same criteria for the definition of cCR[14,15]. In the attempt to standardise the definition of a clinical response, Memorial Sloan Kettering graded response as complete, near-complete, or incomplete based on the findings of DRE, endoscopy, and magnetic resonance imaging (MRI) [T2-weighted and diffusion-weighted imaging (DWI) sequences][16]. They classified ncCR as tumours that showed a marked response to neoadjuvant therapy but did not fulfil all the criteria of cCR at the time of response assessment, such as: (1) Smooth induration or minor mucosal abnormalities on DRE; (2) Irregular mucosa, small mucosal nodules, or minor mucosal abnormalities, superficial ulceration or mild persisting erythema of the scar on endoscopy; and (3) Mostly dark T2 signal, some remaining intermediate signal, and/or partial regression of the lymph nodes on MRI. If patients did not meet all these criteria and those for cCR, they were regarded as incomplete responders. This 3-tiered response/regression schema was tested prospectively in the OPRA trial[17]. Maas *et al*[18] and Martens *et al*[19] provided a pragmatic definition of cCR, ncCR, and non-complete response. This classification has recently been recommended by a panel of experts for use in the definition of tumour response (Table 1; Figures 1-4)[20].

Table 1 Recommended tumour response schema for rectal cancer after neoadjuvant chemoradiotherapy

	cCR	ncCR	Poor response
DRE	No palpable tumour material present	Minor mucosal abnormalities	Palpable tumour mass; Cases who do not fulfill the criteria for either a cCR or ncCR
Endoscopy	No residual tumour material or only a small residual erythematous ulcer or scar; Endoscopic biopsy not mandatory to define a cCR, biopsy should not be performed, especially if the DRE, rectoscopy and MRI criteria for a cCR are all fulfilled	Small and smooth regular irregularities including residual ulcer, or small mucosal nodules or minor mucosal abnormalities, with mild persisting erythema of the scar; Endoscopic biopsy not mandatory	Visible macroscopic tumour; Cases who do not fulfill the criteria for either a cCR or ncCR
MRI	Substantial downsizing with no observable residual tumour material, or residual fibrosis only (with limited signal on diffusion weighted imaging), sometimes associated with residual wall thickening owing to oedema, no suspicious lymph nodes	Obvious downstaging with residual fibrosis but heterogeneous or irregular aspects and signal or regression of lymph nodes with no malignant enhancement features, but with a size > 5 mm	Visible macroscopic tumour and/or lack of regression of involved lymph nodes; Cases who do not fulfill the criteria for either a cCR or ncCR

DRE: Digital rectal exam; cCR: Clinical complete response; ncCR: Near clinical complete response; MRI: Magnetic resonance imaging.

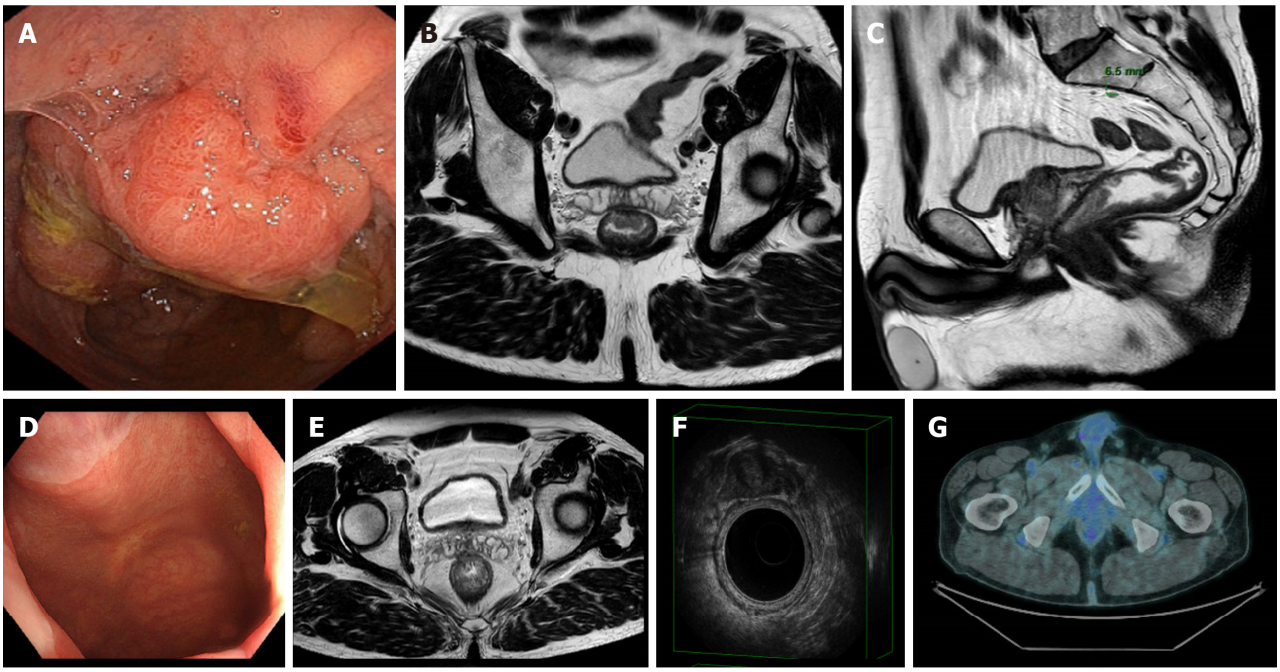

DOI: 10.4251/wjgo.v15.i5.700

Figure 1 A case of clinical complete response confirmed at pathology. A-C: A 61-year-old male patient with rectal cancer. Endoscopy (A) and magnetic resonance imaging (MRI) (B and C) findings staged a tumour of the low rectum (cT3aN1, mesorectal fascia negative, extramural venous invasion negative, pelvic nodes negative). The patient underwent neoadjuvant chemoradiotherapy; D-G: Restaging at 15 wk after the beginning of the neoadjuvant chemoradiotherapy showed a clinical complete response at endoscopy (D), MRI (E), endorectal ultrasound (F), and 18-fluorodeoxyglucose-computed tomography/positron emission tomography (G).

WHEN TO CARRY OUT RESTAGING

Evidence regarding the optimal timing of restaging is not yet available. The ideal interval should allow for the safe identification of responders and non-responders by balancing the time to fully express the maximal effects of the therapy and the time to avoid tumour repopulation or disease progression. In effect, tumour response is a dynamic process associated with tumour-related factors (*e.g.*, size, histology, and molecular profile) and treatment-related factors (*e.g.*, radiotherapy dose and fractionation, chemotherapy, and the time interval between preoperative and/or definitive treatment and the decision to proceed to non-operative management or local excision or TME)[21]. Knowledge of the kinetics of tumour response comes primarily comes from the operative context.

Several trials have shown how lengthening the interval between radiation therapy and surgery and adding systemic therapy leads to higher rates of pCR. In the historic Lyon R90-01 randomised trial, a longer interval (6-8 wk *vs* 2 wk) between completion of the radiotherapy and surgery led to a significant increase in number of patients having a major pathological response (pCR or few residual cells)[22]. In

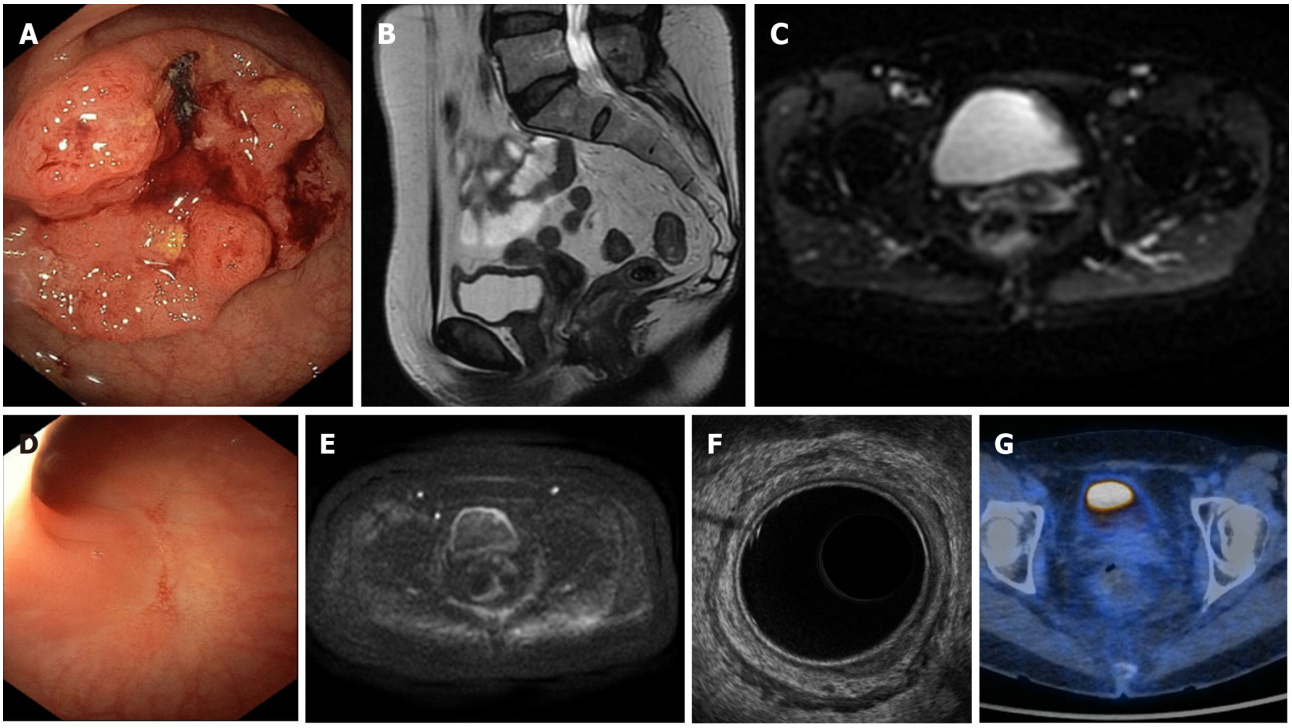

DOI: 10.4251/wjgo.v15.i5.700 **Copyright** ©The Author(s) 2023.

Figure 2 A case of clinical complete response confirmed at pathology. A-C: A 57-year-old female patient with rectal cancer. Endoscopy (A) and magnetic resonance imaging (MRI) (B and C) findings staged a tumour of the low of rectum (cT3aN0 mesorectal fascia negative, extramural vascular invasion negative, pelvic nodes negative). The patient underwent neoadjuvant chemoradiotherapy; D-G: Restaging at 15 wk after the beginning of therapy showed a clinical complete response at endoscopy (D), MRI (E), endorectal ultrasound (F), and 18-fluorodeoxyglucose-computed tomography/positron emission tomography (G).

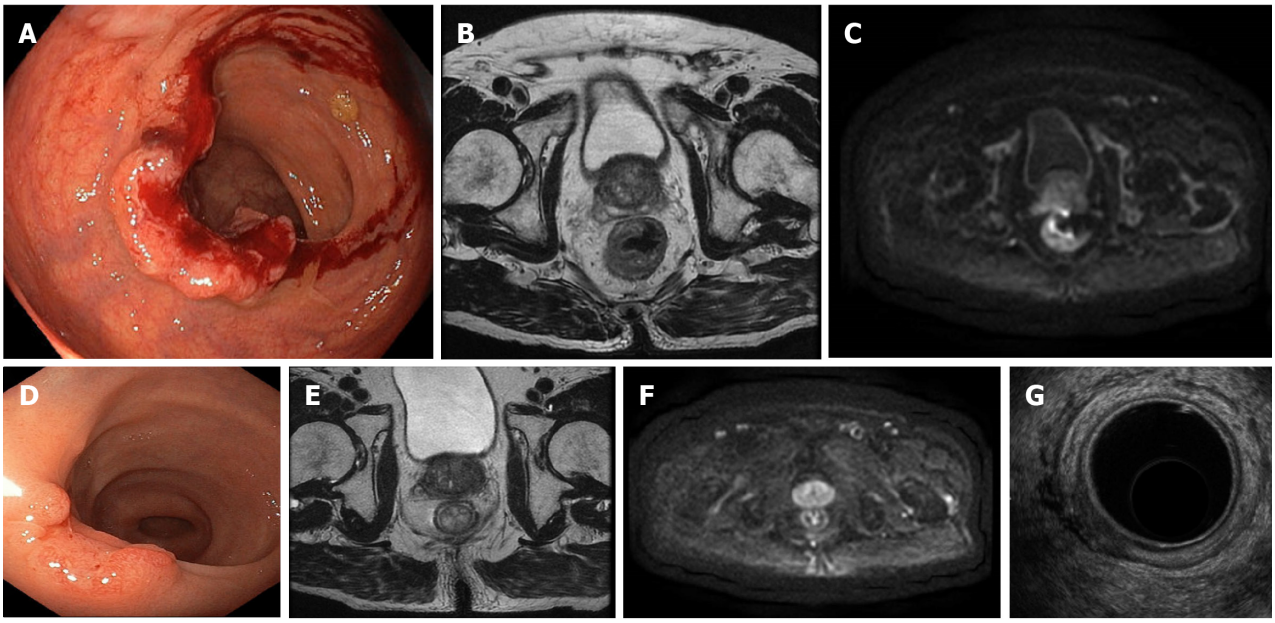

DOI: 10.4251/wjgo.v15.i5.700 **Copyright** ©The Author(s) 2023.

Figure 3 A case of near clinical complete response confirmed at pathology (ypT1N0). A-C: An 84-year-old male patient with rectal cancer. Endoscopy (A) and magnetic resonance imaging (MRI) (B and C) staged a tumour of the low rectum (cT3aN0M0, mesorectal fascia negative, extramural vascular invasion negative, pelvic nodes negative). The patient underwent short-course radiotherapy; D-G: The restaging at 15 wk after the beginning of neoadjuvant radiotherapy showed a near clinical complete response at endoscopy (D), MRI (E and F), and endorectal ultrasound (G).

the phase 3 Stockholm III trial, the rate of complete pathological response in the short course radiation-delay arm (4-8 wk) was 11.8%, as compared to 1.7% for the short course radiation-immediate arm (within 1 wk)[23]. An additional extension beyond 8 wk was subsequently tested in the prospective trials. The GRECCAR-6 trial (7 wk *vs* 11 wk) showed that the longer interval did not increase the pCR

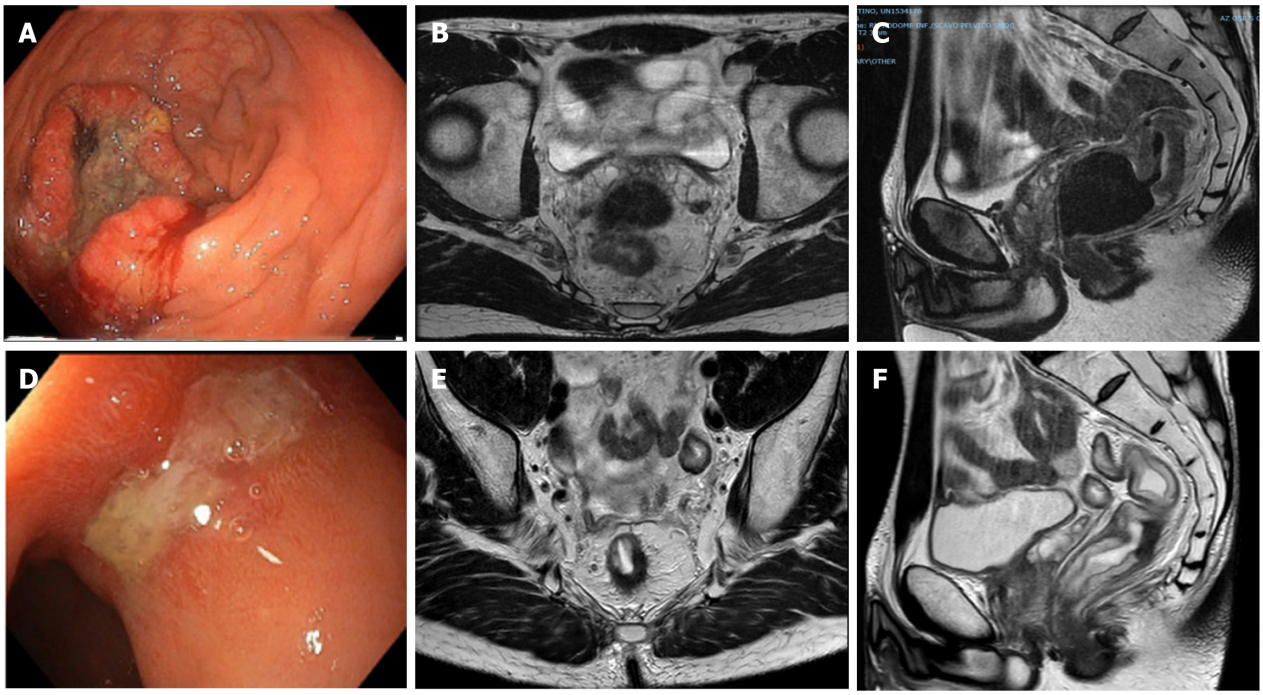

DOI: 10.4251/wjgo.v15.i5.700 **Copyright** ©The Author(s) 2023.

Figure 4 A case of poor response confirmed at pathology (ypT2N0). A-C: A 42-year-old male with rectal cancer. Endoscopy (A) and MRI (B and C) staged a tumour of the middle rectum (cT3bN2, mesorectal fascia negative, extramural vascular invasion positive, pelvic nodes negative). The patient underwent total neoadjuvant therapy; D-F: Restaging at 20 wk after the beginning of neoadjuvant radiotherapy showed a poor response at endoscopy (D) and MRI (E and F).

rate (15% *vs* 17.4%; $P = 0.59$)[24]. In contrast, a British trial (6 wk *vs* 12 wk) found a significant increase in the pCR rate (9% *vs* 20%, $P < 0.05$)[25]. Similarly, an increased pCR rate (18% *vs* 10%; $P = 0,027$) was also reported by a Turkish trial for an interval of more than 8 wk *vs* less than 8 wk after chemoradiotherapy [26]. A large retrospective series of patients revealed the highest pCR rates in patients operated on 9-13 wk from the end of CRT[27-29]. Analogously, a pooled analysis of international randomised trials (Accord12/0405, EORTC22921, FFCD9203, CAO/ARO/AIO-94, CAO-ARO-AIO-04, INTERACT, and TROG01.04) has also suggested that the best time to achieve pCR is at 10 wk, and the lengthening of the surgical interval was not detrimental with respect to survival outcomes[30]. The Timing of Rectal Cancer Response to Chemoradiation Consortium trial, a prospective phase 2 cohort trial in which preoperative chemoradiotherapy and sequentially increased timing of surgery were evaluated, showed an increase in pCR rates when the average time from radiotherapy to surgery was progressively increased from 6 wk to 11 wk, 15 wk, and 19 wk (18%, 25%, 30%, and 38%, respectively)[6].

Whether these differences can be explained by the use of intensified chemotherapy or by the prolonged interval before surgery remains uncertain, as patients operated on after 11-19 wk received 2 to 6 cycles of FOLFOX during the waiting period before surgery. In any case, consolidation chemotherapy in the TNT approach has recently emerged as the new option for optimizing tumour response; however, it made the detection of the optimal timing of restaging even more complex[31,32].

Moreover, with regard to patients who eventually did not experience a complete or a good response, the benefits related to waiting up to 11-12 wk before proceeding to surgical resection appeared less obvious. Studies evaluating the effects of the delayed time interval did not report a negative impact on long-term cancer outcomes[30,33]. However, not all the studies carried out a sub-analysis by tumour stage; therefore, the favourable long-term outcomes of the responder group may have masked or mitigated the adverse effects occurring in the non-responder group. In the RAPIDO trial, the authors suggested that an early response assessment should be encouraged in order to identify, at an earlier point in time, poor responders and, above all, patients with disease progression during preoperative treatment[3]. A large retrospective series of patients from the population-based Dutch Surgical Colorectal Audit found that the proportion of T4 tumours and metastatic disease increased with a longer time interval to surgery; this was particularly evident in the group resected beyond 10-11 wk from the end of CRT[27]. In a large multicentre retrospective cohort study of 1064 patients with a minor or null tumour response to neoadjuvant chemoradiotherapy, a wait time longer than 8 wk before surgery was associated with significantly worse overall outcome and DFS at 5 y and 10 y (reaching almost a 20% difference at 10 y for the overall survival)[10]. Unfortunately, it is not possible to identify poor responders up-front.

Patient selection based on pre-treatment characteristics is challenging, although some features, including a < 1 mm circumferential margin, extramural venous invasion, and extensive mesorectal and

pelvic lymph node involvement, are associated with lower cCR rates[34-36]. Currently, there is insufficient evidence to recommend proper timing for the earlier identification of patients with a poor response before the conventional time. Nevertheless, experts advise caution and selective earlier imaging in patients with tumours featuring certain high-risk characteristics (*e.g.*, advanced clinical T stage)[20]. Moreover, owing to variations in preoperative treatment design and duration across the different trials, they agreed that defining a specific time point for assessing cCR was impossible, and recommended that the response assessment should be determined from the start of treatment[20]. Thus, for patients with early-stage tumours receiving CRT or short-course radiotherapy, they recommended a 2-step approach comprising a response assessment at 12 wk and 16-20 wk after starting treatment; for patients receiving TNT, they recommended that the timing of the cCR assessments should be adapted according to the duration of the treatment (*i.e.* 20-38 wk after commencing treatment)[20]. In the end, if restaging after preoperative treatment reveals ncCR, taking into account initial tumour stage and treatment approach, the panel supported waiting longer (*e.g.*, 3 mo later as was reported in several case studies) if organ preservation was a priority[20].

HOW TO CARRY OUT RESTAGING

The standard methods of response assessment following preoperative therapy rely on clinical examination using DRE, endoscopy, MRI, endorectal ultrasound (EUS), and CT. However, each of these tools has limitations in predicting pathological findings after a surgical resection. These limitations stem from the inability of these imaging methods to differentiate residual tumour from radiation-induced fibrosis; this leads to erring on the safe side, overestimating the amount of tumour. Nevertheless, the current aim of local response assessment is not to correct T-staging but to differentiate between "good responders" (who are ypT0N0 or ypT1N0) and "poor responders." In the latter, the risk of incomplete resection [*e.g.*, mesorectal fascia (MRF) positivity, adjacent organ or anal sphincter infiltration, and residual lateral pelvic node involvement] should also be identified.

Pelvic MRI

MRI is the modality of choice for local staging of LARC due to its excellent soft-tissue resolution. It also plays an essential role in the evaluation of treatment response[37,38]. In a recent meta-analysis, the reported global sensitivity and specificity for T-staging were 81% and 67%, respectively and, for N-staging, they were both 77%[39]. These results confirmed those of a previous meta-analysis in which the pooled sensitivity and specificity were 50.4% and 91.2%, respectively for the T-stage, and the sensitivity for the prediction of a complete response was even lower (19%)[40]. The addition of diffusion-weighted (DWI) MRI improved the results, increasing the sensitivity and specificity for T-stage to 83.6% and 84.8%, respectively[40,41]. Nevertheless, many complete responses were still missed. The magnetic resonance tumour regression grade (TRG) system and a pattern-based approach have been proposed to improve diagnostic performance[42,43]. In experienced hands, the sensitivity of detecting a complete response was 74% when using the former system and 94% with the latter approach[42,43]. To properly identify "good responders," accurate nodal restaging is also important. A pooled analysis showed that the incidence of positive lymph nodes in ypT0 patients was approximately 5%[44]. Although nodal restaging remains a challenge, it seems to be more accurate than primary staging[45]. According to Heijnen *et al*[46], this could be explained by the following: First, after CRT, approximately 40% of lymph nodes decrease in size and approximately 44% disappear on MRI; and second, the prevalence of pathological positive nodes is lower as compared with the initial staging, leading to a higher negative predictive value (95%) and increased accuracy of nodal staging after CRT[46]. However, in cases of ypT0, the sensitivity, specificity, positive predictive value, and negative predictive value for predicting remaining lymph node metastasis with MRI were quite low (37%, 84%, 70%, and 57%, respectively)[47]; this may be attributable to the fact that residual disease occurs within very small nodes. van Heeswijk and colleagues showed that the absence of lymph nodes on restaging DWI MRI was highly predictive of ypN0 status[48]. Nevertheless, the role of DWI in this setting is still under debate[45]; MRI also plays a pivotal role in identifying the risk factors for incomplete resection. The evaluation of MRF status is less accurate than that of the pretreatment assessment (66%)[40,49,50]. In the case of residual involvement of the adjacent organs or mesorectal fascia, radiologists tend to overstage, as fibrotic strands of prior tumour invasion are challenging to differentiate from residual tumour tissue, unless an intact fat plane becomes visible between the tumour and the MRF or adjacent organs. Moreover, in distal tumours, invasion of the internal sphincter, intersphincteric plane, and external sphincter/levator ani has to be assessed to determine the feasibility of sphincter preservation. Furthermore, careful attention should be paid to identifying the lateral nodes, as these nodes, when involved, have an important influence on long-term outcome. A recent large multicentre cohort study evaluating the lateral nodes before and after CRT showed that nodes 7 mm or greater before CRT (short axis) had a higher risk for local recurrence than smaller nodes[51]. Moreover, in the case of shrinkage of the lateral nodes from 7 mm on a primary MRI to a short axis measurement of 4 mm, lateral lymph node dissection can be avoided[52].

EUS

Similar to MRI, the accuracy of EUS is disappointing in restaging. A number of studies on this topic have shown that the overall accuracy of EUS for ypT-stage and ypN-stage was quite variable, ranging from 38% to 75%, and from 59% to 80%, respectively[53-55]. Overstaging was more common in the majority of series, mainly due to the difficulty in differentiating fibrosis from residual cancer; EUS correctly predicted pCR in only approximately 50%-64%of cases[53-55]. These results were confirmed in a meta-analysis in which the sensitivity and specificity for T0-stage were 37% and 94%, respectively[56]. Zhang *et al*[57] have recently evaluated 3-dimensional EUS (3D-EUS) parameters to improve accuracy in tumour response assessment. They found that a value of 3.55 mm for adjusted thickness (*i.e.* the difference between the thickness of the muscularis on the residual side and the thickness of contralateral muscularis) correctly detected the TRG 0 cases with a sensitivity of 73%, a specificity of 81%, and an accuracy of 78%. Moreover, they concluded that utilising the 3D-EUS method as a part of the criteria for cCR would significantly improve the accuracy of the evaluation[57]. Some case-series studies have indicated that optimal accuracy of EUS could be obtained when the tumour location was within 6 cm from the anal verge and the examination was carried out by an experienced operator[54,58,59]. Studies comparing the accuracy of MRI and EUS in the same patients at the same time have reported conflicting results regarding T- and N-staging[59-61]. Nevertheless, EUS was more accurate than MRI for predicting pathologic complete response and anal sphincter infiltration[59-61]. Therefore, EUS is simple and inexpensive tool which, together with MRI and other diagnostic methods, can be useful for restaging rectal cancer. However, this modality is highly operator-dependent and limited to proximal and stenotic rectal tumours and close visual fields that only allow for the evaluation of perirectal lymph nodes.

Endoscopy

Endoscopy only allows for the proper evaluation of the mucosa. Although the healing of the mucosa is generally considered to be a sign of cCR, residual tumour remains deeper in the rectal wall and mesorectum in approximately 27% of cases. On the other hand, the presence of an ulcer on endoscopy, although significantly associated with pathological incomplete response, occurs in 66% of cases with complete response on pathology[62-64]. In clinical practice, to facilitate the decision-making process, additional information can be obtained from the MRI. However, studies that have evaluated this issue have produced contradictory results. Some have shown that a combination of multiple examinations did not improve accuracy[65,66]. In contrast to these findings, in a small prospective cohort study, Maas *et al*[18] showed that when DRE, endoscopy, and MRI together predict CR, this is correct in 98% of cases; when all 3 modalities indicate residual tumour, there still a 15% chance of CR[67]. Advanced endoscopy technologies, such as narrow-spectrum technologies and autofluorescence imaging, may improve the evaluation of the rectal wall mucosa and mucosal vascularity[68]. In the setting of restaging assessment, they may help in differentiating between clinical response and residual tumour.

Biopsies have only a limited clinical value for ruling out residual cancer. They do not provide any additional diagnostic value and could lead to false-negative results as residual cancer cells are often found in the muscularis propia[69]. Therefore, experts did not recommend biopsy as mandatory for diagnosing a complete or a near complete CR[20].

Contrast-enhanced thoraco-abdominal computed tomography

Although the value of CT in assessing local response is relatively low, this tool plays a role in determining the presence of distant metastases and current guidelines recommend its use in restaging [15]. A recent systematic review showed that restaging identified new metastatic disease in 6% of patients[11]. Although the overall detection rate of disease progression is low, the clinical impact of identifying early disease progression prior to surgical therapy is important to consider. Newly-detected distant disease in such a short period may represent a more biologically aggressive tumour or synchronous distant metastases that were not apparent on initial clinical staging, but that become detectable in the few months of the restaging. In any case, its identification requires modifying the therapeutic programme. Singhal and colleagues found that patients with poorly differentiated tumours had a significantly higher rate of systemic disease progression than those with well- or moderately-differentiated tumours (36% *vs* 7%, respectively). Nevertheless, more studies are necessary to identify factors that may predict short-interval disease progression.

18F-fluorodeoxyglucose positron emission tomography/CT

According to the guideline, positron emission tomography (PET) should not be routinely used as a tool to determine tumour response[15]. The pooled sensitivity and specificity reported for complete response were 71% and 76%, respectively[70]. Moreover, the metabolic grade [max standardised uptake value (SUVmax)] of the tumour at initial staging did not predict response to chemoradiotherapy; as with pretreatment SUVmax, the arithmetic difference between pre- and post-SUVmax was also not statistically significant[70]. A systematic review showed that PET/CT had higher accuracy in detecting extra-hepatic and hepatic colorectal metastatic disease than CT alone[71].

Table 2 Take-home message

Re-staging	
Why	It allows for the development of a tailored surgical treatment with the goal of avoiding poor oncological outcomes and overtreatment
When	It remains unclear. Experts recommend: (1) For patients receiving neoadjuvant chemoradiotherapy or short-course radiotherapy, the 2-step approach, at 12 wk and 16-20 wk after starting treatment if organ preservation is a priority; (2) For patients receiving total neoadjuvant therapy, assessment at 20-38 wk after commencing treatment according to the duration of the treatment; and (3) In case of ncCR, a second assessment 3 mo later taking into account initial tumour stage and treatment approach, if organ preservation is a priority. There is insufficient evidence to recommend proper timing for the earlier identification of patients with a poor response before the conventional time. Nevertheless, experts advise caution and selective earlier imaging in patients with tumours featuring certain high-risk characteristics (such as advanced cT stage)
How	Digital rectal examination, endoscopy and pelvic MRI for local tumour restaging; Chest and abdominal CT for distant disease. The current aim of local response assessment is not correct T-staging but the accurate differentiation between "good responders" (who are ypT0N0 or ypT1N0) and "poor responders." In the latter, the risk of incomplete resection, such as MRF positivity, adjacent organ or anal sphincter infiltration, and residual lateral pelvic node involvement should also be identified

CT: Computed tomography; ncCR: Near clinical complete response; MRI: Magnetic resonance imaging.

Future directions and research

Combined 18F-fluorodeoxyglucose (18F-FDG) PET/MRI has recently been proposed as an effective imaging modality for rectal cancer patients, owing to its ability to provide high-resolution anatomical and functional features. Although the role of 18F-FDG PET/MRI in rectal cancer has yet to be established, the evidence in a recent review has suggested that 18F-FDG PET/MRI could be used for rectal cancer restaging due to its better accuracy in T- and N-staging as compared to PET/CT or MRI alone; for M staging, on the other hand, it performed less well than other techniques for lung metastases [72].

Some novel MRI techniques, such as dynamic contrast-enhanced MRI, magnetisation transfer ratio, and textural analysis (*e.g.*, radiomics), have been studied to overcome the limitations of MRI in the restaging of rectal cancer. These tools have been evaluated in promising small retrospective studies; however, they are not currently used in routine clinical practice as they still need large-scale prospective validation.

Circulating biomarkers such as cell-free DNA have been tested to predict cCR and/or tumour regrowth. These have not been incorporated into current practice due to limited data, but represent a promising direction for future investigation and validation.

CONCLUSION

The ultimate goal of restaging is to determine the possibility of changing the planned treatment strategy. DRE, endoscopy, and pelvic MRI are the recommended modalities for local tumour restaging, while chest and abdominal CT are used for assessing distant disease. Nevertheless, the most practical and cost-efficient strategy for assessing tumour response also depends on local logistics and expertise. The optimal length of time between commencing treatment and restaging, in terms of both oncological safety and clinical effectiveness of treatment, remains unclear, especially in patients receiving prolonged TNT. The timely identification of patients who are radioresistant and at risk of disease progression is challenging. Table 2 summarizes the key points discussed in this review.

FOOTNOTES

Author contributions: Cuicchi D, Castagna G, Larotonda C, Cardelli S and Petrello B collected data, drafted the initial manuscript, and approved the final version to be submitted; Poggioli G reviewed and revised the manuscript, and approved the final version to be submitted.

Conflict-of-interest statement: The authors declare having no conflicts of interest.

Country/Territory of origin: Italy

ORCID number: Dajana Cuicchi 0000-0002-1504-4888.

S-Editor: Zhang H
L-Editor: Filipodia
P-Editor: Zhang XD

REFERENCES

1 **Sauer R**, Becker H, Hohenberger W, Rödel C, Wittekind C, Fietkau R, Martus P, Tschmelitsch J, Hager E, Hess CF, Karstens JH, Liersch T, Schmidberger H, Raab R; German Rectal Cancer Study Group. Preoperative versus postoperative chemoradiotherapy for rectal cancer. *N Engl J Med* 2004; **351**: 1731-1740 [PMID: 15496622 DOI: 10.1056/NEJMoa040694]

2 **Kapiteijn E**, Marijnen CA, Nagtegaal ID, Putter H, Steup WH, Wiggers T, Rutten HJ, Pahlman L, Glimelius B, van Krieken JH, Leer JW, van de Velde CJ; Dutch Colorectal Cancer Group. Preoperative radiotherapy combined with total mesorectal excision for resectable rectal cancer. *N Engl J Med* 2001; **345**: 638-646 [PMID: 11547717 DOI: 10.1056/NEJMoa010580]

3 **Bahadoer RR**, Dijkstra EA, van Etten B, Marijnen CAM, Putter H, Kranenbarg EM, Roodvoets AGH, Nagtegaal ID, Beets-Tan RGH, Blomqvist LK, Fokstuen T, Ten Tije AJ, Capdevila J, Hendriks MP, Edhemovic I, Cervantes A, Nilsson PJ, Glimelius B, van de Velde CJH, Hospers GAP; RAPIDO collaborative investigators. Short-course radiotherapy followed by chemotherapy before total mesorectal excision (TME) versus preoperative chemoradiotherapy, TME, and optional adjuvant chemotherapy in locally advanced rectal cancer (RAPIDO): a randomised, open-label, phase 3 trial. *Lancet Oncol* 2021; **22**: 29-42 [PMID: 33301740 DOI: 10.1016/S1470-2045(20)30555-6]

4 **Conroy T**, Bosset JF, Etienne PL, Rio E, François É, Mesgouez-Nebout N, Vendrely V, Artignan X, Bouché O, Gargot D, Boige V, Bonichon-Lamichhane N, Louvet C, Morand C, de la Fouchardière C, Lamfichekh N, Juzyna B, Jouffroy-Zeller C, Rullier E, Marchal F, Gourgou S, Castan F, Borg C; Unicancer Gastrointestinal Group and Partenariat de Recherche en Oncologie Digestive (PRODIGE) Group. Neoadjuvant chemotherapy with FOLFIRINOX and preoperative chemoradiotherapy for patients with locally advanced rectal cancer (UNICANCER-PRODIGE 23): a multicentre, randomised, open-label, phase 3 trial. *Lancet Oncol* 2021; **22**: 702-715 [PMID: 33862000 DOI: 10.1016/S1470-2045(21)00079-6]

5 **Capelli G**, De Simone I, Spolverato G, Cinquini M, Moschetti I, Lonardi S, Masi G, Carlomagno C, Corsi D, Luppi G, Gambacorta MA, Valvo F, Cannizzaro R, Grillo F, Barbaro B, Restivo A, Messina M, Pastorino A, Aschele C, Pucciarelli S. Non-Operative Management Versus Total Mesorectal Excision for Locally Advanced Rectal Cancer with Clinical Complete Response After Neoadjuvant Chemoradiotherapy: a GRADE Approach by the Rectal Cancer Guidelines Writing Group of the Italian Association of Medical Oncology (AIOM). *J Gastrointest Surg* 2020; **24**: 2150-2159 [PMID: 32394125 DOI: 10.1007/s11605-020-04635-1]

6 **Garcia-Aguilar J**, Chow OS, Smith DD, Marcet JE, Cataldo PA, Varma MG, Kumar AS, Oommen S, Coutsoftides T, Hunt SR, Stamos MJ, Ternent CA, Herzig DO, Fichera A, Polite BN, Dietz DW, Patil S, Avila K; Timing of Rectal Cancer Response to Chemoradiation Consortium. Effect of adding mFOLFOX6 after neoadjuvant chemoradiation in locally advanced rectal cancer: a multicentre, phase 2 trial. *Lancet Oncol* 2015; **16**: 957-966 [PMID: 26187751 DOI: 10.1016/S1470-2045(15)00004-2]

7 **Giunta EF**, Bregni G, Pretta A, Deleporte A, Liberale G, Bali AM, Moretti L, Troiani T, Ciardiello F, Hendlisz A, Sclafani F. Total neoadjuvant therapy for rectal cancer: Making sense of the results from the RAPIDO and PRODIGE 23 trials. *Cancer Treat Rev* 2021; **96**: 102177 [PMID: 33798955 DOI: 10.1016/j.ctrv.2021.102177]

8 **Martin ST**, Heneghan HM, Winter DC. Systematic review and meta-analysis of outcomes following pathological complete response to neoadjuvant chemoradiotherapy for rectal cancer. *Br J Surg* 2012; **99**: 918-928 [PMID: 22362002 DOI: 10.1002/bjs.8702]

9 **van der Valk MJM**, Hilling DE, Bastiaannet E, Meershoek-Klein Kranenbarg E, Beets GL, Figueiredo NL, Habr-Gama A, Perez RO, Renehan AG, van de Velde CJH; IWWD Consortium. Long-term outcomes of clinical complete responders after neoadjuvant treatment for rectal cancer in the International Watch & Wait Database (IWWD): an international multicentre registry study. *Lancet* 2018; **391**: 2537-2545 [PMID: 29976470 DOI: 10.1016/S0140-6736(18)31078-X]

10 **Deidda S**, Elmore U, Rosati R, De Nardi P, Vignali A, Puccetti F, Spolverato G, Capelli G, Zuin M, Muratore A, Danna R, Calabrò M, Guerrieri M, Ortenzi M, Ghiselli R, Scabini S, Aprile A, Pertile D, Sammarco G, Gallo G, Sena G, Coco C, Rizzo G, Pafundi DP, Belluco C, Innocente R, Degiuli M, Reddavid R, Puca L, Delrio P, Rega D, Conti P, Pastorino A, Zorcolo L, Pucciarelli S, Aschele C, Restivo A. Association of Delayed Surgery With Oncologic Long-term Outcomes in Patients With Locally Advanced Rectal Cancer Not Responding to Preoperative Chemoradiation. *JAMA Surg* 2021; **156**: 1141-1149 [PMID: 34586340 DOI: 10.1001/jamasurg.2021.4566]

11 **Hendrick LE**, Levesque RL, Hinkle NM, Monroe JJ, Glazer ES, Deneve JL, Yakoub D, Shibata D, Dickson PV. Restaging Patients with Rectal Cancer Following Neoadjuvant Chemoradiation: A Systematic Review. *World J Surg* 2020; **44**: 973-979 [PMID: 31788724 DOI: 10.1007/s00268-019-05309-z]

12 **Habr-Gama A**, Perez RO, Wynn G, Marks J, Kessler H, Gama-Rodrigues J. Complete clinical response after neoadjuvant chemoradiation therapy for distal rectal cancer: characterization of clinical and endoscopic findings for standardization. *Dis Colon Rectum* 2010; **53**: 1692-1698 [PMID: 21178866 DOI: 10.1007/DCR.0b013e3181f42b89]

13 **Habr-Gama A**, São Julião GP, Vailati BB, Sabbaga J, Aguilar PB, Fernandez LM, Araújo SEA, Perez RO. Organ Preservation in cT2N0 Rectal Cancer After Neoadjuvant Chemoradiation Therapy: The Impact of Radiation Therapy Dose-escalation and Consolidation Chemotherapy. *Ann Surg* 2019; **269**: 102-107 [PMID: 28742703 DOI: 10.1097/SLA.0000000000002447]

14 **Glynne-Jones R**, Wyrwicz L, Tiret E, Brown G, Rödel C, Cervantes A, Arnold D; ESMO Guidelines Committee. Rectal cancer: ESMO Clinical Practice Guidelines for diagnosis, treatment and follow-up. *Ann Oncol* 2017; **28**: iv22-iv40

[PMID: 28881920 DOI: 10.1093/annonc/mdx224]

15 **Benson AB**, Venook AP, Al-Hawary MM, Azad N, Chen YJ, Ciombor KK, Cohen S, Cooper HS, Deming D, Garrido-Laguna I, Grem JL, Gunn A, Hecht JR, Hoffe S, Hubbard J, Hunt S, Jeck W, Johung KL, Kirilcuk N, Krishnamurthi S, Maratt JK, Messersmith WA, Meyerhardt J, Miller ED, Mulcahy MF, Nurkin S, Overman MJ, Parikh A, Patel H, Pedersen K, Saltz L, Schneider C, Shibata D, Skibber JM, Sofocleous CT, Stotsky-Himelfarb E, Tavakkoli A, Willett CG, Gregory K, Gurski L. Rectal Cancer, Version 2.2022, NCCN Clinical Practice Guidelines in Oncology. *J Natl Compr Canc Netw* 2022; **20**: 1139-1167 [PMID: 36240850 DOI: 10.6004/jnccn.2022.0051]

16 **Smith JJ**, Chow OS, Gollub MJ, Nash GM, Temple LK, Weiser MR, Guillem JG, Paty PB, Avila K, Garcia-Aguilar J; Rectal Cancer Consortium. Organ Preservation in Rectal Adenocarcinoma: a phase II randomized controlled trial evaluating 3-year disease-free survival in patients with locally advanced rectal cancer treated with chemoradiation plus induction or consolidation chemotherapy, and total mesorectal excision or nonoperative management. *BMC Cancer* 2015; **15**: 767 [PMID: 26497495 DOI: 10.1186/s12885-015-1632-z]

17 **Garcia-Aguilar J**, Patil S, Gollub MJ, Kim JK, Yuval JB, Thompson HM, Verheij FS, Omer DM, Lee M, Dunne RF, Marcet J, Cataldo P, Polite B, Herzig DO, Liska D, Oommen S, Friel CM, Ternent C, Coveler AL, Hunt S, Gregory A, Varma MG, Bello BL, Carmichael JC, Krauss J, Gleisner A, Paty PB, Weiser MR, Nash GM, Pappou E, Guillem JG, Temple L, Wei IH, Widmar M, Lin S, Segal NH, Cercek A, Yaeger R, Smith JJ, Goodman KA, Wu AJ, Saltz LB. Organ Preservation in Patients With Rectal Adenocarcinoma Treated With Total Neoadjuvant Therapy. *J Clin Oncol* 2022; **40**: 2546-2556 [PMID: 35483010 DOI: 10.1200/JCO.22.00032]

18 **Maas M**, Beets-Tan RG, Lambregts DM, Lammering G, Nelemans PJ, Engelen SM, van Dam RM, Jansen RL, Sosef M, Leijtens JW, Hulsewé KW, Buijsen J, Beets GL. Wait-and-see policy for clinical complete responders after chemoradiation for rectal cancer. *J Clin Oncol* 2011; **29**: 4633-4640 [PMID: 22067400 DOI: 10.1200/JCO.2011.37.7176]

19 **Martens MH**, Maas M, Heijnen LA, Lambregts DM, Leijtens JW, Stassen LP, Breukink SO, Hoff C, Belgers EJ, Melenhorst J, Jansen R, Buijsen J, Hoofwijk TG, Beets-Tan RG, Beets GL. Long-term Outcome of an Organ Preservation Program After Neoadjuvant Treatment for Rectal Cancer. *J Natl Cancer Inst* 2016; **108** [PMID: 27509881 DOI: 10.1093/jnci/djw171]

20 **Fokas E**, Appelt A, Glynne-Jones R, Beets G, Perez R, Garcia-Aguilar J, Rullier E, Smith JJ, Marijnen C, Peters FP, van der Valk M, Beets-Tan R, Myint AS, Gerard JP, Bach SP, Ghadimi M, Hofheinz RD, Bujko K, Gani C, Haustermans K, Minsky BD, Ludmir E, West NP, Gambacorta MA, Valentini V, Buyse M, Renehan AG, Gilbert A, Sebag-Montefiore D, Rödel C. International consensus recommendations on key outcome measures for organ preservation after (chemo)radiotherapy in patients with rectal cancer. *Nat Rev Clin Oncol* 2021; **18**: 805-816 [PMID: 34349247 DOI: 10.1038/s41571-021-00538-5]

21 **Fokas E**, Glynne-Jones R, Appelt A, Beets-Tan R, Beets G, Haustermans K, Marijnen C, Minsky BD, Ludmir E, Quirke P, Sebag-Montefiore D, Garcia-Aguilar J, Gambacorta MA, Valentini V, Buyse M, Rödel C. Outcome measures in multimodal rectal cancer trials. *Lancet Oncol* 2020; **21**: e252-e264 [PMID: 32359501 DOI: 10.1016/S1470-2045(20)30024-3]

22 **Francois Y**, Nemoz CJ, Baulieux J, Vignal J, Grandjean JP, Partensky C, Souquet JC, Adeleine P, Gerard JP. Influence of the interval between preoperative radiation therapy and surgery on downstaging and on the rate of sphincter-sparing surgery for rectal cancer: the Lyon R90-01 randomized trial. *J Clin Oncol* 1999; **17**: 2396 [PMID: 10561302 DOI: 10.1200/JCO.1999.17.8.2396]

23 **Pettersson D**, Lörinc E, Holm T, Iversen H, Cedermark B, Glimelius B, Martling A. Tumour regression in the randomized Stockholm III Trial of radiotherapy regimens for rectal cancer. *Br J Surg* 2015; **102**: 972-8; discussion 978 [PMID: 26095256 DOI: 10.1002/bjs.9811]

24 **Lefevre JH**, Mineur L, Kotti S, Rullier E, Rouanet P, de Chaisemartin C, Meunier B, Mehrdad J, Cotte E, Desrame J, Karoui M, Benoist S, Kirzin S, Berger A, Panis Y, Piessen G, Saudemont A, Prudhomme M, Peschaud F, Dubois A, Loriau J, Tuech JJ, Meurette G, Lupinacci R, Goasgen N, Parc Y, Simon T, Tiret E. Effect of Interval (7 or 11 weeks) Between Neoadjuvant Radiochemotherapy and Surgery on Complete Pathologic Response in Rectal Cancer: A Multicenter, Randomized, Controlled Trial (GRECCAR-6). *J Clin Oncol* 2016; **34**: 3773-3780 [PMID: 27432930 DOI: 10.1200/JCO.2016.67.6049]

25 **Evans J**, Bhoday B, Sizer B, Tekkis P, Swift R, Perez R, Tait D and Brown G. Results of a prospective randomised control 6 vs 12 trial: is greater tumour downstaging observed on post treatment MRI if surgery is delayed to 12-weeks vs 6-weeks after completion of neoadjuvant chemoradiotherapy? *Ann Oncol* **27**: 4520 [DOI: 10.1093/ANNONC/MDW370.01]

26 **Akgun E**, Caliskan C, Bozbiyik O, Yoldas T, Sezak M, Ozkok S, Kose T, Karabulut B, Harman M, Ozutemiz O. Randomized clinical trial of short or long interval between neoadjuvant chemoradiotherapy and surgery for rectal cancer. *Br J Surg* 2018; **105**: 1417-1425 [PMID: 30155949 DOI: 10.1002/bjs.10984]

27 **Sloothaak DA**, Geijsen DE, van Leersum NJ, Punt CJ, Buskens CJ, Bemelman WA, Tanis PJ; Dutch Surgical Colorectal Audit. Optimal time interval between neoadjuvant chemoradiotherapy and surgery for rectal cancer. *Br J Surg* 2013; **100**: 933-939 [PMID: 23536485 DOI: 10.1002/bjs.9112]

28 **Macchia G**, Gambacorta MA, Masciocchi C, Chiloiro G, Mantello G, di Benedetto M, Lupattelli M, Palazzari E, Belgioia L, Bacigalupo A, Sainato A, Montrone S, Turri L, Caroli A, De Paoli A, Matrone F, Capirci C, Montesi G, Niespolo RM, Osti MF, Caravatta L, Galardi A, Genovesi D, Rosetto ME, Boso C, Sciacero P, Giaccherini L, Parisi S, Fontana A, Filippone FR, Picardi V, Morganti AG, Valentini V. Time to surgery and pathologic complete response after neoadjuvant chemoradiation in rectal cancer: A population study on 2094 patients. *Clin Transl Radiat Oncol* 2017; **4**: 8-14 [PMID: 29594202 DOI: 10.1016/j.ctro.2017.04.004]

29 **Probst CP**, Becerra AZ, Aquina CT, Tejani MA, Wexner SD, Garcia-Aguilar J, Remzi FH, Dietz DW, Monson JR, Fleming FJ; Consortium for Optimizing the Surgical Treatment of Rectal Cancer (OSTRiCh). Extended Intervals after Neoadjuvant Therapy in Locally Advanced Rectal Cancer: The Key to Improved Tumor Response and Potential Organ Preservation. *J Am Coll Surg* 2015; **221**: 430-440 [PMID: 26206642 DOI: 10.1016/j.jamcollsurg.2015.04.010]

30 **Gambacorta MA**, Masciocchi C, Chiloiro G, Meldolesi E, Macchia G, van Soest J, Peters F, Collette L, Gérard JP, Ngan

S, Rödel CC, Damiani A, Dekker A, Valentini V. Timing to achieve the highest rate of pCR after preoperative radiochemotherapy in rectal cancer: a pooled analysis of 3085 patients from 7 randomized trials. *Radiother Oncol* 2021; **154**: 154-160 [PMID: 32966845 DOI: 10.1016/j.radonc.2020.09.026]

31 **Fokas E**, Allgäuer M, Polat B, Klautke G, Grabenbauer GG, Fietkau R, Kuhnt T, Staib L, Brunner T, Grosu AL, Schmiegel W, Jacobasch L, Weitz J, Folprecht G, Schlenska-Lange A, Flentje M, Germer CT, Grützmann R, Schwarzbach M, Paolucci V, Bechstein WO, Friede T, Ghadimi M, Hofheinz RD, Rödel C; German Rectal Cancer Study Group. Randomized Phase II Trial of Chemoradiotherapy Plus Induction or Consolidation Chemotherapy as Total Neoadjuvant Therapy for Locally Advanced Rectal Cancer: CAO/ARO/AIO-12. *J Clin Oncol* 2019; **37**: 3212-3222 [PMID: 31150315 DOI: 10.1200/JCO.19.00308]

32 **Garcia-Aguilar JPS**, Patil S, Kim JK, Yuval JB, Thompson H, Verheij F, Lee M, Saltz L. Preliminary results of the organ preservation of rectal adenocarcinoma (OPRA) trial. *J Clin Oncol* 2020; **38**: 4008 [DOI: 10.1200/jco.2020.38.15_suppl.4008]

33 **Ryan ÉJ**, O'Sullivan DP, Kelly ME, Syed AZ, Neary PC, O'Connell PR, Kavanagh DO, Winter DC, O'Riordan JM. Meta-analysis of the effect of extending the interval after long-course chemoradiotherapy before surgery in locally advanced rectal cancer. *Br J Surg* 2019; **106**: 1298-1310 [PMID: 31216064 DOI: 10.1002/bjs.11220]

34 **Smith N**, Brown G. Preoperative staging of rectal cancer. *Acta Oncol* 2008; **47**: 20-31 [PMID: 17957502 DOI: 10.1080/02841860701697720]

35 **Kim YI**, Jang JK, Park IJ, Park SH, Kim JB, Park JH, Kim TW, Ro JS, Lim SB, Yu CS, Kim JC. Lateral lymph node and its association with distant recurrence in rectal cancer: A clue of systemic disease. *Surg Oncol* 2020; **35**: 174-181 [PMID: 32889250 DOI: 10.1016/j.suronc.2020.08.013]

36 **Chadi SA**, Malcomson L, Ensor J, Riley RD, Vaccaro CA, Rossi GL, Daniels IR, Smart NJ, Osborne ME, Beets GL, Maas M, Bitterman DS, Du K, Gollins S, Sun Myint A, Smith FM, Saunders MP, Scott N, O'Dwyer ST, de Castro Araujo RO, Valadao M, Lopes A, Hsiao CW, Lai CL, Smith RK, Paulson EC, Appelt A, Jakobsen A, Wexner SD, Habr-Gama A, Sao Julião G, Perez R, Renehan AG. Factors affecting local regrowth after watch and wait for patients with a clinical complete response following chemoradiotherapy in rectal cancer (InterCoRe consortium): an individual participant data meta-analysis. *Lancet Gastroenterol Hepatol* 2018; **3**: 825-836 [PMID: 30318451 DOI: 10.1016/S2468-1253(18)30301-7]

37 **Beets-Tan RGH**, Lambregts DMJ, Maas M, Bipat S, Barbaro B, Curvo-Semedo L, Fenlon HM, Gollub MJ, Gourtsoyianni S, Halligan S, Hoeffel C, Kim SH, Laghi A, Maier A, Rafaelsen SR, Stoker J, Taylor SA, Torkzad MR, Blomqvist L. Magnetic resonance imaging for clinical management of rectal cancer: Updated recommendations from the 2016 European Society of Gastrointestinal and Abdominal Radiology (ESGAR) consensus meeting. *Eur Radiol* 2018; **28**: 1465-1475 [PMID: 29043428 DOI: 10.1007/s00330-017-5026-2]

38 **Gollub MJ**, Arya S, Beets-Tan RG, dePrisco G, Gonen M, Jhaveri K, Kassam Z, Kaur H, Kim D, Knezevic A, Korngold E, Lall C, Lalwani N, Blair Macdonald D, Moreno C, Nougaret S, Pickhardt P, Sheedy S, Harisinghani M. Use of magnetic resonance imaging in rectal cancer patients: Society of Abdominal Radiology (SAR) rectal cancer disease-focused panel (DFP) recommendations 2017. *Abdom Radiol (NY)* 2018; **43**: 2893-2902 [PMID: 29785540 DOI: 10.1007/s00261-018-1642-9]

39 **Wei MZ**, Zhao ZH, Wang JY. The Diagnostic Accuracy of Magnetic Resonance Imaging in Restaging of Rectal Cancer After Preoperative Chemoradiotherapy: A Meta-Analysis and Systematic Review. *J Comput Assist Tomogr* 2020; **44**: 102-110 [PMID: 31939890 DOI: 10.1097/RCT.0000000000000964]

40 **van der Paardt MP**, Zagers MB, Beets-Tan RG, Stoker J, Bipat S. Patients who undergo preoperative chemoradiotherapy for locally advanced rectal cancer restaged by using diagnostic MR imaging: a systematic review and meta-analysis. *Radiology* 2013; **269**: 101-112 [PMID: 23801777 DOI: 10.1148/radiol.13122833]

41 **Lambregts DM**, Vandecaveye V, Barbaro B, Bakers FC, Lambrecht M, Maas M, Haustermans K, Valentini V, Beets GL, Beets-Tan RG. Diffusion-weighted MRI for selection of complete responders after chemoradiation for locally advanced rectal cancer: a multicenter study. *Ann Surg Oncol* 2011; **18**: 2224-2231 [PMID: 21347783 DOI: 10.1245/s10434-011-1607-5]

42 **Sclafani F**, Brown G, Cunningham D, Wotherspoon A, Mendes LST, Balyasnikova S, Evans J, Peckitt C, Begum R, Tait D, Tabernero J, Glimelius B, Roselló S, Thomas J, Oates J, Chau I. Comparison between MRI and pathology in the assessment of tumour regression grade in rectal cancer. *Br J Cancer* 2017; **117**: 1478-1485 [PMID: 28934761 DOI: 10.1038/bjc.2017.320]

43 **Lambregts DMJ**, Delli Pizzi A, Lahaye MJ, van Griethuysen JJM, Maas M, Beets GL, Bakers FCH, Beets-Tan RGH. A Pattern-Based Approach Combining Tumor Morphology on MRI With Distinct Signal Patterns on Diffusion-Weighted Imaging to Assess Response of Rectal Tumors After Chemoradiotherapy. *Dis Colon Rectum* 2018; **61**: 328-337 [PMID: 29369900 DOI: 10.1097/DCR.0000000000000915]

44 **Maas M**, Nelemans PJ, Valentini V, Das P, Rödel C, Kuo LJ, Calvo FA, García-Aguilar J, Glynne-Jones R, Haustermans K, Mohiuddin M, Pucciarelli S, Small W Jr, Suárez J, Theodoropoulos G, Biondo S, Beets-Tan RG, Beets GL. Long-term outcome in patients with a pathological complete response after chemoradiation for rectal cancer: a pooled analysis of individual patient data. *Lancet Oncol* 2010; **11**: 835-844 [PMID: 20692872 DOI: 10.1016/S1470-2045(10)70172-8]

45 **Fernandes MC**, Gollub MJ, Brown G. The importance of MRI for rectal cancer evaluation. *Surg Oncol* 2022; **43**: 101739 [PMID: 35339339 DOI: 10.1016/j.suronc.2022.101739]

46 **Heijnen LA**, Maas M, Beets-Tan RG, Berkhof M, Lambregts DM, Nelemans PJ, Riedl R, Beets GL. Nodal staging in rectal cancer: why is restaging after chemoradiation more accurate than primary nodal staging? *Int J Colorectal Dis* 2016; **31**: 1157-1162 [PMID: 27055660 DOI: 10.1007/s00384-016-2576-8]

47 **Loftås P**, Sturludóttir M, Hallböök O, Almlöv K, Arbman G, Blomqvist L. Assessment of remaining tumour involved lymph nodes with MRI in patients with complete luminal response after neoadjuvant treatment of rectal cancer. *Br J Radiol* 2018; **91**: 20170938 [PMID: 29668301 DOI: 10.1259/bjr.20170938]

48 **van Heeswijk MM**, Lambregts DM, Palm WM, Hendriks BM, Maas M, Beets GL, Beets-Tan RG. DWI for Assessment of Rectal Cancer Nodes After Chemoradiotherapy: Is the Absence of Nodes at DWI Proof of a Negative Nodal Status? *AJR Am J Roentgenol* 2017; **208**: W79-W84 [PMID: 27959622 DOI: 10.2214/AJR.16.17117]

49 **Vliegen RF**, Beets GL, Lammering G, Dresen RC, Rutten HJ, Kessels AG, Oei TK, de Bruïne AP, van Engelshoven JM, Beets-Tan RG. Mesorectal fascia invasion after neoadjuvant chemotherapy and radiation therapy for locally advanced rectal cancer: accuracy of MR imaging for prediction. *Radiology* 2008; **246**: 454-462 [PMID: 18227541 DOI: 10.1148/radiol.2462070042]

50 **Oberholzer K**, Junginger T, Heintz A, Kreft A, Hansen T, Lollert A, Ebert M, Düber C. Rectal Cancer: MR imaging of the mesorectal fascia and effect of chemoradiation on assessment of tumor involvement. *J Magn Reson Imaging* 2012; **36**: 658-663 [PMID: 22592948 DOI: 10.1002/jmri.23687]

51 **Ogura A**, Konishi T, Cunningham C, Garcia-Aguilar J, Iversen H, Toda S, Lee IK, Lee HX, Uehara K, Lee P, Putter H, van de Velde CJH, Beets GL, Rutten HJT, Kusters M; Lateral Node Study Consortium. Neoadjuvant (Chemo)radiotherapy With Total Mesorectal Excision Only Is Not Sufficient to Prevent Lateral Local Recurrence in Enlarged Nodes: Results of the Multicenter Lateral Node Study of Patients With Low cT3/4 Rectal Cancer. *J Clin Oncol* 2019; **37**: 33-43 [PMID: 30403572 DOI: 10.1200/JCO.18.00032]

52 **Ogura A**, Konishi T, Beets GL, Cunningham C, Garcia-Aguilar J, Iversen H, Toda S, Lee IK, Lee HX, Uehara K, Lee P, Putter H, van de Velde CJH, Rutten HJT, Tuynman JB, Kusters M; Lateral Node Study Consortium. Lateral Nodal Features on Restaging Magnetic Resonance Imaging Associated With Lateral Local Recurrence in Low Rectal Cancer After Neoadjuvant Chemoradiotherapy or Radiotherapy. *JAMA Surg* 2019; **154**: e192172 [PMID: 31268504 DOI: 10.1001/jamasurg.2019.2172]

53 **Pastor C**, Subtil JC, Sola J, Baixauli J, Beorlegui C, Arbea L, Aristu J, Hernandez-Lizoain JL. Accuracy of endoscopic ultrasound to assess tumor response after neoadjuvant treatment in rectal cancer: can we trust the findings? *Dis Colon Rectum* 2011; **54**: 1141-1146 [PMID: 21825895 DOI: 10.1097/DCR.0b013e31821c4a60]

54 **Huh JW**, Park YA, Jung EJ, Lee KY, Sohn SK. Accuracy of endorectal ultrasonography and computed tomography for restaging rectal cancer after preoperative chemoradiation. *J Am Coll Surg* 2008; **207**: 7-12 [PMID: 18589355 DOI: 10.1016/j.jamcollsurg.2008.01.002]

55 **Marone P**, de Bellis M, D'Angelo V, Delrio P, Passananti V, Di Girolamo E, Rossi GB, Rega D, Tracey MC, Tempesta AM. Role of endoscopic ultrasonography in the loco-regional staging of patients with rectal cancer. *World J Gastrointest Endosc* 2015; **7**: 688-701 [PMID: 26140096 DOI: 10.4253/wjge.v7.i7.688]

56 **Zhao RS**, Wang H, Zhou ZY, Zhou Q, Mulholland MW. Restaging of locally advanced rectal cancer with magnetic resonance imaging and endoluminal ultrasound after preoperative chemoradiotherapy: a systemic review and meta-analysis. *Dis Colon Rectum* 2014; **57**: 388-395 [PMID: 24509465 DOI: 10.1097/DCR.0000000000000022]

57 **Zhang X**, Fan J, Zhang L, Wang J, Wang M, Zhu J. Association Between Three-Dimensional Transrectal Ultrasound Findings and Tumor Response to Neoadjuvant Chemoradiotherapy in Locally Advanced Rectal Cancer: An Observational Study. *Front Oncol* 2021; **11**: 648839 [PMID: 34178635 DOI: 10.3389/fonc.2021.648839]

58 **Ren Y**, Ye J, Wang Y, Xiong W, Xu J, He Y, Cai S, Tan M, Yuan Y. The Optimal Application of Transrectal Ultrasound in Staging of Rectal Cancer Following Neoadjuvant Therapy: A Pragmatic Study for Accuracy Investigation. *J Cancer* 2018; **9**: 784-791 [PMID: 29581756 DOI: 10.7150/jca.22661]

59 **Martellucci J**, Scheiterle M, Lorenzi B, Roviello F, Cetta F, Pinto E, Tanzini G. Accuracy of transrectal ultrasound after preoperative radiochemotherapy compared to computed tomography and magnetic resonance in locally advanced rectal cancer. *Int J Colorectal Dis* 2012; **27**: 967-973 [PMID: 22297865 DOI: 10.1007/s00384-012-1419-5]

60 **Pomerri F**, Pucciarelli S, Maretto I, Zandonà M, Del Bianco P, Amadio L, Rugge M, Nitti D, Muzzio PC. Prospective assessment of imaging after preoperative chemoradiotherapy for rectal cancer. *Surgery* 2011; **149**: 56-64 [PMID: 20452636 DOI: 10.1016/j.surg.2010.03.025]

61 **Kye BH**, Kim HJ, Kim G, Kim JG, Cho HM. Multimodal Assessments Are Needed for Restaging after Neoadjunvant Chemoradiation Therapy in Rectal Cancer Patients. *Cancer Res Treat* 2016; **48**: 561-566 [PMID: 26323642 DOI: 10.4143/crt.2015.114]

62 **Duldulao MP**, Lee W, Streja L, Chu P, Li W, Chen Z, Kim J, Garcia-Aguilar J. Distribution of residual cancer cells in the bowel wall after neoadjuvant chemoradiation in patients with rectal cancer. *Dis Colon Rectum* 2013; **56**: 142-149 [PMID: 23303141 DOI: 10.1097/DCR.0b013e31827541e2]

63 **Smith FM**, Wiland H, Mace A, Pai RK, Kalady MF. Clinical criteria underestimate complete pathological response in rectal cancer treated with neoadjuvant chemoradiotherapy. *Dis Colon Rectum* 2014; **57**: 311-315 [PMID: 24509452 DOI: 10.1097/DCR.0b013e3182a84eba]

64 **van der Sande ME**, Maas M, Melenhorst J, Breukink SO, van Leerdam ME, Beets GL. Predictive Value of Endoscopic Features for a Complete Response After Chemoradiotherapy for Rectal Cancer. *Ann Surg* 2021; **274**: e541-e547 [PMID: 31851000 DOI: 10.1097/SLA.0000000000003718]

65 **Nahas SC**, Rizkallah Nahas CS, Sparapan Marques CF, Ribeiro U Jr, Cotti GC, Imperiale AR, Capareli FC, Chih Chen AT, Hoff PM, Cecconello I. Pathologic Complete Response in Rectal Cancer: Can We Detect It? *Dis Colon Rectum* 2016; **59**: 255-263 [PMID: 26953983 DOI: 10.1097/DCR.0000000000000558]

66 **Liu S**, Zhong GX, Zhou WX, Xue HD, Pan WD, Xu L, Lu JY, Wu B, Lin GL, Qiu HZ, Xiao Y. Can Endorectal Ultrasound, MRI, and Mucosa Integrity Accurately Predict the Complete Response for Mid-Low Rectal Cancer After Preoperative Chemoradiation? *Dis Colon Rectum* 2018; **61**: 903-910 [PMID: 29944579 DOI: 10.1097/DCR.0000000000001135]

67 **Maas M**, Lambregts DM, Nelemans PJ, Heijnen LA, Martens MH, Leijtens JW, Sosef M, Hulsewé KW, Hoff C, Breukink SO, Stassen L, Beets-Tan RG, Beets GL. Assessment of Clinical Complete Response After Chemoradiation for Rectal Cancer with Digital Rectal Examination, Endoscopy, and MRI: Selection for Organ-Saving Treatment. *Ann Surg Oncol* 2015; **22**: 3873-3880 [PMID: 26198074 DOI: 10.1245/s10434-015-4687-9]

68 **East JE**, Vleugels JL, Roelandt P, Bhandari P, Bisschops R, Dekker E, Hassan C, Horgan G, Kiesslich R, Longcroft-Wheaton G, Wilson A, Dumonceau JM. Advanced endoscopic imaging: European Society of Gastrointestinal Endoscopy (ESGE) Technology Review. *Endoscopy* 2016; **48**: 1029-1045 [PMID: 27711949 DOI: 10.1055/s-0042-118087]

69 **Perez RO**, Habr-Gama A, Pereira GV, Lynn PB, Alves PA, Proscurshim I, Rawet V, Gama-Rodrigues J. Role of biopsies in patients with residual rectal cancer following neoadjuvant chemoradiation after downsizing: can they rule out persisting

cancer? *Colorectal Dis* 2012; **14**: 714-720 [PMID: 22568644 DOI: 10.1111/j.1463-1318.2011.02761.x]

70 **Maffione AM**, Marzola MC, Capirci C, Colletti PM, Rubello D. Value of (18)F-FDG PET for Predicting Response to Neoadjuvant Therapy in Rectal Cancer: Systematic Review and Meta-Analysis. *AJR Am J Roentgenol* 2015; **204**: 1261-1268 [PMID: 26001237 DOI: 10.2214/AJR.14.13210]

71 **Patel S**, McCall M, Ohinmaa A, Bigam D, Dryden DM. Positron emission tomography/computed tomographic scans compared to computed tomographic scans for detecting colorectal liver metastases: a systematic review. *Ann Surg* 2011; **253**: 666-671 [PMID: 21475005 DOI: 10.1097/SLA.0b013e31821110c9]

72 **Crimì F**, Valeggia S, Baffoni L, Stramare R, Lacognata C, Spolverato G, Albertoni L, Spimpolo A, Evangelista L, Zucchetta P, Cecchin D, Pucciarelli S. [18F]FDG PET/MRI in rectal cancer. *Ann Nucl Med* 2021; **35**: 281-290 [PMID: 33517562 DOI: 10.1007/s12149-021-01580-0]

World Journal of Gastrointestinal Oncology

Submit a Manuscript: https://www.f6publishing.com

World J Gastrointest Oncol 2023 May 15; 15(5): 713-730

DOI: 10.4251/wjgo.v15.i5.713

ISSN 1948-5204 (online)

REVIEW

Intratumour microbiome of pancreatic cancer

Shi-Wei Guan, Quan Lin, Hai-Bo Yu

Specialty type: Oncology

Provenance and peer review: Invited article; Externally peer reviewed.

Peer-review model: Single blind

Peer-review report's scientific quality classification

Grade A (Excellent): A
Grade B (Very good): B
Grade C (Good): C
Grade D (Fair): 0
Grade E (Poor): 0

P-Reviewer: Nakahodo J, Japan; Solimando AG, Italy

Received: December 2, 2022
Peer-review started: December 2, 2022
First decision: January 16, 2023
Revised: January 26, 2023
Accepted: April 4, 2023
Article in press: April 4, 2023
Published online: May 15, 2023

Shi-Wei Guan, Quan Lin, Hai-Bo Yu, Department of Surgery, Wenzhou Central Hospital, The Dingli Clinical Institute of Wenzhou Medical University, Wenzhou 325000, Zhejiang Province, China

Corresponding author: Hai-Bo Yu, MD, Chief Doctor, Department of Surgery, Wenzhou Central Hospital, The Dingli Clinical Institute of Wenzhou Medical University, No. 252 Baili East Road, Wenzhou 325000, Zhejiang Province, China. yuhaibozjwz@163.com

Abstract

Pancreatic cancer is a high mortality malignancy with almost equal mortality and morbidity rates. Both normal and tumour tissues of the pancreas were previously considered sterile. In recent years, with the development of technologies for high-throughput sequencing, a variety of studies have revealed that pancreatic cancer tissues contain small amounts of bacteria and fungi. The intratumour microbiome is being revealed as an influential contributor to carcinogenesis. The intratumour microbiome has been identified as a crucial factor for pancreatic cancer progression, diagnosis, and treatment, chemotherapy resistance, and immune response. A better understanding of the biology of the intratumour microbiome of pancreatic cancer contributes to the establishment of better early cancer screening and treatment strategies. This review focuses on the possible origins of the intratumour microbiome in pancreatic cancer, the intratumour localization, the interaction with the tumour microenvironment, and strategies for improving the outcome of pancreatic cancer treatment. Thus, this review offers new perspectives for improving the prognosis of pancreatic cancer.

Key Words: Intratumour microbiome; Pancreatic cancer; Tumour microenvironment; Chemoresistance; Diagnosis; Prognosis

Core Tip: Recently, with the development of high-throughput sequencing, tumour tissues, which were previously believed to be sterile, have been shown to harbor a low microbiome biomass. The intratumour microbiome is crucial for pancreatic ductal adenocarcinoma (PDAC) diagnosis, treatment, chemotherapy resistance, and immune response. Establishing an awareness of the biology of the tumour microbiome in PDAC supports the establishment of better strategies for PDAC. This review focuses on the possible origins of the microbiome, the localization, the interaction with the tumour microenvironment and the strategies for improving the outcomes of treatment. This review offers new perspectives for improving the prognosis of PDAC.

Citation: Guan SW, Lin Q, Yu HB. Intratumour microbiome of pancreatic cancer. *World J Gastrointest Oncol* 2023; 15(5): 713-730
URL: https://www.wjgnet.com/1948-5204/full/v15/i5/713.htm
DOI: https://dx.doi.org/10.4251/wjgo.v15.i5.713

INTRODUCTION

Pancreatic ductal adenocarcinoma (PDAC) is a malignant tumour that originates from pancreatic ductal cells. Although medical technology has improved the mortality of PDAC patients, the five-year survival remains less than 10%[1]. Since early PDAC patients lack specific clinical manifestations, the detection of PDAC usually occurs in the middle or late stages. Furthermore, advanced-stage PDAC usually cannot be eradicated by surgery, and these patients fail to respond to immunotherapy, chemotherapy or radiotherapy[2]. Therefore, it remains a huge challenge to improve the outlook for individuals with PDAC.

The traditional approaches for PDAC research are centred on the factors of PDAC only while ignoring the role of the microbiome in the tumour microenvironment (TME). Investigation revealed that the host microbiome, particularly the gut microbiome, interacts to influence cellular biological activity and regulate inflammation, immunity and cancer progression[3-6]. Of the 1012 different microbial species known today, only 11 are labeled human carcinogens by the International Association for Cancer Registries[7,8]. A broader range of microbiomes may contribute to carcinogenesis as an important class of 'coconspirators' but is not enough to cause cancer[9-11]. Recently, with increasing research on PDAC, tumour tissues, previously believed to be sterile, have been found to harbour a low microbiome biomass. The tumour microbiome was first proposed in the 19th century, but little progress in this field was made for a considerable period of time[12]. With advances in sequencing technology and a better understanding of the TME, it has been revealed that the intratumour microbiome plays an influential role in tumour progression[8]. However, the abundance of the intratumour microbiome is substantially lower than that of tumour cells. The bacterial portion of the tumour tissue was calculated to be approximately 0.68%. In the case of a three-dimensional or flat tumour environment, this equates to approximately 10^5 to 10^6 bacteria per 1 cm^3 or approximately 34 bacteria per 1 mm^2[8,13]. However, research has revealed that the intratumour microbiome exerts influential impacts on the progression, diagnosis, treatment, chemotherapy resistance, and modulation of immune tone in PDAC[14-17].

Despite the progress made in the study of the intratumour microbiome, there are still many unanswered questions in this emerging field. Furthermore, the understanding of the PDAC intratumour microbiome is far from complete, partly due to the limitations of research techniques[18]. Establishing an awareness of the biology of the tumour microbiome in PDAC supports the establishment of better strategies for early cancer screening and treatment. This review focuses on the possible origins of the intratumour microbiome in PDAC, the intratumour localization, the interaction with the TME, and the roles or strategies in improving the outcomes of PDAC treatment, offering new perspectives for improving the prognosis of PDAC.

THE ORIGIN OF THE PDAC INTRATUMOUR MICROBIOME

The mainstream view holds that the microbiome in PDAC may originate from the gut and the oral cavity, but this remains controversial (Figure 1). The pancreatic duct and common bile duct open together at the duodenal papilla. The innate anatomy allows microorganisms from the gut to enter the pancreatic tissue retrogradely through the pancreatic duct. Additionally, Okuda *et al*[19] showed that representative bacteria in pancreatic juice strongly colocalized in PDAC tissue[19]. Bacterial signals were detected in pancreatic tissue of wild-type (WT) mice by gavaging fluorescently labelled *Enterococcus faecalis* and GFP-labelled *Escherichia coli* (*E. coli*)[20]. Similarly, when PDAC mice were gavaged with fungi, the presence of fungi in the tumour tissue was confirmed by staining or fluorescence[17,21]. However, in another design, the presence of bacteria in normal pancreatic tissue was not detected in

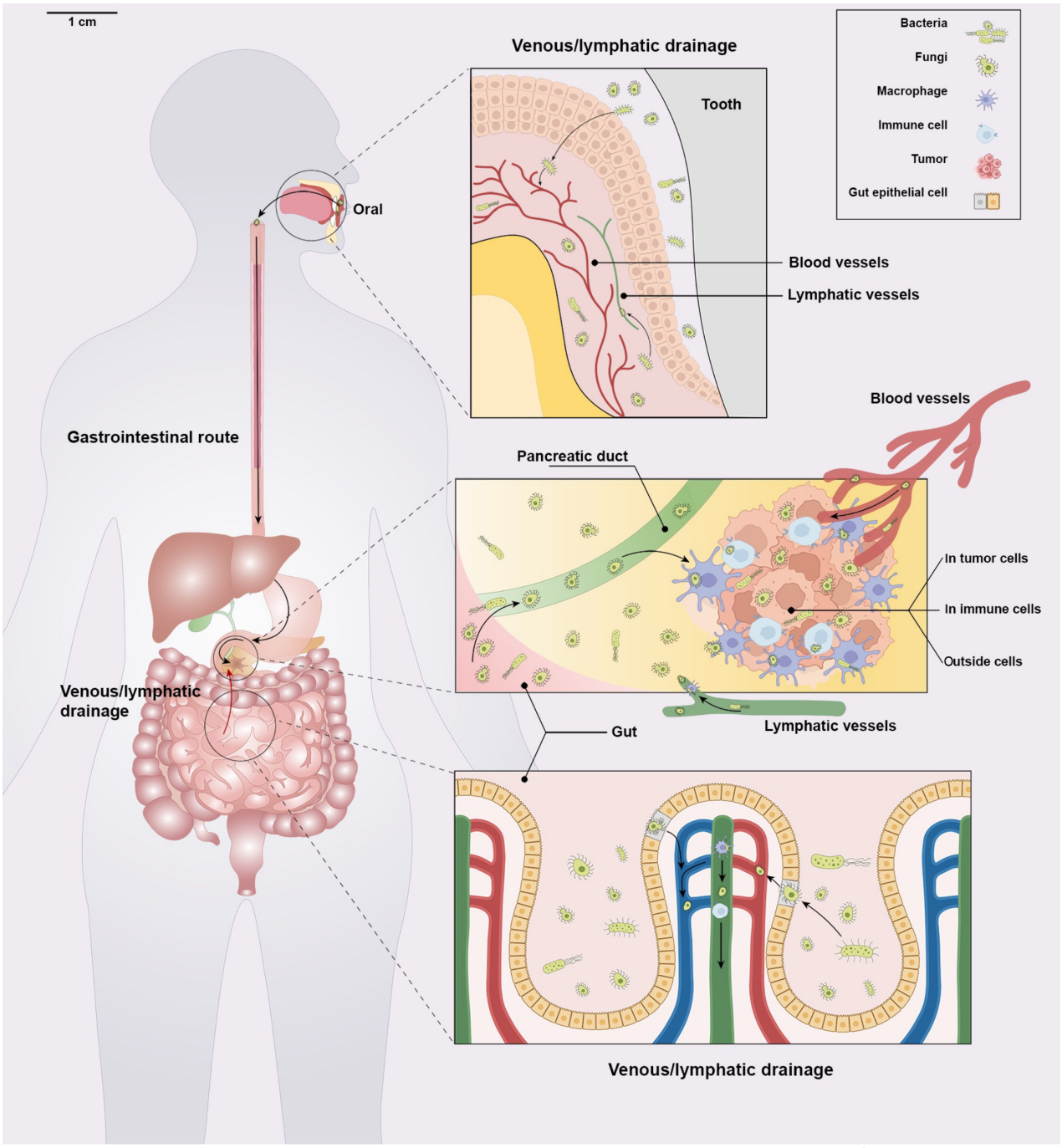

DOI: 10.4251/wjgo.v15.i5.713

Figure 1 The origin and localization of the intratumour microbiome in pancreatic cancer. The microbiome in pancreatic ductal adenocarcinoma (PDAC) may originate from the gut and the oral cavity. The microbiome located in the oral cavity and gut can reach the pancreas *via* the pancreatic duct. But also exists the possibility of drainage *via* blood and lymph. The microbiome located in the gut migrates through the damaged intestinal epithelial barrier into the pancreas *via* venous blood, especially in the inferior gastrointestinal tract. In the case of oral microbiome, it can also enter the pancreas *via* the venous or lymphatic drainage. And the PDAC intratumour microbiome locates in tumour cells, immune cells and outside cells.

germ-free GF 129SvEv mice after gavage with relatively low doses and frequencies of specific pathogen-free bacteria[22]. This reflects the problem that although animal experiments have indicated that gastrointestinal flora can enter the pancreatic tissue *via* the gastrointestinal route, gavage by specific microbiota at high concentrations and frequencies does not seem to be proportionate to the normal human physiological situation[23]. In 16S rRNA sequencing of intratumour bacteria from PDAC in humans and mice, the bacterial compositions of PDAC and duodenal tissue were quite similar. The highest abundance of bacteria in human PDAC at the phylum level was *Proteobacteria*, which was the same as the highest abundance of bacteria in the duodenum, and patients who received invasive endoscopic procedures (IEP) had a higher abundance of intratumour bacteria than those who did not [15,24-26]. Significantly more abundant 16S rDNA copies were also observed in the pancreatic cyst fluid of intraductal papillary mucinous neoplasm (IPMN) and PDAC in patients with a preoperative history

of IEP[27]. When comparing the microbiomes of PDAC tissue, duodenal fluid, and duodenal tissue from postoperative pancreatic patients, extensive similarities between duodenal and PDAC microbiomes were shown, but some of the microbiome of PDAC was not present in the duodenum[28,29]. Riquelme *et al*[14] also demonstrated that approximately 50% of the intratumour bacteria of PDAC could not be explained by gastrointestinal or adjacent tissue[14]. Even though human-derived bacteria were detected in PDAC in mice that had been gavaged with faeces from PDAC patients, more than half of the intratumour bacteria in mouse PDAC remained unexplained[14]. This suggests that the microbiome in PDAC may have other sources.

Part of the oral microbiome of PDAC patients is also present in PDAC. Normally, the oral microbiome continues to spread to the distal gastrointestinal tract through oral intake alone and exceeds the expected abundance[30]. Coabundance of oral pathogens was found in the pancreatic cyst fluid of IPMN and PDAC[27]. At the phylum level, the intratumour and oral microbiomes of PDAC patients are dominated by *Firmicutes*, *Protebacteria* and *Bacteroidota*. However, *Protebacteria*, highly abundant in PDAC tissues, are not highly enriched in the oral cavity[25]. *Porphyromonas gingivalis* (*P. gingivalis*), an oral disease bacterium strongly associated with periodontitis and other oral diseases, has been most studied in relation to PDAC. Multiple findings indicate that *P. gingivalis* is also available in the PDAC microenvironment[25,29]. By gavaging calcein AM-labelled *P. gingivalis* for 2 weeks in C57BL/6 mice, the presence of *P. gingivalis* in the pancreas and faeces was confirmed by flow cytometry and fluorescence in situ hybridization (FISH)[25]. Thus, it is also possible for the microbiome from the oral cavity to reach the pancreas *via* the gastrointestinal route passing through the pancreatic duct.

Existing studies have indicated that the intratumour microbiome in PDAC has the potential to enter the pancreas through the gastrointestinal anatomy, but the possibility that the microbiome from the oral cavity or gastrointestinal cavity could enter the pancreas through blood and lymphatic drainage is not excluded[23]. *Fusobacterium nucleatum* (*F. nucleatum*), an oral colonizing anaerobic bacterium found in the same PDAC microenvironment as *P. gingivalis*, was injected into the tail vein of mice with rectal cancer and showed an enrichment of *F. nucleatum* in rectal cancer tumour tissue by plate culture or quantitative real-time polymerase chain reaction (qPCR)[31,32]. Tumours of nondigestive tract origin, such as breast cancer, are more likely to have an intratumour microbiome originating *via* blood or lymphatic drainage than tumours of digestive tract origin[33,34]. Although there is no experimental evidence at present that the microbiome can reach PDAC from microbial-rich sites such as the oral cavity or gastrointestinal tract by blood or lymph, much indirect evidence has shown the feasibility of such a transport route. Under healthy conditions, portal blood may contain small amounts of potential pathogens[35]. In cats, *E. coli* enter from the transmural wall of the colon and spread through the bloodstream to the pancreas, especially in cats with acute pancreatitis[36]. Bacterial translocation was detectable in blood from patients with acute pancreatitis by 16S rDNA sequencing[37]. However, this blood drainage seems to be difficult to achieve in disease-free conditions. In germ-free Il10-/- mice with no pancreatic lesions, a mouse with defects in intestinal permeability, oral infection with *Campylobacter jejuni* to accelerate such permeability defects caused them to develop severe colitis, but there appears to be no evidence of bacterial presence in the corresponding mouse pancreas by qPCR or culture[22].

In terms of lymphatic drainage, there is evidence of transfer of the gastrointestinal microbiome to mesenteric lymph nodes and transport *via* immune cells[38-40]. Commensal bacteria modulate intestinal immune surveillance by transporting CX3CR1^{hi} mononuclear phagocytes to mesenteric lymph nodes along with bacteria captured in the intestinal lumen[38]. During this process, bacteria are screened and transported from the intestine to the mesenteric lymph nodes, which may provide an opportunity for bacteria to enter the pancreas *via* anatomical lymphatic drainage. Although the mechanism is unclear, microbial staining of a variety of tumours in different ways revealed that the intracellular microbiome was found in macrophages[16,24]. Consequently, it is possible that the microbiome within the tumour is transferred to the pancreas by lymphatic drainage through such a mechanism of macrophage transport. Unfortunately, Nejman *et al*[24] did not perform lipopolysaccharide (LPS) staining of PDAC. Furthermore, the immunohistochemistry (IHC) staining of LPS within macrophages may also be due to phagocytosis of local microbiota by macrophages. Macrophages exhibiting positive IHC in LPS rarely exhibit positive 16S rRNA FISH. Thus, the possibility is not excluded that the bacterial LPS staining present in macrophages originates from bacterial components that are not fully processed[16,41]. Bacteria present in the oral cavity, such as *P. gingivalis*, may be captured by lymphatic vasculature during the flow from the oral cavity to the bloodstream and then enter the systemic bloodstream[42]. Sakamoto *et al*[43] analysed microbiota in 153 lymph nodes collected from oral cancer patients and found viable bacteria in 45% of the lymph nodes from 83% of the patients[43]. Overall, the origin of the PDAC intratumour microbiome is still not entirely clear, but the possibility of multiple sources exists. Probing the origin of such a microbiome will facilitate the utilization of diverse approaches to target the intratumour microbiome for the treatment of PDAC patients in the future.

THE LOCATION IN PDAC

The intratumoural microbiome is a novel member of the PDAC tumour ecosystem, and its localization,

especially its subcellular localization, remains unclear (Figure 1). Nejman *et al*[24] performed IHC for LPS and lipoteichoic acid of bacteria in five cancers, including breast, bone, lung, glioblastoma and ovarian cancers, and found that bacteria were predominantly present in tumour cells and immune cells and localized in the cytoplasm and nucleus of cancer cells. FISH was performed on bacterial 16S rRNA; however, bacterial 16S rRNA was mainly localized in the cytoplasm[24]. In multimethod staining of pancreatic, melanoma, ovarian, breast, and lung cancers, Narunsky-Haziza *et al*[16] reported that the fungi were predominantly present in cancer cells of pancreatic, breast, and ovarian cancers, as well as in macrophages of melanoma and lung cancers, and that very few fungi were extracellularly localized[16]. Although Nejman *et al*[24] did not report the dominant localization of bacteria within pancreatic cancer tumours, the results would be expected to be similar. An *in vitro* experiment revealed that *P. gingivalis* could exert tumour-promoting effects in PANC1 cells after *P. gingivalis* infection[44]. Another *in vitro* experiment reported that after coculture of bacteria from IPMN cyst fluid with pancreatic normal cells or pancreatic cancer cell lines for 2 h, most bacterial isolates were discovered to enter and survive in human pancreatic cells[45]. Another line of indirect evidence of the intracellular localization of bacteria was the discovery of bacteria in PDAC tissue-derived extracellular vesicles[46]. However, it is possible that some of these vesicles may also originate in the blood or lymph of the circulation.

Insights into microbial localization inside and outside cells suggest that the microbiome inside cancer cells can alter the transcriptional state, proteome, and metabolic reserve of cancer cells and that the microbiome outside cancer cells can cause metabolic alterations, immune editing, clonal expansion and metastasis, and mutagenesis in cancer cells[13]. Intracellular and extracellular microbial localization studies may also have clinical implications for the selection of antibiotics with different bactericidal mechanisms. In breast cancer, intracellular bacteria can survive cell-impermeable antibiotic treatment (ampicillin and gentamicin) but not cell-penetrating doxycycline treatment[34]. However, it seems to be crucial to elucidate the subcellular localization of the microbiome in tumours. For example, the biological characteristics of microbiomes with different subcellular localizations may differ. Bacteria present in the cytosol can obtain nutrients directly from the interior of the host cell, while the source of nutrients for bacteria present in intracellular vesicles requires input through the membrane[47]. In addition, bacteria in the cytosol spread directly between cells by forming membrane protrusions that eventually enter adjacent cells, thus avoiding the harm of humoural immunity, while vacuolar bacteria can remain free from cytosolic sensors and autophagy[47]. However, the intensity of bacterial effects on target cells depends on the cell type and bacterial strain. The microbiome in PDAC cells is not fully characterized by studies involving normal cells or specific microbiomes[48]. In conclusion, the localization of the intratumoural microbiome within PDAC tumours requires further revelation, and such revelation is of great importance.

PDAC-SPECIFIC INTRATUMOUR MICROBIOME

The "genomics era" has accelerated various fields of biological research, and the impact is particularly noticeable with respect to the human microbiome. As a 'second genome' for cancer, each tumour type was detected to have its own specific intratumour microbiota in approximately 7.2% of sequenced reads in The Cancer Genome Atlas (TCGA) that were not attributed to human origin[16,49-52]. Despite the unavoidable contamination of TCGA-sourced data, the in silico decontamination method and a machine learning (ML) approach to build diagnostic models could effectively distinguish the cancers of TCGA, regardless of the stringency of decontamination[16,49]. Nejman *et al*[24] sequenced 1010 tumour samples with a critical decontamination process and similarly concluded that different tumour types have different microbial compositions[24]. Analogous to the specific microbial community characteristics of ecological differences in nature, in the tumour ecosystem, the specificity of the PDAC intratumour microbiome is reflected not only in the pancancer aspect but also between PDAC patients and normal individuals and between PDAC and the gut.

The intratumour bacterial 16S rDNA of PDAC is abundant, with great differences with respect to glioblastoma and bone cancer, while the Shannon diversity of intratumour bacteria is moderate, between that of ovarian cancer and melanoma[24]. Similar to bacteria, PDAC fungi have higher contents intermediate between breast and ovarian cancers[16]. At the phylum level, *Proteobacteria*, *Bacteroidetes* and *Firmicutes* are prevalent in the bacterial composition of PDAC[15,20,28,29,53]. Moreover, the abundance of Proteobacteria is also higher in PDAC than in breast cancer, glioblastoma, lung cancer, colorectal cancer and melanoma[24]. A similar specificity was also observed in PDAC intratumour fungi, with *Ascomycota* and *Basidiomycota* dominating the panintratumour fungal community at the phylum level. *Ascomycota* is slightly more abundant than *Basidiomycota* in PDAC, and *Yarrowia bubula*, a type of fungus belonging to *Ascomycota*, is the most differentiated fungus between PDAC and other tumours[16]. There was no considerable difference in the abundance of *Malassezia* across cancers, but important differences were shown in the human or mouse intestine *vs* PDAC[17,21].

Comparing PDAC with normal pancreas, the results seem to vary depending on the definition of "normal". When the pancreatic tissue in normal individuals is considered "normal", there are differences in the composition of the intratumour microbiome and a high alpha diversity of the microbiome in

PDAC[17,20,21,54]. The increase in intratumour bacteria in PDAC is 1000-fold compared to the normal pancreas, while the expansion of intratumour fungi is even more remarkable, with a 3000-fold increase compared to the normal pancreas[20,21]. Interestingly, the amount of bacteria in PDAC is considerably higher than the amount of fungi[16]. The gut microbiome from *Pdx1*^{Cre}; *LSL-Kras*^{G12D}; *Trp53*^{R172H} (KPC) mice, which have a higher degree of PDAC malignancy, has a higher capacity to translocate to the pancreas than that of WT mice[20]. Furthermore, the ability of the intratumour microbiome to enter the pancreas seems to be correlated with the level of pathological alterations of the pancreas. The percentage of bacterial DNA positivity in pancreatic cysts increases from 33.0% in non-IPMN to 59.6% in IPMN and 81.5% in cancer[27]. The mechanism of microbial enrichment within the tumour may be attributed to: (1) A hypoxic TME favouring the growth of anaerobic and parthenogenetic bacteria; (2) chemotactic effects of bacterial nutrients present in the necrotic region of the tumour and chemoattractive compounds present in the necrotic region of the resting cancer cells; (3) entry of circulating bacteria into the tumour tissue through an abnormally proliferating leaky tumour vascular system; (4) an immunosuppressive TME providing a refuge for microbial immune evasion; and (5) the impaired pancreatic barrier function, which facilitates microbial colonization[23,54,55]. Broad similarity in microbiome composition exists between PDAC and NAT when "normal" pancreas is defined as NAT, but differences also exist[19,25,26,28]. Interestingly, when comparing the microbial compositions of ductal adenocarcinomas in different parts of the pancreas, no differences in the composition or diversity of the microbial community were shown[25,45,56]. Upon comparing different subtypes of PDAC, the 'basal-like' subtype had higher microbial abundance than the 'classical' or 'hybrid' subtypes but was dominated by a few very-high-abundance species[57].

As a possible source of the PDAC intratumour microbiome, several reports have demonstrated significantly higher gut fungal and bacterial alpha diversity than tumours[21,29]. For bacteria, *Proteobacteria*, which account for only 8% of the gut bacteria in PDAC patients, account for nearly 50% in PDAC[20]. Regarding fungi, at the genus level, *Malassezia* was more prevalent in PDAC than in the gut [17,21]. The faeces seem to be incapable of referring to the microbial composition of the gut in different locations. However, comparing bacterial differences between duodenal and PDAC using endoscopic ultrasound-guided fine-needle aspiration (EUS-FNA) also confirmed the higher abundance of *Proteobacteria* in PDAC than in the duodenum[53]. In other words, the enrichment of the gut microbiome in PDAC may be specific as well.

THE INTRATUMOUR MICROBIOME AND THE DIAGNOSIS AND PROGNOSIS OF PDAC

Due to the paucity and nonspecificity of symptoms in patients with early PDAC, early detection of PDAC in clinical practice involves many challenges[58]. Poore *et al*[49], Nejman *et al*[24] and Narunsky-Haziza *et al*[16] provide the most comprehensive analysis of the blood microbiome and solid tumour diagnosis thus far[16,24,49]. Liquid biopsy in cancer allows the detection of miniature amounts of analytes (*e.g.*, DNA, RNA, proteins) shed from the tumour, which enables diagnostic and prognostic analysis of cancer[59] and earlier and more sensitive detection of PDAC by liquid biopsy compared to traditional PDAC examination techniques[60,61]. Traditional liquid biopsy-based diagnostic models have failed to address the presence of the intratumour microbiome. Poore *et al*[49] and Narunsky-Haziza *et al*[16] analysed blood-derived microorganisms from the TCGA and Hopkins cohorts and concluded that ML models based on the blood-derived microbiome can widely distinguish between multiple cancer types[16,49]. In the Hopkins cohort, the ML classification of untreated PDAC in phase I *vs* healthy controls revealed that decontaminated fungal species provided significant performance. This provides a new landscape for cell-free microbial DNA (cf.-mb DNA) models based on multispecies (*e.g.*, tumour, bacterial, fungal) sources in the early clinical diagnosis of PDAC. Despite rigorous computerized decontamination, further examination of decontaminated samples in a rigorous laboratory is required. It is also questionable whether the origin of cf.-mb DNA remains uncertain, although possible sources include oral, gut, and intratumour microbiomes[8].

TCGA microbiome data of solid tumours allow excellent differentiation of tumours by ML[16,49]. Regardless of the low abundance of the intratumour microbiome when compared to the tumour genome, species presence, whether involved in tumour pathogenesis or as opportunistic occupants, potentially contributes to the diagnosis of PDAC. EUS-FNA is a safe histological procedure for the diagnosis of patients with suspected PDAC[62]. Fast frozen EUS-FNA biopsy significantly enhances the diagnostic accuracy of current standard procedures by providing comprehensive genomic and transcriptomic analysis of PDAC patients at all stages[63]. Likewise, this technique is valuable for the evaluation of the intratumour microbiome of PDAC[53,56,64]. The strength of EUS-FNA is the ability to capture microbiome information in inoperable patients with no significant differences in alpha diversity, beta diversity, or taxonomic characteristics between EUS-FNA and surgically resected samples[64]. Since the early phase of intratumour microbiome research, there has been no more application of EUS-FNA for PDAC intratumour microbiology-related diagnosis. The diagnostic idea may be similar to genomic and transcriptional analysis: (1) By using the PDAC-specific microbiome for differentiation; and (2) building a strongly robust diagnostic model of multiple microbiomes, Narunsky-

Haziza *et al*[16] concluded that the TME may be a noncompetitive space for multidomain microbial colonization based on the strong positive correlation observed between fungal and bacterial diversity, abundance and cooccurrence in multiple cancer types[16]. Consequently, utilizing multifeature-based ML seems to be a better choice for diagnosis.

The essential role of the intratumoural microbiome in regulating the immune tone of the tumour TME makes it a favourable predictor of prognosis in PDAC patients. When comparing the alpha diversity of the intratumour microbiome in long-term survival (LTS) PDAC patients [overall survival (OS) > 5 years] *vs* short-term survival (STS) PDAC patients (OS < 5 years), patients with LTS had higher diversity than those with STS[14]. LTS patients showed a predominance of *Alphaproteobacteria*, *Sphingobacteria* and *Flavobacteria* at the class level, while STS patients presented with *Clostridia* and *Bacteroidea*. Similarly, another study on the prognosis-related intratumoural microbiome of Chinese PDAC patients reported higher alpha diversity in LTS patients than in STS patients, although the two studies did not have the same threshold for OS time[65]. It seems, however, that the role of high microbiome diversity in predicting the prognosis of PDAC tumours is not common to all tumours. For instance, high microbial diversity in gastric adenocarcinoma tumours is associated with poor survival[66]. Most likely due to genetic, ethnic, dietary, and geographical variability, the dominant species between LTS and STS obtained from these two cohorts were not identical[65,67]. Similar to the aforementioned diagnostic approach using the intratumour microbiome, microbiome data from TCGA were found to be a better prognostic predictor than clinical covariates alone in adrenocortical carcinoma, cervical squamous cell carcinoma, low-grade glioma and subcutaneous melanoma by the ML approach[68]. The combination of tumour microbiome abundance data and gene expression data allowed for modest improvements in predictive performance. In PDAC, Riquelme *el al*[14] constructed a prognostic signature employing *Pseudoxanthomonas*, *Saccharopolyspora* and *Streptomyces*, together with *Bacillus clausii*, that effectively predicted the prognosis of patients in the MD Anderson Cancer Center cohort (AUC = 97.51) and Johns Hopkins Hospital cohort (AUC = 99.17)[14].

Overall, the PDAC microbiome has shown incipient clinical relevance in diagnosis and prognosis, but the low biomass of the tumour microbiome makes decontamination particularly critical[69]. Laboratory means and computerized decontamination to achieve more reliable and reproducible results make the use of intratumour microbiome information for PDAC cancer diagnosis and prognosis more reliable. However, few studies have applied strict contamination controls to the cancer genome, although the efficiency of the application can be increased by adding samples or performing computerized decontamination[13]. Furthermore, genetic, ethnic, and geographical differences create heterogeneity in the microbiome composition of populations in different regions, which adds limitations in the use of microbial information for diagnostic and prognostic judgements. However, recently, one of the methods using transfer learning to overcome regional effects has yielded better robustness in cross-regional disease diagnosis using gut microbial features[70]. In other words, the microbial information within the tumour seems not to lose its meaning due to the presence of various restrictions. Further investigation of the meaning of the intratumour microbiome of PDAC in diagnosis and prognosis is desirable.

THE INTRATUMOUR MICROBIOME-IMMUNE-PANCREATIC CANCER AXIS

Innate and adaptive immunity comprise the body's powerful immune system, and they serve in the surveillance, recognition and elimination of tumours. The innate immune system reacts rapidly and nonspecifically when the body encounters pathogens, while adaptive immune responses develop more slowly but specifically and lead to classical immune memory[71]. Research over the years has focused on the adaptive immune system; however, studies of the adaptive immune system have led researchers to reassess the role of innate immunity as an essential hub for adaptive immune activation[71-73]. The human gut microbiome, as the largest microbial reservoir in the body, coevolved with the immune system and interacts directly through metabolic crosstalk[74]. The gut microbiome regulates host innate and adaptive immunity and influences disease development through its metabolic and microbial intrinsic components[75]. Similarly, in tumours, microbial mechanisms exist that are known to manipulate components of the intestinal epithelial barrier, regulate the activity of lymphoid organs, and modulate the immune tone of the TME[76]. For PDAC, immune cells, as an important component of the PDAC microenvironment, serve influential roles in regulating the growth, metastasis and treatment of PDAC[77-79]. Current findings demonstrated that the PDAC intratumour microbiome, by regulating immune tone in the TME, impacts PDAC progression and the immunotherapeutic response[14,20-22]. This mechanism of intratumour microbiome regulation of PDAC by influencing TME immune tone can be described as the intratumour microbial-immune-pancreatic cancer axis[8] (Figure 2). The intratumour microbiome similarly influences PDAC by modulating adaptive and innate immunity in the TME.

The complement system is a member of innate immunity and consists of approximately 20 different serine proteases. Similar to the coagulation pathway, complement activation entails several steps that are tightly regulated[80,81]. The complement system is activated in three major ways: The "classical activation pathway", the "bypass activation pathway" and the "lectin activation pathway"[80,82]. The convergence point for all complement activation pathways is the formation of C3 convertase complexes

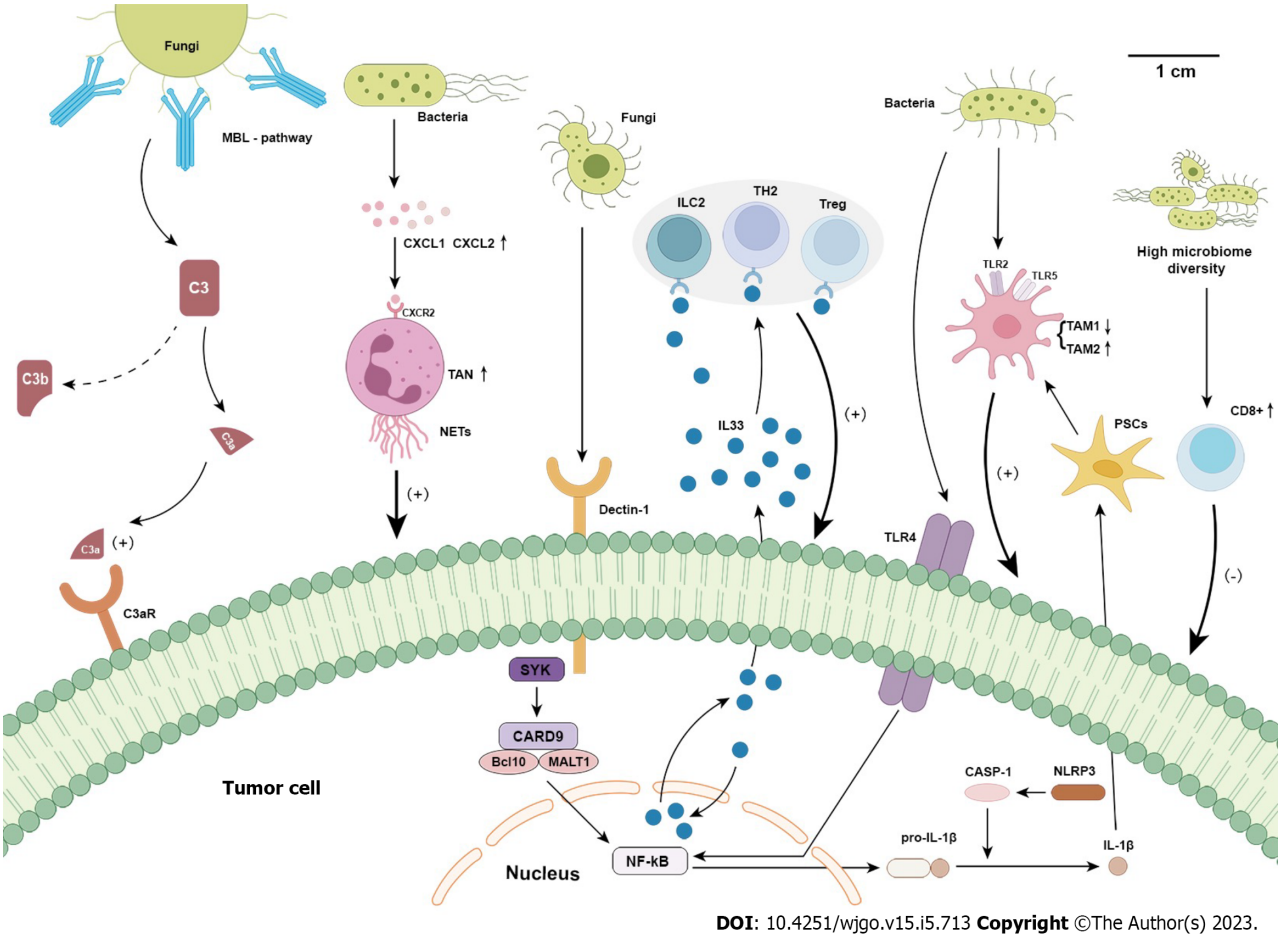

DOI: 10.4251/wjgo.v15.i5.713 **Copyright** ©The Author(s) 2023.

Figure 2 The intratumour microbiome-immune-pancreatic cancer axis. The intratumour fungi can activate the complement 3 (C3) complement cascade through the "lectin activation pathway". And C3a, as a fragment after C3 complement cascade reaction, promotes pancreatic ductal adenocarcinoma (PDAC) cells proliferation by binding to C3a receptors on the surface of cancer cells. Moreover, the intratumour fungi (*Malassezia globosa* or *Alternaria alternata*) and their cell-free extracts facilitate interleukin (IL)-33 secretion through activation of the dectin-1 receptor-mediated Src-Syk-CARD9 pathway. And IL-33 secretion promotes T helper 2 cell, group 2 innate lymphoid cells and Tregs enrichment in tumour microenvironment (TME), thus promoting PDAC progression. The intratumour bacteria promotes the secretion of neutrophil chemokines in the TME of PDAC thereby promoting tumour-associated neutrophils 2 (TAN2) enrichment in the TME. A portion of the effect of TAN2 may be through neutrophil extracellular traps. The PDAC intratumour bacteria also reduces the TAM1 polarization and decreased the antigen-presenting ability of TAM1 though through activation of toll-like receptors (TLR)2 and TLR4 on the surface of cells. TAM1 inhibition is accompanied by an increase in TAM to TAM2 conversion. It also promotes the secretion of IL-1β through TLR4 on the surface of PDAC cells. And IL-1β secretion promotes TAM2 activation through an indirect pathway that activates pancreatic stellate cells. Finally, the high diversity of intratumour microbiome promotes the activation of $CD8^+$ T cells, which inhibits PDAC. C3: Complement 3; PDAC: Pancreatic ductal adenocarcinoma; Th2: T helper 2 cell; ILC2: Group 2 innate lymphoid cells; TME: Tumour microenvironment; TAN2: Tumour-associated neutrophils 2; NETs: Neutrophil extracellular traps; TAM: Tumour-associated macrophages; TLR: Toll-like receptors; PSCs: Pancreatic stellate cells.

on the surface of target cells, and upon formation of C3 convertase, the complement system is able to perform its duties. C3 is primarily synthesized by hepatocytes, but increasing evidence suggests that C3 is also locally secreted by a variety of cell types, including monocytes/macrophages, fibroblasts, endothelial cells, epithelial cells, and cancer cells, including PDAC[83-85]. The positive role of the complement system in fighting heterologous pathogens has been extensively studied, but it appears to serve as a promoter of tumour growth in a variety of tumours[82,83]. On the one hand, tumour-associated macrophages (TAMs) in the PDAC microenvironment can protect pancreatic cancer cells from complement-dependent cytotoxicity by regulating CD59, and on the other hand, intratumour fungi can promote fungal-tumour cohabitations using complement cascade reactions[21,86]. In preclinical experiments, the intratumour fungi of KPC mice, especially *Malassezia*, can activate the C3 complement cascade through the "lectin activation pathway"[21]. C3a, as a fragment produced after the C3 complement cascade reaction, promotes PDAC cell proliferation by binding to C3a receptors on the surface of cancer cells[21]. However, the role of the MBL-C3 mechanism of intratumoural fungi may be more significant than that[87]. An *in vitro* experiment showed that C3a-C3a receptor binding could promote the epithelial-to-mesenchymal transition (EMT) by activating the ERK pathway in PDAC cells [88]. Additionally, C3a receptors are expressed not only in tumour cells, but also on myeloid cells and CD4+ T lymphocytes[89-93]. This suggests that the intratumour fungal MBL-C3 mechanism in PDAC may have a broader role in the TME and necessitates further investigation.

Neutrophils, as the predominant specialized phagocytes in the body, play an important role in the body's resistance to pathogens such as bacteria, fungi, viruses and parasites[87,94-96]. Neutrophils function primarily through three major strategies: Phagocytosis, degranulation and the release of neutrophil extracellular traps (NETs)[97]. NETs are reticular structures composed of nuclear or mitochondrial DNA fibres decorated with antimicrobial enzymes and histones that are released to trap and kill pathogens[87,98]. NETs in tumours induce tumour recurrence, enhance tumour migration and invasiveness, and promote tumour cell proliferation[99]. The interaction between neutrophils and the microbiome is also reflected in PDAC. It was recently reported that *P. gingivalis* promotes the secretion of neutrophil chemokines (CXCL1 and CXCL2) in the TME of PDAC, thereby promoting tumour-associated neutrophil 2 (TAN2) enrichment in the TME[25]. In addition, the enrichment of TAN2 and the progression of PDAC can be blocked by CXCR2 inhibitors. In addition, neutrophil elastase (NE) in the TME was observed to be coexpressed with myeloperoxidase, a component of NETs[25]. However, the mechanism of increased neutrophil-associated chemokines and NE in the PDAC microenvironment caused by intratumour *P. gingivalis* is unclear. However, the toxicity factors of *P. gingivalis*, such as gingipains, serine proteases, lipid phosphatases or fimbriae, have been reported to manipulate the immune response of neutrophils in periodontitis[100].

Group 2 innate lymphoid cells (ILC2s), initially identified as important cells that protect the host from worm infection, also appear to play roles in asthma, inflammation and cancer. It was revealed that ILC2s seem to serve as ”bipartisan politicians” in different tumours, and this feature was also likely exhibited in different immunogenic pancreatic cancers[17,101,102]. Kras-mutated PDAC promotes the infiltration of Th2 cells, ILC2 cells and Tregs in the TME through interleukin (IL)-33 secretion mediated by the Kras-MEK-ERK pathway. Meanwhile, intratumour fungi (*Malassezia globosa* or *Alternaria alternata*) and their cell-free extracts facilitate IL-33 secretion through activation of the dectin-1 receptor-mediated Src-Syk-CARD9 pathway[17]. PDAC infiltrates into tumour-promoting immune cells, including Th2 and ILC2 cells, to contribute to the protumourigenic program through their cytokine networks, leading to PDAC progression[103-105]. However, ILC2 cells in PDAC may have opposite effects. From another study, ILC2 was reported to inhibit PDAC tumour progression through the ILC2-CD103$^+$DC-CD8$^+$T axis[102]. High/Low TME immunogenicity apparently leads to distinct effects of ILC2 cells in PDAC. In other words, although there are no reports on the inhibition of PDAC by intratumour fungi, the bifacial impact of ILC2 cells in PDAC provides a clue to the antitumour effects of intratumour fungi in PDAC with respect to the pro/inhibitory effects of the intratumour microbiome under different immunogenicities.

The spectrum of macrophage activation states in tumour tissues is complicated, and TAMs are typically classified into two categories: M1 classically activated macrophages (TAM1) or M2 alternatively activated macrophages (TAM2)[106]. TAM1 promotes tumour remission and the Th1 response by secreting tumour necrosis factor-α and IL-12, while TAM2 exhibits an immunosuppressive phenotype and releases cytokines such as IL-4, IL-13, and IL-10 to promote the Th2 response[107]. A complex mechanism exists for the interaction between the intratumour microbiome and TAMs. Ablation of the microbiota with antibiotics leads to a decrease in TAM2 in KPC mice in situ and a concomitant increase in TAM1. Moreover, cell-free extracts from *Bifidobacterium pseudolongum*, a member of the PDAC intratumour microbiota, reduced TAM1 polarization and decreased the antigen-presenting ability of TAM1[20]. TAM2 tumour-promoting efficacy weakens when Toll-like receptor (TLR) signalling is eliminated *in vivo*. However, the TLR signalling-mediated effects do not seem to be limited to TAMs. According to a separate study, the pro-oncogenic effect of the intratumour microbiome in PDAC probably results partly from TLR4-mediated IL-1β production in PDAC cells[108]. Tumour-derived IL-1β partially contributes to the upregulation of TAM2 by regulating the activation and secretory phenotype of pancreatic stellate cells. In addition, the concentration of IL-1β seems to be positively correlated with the number of bacterial 16S rDNA copies in PDAC and IPMN cyst fluid[27].

In regard to adaptive immunity, CD8$^+$ T cells are an essential component. CD8+ T cells are recruited to infiltrate the TME and specifically kill target cells through recognition of antigens presented by MHC class I molecules[109]. Antibiotic ablation of the microbiota significantly increased the proportion of intratumour T cells in KPC mice. In parallel, the decrease in the microbiome increased the CD8$^+$:CD4$^+$ T-cell ratio and the number of cytotoxic phenotypic CD8$^+$ T cells[20]. A significant reduction in CD8$^+$ T cells in the TME was observed in PDAC mice gavaged with *Alternaria alternata* and *P. gingivalis*[17,25]. However, the effects of the intratumoural microbiome on CD8$^+$ T cells in the TME may be associated with the heterogeneity of the PDAC microbial community. The LTS patients had higher alpha diversity and a higher density of CD3+ and CD8+ T cells than STS patients. Furthermore, the enrichment of *Saccharopolyspora*, *Pseudoxanthomonas* and *Streptomyces* in LTS patients was positively correlated with CD8$^+$ T-cell density[14]. This may imply that the intratumour microbiome is not just tumour-promoting. The recruitment mechanism of the PDAC intratumour microbiome is still unclear, but it seems that the PDAC ecosystem allows "co-occurrence" of microbiomes that are beneficial to PDAC[16]. The evidence derived from pancreatic cancer mice with Col1 gene knockout showed reduced *Bacteroidales*, increased *Campylobacterales* and high infiltration of CD8$^+$ T cells compared to the tumour ecosystem of control mice[54]. Knockdown of the Col1 gene resulted in reduced malignancy of PDAC and altered intratumour microbial composition. Meanwhile, the ablation of the microbiome at this time resulted in shorter survival time and reduced infiltration of CD8+ T cells in the TME of the knockout Col1 mice.

In conclusion, complex interactions exist in the intratumour microbiome-immune-pancreatic cancer axis, which may more predominantly act as contributors to PDAC progression by modulating immune tone and thus influencing PDAC progression. However, the impact of the PDAC intratumour microbiome exceeds that of promoting the production of an immunosuppressive TME; depending on the PDAC ecosystem, it may also help to form an immune-promoting TME. At present, problems remain in the study of the PDAC intratumour microbiome: For example, the gavage of the microbiome or the oral administration of antibiotics cannot rule out the effects of the gut microbiome in mice[22]. Therefore, the mechanisms related to bacteria and fungi in PDAC still need to be further investigated.

THE INTRATUMOUR MICROBIOME AND CANCER THERAPY

Chemotherapy resistance

Gemcitabine, the classic chemotherapy regimen for PDAC, is also used in other solid tumours, such as ovarian cancer, bladder cancer and non-small cell lung cancer[110-113]. Gemcitabine is a cytidine analogue for which clearance is mainly due to the rapid and extensive inactivation of its main metabolite, 2',2'-difluorodeoxyuridine, by cytidine deaminase (CDD)[110]. CDD was recently identified by Geller *et al*[15] as a potential contributor to microbial-induced chemoresistance[15]. They classified bacteria according to the length of the bacterial CDD gene into 880-nucleotide-long CDD (CDD_L), 400-nucleotide-long short form CDD (CDD_S) and CDD-deficient bacteria. All species expressing CDD_L were resistant to gemcitabine, whereas only a minority of CDD_S and CDD-deficient bacteria mediated this effect. *In vivo* experiments confirmed that CDD_L-expressing *E. coli* increased tumour resistance to gemcitabine. Instead, the combination of gemcitabine and the antibiotic ciprofloxacin impeded resistance to this anticancer drug. Finally, by culturing bacteria from 15 fresh human PDAC tumours, they observed that bacteria from 14 PDAC samples enabled human colon cancer cell lines to become fully resistant to gemcitabine. This bacterial-driven gemcitabine deamination could be restored by exogenous delivery of the CDD inhibitor tetrahydrouridine[114]. Geller *et al*[15] also reported that bacterial suspensions also reduced the efficacy of oxaliplatin; however, this effect was not mediated by CDD. Although the enzyme or bacterial product that mediates oxaliplatin catabolism remains elusive, it is clear that bacteria can confer oxaliplatin resistance to cancer cells in a similar manner[15]. Nevertheless, *Clostridium nucleatum* was also revealed to induce resistance to oxaliplatin in colorectal cancer indirectly through the TLR4/MYD88 pathway[115]. It seems that the application of chemotherapeutic agents also altered the intratumour microbial composition of PDAC patients and affected the efficacy of chemotherapeutic agents. Significantly higher relative abundance of *Enterobacteriaceae* was observed in samples from patients treated with the combination of gemcitabine and paclitaxel compared to those treated with gemcitabine only and those not receiving neoadjuvant chemotherapy at all[26]. These *Enterobacteriaceae* are believed to be associated with chemotherapy resistance. Consequently, there may be various mechanisms involved in the chemotherapy resistance of PDAC with respect to the intratumour microbiome, showing the potential to improve tumour treatment outcomes by influencing the microbiome.

The strategy of applying antibiotics

In preclinical studies, the administration of antibiotics to PDAC mice to ablate the gut and intratumour microbiota of mice achieved inhibition or promotion of tumour progression[20,21]. In clinical trials, antibiotic monotherapy seems to improve the prognosis of patients with PDAC. In a retrospective clinical study enrolling 580 patients, patients with metastatic PDAC with a history of antibiotic use beyond 48 h had longer OS and progression-free survival (PFS) than patients with metastatic PDAC who did not use antibiotics but were not dependent on the use of preoperative antibiotics[116]. However, such an effect may be limited to specific patients. Another study noted that postoperative quinolones improved postoperative survival for patients with positive *Klebsiella pneumoniae* cultures in the bile but failed to show statistically significant improvement in postoperative survival for patients with negative *Klebsiella pneumoniae* cultures[117].

The combination of antibiotics with gemcitabine to reduce microbial-induced chemoresistance seems to be an effective strategy for the treatment of PDAC patients. The combination of antibiotics with gemcitabine improved OS and PFS in patients with metastatic PDAC, and improvement in PFS was observed in patients using FOLFIRINOX in combination with antibiotics[116]. Similarly, a retrospective study of 430 patients with PDAC reported that patient treatment with the combination of gemcitabine and antibiotics was more effective than monotherapy with gemcitabine[118]. In other words, the combination of antimicrobials with gemcitabine may increase the efficacy of gemcitabine while probably also increasing gastrointestinal and haematological adverse effects. Furthermore, the combination of quinolones with gemcitabine increased the incidence of haematological, gastrointestinal, obesity, and transaminase elevations, while the combination of β-lactam antibiotics with gemcitabine increased the incidence of haematological adverse events[118]. However, the combination of quinolones with gemcitabine improved PFS in patients with negative *Klebsiella pneumoniae* bile cultures[117]. Apart from aggravating the adverse effects of chemotherapeutic drugs, the combination of antibiotics and

chemotherapeutic drugs may lead to the development of drug-resistant bacteria and disrupt the commensal relationships of microbiota in the long-term use of antibiotics[119]. Research has shown that 7 d of continuous antibiotic use in healthy individuals will perturb gut microbes and require at least 1 year to return to normal[120]. Therefore, it is imperative to investigate antibiotic strategies that target microbiota to improve the prognosis of PDAC patients and preserve the beneficial microbiota.

Despite the limited efficacy of immunotherapy in PDAC, the significance of the intratumour microbiota in altering the immune tone of PDAC offers new therapeutic options[121,122]. The complex relationship between the microbiota and immune regulation within PDAC tumours makes the outcome of antibiotic combination immunotherapy unclear. In a meta-analysis enrolling 2740 cancer patients, antibiotic use was associated with significantly lower OS and PFS in patients treated with immune checkpoint inhibitors[123]. Moreover, the modulatory mechanism of the intratumour microbiome on the TME in PDAC may not be dependent on the surviving microbiome. The application of cell-free extracts of microbiota in preclinical studies also achieved the modulation of TME immune tone[17,65]. Therefore, the strategy of applying antibiotics in combination with immune checkpoint inhibitors in PDAC also faces some urgent challenges to be solved.

The application of probiotics

In view of the access of the PDAC microbiome to the pancreas *via* the pancreatic duct, oral administration of probiotics offers a potentially effective strategy. While this strategy needs to be confirmed by clinical trials, the role of the gut/pancreatic microbiome and its metabolites in PDAC has been demonstrated in many preclinical studies. For example, *Lactobacillus* can decrease the number and grade of pancreatic precancerous lesions, retard the growth of pancreatic cancer cells in Kras mutant mice, and inhibit the EMT process in cancer cells[124]. Heptelidic acid, a metabolite of the probiotic *Aspergillus oryzae*, activates the p38 MAPK signalling pathway and induces apoptosis in pancreatic cancer cells [125]. *Megasphaera* and the short-chain fatty acids derived from its metabolism enriched in LTS PDAC patients stimulated macrophage activation *in vitro* and improved the efficacy of programmed cell death protein 1 inhibitors *in vivo*[65]. However, the use of probiotics in PDAC is also problematic. Probiotics may not only destroy the ecosystem of innately colonized microbiota but could also hinder the re-establishment of the microbial ecosystem after antibiotic treatment[126]. It is also noted that probiotics may induce infections in patients, especially those who suffer from immune deficiency[122,127]. Incorporating the once-unappreciated intratumour microbiome into research would provide a good direction to improve the prognosis of pancreatic cancer patients.

CONCLUSION

In recent years, the field of the intratumour microbiome has provided new insights into the field of oncology. PDAC is a highly malignant tumour, and some of the biological processes in PDAC are tied to the intratumour microbiome. Investigating the causal relationship and molecular interactions between PDAC and the commensal microbes in the TME is expected to provide new ideas for mankind in the conquest of PDAC. In this review, we reveal that the microorganisms within PDAC tissues may originate from the gut and oral cavity *via* circulation, the lymphatic system, and the gastrointestinal system. The microbial enrichment within PDAC tissues is specific. The PDAC intratumour microbiome is capable of regulating immune tone through immune cells, such as TAMs, TANs and lymphocytes, and the complement system. In addition, targeting the microbiota associated with PDAC has potential clinical applications in the diagnosis and treatment of tumours. Overall, the study of the intratumour microbiome is still at an early stage, and many issues remain to be addressed. For example, the origin and pathways of the intratumour microbiome in PDAC have not been fully explained. The details about the specific intratissue localization of the microbiome and its subcellular localization are unclear. The complex interactions between specific microbiomes and the TME have not been fully revealed. Alternatively, the majority of microbiota appears not to be culturable from tumours in a straightforward manner, limiting the ability to directly utilize intratumour microbiota for studies[128]. Furthermore, fundamental and clinical research on the association between the intratumour microbiome and genomic mutations in PDAC is still inadequate. However, based on the previously described mechanism by which intratumoural fungi enhance KRAS mutations mediating IL-33 secretion by PDAC, the existence of interactions between genomic alterations in PDAC and intratumoural microbes has been shown[17]. In addition, current research mainly focuses on intratumoural bacteria and fungi, and there is less research on the interactions between viruses and tumours. An association between hepatitis B virus (HBV) and hepatitis C virus and PDAC risk has been shown, and HBV expression can be found in PDAC tissue[129,130].

In the future, it is essential to investigate the causal relationship between PDAC and intratumoural microbial interactions and to use more advanced technologies, such as single-cell sequencing, for related research. Furthermore, KRAS mutations are a major burden in the conversion of pancreatic precancerous lesions to PDAC; thus, the relevance of KRAS mutations in the intratumour microbiome of PDAC needs further investigation[131]. Additionally, the mechanisms of virus-host interactions are still

not available, and it is essential to investigate the mechanisms associated with viruses in tumours to improve the theoretical system of tumour microbiology. Finally, a more precise and personalized application of antibiotics or probiotics to improve chemoresistance and immunotherapy in PDAC patients is a huge challenge. Thus, more sophisticated and effective clinical trials are required in the future to identify such potentially beneficial patients and improve their prognosis.

FOOTNOTES

Author contributions: All authors contributed to the original ideas and writing of this paper; Guan SW wrote the paper; Lin Q draw figures; Yu HB made critical revisions of this paper; all authors have read and approve the final manuscript.

Conflict-of-interest statement: All the authors report no relevant conflicts of interest for this article.

Country/Territory of origin: China

ORCID number: Shi-Wei Guan 0000-0001-6046-8383; Quan Lin 0000-0001-5842-8032; Hai-Bo Yu 0000-0001-7616-3891.

S-Editor: Fan JR
L-Editor: A
P-Editor: Zhang XD

REFERENCES

1 **Park W**, Chawla A, O'Reilly EM. Pancreatic Cancer: A Review. *JAMA* 2021; **326**: 851-862 [PMID: 34547082 DOI: 10.1001/jama.2021.13027]
2 **Mizrahi JD**, Surana R, Valle JW, Shroff RT. Pancreatic cancer. *Lancet* 2020; **395**: 2008-2020 [PMID: 32593337 DOI: 10.1016/S0140-6736(20)30974-0]
3 **Koh A**, De Vadder F, Kovatcheva-Datchary P, Bäckhed F. From Dietary Fiber to Host Physiology: Short-Chain Fatty Acids as Key Bacterial Metabolites. *Cell* 2016; **165**: 1332-1345 [PMID: 27259147 DOI: 10.1016/j.cell.2016.05.041]
4 **Wang Y**, Du J, Wu X, Abdelrehem A, Ren Y, Liu C, Zhou X, Wang S. Crosstalk between autophagy and microbiota in cancer progression. *Mol Cancer* 2021; **20**: 163 [PMID: 34895252 DOI: 10.1186/s12943-021-01461-0]
5 **Tilg H**, Zmora N, Adolph TE, Elinav E. The intestinal microbiota fuelling metabolic inflammation. *Nat Rev Immunol* 2020; **20**: 40-54 [PMID: 31388093 DOI: 10.1038/s41577-019-0198-4]
6 **Shi N**, Li N, Duan X, Niu H. Interaction between the gut microbiome and mucosal immune system. *Mil Med Res* 2017; **4**: 14 [PMID: 28465831 DOI: 10.1186/s40779-017-0122-9]
7 **Locey KJ**, Lennon JT. Scaling laws predict global microbial diversity. *Proc Natl Acad Sci U S A* 2016; **113**: 5970-5975 [PMID: 27140646 DOI: 10.1073/pnas.1521291113]
8 **Sepich-Poore GD**, Zitvogel L, Straussman R, Hasty J, Wargo JA, Knight R. The microbiome and human cancer. *Science* 2021; **371** [PMID: 33766858 DOI: 10.1126/science.abc4552]
9 **Jin C**, Lagoudas GK, Zhao C, Bullman S, Bhutkar A, Hu B, Ameh S, Sandel D, Liang XS, Mazzilli S, Whary MT, Meyerson M, Germain R, Blainey PC, Fox JG, Jacks T. Commensal Microbiota Promote Lung Cancer Development *via* γδ T Cells. *Cell* 2019; **176**: 998-1013.e16 [PMID: 30712876 DOI: 10.1016/j.cell.2018.12.040]
10 **Tsay JJ**, Wu BG, Sulaiman I, Gershner K, Schluger R, Li Y, Yie TA, Meyn P, Olsen E, Perez L, Franca B, Carpenito J, Iizumi T, El-Ashmawy M, Badri M, Morton JT, Shen N, He L, Michaud G, Rafeq S, Bessich JL, Smith RL, Sauthoff H, Felner K, Pillai R, Zavitsanou AM, Koralov SB, Mezzano V, Loomis CA, Moreira AL, Moore W, Tsirigos A, Heguy A, Rom WN, Sterman DH, Pass HI, Clemente JC, Li H, Bonneau R, Wong KK, Papagiannakopoulos T, Segal LN. Lower Airway Dysbiosis Affects Lung Cancer Progression. *Cancer Discov* 2021; **11**: 293-307 [PMID: 33177060 DOI: 10.1158/2159-8290.CD-20-0263]
11 **Dejea CM**, Fathi P, Craig JM, Boleij A, Taddese R, Geis AL, Wu X, DeStefano Shields CE, Hechenbleikner EM, Huso DL, Anders RA, Giardiello FM, Wick EC, Wang H, Wu S, Pardoll DM, Housseau F, Sears CL. Patients with familial adenomatous polyposis harbor colonic biofilms containing tumorigenic bacteria. *Science* 2018; **359**: 592-597 [PMID: 29420293 DOI: 10.1126/science.aah3648]
12 **Gagliani N**, Hu B, Huber S, Elinav E, Flavell RA. The fire within: microbes inflame tumors. *Cell* 2014; **157**: 776-783 [PMID: 24813605 DOI: 10.1016/j.cell.2014.03.006]
13 **Sepich-Poore GD**, Guccione C, Laplane L, Pradeu T, Curtius K, Knight R. Cancer's second genome: Microbial cancer diagnostics and redefining clonal evolution as a multispecies process: Humans and their tumors are not aseptic, and the multispecies nature of cancer modulates clinical care and clonal evolution: Humans and their tumors are not aseptic, and the multispecies nature of cancer modulates clinical care and clonal evolution. *Bioessays* 2022; **44**: e2100252 [PMID:

35253252 DOI: 10.1002/bies.202100252]

14 **Riquelme E**, Zhang Y, Zhang L, Montiel M, Zoltan M, Dong W, Quesada P, Sahin I, Chandra V, San Lucas A, Scheet P, Xu H, Hanash SM, Feng L, Burks JK, Do KA, Peterson CB, Nejman D, Tzeng CD, Kim MP, Sears CL, Ajami N, Petrosino J, Wood LD, Maitra A, Straussman R, Katz M, White JR, Jenq R, Wargo J, McAllister F. Tumor Microbiome Diversity and Composition Influence Pancreatic Cancer Outcomes. *Cell* 2019; **178**: 795-806.e12 [PMID: 31398337 DOI: 10.1016/j.cell.2019.07.008]

15 **Geller LT**, Barzily-Rokni M, Danino T, Jonas OH, Shental N, Nejman D, Gavert N, Zwang Y, Cooper ZA, Shee K, Thaiss CA, Reuben A, Livny J, Avraham R, Frederick DT, Ligorio M, Chatman K, Johnston SE, Mosher CM, Brandis A, Fuks G, Gurbatri C, Gopalakrishnan V, Kim M, Hurd MW, Katz M, Fleming J, Maitra A, Smith DA, Skalak M, Bu J, Michaud M, Trauger SA, Barshack I, Golan T, Sandbank J, Flaherty KT, Mandinova A, Garrett WS, Thayer SP, Ferrone CR, Huttenhower C, Bhatia SN, Gevers D, Wargo JA, Golub TR, Straussman R. Potential role of intratumor bacteria in mediating tumor resistance to the chemotherapeutic drug gemcitabine. *Science* 2017; **357**: 1156-1160 [PMID: 28912244 DOI: 10.1126/science.aah5043]

16 **Narunsky-Haziza L**, Sepich-Poore GD, Livyatan I, Asraf O, Martino C, Nejman D, Gavert N, Stajich JE, Amit G, González A, Wandro S, Perry G, Ariel R, Meltser A, Shaffer JP, Zhu Q, Balint-Lahat N, Barshack I, Dadiani M, Gal-Yam EN, Patel SP, Bashan A, Swafford AD, Pilpel Y, Knight R, Straussman R. Pan-cancer analyses reveal cancer-type-specific fungal ecologies and bacteriome interactions. *Cell* 2022; **185**: 3789-3806.e17 [PMID: 36179670 DOI: 10.1016/j.cell.2022.09.005]

17 **Alam A**, Levanduski E, Denz P, Villavicencio HS, Bhatta M, Alhorebi L, Zhang Y, Gomez EC, Morreale B, Senchanthisai S, Li J, Turowski SG, Sexton S, Sait SJ, Singh PK, Wang J, Maitra A, Kalinski P, DePinho RA, Wang H, Liao W, Abrams SI, Segal BH, Dey P. Fungal mycobiome drives IL-33 secretion and type 2 immunity in pancreatic cancer. *Cancer Cell* 2022; **40**: 153-167.e11 [PMID: 35120601 DOI: 10.1016/j.ccell.2022.01.003]

18 **Lloréns-Rico V**, Simcock JA, Huys GRB, Raes J. Single-cell approaches in human microbiome research. *Cell* 2022; **185**: 2725-2738 [PMID: 35868276 DOI: 10.1016/j.cell.2022.06.040]

19 **Okuda S**, Hirose Y, Takihara H, Okuda A, Ling Y, Tajima Y, Shimada Y, Ichikawa H, Takizawa K, Sakata J, Wakai T. Unveiling microbiome profiles in human inner body fluids and tumor tissues with pancreatic or biliary tract cancer. *Sci Rep* 2022; **12**: 8766 [PMID: 35610303 DOI: 10.1038/s41598-022-12658-8]

20 **Pushalkar S**, Hundeyin M, Daley D, Zambirinis CP, Kurz E, Mishra A, Mohan N, Aykut B, Usyk M, Torres LE, Werba G, Zhang K, Guo Y, Li Q, Akkad N, Lall S, Wadowski B, Gutierrez J, Kochen Rossi JA, Herzog JW, Diskin B, Torres-Hernandez A, Leinwand J, Wang W, Taunk PS, Savadkar S, Janal M, Saxena A, Li X, Cohen D, Sartor RB, Saxena D, Miller G. The Pancreatic Cancer Microbiome Promotes Oncogenesis by Induction of Innate and Adaptive Immune Suppression. *Cancer Discov* 2018; **8**: 403-416 [PMID: 29567829 DOI: 10.1158/2159-8290.CD-17-1134]

21 **Aykut B**, Pushalkar S, Chen R, Li Q, Abengozar R, Kim JI, Shadaloey SA, Wu D, Preiss P, Verma N, Guo Y, Saxena A, Vardhan M, Diskin B, Wang W, Leinwand J, Kurz E, Kochen Rossi JA, Hundeyin M, Zambrinis C, Li X, Saxena D, Miller G. The fungal mycobiome promotes pancreatic oncogenesis *via* activation of MBL. *Nature* 2019; **574**: 264-267 [PMID: 31578522 DOI: 10.1038/s41586-019-1608-2]

22 **Thomas RM**, Gharaibeh RZ, Gauthier J, Beveridge M, Pope JL, Guijarro MV, Yu Q, He Z, Ohland C, Newsome R, Trevino J, Hughes SJ, Reinhard M, Winglee K, Fodor AA, Zajac-Kaye M, Jobin C. Intestinal microbiota enhances pancreatic carcinogenesis in preclinical models. *Carcinogenesis* 2018; **39**: 1068-1078 [PMID: 29846515 DOI: 10.1093/carcin/bgy073]

23 **Thomas RM**, Jobin C. Microbiota in pancreatic health and disease: the next frontier in microbiome research. *Nat Rev Gastroenterol Hepatol* 2020; **17**: 53-64 [PMID: 31811279 DOI: 10.1038/s41575-019-0242-7]

24 **Nejman D**, Livyatan I, Fuks G, Gavert N, Zwang Y, Geller LT, Rotter-Maskowitz A, Weiser R, Mallel G, Gigi E, Meltser A, Douglas GM, Kamer I, Gopalakrishnan V, Dadosh T, Levin-Zaidman S, Avnet S, Atlan T, Cooper ZA, Arora R, Cogdill AP, Khan MAW, Ologun G, Bussi Y, Weinberger A, Lotan-Pompan M, Golani O, Perry G, Rokah M, Bahar-Shany K, Rozeman EA, Blank CU, Ronai A, Shaoul R, Amit A, Dorfman T, Kremer R, Cohen ZR, Harnof S, Siegal T, Yehuda-Shnaidman E, Gal-Yam EN, Shapira H, Baldini N, Langille MGI, Ben-Nun A, Kaufman B, Nissan A, Golan T, Dadiani M, Levanon K, Bar J, Yust-Katz S, Barshack I, Peeper DS, Raz DJ, Segal E, Wargo JA, Sandbank J, Shental N, Straussman R. The human tumor microbiome is composed of tumor type-specific intracellular bacteria. *Science* 2020; **368**: 973-980 [PMID: 32467386 DOI: 10.1126/science.aay9189]

25 **Tan Q**, Ma X, Yang B, Liu Y, Xie Y, Wang X, Yuan W, Ma J. Periodontitis pathogen Porphyromonas gingivalis promotes pancreatic tumorigenesis *via* neutrophil elastase from tumor-associated neutrophils. *Gut Microbes* 2022; **14**: 2073785 [PMID: 35549648 DOI: 10.1080/19490976.2022.2073785]

26 **Nalluri H**, Jensen E, Staley C. Role of biliary stent and neoadjuvant chemotherapy in the pancreatic tumor microbiome. *BMC Microbiol* 2021; **21**: 280 [PMID: 34656097 DOI: 10.1186/s12866-021-02339-3]

27 **Gaiser RA**, Halimi A, Alkharaan H, Lu L, Davanian H, Healy K, Hugerth LW, Ateeb Z, Valente R, Fernández Moro C, Del Chiaro M, Sällberg Chen M. Enrichment of oral microbiota in early cystic precursors to invasive pancreatic cancer. *Gut* 2019; **68**: 2186-2194 [PMID: 30872392 DOI: 10.1136/gutjnl-2018-317458]

28 **Kohi S**, Macgregor-Das A, Dbouk M, Yoshida T, Chuidian M, Abe T, Borges M, Lennon AM, Shin EJ, Canto MI, Goggins M. Alterations in the Duodenal Fluid Microbiome of Patients With Pancreatic Cancer. *Clin Gastroenterol Hepatol* 2022; **20**: e196-e227 [PMID: 33161160 DOI: 10.1016/j.cgh.2020.11.006]

29 **Del Castillo E**, Meier R, Chung M, Koestler DC, Chen T, Paster BJ, Charpentier KP, Kelsey KT, Izard J, Michaud DS. The Microbiomes of Pancreatic and Duodenum Tissue Overlap and Are Highly Subject Specific but Differ between Pancreatic Cancer and Noncancer Subjects. *Cancer Epidemiol Biomarkers Prev* 2019; **28**: 370-383 [PMID: 30373903 DOI: 10.1158/1055-9965.EPI-18-0542]

30 **Schmidt TS**, Hayward MR, Coelho LP, Li SS, Costea PI, Voigt AY, Wirbel J, Maistrenko OM, Alves RJ, Bergsten E, de Beaufort C, Sobhani I, Heintz-Buschart A, Sunagawa S, Zeller G, Wilmes P, Bork P. Extensive transmission of microbes along the gastrointestinal tract. *Elife* 2019; **8** [PMID: 30747106 DOI: 10.7554/eLife.42693]

31 **Mitsuhashi K**, Nosho K, Sukawa Y, Matsunaga Y, Ito M, Kurihara H, Kanno S, Igarashi H, Naito T, Adachi Y,

Tachibana M, Tanuma T, Maguchi H, Shinohara T, Hasegawa T, Imamura M, Kimura Y, Hirata K, Maruyama R, Suzuki H, Imai K, Yamamoto H, Shinomura Y. Association of Fusobacterium species in pancreatic cancer tissues with molecular features and prognosis. *Oncotarget* 2015; **6**: 7209-7220 [PMID: 25797243 DOI: 10.18632/oncotarget.3109]

32 **Abed J**, Emgård JE, Zamir G, Faroja M, Almogy G, Grenov A, Sol A, Naor R, Pikarsky E, Atlan KA, Mellul A, Chaushu S, Manson AL, Earl AM, Ou N, Brennan CA, Garrett WS, Bachrach G. Fap2 Mediates Fusobacterium nucleatum Colorectal Adenocarcinoma Enrichment by Binding to Tumor-Expressed Gal-GalNAc. *Cell Host Microbe* 2016; **20**: 215-225 [PMID: 27512904 DOI: 10.1016/j.chom.2016.07.006]

33 **Parhi L**, Alon-Maimon T, Sol A, Nejman D, Shhadeh A, Fainsod-Levi T, Yajuk O, Isaacson B, Abed J, Maalouf N, Nissan A, Sandbank J, Yehuda-Shnaidman E, Ponath F, Vogel J, Mandelboim O, Granot Z, Straussman R, Bachrach G. Breast cancer colonization by Fusobacterium nucleatum accelerates tumor growth and metastatic progression. *Nat Commun* 2020; **11**: 3259 [PMID: 32591509 DOI: 10.1038/s41467-020-16967-2]

34 **Fu A**, Yao B, Dong T, Chen Y, Yao J, Liu Y, Li H, Bai H, Liu X, Zhang Y, Wang C, Guo Y, Li N, Cai S. Tumor-resident intracellular microbiota promotes metastatic colonization in breast cancer. *Cell* 2022; **185**: 1356-1372.e26 [PMID: 35395179 DOI: 10.1016/j.cell.2022.02.027]

35 **Tilg H**, Adolph TE, Trauner M. Gut-liver axis: Pathophysiological concepts and clinical implications. *Cell Metab* 2022; **34**: 1700-1718 [PMID: 36208625 DOI: 10.1016/j.cmet.2022.09.017]

36 **Widdison AL**, Karanjia ND, Reber HA. Routes of spread of pathogens into the pancreas in a feline model of acute pancreatitis. *Gut* 1994; **35**: 1306-1310 [PMID: 7959243 DOI: 10.1136/gut.35.9.1306]

37 **Liu J**, Huang L, Luo M, Xia X. Bacterial translocation in acute pancreatitis. *Crit Rev Microbiol* 2019; **45**: 539-547 [PMID: 31851854 DOI: 10.1080/1040841X.2019.1621795]

38 **Diehl GE**, Longman RS, Zhang JX, Breart B, Galan C, Cuesta A, Schwab SR, Littman DR. Microbiota restricts trafficking of bacteria to mesenteric lymph nodes by CX(3)CR1(hi) cells. *Nature* 2013; **494**: 116-120 [PMID: 23334413 DOI: 10.1038/nature11809]

39 **Bravo-Blas A**, Utriainen L, Clay SL, Kästele V, Cerovic V, Cunningham AF, Henderson IR, Wall DM, Milling SWF. Salmonella enterica Serovar Typhimurium Travels to Mesenteric Lymph Nodes Both with Host Cells and Autonomously. *J Immunol* 2019; **202**: 260-267 [PMID: 30487173 DOI: 10.4049/jimmunol.1701254]

40 **Fritz S**, Hackert T, Hartwig W, Rossmanith F, Strobel O, Schneider L, Will-Schweiger K, Kommerell M, Büchler MW, Werner J. Bacterial translocation and infected pancreatic necrosis in acute necrotizing pancreatitis derives from small bowel rather than from colon. *Am J Surg* 2010; **200**: 111-117 [PMID: 20637344 DOI: 10.1016/j.amjsurg.2009.08.019]

41 **Forestier C**, Moreno E, Pizarro-Cerda J, Gorvel JP. Lysosomal accumulation and recycling of lipopolysaccharide to the cell surface of murine macrophages, an in vitro and in vivo study. *J Immunol* 1999; **162**: 6784-6791 [PMID: 10352299]

42 **Iwai T**. Periodontal bacteremia and various vascular diseases. *J Periodontal Res* 2009; **44**: 689-694 [PMID: 19874452 DOI: 10.1111/j.1600-0765.2008.01165.x]

43 **Sakamoto H**, Naito H, Ohta Y, Tanakna R, Maeda N, Sasaki J, Nord CE. Isolation of bacteria from cervical lymph nodes in patients with oral cancer. *Arch Oral Biol* 1999; **44**: 789-793 [PMID: 10530911 DOI: 10.1016/s0003-9969(99)00079-5]

44 **Gnanasekaran J**, Binder Gallimidi A, Saba E, Pandi K, Eli Berchoer L, Hermano E, Angabo S, Makkawi HA, Khashan A, Daoud A, Elkin M, Nussbaum G. Intracellular Porphyromonas gingivalis Promotes the Tumorigenic Behavior of Pancreatic Carcinoma Cells. *Cancers (Basel)* 2020; **12** [PMID: 32824786 DOI: 10.3390/cancers12082331]

45 **Halimi A**, Gabarrini G, Sobkowiak MJ, Ateeb Z, Davanian H, Gaiser RA, Arnelo U, Valente R, Wong AYW, Moro CF, Del Chiaro M, Özenci V, Chen MS. Isolation of pancreatic microbiota from cystic precursors of pancreatic cancer with intracellular growth and DNA damaging properties. *Gut Microbes* 2021; **13**: 1983101 [PMID: 34816784 DOI: 10.1080/19490976.2021.1983101]

46 **Jeong JY**, Kim TB, Kim J, Choi HW, Kim EJ, Yoo HJ, Lee S, Jun HR, Yoo W, Kim S, Kim SC, Jun E. Diversity in the Extracellular Vesicle-Derived Microbiome of Tissues According to Tumor Progression in Pancreatic Cancer. *Cancers (Basel)* 2020; **12** [PMID: 32825137 DOI: 10.3390/cancers12092346]

47 **Petit TJP**, Lebreton A. Adaptations of intracellular bacteria to vacuolar or cytosolic niches. *Trends Microbiol* 2022; **30**: 736-748 [PMID: 35168833 DOI: 10.1016/j.tim.2022.01.015]

48 **Strobel M**, Pförtner H, Tuchscherr L, Völker U, Schmidt F, Kramko N, Schnittler HJ, Fraunholz MJ, Löffler B, Peters G, Niemann S. Post-invasion events after infection with Staphylococcus aureus are strongly dependent on both the host cell type and the infecting S. aureus strain. *Clin Microbiol Infect* 2016; **22**: 799-809 [PMID: 27393124 DOI: 10.1016/j.cmi.2016.06.020]

49 **Poore GD**, Kopylova E, Zhu Q, Carpenter C, Fraraccio S, Wandro S, Kosciolek T, Janssen S, Metcalf J, Song SJ, Kanbar J, Miller-Montgomery S, Heaton R, Mckay R, Patel SP, Swafford AD, Knight R. Microbiome analyses of blood and tissues suggest cancer diagnostic approach. *Nature* 2020; **579**: 567-574 [PMID: 32214244 DOI: 10.1038/s41586-020-2095-1]

50 **Robinson KM**, Crabtree J, Mattick JS, Anderson KE, Dunning Hotopp JC. Distinguishing potential bacteria-tumor associations from contamination in a secondary data analysis of public cancer genome sequence data. *Microbiome* 2017; **5**: 9 [PMID: 28118849 DOI: 10.1186/s40168-016-0224-8]

51 **Dohlman AB**, Arguijo Mendoza D, Ding S, Gao M, Dressman H, Iliev ID, Lipkin SM, Shen X. The cancer microbiome atlas: a pan-cancer comparative analysis to distinguish tissue-resident microbiota from contaminants. *Cell Host Microbe* 2021; **29**: 281-298.e5 [PMID: 33382980 DOI: 10.1016/j.chom.2020.12.001]

52 **Dohlman AB**, Klug J, Mesko M, Gao IH, Lipkin SM, Shen X, Iliev ID. A pan-cancer mycobiome analysis reveals fungal involvement in gastrointestinal and lung tumors. *Cell* 2022; **185**: 3807-3822.e12 [PMID: 36179671 DOI: 10.1016/j.cell.2022.09.015]

53 **Nakano S**, Kawamoto Y, Komatsu Y, Saito R, Ito K, Yamamura T, Harada K, Yuki S, Kawakubo K, Sugiura R, Kato S, Hirata K, Hirata H, Nakajima M, Furukawa R, Takishin Y, Nagai K, Yokota I, Ota KH, Nakaoka S, Kuwatani M, Sakamoto N. Analysis of the Pancreatic Cancer Microbiome Using Endoscopic Ultrasound-Guided Fine-Needle Aspiration-Derived Samples. *Pancreas* 2022; **51**: 351-357 [PMID: 35695806 DOI: 10.1097/MPA.0000000000002028]

54 **Chen Y**, Yang S, Tavormina J, Tampe D, Zeisberg M, Wang H, Mahadevan KK, Wu CJ, Sugimoto H, Chang CC, Jenq

RR, McAndrews KM, Kalluri R. Oncogenic collagen I homotrimers from cancer cells bind to α3β1 integrin and impact tumor microbiome and immunity to promote pancreatic cancer. *Cancer Cell* 2022; **40**: 818-834.e9 [PMID: 35868307 DOI: 10.1016/j.ccell.2022.06.011]

55 **Cummins J**, Tangney M. Bacteria and tumours: causative agents or opportunistic inhabitants? *Infect Agent Cancer* 2013; **8**: 11 [PMID: 23537317 DOI: 10.1186/1750-9378-8-11]

56 **Gleeson FC**, Jeraldo P, Levy MJ, Murphy SJ, Mendes-Soares H, Karagouga G, Mccune AF, Garcia Garcia Deparedes A, Kipp BR, Song SD, Khanna S, Pardi DS, Chia N. Composition, diversity and potential utility of intervention-naïve pancreatic cancer intratumoral microbiome signature profiling *via* endoscopic ultrasound. *Gut* 2022; **71**: 441-443 [PMID: 33753418 DOI: 10.1136/gutjnl-2021-324031]

57 **Guo W**, Zhang Y, Guo S, Mei Z, Liao H, Dong H, Wu K, Ye H, Zhu Y, Lang J, Hu L, Jin G, Kong X. Tumor microbiome contributes to an aggressive phenotype in the basal-like subtype of pancreatic cancer. *Commun Biol* 2021; **4**: 1019 [PMID: 34465850 DOI: 10.1038/s42003-021-02557-5]

58 **Zhou B**, Xu JW, Cheng YG, Gao JY, Hu SY, Wang L, Zhan HX. Early detection of pancreatic cancer: Where are we now and where are we going? *Int J Cancer* 2017; **141**: 231-241 [PMID: 28240774 DOI: 10.1002/ijc.30670]

59 **Avanzini S**, Kurtz DM, Chabon JJ, Moding EJ, Hori SS, Gambhir SS, Alizadeh AA, Diehn M, Reiter JG. A mathematical model of ctDNA shedding predicts tumor detection size. *Sci Adv* 2020; **6** [PMID: 33310847 DOI: 10.1126/sciadv.abc4308]

60 **Mellby LD**, Nyberg AP, Johansen JS, Wingren C, Nordestgaard BG, Bojesen SE, Mitchell BL, Sheppard BC, Sears RC, Borrebaeck CAK. Serum Biomarker Signature-Based Liquid Biopsy for Diagnosis of Early-Stage Pancreatic Cancer. *J Clin Oncol* 2018; **36**: 2887-2894 [PMID: 30106639 DOI: 10.1200/JCO.2017.77.6658]

61 **Sausen M**, Phallen J, Adleff V, Jones S, Leary RJ, Barrett MT, Anagnostou V, Parpart-Li S, Murphy D, Kay Li Q, Hruban CA, Scharpf R, White JR, O'Dwyer PJ, Allen PJ, Eshleman JR, Thompson CB, Klimstra DS, Linehan DC, Maitra A, Hruban RH, Diaz LA Jr, Von Hoff DD, Johansen JS, Drebin JA, Velculescu VE. Clinical implications of genomic alterations in the tumour and circulation of pancreatic cancer patients. *Nat Commun* 2015; **6**: 7686 [PMID: 26154128 DOI: 10.1038/ncomms8686]

62 **Hamada T**, Yasunaga H, Nakai Y, Isayama H, Horiguchi H, Matsuda S, Fushimi K, Koike K. Severe bleeding and perforation are rare complications of endoscopic ultrasound-guided fine needle aspiration for pancreatic masses: an analysis of 3,090 patients from 212 hospitals. *Gut Liver* 2014; **8**: 215-218 [PMID: 24672664 DOI: 10.5009/gnl.2014.8.2.215]

63 **Lundy J**, Gao H, Berry W, Masoumi-Moghoddam S, Jenkins BJ, Croagh D. Targeted Transcriptome and KRAS Mutation Analysis Improve the Diagnostic Performance of EUS-FNA Biopsies in Pancreatic Cancer. *Clin Cancer Res* 2021; **27**: 5900-5911 [PMID: 34400416 DOI: 10.1158/1078-0432.CCR-21-1107]

64 **Masi AC**, Oppong YEA, Haugk B, Lamb CA, Sharp L, Shaw JM, Stewart CJ, Oppong KW. Endoscopic ultrasound (EUS)-guided fine needle biopsy (FNB) formalin fixed paraffin-embedded (FFPE) pancreatic tissue samples are a potential resource for microbiota analysis. *Gut* 2021; **70**: 999-1001 [PMID: 32816963 DOI: 10.1136/gutjnl-2020-322457]

65 **Huang Y**, Zhu N, Zheng X, Liu Y, Lu H, Yin X, Hao H, Tan Y, Wang D, Hu H, Liang Y, Li X, Hu Z, Yin Y. Intratumor Microbiome Analysis Identifies Positive Association Between Megasphaera and Survival of Chinese Patients With Pancreatic Ductal Adenocarcinomas. *Front Immunol* 2022; **13**: 785422 [PMID: 35145519 DOI: 10.3389/fimmu.2022.785422]

66 **Rodriguez RM**, Menor M, Hernandez BY, Deng Y, Khadka VS. Bacterial Diversity Correlates with Overall Survival in Cancers of the Head and Neck, Liver, and Stomach. *Molecules* 2021; **26** [PMID: 34577130 DOI: 10.3390/molecules26185659]

67 **Luo M**, Liu Y, Hermida LC, Gertz EM, Zhang Z, Li Q, Diao L, Ruppin E, Han L. Race is a key determinant of the human intratumor microbiome. *Cancer Cell* 2022; **40**: 901-902 [PMID: 36099885 DOI: 10.1016/j.ccell.2022.08.007]

68 **Hermida LC**, Gertz EM, Ruppin E. Predicting cancer prognosis and drug response from the tumor microbiome. *Nat Commun* 2022; **13**: 2896 [PMID: 35610202 DOI: 10.1038/s41467-022-30512-3]

69 **Eisenhofer R**, Minich JJ, Marotz C, Cooper A, Knight R, Weyrich LS. Contamination in Low Microbial Biomass Microbiome Studies: Issues and Recommendations. *Trends Microbiol* 2019; **27**: 105-117 [PMID: 30497919 DOI: 10.1016/j.tim.2018.11.003]

70 **Wang N**, Cheng M, Ning K. Overcoming regional limitations: transfer learning for cross-regional microbial-based diagnosis of diseases. *Gut* 2022 [PMID: 36307182 DOI: 10.1136/gutjnl-2022-328216]

71 **Netea MG**, Joosten LA, Latz E, Mills KH, Natoli G, Stunnenberg HG, O'Neill LA, Xavier RJ. Trained immunity: A program of innate immune memory in health and disease. *Science* 2016; **352**: aaf1098 [PMID: 27102489 DOI: 10.1126/science.aaf1098]

72 **Deets KA**, Vance RE. Inflammasomes and adaptive immune responses. *Nat Immunol* 2021; **22**: 412-422 [PMID: 33603227 DOI: 10.1038/s41590-021-00869-6]

73 **Medzhitov R**. Recognition of microorganisms and activation of the immune response. *Nature* 2007; **449**: 819-826 [PMID: 17943118 DOI: 10.1038/nature06246]

74 **Sethi V**, Vitiello GA, Saxena D, Miller G, Dudeja V. The Role of the Microbiome in Immunologic Development and its Implication For Pancreatic Cancer Immunotherapy. *Gastroenterology* 2019; **156**: 2097-2115.e2 [PMID: 30768986 DOI: 10.1053/j.gastro.2018.12.045]

75 **Rooks MG**, Garrett WS. Gut microbiota, metabolites and host immunity. *Nat Rev Immunol* 2016; **16**: 341-352 [PMID: 27231050 DOI: 10.1038/nri.2016.42]

76 **Helmink BA**, Khan MAW, Hermann A, Gopalakrishnan V, Wargo JA. The microbiome, cancer, and cancer therapy. *Nat Med* 2019; **25**: 377-388 [PMID: 30842679 DOI: 10.1038/s41591-019-0377-7]

77 **Pandey V**, Storz P. Targeting the tumor microenvironment in pancreatic ductal adenocarcinoma. *Expert Rev Anticancer Ther* 2019; **19**: 473-482 [PMID: 31148495 DOI: 10.1080/14737140.2019.1622417]

78 **Amedei A**, Niccolai E, Prisco D. Pancreatic cancer: role of the immune system in cancer progression and vaccine-based immunotherapy. *Hum Vaccin Immunother* 2014; **10**: 3354-3368 [PMID: 25483688 DOI: 10.4161/hv.34392]

79 **Bear AS**, Vonderheide RH, O'Hara MH. Challenges and Opportunities for Pancreatic Cancer Immunotherapy. *Cancer Cell* 2020; **38**: 788-802 [PMID: 32946773 DOI: 10.1016/j.ccell.2020.08.004]

80 **Sjöberg AP**, Trouw LA, Blom AM. Complement activation and inhibition: a delicate balance. *Trends Immunol* 2009; **30**: 83-90 [PMID: 19144569 DOI: 10.1016/j.it.2008.11.003]

81 **Zipfel PF**, Skerka C. Complement regulators and inhibitory proteins. *Nat Rev Immunol* 2009; **9**: 729-740 [PMID: 19730437 DOI: 10.1038/nri2620]

82 **Afshar-Kharghan V**. The role of the complement system in cancer. *J Clin Invest* 2017; **127**: 780-789 [PMID: 28248200 DOI: 10.1172/JCI90962]

83 **Cho MS**, Vasquez HG, Rupaimoole R, Pradeep S, Wu S, Zand B, Han HD, Rodriguez-Aguayo C, Bottsford-Miller J, Huang J, Miyake T, Choi HJ, Dalton HJ, Ivan C, Baggerly K, Lopez-Berestein G, Sood AK, Afshar-Kharghan V. Autocrine effects of tumor-derived complement. *Cell Rep* 2014; **6**: 1085-1095 [PMID: 24613353 DOI: 10.1016/j.celrep.2014.02.014]

84 **Chen J**, Wu W, Zhen C, Zhou H, Yang R, Chen L, Hu L. Expression and clinical significance of complement C3, complement C4b1 and apolipoprotein E in pancreatic cancer. *Oncol Lett* 2013; **6**: 43-48 [PMID: 23946775 DOI: 10.3892/ol.2013.1326]

85 **Andoh A**, Shimada M, Takaya H, Hata K, Fujiyama Y, Bamba T. Transforming growth factor-beta1 acts as a potent inhibitor of complement C3 biosynthesis in human pancreatic cancer cell lines. *Pancreas* 2000; **20**: 138-145 [PMID: 10707928 DOI: 10.1097/00006676-200003000-00005]

86 **Zhang R**, Liu Q, Peng J, Wang M, Gao X, Liao Q, Zhao Y. Pancreatic cancer-educated macrophages protect cancer cells from complement-dependent cytotoxicity by up-regulation of CD59. *Cell Death Dis* 2019; **10**: 836 [PMID: 31685825 DOI: 10.1038/s41419-019-2065-4]

87 **Brinkmann V**, Reichard U, Goosmann C, Fauler B, Uhlemann Y, Weiss DS, Weinrauch Y, Zychlinsky A. Neutrophil extracellular traps kill bacteria. *Science* 2004; **303**: 1532-1535 [PMID: 15001782 DOI: 10.1126/science.1092385]

88 **Suzuki R**, Okubo Y, Takagi T, Sugimoto M, Sato Y, Irie H, Nakamura J, Takasumi M, Kato T, Hashimoto M, Kobashi R, Hikichi T, Ohira H. The Complement C3a-C3a Receptor Axis Regulates Epithelial-to-Mesenchymal Transition by Activating the ERK Pathway in Pancreatic Ductal Adenocarcinoma. *Anticancer Res* 2022; **42**: 1207-1215 [PMID: 35220210 DOI: 10.21873/anticanres.15587]

89 **Dahinden CA**, Bischoff SC, Brunner T, Krieger M, Takafuji S, de Weck AL. Regulation of mediator release by human basophils: importance of the sequence and time of addition in the combined action of different agonists. *Int Arch Allergy Appl Immunol* 1991; **94**: 161-164 [PMID: 1718886 DOI: 10.1159/000235350]

90 **Elsner J**, Oppermann M, Czech W, Dobos G, Schöpf E, Norgauer J, Kapp A. C3a activates reactive oxygen radical species production and intracellular calcium transients in human eosinophils. *Eur J Immunol* 1994; **24**: 518-522 [PMID: 8125125 DOI: 10.1002/eji.1830240304]

91 **Martin U**, Bock D, Arseniev L, Tornetta MA, Ames RS, Bautsch W, Köhl J, Ganser A, Klos A. The human C3a receptor is expressed on neutrophils and monocytes, but not on B or T lymphocytes. *J Exp Med* 1997; **186**: 199-207 [PMID: 9221749 DOI: 10.1084/jem.186.2.199]

92 **Strainic MG**, Shevach EM, An F, Lin F, Medof ME. Absence of signaling into $CD4^+$ cells *via* C3aR and C5aR enables autoinductive TGF-β1 signaling and induction of $Foxp3^+$ regulatory T cells. *Nat Immunol* 2013; **14**: 162-171 [PMID: 23263555 DOI: 10.1038/ni.2499]

93 **Wang Y**, Zhang H, He YW. The Complement Receptors C3aR and C5aR Are a New Class of Immune Checkpoint Receptor in Cancer Immunotherapy. *Front Immunol* 2019; **10**: 1574 [PMID: 31379815 DOI: 10.3389/fimmu.2019.01574]

94 **Urban CF**, Reichard U, Brinkmann V, Zychlinsky A. Neutrophil extracellular traps capture and kill Candida albicans yeast and hyphal forms. *Cell Microbiol* 2006; **8**: 668-676 [PMID: 16548892 DOI: 10.1111/j.1462-5822.2005.00659.x]

95 **Saitoh T**, Komano J, Saitoh Y, Misawa T, Takahama M, Kozaki T, Uehata T, Iwasaki H, Omori H, Yamaoka S, Yamamoto N, Akira S. Neutrophil extracellular traps mediate a host defense response to human immunodeficiency virus-1. *Cell Host Microbe* 2012; **12**: 109-116 [PMID: 22817992 DOI: 10.1016/j.chom.2012.05.015]

96 **Abi Abdallah DS**, Lin C, Ball CJ, King MR, Duhamel GE, Denkers EY. Toxoplasma gondii triggers release of human and mouse neutrophil extracellular traps. *Infect Immun* 2012; **80**: 768-777 [PMID: 22104111 DOI: 10.1128/IAI.05730-11]

97 **Papayannopoulos V**. Neutrophil extracellular traps in immunity and disease. *Nat Rev Immunol* 2018; **18**: 134-147 [PMID: 28990587 DOI: 10.1038/nri.2017.105]

98 **Lood C**, Blanco LP, Purmalek MM, Carmona-Rivera C, De Ravin SS, Smith CK, Malech HL, Ledbetter JA, Elkon KB, Kaplan MJ. Neutrophil extracellular traps enriched in oxidized mitochondrial DNA are interferogenic and contribute to lupus-like disease. *Nat Med* 2016; **22**: 146-153 [PMID: 26779811 DOI: 10.1038/nm.4027]

99 **Demkow U**. Neutrophil Extracellular Traps (NETs) in Cancer Invasion, Evasion and Metastasis. *Cancers (Basel)* 2021; **13** [PMID: 34503307 DOI: 10.3390/cancers13174495]

100 **Sochalska M**, Potempa J. Manipulation of Neutrophils by Porphyromonas gingivalis in the Development of Periodontitis. *Front Cell Infect Microbiol* 2017; **7**: 197 [PMID: 28589098 DOI: 10.3389/fcimb.2017.00197]

101 **Zebboudj A**, Amisaki M, Balachandran VP. ILC2s-Bipartisan politicians in cancer. *Sci Immunol* 2022; **7**: eabq2791 [PMID: 35658014 DOI: 10.1126/sciimmunol.abq2791]

102 **Moral JA**, Leung J, Rojas LA, Ruan J, Zhao J, Sethna Z, Ramnarain A, Gasmi B, Gururajan M, Redmond D, Askan G, Bhanot U, Elyada E, Park Y, Tuveson DA, Gönen M, Leach SD, Wolchok JD, DeMatteo RP, Merghoub T, Balachandran VP. ILC2s amplify PD-1 blockade by activating tissue-specific cancer immunity. *Nature* 2020; **579**: 130-135 [PMID: 32076273 DOI: 10.1038/s41586-020-2015-4]

103 **Mahajan UM**, Langhoff E, Goni E, Costello E, Greenhalf W, Halloran C, Ormanns S, Kruger S, Boeck S, Ribback S, Beyer G, Dombroswki F, Weiss FU, Neoptolemos JP, Werner J, D'Haese JG, Bazhin A, Peterhansl J, Pichlmeier S, Büchler MW, Kleeff J, Ganeh P, Sendler M, Palmer DH, Kohlmann T, Rad R, Regel I, Lerch MM, Mayerle J. Immune Cell and Stromal Signature Associated With Progression-Free Survival of Patients With Resected Pancreatic Ductal Adenocarcinoma. *Gastroenterology* 2018; **155**: 1625-1639.e2 [PMID: 30092175 DOI: 10.1053/j.gastro.2018.08.009]

104 **Liu X**, Xu J, Zhang B, Liu J, Liang C, Meng Q, Hua J, Yu X, Shi S. The reciprocal regulation between host tissue and immune cells in pancreatic ductal adenocarcinoma: new insights and therapeutic implications. *Mol Cancer* 2019; **18**: 184 [PMID: 31831007 DOI: 10.1186/s12943-019-1117-9]

105 **Dey P**, Li J, Zhang J, Chaurasiya S, Strom A, Wang H, Liao WT, Cavallaro F, Denz P, Bernard V, Yen EY, Genovese G, Gulhati P, Liu J, Chakravarti D, Deng P, Zhang T, Carbone F, Chang Q, Ying H, Shang X, Spring DJ, Ghosh B, Putluri N, Maitra A, Wang YA, DePinho RA. Oncogenic KRAS-Driven Metabolic Reprogramming in Pancreatic Cancer Cells Utilizes Cytokines from the Tumor Microenvironment. *Cancer Discov* 2020; **10**: 608-625 [PMID: 32046984 DOI: 10.1158/2159-8290.CD-19-0297]

106 **Mosser DM**, Edwards JP. Exploring the full spectrum of macrophage activation. *Nat Rev Immunol* 2008; **8**: 958-969 [PMID: 19029990 DOI: 10.1038/nri2448]

107 **Mielgo A**, Schmid MC. Impact of tumour associated macrophages in pancreatic cancer. *BMB Rep* 2013; **46**: 131-138 [PMID: 23527856 DOI: 10.5483/bmbrep.2013.46.3.036]

108 **Das S**, Shapiro B, Vucic EA, Vogt S, Bar-Sagi D. Tumor Cell-Derived IL1β Promotes Desmoplasia and Immune Suppression in Pancreatic Cancer. *Cancer Res* 2020; **80**: 1088-1101 [PMID: 31915130 DOI: 10.1158/0008-5472.CAN-19-2080]

109 **Fu C**, Jiang A. Dendritic Cells and CD8 T Cell Immunity in Tumor Microenvironment. *Front Immunol* 2018; **9**: 3059 [PMID: 30619378 DOI: 10.3389/fimmu.2018.03059]

110 **Ciccolini J**, Serdjebi C, Peters GJ, Giovannetti E. Pharmacokinetics and pharmacogenetics of Gemcitabine as a mainstay in adult and pediatric oncology: an EORTC-PAMM perspective. *Cancer Chemother Pharmacol* 2016; **78**: 1-12 [PMID: 27007129 DOI: 10.1007/s00280-016-3003-0]

111 **Konstantinopoulos PA**, Cheng SC, Wahner Hendrickson AE, Penson RT, Schumer ST, Doyle LA, Lee EK, Kohn EC, Duska LR, Crispens MA, Olawaiye AB, Winer IS, Barroilhet LM, Fu S, McHale MT, Schilder RJ, Färkkilä A, Chowdhury D, Curtis J, Quinn RS, Bowes B, D'Andrea AD, Shapiro GI, Matulonis UA. Berzosertib plus gemcitabine versus gemcitabine alone in platinum-resistant high-grade serous ovarian cancer: a multicentre, open-label, randomised, phase 2 trial. *Lancet Oncol* 2020; **21**: 957-968 [PMID: 32553118 DOI: 10.1016/S1470-2045(20)30180-7]

112 **Gontero P**, Frea B. Actual experience and future development of gemcitabine in superficial bladder cancer. *Ann Oncol* 2006; **17** Suppl 5: v123-v128 [PMID: 16807439 DOI: 10.1093/annonc/mdj966]

113 **Wu YL**, Zhou C, Hu CP, Feng J, Lu S, Huang Y, Li W, Hou M, Shi JH, Lee KY, Xu CR, Massey D, Kim M, Shi Y, Geater SL. Afatinib versus cisplatin plus gemcitabine for first-line treatment of Asian patients with advanced non-small-cell lung cancer harbouring EGFR mutations (LUX-Lung 6): an open-label, randomised phase 3 trial. *Lancet Oncol* 2014; **15**: 213-222 [PMID: 24439929 DOI: 10.1016/S1470-2045(13)70604-1]

114 **Vande Voorde J**, Vervaeke P, Liekens S, Balzarini J. Mycoplasma hyorhinis-encoded cytidine deaminase efficiently inactivates cytosine-based anticancer drugs. *FEBS Open Bio* 2015; **5**: 634-639 [PMID: 26322268 DOI: 10.1016/j.fob.2015.07.007]

115 **Yu T**, Guo F, Yu Y, Sun T, Ma D, Han J, Qian Y, Kryczek I, Sun D, Nagarsheth N, Chen Y, Chen H, Hong J, Zou W, Fang JY. Fusobacterium nucleatum Promotes Chemoresistance to Colorectal Cancer by Modulating Autophagy. *Cell* 2017; **170**: 548-563.e16 [PMID: 28753429 DOI: 10.1016/j.cell.2017.07.008]

116 **Mohindroo C**, Hasanov M, Rogers JE, Dong W, Prakash LR, Baydogan S, Mizrahi JD, Overman MJ, Varadhachary GR, Wolff RA, Javle MM, Fogelman DR, Lotze MT, Kim MP, Katz MHG, Pant S, Tzeng CD, McAllister F. Antibiotic use influences outcomes in advanced pancreatic adenocarcinoma patients. *Cancer Med* 2021; **10**: 5041-5050 [PMID: 34250759 DOI: 10.1002/cam4.3870]

117 **Weniger M**, Hank T, Qadan M, Ciprani D, Michelakos T, Niess H, Heiliger C, Ilmer M, D'Haese JG, Ferrone CR, Warshaw AL, Lillemoe KD, Werner J, Liss A, Fernández-Del Castillo C. Influence of Klebsiella pneumoniae and quinolone treatment on prognosis in patients with pancreatic cancer. *Br J Surg* 2021; **108**: 709-716 [PMID: 34157083 DOI: 10.1002/bjs.12003]

118 **Corty RW**, Langworthy BW, Fine JP, Buse JB, Sanoff HK, Lund JL. Antibacterial Use Is Associated with an Increased Risk of Hematologic and Gastrointestinal Adverse Events in Patients Treated with Gemcitabine for Stage IV Pancreatic Cancer. *Oncologist* 2020; **25**: 579-584 [PMID: 32181968 DOI: 10.1634/theoncologist.2019-0570]

119 **Seelbinder B**, Chen J, Brunke S, Vazquez-Uribe R, Santhaman R, Meyer AC, de Oliveira Lino FS, Chan KF, Loos D, Imamovic L, Tsang CC, Lam RP, Sridhar S, Kang K, Hube B, Woo PC, Sommer MOA, Panagiotou G. Antibiotics create a shift from mutualism to competition in human gut communities with a longer-lasting impact on fungi than bacteria. *Microbiome* 2020; **8**: 133 [PMID: 32919472 DOI: 10.1186/s40168-020-00899-6]

120 **Zaura E**, Brandt BW, Teixeira de Mattos MJ, Buijs MJ, Caspers MP, Rashid MU, Weintraub A, Nord CE, Savell A, Hu Y, Coates AR, Hubank M, Spratt DA, Wilson M, Keijser BJ, Crielaard W. Same Exposure but Two Radically Different Responses to Antibiotics: Resilience of the Salivary Microbiome versus Long-Term Microbial Shifts in Feces. *mBio* 2015; **6**: e01693-e01615 [PMID: 26556275 DOI: 10.1128/mBio.01693-15]

121 **O'Reilly EM**, Oh DY, Dhani N, Renouf DJ, Lee MA, Sun W, Fisher G, Hezel A, Chang SC, Vlahovic G, Takahashi O, Yang Y, Fitts D, Philip PA. Durvalumab With or Without Tremelimumab for Patients With Metastatic Pancreatic Ductal Adenocarcinoma: A Phase 2 Randomized Clinical Trial. *JAMA Oncol* 2019; **5**: 1431-1438 [PMID: 31318392 DOI: 10.1001/jamaoncol.2019.1588]

122 **Zhang Z**, Tang D. The huge clinical potential of microbiota in the treatment of pancreatic cancer: The next frontier. *Biochim Biophys Acta Rev Cancer* 2022; **1877**: 188733 [PMID: 35483491 DOI: 10.1016/j.bbcan.2022.188733]

123 **Huang XZ**, Gao P, Song YX, Xu Y, Sun JX, Chen XW, Zhao JH, Wang ZN. Antibiotic use and the efficacy of immune checkpoint inhibitors in cancer patients: a pooled analysis of 2740 cancer patients. *Oncoimmunology* 2019; **8**: e1665973 [PMID: 31741763 DOI: 10.1080/2162402X.2019.1665973]

124 **Chen SM**, Hsu LJ, Lee HL, Lin CP, Huang SW, Lai CJ, Lin CW, Chen WT, Chen YJ, Lin YC, Yang CC, Jan MS. Lactobacillus Attenuate the Progression of Pancreatic Cancer Promoted by Porphyromonas Gingivalis in K-ras(G12D) Transgenic Mice. *Cancers (Basel)* 2020; **12** [PMID: 33255941 DOI: 10.3390/cancers12123522]

125 **Konishi H**, Isozaki S, Kashima S, Moriichi K, Ichikawa S, Yamamoto K, Yamamura C, Ando K, Ueno N, Akutsu H,

Ogawa N, Fujiya M. Probiotic Aspergillus oryzae produces anti-tumor mediator and exerts anti-tumor effects in pancreatic cancer through the p38 MAPK signaling pathway. *Sci Rep* 2021; **11**: 11070 [PMID: 34040123 DOI: 10.1038/s41598-021-90707-4]

126 **Suez J**, Zmora N, Zilberman-Schapira G, Mor U, Dori-Bachash M, Bashiardes S, Zur M, Regev-Lehavi D, Ben-Zeev Brik R, Federici S, Horn M, Cohen Y, Moor AE, Zeevi D, Korem T, Kotler E, Harmelin A, Itzkovitz S, Maharshak N, Shibolet O, Pevsner-Fischer M, Shapiro H, Sharon I, Halpern Z, Segal E, Elinav E. Post-Antibiotic Gut Mucosal Microbiome Reconstitution Is Impaired by Probiotics and Improved by Autologous FMT. *Cell* 2018; **174**: 1406-1423.e16 [PMID: 30193113 DOI: 10.1016/j.cell.2018.08.047]

127 **Cullin N**, Azevedo Antunes C, Straussman R, Stein-Thoeringer CK, Elinav E. Microbiome and cancer. *Cancer Cell* 2021; **39**: 1317-1341 [PMID: 34506740 DOI: 10.1016/j.ccell.2021.08.006]

128 **Watterson WJ**, Tanyeri M, Watson AR, Cham CM, Shan Y, Chang EB, Eren AM, Tay S. Droplet-based high-throughput cultivation for accurate screening of antibiotic resistant gut microbes. *Elife* 2020; **9** [PMID: 32553109 DOI: 10.7554/eLife.56998]

129 **Song C**, Lv J, Liu Y, Chen JG, Ge Z, Zhu J, Dai J, Du LB, Yu C, Guo Y, Bian Z, Yang L, Chen Y, Chen Z, Liu J, Jiang J, Zhu L, Zhai X, Jiang Y, Ma H, Jin G, Shen H, Li L, Hu Z; China Kadoorie Biobank Collaborative Group. Associations Between Hepatitis B Virus Infection and Risk of All Cancer Types. *JAMA Netw Open* 2019; **2**: e195718 [PMID: 31199446 DOI: 10.1001/jamanetworkopen.2019.5718]

130 **Arafa A**, Eshak ES, Abdel Rahman TA, Anwar MM. Hepatitis C virus infection and risk of pancreatic cancer: A meta-analysis. *Cancer Epidemiol* 2020; **65**: 101691 [PMID: 32088651 DOI: 10.1016/j.canep.2020.101691]

131 **Javadrashid D**, Baghbanzadeh A, Derakhshani A, Leone P, Silvestris N, Racanelli V, Solimando AG, Baradaran B. Pancreatic Cancer Signaling Pathways, Genetic Alterations, and Tumor Microenvironment: The Barriers Affecting the Method of Treatment. *Biomedicines* 2021; **9** [PMID: 33918146 DOI: 10.3390/biomedicines9040373]

World Journal of Gastrointestinal Oncology

Submit a Manuscript: https://www.f6publishing.com

World J Gastrointest Oncol 2023 May 15; 15(5): 731-756

DOI: 10.4251/wjgo.v15.i5.731

ISSN 1948-5204 (online)

REVIEW

Exosomes in metastasis of colorectal cancers: Friends or foes?

Zheng Wu, Ze-Xuan Fang, Yan-Yu Hou, Bing-Xuan Wu, Yu Deng, Hua-Tao Wu, Jing Liu

Specialty type: Oncology

Provenance and peer review: Invited article; Externally peer reviewed.

Peer-review model: Single blind

Peer-review report's scientific quality classification

Grade A (Excellent): 0
Grade B (Very good): 0
Grade C (Good): C, C
Grade D (Fair): 0
Grade E (Poor): 0

P-Reviewer: Mu Y, China; Zhang L, China

Received: December 7, 2022
Peer-review started: December 7, 2022
First decision: February 23, 2023
Revised: March 7, 2023
Accepted: April 4, 2023
Article in press: April 4, 2023
Published online: May 15, 2023

Zheng Wu, Ze-Xuan Fang, Yan-Yu Hou, Jing Liu, Guangdong Provincial Key Laboratory for Diagnosis and Treatment of Breast Cancer, Cancer Hospital of Shantou University Medical College, Shantou 515041, Guangdong Province, China

Bing-Xuan Wu, Yu Deng, Hua-Tao Wu, Department of General Surgery, The First Affiliated Hospital of Shantou University Medical College, Shantou 515041, Guangdong Province, China

Corresponding author: Jing Liu, MD, PhD, Academic Research, Associate Professor, Research Scientist, Senior Scientist, Guangdong Provincial Key Laboratory for Diagnosis and Treatment of Breast Cancer, Cancer Hospital of Shantou University Medical College, No. 22 Xinling Road, Shantou 515041, Guangdong Province, China. jliu12@stu.edu.cn

Abstract

Colorectal cancer (CRC), the third most common type of cancer worldwide, threaten human health and quality of life. With multidisciplinary, including surgery, chemotherapy and/or radiotherapy, patients with an early diagnosis of CRC can have a good prognosis. However, metastasis in CRC patients is the main risk factor causing cancer-related death. To elucidate the underlying molecular mechanisms of CRC metastasis is the difficult and research focus on the investigation of the CRC mechanism. On the other hand, the tumor microenvironment (TME) has been confirmed as having an essential role in the tumorigenesis and metastasis of malignancies, including CRCs. Among the different factors in the TME, exosomes as extracellular vesicles, function as bridges in the communication between cancer cells and different components of the TME to promote the progression and metastasis of CRC. MicroRNAs packaged in exosomes can be derived from different sources and transported into the TME to perform oncogenic or tumor-suppressor roles accordingly. This article focuses on CRC exosomes and illustrates their role in regulating the metastasis of CRC, especially through the packaging of miRNAs, to evoke exosomes as novel biomarkers for their impact on the metastasis of CRC progression.

Key Words: Exosome; Colorectal cancer; Metastasis; miRNA; Biomarker

Core Tip: Exosomes, the extracellular vesicles function as connectors in communication between cancer cells and different components of the tumor microenvironment (TME). The miRNAs packaged into exosomes were derived from different sources and transported into the TME, performing oncogenesis or tumor-suppressor roles.

Citation: Wu Z, Fang ZX, Hou YY, Wu BX, Deng Y, Wu HT, Liu J. Exosomes in metastasis of colorectal cancers: Friends or foes? *World J Gastrointest Oncol* 2023; 15(5): 731-756
URL: https://www.wjgnet.com/1948-5204/full/v15/i5/731.htm
DOI: https://dx.doi.org/10.4251/wjgo.v15.i5.731

INTRODUCTION

Colorectal cancer (CRC) is a common malignant tumor of the digestive system, which has a high incidence and mortality, accounting for 10% of all cancer incidences and 9.4% of deaths worldwide[1]. The major reason for the high mortality rate of patients with CRC is the high heterogeneity and metastasis. Tumor microenvironment (TME) provides the environment for the growing, developing and maturing processes of cancer cells, whose special structure and composition have a great influence on the growth and metastasis of malignancies, including CRC[2]. Therefore, the study of the CRC microenvironment enables us to have a deep understanding of the mechanism of tumorigenesis and metastasis of CRC and is of great significance for evoking novel therapeutic strategies for metastatic CRC.

Exosomes are extracellular vesicles (EVs) secreted by various cells, which are actively involved in biological growth and development, immune system response, anti-tumor activity, mediating tumor metastasis and other biochemical reactions *in vivo* and *in vitro*[3]. Exosomes originate from the endocytosis of cells and are released after a series of transport to form intralumenal vesicles (ILVs)[4]. It is confirmed that exosomes carry cargo, such as proteins and miRNAs, that promotes tumor initiation, metastasis, and therapeutic resistance of cancer cells through intercellular communication in TME[5]. In different types of exosome-loaded biomolecules, miRNA plays the main regulatory role in the expression of downstream genes. As one kind of non-coding single-stranded RNA molecule, miRNAs was proved to be involved in regulating the process of protein synthesis[6,7]. A large number of studies have shown that exosomal miRNAs are highly expressed in a variety of tumors, and since exosomal miRNAs can be isolated and detected from body fluids, the exosomal miRNAs may become novel markers for tumor diagnosis[8].

Exosomes, on the other hand, act as communication mediators, carrying contents that function not only between cancer cells, but also between cancer cells and stromal cells, which is one of the main mechanisms by which exosomes participates in tumor metastasis. In colon cancer cells, exosome miRNAs can play a regulatory role in the initiation and metastasis of colon cancer through different signaling pathways, such as WNT pathway[9] and transforming growth factor beta (TGF-β) pathway [10]. It also plays an essential role in regulating epithelial-mesenchymal transition (EMT) formation, extracellular matrix (ECM) remodeling and premetastatic niches (PMN) formation, which are vital for tumor metastasis. Therefore, this article focused on the investigation of miRNA in exosomes, comprehensively analyzed the function and mechanism of miRNA in CRC metastasis and its effects on ECM remodeling, EMT, angiogenesis and PMN formation during metastatic processes and described the application of miRNA in exosomes as the novel biomarkers for the diagnosis and treatment of metastatic CRC.

TME PLAYS AN ESSENTIAL ROLE IN THE METASTASIS OF CRC

The construction and function of TME

TME, a complex and constantly changing system as the "soil" of tumor cell growth and development, is mainly composed of ECM, stromal cells and immune cells, which can be divided into an immune microenvironment dominated by immune cells and the non-immune microenvironment dominated by stromal cells[5]. The former contains both innate and adaptive immune cells, such as macrophages/dendritic cells (DC) and T lymphocytes, mediating the immunosuppressive function. Among them, tumor-associated macrophages (TAMs) and regulatory T cells (Tregs) performed the main immunosuppressive role by helping the immune escape of tumor cells and promoting the malignant development of tumors. On the other hand, the non-immune microenvironment mainly including fibroblasts, stromal cells and endothelial cells, was also involved in the development of malignancies. Cancer-associated fibroblasts (CAFs) were found to release stromal cell-derived factors and pro-angiogenic factors to promote tumor cell growth and angiogenesis process, while vascular endothelial cells mainly mediate

tumor angiogenesis, jointly contributing to tumorigenesis and metastasis. Due to its complexity and heterogeneity with a close impact on tumor cells, TME has been widely studied in the field of cancer therapy[11].

Since the role of TME in cancer has been reported before, the effect of T lymphocyte migration in TME was the focus of the research on tumorigenesis. It is discovered that innate immune responses not only indirectly control the production of T lymphocytes, but also directly shape TME through the production of cytokines. The following section will demonstrate the solely different roles of innate immune response cells in TME, including macrophages, DC, neutrophils, natural killer cells (NK) and bone marrow-derived suppressor cells (MDSC), as well as the non-immune microenvironment.

The role of TME in mediating the metastasis of CRCs

Immune cells: Among all innate immune cells, there is no doubted that macrophages derived from monocytes play an indispensable role, which is the first activated by pathogens and subsequently evoking the immune activation state[12]. During the tumorigenesis and development processes, TAMs are classified into classical inflammatory "M1" and alternative immunosuppressive "M2" activation modes[13].

M1 macrophages have pro-inflammatory, immune-stimulating and anti-tumor properties, which produce interleukin (IL)-1β, IL-6 and tumor necrosis factor α (TNF-α), participating in immune stress of the body[14]. Nevertheless, in the colitis model, the proinflammatory effect of M1 TAMs inducing an inflammatory response, is a risk factor for CRC, indicating that the effect of M1 TAMs on CRC will be judged by the specific environment[15]. M2 macrophages, highly infiltrated in most types of cancers, have immunosuppressive and tumor-promoting properties[16-18]. In colitis models, Wang *et al*[19] discovered that the density of M1 and M2 TAMs changed in the inflammation-carcinoma sequence, and the total number of TAMs gradually increased along with tumor metastasis[19]. Cultured with M1 TAMs conditioned medium, CRC cells were found to accelerate pro-apoptotic morphological changes, while those in the M2 TAMs medium promoted cell proliferation and increased the expression of anti-apoptotic markers[20]. TME with increased IL-4 cytokines, enhanced the immunosuppressive effect of M2 TAMs, promoting tumor growth and progression as well as the increase of M2 TAMs[21]. Vascular endothelial growth factor (VEGF) was also secreted by M2 TAMs to promote tumor angiogenesis through conjunction with other cells in TME[22,23].

On the flip side, M2 TAMs was also found to be involved in remodeling ECM and promoting EMT, to accelerate the invasion and metastasis of CRC[24,25]. Afik *et al*[26] conducted transcriptome and proteomic analyses in TAM of CRC and found that they are enriched in molecular features related to ECM remodeling[26], especially the expression of matrix metalloproteinase (MMP)[27]. TGF-β was also contributed to enhancing ECM remodeling and the EMT process, which is produced by M2 TAMs[28]. Herbeuval *et al*[29] demonstrated the production of IL-10 by CRC cells, which was induced by TAM-derived IL-6 and recruited transcription factor, signal transducers and activators of transduction3 (STAT3)[29], while M2 TAMs could promote CRC immune evasion by secreting immunosuppressive cytokines, IL-10 and TGF-β, and suppress the activities of T lymphocytes[30]. These findings indicate the promoting role of M2 TAMs in TME to accelerate CRC progression and invasion.

DCs, key players in the innate immune system, have high antigen presentation, through recognizing, capturing, and presenting the antigens to T cells in lymphoid organs. In cancer, DCs are specifically referred to as tumor-infiltrating DCs, which often exhibit immune stimulatory phenotypes in TME, through secreting inflammatory cytokines and prime effector T cells[31]. Orsini *et al*[32] confirmed that the antigen presentation ability of DCs was impaired in CRC patients, suggesting the immune stimulatory capacity of DCs can be inhibited by CRC cells to promote the development of cancers[32], while removed from the such environment, the ability to process antigens to T cells of DCs will be regained[33]. It is found that immunosuppressive factors, such as VEGF, IL-10, and TGF-β secreted by cancer cells were involved in inhibiting DCs maturation and antigen presentation[34,35]. In CRC, myeloid DCs are the most common subtypes, which are increased in frequency at the leading edge of tumor invasion and associated with lymph node invasion[36]. Hsu *et al*[37] found the high expression of C-X-C motif chemokine ligand 1 (CXCL1) in DCs obtained from CRC patients, enhancing the migration and stemness of cancer cells[37]. Additionally, the composition and function of DCs can be influenced by the unique TME of different types of cancer, even in different subtypes within the same malignancies [38,39].

Neutrophils, the primary responders in acute inflammation, are the first line of defense against pathogens, by producing neutrophil extracellular traps (NETs) and engulfing invading microorganisms [40]. It is reported that NETs dissolved ECM through MMP8/9 protease and improved tumor invasion and angiogenesis by releasing VEGF[41,42]. The EMT process was also induced by NETs for tumor cells to break through the vascular wall and enter the circulatory system, thus promoting the immune escape of tumor cells[40,41]. As part of the innate immune response, tumor-associated neutrophils (TANs) are similarly classified into the tumor-suppressive N1 and tumor-promoting N2 phenotypes. N1 TANs are the main type in the early stage of tumorigenesis, performing anti-tumor function through secreting type I interferon and activating IL-18 from NKs, while N2 TANs increase during the tumor development gradually, promoting tumor progression through increasing the level of reactive oxygen species and inhibiting the function of T and NK cells[43]. Interestingly, in CRC, the production of TGF-β

in TME polarized TANs from N1 to N2 phenotype, contributing the immune evasion by activating TAN-secreted MMP-9 and inhibiting the proliferation of T cells[33,44].

In addition, other immune cells, such as MDSCs, NK and Tregs also have been reported to be involved in the occurrence, development and metastasis of CRC. The function of MDSCs in TME was confirmed as suppressing the immune by inhibiting T cells and innate immune regulation, as well as contributing to the formation of PMN, maintenance of tumor stemness and promotion of angiogenesis [45]. As non-specific innate immune cells, NKs performed cytotoxic effects through secreting killing mediators, such as perforin, NK cytotoxic factor, and TNF-α, thereby limiting the metastatic growth of tumor cells rather than the proliferation of primary tumor cells[46,47]. Enhancing NK cytotoxicity is speculated as a novel way to prevent cancer metastasis. Tregs, one of the important factors for maintaining immune tolerance, are effective mediators of immunosuppression, negatively correlated with the prognosis of patients with malignant tumors[48]. In CRC, the contradictory effects of Tregs were reported, which were related to TME status[49].

Stromal cells: CAFs are one of the most abundant stromal components in solid tumors, which play an important role in tumorigenesis, angiogenesis, metastasis and invasion, and chemotherapy resistance of malignancies[50]. Similar to TAMs, CAFs promote the metastasis of cancer cells through remodeling ECM and promoting EMT[51]. By secreting collagen, fibronectin and MMP, as well as increasing VEGF levels, CAFs reorganize ECM components and form a directional migration trajectory available to tumor cells[52,53]. Additionally, expression of the collagen cross-linking enzyme lysine oxidase-like 2 (LOXL2) in CAFs is, to a certain extent, associated with a high recurrence rate, poor overall and disease-free survival in patients with CRC, since CAFs stimulate the EMT process through LOXL2 elevation[54]. Moreover, CAFs also promote immune evasion by restraining T cell function and promoting the polarization of TAMs, which was also inhibited by the high levels of TGF-β present at the edge of tumor invasion, derived from CAFs mainly[44,55]. Zhang *et al*[56] revealed that CXCL8 secreted by CAFs attracts monocytes to TME of CRC and promotes the polarization of M2 TAMs, further promoting immune suppression[56].

Mesenchymal stem cells (MSCs) are a kind of pluripotent stem cells with self-renewal and multidirectional differentiation abilities, participating in tissue generation and repair in a variety of tissues. In many types of tumors, the cancer-associated MSCs are reprogrammed by tumors and have significant effects on the structure and function of TME through enhancing EMT and angiogenesis processes. What is noteworthy is that MSCs are the only one capable to produce large amounts of exosomes[57]. Utilizing secreting exosomes, MSCs transfer genes carried by cancer cells to other tissues and promote the formation of PMN, thus affecting the proliferation and metastasis of cancer cells[58]. However, the function of MSC-derived exosomes in cancers is controversial and needs further investigation[59].

ECM: Along with immune and stromal cells, ECM is also the important structural and biochemical support in TME, composed of a variety of extracellular proteins and macromolecules, participating in and controlling cell growth, migration, metabolism and other activities. It is found that ECM is mainly composed of collagen, non-collagen, elastin, and proteoglycans[60]. During tumor progression, the structure and function of ECM can be remodeled by the cells in TME, including immune and stromal cells[61]. Regarding cancer metastasis, the remodeling enzymes MMP-2/9 against collagenase in CRC was increased to degrade type IV collagen, resulting in the loss of ECM support and enhancement of tumor cell viability and aggressiveness[62,63]. The fibrotic response is another reason for biomechanical changes, like tumor sclerosis, which is mainly caused by the TGF-β-mediated activation of CAFs[64]. Stiffness in CRC, usually in collagen-rich regions, is associated with metastasis and the EMT process[65, 66].

As mentioned above, immune cells, stromal cells and ECM in TME all mediate the tumorigenesis, development and metastasis of types of cancer. During different processes, exosomes as bilayer vesicles containing complex RNA and proteins, have a non-negligible function in intercellular communication in the process of tumor metastasis. Uncovering the function and mechanism of exosomes will provide a new trend for anti-cancer research and benefit patients with CRC.

EXOSOMES INTERACTING BETWEEN CANCER AND TME

In recent years, exosomes, as a newly proposed concept, have attracted much interest in their role in tumor growth and metastasis. Numerous studies have shown that exosomes and their cargoes promote tumor cell genesis and metastasis through cell-to-cell communication in TMEs[5,67,68]. Under normal conditions, the individual cells and extracellular matrix of the body complement each other to form a healthy ecological niche[69,70]. When pre-metastasis niches are formed in the body, tumor stem cells begin to survive and proliferate, and induce other cells to participate in tumor formation and metastasis [71], so as to construct a TME suitable for tumor cell growth and propagation. It is confirmed that exosomes play an important role in this process. It can have large or small effects on different tumorigenic pathways in TME, including tumor dryness, angiogenesis, tumor metastasis and EMT formation[72]. In addition, other studies have shown that the trigger of tumor is not only caused by

sufficient gene mutations, but more by functional changes of different interacting mediators in TME[73, 74]. In view of the important role of exosomes in the occurrence, development and metastasis of cancer, we will elaborate on the origin, development, cargos and function of exosomes, as well as the role of cell-to-cell communication of exosomes in cancer.

The development and concept of exosomes

Exosomes, first discovered in sheep reticulocytes, were simply considered as cellular vesicles for excreting cellular wastes. Soon, the new intercellular communication mode represented has made outstanding contributions to the monitoring, diagnosis and treatment of diseases. Particularly, tumor-derived exosomes (TDEs), are the main focus of the research in cancers. Exosomes and/or their vectors have been reported as biomarkers, therapeutic targets and even vectors for anti-cancer drugs[75]. Therefore, understanding the formation and transport of exosomes and their relationship with the TME is of great significance for studying the function of exosomes in cancer.

Exosomes are EVs encapsulated by lipid bilayers with a diameter of 40-160 nm, originating from the endocytic pathway of cells[75]. The biogenesis of exosomes includes four processes, that is membrane invagination, endosome formation, endosome maturation, and multivesicle bodies (MVBs) release (Figure 1). First, the cell membrane invaginates and generates small vesicles by endocytosis, which contain cell surface proteins and soluble proteins related to the extracellular environment. Next, the vesicles fuse to form early endosomes (EEs), which share their contents and membrane composition through clathrin and vesicle protein pathways, which is the main reason for the diversity and heterogeneity of exosomes. At the same time, the trans-Golgi network and endoplasmic reticulum also contribute to the formation of EEs. Along with the acidification of the contents and the entry of some "cargoes", such as cytoplasmic miRNAs, enzyme molecules and heat shock proteins (HSP), EEs gradually become mature late endosomes, also known as cellular MVBs containing ILVs. Finally, MVBs fuse with the plasma membrane and release ILVs to form exosomes, while the rest part fused with lysosomes or autophagosomes for degradation[76,77].

The endosomal sorting complex required for transport (ESCRT) is essential for the classical pathways to facilitate the formation of ILVs, composed of four complexes, ESCRT-0, -I, -II and -III[78]. Among them, ESCRT-0 and –I is responsible for the recognition of ubiquitinated proteins, while the combination of ESCRT-I/II initiates the activation of ESCRT-III, which combined with the ESCRT-I/II complex, cleaved the plasma membrane and releases buds into the endosomes to form ILVs[79].

Interestingly, ESCRT-independent exosome was first found in melanoma, involving CD63, one tetraspanin in the lysosome/endosome-associated organelle melanosomes[80]. Recently, Wei *et al*[81] reported an ESCRT-independent exosome pathway and demonstrated Ras-related protein Rab-31 (RAB31), a small GTP-binding protein related to vesicle-mediated transport, drives ILVs formation *via* the Flotillin domain of flotillin proteins and recruited GTPase-activating protein to prevent the fusion of MVEs with lysosomes and suppress MVEs degradation, thereby enabling the secretion of ILVs as exosomes[81].

Meanwhile, lipids, as the basic construction of exosome formation, located in the inner membrane of cellular MVBs with high density, such as lysobisphosphatidic acid (LBPA), leads to the composition of ILVs and then the exosomes[82]. Programmed cell death 6 interacting protein (PDCD6IP), functioning within the ESCRT pathway in the abscission stage of cytokinesis, interacted with LBPA, promoting the internal germination of the MVB membrane[83]. It is found that exosomes can alter the lipid composition of target cells by transferring molecules to them, especially cholesterol and sphingolipids, and subsequently affect the cellular homeostasis of targets[84]. Since the ceramide-rich fraction of endosomes is highly sensitive to inward plasma membrane germination, loss of sphingomyelin and subsequent converter of sphingomyelin to ceramide results in inhibition of ILVs formation[85].

Exosomes have different functions in different physiological and pathological processes, according to their size, content, origin, contents and influence on recipient cells, which is called exosome heterogeneity. In the process of MVBs formation, it restricts the uneven invaginations of the membrane, resulting in different total contents of liquid and solid contained in the vesicles formed by MVBs, which may be the cause of the size and content heterogeneity of exosomes[86]. Proteomic analysis of breast cancer cells and their exosomes identified epithelioid or mesenchymal origin cells according to the enrichment degree of different proteins and nucleic acids in exosomes, which reflects the specific sorting mechanism in the formation of exosomes[87]. Exosome heterogeneity gives them unique characteristics based on different types of cells or tissues of their origin, including absorption by specific cells and tendency to certain organs, which also provides the possibility for the location and migration of cancer cell metastasis[87].

The function of cargos carried by exosomes in physiological and pathological situations

Exosomes, involved in diverse processes as communicators between cells, are dependent on the presence of a great of biologically vital "cargos" in them, such as proteins, mRNAs, non-coding RNAs (ncRNAs) and various metabolic enzymes, all of which are bioactive substances to determine the type and function of exosomes[86]. The proteins in exosomes can be divided into the following four types, according to the discrepant structure and function, that is membrane transport and fusion-related proteins, tetraspanins, MVBs-related proteins and other proteins involved in cell adhesion and skeleton

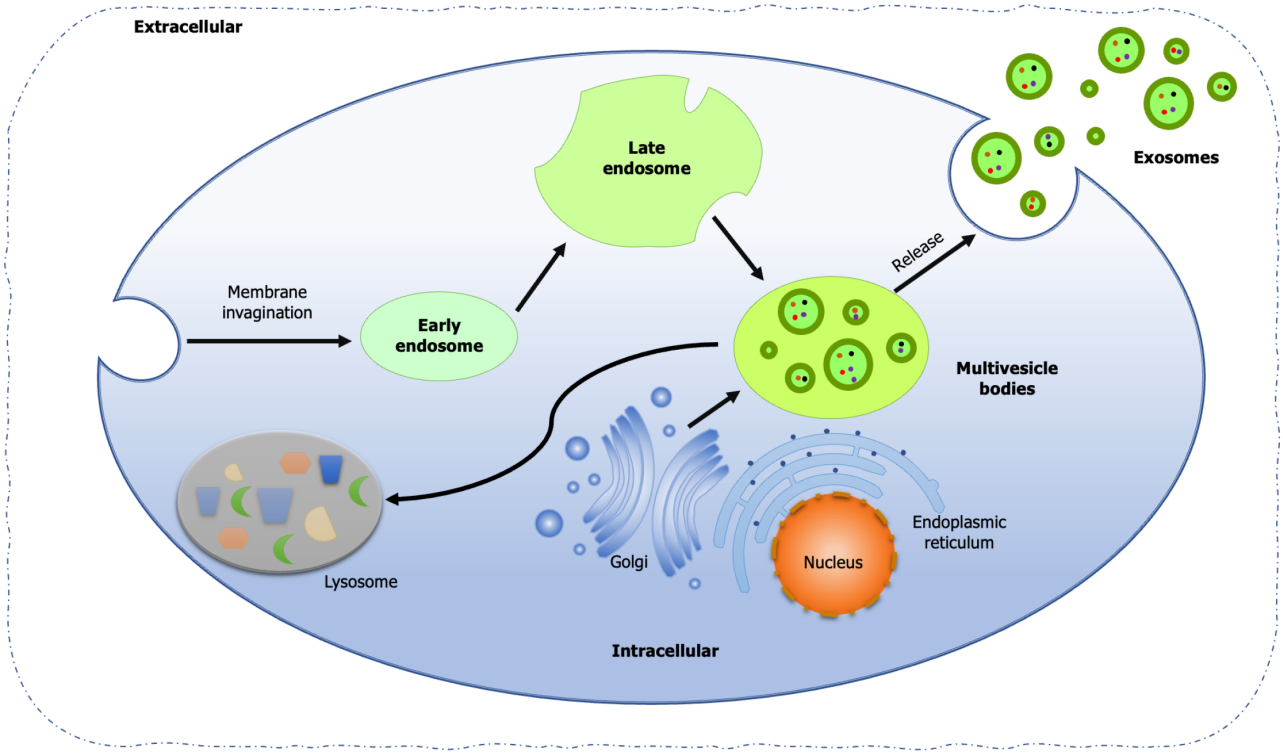

DOI: 10.4251/wjgo.v15.i5.731

Figure 1 The biogenesis of exosomes.

construction[88].

Membrane transport and fusion-related proteins include annexin, RAB and HSPs, which were involved in regulating plasma membrane fusion and release during exosome formation[89]. Among them, the regulating function of the RAB family is dependent on the surrounding environment and cell types. For example, Ostrowski *et al*[89] found that RAB27a and RAB27b control the exosome secretion pathway in different steps in cervical cancer[89], while in breast cancer, RAB7 was identified as the key regulator for exosome release in cancer cells[90]. However, in the central nervous system, the inhibition of RAB35 function leads to intracellular accumulation of endosomal vesicles and impairs exosome secretion in oligodendrocytes[91]. In the HSP family, HSP90 is a major intercellular chaperone protein, ensuring the normal folding and function of protein under normal conditions. However, in tumors, HSP90 plays the anti-apoptotic function by promoting abnormal protein folding, protein balance and proteolysis[92]. Lauwers *et al*[93] found that HSP90 is membrane-deformable to mediate the fusion of MVBs and plasma membranes and facilitate the exosome release[93], while exosomes lacking HSP90α, a key subtype of Hsp90, will lose important cell-to-cell communication from tumor cells to stromal cells to promote cell movement[94].

Tetraspanins are demonstrated to facilitate the entry of specific cargos into exosomes, including CD9, CD63, CD81, CD82, CD106, tetraspanin 8 (Tspan8), and intercellular adhesion molecules-1 (ICAM-1)[95]. PDCD6IP and TSG101 are the main MVBs-related proteins to regulate exosome formation in MVBs[96]. The analysis of exosomal protein composition displayed that a series of fusion and transfer proteins, as well as cytoskeletal proteins, such as actin, myosin, and tubulin, are non-specific and common in all exosomes[97]. Generally, the proteome of exosomes mirrors that of the protocell, but it is worth noting that the proteins in exosomes from cancer cells can selectively induce specific signals in the recipient cells, leading to the occurrence of carcinogenic changes[98,99].

Apart from proteins, ncRNAs referring to functional RNAs without encoding potential, also play an indispensable role in exosomes, including miRNAs, long ncRNAs (lncRNAs) and circular RNAs (circRNAs). Through binding to the 3' non-coding region of target mRNA, miRNA induced the inhibition of protein translation, involved in precise, fine and dynamic intercellular communication during human reproduction, pregnancy and embryonic development[6,7]. Molecular profiling indicated that miR-148a, let-7b, miR-148a, miR-375, and miR-99a associated with the expression of IL-10/13 in spermatogenic exosomes from multiple human donors are enriched, suggesting that exosomes may be involved in reproductive immunity through secreting miRNAs[100].

The analysis of tumor-related studies manifested that miRNA in exosomes is highly expressed during the development of lung cancer, prostate cancer and other cancers, therefore, it may be used as a potential biomarker or grading basis for cancer prognosis[101-103]. Moreover, miRNAs in exosomes can be isolated from body fluids and detected, which means that exosomal miRNAs have an advantage in

becoming novel biomarkers for non-invasive utilization *in vivo*[8]. Puik *et al*[104] use miRNA profiling to identify miR-21, miR-26, miR-122 and miR-150 as potential blood biomarkers for the non-invasive diagnosis of cholangiocarcinoma[104]. In addition to being used as diagnostic markers, exosomes can also be used as predictive therapeutic markers. Sun *et al*[105] found that in the exosomes secreted by CSCs and corresponding mother cells, six miRNAs including miR-1246, miR-424-5p, miR628-5p, miR-1290, miR-675-3p and miR-590-3p were up-regulated, whereas five miRNAs such as miR-224-5p, let-7b-5p, miR-615-3p, miR-122-5p and miR-5787 were the opposite, which suggest that miRNAs may contribute to the early diagnosis of gastric cancers and are expected to be a potential biomarker for predicting patients with a high risk of gastric cancer[105]. Furthermore, exosomal miR-222-3p can be used as a predictive biomarker of gemcitabine sensitivity, while miR-208a can be used as a predictive biomarker of radiation response[106,107].

LncRNA is a kind of ncRNA with a transcription length of more than 200 nucleotides, which plays essential roles in a series of life activities, such as dose compensation effect, epigenetic regulation, cell cycle regulation and cell differentiation regulation[108]. In cancer cells, lncRNA has the function of "cell messenger", which can be selectively packaged into exosomes to regulate tumor growth, metastasis and angiogenesis[109]. For example, Conigliaro *et al*[110] discovered that exosomes secreted by CD90 cells and CSCs can be taken up by human umbilical vein endothelial cells (HUVECs) and deliver lncRNA H19 to the corresponding target cells through adhesion to CD90 cells and HUVECs, and subsequently, synthesis and release of VEGF to stimulate angiogenesis[110].

CircRNAs are another main type of ncRNA in exosomes, as endogenous RNAs in all eukaryotic cells. Different from traditional linear RNAs containing 5' and 3' ends, circRNA molecules presenting as a closed ring structure is not affected by RNA exonuclease, so their expression is more stable and not easily degraded. This strong stability may enable non-invasive detection in body fluids, and the absence of the 5′ to 3′ polar structure and poly-adenosine tail makes it inherently resistant to nucleic acid degrading enzymes targeting the 5′ and 3′ ends[111]. Recently, circRNAs rich in miRNA binding sites, are reported to serve as the miRNA sponge in cells, which dissolves the inhibitory effect of miRNA on its target genes and increases the expression level of target genes, making circRNA as a competitive inhibitor of miRNA to regulate the translation and function of the downstream protein[112]. Through regulating target genes and miRNA, circRNA plays an important role in the proliferation, invasion, metastasis and progression of tumor cells in a variety of cancer biological processes. For example, circ-IARS expression in exosomes is up-regulated in the plasma of patients with in situ metastatic lung cancer, which, however, down-regulate the levels of miR-122 and tight junction protein 1 (TJP1) significantly but up-regulate the levels of RhoA and RhoA-GTP in exosome, thereby increasing the expression and adhesion of F-actin, enhancing endothelial permeability and promoting tumor invasion and metastasis[113], suggesting that the expression level of circRNA is highly correlated with clinicopathology and may serve as biomarkers with diagnostic, prognostic and predictive properties [111].

The intercellular communication of exosomes contributed to tumorigenesis and metastasis

The release of exosomes and uptake by recipient cells provides the basic mechanism of the intercellular communication function of exosomes, which is occurred in almost all types of cells in mammals[114]. After being released by cells, exosomes enter the blood, saliva, urine, cerebrospinal fluid, breast milk and other body fluids through autocrine and paracrine methods, after which reach other cells and tissues in the distance, producing a remote regulation effect. Interestingly, exosomes also influence the origin cell itself through the autocrine pathway based on specific receptors.

Within the exosome of chronic myeloid leukemia cells, cytokine TGF-β1 binds to its receptor and promotes tumor growth through an autocrine mechanism by activating anti-apoptotic pathways[115]. The exosomes were also involved in maintaining cellular homeostasis, through exosome secretion with harmful cytoplasmic DNA from cells[116]. The inhibition of exosomes will cause accumulated DNA in the cytoplasm, associated with increased reactive oxygen species-dependent DNA damage reaction, thus leading to cell cycle arrest or apoptosis. Therefore, cell secretion of such DNA-containing exosomes contributes to cell survival and homeostasis maintenance[116].

Through the paracrine pathway, exosomes mediate intercellular information transmission and microenvironment regulation, especially in the field of tumor therapy. Exosomes contain cargoes such as proteins, DNA, mRNA, ncRNA and metabolic enzymes described above, acting as external stimuli for recipient cells, triggering the uptake of exosomes and changing their biological phenotypes. The uptake of exosomes by recipient cells is not random but is accomplished through the recognition of exosome surface proteins that trigger interactions including endocytosis, receptor-ligand binding, and membrane fusion. Yang *et al*[117] found that breast cancer cells release and transfer exosomes containing programmed cell death ligand 1 (PD-L1) to other cancer cells with low or even no PD-L1 through the secretory pathway, to help cancer cells escape immune monitoring[117]. In CRC, Demory *et al*[118] reported that the transfer of mutant Kirsten rat sarcoma viral proto-oncogene (KRAS) to cancer cells with wild-type KRAS receptors *via* exosomes can promote the invasion of cancer cells[118].

In cancers, the intercellular communication of exosomes is not only limited between cancer cells but also occurred between cancer cells and stromal cells, which is one of the important mechanisms of distant metastasis of tumors. Shimoda *et al*[119] investigated the molecular mechanism of CAF-derived

tumor progression and demonstrated the metalloproteinase ADAM10 as the important factor in CAF-derived exosomes to enhance the viability of cancer cells through activating Notch receptor and increasing aldehyde dehydrogenase expression[119]. Moreover, the absorption of CAF-derived exosomes by cancer cells caused the increase of glycolysis and glutamine-dependent reductive carboxylation, which promotes the growth of tumors under nutrients deficiency or nutrient stress, as the carry of amino acids, lipids and intermediates in exosomes[120].

Conversely, exosomes from cancer cells also act on stromal cells, imbuing them with the properties to be transformed into cancer cells and inducing the formation of pro-TME. Cho *et al*[121] demonstrated that exosomes from breast cancer cells triggered the transformation of MSCs in fat into tumor-associated myoblasts *via* the TGF-β-mediated signaling pathway[121]. Also, miR-9 in exosomes derived from triple-negative breast cancer can induce EMT in tumor cells through down-regulating E-cadherin in fibroblasts, and promote the transformation of fibroblasts into CAFs, thus stimulating tumor migration [122]. The hallmark, angiogenesis in cancer was also promoted by TDEs promoting endothelial cell proliferation and angiogenesis[123]. Nazarenko *et al*[123] found the cell surface Tspan8 as the contributor to exosome-induced endothelial cell activation, in which Tspan8-α4 integrin in exosomes facilitates the binding and absorption of exosomes to endothelial cells and promotes angiogenesis accordingly[123]. Even under hypoxia conditions, the stimulating effect of exosomes on angiogenesis was enhanced in cancers[124]. Hsu *et al*[125] found that hypoxic lung cancer-secreted exosomes with miR-23a not only cause the accumulation of hypoxia-inducing factor-1α (HIF-1α) in endothelial cells but also target TJP1 to increase vascular permeability and cancer migration possibility[125].

Interestingly, mRNA delivery by exosomes to recipient cells is a rare case, while it was increased in those with acute inflammation (peritonitis) or chronic inflammation (subcutaneous tumors)[126]. Engineered exosomes have been found to conduct certain functions in inducing innate and adaptive immune responses in cancers[127]. The mechanism mainly involves the antigen presentation, activation of the intracellular cGAS-STING signaling pathway, intercellular miRNA transfer, and immunoregulation of exosome surface presenting molecules, which may be related to different contents wrapped in exosomes and their effects on the recipient cells[114].

First, the antigen-presenting peptides were direct presented by antigen-presenting cells (APCs), such as DCs or Tregs to specific T cells and induce activation of them *via* carrying exosomes containing co-stimulatory signals[114]. A single intradermal injection of APC-derived exosomes significantly induced tumor eradication and growth delay in the mouse model[114]. Simultaneously, exosomes secreted by human DCs promote the production of interferon (IFN) production and thus enhance antigen presentation, regardless of the maturation of the exosomal origin cells[128].

Then, the activation of the intracellular cGAS-STING signaling pathway was induced by genomic DNA in exosomes to generate an anti-tumor response[129]. The production of IFN was enhanced after the contact between DCs and T cells with the uptake of exosomes through the activated cGAS-STING signaling pathway[130]. Although the uptake of exosomal DNA by recipient cells may change their signaling, such alternations may be beneficial in the context of cancer[116], as the inhibition of epidermal growth factor receptor (EGFR) in cancer cells may lead to an increase in DNA in their secreted exosomes, helping to induce cGAS-STING signaling in DCs to inhibit tumor growth[131]. In contrast, the uptake of tumor-derived exosomal DNA by circulating neutrophils enhances the production of tissue factors and IL-8, which may indirectly worsen cancer by promoting inflammatory responses[132].

Next, in the process of cell-to-cell communication, exosomes influence signaling pathways and gene expression in recipient cells through miRNA transfer to regulate the immune response. Immature DCs have a strong ability to phagocytose antigen, but their weak ability to present antigen makes the activation of DCs to specific T cells limited. In addition, miR-212-3p in TDEs promoted the immune escape of cancer cells by suppressing transcription factor RFXAP in DCs[133]. However, miR-222-3p promoted the polarization of TAMs to M2 phenotype and generated an immunosuppressive microenvironment through a down-regulating suppressor of cytokine signaling 3 (SOCS3)[134].

Finally, immunomodulatory molecules such as PD-L1 and Fas cell surface death receptor ligand (FasL) on TDEs accelerate the failure and apoptosis of T cells, thus regulating the immune response and promoting the progression of tumors[135,136]. On the contrary, mast cell-derived exosomes with CD86, lymphocyte function-associated antigen 1, and ICAM-1 on their surface, induce the proliferation of B and T immune cells and enhance anti-tumor activities[137].

Despite how the cargoes carried in exosomes act and affect recipient cells have been extensively studied, the mechanism of how exosomes selectively package those cargoes remains unclear. Through comparing miRNA content in CRCs exosomes of mutant and wild-type KRAS, Cha *et al*[138] found that the exosomes of wild-type KRAS cancer cells were enriched with miR-10b, while the others were enriched with miR-100[138], suggesting that exosomes selectively pack the cargo under an unknown condition for further investigation.

THE MECHANISM OF THE METASTASIS OF CRC RESULTING FROM THE EXOSOMES BY MIRNA

As described above, miRNA, a vital ncRNA, is responsible for negatively regulating the expression of up to 60% of the protein-coding genes, and play important role in the processes of malignancies[139]. Since Michael *et al*[140] described the association between miRNAs and CRC, the involvement of miRNAs in the occurrence of CRC evoked plenty of investigation to explore the molecular mechanism of miRNA regulating CRC[140,141]. As the main content of exosomes, miRNAs are also involved in certain control and regulatory functions on tumor proliferation, EMT and ECM remodeling, and the formation of PMNs.

EMT promotes the metastasis of CRC through miRNAs

It is accepted that EMT is an important biological process in which epithelial cells become cells with mesenchymal phenotypic characteristics and acquire the ability to migrate[142]. During the EMT process, epithelial cells lose cell polarity and the ability to connect with the basement membrane, so that the genome of cancer cells can be transferred between cells through exosomes, thus gaining aggressive abilities of migration and invasion, anti-apoptosis and ECM degradation[143]. First, epithelial cell-associated proteins located in the primary tumor of CRC are down-regulated, while mesenchymal adhesion proteins are up-regulated, and cancer cells, especially with mesenchymal characteristics, secrete abundant exosomes to invade local tissues[144]. Next, the locally proliferating cancer cells break through the basement membrane and propagate through the circulatory system to distant organs through specific signaling mechanisms involving exosomal miRNAs. Finally, these mesenchymal cells reprogram the microenvironment of distant metastases, inducing the formation of metastatic TMEs and angiogenesis[145,146].

EMT-related transcription factors are confirmed as the key regulators during this process. Snail family transcriptional repressor (Snail1/2), belonging to the Zinc finger transcription factor, can destroy the normal tight junction between cells, while zinc finger E-box binding homeobox (ZEB1/2) can inhibit the expression of adhesion protein in epithelial cells and promote the initiation of EMT, all of which can be regulated by miRNAs. In cancers, the inhibition of EMT by p53 to prevent metastasis, down-regulated Snail and ZEB1 *via* induction of miR-34, which also suppresses the expression of the stemness factors, BMI1, CD44, CD133 and c-MYC. Interestingly, Siemens *et al*[147] reported a double-negative feedback loop between miR-34 and Snail, that is Snail and ZEB1 conversely inhibit the expression of miR-34 through binding to E-box regions in miR-34 promoters[147]. MiR-200 family members are another group involved in the regulation of ZEB1 by forming a double-negative feedback loop, to reduce the migration and invasion of CRC cells[148]. Also, miR-429, the member of the miR-200 family, was found to reverse TGF-β-induced EMT by targeting one cut homeobox 2 (ONECUT2), thereby inhibiting cell migration and invasion, and its activity is significantly down-regulated in CRC[149]. The downregulation of other tumor suppressor factors, mainly miR-335, miR-132 and miR-192, is associated with the invasion and metastasis of CRC by increasing the expression of their ZEB2 target genes[150-152].

Additionally, twist family basic helix-loop-helix (bHLH) transcription factor (TWIST), containing the bHLH domain, inhibits mesenchymal cell protein expression to promote the EMT process[153], which can be suppressed by miR-145[154]. Prospero homeobox 1, another transcription factor, inhibit the expression of E-cadherin to promote the occurrence of EMT, which was achieved by binding to the promoter of pre-miR-9 and triggering its expression[155]. The FOX family of transcription factors, FOXQ1 and FOXM1, are also involved in the induction of EMT, and their expressions are negatively correlated with the low expression of miR-320 in CRC, which reduces the expression of E-cadherin[156].

TGF-β, the acceptable EMT-inducer, can activate the EMT process by regulating downstream factors, such as miR-187, which inhibit the expression of SMAD family member 4 (SMAD4), the maintainer of epithelial phenotype in CRC[10]. Furthermore, miR-20a overexpression can also facilitate EMT by inhibiting SMAD4 expression to promote the metastasis of CRC[157]. Interestingly, SMAD7 is the inhibitor of SMAD4, and the inhibition of SMAD7 can initiate TGF-β-induced EMT. A series of miRNAs, like miR-4775, miR-1269, and miR21 have been approved to promote the metastasis of CRC in a SMAD7/TGF-β-dependent manner[158-160].

Regarding the Wnt/β-catenin signaling pathway, the enhanced effect of miR-150 on EMT in CRC is generated by targeting the cAMP response element-binding protein signaling pathway[9]. Interestingly, Wnt-induced EMT is not only through the Wnt/β-catenin signaling pathway, but also partially activated through inhibiting negative transcription factors by miR-34a, miR-145 and miR-29b[161,162]. The loss of miR-145 function is negatively correlated with the EMT process and the downregulation of E-cadherin expression[163], while miR-29b inhibits β-catenin co-activators to block multiple β-catenin target genes and achieve the regulation of EMT in CRC[164].

After breaking through the basement membrane, CRC cells enter the circulation turning into circulating tumor cells (CTCs), responding to distant metastasis, referring to EMT-MET plasticity with promoting new invasion and metastasis, the important marker of metastasis when this characteristic exists in CTCs[165]. Increased activity of MMP or decrease the function of tissue inhibitors of metallo-

proteinases (TIMPs) promote CTCs detachment from the primary location, which can be regulated by miR-375 to suppress MMP2 level in CRC cells and correspondingly inhibit the proliferation, migration and invasion of CRC[166]. Cai *et al*[167] revealed that miR-194 promoted EMT-mediated metastasis in CRC through activating MMP2 function, while Xu *et al*[168] found that miR-20a performed a facilitated role during the EMT process through inhibiting TIMP2, resulting in increased activities of MMP2 and MMP9[167,168].

PMN formation is an important step in CRC metastasis, involving exosomal miRNAs

As distant metastasis of CRC is a major reason for clinical treatment failure and death in cancer patients, PMN is found to be a crucial factor of CRC metastasis, which is the formation of a microenvironment conducive to tumor metastasis at a specific site in the distant organ[169,170]. Tumor secretory factors, recruitment of inhibitory immune cells and inflammatory polarization of matrix components are key factors involved in the formation of PMN[171].

TDEs are the main component of tumor secretory factors, secreted by cancer cells at the primary site of the tumor and transmitted to distant sites through autocrine or paracrine to recruit immune cells [171]. The recruited immune cells, such as MDSCs, TAMs, and Tregs, induce the formation of the immunosuppressive microenvironment and subsequently secrete inflammatory cytokines to produce an inflammatory response and form an inflammatory microenvironment, which is conducive to the colonization and growth of CTCs. During this process, the increased tumor volume with a continuous proliferation of CRC cells leads to cells prone to hypoxia and nutrient deficiency, hence rapid angiogenesis can be found in the primary lesion. The pro-angiogenic factors secreted by the neovascularization will circulate with TDEs to the distant metastasis, promote angiogenesis at distant sites, and construct a perfect PMN to bear more tumor cells from distant metastasis[171]. So Liu *et al*[171] proposed immunosuppression, inflammatory response, angiogenesis and increased permeability, lymphangiogenesis, organicity and reprogramming as the six characteristics of PMN, which make PMN the best choice for the settlement and proliferation of metastatic cancer cells[171].

Immunosuppression, an important contributor to the formation and development of PMN, is also the major reason for the survival and development of tumors *in vivo*. Takano *et al*[172] found that plasma-derived exosome miR-203 induced the differentiation of monocytes in distal organs into M2 TAMs of immunosuppressant phenotype, while Zhao *et al*[173] reported that exosomal miR-934 also induced the differentiation of normal phenotype M1 TAMs into M2 TAMs, inducing the formation of immunosuppressive microenvironment[172,173]. SOCS3 was down-regulated by miR-222-3p in TDEs, which promoted STAT3-mediated M2 polarization of TAMs and contributed to the immunosuppressive microenvironment[134]. Wang *et al*[174] also demonstrated the enhancing role of exosomal miR-425-5p and miR-25-3p on M2 TAMs expression through the PI3K/AKT signaling pathway, to promote CRC metastasis to distant metastases[174].

TDEs in CRC were also reported to be involved in promoting T cell differentiation into Tregs, inhibiting normal immune cell function, and recruiting immunosuppressive cells into PMN[175]. Other immune cells, such as MDSCs, DCs, and NKs can also be transformed into immunosuppressive phenotypes in TME, together constituting the immunosuppressive microenvironment for tumor metastasis[176]. In addition to recruiting immunosuppressive cells to PMN, the immune escape of tumors ultimately needs to be realized by destroying the normal immunity of the body[177]. Inhibition of T cell function, disturbance of normal NK cell function and immature reversal of DCs are all able to lead to the destruction of the normal immune mechanism of the body[133]. Huang *et al*[178] demonstrated that lncRNA SNHG10 in TDEs participated in the TGF-β signaling pathway, inhibited the activity of NK cells, and damaged the normal anti-tumor immune function in CRC[178].

It should be noted that the activation of immune checkpoints is an effective pathway for the development of immunosuppression. PD-L1 derived from TDEs with highly similar function to the surface of tumor cells, can bind to its receptor on T cells to generate an immune examination response, effectively inhibiting the proliferation of T cells and inducing apoptosis, and destroying the anti-tumor function of positive T cells[136,179]. In addition, CSCs-derived exosomal miRNA-17-5p inhibits normal immune cell function and promotes immunosuppression by targeting speckle-type POZ protein and promoting the expression of PD-L1[180].

During the formation of PMN, ECM remodeling is one of the essential links. In situ tumor cells colonize and proliferate in distant metastases, secreting exosomes and producing inflammatory cytokines, causing hypoxia and inflammatory responses in normal cells of metastases. In such an environment, a large number of cytokines such as VEGF, macrophage migration inhibitory factor, TGF-β, and immunosuppressive cells are recruited to participate in the formation of PMN[181]. Similar to the ECM remodeling mechanism in the primary site, CAFs activated by TGF-β promote the fibrosis of ECM through the secretion of collagen and fibronectin, increase the hardness of ECM, and change its biomechanics[182]. It is found that CRC-derived exosomal miR-10b promotes CAFs formation and leads to ECM fibronectin through the PI3K/Akt/mTOR pathway[183]. Exosomal miR-1246 and miR-1290 advance the development of interstitial fibrosis by activating the expression of actin alpha 2 and pro-fibrotic factors[184], while exosomal miR-139-5p and miR-21-5p degrade ECM proteins by promoting the expression of MMP2 and MMP13, thus accelerating the formation of PMN[185].

Interestingly, inflammation is not only involved in inhibiting the process of cancer but also found to promote tumor occurrence and metastasis. Inflammatory M1 TAMs, as a pro-inflammatory, immunostimulating and anti-tumor factor producing IL-1β, IL-6 and TNF-α, contributed to the development of CRC in colitis[15]. Therefore, the inflammatory microenvironment caused by chronic inflammation significantly promotes the formation of PMN in distant organs during tumor growth and metastasis [186]. Pro-inflammatory cytokines such as IL-1β, IL-6 and TNF-α are important factors in the inflammatory microenvironment, which directly or indirectly stimulate tumor survival, proliferation and metastasis[187]. It is shown that low-density IL-1β, an important pro-inflammatory factor involved in innate immunity, could induce local inflammatory responses and lead to protective immune responses, while high concentration would result in inflammation-related cancer tissue damage[188].

Another chemokine, IL-6 stimulates the activation of T and B cells during the immune response to perform an anti-inflammatory role[189]. Pucci *et al*[190] found that CRC tumor cell-derived exosomal miRNAs increase IL-6 secretion, thereby promoting inflammatory responses[190]. High levels of IL-6 have been detected in serum detected in live tumors or biopsies from cancer patients, suggesting that the inflammatory effects of this cytokine may be related to the occurrence of cancer[191]. MiR-21 carried by exosomes promotes the release of pro-inflammatory IL-6 and IL-21 and induces them into circulation, thus inducing the formation of an inflammatory microenvironment[192].

Although originally TNF-α was reported as an anti-tumor cytokine, high-dose recombinant TNF-α has been verified to induce tumor necrosis and promote the progression of tumors *in vivo*[193]. In addition, owing to the special biological environment of CRC, intestinal bacteria also promote the formation of an inflammatory microenvironment through secreting exosomes. The induction of E.coli-derived exosome with miRNAs on the inflammatory microenvironment is achieved by increasing the expression of toll-like receptor (TLR) and promoting the secretion of pro-inflammatory cytokine IL-8 [194]. The exosomal miR-149-3p derived from enterotoxin bacteria disrupts normal gene transcription and leads to DNA damage and oxidative stress, which promotes the formation of an inflammatory microenvironment[195]. Exosomal miRNA-21 and miRNA-29a promote CRC metastasis by acting on TLR7/TLR8 and inducing the formation of an inflammatory microenvironment in PMN[196].

Angiogenesis is another critical factor in PMN formation in CRC, which rapidly generates tumor cells providing oxygen, energy and nutrients for survival and metastasis in the case of hypoxia and nutrient deficiency. To form a suitable PMN for the metastasis of CRC, a variety of pro-angiogenic factors must reach the distal metastasis *via* exosomes through blood circulation and be expressed. VEGF, fibroblast growth factor, platelet-derived growth factor, basic fibroblast growth factor, TGF-β, TNF-α, and IL-8 are the main angiogenic stimulator carried by TDEs[197]. VEGF signaling pathway is the most promising target for angiogenesis and plays a key role in angiogenesis[198]. Equally important to these pro-angiogenic factors are cell- or plasma-derived exosomes from various human tumors identified as effective inducers of angiogenesis *in vitro* and *in vivo*, which have the function of inducing closely related to the miRNA carried in exosomes[199]. For instance, CRC-derived exosomal miR-21-5p improves the expression of VEGF and Cyclin D1, enhances vascular permeability and promotes angiogenesis[145]. Exosome miR-25-3p promotes the expression of VEGF receptor 2, and regulates tight junction protein Claudin-5, resulting in the production of PMN in the liver and other sites of CRC patients[200]. In addition, exosomal miRNA-92a-3p stimulates angiogenesis by increasing vascular endothelial cell division and participating in the regulation of the binding protein, Claudin-11[201]. Zhao *et al*[202] reported that CRC-derived exosome miR-1229 promoted metastasis of CRC by activating VEGF production and promoting angiogenesis[202]. Exosome-derived miRNA-183-5p accelerates the generation of neovascularization in CRC metastasis, whereas exosomes secreted by neovascularization in PMN promote the metastasis of tumor cells from the primary site to specific organs and tissues[143].

MECHANISMS AND INFLUENCING FACTORS OF DRUG RESISTANCE INDUCED BY EXOSOMES

It is worth mentioning that exosomes have the role of inducing tumor drug resistance, which provides a new research direction to solve the drug resistance problem that has puzzled doctors and researchers for a long time. Exosomes secreted by drug-resistant cancer cells encapsulate chemotherapeutic drugs and transport them out of tumor cells[203], and the interaction of exosomes containing miRNA, mRNA and protein from cancer cells is also associated with tumor drug resistance[204]. In summary, the mechanism of exosomes inducing drug resistance mainly involves drug expulsion, activation of anti-apoptotic pathways, changes in signal transduction, and promotion of survival and proliferation of CSCs.

First of all, exosomes released by tumor cells help cells to expel cytotoxic drugs, related to the overexpression of P-glycoprotein[205]. Although no reports on CRC, it is demonstrated that exosomes directly or indirectly regulate drug efflux pumps and thus influence drug resistance by regulating P-glycoprotein expression in breast and ovarian cancers[203,206]. Second, acquired or intrinsic resistance to chemotherapy often prevents tumor cells from undergoing adequate levels of apoptosis, resulting in poor survival and treatment[207]. Inhibitors of the apoptotic pathway are used to sensitize tumor cells

to chemotherapy. In the clinical treatment of CRC, cetuximab-resistant CRC cells RKO have been found to induce cetuximab resistance by down-regulating PTEN and increasing AKT phosphorylation, which is related to apoptosis escape[208]. Third, signaling pathways in drug-sensitive cells are altered by the uptake of drug-resistant cell-derived exosomes, including EGFR, Wnt/β-catenin, PI3K/AKT, PTEN, and mTORC signaling pathways that play important roles in tumor progression and drug resistance, whose abnormalities are associated with chemotherapy resistance[209,210]. Hu *et al*[211] reported that CRC cells secreted exosomes capable of inducing chemotherapy resistance, which caused drug resistance by promoting β-catenin stabilization and nuclear translocation and activating the Wnt/β-catenin pathway [211]. Furthermore, miR-30a, miR-222, or miR-100-5p carried by exosomes may induce drug resistance in drug-sensitive cells by regulating MAPK or mTOR pathways[212]. Lastly, exosomes induce drug resistance by promoting the growth and proliferation of CSCs[213]. Plenty of stromal cells, such as CAFs and MSCs, promote the growth of CSCs by secreting exosomes[214]. Exosomes derived from MSCs increase the proportion of CSCs by activating the Wnt signaling pathway and activating the 1/2 extracellular signal (ERK1/2), thus endowing CSCs with phenotypes, and inducing drug resistance in CRC[215].

Notably, CSC self-derived exosomes maintain stemness within TME by transporting their cargoes, thus enhancing resistance to different cancer therapies[216]. The cargos include Hedgehog, Wnt, β-catenin, and other CSC-specific mRNAs, as well as proteins needed by CSCs to maintain self-renewal and other stemness. TDEs have been reported to carry different types of integrins and related ligands that are involved in the formation of cancer cell colonization and PMN, while integrin is the key drug resistance factor in cancer therapy in maintaining the phenotype and behavior of stem cells[217].

CLINICAL PERSPECTIVES

CRC is a highly heterogeneous, highly metastatic and fatal cancer, and tumor cell metastasis is the main reason for the high mortality rate of this cancer. In the process of diagnosis and treatment of CRC, the lack of specific symptoms causes great difficulties in the early diagnosis of CRC due to its similarity to non-cancerous intestinal diseases. At present, the diagnosis of CRC depends on clinical evaluation and imaging diagnosis. However, routine diagnosis such as radiographic imaging or histopathological analysis fails to detect early systemic spread of CRC[218], and colon cancer markers such as carcinoembryonic antigen (CEA) and CA19-9 have low sensitivity and specificity[219]. In most clinical cases of CRC, surgery is the best treatment option, sometimes accompanied by chemoradiotherapy. However, due to limited diagnostic means, most patients are often diagnosed with advanced CRC and miss the optimal surgical opportunity. Therefore, the development of new and effective diagnostic biomarkers for CRC is essential for early detection and reduction of CRC mortality.

As EVs that play a key role in intercellular communication, exosomes contain proteins, miRNAs and other substances that are closely related to tumorigenesis, tumor cell survival, chemotherapy resistance and metastasis. Due to their non-invasive, high sensitivity and specificity, exosomes have advantages in being ideal biomarkers for early cancer screening and diagnosis at this stage[220]. In addition, some studies have shown that exosomal miRNAs can be used as drug carriers to transport drugs and participate in the immunotherapy of CRC[221]. Next, we describe the advantages of exosomes in CRC screening, diagnosis, treatment, and prognosis.

Exosomes as biomarkers for early screening, diagnosis, and prognosis of CRC

It is interesting and useful that exosomes can be detected by taking body fluids, such as blood, urine, saliva and cerebrospinal fluid for analysis, suggesting that exosomes could be an ideal non-invasive or less invasive biomarker for early cancer screening and diagnosis, with high specificity and sensitivity at an early stage[220]. Recently, transcriptomics research revealed that ncRNAs in exosomes are involved in different biological processes of CRC, and the high stability of exosome miRNAs in a variety of biological samples makes them an important candidate molecule for the discovery of new cancer biomarkers for CRC[222-224]. Wang *et al*[225] reported a group of six miRNAs including miR-21, let-7g, miR-31, miR-92a, miR-181b, and miR-203 as reliable biomarkers for CRC diagnosis, whose specificity and sensitivity exceed 40% compared to classical biomarkers, CEA and CA19-9[225], while the sensitivity of exosomes miR-1229, miR-223, miR-1224-5p and miR-150 are reach to 50%, whose expressions were significantly different between CRC patients and healthy individuals[226]. Increased serum levels of exosome miR-200 were significantly associated with CRC progression and liver metastasis[227]. Wang *et al*[158] confirmed that miR-125A-3p is highly expressed in the plasma of patients with early CRC but not in normal subjects, suggesting that miRNA in exosomes can be used as a biomarker for early CRC screening[158]. Moreover, compared with normal people, the expression of exosomal miR-92b is significantly decreased in CRC patients, indicating its higher accuracy in early CRC screening[228]. The expression of miR-23a and miR-1246 in exosomes was abundant in CRC patients. Decreased expression of exosome miRNA-23a and miRNA-1246 can be used as diagnostic markers for CRC in patients with primary resection[229]. In addition, circulating exosomal miR-17-5p and miR-92a-3p are associated with pathological staging and grading of CRC[230].

Apart from being biomarkers for CRC screening and diagnosis, exosomal miRNAs are also closely related to the prognosis of CRC and can be used as biomarkers for postoperative or therapeutic evaluation. Liu *et al*[231] found that low expression of plasma exosomal miR-4772-3p was closely associated with less lymph node metastasis, less tumor recurrence, and better prognosis in CRC patients [231]. Plasmid-derived exosome miRNA-193a is highly expressed in patients with middle and advanced CRC, suggesting that CRC patients have a longer survival time and a higher survival rate, since exosomal miR-193a could inhibit the mitosis and proliferation of tumor cells and induce cell apoptosis [232]. Peng *et al*[233] found that low expression of exosome miR-548-3c suggested poor prognosis, and its low expression in CRC liver metastases was positively correlated with angiogenesis and reduced overall survival rate[233].

Despite a large number of studies that have shown that exosomal miRNAs are potential biomarkers for a variety of cancers, their application in clinical biomarkers still faces many problems. Most current exosome miRNA studies have been limited to small patient cohorts or mice models, which means that miRNA levels in plasma exosomes vary widely in a single cohort and results are inconsistent across groups even when studying the same cancer type. Another common drawback is that the methods used to isolate exosomes from plasma are different from those used to extract miRNAs from exosomes. Studies lack common endogenous miRNA controls for quantifying exosome miRNAs. These problems affect the reliability of circulating exosome miRNAs as cancer biomarkers in clinical diagnosis or prognosis. Therefore, the techniques for isolating exosomes from body fluids and the methods for quantifying miRNAs or proteins also need to be further standardized.

In order to explore the potential of exosomes as novel biomarkers in clinical practice, the most important aspect is to optimize or standardize the measurement of exosomes. Nonetheless, to date, the isolation and purification of exosomes lacks a universally accepted gold standard. At present, the common method for exosome separation is ultra-centrifugation[234], which is controlled by different centrifugal forces and durations according to the density and size differences between exosomes and other components. However, the effectiveness of exosomes is limited due to many reasons such as excessive pressure, long time, high equipment requirements and the specificity of precipitation for separation during the centrifugation process[235]. Size exclusion chromatography is another common method for exosome separation[236], but owing to the high dilution degree of samples, this method cannot be used in applications requiring high concentration of exosomes. Additionally, quantitative reverse transcription polymerase chain reaction (qRT-PCR) is commonly used for the quantitative detection of exosome miRNAs[237], but this method is prone to produce false positive signals. Subsequently, researchers developed non-PCR miRNA quantitative spectroscopy based on proportional electrochemistry, local surface Plasma Resonance[238] and Surface-enhanced Raman spectroscopy[239, 240]. Yet, its application has been hampered by expensive instruments and complex operation. Currently, it is attempted to detect exosome miRNAs using fluorescence method have achieved varying degrees of success, and this method has been attached great importance by researchers due to its inherent advantages of simple instruments, high sensitivity, and high throughput screening[241]. The only fly in the ointment is that the complexity of biological systems makes it necessary to develop fluorescent systems with anti-interference for exosome miRNAs as diagnostic biomarkers. It is worth noting that environmental fluctuations caused by such experimental conditions can be offset by ratio fluorescence measurements by calculating the emission intensity ratio of two different wavelengths. In general, the isolation and measurement methods of exosome miRNAs are under constant research and innovation, and the increasingly mature technological conditions make it possible for exosome miRNAs to be used as novel biomarkers for cancer.

In fact, the key obstacle to exosome research to date has not been the separation of impurities from exosome samples, but rather the lack of information on the ratio of actual exosomes to exovesicles in the "exosomes" collected by experimental techniques. Since exosomes overlap with these cellular microvesicles in structure and characteristics[242,243], the reliability of the analysis can be ensured as long as the composition of exosomes in the extracted samples can be accurately determined. From the perspective of exosome drug development, the current drug approval system in most countries only requires a high proportion and quantification of exosomes to meet the requirements for quality control and safety assessment of cell-derived compounds[242]. Therefore, how to effectively quantify the individual components of exosomes in collected samples will facilitate the utilization and clinical application of exosomes in the future.

Exosomes as anticancer agents for the treatment of CRC

At present, the treatment of CRC mainly includes surgery, adjuvant chemotherapy, radiotherapy and immunotherapy. Exosomes can be used as drug carriers to transport drugs or directly transport miRNA small molecules to participate in CRC chemotherapy, radiotherapy and immunotherapy[221]. Zaharie *et al*[244] demonstrated that exosome miR-375 promoted tumor cell apoptosis and inhibited CRC proliferation, invasion and metastasis by participating in the Bcl-2 signaling pathway[244]. Similarly, exosomal miR-140-3p inhibits CRC proliferation, growth, and liver metastasis by involving the Bcl-2 and Bcl-9 pathways[245]. Yan *et al*[246] found that CRC patients with high expression of exosome miR-548c-5p capable to inhibit the proliferation, invasion and metastasis of CRC cells by enhancing the expression of HIF-1α, had a better prognosis, predicting miR-548c-5p as an indicator for prognostic

analysis[246]. In addition, Hu *et al*[247] demonstrated that exosome miR-214 inhibits CRC autophagy and promotes its sensitivity to radiotherapy[247].

Recently, due to the rapid development of therapeutic methods, targeted therapy has become an effective strategy for the treatment of CRC. Exosomes are natural nanoparticle biological carriers that have emerged as promising therapeutic tools for the delivery and transfer of drugs, miRNAs, small interfering RNAs (siRNA), short hairpin RNAs, and other compounds that remain stable in exosomes used to treat cancer and other diseases, based on their non-toxicity and non-immunogenicity[248]. As delivery carriers of natural drugs and functional RNA, exosomes have their natural advantages[249].

First, exosomes can be produced and absorbed, and are capable of stable delivery of therapeutic drugs, such as therapeutic miRNAs and proteins[250]. Currently, doxorubicin and paclitaxel have been used in targeted cancer therapy *via* exosomes with minimal immunogenicity and toxicity compared to liposome, metal and polymer nanomaterials[251-254]. Second, exosomes enhance endocytosis by targeting specific cells and tissues with specific proteins, thus promoting the transfer of their contents [255]. In animal tumor models, exosome-mediated chemotherapy is more effective than free agents. For example, the anti-mitotic chemotherapy drug paclitaxel can be ultrasound-loaded into exosomes and is 50 times more cytotoxic to drug-resistant cancer cells *in vitro* than free paclitaxel[256]. Also, it is found that exosomes coated with different chemotherapeutic drugs inhibit tumor growth when delivered to mice tumor tissues, but no equivalent side effects have been observed in free drugs[257]. Bioengineered exosomes have been used to deliver anticancer drugs and functional RNAs to cancer cells, including CSCs, in a cell-specific manner. Several strategies have been reported to improve the targeting specificity and tumor absorption of the exosome, for instance, transforming the exosome into lysosome-associated membrane protein 2b and tumor-targeting integrin to express target ligands[253]. Exosomes are surface modified through oligonucleotide binding, which could potentially alter not only cell function, but also transport between cells. Third, exosomes deliver therapeutic goods with better efficacy and fewer off-target effects than other biological carriers, such as liposomes, due to their small size, membrane-permeability, ease of crossing the blood-brain barrier, and faster penetration of tumor cells than liposomes[258]. Kim *et al*[256] found that macrophage-derived exosomes loaded with paclitaxel significantly increased cellular uptake of Lewis lung cancer cell line compared to paclitaxel-loaded liposomes[256,259].

Remarkably, exosome targeting of CSCs is a promising approach for the development of cancer therapy, as the growth of CSCs causes drug-sensitive cells to transform into drug-resistant cells, reducing the sensitivity of anti-cancer drug therapy. CSC signaling pathways such as Wnt, Notch, Hippo, Hedgehog, NF-κB and TGF-β are significant for maintaining a series of biological functions such as self-renewal, differentiation and tumorigenesis, which, therefore, is also the main way for exosome loaded inhibitors (miRNA or siRNA) to selectively target CSCs[213]. Previous studies have indicated that fibroblast-derived exosome with Wnt could induce dedifferentiation of tumor cells and thus increase chemotherapy resistance to CRC, suggesting that interference with the exosomal Wnt signaling pathway is helpful to improve chemotherapy sensitivity and treatment window[211]. Furthermore, specific producers of CSCs, such as CD44, CD24, CD133, and CD200 can also be used as exosome targets using bioengineering techniques[260]. Liu *et al*[261] manifested that exosomes designed to carry miR-21 inhibitors and chemotherapeutic agents enhance the killing effect on CRC tumor cells and inhibit CRC resistance[261]. RDEs carrying miR-3a improve immunosuppression and inhibit CRC proliferation and metastasis[262].

In addition to being a transport vehicle for targeted drugs, another promising clinical application area for exosomes is anti-cancer vaccination. Taking the DC exosome vaccine as an example, DC-derived exosomes express MHC-I and MHC-II molecules, which can effectively activate cytotoxic T cells and induce anti-tumor immunity. Currently, DC-derived exosome vaccines have been tested in phase I clinical trials[263,264]. The results showed that no grade 2 or higher toxicity was observed in these clinical trials, proving that exosome administration is safe. In one of the Phase I trials, exosomes were isolated from the ascites of colon cancer patients and injected into the patients as a vaccine. Ascites-derived exosomes were found to be safe, well tolerated, and capable of producing tumor-specific antitumor cytotoxic T cell responses after the granulocyte-macrophage colony-stimulating factor use in the immunotherapy of CRC[265]. However, the safety of TDE vaccines remains uncertain because TDEs carry a large number of oncogenes, mRNAs, and miRNAs that induce tumor progression and metastasis.

Though a large number of experimental models support the use of exosomes in cancer therapy, only a few clinical trials are in progress, thus the clinical use of exosomes in cancer and other diseases still needs to solve many challenges. First, how to effectively load exogenous therapeutic miRNAs or therapeutic agents into exosomes and enhance cell-specific delivery. Second, how to prevent autoimmune reactions when using non-autologous exosomes carrying MHC-I or II, and how to control the degree of cytotoxic T cell activation in vaccine use. Furthermore, how to prolong the half-life of bioengineered exosomes *in vivo* to avoid the rapid clearance of immune cells, liver or kidney, *etc.* Finally, it remains to be seen whether exosomes can overcome the digestive effects of the gut and be used as oral agents to treat cancer. Therefore, before the widespread use of exosomes in clinical trials, the quality standards of exosomes should be carefully established to improve their efficacy *in vivo*.

CONCLUSION

To sum up, exosomes have been successfully used as drug carriers in clinical therapy, and their safety and clinical application in targeted therapy and so on still need further exploration and research. In this review, the mechanism of exosomes in CRC metastasis was comprehensively described, including the formation and influencing factors of TME, the formation, function and role of exosomes in cancer, as well as the role of exosome miRNAs in the process of CRC metastasis. In TME, exosomes secreted by tumor-derived immune cells such as TAMs, DCs, MDSCs and NKs are critical for tumor growth and metastasis. In addition, stromal cells such as CAFs and MSCs as well as the ECM also play a significant role in tumor metastasis. Exosomes, as EVs carrying biological cargos, exert their function in primary tumors and metastases mainly of intercellular communication. In exosomes, DNA, mRNA, ncRNA and protein have different biological meanings and participate in the regulation of the body together. The role of exosome miRNA in early screening, diagnosis and prognosis of CRC, as well as in the treatment strategies for CRC along with chemotherapy, radiotherapy, immunotherapy and targeted therapy, provides a promising way for preventing and treating the metastasis in patients with CRC.

FOOTNOTES

Author contributions: Wu Z contributed to this work; Fang ZX, Hou YY, Wu BX and Deng Y participated in the writing of the manuscript; Wu HT and Liu J reviewed the manuscript and contacted the journals; All authors have read and approve the final manuscript.

Supported by National Natural Science Foundation of China, No. 82273457; Natural Science Foundation of Guangdong Province, No. 2021A1515012180 and 2016A030312008; Special Grant for Key Area Programs of Guangdong Department of Education, No. 2021ZDZX2040; and Science and Technology Special Project of Guangdong Province, No. 210715216902829.

Conflict-of-interest statement: All the authors report no relevant conflicts of interest for this article.

Country/Territory of origin: China

ORCID number: Zheng Wu 0000-0002-1393-7586; Ze-Xuan Fang 0000-0002-6100-9012; Yan-Yu Hou 0000-0002-4249-8770; Bing-Xuan Wu 0000-0002-1212-7936; Yu Deng 0000-0002-0950-6169; Hua-Tao Wu 0000-0002-1640-6094; Jing Liu 0000-0002-7483-4572.

S-Editor: Fan JR
L-Editor: A
P-Editor: Zhang XD

REFERENCES

1 **Xi Y**, Xu P. Global colorectal cancer burden in 2020 and projections to 2040. *Transl Oncol* 2021; **14**: 101174 [PMID: 34243011 DOI: 10.1016/j.tranon.2021.101174]
2 **Chen H**, Yao J, Bao R, Dong Y, Zhang T, Du Y, Wang G, Ni D, Xun Z, Niu X, Ye Y, Li HB. Cross-talk of four types of RNA modification writers defines tumor microenvironment and pharmacogenomic landscape in colorectal cancer. *Mol Cancer* 2021; **20**: 29 [PMID: 33557837 DOI: 10.1186/s12943-021-01322-w]
3 **Xu Z**, Zeng S, Gong Z, Yan Y. Exosome-based immunotherapy: a promising approach for cancer treatment. *Mol Cancer* 2020; **19**: 160 [PMID: 33183286 DOI: 10.1186/s12943-020-01278-3]
4 **Kahroba H**, Hejazi MS, Samadi N. Exosomes: from carcinogenesis and metastasis to diagnosis and treatment of gastric cancer. *Cell Mol Life Sci* 2019; **76**: 1747-1758 [PMID: 30734835 DOI: 10.1007/s00018-019-03035-2]
5 **Quail DF**, Joyce JA. Microenvironmental regulation of tumor progression and metastasis. *Nat Med* 2013; **19**: 1423-1437 [PMID: 24202395 DOI: 10.1038/nm.3394]
6 **Yang F**, Ning Z, Ma L, Liu W, Shao C, Shu Y, Shen H. Exosomal miRNAs and miRNA dysregulation in cancer-associated fibroblasts. *Mol Cancer* 2017; **16**: 148 [PMID: 28851377 DOI: 10.1186/s12943-017-0718-4]
7 **Treiber T**, Treiber N, Meister G. Regulation of microRNA biogenesis and its crosstalk with other cellular pathways. *Nat Rev Mol Cell Biol* 2019; **20**: 5-20 [PMID: 30228348 DOI: 10.1038/s41580-018-0059-1]
8 **Nedaeinia R**, Manian M, Jazayeri MH, Ranjbar M, Salehi R, Sharifi M, Mohaghegh F, Goli M, Jahednia SH, Avan A, Ghayour-Mobarhan M. Circulating exosomes and exosomal microRNAs as biomarkers in gastrointestinal cancer. *Cancer*

Gene Ther 2017; **24**: 48-56 [PMID: 27982021 DOI: 10.1038/cgt.2016.77]
9 **Guo YH**, Wang LQ, Li B, Xu H, Yang JH, Zheng LS, Yu P, Zhou AD, Zhang Y, Xie SJ, Liang ZR, Zhang CM, Zhou H, Qu LH. Wnt/β-catenin pathway transactivates microRNA-150 that promotes EMT of colorectal cancer cells by suppressing CREB signaling. *Oncotarget* 2016; **7**: 42513-42526 [PMID: 27285761 DOI: 10.18632/oncotarget.9893]
10 **Zhang F**, Luo Y, Shao Z, Xu L, Liu X, Niu Y, Shi J, Sun X, Liu Y, Ding Y, Zhao L. MicroRNA-187, a downstream effector of TGFβ pathway, suppresses Smad-mediated epithelial-mesenchymal transition in colorectal cancer. *Cancer Lett* 2016; **373**: 203-213 [PMID: 26820227 DOI: 10.1016/j.canlet.2016.01.037]
11 **Wang M**, Zhao J, Zhang L, Wei F, Lian Y, Wu Y, Gong Z, Zhang S, Zhou J, Cao K, Li X, Xiong W, Li G, Zeng Z, Guo C. Role of tumor microenvironment in tumorigenesis. *J Cancer* 2017; **8**: 761-773 [PMID: 28382138 DOI: 10.7150/jca.17648]
12 **Chen H**, Shi R, Luo B, Yang X, Qiu L, Xiong J, Jiang M, Liu Y, Zhang Z, Wu Y. Macrophage peroxisome proliferator-activated receptor γ deficiency delays skin wound healing through impairing apoptotic cell clearance in mice. *Cell Death Dis* 2015; **6**: e1597 [PMID: 25590807 DOI: 10.1038/cddis.2014.544]
13 **Yang L**, Zhang Y. Tumor-associated macrophages: from basic research to clinical application. *J Hematol Oncol* 2017; **10**: 58 [PMID: 28241846 DOI: 10.1186/s13045-017-0430-2]
14 **Grivennikov SI**. Inflammation and colorectal cancer: colitis-associated neoplasia. *Semin Immunopathol* 2013; **35**: 229-244 [PMID: 23161445 DOI: 10.1007/s00281-012-0352-6]
15 **Zhu W**, Yu J, Nie Y, Shi X, Liu Y, Li F, Zhang XL. Disequilibrium of M1 and M2 macrophages correlates with the development of experimental inflammatory bowel diseases. *Immunol Invest* 2014; **43**: 638-652 [PMID: 24921428 DOI: 10.3109/08820139.2014.909456]
16 **Cardoso AP**, Pinto ML, Pinto AT, Oliveira MI, Pinto MT, Gonçalves R, Relvas JB, Figueiredo C, Seruca R, Mantovani A, Mareel M, Barbosa MA, Oliveira MJ. Macrophages stimulate gastric and colorectal cancer invasion through EGFR Y(1086), c-Src, Erk1/2 and Akt phosphorylation and smallGTPase activity. *Oncogene* 2014; **33**: 2123-2133 [PMID: 23644655 DOI: 10.1038/onc.2013.154]
17 **Wang N**, Liu W, Zheng Y, Wang S, Yang B, Li M, Song J, Zhang F, Zhang X, Wang Q, Wang Z. CXCL1 derived from tumor-associated macrophages promotes breast cancer metastasis *via* activating NF-κB/SOX4 signaling. *Cell Death Dis* 2018; **9**: 880 [PMID: 30158589 DOI: 10.1038/s41419-018-0876-3]
18 **Zhao X**, Qu J, Sun Y, Wang J, Liu X, Wang F, Zhang H, Wang W, Ma X, Gao X, Zhang S. Prognostic significance of tumor-associated macrophages in breast cancer: a meta-analysis of the literature. *Oncotarget* 2017; **8**: 30576-30586 [PMID: 28427165 DOI: 10.18632/oncotarget.15736]
19 **Wang W**, Li X, Zheng D, Zhang D, Peng X, Zhang X, Ai F, Wang X, Ma J, Xiong W, Li G, Zhou Y, Shen S. Dynamic changes and functions of macrophages and M1/M2 subpopulations during ulcerative colitis-associated carcinogenesis in an AOM/DSS mouse model. *Mol Med Rep* 2015; **11**: 2397-2406 [PMID: 25434400 DOI: 10.3892/mmr.2014.3018]
20 **Lee YS**, Song SJ, Hong HK, Oh BY, Lee WY, Cho YB. The FBW7-MCL-1 axis is key in M1 and M2 macrophage-related colon cancer cell progression: validating the immunotherapeutic value of targeting PI3Kγ. *Exp Mol Med* 2020; **52**: 815-831 [PMID: 32444799 DOI: 10.1038/s12276-020-0436-7]
21 **Kim J**, Bae JS. Tumor-Associated Macrophages and Neutrophils in Tumor Microenvironment. *Mediators Inflamm* 2016; **2016**: 6058147 [PMID: 26966341 DOI: 10.1155/2016/6058147]
22 **Barbera-Guillem E**, Nyhus JK, Wolford CC, Friece CR, Sampsel JW. Vascular endothelial growth factor secretion by tumor-infiltrating macrophages essentially supports tumor angiogenesis, and IgG immune complexes potentiate the process. *Cancer Res* 2002; **62**: 7042-7049 [PMID: 12460925]
23 **Suarez-Lopez L**, Sriram G, Kong YW, Morandell S, Merrick KA, Hernandez Y, Haigis KM, Yaffe MB. MK2 contributes to tumor progression by promoting M2 macrophage polarization and tumor angiogenesis. *Proc Natl Acad Sci U S A* 2018; **115**: E4236-E4244 [PMID: 29666270 DOI: 10.1073/pnas.1722020115]
24 **Wyckoff J**, Wang W, Lin EY, Wang Y, Pixley F, Stanley ER, Graf T, Pollard JW, Segall J, Condeelis J. A paracrine loop between tumor cells and macrophages is required for tumor cell migration in mammary tumors. *Cancer Res* 2004; **64**: 7022-7029 [PMID: 15466195 DOI: 10.1158/0008-5472.CAN-04-1449]
25 **Wei C**, Yang C, Wang S, Shi D, Zhang C, Lin X, Liu Q, Dou R, Xiong B. Crosstalk between cancer cells and tumor associated macrophages is required for mesenchymal circulating tumor cell-mediated colorectal cancer metastasis. *Mol Cancer* 2019; **18**: 64 [PMID: 30927925 DOI: 10.1186/s12943-019-0976-4]
26 **Afik R**, Zigmond E, Vugman M, Klepfish M, Shimshoni E, Pasmanik-Chor M, Shenoy A, Bassat E, Halpern Z, Geiger T, Sagi I, Varol C. Tumor macrophages are pivotal constructors of tumor collagenous matrix. *J Exp Med* 2016; **213**: 2315-2331 [PMID: 27697834 DOI: 10.1084/jem.20151193]
27 **Illemann M**, Bird N, Majeed A, Sehested M, Laerum OD, Lund LR, Danø K, Nielsen BS. MMP-9 is differentially expressed in primary human colorectal adenocarcinomas and their metastases. *Mol Cancer Res* 2006; **4**: 293-302 [PMID: 16687484 DOI: 10.1158/1541-7786.MCR-06-0003]
28 **Cai J**, Xia L, Li J, Ni S, Song H, Wu X. Tumor-Associated Macrophages Derived TGF-β–Induced Epithelial to Mesenchymal Transition in Colorectal Cancer Cells through Smad2,3-4/Snail Signaling Pathway. *Cancer Res Treat* 2019; **51**: 252-266 [PMID: 29690747 DOI: 10.4143/crt.2017.613]
29 **Herbeuval JP**, Lelievre E, Lambert C, Dy M, Genin C. Recruitment of STAT3 for production of IL-10 by colon carcinoma cells induced by macrophage-derived IL-6. *J Immunol* 2004; **172**: 4630-4636 [PMID: 15034082 DOI: 10.4049/jimmunol.172.7.4630]
30 **Lewis CE**, Pollard JW. Distinct role of macrophages in different tumor microenvironments. *Cancer Res* 2006; **66**: 605-612 [PMID: 16423985 DOI: 10.1158/0008-5472.CAN-05-4005]
31 **Sumpter TL**, Dangi A, Matta BM, Huang C, Stolz DB, Vodovotz Y, Thomson AW, Gandhi CR. Hepatic stellate cells undermine the allostimulatory function of liver myeloid dendritic cells *via* STAT3-dependent induction of IDO. *J Immunol* 2012; **189**: 3848-3858 [PMID: 22962681 DOI: 10.4049/jimmunol.1200819]
32 **Orsini G**, Legitimo A, Failli A, Ferrari P, Nicolini A, Spisni R, Miccoli P, Consolini R. Defective generation and maturation of dendritic cells from monocytes in colorectal cancer patients during the course of disease. *Int J Mol Sci* 2013;

14: 22022-22041 [PMID: 24213603 DOI: 10.3390/ijms141122022]

33 **Fridlender ZG**, Sun J, Kim S, Kapoor V, Cheng G, Ling L, Worthen GS, Albelda SM. Polarization of tumor-associated neutrophil phenotype by TGF-beta: "N1" versus "N2" TAN. *Cancer Cell* 2009; **16**: 183-194 [PMID: 19732719 DOI: 10.1016/j.ccr.2009.06.017]

34 **Motta JM**, Rumjanek VM. Sensitivity of Dendritic Cells to Microenvironment Signals. *J Immunol Res* 2016; **2016**: 4753607 [PMID: 27088097 DOI: 10.1155/2016/4753607]

35 **Kobie JJ**, Wu RS, Kurt RA, Lou S, Adelman MK, Whitesell LJ, Ramanathapuram LV, Arteaga CL, Akporiaye ET. Transforming growth factor beta inhibits the antigen-presenting functions and antitumor activity of dendritic cell vaccines. *Cancer Res* 2003; **63**: 1860-1864 [PMID: 12702574]

36 **Pryczynicz A**, Cepowicz D, Zaręba K, Gryko M, Hołody-Zaręba J, Kędra B, Kemona A, Guzińska-Ustymowicz K. Dysfunctions in the Mature Dendritic Cells Are Associated with the Presence of Metastases of Colorectal Cancer in the Surrounding Lymph Nodes. *Gastroenterol Res Pract* 2016; **2016**: 2405437 [PMID: 26839537 DOI: 10.1155/2016/2405437]

37 **Hsu YL**, Chen YJ, Chang WA, Jian SF, Fan HL, Wang JY, Kuo PL. Interaction between Tumor-Associated Dendritic Cells and Colon Cancer Cells Contributes to Tumor Progression *via* CXCL1. *Int J Mol Sci* 2018; **19** [PMID: 30115896 DOI: 10.3390/ijms19082427]

38 **Chaput N**, Conforti R, Viaud S, Spatz A, Zitvogel L. The Janus face of dendritic cells in cancer. *Oncogene* 2008; **27**: 5920-5931 [PMID: 18836473 DOI: 10.1038/onc.2008.270]

39 **Michea P**, Noël F, Zakine E, Czerwinska U, Sirven P, Abouzid O, Goudot C, Scholer-Dahirel A, Vincent-Salomon A, Reyal F, Amigorena S, Guillot-Delost M, Segura E, Soumelis V. Adjustment of dendritic cells to the breast-cancer microenvironment is subset specific. *Nat Immunol* 2018; **19**: 885-897 [PMID: 30013147 DOI: 10.1038/s41590-018-0145-8]

40 **Uribe-Querol E**, Rosales C. Neutrophils in Cancer: Two Sides of the Same Coin. *J Immunol Res* 2015; **2015**: 983698 [PMID: 26819959 DOI: 10.1155/2015/983698]

41 **Chen Q**, Zhang L, Li X, Zhuo W. Neutrophil Extracellular Traps in Tumor Metastasis: Pathological Functions and Clinical Applications. *Cancers (Basel)* 2021; **13** [PMID: 34204148 DOI: 10.3390/cancers13112832]

42 **Schauer C**, Janko C, Munoz LE, Zhao Y, Kienhöfer D, Frey B, Lell M, Manger B, Rech J, Naschberger E, Holmdahl R, Krenn V, Harrer T, Jeremic I, Bilyy R, Schett G, Hoffmann M, Herrmann M. Aggregated neutrophil extracellular traps limit inflammation by degrading cytokines and chemokines. *Nat Med* 2014; **20**: 511-517 [PMID: 24784231 DOI: 10.1038/nm.3547]

43 **Zhou J**, Nefedova Y, Lei A, Gabrilovich D. Neutrophils and PMN-MDSC: Their biological role and interaction with stromal cells. *Semin Immunol* 2018; **35**: 19-28 [PMID: 29254756 DOI: 10.1016/j.smim.2017.12.004]

44 **Germann M**, Zangger N, Sauvain MO, Sempoux C, Bowler AD, Wirapati P, Kandalaft LE, Delorenzi M, Tejpar S, Coukos G, Radtke F. Neutrophils suppress tumor-infiltrating T cells in colon cancer *via* matrix metalloproteinase-mediated activation of TGFβ. *EMBO Mol Med* 2020; **12**: e10681 [PMID: 31793740 DOI: 10.15252/emmm.201910681]

45 **Condamine T**, Dominguez GA, Youn JI, Kossenkov AV, Mony S, Alicea-Torres K, Tcyganov E, Hashimoto A, Nefedova Y, Lin C, Partlova S, Garfall A, Vogl DT, Xu X, Knight SC, Malietzis G, Lee GH, Eruslanov E, Albelda SM, Wang X, Mehta JL, Bewtra M, Rustgi A, Hockstein N, Witt R, Masters G, Nam B, Smirnov D, Sepulveda MA, Gabrilovich DI. Lectin-type oxidized LDL receptor-1 distinguishes population of human polymorphonuclear myeloid-derived suppressor cells in cancer patients. *Sci Immunol* 2016; **1** [PMID: 28417112 DOI: 10.1126/sciimmunol.aaf8943]

46 **Glasner A**, Levi A, Enk J, Isaacson B, Viukov S, Orlanski S, Scope A, Neuman T, Enk CD, Hanna JH, Sexl V, Jonjic S, Seliger B, Zitvogel L, Mandelboim O. NKp46 Receptor-Mediated Interferon-γ Production by Natural Killer Cells Increases Fibronectin 1 to Alter Tumor Architecture and Control Metastasis. *Immunity* 2018; **48**: 396-398 [PMID: 29466761 DOI: 10.1016/j.immuni.2018.01.010]

47 **Eyles J**, Puaux AL, Wang X, Toh B, Prakash C, Hong M, Tan TG, Zheng L, Ong LC, Jin Y, Kato M, Prévost-Blondel A, Chow P, Yang H, Abastado JP. Tumor cells disseminate early, but immunosurveillance limits metastatic outgrowth, in a mouse model of melanoma. *J Clin Invest* 2010; **120**: 2030-2039 [PMID: 20501944 DOI: 10.1172/JCI42002]

48 **Olguín JE**, Medina-Andrade I, Rodríguez T, Rodríguez-Sosa M, Terrazas LI. Relevance of Regulatory T Cells during Colorectal Cancer Development. *Cancers (Basel)* 2020; **12** [PMID: 32674255 DOI: 10.3390/cancers12071888]

49 **Saito T**, Nishikawa H, Wada H, Nagano Y, Sugiyama D, Atarashi K, Maeda Y, Hamaguchi M, Ohkura N, Sato E, Nagase H, Nishimura J, Yamamoto H, Takiguchi S, Tanoue T, Suda W, Morita H, Hattori M, Honda K, Mori M, Doki Y, Sakaguchi S. Two FOXP3(+)CD4(+) T cell subpopulations distinctly control the prognosis of colorectal cancers. *Nat Med* 2016; **22**: 679-684 [PMID: 27111280 DOI: 10.1038/nm.4086]

50 **Garvey CM**, Lau R, Sanchez A, Sun RX, Fong EJ, Doche ME, Chen O, Jusuf A, Lenz HJ, Larson B, Mumenthaler SM. Anti-EGFR Therapy Induces EGF Secretion by Cancer-Associated Fibroblasts to Confer Colorectal Cancer Chemoresistance. *Cancers (Basel)* 2020; **12** [PMID: 32481658 DOI: 10.3390/cancers12061393]

51 **Yu Y**, Xiao CH, Tan LD, Wang QS, Li XQ, Feng YM. Cancer-associated fibroblasts induce epithelial-mesenchymal transition of breast cancer cells through paracrine TGF-β signalling. *Br J Cancer* 2014; **110**: 724-732 [PMID: 24335925 DOI: 10.1038/bjc.2013.768]

52 **Gaggioli C**, Hooper S, Hidalgo-Carcedo C, Grosse R, Marshall JF, Harrington K, Sahai E. Fibroblast-led collective invasion of carcinoma cells with differing roles for RhoGTPases in leading and following cells. *Nat Cell Biol* 2007; **9**: 1392-1400 [PMID: 18037882 DOI: 10.1038/ncb1658]

53 **Erdogan B**, Ao M, White LM, Means AL, Brewer BM, Yang L, Washington MK, Shi C, Franco OE, Weaver AM, Hayward SW, Li D, Webb DJ. Cancer-associated fibroblasts promote directional cancer cell migration by aligning fibronectin. *J Cell Biol* 2017; **216**: 3799-3816 [PMID: 29021221 DOI: 10.1083/jcb.201704053]

54 **Torres S**, Garcia-Palmero I, Herrera M, Bartolomé RA, Peña C, Fernandez-Aceñero MJ, Padilla G, Peláez-García A, Lopez-Lucendo M, Rodriguez-Merlo R, García de Herreros A, Bonilla F, Casal JI. LOXL2 Is Highly Expressed in Cancer-Associated Fibroblasts and Associates to Poor Colon Cancer Survival. *Clin Cancer Res* 2015; **21**: 4892-4902 [PMID: 26206869 DOI: 10.1158/1078-0432.CCR-14-3096]

55 **Tauriello DVF**, Palomo-Ponce S, Stork D, Berenguer-Llergo A, Badia-Ramentol J, Iglesias M, Sevillano M, Ibiza S, Cañellas A, Hernando-Momblona X, Byrom D, Matarin JA, Calon A, Rivas EI, Nebreda AR, Riera A, Attolini CS, Batlle E. TGFβ drives immune evasion in genetically reconstituted colon cancer metastasis. *Nature* 2018; **554**: 538-543 [PMID: 29443964 DOI: 10.1038/nature25492]

56 **Zhang R**, Qi F, Zhao F, Li G, Shao S, Zhang X, Yuan L, Feng Y. Cancer-associated fibroblasts enhance tumor-associated macrophages enrichment and suppress NK cells function in colorectal cancer. *Cell Death Dis* 2019; **10**: 273 [PMID: 30894509 DOI: 10.1038/s41419-019-1435-2]

57 **Gassmann P**, Hemping-Bovenkerk A, Mees ST, Haier J. Metastatic tumor cell arrest in the liver-lumen occlusion and specific adhesion are not exclusive. *Int J Colorectal Dis* 2009; **24**: 851-858 [PMID: 19319542 DOI: 10.1007/s00384-009-0694-2]

58 **Matsumura H**, Kondo T, Ogawa K, Tamura T, Fukunaga K, Murata S, Ohkohchi N. Kupffer cells decrease metastasis of colon cancer cells to the liver in the early stage. *Int J Oncol* 2014; **45**: 2303-2310 [PMID: 25231346 DOI: 10.3892/ijo.2014.2662]

59 **Tsilimigras DI**, Brodt P, Clavien PA, Muschel RJ, D'Angelica MI, Endo I, Parks RW, Doyle M, de Santibañes E, Pawlik TM. Liver metastases. *Nat Rev Dis Primers* 2021; **7**: 27 [PMID: 33859205 DOI: 10.1038/s41572-021-00261-6]

60 **Frantz C**, Stewart KM, Weaver VM. The extracellular matrix at a glance. *J Cell Sci* 2010; **123**: 4195-4200 [PMID: 21123617 DOI: 10.1242/jcs.023820]

61 **Egeblad M**, Rasch MG, Weaver VM. Dynamic interplay between the collagen scaffold and tumor evolution. *Curr Opin Cell Biol* 2010; **22**: 697-706 [PMID: 20822891 DOI: 10.1016/j.ceb.2010.08.015]

62 **Dong W**, Li H, Zhang Y, Yang H, Guo M, Li L, Liu T. Matrix metalloproteinase 2 promotes cell growth and invasion in colorectal cancer. *Acta Biochim Biophys Sin (Shanghai)* 2011; **43**: 840-848 [PMID: 21968416 DOI: 10.1093/abbs/gmr085]

63 **Zeng ZS**, Cohen AM, Guillem JG. Loss of basement membrane type IV collagen is associated with increased expression of metalloproteinases 2 and 9 (MMP-2 and MMP-9) during human colorectal tumorigenesis. *Carcinogenesis* 1999; **20**: 749-755 [PMID: 10334190 DOI: 10.1093/carcin/20.5.749]

64 **Levental KR**, Yu H, Kass L, Lakins JN, Egeblad M, Erler JT, Fong SF, Csiszar K, Giaccia A, Weninger W, Yamauchi M, Gasser DL, Weaver VM. Matrix crosslinking forces tumor progression by enhancing integrin signaling. *Cell* 2009; **139**: 891-906 [PMID: 19931152 DOI: 10.1016/j.cell.2009.10.027]

65 **Brauchle E**, Kasper J, Daum R, Schierbaum N, Falch C, Kirschniak A, Schäffer TE, Schenke-Layland K. Biomechanical and biomolecular characterization of extracellular matrix structures in human colon carcinomas. *Matrix Biol* 2018; **68-69**: 180-193 [PMID: 29605717 DOI: 10.1016/j.matbio.2018.03.016]

66 **Bauer J**, Emon MAB, Staudacher JJ, Thomas AL, Zessner-Spitzenberg J, Mancinelli G, Krett N, Saif MT, Jung B. Author Correction: Increased stiffness of the tumor microenvironment in colon cancer stimulates cancer associated fibroblast-mediated prometastatic activin A signaling. *Sci Rep* 2020; **10**: 7606 [PMID: 32355318 DOI: 10.1038/s41598-020-64239-2]

67 **Zhang HG**, Grizzle WE. Exosomes: a novel pathway of local and distant intercellular communication that facilitates the growth and metastasis of neoplastic lesions. *Am J Pathol* 2014; **184**: 28-41 [PMID: 24269592 DOI: 10.1016/j.ajpath.2013.09.027]

68 **Azmi AS**, Bao B, Sarkar FH. Exosomes in cancer development, metastasis, and drug resistance: a comprehensive review. *Cancer Metastasis Rev* 2013; **32**: 623-642 [PMID: 23709120 DOI: 10.1007/s10555-013-9441-9]

69 **Plaks V**, Kong N, Werb Z. The cancer stem cell niche: how essential is the niche in regulating stemness of tumor cells? *Cell Stem Cell* 2015; **16**: 225-238 [PMID: 25748930 DOI: 10.1016/j.stem.2015.02.015]

70 **Riches A**, Campbell E, Borger E, Powis S. Regulation of exosome release from mammary epithelial and breast cancer cells - a new regulatory pathway. *Eur J Cancer* 2014; **50**: 1025-1034 [PMID: 24462375 DOI: 10.1016/j.ejca.2013.12.019]

71 **Miyoshi H**, Ajima R, Luo CT, Yamaguchi TP, Stappenbeck TS. Wnt5a potentiates TGF-β signaling to promote colonic crypt regeneration after tissue injury. *Science* 2012; **338**: 108-113 [PMID: 22956684 DOI: 10.1126/science.1223821]

72 **Deep G**, Panigrahi GK. Hypoxia-Induced Signaling Promotes Prostate Cancer Progression: Exosomes Role as Messenger of Hypoxic Response in Tumor Microenvironment. *Crit Rev Oncog* 2015; **20**: 419-434 [PMID: 27279239 DOI: 10.1615/CritRevOncog.v20.i5-6.130]

73 **DeCosse JJ**, Gossens CL, Kuzma JF, Unsworth BR. Breast cancer: induction of differentiation by embryonic tissue. *Science* 1973; **181**: 1057-1058 [PMID: 4269415 DOI: 10.1126/science.181.4104.1057]

74 **Fujii H**, Cunha GR, Norman JT. The induction of adenocarcinomatous differentiation in neoplastic bladder epithelium by an embryonic prostatic inductor. *J Urol* 1982; **128**: 858-861 [PMID: 7143620 DOI: 10.1016/s0022-5347(17)53221-8]

75 **Kalluri R**, LeBleu VS. The biology, function, and biomedical applications of exosomes. *Science* 2020; **367** [PMID: 32029601 DOI: 10.1126/science.aau6977]

76 **van Niel G**, D'Angelo G, Raposo G. Shedding light on the cell biology of extracellular vesicles. *Nat Rev Mol Cell Biol* 2018; **19**: 213-228 [PMID: 29339798 DOI: 10.1038/nrm.2017.125]

77 **McAndrews KM**, Kalluri R. Mechanisms associated with biogenesis of exosomes in cancer. *Mol Cancer* 2019; **18**: 52 [PMID: 30925917 DOI: 10.1186/s12943-019-0963-9]

78 **Henne WM**, Stenmark H, Emr SD. Molecular mechanisms of the membrane sculpting ESCRT pathway. *Cold Spring Harb Perspect Biol* 2013; **5** [PMID: 24003212 DOI: 10.1101/cshperspect.a016766]

79 **Wollert T**, Wunder C, Lippincott-Schwartz J, Hurley JH. Membrane scission by the ESCRT-III complex. *Nature* 2009; **458**: 172-177 [PMID: 19234443 DOI: 10.1038/nature07836]

80 **van Niel G**, Charrin S, Simoes S, Romao M, Rochin L, Saftig P, Marks MS, Rubinstein E, Raposo G. The tetraspanin CD63 regulates ESCRT-independent and -dependent endosomal sorting during melanogenesis. *Dev Cell* 2011; **21**: 708-721 [PMID: 21962903 DOI: 10.1016/j.devcel.2011.08.019]

81 **Wei D**, Zhan W, Gao Y, Huang L, Gong R, Wang W, Zhang R, Wu Y, Gao S, Kang T. RAB31 marks and controls an ESCRT-independent exosome pathway. *Cell Res* 2021; **31**: 157-177 [PMID: 32958903 DOI: 10.1038/s41422-020-00409-1]

82 **Bissig C**, Lenoir M, Velluz MC, Kufareva I, Abagyan R, Overduin M, Gruenberg J. Viral infection controlled by a

calcium-dependent lipid-binding module in ALIX. *Dev Cell* 2013; **25**: 364-373 [PMID: 23664863 DOI: 10.1016/j.devcel.2013.04.003]

83 **Laulagnier K**, Motta C, Hamdi S, Roy S, Fauvelle F, Pageaux JF, Kobayashi T, Salles JP, Perret B, Bonnerot C, Record M. Mast cell- and dendritic cell-derived exosomes display a specific lipid composition and an unusual membrane organization. *Biochem J* 2004; **380**: 161-171 [PMID: 14965343 DOI: 10.1042/BJ20031594]

84 **Mathivanan S**, Fahner CJ, Reid GE, Simpson RJ. ExoCarta 2012: database of exosomal proteins, RNA and lipids. *Nucleic Acids Res* 2012; **40**: D1241-D1244 [PMID: 21989406 DOI: 10.1093/nar/gkr828]

85 **McGough IJ**, Vincent JP. Exosomes in developmental signalling. *Development* 2016; **143**: 2482-2493 [PMID: 27436038 DOI: 10.1242/dev.126516]

86 **Bebelman MP**, Smit MJ, Pegtel DM, Baglio SR. Biogenesis and function of extracellular vesicles in cancer. *Pharmacol Ther* 2018; **188**: 1-11 [PMID: 29476772 DOI: 10.1016/j.pharmthera.2018.02.013]

87 **Wen SW**, Lima LG, Lobb RJ, Norris EL, Hastie ML, Krumeich S, Möller A. Breast Cancer-Derived Exosomes Reflect the Cell-of-Origin Phenotype. *Proteomics* 2019; **19**: e1800180 [PMID: 30672117 DOI: 10.1002/pmic.201800180]

88 **Mathieu M**, Martin-Jaular L, Lavieu G, Théry C. Specificities of secretion and uptake of exosomes and other extracellular vesicles for cell-to-cell communication. *Nat Cell Biol* 2019; **21**: 9-17 [PMID: 30602770 DOI: 10.1038/s41556-018-0250-9]

89 **Ostrowski M**, Carmo NB, Krumeich S, Fanget I, Raposo G, Savina A, Moita CF, Schauer K, Hume AN, Freitas RP, Goud B, Benaroch P, Hacohen N, Fukuda M, Desnos C, Seabra MC, Darchen F, Amigorena S, Moita LF, Thery C. Rab27a and Rab27b control different steps of the exosome secretion pathway. *Nat Cell Biol* 2010; **12**: 19-30; sup pp 1 [PMID: 19966785 DOI: 10.1038/ncb2000]

90 **Baietti MF**, Zhang Z, Mortier E, Melchior A, Degeest G, Geeraerts A, Ivarsson Y, Depoortere F, Coomans C, Vermeiren E, Zimmermann P, David G. Syndecan-syntenin-ALIX regulates the biogenesis of exosomes. *Nat Cell Biol* 2012; **14**: 677-685 [PMID: 22660413 DOI: 10.1038/ncb2502]

91 **Hsu C**, Morohashi Y, Yoshimura S, Manrique-Hoyos N, Jung S, Lauterbach MA, Bakhti M, Grønborg M, Möbius W, Rhee J, Barr FA, Simons M. Regulation of exosome secretion by Rab35 and its GTPase-activating proteins TBC1D10A-C. *J Cell Biol* 2010; **189**: 223-232 [PMID: 20404108 DOI: 10.1083/jcb.200911018]

92 **Taha EA**, Ono K, Eguchi T. Roles of Extracellular HSPs as Biomarkers in Immune Surveillance and Immune Evasion. *Int J Mol Sci* 2019; **20** [PMID: 31533245 DOI: 10.3390/ijms20184588]

93 **Lauwers E**, Wang YC, Gallardo R, Van der Kant R, Michiels E, Swerts J, Baatsen P, Zaiter SS, McAlpine SR, Gounko NV, Rousseau F, Schymkowitz J, Verstreken P. Hsp90 Mediates Membrane Deformation and Exosome Release. *Mol Cell* 2018; **71**: 689-702.e9 [PMID: 30193096 DOI: 10.1016/j.molcel.2018.07.016]

94 **Tang X**, Chang C, Guo J, Lincoln V, Liang C, Chen M, Woodley DT, Li W. Tumour-Secreted Hsp90α on External Surface of Exosomes Mediates Tumour - Stromal Cell Communication *via* Autocrine and Paracrine Mechanisms. *Sci Rep* 2019; **9**: 15108 [PMID: 31641193 DOI: 10.1038/s41598-019-51704-w]

95 **Mazurov D**, Barbashova L, Filatov A. Tetraspanin protein CD9 interacts with metalloprotease CD10 and enhances its release *via* exosomes. *FEBS J* 2013; **280**: 1200-1213 [PMID: 23289620 DOI: 10.1111/febs.12110]

96 **Bobrie A**, Colombo M, Krumeich S, Raposo G, Théry C. Diverse subpopulations of vesicles secreted by different intracellular mechanisms are present in exosome preparations obtained by differential ultracentrifugation. *J Extracell Vesicles* 2012; **1** [PMID: 24009879 DOI: 10.3402/jev.v1i0.18397]

97 **Poliakov A**, Spilman M, Dokland T, Amling CL, Mobley JA. Structural heterogeneity and protein composition of exosome-like vesicles (prostasomes) in human semen. *Prostate* 2009; **69**: 159-167 [PMID: 18819103 DOI: 10.1002/pros.20860]

98 **Cossetti C**, Iraci N, Mercer TR, Leonardi T, Alpi E, Drago D, Alfaro-Cervello C, Saini HK, Davis MP, Schaeffer J, Vega B, Stefanini M, Zhao C, Muller W, Garcia-Verdugo JM, Mathivanan S, Bachi A, Enright AJ, Mattick JS, Pluchino S. Extracellular vesicles from neural stem cells transfer IFN-γ *via* Ifngr1 to activate Stat1 signaling in target cells. *Mol Cell* 2014; **56**: 193-204 [PMID: 25242146 DOI: 10.1016/j.molcel.2014.08.020]

99 **Choi D**, Montermini L, Kim DK, Meehan B, Roth FP, Rak J. The Impact of Oncogenic EGFRvIII on the Proteome of Extracellular Vesicles Released from Glioblastoma Cells. *Mol Cell Proteomics* 2018; **17**: 1948-1964 [PMID: 30006486 DOI: 10.1074/mcp.RA118.000644]

100 **Vojtech L**, Woo S, Hughes S, Levy C, Ballweber L, Sauteraud RP, Strobl J, Westerberg K, Gottardo R, Tewari M, Hladik F. Exosomes in human semen carry a distinctive repertoire of small non-coding RNAs with potential regulatory functions. *Nucleic Acids Res* 2014; **42**: 7290-7304 [PMID: 24838567 DOI: 10.1093/nar/gku347]

101 **Kanaoka R**, Iinuma H, Dejima H, Sakai T, Uehara H, Matsutani N, Kawamura M. Usefulness of Plasma Exosomal MicroRNA-451a as a Noninvasive Biomarker for Early Prediction of Recurrence and Prognosis of Non-Small Cell Lung Cancer. *Oncology* 2018; **94**: 311-323 [PMID: 29533963 DOI: 10.1159/000487006]

102 **Fortunato O**, Gasparini P, Boeri M, Sozzi G. Exo-miRNAs as a New Tool for Liquid Biopsy in Lung Cancer. *Cancers (Basel)* 2019; **11** [PMID: 31242686 DOI: 10.3390/cancers11060888]

103 **Endzeliņš E**, Berger A, Melne V, Bajo-Santos C, Soboļevska K, Ābols A, Rodriguez M, Šantare D, Rudņickiha A, Lietuvietis V, Llorente A, Linē A. Detection of circulating miRNAs: comparative analysis of extracellular vesicle-incorporated miRNAs and cell-free miRNAs in whole plasma of prostate cancer patients. *BMC Cancer* 2017; **17**: 730 [PMID: 29121858 DOI: 10.1186/s12885-017-3737-z]

104 **Puik JR**, Meijer LL, Le Large TY, Prado MM, Frampton AE, Kazemier G, Giovannetti E. miRNA profiling for diagnosis, prognosis and stratification of cancer treatment in cholangiocarcinoma. *Pharmacogenomics* 2017; **18**: 1343-1358 [PMID: 28832247 DOI: 10.2217/pgs-2017-0010]

105 **Sun ZP**, Li AQ, Jia WH, Ye S, Van Eps G, Yu JM, Yang WJ. MicroRNA expression profiling in exosomes derived from gastric cancer stem-like cells. *Oncotarget* 2017; **8**: 93839-93855 [PMID: 29212193 DOI: 10.18632/oncotarget.21288]

106 **Tang Y**, Cui Y, Li Z, Jiao Z, Zhang Y, He Y, Chen G, Zhou Q, Wang W, Zhou X, Luo J, Zhang S. Radiation-induced miR-208a increases the proliferation and radioresistance by targeting p21 in human lung cancer cells. *J Exp Clin Cancer Res* 2016; **35**: 7 [PMID: 26754670 DOI: 10.1186/s13046-016-0285-3]

107 **Wei F**, Ma C, Zhou T, Dong X, Luo Q, Geng L, Ding L, Zhang Y, Zhang L, Li N, Li Y, Liu Y. Exosomes derived from gemcitabine-resistant cells transfer malignant phenotypic traits *via* delivery of miRNA-222-3p. *Mol Cancer* 2017; **16**: 132 [PMID: 28743280 DOI: 10.1186/s12943-017-0694-8]

108 **Zhao W**, Shan B, He D, Cheng Y, Li B, Zhang C, Duan C. Recent Progress in Characterizing Long Noncoding RNAs in Cancer Drug Resistance. *J Cancer* 2019; **10**: 6693-6702 [PMID: 31777598 DOI: 10.7150/jca.30877]

109 **Wang M**, Zhou L, Yu F, Zhang Y, Li P, Wang K. The functional roles of exosomal long non-coding RNAs in cancer. *Cell Mol Life Sci* 2019; **76**: 2059-2076 [PMID: 30683984 DOI: 10.1007/s00018-019-03018-3]

110 **Conigliaro A**, Costa V, Lo Dico A, Saieva L, Buccheri S, Dieli F, Manno M, Raccosta S, Mancone C, Tripodi M, De Leo G, Alessandro R. CD90+ liver cancer cells modulate endothelial cell phenotype through the release of exosomes containing H19 lncRNA. *Mol Cancer* 2015; **14**: 155 [PMID: 26272696 DOI: 10.1186/s12943-015-0426-x]

111 **Kristensen LS**, Andersen MS, Stagsted LVW, Ebbesen KK, Hansen TB, Kjems J. The biogenesis, biology and characterization of circular RNAs. *Nat Rev Genet* 2019; **20**: 675-691 [PMID: 31395983 DOI: 10.1038/s41576-019-0158-7]

112 **Cheng X**, Zhang L, Zhang K, Zhang G, Hu Y, Sun X, Zhao C, Li H, Li YM, Zhao J. Circular RNA VMA21 protects against intervertebral disc degeneration through targeting miR-200c and X linked inhibitor-of-apoptosis protein. *Ann Rheum Dis* 2018; **77**: 770-779 [PMID: 29343508 DOI: 10.1136/annrheumdis-2017-212056]

113 **Li J**, Li Z, Jiang P, Peng M, Zhang X, Chen K, Liu H, Bi H, Liu X, Li X. Circular RNA IARS (circ-IARS) secreted by pancreatic cancer cells and located within exosomes regulates endothelial monolayer permeability to promote tumor metastasis. *J Exp Clin Cancer Res* 2018; **37**: 177 [PMID: 30064461 DOI: 10.1186/s13046-018-0822-3]

114 **Zitvogel L**, Regnault A, Lozier A, Wolfers J, Flament C, Tenza D, Ricciardi-Castagnoli P, Raposo G, Amigorena S. Eradication of established murine tumors using a novel cell-free vaccine: dendritic cell-derived exosomes. *Nat Med* 1998; **4**: 594-600 [PMID: 9585234 DOI: 10.1038/nm0598-594]

115 **Raimondo S**, Saieva L, Corrado C, Fontana S, Flugy A, Rizzo A, De Leo G, Alessandro R. Chronic myeloid leukemia-derived exosomes promote tumor growth through an autocrine mechanism. *Cell Commun Signal* 2015; **13**: 8 [PMID: 25644060 DOI: 10.1186/s12964-015-0086-x]

116 **Takahashi A**, Okada R, Nagao K, Kawamata Y, Hanyu A, Yoshimoto S, Takasugi M, Watanabe S, Kanemaki MT, Obuse C, Hara E. Exosomes maintain cellular homeostasis by excreting harmful DNA from cells. *Nat Commun* 2017; **8**: 15287 [PMID: 28508895 DOI: 10.1038/ncomms15287]

117 **Yang Y**, Li CW, Chan LC, Wei Y, Hsu JM, Xia W, Cha JH, Hou J, Hsu JL, Sun L, Hung MC. Exosomal PD-L1 harbors active defense function to suppress T cell killing of breast cancer cells and promote tumor growth. *Cell Res* 2018; **28**: 862-864 [PMID: 29959401 DOI: 10.1038/s41422-018-0060-4]

118 **Demory Beckler M**, Higginbotham JN, Franklin JL, Ham AJ, Halvey PJ, Imasuen IE, Whitwell C, Li M, Liebler DC, Coffey RJ. Proteomic analysis of exosomes from mutant KRAS colon cancer cells identifies intercellular transfer of mutant KRAS. *Mol Cell Proteomics* 2013; **12**: 343-355 [PMID: 23161513 DOI: 10.1074/mcp.M112.022806]

119 **Shimoda M**, Principe S, Jackson HW, Luga V, Fang H, Molyneux SD, Shao YW, Aiken A, Waterhouse PD, Karamboulas C, Hess FM, Ohtsuka T, Okada Y, Ailles L, Ludwig A, Wrana JL, Kislinger T, Khokha R. Loss of the Timp gene family is sufficient for the acquisition of the CAF-like cell state. *Nat Cell Biol* 2014; **16**: 889-901 [PMID: 25150980 DOI: 10.1038/ncb3021]

120 **Achreja A**, Zhao H, Yang L, Yun TH, Marini J, Nagrath D. Exo-MFA - A 13C metabolic flux analysis framework to dissect tumor microenvironment-secreted exosome contributions towards cancer cell metabolism. *Metab Eng* 2017; **43**: 156-172 [PMID: 28087332 DOI: 10.1016/j.ymben.2017.01.001]

121 **Cho JA**, Park H, Lim EH, Lee KW. Exosomes from breast cancer cells can convert adipose tissue-derived mesenchymal stem cells into myofibroblast-like cells. *Int J Oncol* 2012; **40**: 130-138 [PMID: 21904773 DOI: 10.3892/ijo.2011.1193]

122 **Baroni S**, Romero-Cordoba S, Plantamura I, Dugo M, D'Ippolito E, Cataldo A, Cosentino G, Angeloni V, Rossini A, Daidone MG, Iorio MV. Exosome-mediated delivery of miR-9 induces cancer-associated fibroblast-like properties in human breast fibroblasts. *Cell Death Dis* 2016; **7**: e2312 [PMID: 27468688 DOI: 10.1038/cddis.2016.224]

123 **Nazarenko I**, Rana S, Baumann A, McAlear J, Hellwig A, Trendelenburg M, Lochnit G, Preissner KT, Zöller M. Cell surface tetraspanin Tspan8 contributes to molecular pathways of exosome-induced endothelial cell activation. *Cancer Res* 2010; **70**: 1668-1678 [PMID: 20124479 DOI: 10.1158/0008-5472.CAN-09-2470]

124 **Gesierich S**, Berezovskiy I, Ryschich E, Zöller M. Systemic induction of the angiogenesis switch by the tetraspanin D6.1A/CO-029. *Cancer Res* 2006; **66**: 7083-7094 [PMID: 16849554 DOI: 10.1158/0008-5472.CAN-06-0391]

125 **Hsu YL**, Hung JY, Chang WA, Lin YS, Pan YC, Tsai PH, Wu CY, Kuo PL. Hypoxic lung cancer-secreted exosomal miR-23a increased angiogenesis and vascular permeability by targeting prolyl hydroxylase and tight junction protein ZO-1. *Oncogene* 2017; **36**: 4929-4942 [PMID: 28436951 DOI: 10.1038/onc.2017.105]

126 **Ridder K**, Keller S, Dams M, Rupp AK, Schlaudraff J, Del Turco D, Starmann J, Macas J, Karpova D, Devraj K, Depboylu C, Landfried B, Arnold B, Plate KH, Höglinger G, Sültmann H, Altevogt P, Momma S. Extracellular vesicle-mediated transfer of genetic information between the hematopoietic system and the brain in response to inflammation. *PLoS Biol* 2014; **12**: e1001874 [PMID: 24893313 DOI: 10.1371/journal.pbio.1001874]

127 **Kurywchak P**, Tavormina J, Kalluri R. The emerging roles of exosomes in the modulation of immune responses in cancer. *Genome Med* 2018; **10**: 23 [PMID: 29580275 DOI: 10.1186/s13073-018-0535-4]

128 **Tkach M**, Kowal J, Zucchetti AE, Enserink L, Jouve M, Lankar D, Saitakis M, Martin-Jaular L, Théry C. Qualitative differences in T-cell activation by dendritic cell-derived extracellular vesicle subtypes. *EMBO J* 2017; **36**: 3012-3028 [PMID: 28923825 DOI: 10.15252/embj.201696003]

129 **Kitai Y**, Kawasaki T, Sueyoshi T, Kobiyama K, Ishii KJ, Zou J, Akira S, Matsuda T, Kawai T. DNA-Containing Exosomes Derived from Cancer Cells Treated with Topotecan Activate a STING-Dependent Pathway and Reinforce Antitumor Immunity. *J Immunol* 2017; **198**: 1649-1659 [PMID: 28069806 DOI: 10.4049/jimmunol.1601694]

130 **Torralba D**, Baixauli F, Villarroya-Beltri C, Fernández-Delgado I, Latorre-Pellicer A, Acín-Pérez R, Martín-Cófreces NB, Jaso-Tamame ÁL, Iborra S, Jorge I, González-Aseguinolaza G, Garaude J, Vicente-Manzanares M, Enríquez JA,

Mittelbrunn M, Sánchez-Madrid F. Priming of dendritic cells by DNA-containing extracellular vesicles from activated T cells through antigen-driven contacts. *Nat Commun* 2018; **9**: 2658 [PMID: 29985392 DOI: 10.1038/s41467-018-05077-9]

131 **Montermini L**, Meehan B, Garnier D, Lee WJ, Lee TH, Guha A, Al-Nedawi K, Rak J. Inhibition of oncogenic epidermal growth factor receptor kinase triggers release of exosome-like extracellular vesicles and impacts their phosphoprotein and DNA content. *J Biol Chem* 2015; **290**: 24534-24546 [PMID: 26272609 DOI: 10.1074/jbc.M115.679217]

132 **Chennakrishnaiah S**, Meehan B, D'Asti E, Montermini L, Lee TH, Karatzas N, Buchanan M, Tawil N, Choi D, Divangahi M, Basik M, Rak J. Leukocytes as a reservoir of circulating oncogenic DNA and regulatory targets of tumor-derived extracellular vesicles. *J Thromb Haemost* 2018; **16**: 1800-1813 [PMID: 29971917 DOI: 10.1111/jth.14222]

133 **Ding G**, Zhou L, Qian Y, Fu M, Chen J, Xiang J, Wu Z, Jiang G, Cao L. Pancreatic cancer-derived exosomes transfer miRNAs to dendritic cells and inhibit RFXAP expression *via* miR-212-3p. *Oncotarget* 2015; **6**: 29877-29888 [PMID: 26337469 DOI: 10.18632/oncotarget.4924]

134 **Ying X**, Wu Q, Wu X, Zhu Q, Wang X, Jiang L, Chen X. Epithelial ovarian cancer-secreted exosomal miR-222-3p induces polarization of tumor-associated macrophages. *Oncotarget* 2016; **7**: 43076-43087 [PMID: 27172798 DOI: 10.18632/oncotarget.9246]

135 **Chen G**, Huang AC, Zhang W, Zhang G, Wu M, Xu W, Yu Z, Yang J, Wang B, Sun H, Xia H, Man Q, Zhong W, Antelo LF, Wu B, Xiong X, Liu X, Guan L, Li T, Liu S, Yang R, Lu Y, Dong L, McGettigan S, Somasundaram R, Radhakrishnan R, Mills G, Kim J, Chen YH, Dong H, Zhao Y, Karakousis GC, Mitchell TC, Schuchter LM, Herlyn M, Wherry EJ, Xu X, Guo W. Exosomal PD-L1 contributes to immunosuppression and is associated with anti-PD-1 response. *Nature* 2018; **560**: 382-386 [PMID: 30089911 DOI: 10.1038/s41586-018-0392-8]

136 **Poggio M**, Hu T, Pai CC, Chu B, Belair CD, Chang A, Montabana E, Lang UE, Fu Q, Fong L, Blelloch R. Suppression of Exosomal PD-L1 Induces Systemic Anti-tumor Immunity and Memory. *Cell* 2019; **177**: 414-427.e13 [PMID: 30951669 DOI: 10.1016/j.cell.2019.02.016]

137 **Skokos D**, Le Panse S, Villa I, Rousselle JC, Peronet R, David B, Namane A, Mécheri S. Mast cell-dependent B and T lymphocyte activation is mediated by the secretion of immunologically active exosomes. *J Immunol* 2001; **166**: 868-876 [PMID: 11145662 DOI: 10.4049/jimmunol.166.2.868]

138 **Cha DJ**, Franklin JL, Dou Y, Liu Q, Higginbotham JN, Demory Beckler M, Weaver AM, Vickers K, Prasad N, Levy S, Zhang B, Coffey RJ, Patton JG. KRAS-dependent sorting of miRNA to exosomes. *Elife* 2015; **4**: e07197 [PMID: 26132860 DOI: 10.7554/eLife.07197]

139 **Lewis BP**, Burge CB, Bartel DP. Conserved seed pairing, often flanked by adenosines, indicates that thousands of human genes are microRNA targets. *Cell* 2005; **120**: 15-20 [PMID: 15652477 DOI: 10.1016/j.cell.2004.12.035]

140 **Michael MZ**, O' Connor SM, van Holst Pellekaan NG, Young GP, James RJ. Reduced accumulation of specific microRNAs in colorectal neoplasia. *Mol Cancer Res* 2003; **1**: 882-891 [PMID: 14573789]

141 **Bartley AN**, Yao H, Barkoh BA, Ivan C, Mishra BM, Rashid A, Calin GA, Luthra R, Hamilton SR. Complex patterns of altered MicroRNA expression during the adenoma-adenocarcinoma sequence for microsatellite-stable colorectal cancer. *Clin Cancer Res* 2011; **17**: 7283-7293 [PMID: 21948089 DOI: 10.1158/1078-0432.CCR-11-1452]

142 **Becker A**, Thakur BK, Weiss JM, Kim HS, Peinado H, Lyden D. Extracellular Vesicles in Cancer: Cell-to-Cell Mediators of Metastasis. *Cancer Cell* 2016; **30**: 836-848 [PMID: 27960084 DOI: 10.1016/j.ccell.2016.10.009]

143 **Syn N**, Wang L, Sethi G, Thiery JP, Goh BC. Exosome-Mediated Metastasis: From Epithelial-Mesenchymal Transition to Escape from Immunosurveillance. *Trends Pharmacol Sci* 2016; **37**: 606-617 [PMID: 27157716 DOI: 10.1016/j.tips.2016.04.006]

144 **Whiteside TL**. The role of tumor-derived exosomes in epithelial mesenchymal transition (EMT). *Transl Cancer Res* 2017; **6**: S90-S92 [PMID: 31080768 DOI: 10.21037/tcr.2017.02.13]

145 **Webber J**, Steadman R, Mason MD, Tabi Z, Clayton A. Cancer exosomes trigger fibroblast to myofibroblast differentiation. *Cancer Res* 2010; **70**: 9621-9630 [PMID: 21098712 DOI: 10.1158/0008-5472.CAN-10-1722]

146 **Cao H**, Xu E, Liu H, Wan L, Lai M. Epithelial-mesenchymal transition in colorectal cancer metastasis: A system review. *Pathol Res Pract* 2015; **211**: 557-569 [PMID: 26092594 DOI: 10.1016/j.prp.2015.05.010]

147 **Siemens H**, Jackstadt R, Hünten S, Kaller M, Menssen A, Götz U, Hermeking H. miR-34 and SNAIL form a double-negative feedback loop to regulate epithelial-mesenchymal transitions. *Cell Cycle* 2011; **10**: 4256-4271 [PMID: 22134354 DOI: 10.4161/cc.10.24.18552]

148 **Hur K**, Toiyama Y, Takahashi M, Balaguer F, Nagasaka T, Koike J, Hemmi H, Koi M, Boland CR, Goel A. MicroRNA-200c modulates epithelial-to-mesenchymal transition (EMT) in human colorectal cancer metastasis. *Gut* 2013; **62**: 1315-1326 [PMID: 22735571 DOI: 10.1136/gutjnl-2011-301846]

149 **Sun Y**, Shen S, Liu X, Tang H, Wang Z, Yu Z, Li X, Wu M. MiR-429 inhibits cells growth and invasion and regulates EMT-related marker genes by targeting Onecut2 in colorectal carcinoma. *Mol Cell Biochem* 2014; **390**: 19-30 [PMID: 24402783 DOI: 10.1007/s11010-013-1950-x]

150 **Sun Z**, Zhang Z, Liu Z, Qiu B, Liu K, Dong G. MicroRNA-335 inhibits invasion and metastasis of colorectal cancer by targeting ZEB2. *Med Oncol* 2014; **31**: 982 [PMID: 24829139 DOI: 10.1007/s12032-014-0982-8]

151 **Zheng YB**, Luo HP, Shi Q, Hao ZN, Ding Y, Wang QS, Li SB, Xiao GC, Tong SL. miR-132 inhibits colorectal cancer invasion and metastasis *via* directly targeting ZEB2. *World J Gastroenterol* 2014; **20**: 6515-6522 [PMID: 24914372 DOI: 10.3748/wjg.v20.i21.6515]

152 **Geng L**, Chaudhuri A, Talmon G, Wisecarver JL, Are C, Brattain M, Wang J. MicroRNA-192 suppresses liver metastasis of colon cancer. *Oncogene* 2014; **33**: 5332-5340 [PMID: 24213572 DOI: 10.1038/onc.2013.478]

153 **Solanes-Casado S**, Cebrián A, Rodríguez-Remírez M, Mahíllo I, García-García L, Río-Vilariño A, Baños N, de Cárcer G, Monfort-Vengut A, Castellano V, Fernández-Aceñero MJ, García-Foncillas J, Del Puerto-Nevado L. Overcoming PLK1 inhibitor resistance by targeting mevalonate pathway to impair AXL-TWIST axis in colorectal cancer. *Biomed Pharmacother* 2021; **144**: 112347 [PMID: 34700228 DOI: 10.1016/j.biopha.2021.112347]

154 **Shen X**, Jiang H, Chen Z, Lu B, Zhu Y, Mao J, Chai K, Chen W. MicroRNA-145 Inhibits Cell Migration and Invasion in Colorectal Cancer by Targeting TWIST. *Onco Targets Ther* 2019; **12**: 10799-10809 [PMID: 31849487 DOI: 10.2147/OTT.S216147]

155 **Lu MH**, Huang CC, Pan MR, Chen HH, Hung WC. Prospero homeobox 1 promotes epithelial-mesenchymal transition in colon cancer cells by inhibiting E-cadherin *via* miR-9. *Clin Cancer Res* 2012; **18**: 6416-6425 [PMID: 23045246 DOI: 10.1158/1078-0432.CCR-12-0832]

156 **Vishnubalaji R**, Hamam R, Yue S, Al-Obeed O, Kassem M, Liu FF, Aldahmash A, Alajez NM. MicroRNA-320 suppresses colorectal cancer by targeting SOX4, FOXM1, and FOXQ1. *Oncotarget* 2016; **7**: 35789-35802 [PMID: 27119506 DOI: 10.18632/oncotarget.8937]

157 **Zhang GJ**, Li Y, Zhou H, Xiao HX, Zhou T. miR20a is an independent prognostic factor in colorectal cancer and is involved in cell metastasis. *Mol Med Rep* 2014; **10**: 283-291 [PMID: 24737193 DOI: 10.3892/mmr.2014.2144]

158 **Wang J**, Yan F, Zhao Q, Zhan F, Wang R, Wang L, Zhang Y, Huang X. Circulating exosomal miR-125a-3p as a novel biomarker for early-stage colon cancer. *Sci Rep* 2017; **7**: 4150 [PMID: 28646161 DOI: 10.1038/s41598-017-04386-1]

159 **Zhao S**, Sun H, Jiang W, Mi Y, Zhang D, Wen Y, Cheng D, Tang H, Wu S, Yu Y, Liu X, Cui W, Zhang M, Sun X, Zhou Z, Peng Z, Yan D. miR-4775 promotes colorectal cancer invasion and metastasis *via* the Smad7/TGFβ-mediated epithelial to mesenchymal transition. *Mol Cancer* 2017; **16**: 12 [PMID: 28095858 DOI: 10.1186/s12943-017-0585-z]

160 **Bu P**, Wang L, Chen KY, Rakhilin N, Sun J, Closa A, Tung KL, King S, Kristine Varanko A, Xu Y, Huan Chen J, Zessin AS, Shealy J, Cummings B, Hsu D, Lipkin SM, Moreno V, Gümüş ZH, Shen X. miR-1269 promotes metastasis and forms a positive feedback loop with TGF-β. *Nat Commun* 2015; **6**: 6879 [PMID: 25872451 DOI: 10.1038/ncomms7879]

161 **Hahn S**, Jackstadt R, Siemens H, Hünten S, Hermeking H. SNAIL and miR-34a feed-forward regulation of ZNF281/ZBP99 promotes epithelial-mesenchymal transition. *EMBO J* 2013; **32**: 3079-3095 [PMID: 24185900 DOI: 10.1038/emboj.2013.236]

162 **Kim NH**, Kim HS, Kim NG, Lee I, Choi HS, Li XY, Kang SE, Cha SY, Ryu JK, Na JM, Park C, Kim K, Lee S, Gumbiner BM, Yook JI, Weiss SJ. p53 and microRNA-34 are suppressors of canonical Wnt signaling. *Sci Signal* 2011; **4**: ra71 [PMID: 22045851 DOI: 10.1126/scisignal.2001744]

163 **Sanchez-Mejias A**, Kwon J, Chew XH, Siemens A, Sohn HS, Jing G, Zhang B, Yang H, Tay Y. A novel SOCS5/miR-18/miR-25 axis promotes tumorigenesis in liver cancer. *Int J Cancer* 2019; **144**: 311-321 [PMID: 30191950 DOI: 10.1002/ijc.31857]

164 **Subramanian M**, Rao SR, Thacker P, Chatterjee S, Karunagaran D. MiR-29b downregulates canonical Wnt signaling by suppressing coactivators of β-catenin in human colorectal cancer cells. *J Cell Biochem* 2014; **115**: 1974-1984 [PMID: 24913975 DOI: 10.1002/jcb.24869]

165 **Jolly MK**, Tripathi SC, Somarelli JA, Hanash SM, Levine H. Epithelial/mesenchymal plasticity: how have quantitative mathematical models helped improve our understanding? *Mol Oncol* 2017; **11**: 739-754 [PMID: 28548388 DOI: 10.1002/1878-0261.12084]

166 **Cui F**, Wang S, Lao I, Zhou C, Kong H, Bayaxi N, Li J, Chen Q, Zhu T, Zhu H. miR-375 inhibits the invasion and metastasis of colorectal cancer *via* targeting SP1 and regulating EMT-associated genes. *Oncol Rep* 2016; **36**: 487-493 [PMID: 27222350 DOI: 10.3892/or.2016.4834]

167 **Cai HK**, Chen X, Tang YH, Deng YC. MicroRNA-194 modulates epithelial-mesenchymal transition in human colorectal cancer metastasis. *Onco Targets Ther* 2017; **10**: 1269-1278 [PMID: 28280361 DOI: 10.2147/OTT.S125172]

168 **Xu T**, Jing C, Shi Y, Miao R, Peng L, Kong S, Ma Y, Li L. microRNA-20a enhances the epithelial-to-mesenchymal transition of colorectal cancer cells by modulating matrix metalloproteinases. *Exp Ther Med* 2015; **10**: 683-688 [PMID: 26622375 DOI: 10.3892/etm.2015.2538]

169 **Hood JL**, San RS, Wickline SA. Exosomes released by melanoma cells prepare sentinel lymph nodes for tumor metastasis. *Cancer Res* 2011; **71**: 3792-3801 [PMID: 21478294 DOI: 10.1158/0008-5472.CAN-10-4455]

170 **Rana S**, Malinowska K, Zöller M. Exosomal tumor microRNA modulates premetastatic organ cells. *Neoplasia* 2013; **15**: 281-295 [PMID: 23479506 DOI: 10.1593/neo.122010]

171 **Liu Y**, Cao X. Characteristics and Significance of the Pre-metastatic Niche. *Cancer Cell* 2016; **30**: 668-681 [PMID: 27846389 DOI: 10.1016/j.ccell.2016.09.011]

172 **Takano Y**, Masuda T, Iinuma H, Yamaguchi R, Sato K, Tobo T, Hirata H, Kuroda Y, Nambara S, Hayashi N, Iguchi T, Ito S, Eguchi H, Ochiya T, Yanaga K, Miyano S, Mimori K. Circulating exosomal microRNA-203 is associated with metastasis possibly *via* inducing tumor-associated macrophages in colorectal cancer. *Oncotarget* 2017; **8**: 78598-78613 [PMID: 29108252 DOI: 10.18632/oncotarget.20009]

173 **Zhao S**, Mi Y, Guan B, Zheng B, Wei P, Gu Y, Zhang Z, Cai S, Xu Y, Li X, He X, Zhong X, Li G, Chen Z, Li D. Tumor-derived exosomal miR-934 induces macrophage M2 polarization to promote liver metastasis of colorectal cancer. *J Hematol Oncol* 2020; **13**: 156 [PMID: 33213490 DOI: 10.1186/s13045-020-00991-2]

174 **Wang D**, Wang X, Si M, Yang J, Sun S, Wu H, Cui S, Qu X, Yu X. Exosome-encapsulated miRNAs contribute to CXCL12/CXCR4-induced liver metastasis of colorectal cancer by enhancing M2 polarization of macrophages. *Cancer Lett* 2020; **474**: 36-52 [PMID: 31931030 DOI: 10.1016/j.canlet.2020.01.005]

175 **Yamada N**, Kuranaga Y, Kumazaki M, Shinohara H, Taniguchi K, Akao Y. Colorectal cancer cell-derived extracellular vesicles induce phenotypic alteration of T cells into tumor-growth supporting cells with transforming growth factor-β1-mediated suppression. *Oncotarget* 2016; **7**: 27033-27043 [PMID: 27081032 DOI: 10.18632/oncotarget.7041]

176 **Whiteside TL**. Exosomes and tumor-mediated immune suppression. *J Clin Invest* 2016; **126**: 1216-1223 [PMID: 26927673 DOI: 10.1172/JCI81136]

177 **Wang J**, De Veirman K, De Beule N, Maes K, De Bruyne E, Van Valckenborgh E, Vanderkerken K, Menu E. The bone marrow microenvironment enhances multiple myeloma progression by exosome-mediated activation of myeloid-derived suppressor cells. *Oncotarget* 2015; **6**: 43992-44004 [PMID: 26556857 DOI: 10.18632/oncotarget.6083]

178 **Huang Y**, Luo Y, Ou W, Wang Y, Dong D, Peng X. Exosomal lncRNA SNHG10 derived from colorectal cancer cells suppresses natural killer cell cytotoxicity by upregulating INHBC. *Cancer Cell Int* 2021; **21**: 528 [PMID: 34641864 DOI: 10.1186/s12935-021-02221-2]

179 **Liu J**, Chen Z, Li Y, Zhao W, Wu J, Zhang Z. PD-1/PD-L1 Checkpoint Inhibitors in Tumor Immunotherapy. *Front Pharmacol* 2021; **12**: 731798 [PMID: 34539412 DOI: 10.3389/fphar.2021.731798]

180 **Sun W**, Cui J, Ge Y, Wang J, Yu Y, Han B, Liu B. Tumor stem cell-derived exosomal microRNA-17-5p inhibits anti-

tumor immunity in colorectal cancer *via* targeting SPOP and overexpressing PD-L1. *Cell Death Discov* 2022; **8**: 223 [PMID: 35461336 DOI: 10.1038/s41420-022-00919-4]

181 **Høye AM**, Erler JT. Structural ECM components in the premetastatic and metastatic niche. *Am J Physiol Cell Physiol* 2016; **310**: C955-C967 [PMID: 27053524 DOI: 10.1152/ajpcell.00326.2015]

182 **Najafi M**, Farhood B, Mortezaee K. Extracellular matrix (ECM) stiffness and degradation as cancer drivers. *J Cell Biochem* 2019; **120**: 2782-2790 [PMID: 30321449 DOI: 10.1002/jcb.27681]

183 **Dai G**, Yao X, Zhang Y, Gu J, Geng Y, Xue F, Zhang J. Colorectal cancer cell-derived exosomes containing miR-10b regulate fibroblast cells *via* the PI3K/Akt pathway. *Bull Cancer* 2018; **105**: 336-349 [PMID: 29496262 DOI: 10.1016/j.bulcan.2017.12.009]

184 **Masamune A**, Yoshida N, Hamada S, Takikawa T, Nabeshima T, Shimosegawa T. Exosomes derived from pancreatic cancer cells induce activation and profibrogenic activities in pancreatic stellate cells. *Biochem Biophys Res Commun* 2018; **495**: 71-77 [PMID: 29111329 DOI: 10.1016/j.bbrc.2017.10.141]

185 **Sánchez CA**, Andahur EI, Valenzuela R, Castellón EA, Fullá JA, Ramos CG, Triviño JC. Exosomes from bulk and stem cells from human prostate cancer have a differential microRNA content that contributes cooperatively over local and pre-metastatic niche. *Oncotarget* 2016; **7**: 3993-4008 [PMID: 26675257 DOI: 10.18632/oncotarget.6540]

186 **Guo Y**, Ji X, Liu J, Fan D, Zhou Q, Chen C, Wang W, Wang G, Wang H, Yuan W, Ji Z, Sun Z. Effects of exosomes on pre-metastatic niche formation in tumors. *Mol Cancer* 2019; **18**: 39 [PMID: 30857545 DOI: 10.1186/s12943-019-0995-1]

187 **Grivennikov SI**, Greten FR, Karin M. Immunity, inflammation, and cancer. *Cell* 2010; **140**: 883-899 [PMID: 20303878 DOI: 10.1016/j.cell.2010.01.025]

188 **Lust JA**, Lacy MQ, Zeldenrust SR, Dispenzieri A, Gertz MA, Witzig TE, Kumar S, Hayman SR, Russell SJ, Buadi FK, Geyer SM, Campbell ME, Kyle RA, Rajkumar SV, Greipp PR, Kline MP, Xiong Y, Moon-Tasson LL, Donovan KA. Induction of a chronic disease state in patients with smoldering or indolent multiple myeloma by targeting interleukin 1{beta}-induced interleukin 6 production and the myeloma proliferative component. *Mayo Clin Proc* 2009; **84**: 114-122 [PMID: 19181644 DOI: 10.4065/84.2.114]

189 **Hong DS**, Angelo LS, Kurzrock R. Interleukin-6 and its receptor in cancer: implications for translational therapeutics. *Cancer* 2007; **110**: 1911-1928 [PMID: 17849470 DOI: 10.1002/cncr.22999]

190 **Pucci M**, Raimondo S, Urzì O, Moschetti M, Di Bella MA, Conigliaro A, Caccamo N, La Manna MP, Fontana S, Alessandro R. Tumor-Derived Small Extracellular Vesicles Induce Pro-Inflammatory Cytokine Expression and PD-L1 Regulation in M0 Macrophages *via* IL-6/STAT3 and TLR4 Signaling Pathways. *Int J Mol Sci* 2021; **22** [PMID: 34829995 DOI: 10.3390/ijms222212118]

191 **Guillerey C**, Nakamura K, Vuckovic S, Hill GR, Smyth MJ. Immune responses in multiple myeloma: role of the natural immune surveillance and potential of immunotherapies. *Cell Mol Life Sci* 2016; **73**: 1569-1589 [PMID: 26801219 DOI: 10.1007/s00018-016-2135-z]

192 **Shi C**, Yang Y, Xia Y, Okugawa Y, Yang J, Liang Y, Chen H, Zhang P, Wang F, Han H, Wu W, Gao R, Gasche C, Qin H, Ma Y, Goel A. Novel evidence for an oncogenic role of microRNA-21 in colitis-associated colorectal cancer. *Gut* 2016; **65**: 1470-1481 [PMID: 25994220 DOI: 10.1136/gutjnl-2014-308455]

193 **Balkwill F**. Tumour necrosis factor and cancer. *Nat Rev Cancer* 2009; **9**: 361-371 [PMID: 19343034 DOI: 10.1038/nrc2628]

194 **Patten DA**, Hussein E, Davies SP, Humphreys PN, Collett A. Commensal-derived OMVs elicit a mild proinflammatory response in intestinal epithelial cells. *Microbiology (Reading)* 2017; **163**: 702-711 [PMID: 28530169 DOI: 10.1099/mic.0.000468]

195 **Cao Y**, Wang Z, Yan Y, Ji L, He J, Xuan B, Shen C, Ma Y, Jiang S, Ma D, Tong T, Zhang X, Gao Z, Zhu X, Fang JY, Chen H, Hong J. Enterotoxigenic Bacteroidesfragilis Promotes Intestinal Inflammation and Malignancy by Inhibiting Exosome-Packaged miR-149-3p. *Gastroenterology* 2021; **161**: 1552-1566.e12 [PMID: 34371001 DOI: 10.1053/j.gastro.2021.08.003]

196 **Fabbri M**, Paone A, Calore F, Galli R, Gaudio E, Santhanam R, Lovat F, Fadda P, Mao C, Nuovo GJ, Zanesi N, Crawford M, Ozer GH, Wernicke D, Alder H, Caligiuri MA, Nana-Sinkam P, Perrotti D, Croce CM. MicroRNAs bind to Toll-like receptors to induce prometastatic inflammatory response. *Proc Natl Acad Sci U S A* 2012; **109**: E2110-E2116 [PMID: 22753494 DOI: 10.1073/pnas.1209414109]

197 **Katoh M**. Therapeutics targeting angiogenesis: genetics and epigenetics, extracellular miRNAs and signaling networks (Review). *Int J Mol Med* 2013; **32**: 763-767 [PMID: 23863927 DOI: 10.3892/ijmm.2013.1444]

198 **Momeny M**, Sabourinejad Z, Zarrinrad G, Moghaddaskho F, Eyvani H, Yousefi H, Mirshahvaladi S, Poursani EM, Barghi F, Poursheikhani A, Dardaei L, Bashash D, Ghazi-Khansari M, Tavangar SM, Dehpour AR, Yaghmaie M, Alimoghaddam K, Ghavamzadeh A, Ghaffari SH. Anti-tumour activity of tivozanib, a pan-inhibitor of VEGF receptors, in therapy-resistant ovarian carcinoma cells. *Sci Rep* 2017; **7**: 45954 [PMID: 28383032 DOI: 10.1038/srep45954]

199 **Skog J**, Würdinger T, van Rijn S, Meijer DH, Gainche L, Sena-Esteves M, Curry WT Jr, Carter BS, Krichevsky AM, Breakefield XO. Glioblastoma microvesicles transport RNA and proteins that promote tumour growth and provide diagnostic biomarkers. *Nat Cell Biol* 2008; **10**: 1470-1476 [PMID: 19011622 DOI: 10.1038/ncb1800]

200 **Zhang Q**, Peng C. Cancer-associated fibroblasts regulate the biological behavior of cancer cells and stroma in gastric cancer. *Oncol Lett* 2018; **15**: 691-698 [PMID: 29399141 DOI: 10.3892/ol.2017.7385]

201 **Richards KE**, Zeleniak AE, Fishel ML, Wu J, Littlepage LE, Hill R. Cancer-associated fibroblast exosomes regulate survival and proliferation of pancreatic cancer cells. *Oncogene* 2017; **36**: 1770-1778 [PMID: 27669441 DOI: 10.1038/onc.2016.353]

202 **Zhao H**, Yang L, Baddour J, Achreja A, Bernard V, Moss T, Marini JC, Tudawe T, Seviour EG, San Lucas FA, Alvarez H, Gupta S, Maiti SN, Cooper L, Peehl D, Ram PT, Maitra A, Nagrath D. Tumor microenvironment derived exosomes pleiotropically modulate cancer cell metabolism. *Elife* 2016; **5**: e10250 [PMID: 26920219 DOI: 10.7554/eLife.10250]

203 **Safaei R**, Larson BJ, Cheng TC, Gibson MA, Otani S, Naerdemann W, Howell SB. Abnormal lysosomal trafficking and enhanced exosomal export of cisplatin in drug-resistant human ovarian carcinoma cells. *Mol Cancer Ther* 2005; **4**: 1595-1604 [PMID: 16227410 DOI: 10.1158/1535-7163.MCT-05-0102]

204 **Shedden K**, Xie XT, Chandaroy P, Chang YT, Rosania GR. Expulsion of small molecules in vesicles shed by cancer cells: association with gene expression and chemosensitivity profiles. *Cancer Res* 2003; **63**: 4331-4337 [PMID: 12907600]

205 **Bebawy M**, Combes V, Lee E, Jaiswal R, Gong J, Bonhoure A, Grau GE. Membrane microparticles mediate transfer of P-glycoprotein to drug sensitive cancer cells. *Leukemia* 2009; **23**: 1643-1649 [PMID: 19369960 DOI: 10.1038/leu.2009.76]

206 **Yang SJ**, Wang DD, Li J, Xu HZ, Shen HY, Chen X, Zhou SY, Zhong SL, Zhao JH, Tang JH. Predictive role of GSTP1-containing exosomes in chemotherapy-resistant breast cancer. *Gene* 2017; **623**: 5-14 [PMID: 28438694 DOI: 10.1016/j.gene.2017.04.031]

207 **Wilson TR**, Johnston PG, Longley DB. Anti-apoptotic mechanisms of drug resistance in cancer. *Curr Cancer Drug Targets* 2009; **9**: 307-319 [PMID: 19442051 DOI: 10.2174/156800909788166547]

208 **Zhang S**, Zhang Y, Qu J, Che X, Fan Y, Hou K, Guo T, Deng G, Song N, Li C, Wan X, Qu X, Liu Y. Exosomes promote cetuximab resistance *via* the PTEN/Akt pathway in colon cancer cells. *Braz J Med Biol Res* 2017; **51**: e6472 [PMID: 29160412 DOI: 10.1590/1414-431X20176472]

209 **McCubrey JA**, Abrams SL, Fitzgerald TL, Cocco L, Martelli AM, Montalto G, Cervello M, Scalisi A, Candido S, Libra M, Steelman LS. Roles of signaling pathways in drug resistance, cancer initiating cells and cancer progression and metastasis. *Adv Biol Regul* 2015; **57**: 75-101 [PMID: 25453219 DOI: 10.1016/j.jbior.2014.09.016]

210 **Zheng P**, Luo Q, Wang W, Li J, Wang T, Wang P, Chen L, Zhang P, Chen H, Liu Y, Dong P, Xie G, Ma Y, Jiang L, Yuan X, Shen L. Tumor-associated macrophages-derived exosomes promote the migration of gastric cancer cells by transfer of functional Apolipoprotein E. *Cell Death Dis* 2018; **9**: 434 [PMID: 29567987 DOI: 10.1038/s41419-018-0465-5]

211 **Hu YB**, Yan C, Mu L, Mi YL, Zhao H, Hu H, Li XL, Tao DD, Wu YQ, Gong JP, Qin JC. Exosomal Wnt-induced dedifferentiation of colorectal cancer cells contributes to chemotherapy resistance. *Oncogene* 2019; **38**: 1951-1965 [PMID: 30390075 DOI: 10.1038/s41388-018-0557-9]

212 **Qin X**, Yu S, Zhou L, Shi M, Hu Y, Xu X, Shen B, Liu S, Yan D, Feng J. Cisplatin-resistant lung cancer cell-derived exosomes increase cisplatin resistance of recipient cells in exosomal miR-100-5p-dependent manner. *Int J Nanomedicine* 2017; **12**: 3721-3733 [PMID: 28553110 DOI: 10.2147/IJN.S131516]

213 **Wang J**, Zheng Y, Zhao M. Exosome-Based Cancer Therapy: Implication for Targeting Cancer Stem Cells. *Front Pharmacol* 2016; **7**: 533 [PMID: 28127287 DOI: 10.3389/fphar.2016.00533]

214 **Hu Y**, Yan C, Mu L, Huang K, Li X, Tao D, Wu Y, Qin J. Fibroblast-Derived Exosomes Contribute to Chemoresistance through Priming Cancer Stem Cells in Colorectal Cancer. *PLoS One* 2015; **10**: e0125625 [PMID: 25938772 DOI: 10.1371/journal.pone.0125625]

215 **Seo M**, Kim SM, Woo EY, Han KC, Park EJ, Ko S, Choi EW, Jang M. Stemness-Attenuating miR-503-3p as a Paracrine Factor to Regulate Growth of Cancer Stem Cells. *Stem Cells Int* 2018; **2018**: 4851949 [PMID: 29849663 DOI: 10.1155/2018/4851949]

216 **Fatima F**, Nawaz M. Stem cell-derived exosomes: roles in stromal remodeling, tumor progression, and cancer immunotherapy. *Chin J Cancer* 2015; **34**: 541-553 [PMID: 26369565 DOI: 10.1186/s40880-015-0051-5]

217 **Paolillo M**, Schinelli S. Integrins and Exosomes, a Dangerous Liaison in Cancer Progression. *Cancers (Basel)* 2017; **9** [PMID: 28933725 DOI: 10.3390/cancers9080095]

218 **Norcic G**. Liquid Biopsy in Colorectal Cancer-Current Status and Potential Clinical Applications. *Micromachines (Basel)* 2018; **9** [PMID: 30424233 DOI: 10.3390/mi9060300]

219 **Duffy MJ**, van Dalen A, Haglund C, Hansson L, Holinski-Feder E, Klapdor R, Lamerz R, Peltomaki P, Sturgeon C, Topolcan O. Tumour markers in colorectal cancer: European Group on Tumour Markers (EGTM) guidelines for clinical use. *Eur J Cancer* 2007; **43**: 1348-1360 [PMID: 17512720 DOI: 10.1016/j.ejca.2007.03.021]

220 **Bach DH**, Hong JY, Park HJ, Lee SK. The role of exosomes and miRNAs in drug-resistance of cancer cells. *Int J Cancer* 2017; **141**: 220-230 [PMID: 28240776 DOI: 10.1002/ijc.30669]

221 **Umwali Y**, Yue CB, Gabriel ANA, Zhang Y, Zhang X. Roles of exosomes in diagnosis and treatment of colorectal cancer. *World J Clin Cases* 2021; **9**: 4467-4479 [PMID: 34222415 DOI: 10.12998/wjcc.v9.i18.4467]

222 **Weber JA**, Baxter DH, Zhang S, Huang DY, Huang KH, Lee MJ, Galas DJ, Wang K. The microRNA spectrum in 12 body fluids. *Clin Chem* 2010; **56**: 1733-1741 [PMID: 20847327 DOI: 10.1373/clinchem.2010.147405]

223 **Lan H**, Lu H, Wang X, Jin H. MicroRNAs as potential biomarkers in cancer: opportunities and challenges. *Biomed Res Int* 2015; **2015**: 125094 [PMID: 25874201 DOI: 10.1155/2015/125094]

224 **Chen B**, Xia Z, Deng YN, Yang Y, Zhang P, Zhu H, Xu N, Liang S. Emerging microRNA biomarkers for colorectal cancer diagnosis and prognosis. *Open Biol* 2019; **9**: 180212 [PMID: 30958116 DOI: 10.1098/rsob.180212]

225 **Wang J**, Huang SK, Zhao M, Yang M, Zhong JL, Gu YY, Peng H, Che YQ, Huang CZ. Identification of a circulating microRNA signature for colorectal cancer detection. *PLoS One* 2014; **9**: e87451 [PMID: 24709885 DOI: 10.1371/journal.pone.0087451]

226 **Ogata-Kawata H**, Izumiya M, Kurioka D, Honma Y, Yamada Y, Furuta K, Gunji T, Ohta H, Okamoto H, Sonoda H, Watanabe M, Nakagama H, Yokota J, Kohno T, Tsuchiya N. Circulating exosomal microRNAs as biomarkers of colon cancer. *PLoS One* 2014; **9**: e92921 [PMID: 24705249 DOI: 10.1371/journal.pone.0092921]

227 **Toiyama Y**, Hur K, Tanaka K, Inoue Y, Kusunoki M, Boland CR, Goel A. Serum miR-200c is a novel prognostic and metastasis-predictive biomarker in patients with colorectal cancer. *Ann Surg* 2014; **259**: 735-743 [PMID: 23982750 DOI: 10.1097/SLA.0b013e3182a6909d]

228 **Min L**, Chen L, Liu S, Yu Y, Guo Q, Li P, Zhu S. Loss of Circulating Exosomal miR-92b is a Novel Biomarker of Colorectal Cancer at Early Stage. *Int J Med Sci* 2019; **16**: 1231-1237 [PMID: 31588188 DOI: 10.7150/ijms.34540]

229 **Baassiri A**, Nassar F, Mukherji D, Shamseddine A, Nasr R, Temraz S. Exosomal Non Coding RNA in LIQUID Biopsies as a Promising Biomarker for Colorectal Cancer. *Int J Mol Sci* 2020; **21** [PMID: 32092975 DOI: 10.3390/ijms21041398]

230 **Fu F**, Jiang W, Zhou L, Chen Z. Circulating Exosomal miR-17-5p and miR-92a-3p Predict Pathologic Stage and Grade of Colorectal Cancer. *Transl Oncol* 2018; **11**: 221-232 [PMID: 29367070 DOI: 10.1016/j.tranon.2017.12.012]

231 **Liu C**, Eng C, Shen J, Lu Y, Takata Y, Mehdizadeh A, Chang GJ, Rodriguez-Bigas MA, Li Y, Chang P, Mao Y, Hassan MM, Wang F, Li D. Serum exosomal miR-4772-3p is a predictor of tumor recurrence in stage II and III colon cancer.

Oncotarget 2016; **7**: 76250-76260 [PMID: 27788488 DOI: 10.18632/oncotarget.12841]

232 **Teng Y**, Ren Y, Hu X, Mu J, Samykutty A, Zhuang X, Deng Z, Kumar A, Zhang L, Merchant ML, Yan J, Miller DM, Zhang HG. MVP-mediated exosomal sorting of miR-193a promotes colon cancer progression. *Nat Commun* 2017; **8**: 14448 [PMID: 28211508 DOI: 10.1038/ncomms14448]

233 **Peng ZY**, Gu RH, Yan B. Downregulation of exosome-encapsulated miR-548c-5p is associated with poor prognosis in colorectal cancer. *J Cell Biochem* 2019; **120**: 1457-1463 [PMID: 30171732 DOI: 10.1002/jcb.27291]

234 **Li P**, Kaslan M, Lee SH, Yao J, Gao Z. Progress in Exosome Isolation Techniques. *Theranostics* 2017; **7**: 789-804 [PMID: 28255367 DOI: 10.7150/thno.18133]

235 **Johnstone RM**, Bianchini A, Teng K. Reticulocyte maturation and exosome release: transferrin receptor containing exosomes shows multiple plasma membrane functions. *Blood* 1989; **74**: 1844-1851 [PMID: 2790208]

236 **Lathe GH**, Ruthven CR. The separation of substances on the basis of their molecular weights, using columns of starch and water. *Biochem J* 1955; **60**: xxxiv [PMID: 13249976]

237 **Lv LL**, Cao Y, Liu D, Xu M, Liu H, Tang RN, Ma KL, Liu BC. Isolation and quantification of microRNAs from urinary exosomes/microvesicles for biomarker discovery. *Int J Biol Sci* 2013; **9**: 1021-1031 [PMID: 24250247 DOI: 10.7150/ijbs.6100]

238 **Thakur A**, Xu C, Li WK, Qiu G, He B, Ng SP, Wu CL, Lee Y. In vivo liquid biopsy for glioblastoma malignancy by the AFM and LSPR based sensing of exosomal CD44 and CD133 in a mouse model. *Biosens Bioelectron* 2021; **191**: 113476 [PMID: 34246124 DOI: 10.1016/j.bios.2021.113476]

239 **Tao L**, Chen K, Chen Z, Cong C, Qiu C, Chen J, Wang X, Chen H, Yu T, Xie W, Deng S, Xu JB. 1T' Transition Metal Telluride Atomic Layers for Plasmon-Free SERS at Femtomolar Levels. *J Am Chem Soc* 2018; **140**: 8696-8704 [PMID: 29927248 DOI: 10.1021/jacs.8b02972]

240 **Fu JH**, Zhong Z, Xie D, Guo YJ, Kong DX, Zhao ZX, Li M. SERS-Active MIL-100(Fe) Sensory Array for Ultrasensitive and Multiplex Detection of VOCs. *Angew Chem Int Ed Engl* 2020; **59**: 20489-20498 [PMID: 32743925 DOI: 10.1002/anie.202002720]

241 **Kırbaş OK**, Bozkurt BT, Asutay AB, Mat B, Ozdemir B, Öztürkoğlu D, Ölmez H, İşlek Z, Şahin F, Taşlı PN. Optimized Isolation of Extracellular Vesicles From Various Organic Sources Using Aqueous Two-Phase System. *Sci Rep* 2019; **9**: 19159 [PMID: 31844310 DOI: 10.1038/s41598-019-55477-0]

242 **Fais S**, O'Driscoll L, Borras FE, Buzas E, Camussi G, Cappello F, Carvalho J, Cordeiro da Silva A, Del Portillo H, El Andaloussi S, Ficko Trček T, Furlan R, Hendrix A, Gursel I, Kralj-Iglic V, Kaeffer B, Kosanovic M, Lekka ME, Lipps G, Logozzi M, Marcilla A, Sammar M, Llorente A, Nazarenko I, Oliveira C, Pocsfalvi G, Rajendran L, Raposo G, Rohde E, Siljander P, van Niel G, Vasconcelos MH, Yáñez-Mó M, Yliperttula ML, Zarovni N, Zavec AB, Giebel B. Evidence-Based Clinical Use of Nanoscale Extracellular Vesicles in Nanomedicine. *ACS Nano* 2016; **10**: 3886-3899 [PMID: 26978483 DOI: 10.1021/acsnano.5b08015]

243 **Karimi N**, Cvjetkovic A, Jang SC, Crescitelli R, Hosseinpour Feizi MA, Nieuwland R, Lötvall J, Lässer C. Detailed analysis of the plasma extracellular vesicle proteome after separation from lipoproteins. *Cell Mol Life Sci* 2018; **75**: 2873-2886 [PMID: 29441425 DOI: 10.1007/s00018-018-2773-4]

244 **Zaharie F**, Muresan MS, Petrushev B, Berce C, Gafencu GA, Selicean S, Jurj A, Cojocneanu-Petric R, Lisencu CI, Pop LA, Pileczki V, Eniu D, Muresan MA, Zaharie R, Berindan-Neagoe I, Tomuleasa C, Irimie A. Exosome-Carried microRNA-375 Inhibits Cell Progression and Dissemination *via* Bcl-2 Blocking in Colon Cancer. *J Gastrointestin Liver Dis* 2015; **24**: 435-443 [PMID: 26697569 DOI: 10.15403/jgld.2014.1121.244.375]

245 **Liu D**, Chen C, Cui M, Zhang H. miR-140-3p inhibits colorectal cancer progression and its liver metastasis by targeting BCL9 and BCL2. *Cancer Med* 2021; **10**: 3358-3372 [PMID: 33838016 DOI: 10.1002/cam4.3840]

246 **Yan S**, Ren X, Yang J, Wang J, Zhang Q, Xu D. Exosomal miR-548c-5p Regulates Colorectal Cancer Cell Growth and Invasion Through HIF1A/CDC42 Axis. *Onco Targets Ther* 2020; **13**: 9875-9885 [PMID: 33116573 DOI: 10.2147/OTT.S273008]

247 **Hu JL**, He GY, Lan XL, Zeng ZC, Guan J, Ding Y, Qian XL, Liao WT, Ding YQ, Liang L. Inhibition of ATG12-mediated autophagy by miR-214 enhances radiosensitivity in colorectal cancer. *Oncogenesis* 2018; **7**: 16 [PMID: 29459645 DOI: 10.1038/s41389-018-0028-8]

248 **Johnsen KB**, Gudbergsson JM, Skov MN, Pilgaard L, Moos T, Duroux M. A comprehensive overview of exosomes as drug delivery vehicles - endogenous nanocarriers for targeted cancer therapy. *Biochim Biophys Acta* 2014; **1846**: 75-87 [PMID: 24747178 DOI: 10.1016/j.bbcan.2014.04.005]

249 **Ha D**, Yang N, Nadithe V. Exosomes as therapeutic drug carriers and delivery vehicles across biological membranes: current perspectives and future challenges. *Acta Pharm Sin B* 2016; **6**: 287-296 [PMID: 27471669 DOI: 10.1016/j.apsb.2016.02.001]

250 **Gilligan KE**, Dwyer RM. Engineering Exosomes for Cancer Therapy. *Int J Mol Sci* 2017; **18** [PMID: 28538671 DOI: 10.3390/ijms18061122]

251 **Blanco E**, Shen H, Ferrari M. Principles of nanoparticle design for overcoming biological barriers to drug delivery. *Nat Biotechnol* 2015; **33**: 941-951 [PMID: 26348965 DOI: 10.1038/nbt.3330]

252 **Srivastava A**, Amreddy N, Razaq M, Towner R, Zhao YD, Ahmed RA, Munshi A, Ramesh R. Exosomes as Theranostics for Lung Cancer. In: Broome AM, editor Cancer Nanotechnology-Book, 2018: 1-33

253 **Tian Y**, Li S, Song J, Ji T, Zhu M, Anderson GJ, Wei J, Nie G. A doxorubicin delivery platform using engineered natural membrane vesicle exosomes for targeted tumor therapy. *Biomaterials* 2014; **35**: 2383-2390 [PMID: 24345736 DOI: 10.1016/j.biomaterials.2013.11.083]

254 **Yang T**, Martin P, Fogarty B, Brown A, Schurman K, Phipps R, Yin VP, Lockman P, Bai S. Exosome delivered anticancer drugs across the blood-brain barrier for brain cancer therapy in Danio rerio. *Pharm Res* 2015; **32**: 2003-2014 [PMID: 25609010 DOI: 10.1007/s11095-014-1593-y]

255 **Kamerkar S**, LeBleu VS, Sugimoto H, Yang S, Ruivo CF, Melo SA, Lee JJ, Kalluri R. Exosomes facilitate therapeutic targeting of oncogenic KRAS in pancreatic cancer. *Nature* 2017; **546**: 498-503 [PMID: 28607485 DOI: 10.1038/nature22341]

256 **Kim MS**, Haney MJ, Zhao Y, Mahajan V, Deygen I, Klyachko NL, Inskoe E, Piroyan A, Sokolsky M, Okolie O, Hingtgen SD, Kabanov AV, Batrakova EV. Development of exosome-encapsulated paclitaxel to overcome MDR in cancer cells. *Nanomedicine* 2016; **12**: 655-664 [PMID: 26586551 DOI: 10.1016/j.nano.2015.10.012]

257 **Batrakova EV**, Kim MS. Using exosomes, naturally-equipped nanocarriers, for drug delivery. *J Control Release* 2015; **219**: 396-405 [PMID: 26241750 DOI: 10.1016/j.jconrel.2015.07.030]

258 **Alvarez-Erviti L**, Seow Y, Yin H, Betts C, Lakhal S, Wood MJ. Delivery of siRNA to the mouse brain by systemic injection of targeted exosomes. *Nat Biotechnol* 2011; **29**: 341-345 [PMID: 21423189 DOI: 10.1038/nbt.1807]

259 **Luan X**, Sansanaphongpricha K, Myers I, Chen H, Yuan H, Sun D. Engineering exosomes as refined biological nanoplatforms for drug delivery. *Acta Pharmacol Sin* 2017; **38**: 754-763 [PMID: 28392567 DOI: 10.1038/aps.2017.12]

260 **Lu B**, Huang X, Mo J, Zhao W. Drug Delivery Using Nanoparticles for Cancer Stem-Like Cell Targeting. *Front Pharmacol* 2016; **7**: 84 [PMID: 27148051 DOI: 10.3389/fphar.2016.00084]

261 **Liu Y**, Gu Y, Han Y, Zhang Q, Jiang Z, Zhang X, Huang B, Xu X, Zheng J, Cao X. Tumor Exosomal RNAs Promote Lung Pre-metastatic Niche Formation by Activating Alveolar Epithelial TLR3 to Recruit Neutrophils. *Cancer Cell* 2016; **30**: 243-256 [PMID: 27505671 DOI: 10.1016/j.ccell.2016.06.021]

262 **Valencia K**, Luis-Ravelo D, Bovy N, Antón I, Martínez-Canarias S, Zandueta C, Ormazábal C, Struman I, Tabruyn S, Rebmann V, De Las Rivas J, Guruceaga E, Bandrés E, Lecanda F. miRNA cargo within exosome-like vesicle transfer influences metastatic bone colonization. *Mol Oncol* 2014; **8**: 689-703 [PMID: 24593875 DOI: 10.1016/j.molonc.2014.01.012]

263 **Bourderioux M**, Nguyen-Khoa T, Chhuon C, Jeanson L, Tondelier D, Walczak M, Ollero M, Bekri S, Knebelmann B, Escudier E, Escudier B, Edelman A, Guerrera IC. A new workflow for proteomic analysis of urinary exosomes and assessment in cystinuria patients. *J Proteome Res* 2015; **14**: 567-577 [PMID: 25365230 DOI: 10.1021/pr501003q]

264 **Morse MA**, Garst J, Osada T, Khan S, Hobeika A, Clay TM, Valente N, Shreeniwas R, Sutton MA, Delcayre A, Hsu DH, Le Pecq JB, Lyerly HK. A phase I study of dexosome immunotherapy in patients with advanced non-small cell lung cancer. *J Transl Med* 2005; **3**: 9 [PMID: 15723705 DOI: 10.1186/1479-5876-3-9]

265 **Dai S**, Wei D, Wu Z, Zhou X, Wei X, Huang H, Li G. Phase I clinical trial of autologous ascites-derived exosomes combined with GM-CSF for colorectal cancer. *Mol Ther* 2008; **16**: 782-790 [PMID: 18362931 DOI: 10.1038/mt.2008.1]

World Journal of Gastrointestinal Oncology

Submit a Manuscript: https://www.f6publishing.com

World J Gastrointest Oncol 2023 May 15; 15(5): 757-775

DOI: 10.4251/wjgo.v15.i5.757

ISSN 1948-5204 (online)

REVIEW

Immuno-oncology-microbiome axis of gastrointestinal malignancy

Quan Lin, Shi-Wei Guan, Hai-Bo Yu

Specialty type: Oncology

Provenance and peer review: Invited article; Externally peer reviewed.

Peer-review model: Single blind

Peer-review report's scientific quality classification

Grade A (Excellent): 0
Grade B (Very good): B, B
Grade C (Good): 0
Grade D (Fair): 0
Grade E (Poor): 0

P-Reviewer: Ekine-Afolabi B, United Kingdom; Paparoupa M, Germany

Received: December 26, 2022
Peer-review started: December 26, 2022
First decision: March 13, 2023
Revised: March 15, 2023
Accepted: April 14, 2023
Article in press: April 14, 2023
Published online: May 15, 2023

Quan Lin, Shi-Wei Guan, Hai-Bo Yu, Department of Surgery, Wenzhou Central Hospital, The Dingli Clinical Institute of Wenzhou Medical University, Wenzhou 325000, Zhejiang Province, China

Corresponding author: Hai-Bo Yu, MD, Chief Doctor, Department of Surgery, Wenzhou Central Hospital, The Dingli Clinical Institute of Wenzhou Medical University, No. 252 Baili East Road, Wenzhou 325000, Zhejiang Province, China. yuhaibozjwz@163.com

Abstract

Research on the relationship between the microbiome and cancer has been controversial for centuries. Recent works have discovered that the intratumor microbiome is an important component of the tumor microenvironment (TME). Intratumor bacteria, the most studied intratumor microbiome, are mainly localized in tumor cells and immune cells. As the largest bacterial reservoir in human body, the gut microbiome may be one of the sources of the intratumor microbiome in gastrointestinal malignancies. An increasing number of studies have shown that the gut and intratumor microbiome play an important role in regulating the immune tone of tumors. Moreover, it has been recently proposed that the gut and intratumor microbiome can influence tumor progression by modulating host metabolism and the immune and immune tone of the TME, which is defined as the immuno-oncology-microbiome (IOM) axis. The proposal of the IOM axis provides a new target for the tumor microbiome and tumor immunity. This review aims to reveal the mechanism and progress of the gut and intratumor microbiome in gastrointestinal malignancies such as esophageal cancer, gastric cancer, liver cancer, colorectal cancer and pancreatic cancer by exploring the IOM axis. Providing new insights into the research related to gastrointestinal malignancies.

Key Words: Gut microbiome; Intratumor microbiome; Gastrointestinal malignancy; Tumor microenvironment; Immunity; Therapy

Core Tip: The gut and intratumor microbiome can influence tumor progression by modulating host metabolism and the immune and immune tone of the tumor microenvironment, which is defined as the immuno-oncology-microbiome (IOM) axis. The proposed the IOM axis provides a new target for tumor microbiome and tumor immunity. Current studies have shown that immunotherapy with fecal microbiota transplantation or microbial metabolism have certain effects. This review aims to explore the mechanism of the IOM axis of gastrointestinal malignancies, to reveal the mechanism and progress of gut and intratumor microbiome in gastrointestinal malignancies. Providing new insights into the research related to gastrointestinal malignancies.

Citation: Lin Q, Guan SW, Yu HB. Immuno-oncology-microbiome axis of gastrointestinal malignancy. *World J Gastrointest Oncol* 2023; 15(5): 757-775
URL: https://www.wjgnet.com/1948-5204/full/v15/i5/757.htm
DOI: https://dx.doi.org/10.4251/wjgo.v15.i5.757

INTRODUCTION

According to statistics, gastrointestinal tumors were one of the leading causes of death in the United States in 2020[1]. Improving the survival rate of patients with gastrointestinal tumors has always been an urgent task. In recent years, with the deepening of research on tumor immunity, various immune checkpoint inhibitors (ICIs) have shown great effects in clinical practice[2,3]. Among gastrointestinal tumors, there appears to be heterogeneity in the effect of immunotherapy across different tumor types [4,5]. Pembrolizumab improves the prognosis of patients with esophageal cancer (EC)[4]. However, the effect of niraparib plus nivolumab in pancreatic cancer was not satisfactory[5]. Recent studies have described that the gut microbiome can reprogram tumor microenvironment (TME) immunity by participating in innate and/or adaptive immunity[6]. Regulation of the microbiome can enhance the effectiveness of immunotherapy[7]. Of all tumors, gastrointestinal malignancies have received the most attention due to their large number of microbial residues in the gut[8]. Using microorganisms as one of the targets of immunotherapeutic effects seems to be an effective measure.

The human microbiome inhabits every surface and cavity of the body[9], including bacteria, archaea, eukaryotes, and viruses that colonize humans[10]. The microbiome affects overall immune function through many different mechanisms, resulting in a broad response from resistance to immune activation[10]. The gut microbiome has long been recognized as playing a major role in human health and disease[6], influencing host metabolism and shaping the immune system and disease conditions, including cancer[11]. The gut microbiota plays a key role in shaping the immune system[12]. The human gut microbiota can influence the development and progression of gastrointestinal tumors by disrupting DNA, activating oncogenic signaling pathways, producing protumor metabolites, and suppressing antitumor immune responses[13,14]. In recent years, with increasing research on the relationship between tumors and the microbiome, tumor tissues that were previously considered sterile are rich in microorganisms. After statistical analysis, the bacterial composition in tumor tissue is approximately 0.68%, equivalent to approximately 10^5 to 10^6 bacteria per 1 cm^3 of tumor tissue[15,16]. Although the abundance of microorganisms is relatively lower for tumor genomes, this intratumor microbiome is a potentially important player in tumor progression[15]. The intratumor microbiome is mainly intracellular and present in cancer cells and immune cells[17]. The gut and intratumor microbiome can influence tumor progression by modulating host metabolism and the immune and immune tone of the TME, and these immune-mediated interactions and collective feedback loops have been defined as the he immuno-oncology-microbiome (IOM) axis[15]. The proposal of the IOM axis provides a new target for the tumor microbiome and tumor immunity. This review aims to reveal the mechanism and progress of the gut and intratumor microbiome and gastrointestinal malignancies by exploring the mechanism of the IOM axis in gastrointestinal malignancies. Providing new insights into the research related to gastrointestinal malignancies.

COLORECTAL CANCER

Colorectal cancer (CRC) is one of the most common cancers in humans, with a leading incidence rate [18]. The initiation of CRC is a heterogeneous process that is influenced by the environment, microbial exposure, and host immunity[9]. Interactions between CRC and the microbiome have been revealed in numerous studies, with increasing evidence highlighting the critical role of the TME in the initiation and progression of carcinogenesis. In this microenvironment, multiple relationships between tumor development, immune responses, and the microbiome have been identified. All stages of CRC are accompanied by an immune response[19]. The regulation of the tumor immune response by the

microbiome plays an important role in the pathogenesis of CRC (Figure 1).

Tumor-infiltrating lymphocytes (TILs) are beneficial to the survival of human CRC[8,19]. One of the features of CRC is a strong imbalance of T cells[9,20]. One of the features of CRC is a strong imbalance of T cells[21]. Tosolini *et al*[22] analyzed T helper (Th) cell subsets in CRC and found that the expression of immune markers was different in adjacent mucosa and tumor tissue, suggesting that specific Th cell subsets were recruited at the tumor site. Experiments by Cremonesi *et al*[20] showed that infiltration of different T-cell subsets in CRC correlated with the expression of well-defined chemokine genes such as chemokine (C-C motif) ligand (CCL)3, CCL4, and CCL20. Exposure of tumor cells to gut bacteria induced upregulation of most chemokine genes by flow cytometry[20]. Upregulation of chemokines leads to higher T-cell recruitment into tumor xenografts. Therefore, whether CRC cells are exposed to intestinal bacteria and the degree of exposure may be one of the factors that affect the abundance of TILs. However, *Fusobacterium nucleatum* (*F. nucleatum*)[23-25], which is abundantly enriched within CRC tumors, can interact with the immune cell inhibitory receptor T-cell immunoglobulin (Ig) and ITIM domain expressed by TILs through the adhesin Fap2, inhibiting the activity of tumor-infiltrating T cells and protecting tumor cells from immune cell attack[26]. The effect of *F. nucleatum* on T cells may not be limited to this. *In vitro* experiments have shown that *F. nucleatum* inhibitory protein can block human T cells in the G1 phase of the cell cycle to prevent their proliferation[27]. *F. nucleatum* can also use the trimeric autotransporter adhesin CbpF on its surface, inhibiting T-cell function by activating the inhibitory receptor carcinoembryonic antigen cell adhesion molecule 1[28].

Th17 cells were found to be elevated to promote tumorigenesis[29]. Microbial metabolites penetrate tumors, activate tumor-associated bone marrow cells, and mediate interleukin (IL)-23 secretion. In turn, the IL-23-driven Th17 response can promote tumor growth. Enterotoxigenic *Bacteroides fragilis*, on the other hand, increases IL-17 expression by triggering a Th17-type inflammatory response, which shifts the colonic epithelium from an inflammatory to an oncogenic state[30]. The mechanism of bacterial induction of carcinogenesis can be explained by the hypothesis of the "bacterial driver–passenger model", in which "driver bacteria" of CRC promote tumorigenesis by inducing a sustained Th17 type inflammatory response, which is subsequently replaced by opportunistic "passenger bacteria" within the tumor, disrupting local innate immunity and ultimately leading to cancer progression[30]. Group 3 innate lymphoid cells (ILC3s) are the innate counterpart of Th17 cells, which modulate adaptive Th17 cell responses and act with Th17 cells against extracellular microorganisms[31]. ILCs are lymphocytes that do not express multiple antigen receptor types expressed on T and B cells[31] and play a key role in regulating host-microorganism interactions on the intestinal mucosal barrier surface[21,32]. ILC3s are abundant in mucosal sites and are involved in the innate immune response to extracellular bacteria and the suppression of gut commensal bacteria[31], and intestinal T cells control microbiota composition and intestinal immune response[33]. One study found that CRC is characterized by a significant decrease in ILC3s, accompanied by an increase in Th17 cells, suggesting that the progression of CRC is associated with impaired dialog between gut innate and adaptive immunity[21]. Whereas ILC3s and effector T cells interact *via* major histocompatibility complex class II (MHCII), this experiment found that deletion of ILC3-specific MHCII in mice lead to increased CRC invasiveness and susceptibility. Thus, the disruption of the interaction between MHCII^{+} ILC3s, effector T cells, and microbiota may be a mechanism to increase CRC invasiveness. In addition, gut commensal fungi, such as *Candida albicans* (*C. albicans*), promoted CRC tumorigenesis in animal experiments[34]. Commensal fungi activate glycolysis and IL-7 production in macrophages, while IL-7 induces IL-22 production in ILC3s, leading to tumor progression. However, other studies suggest that ILC3s in the TME may have both pro- and antitumor functions, depending on the cytokine types in the microenvironment[35,36].

Macrophages play a vital role in the maintenance of the innate immune response[37]. Tumor-associated macrophages (TAMs) are the main component of immune cells in the TME. On the one hand, M1 TAMs are induced by cytokines such as tumor necrosis factor (TNF)-α, secrete IL-6 and IL-23, participate in the polarized Th1 response, and exert antitumor immunity[37,38]. *Akkermansia muciniphila* (*A. muciniphila*) is a gut probiotic. Compared with the control group, the levels of M1-like TAMs were increased in *A. Muciniphila*-treated Apc$^{Min/+}$ mice, and M1-like TAM-related cytokines, such as IL-23, TNF-α, and IL-27, were significantly induced in CRC[39]. It was also shown that *A. Muciniphila* promotes the enrichment of M1-like macrophages in a nucleotide-binding and oligomerization domain-like receptor thermal protein domain associated protein 3 (NLRP3)-dependent manner *in vivo* and *in vitro*, acting as a suppressor of CRC proliferation. NLRP3 activation and macrophage phenotypic polarization may be induced by toll-like receptor (TLR) 2. On the other hand, M2 is the main phenotype of TAMs. M2 TAMs are induced by IL-4, IL-10, and IL-13, secrete anti-inflammatory cytokines such as IL-10 and IL-1β, and participate in the polarized Th2 response, while activated Th2 cells produce lymphocytes producing IL-4 and IL-13, enhancing the expression of epidermal growth factor in TAMs and promoting the occurrence and development of tumors[37,38]. Gut dysbacteriosis results in increased expression of cathepsin K (CTSK) in colon cancer cells, and CTSK binds to TLR4 to stimulate M2 polarization of TAMs *via* the mechanistic target of rapamycin-dependent pathway[40]. At the same time, CTSK can stimulate M2 TAMs to secrete cytokines, including IL-10 and IL-17, which in turn mediate CRC cell invasion and metastasis through the nuclear factor kappa B (NF-κB) pathway. In addition to dysbacteriosis, *F. nucleatum* can also promote macrophage infiltration through CCL20 activation while inducing polarization of M2 macrophages to promote CRC metastasis[41].

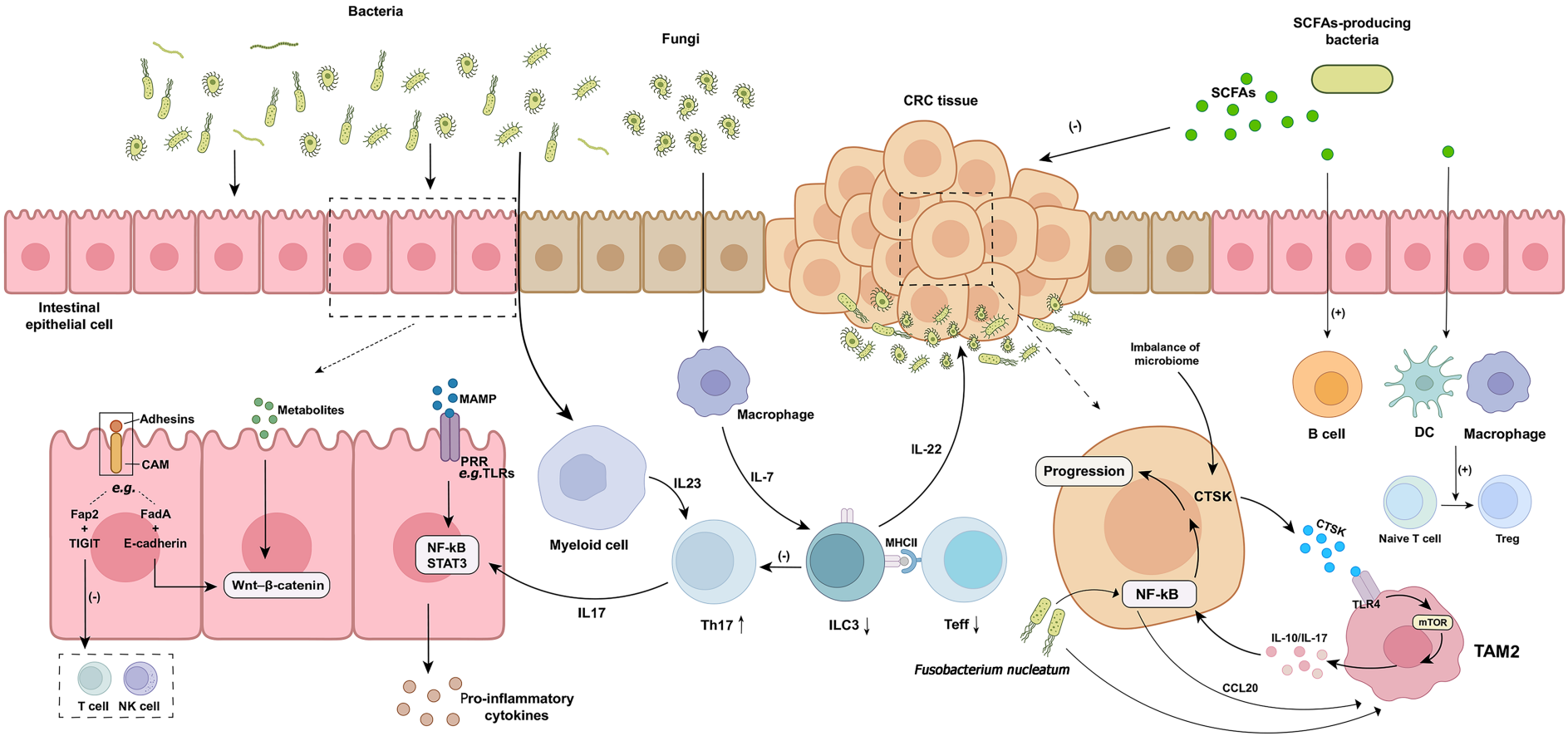

DOI: 10.4251/wjgo.v15.i5.757 **Copyright** ©The Author(s) 2023.

Figure 1 The role of microbiome in the occurrence and development of colorectal cancer. Microbiome influences the occurrence and development of colorectal cancer through a variety of mechanisms. Microbiome and their metabolites can induce tumorigenesis through direct mutagenesis of intestinal epithelial cells or activation of intracellular carcinogenic signals. Bacterial metabolites can also trigger the release of pro-inflammatory signals, which further promote tumorigenesis. Pathogenic bacteria or their products activate tumor-associated myeloid cells and induce tumor-promoting inflammation. Symbiotic fungi activate the production of interleukin (IL)-7 in macrophages and induce the production of IL-22 in ILC3, leading to tumor progression. ILC3s inhibited Th17 cells and intestinal inflammation. ILC3s decreased significantly and Th17 increased in colorectal cancer. The dialogue between ILC3s, effector T cell and major histocompatibility complex class II is disrupted by colorectal cancer and intestinal inflammation, promoting the progress of colorectal cancer. *Fusobacterium nucleatum* upregulates the expression of chemokine (C-C motif) ligand 20 through nuclear factor-κB and induces M2 macrophages to polarize and promote tumor metastasis. Cathepsin K mediates tumor invasion and metastasis. Short chain fatty acids directly inhibits tumor cell growth and induces host macrophage, T and B cell responses to protect colitis-induced colorectal cancer. CRC: Colorectal cancer; CAM: Cell adhesion molecule; FadA: Fusobacterium adhesin A; TIGIT: T-cell immunoglobulin and ITIM domain; MAMP: Microbe-associated molecular pattern; PRR: Pattern recognition receptor; NF-κB: Nuclear factor-κB; STAT3: Signal transducer and activator of transcription 3; MHCII: Major histocompatibility complex class II; Teff: Effector T cell; CTSK: Cathepsin K; TLR4: Toll-like receptor 4; TAM: Tumor-associated macrophages; SCFA: Short chain fatty acid; DC: Dendritic cell; IL: Interleukin; NK: Natural killer; CCL20: Chemokine (C-C motif) ligand 20.

TAMs can also promote the proliferation and invasion of tumor cells by interacting with tumor cells through microbiota-derived exosomes[37]. Microbiota-derived exosomes have the potential to activate macrophages. The extracellular vesicles released from bacteria are named outer membrane vesicles, and the coculture of outer membrane vesicles and macrophages leads to a large production of type M1 and M2 cytokines and chemokines. TLRs are an important component of the host defense mediated by the innate immune system[39] and are also involved in tumorigenesis[40]. Colon epithelial cells can sense the gut microbiome through pattern recognition receptors, including TLRs[42]. Thus, bacterial-induced chemokine gene expression is most likely initiated when TLRs trigger tumor cells[20].

In addition to the microbiome itself, microbiota-derived metabolites are also significant factors in the regulation of TME formation[43]. It is an important mediator of host-microbiome interactions[44]. Short-chain fatty acids (SCFAs), beneficial metabolites of the gut microbiome, are fermented from dietary fiber, including acetic acid, propionic acid, and butyrate[43-46]. SCFAs regulate intestinal motility and energy metabolism by secreting peptides YY and glucagon-like peptide 1 from intestinal endocrine L cells, directly inhibiting tumor cell growth and inducing host macrophage, T-cell and B-cell responses to protect against colitis-induced CRC[45].

Of these, butyrate is the most relevant bacterial metabolite of SCFAs[47] and has important immunomodulatory functions that can mediate the switching of pro-inflammatory cytokine expression by inhibiting histone deacetylases[48]. The significant reduction in butyrate-producing bacteria in the gut microbiome of patients with CRC may constitute a major structural imbalance in the gut microbiome of patients with CRC[49]. Thus, SCFAs play an important role in regulating host energy metabolism and the immune system[50]. Studies have shown that supplementation with probiotics that produce SCFAs can inhibit the development of intestinal tumors[51,52]. However, under certain conditions, butyrate metabolized by microorganisms may have the opposite effect. Several studies have shown that at lower concentrations, butyrate may stimulate the proliferation of colonic epithelial cells and thus promote CRC[53,54]. This discrepancy in the effects of butyrate on CRC is known as the "butyrate paradox"[53,54]. Therefore, increasing metabolites, such as SCFAs, has the potential to be used as an adjuvant treatment and preventive measure for CRC. However, it is necessary to further explore the action threshold of butyrate to avoid the opposite effect. Another gut bacterial metabolite, conjugated linoleic acid (CLA), is one of the most important fatty acids in the gut and is mainly produced by *Roseburia species*[55]. The reduction in *Roseburia species* was closely associated with the occurrence of CRC[49]. CLA also inhibits TNF-α expression and induces the immunomodulatory cytokine transforming growth factor β1 (TGF-β1) to participate in and regulate the pathways of apoptosis and immune response, reducing the risk of CRC[56]. Thus, the antiproliferative and anti-inflammatory capacity of CLA on colon cells may play an important role in CLA's protection of the host against CRC[57].

GASTRIC CANCER

Gastric cancer (GC) is the fifth most common cancer in the world and the third most common cause of cancer death[58]. The host microbiome is closely associated with the occurrence and development of GC. The gastric microbiome affects inflammation and immunity at the local mucosal level and systemically. Disorders in the close interaction between the gastric microbiome and the immune system in the TME may contribute to GC development by triggering a tumor-promoting immune response[59] (Figure 2).

Helicobacter pylori (H. pylori) infection is a risk factor for GC[60]. *H. pylori* colonizes the gastric mucosa of up to 50% of the population, manipulating host tissue to establish and maintain an immunosuppressive environment for chronic infection[61]. *H. pylori* inhibits the effector functions of $CD4^+$ T cells, dendritic cells (DCs), and macrophages by altering the cross-presentation activity of DCs to suppress antitumor $CD8^+$ T-cell responses, thereby suppressing the innate and adaptive immune responses of the infected host[61,62]. During GC formation, *H. pylori* may actively participate in GC by altering gastric mucosal immunity, particularly regulatory T (Treg)/Th17 imbalance[61]. *H. pylori* can also produce virulence factors (*e.g.*, VacA, γ-GT, DupA) to impair immune cell activity[63]. For example, VacA affects the inflammatory response of the host primarily by inhibiting the proliferation and effector functions of T cells[63], but also induces the proinflammatory effects of T cells by activating nuclear factor kappa B and leading to the upregulation of IL-8[64]. γ-GT induces T-cell cycle block by disrupting RAS signaling and inhibits T-cell proliferation[65]. DupA increases the expression of proinflammatory cytokines (*e.g.*, IL-12 and IL-23) *via* monocytes[66]. However, only *H. pylori* colonization in the stomach is not sufficient to induce gastric carcinogenesis[61]. In the past, the human stomach was thought to be the only habitat for *H. pylori* and was considered unsuitable for microbial habitation. However, recently, various studies have demonstrated that different gastric environments result in different microbial ecosystems within the stomach, and changes in specific microbial species may make the gastric microbiome more carcinogenic[67]. Bacteria other than *H. pylori* were previously thought to be unrelated to the development of GC[60]. Lofgren *et al*[68] demonstrated that the presence of a complex microbiome promoted the development of *H. pylori*-induced GC. However, the specific mechanism of the intragastric microbiome interaction with *H. pylori* on immunity remains unclear.

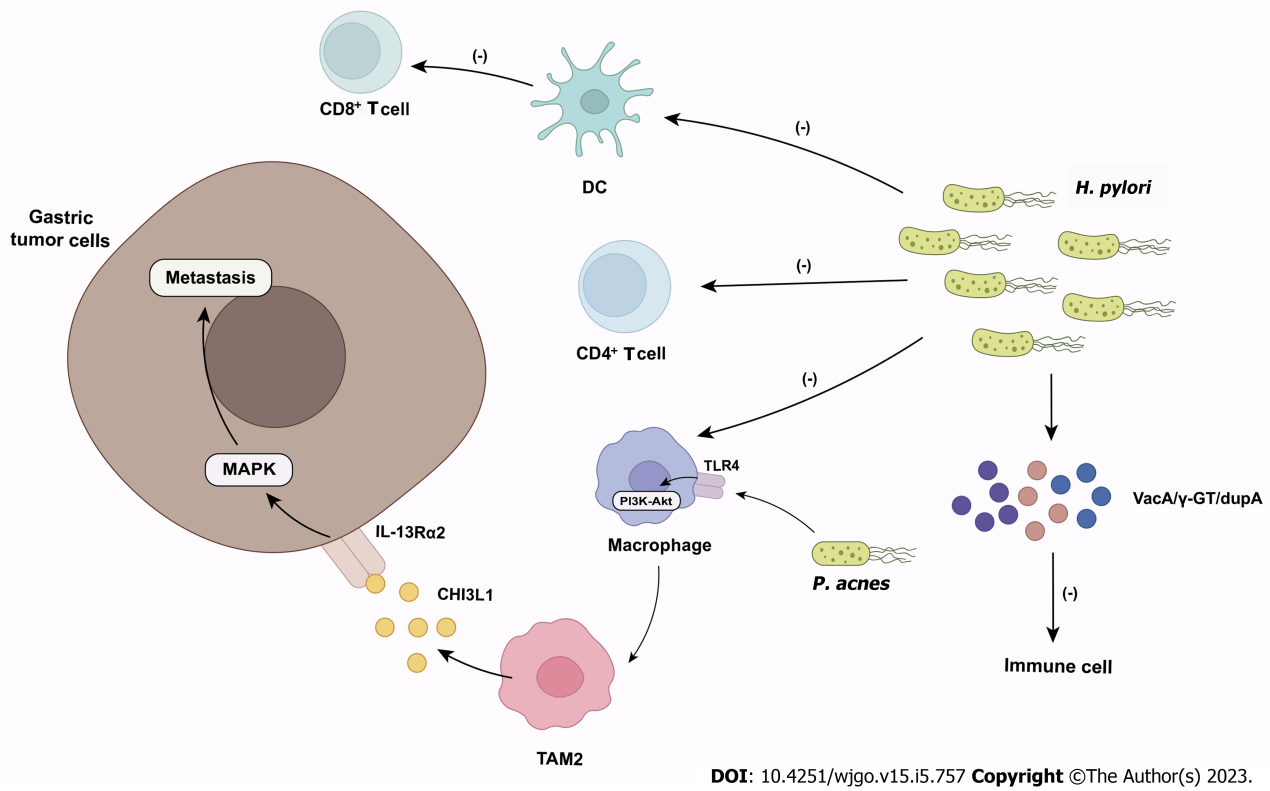

DOI: 10.4251/wjgo.v15.i5.757

Figure 2 The role of microbiome in gastric cancer. *Helicobacter pylori* inhibits the effector functions of CD4⁺ T cells, dendritic cells and macrophages and suppresses antitumor CD8⁺ T cell responses by altering the cross-presentation activity of dendritic cells. *Helicobacter pylori* also produce virulence factors (*e.g.*, VacA, γ-GT, dupA) to impair immune cell activity. *Propionibacterium acnes* promote M2 polarization of macrophages *via* toll-like receptor 4/PI3K/Akt signaling. M2 macrophages secrete chitinase 3-like protein 1 that binds specifically to the interleukin-13 receptor α2 chai of tumor cells, triggering the mitogen-activated protein kinase signaling pathway and promoting gastric cancer metastasis. DC: Dendritic cell; TLR4: Toll-like receptor 4; TAM: Tumor-associated macrophages; CHI3L1: Chitinase 3-like protein 1; IL-13Rα2: Interleukin-13 receptor α2 chain; MAPK: Mitogen-activated protein kinase; *H. pylori*: *Helicobacter pylori*; *P. acnes*: *Propionibacterium acnes*.

The microbial diversity and abundance in GC tumors were higher than those in nontumor tissues[67, 69]. The intratumoral microbiome influences GC by modulating immune responses in the TME. A recent study by Peng *et al*[59] found that the infiltration of CD8⁺ tissue-resident memory T cells (TRM cells) in the TME of patients with GC is negatively correlated with the abundance of *Methylobacterium* in gastric tumors. The population of memory T cells in TILs, known as TRM cells, is derived from T cells that enter tissues during the primary response (such as in response to viral invasion) and plays a role in tumor immune surveillance[70]. CD8⁺ TRM cells produce and release various cytokines, such as interferon-γ (IFN-γ), which promote the activation of other immune cells and play an important role in antitumor immunity[71]. Intratumor *Methylobacterium* may promote the development of GC by inhibiting the immune infiltration of CD8⁺ TRM cells in the TME, leading to poor prognosis[59]. Furthermore, the abundance of *Methylobacterium* was also found to be significantly negatively correlated with TGF-β and IL-2[59]. TGF-β induces the expression of CD103, which plays an essential role in the permanent residence of TRM cells in epithelial tissues[71]. This may provide a new target for the development of immunotherapy for GC.

TAMs, mainly M2 TAMs (*i.e.*, polarized M2 macrophages), are important in the progression of GC [72]. Recent experiments have shown that *Propionibacterium acnes* (*P. acnes*) is significantly increased in GC tissues, especially in *H. pylori*-negative tissue, and promotes M2 polarization of macrophages *via* TLR4/PI3K/Akt signaling when comparing microbial communities in GC tissues and adjacent normal tissues[73]. M2 macrophages secrete chitinase 3-like protein 1, which binds specifically to the interleukin-13 receptor α2 chain of cancer cells and triggers the mitogen-activated protein kinase signaling pathway to promote regional or distal metastasis of GC[72]. The abundance of *P. acnes* is positively correlated with M2 macrophages in GC tissues[73]. Therefore, *P. acnes* may be one of the possible factors for GC progression beyond *H. pylori*. Recent reports have shown a sustained increase in the abundance of lactic acid bacteria (LAB) in GC patients. LAB can increase exogenous lactate production[74]. Lactate produced by the glycolytic pathway leads to the formation of an acidic TME [75], which is involved in cancer progression. Lactate mediates M2-like polarization of TAMs and increases vascular endothelial growth factor and arginase 1 expression in these cells, thereby facilitating immune escape[74]. Lactate also inhibits the function and survival of T cells and natural killer (NK) cells and increases the number of myeloid-derived suppressor cells, which further inhibits the cytotoxicity of

NK cells. Because LAB can produce large amounts of lactate in a short period of time[76], it is possible that microbial lactate can shape the TME like host lactate, altering the immune response[74].

In addition to bacteria, intratumoral fungi can also affect GC progression through the IOM axis. Yang *et al*[77] analyzed the gastric fungal microbiome in patients with GC and healthy individuals by high-throughput sequencing and noted that the ecological dysbiosis of the gastric fungal microbiota may be related to the occurrence of GC. They also measured the mRNA levels of cytokines and chemokines in tumor and normal tissues. The results showed that the levels of pro-inflammatory cytokines and chemokines such as CXCL9, CXCL10, CXCL11, and TNF-α were significantly increased, while anti-inflammatory cytokines and chemokines such as CCL17, IL-4, IL-6, and IL-8 were significantly decreased in the GC group. It is suggested that fungi that promote the production of proinflammatory cytokines and chemokines may be involved in promoting the tumor immune response, while fungi that promote the production of anti-inflammatory cytokines and chemokines may enhance the anti-inflammatory response in GC. IL-10 is highly expressed in various types of cancer[78,79], and can downregulate the inflammatory cytokines IL-6 and IL-8[77]. Therefore, the decreased levels of IL-6 and IL-8 in the GC group may be due to the increase in IL-10 levels in the local area of the tumor. IL-10 is released by TAMs, and IL-10+ TAMs infiltrate the tumor, which drives immune escape from the TME characterized by Treg-cell infiltration and $CD8^+$ T-cell dysfunction[80]. *C. albicans* is the most studied fungal species in GC. *C. albicans* was found to be a fungal marker of GC[81]. *In vitro*, the mannose protein of *C. albicans* could promote tumor adhesion and liver metastasis[82]. Similar to CRC, fungi may have a complex role in the Th17 cell family. On the one hand, Th17 cells produce IL-17 to initiate downstream immunity against *C. albicans*. On the other hand, other cytokines, such as IL-23, produced by Th17 cells can promote tumorigenesis and growth. In addition, Th-17 can promote the progression of GC through an indirect mechanism. IL-17 secreted by Th17 cells can antagonize IL-12. IL-12 induces the production of IFN-γ and promotes the infiltration of cytotoxic T cells, which plays a critical role in the Th1-type antitumor immune response[83,84]. The promotion of cancer progression by IL-17 is also associated with neutrophil recruitment[85]. Additionally, the complement receptor 3-related protein (CR3-RP) of *C. albicans* has antigenic and structural similarity to CR3. CR3 is involved in leukocyte adhesion to endothelial cells and the subsequent extravasation process. Thus, antibodies against *C. albicans* CR3-RP may cross-react with leukocyte CR3 and disrupt the host's antitumor defense[85].

In general, bacteria and fungi in the stomach, which are considered unsuitable for microbial habitation, have an important role in the regulation of GC progression. They can interact with immune cells in the body or the TME, affecting the progression of GC. Moreover, the role of fungi in GC may be underestimated. However, it is not clear whether fungi exist in tumor tissue as viable or partial components.

EC

EC is one of the most invasive malignant diseases[86]. Unlike other luminal organs of the digestive system, the esophagus does not retain food contents. It was first thought that the esophagus was aseptic, but after the study of traditional bacterial culture methods, it was found that the esophagus contained a small number of microorganisms swallowed from the oropharynx or excreted from the stomach through gastroesophageal reflux[87,88]. With the progress of culture technology, increasing evidence shows that the normal esophagus has a unique, stable, resident microbiome[87,88]. The distal esophageal microbiome was divided into two groups: Type I and type II[89]. Among them, the type I microbiome, dominated by *Streptococcus species*, seems to be the main component of the normal esophageal microbiome[89,90]. However, a study found that the microbiome of the normal esophagus is not the same as that of the esophagus with inflammation, Barrett's esophagus (BE), and EC[87]. Type II microbiome, dominated by gram-negative bacteria, is usually associated with an abnormal esophagus [89].

Gastroesophageal reflux disease (GERD) and BE are significant risk factors for esophageal adenocarcinoma (EAC)[91-93]. Gram-negative bacteria that predominate in GERD and BE produce specific components, such as lipopolysaccharide (LPS)[87,88]. LPS directly or indirectly stimulates TLR4[94] in epithelial cells or inflammatory cells, leading to NF-κB activation[87] promote the expression of proinflammatory cytokines and sustain the innate immune response in the esophagus[88,94]. LPS binds plasma-derived LPS-binding protein and transmits to membrane-bound CD14 in monocytes, interacting with CD14[95]. CD14 plays a key role in LPS-mediated signal transduction by enhancing leukocyte adhesion, activation, and cytokine production. LPS stimulation of monocytes or epithelial cells leads to the activation of TLR4 and downstream NF-κB pathways, which triggers an inflammatory response[94]. LPS may also indirectly activate the NF-κB pathway of epithelial cells by triggering the production of inflammatory cytokines such as TNF-α, IL-1, and IL-6 by monocytes and macrophages[94,95].

In addition, *Campylobacter* was experimentally demonstrated to be significantly increased in GERD and BE[96]. Cytokines related to carcinogenesis, such as IL-18, were more highly expressed in the tissues colonized by *Campylobacter*[87]. Studies have shown that there is a very close relationship between esophageal *Campylobacter* colonization and IL-18 epithelial cell production[97]. IL-18 is produced by

gastrointestinal epithelial cells, including squamous esophagus cells, which can stimulate both congenital and adaptive responses (Th1 and Th2) and induce NK cell activity and apoptosis[98]. Another study found that *Campylobacter* infection induced the secretion of IL-8 and TNF-α[99]. However, the increase in IL-8 secretion was not associated with the secretion of TNF-α stimulated by *Campylobacter*. It is not clear whether IL-8 can play a role in the initiation and maintenance of malignant transformation from GERD and BE to EAC. However, *Campylobacter species* is associated with a range of gastrointestinal diseases and may play a role in the progression of EAC similar to *H. pylori* in GC[87,100].

Moreover, the microbiome can also directly promote the occurrence of EAC by stimulating the human systemic immune system. For example, Lopetuso *et al*[90] identified *Leptotrichia* as the main taxon distinguishing EAC by LefSe analysis. *Leptotrichia* can promote the release of proinflammatory cytokines, such as IL-6 and IL-8. In turn, IL-6 and IL-8 can attract granulocytes and lymphocytes, thus inducing the host cellular immune response[101]. Serum antibodies against *Leptotrichia* are very common and belong to the IgG and IgM classes[102]. It is speculated that the immune activity caused by *Leptotrichia* may promote the occurrence of esophageal tumors[90].

Although there are few definitive conclusions about the impact of the microbiome on EAC, the change in the microbiome in the esophagus induces GERD and BE by activating the innate immune system and makes them progress to EAC, which seems to be a very important link in the pathogenesis of EAC. Compared with EAC, the characteristics of the microbiome in esophageal squamous cell carcinoma (ESCC) are not very clear[103]. However, there is growing evidence showing that the microbiome plays an important role in the occurrence and development of ESCC[87]. In a study by NHANES III, an increase in serum IgG of *Porphyromonas gingivalis* (*P. gingivalis*) was associated with increased mortality from oral and gastrointestinal cancers[104]. The results of Gao *et al*[105] showed that *P. gingivalis* infected the cancerous and adjacent esophageal mucosa of patients with ESCC. The titers of IgG and IgA against *P. gingivalis* in patients with ESCC were significantly higher than those in patients with esophagitis and healthy controls, which provided direct evidence for the involvement of *P. gingivalis* in the pathogenesis of ESCC. However, the specific mechanism by which *P. gingivalis* is involved in the progression of ESCC is unknown. Although the mechanism by which *P. gingivalis* affects the progression of ESCC through the IOM axis is still unclear, *P. gingivalis* can promote the infiltration of tumor-associated neutrophil 2 in tumor tissues in pancreatic cancer[106].

The poor prognosis of ESCC is also related to the presence of *F. nucleatum*[107]. In the relationship between *F. nucleatum* and cancer, especially CRC, *F. nucleatum* is considered to selectively amplify myeloid-derived immune cells to regulate the tumor immune microenvironment[23,25]. The immune response mediated by myeloid cells may provide the driving force for inflammation, genotoxicity, and epigenetic changes that lead to cancer[23]. In addition, *F. nucleatum* may promote tumor invasiveness by activating chemokines, such as CCL20, in EC tissue[87]. CCL20 plays a critical role in the migration of Treg lymphocytes. The specific receptor of CCL20 is CCR6, which is highly expressed in immune cells (*e.g.*, Treg and Th17) and epithelial tumors[108]. Treg cells promote migration to tumor tissue in a CCR6-dependent manner in response to CCL20[109], and the concentration of CCL20 in the tumor is positively correlated with the number of tumor-infiltrating Tregs[108,110].

PANCREATIC CANCER

The central position of the pancreas in the abdominal cavity and the surrounding blood vessels and lymphatic vessels promote local and distant tumor spread. The TME of pancreatic cancer is characterized by a high matrix level and low immune activity[111]. This has also become one of the reasons for the poor efficacy of ICIs in pancreatic cancer. Improving this immunosuppressive microenvironment has become an urgent problem to be solved. In recent years, with the deepening of the study of the microbiome and the application of high-throughput sequencing technology[112], it has been found that the gut and intratumor microbiome have an important effect on pancreatic cancer[113-115]. This is especially true in immune-related research. The role of the IOM axis in pancreatic cancer has a dual nature. Most studies have reported the cancer-promoting effect of fungi and bacteria through the IOM axis in pancreatic ductal adenocarcinoma (PDAC).

TAMs have important potential in activating tumor-specific $CD8^+$ T cells, while the important role of the microbiome has long been neglected in research on TAMs in the TME, as well as in pancreatic cancer [116-119]. Pushalkar *et al*[120] reported that ablation of the gut flora of mice with pancreatic cancer resulted in a decrease in immunosuppressive $CD206^+$ M2-like TAMs with a concomitant increase in M1-like TAMs and increased expression of MHCII, CD86, TNF-α, IL-12, and IL-6. Moreover, like other gastrointestinal tumors, microbial ablation increased TLR expression in macrophages. Thus, the effect of the microbiome on PDAC through the IOM axis may be partly caused by acting on TLRs on macrophages. At the same time, their research also reported that the cell-free extract of the gut microbiome from pancreatic cancer mice can also promote the transformation of TAMs to an immunosuppressive phenotype. This suggests that the cellular components or metabolites of the microbiome located in the gut or tumor may play an important role in TAM-related reactions. Indole, a

metabolite of the gut microbiome, such as *Lactobacillus murinus*, was found to activate the aryl hydrocarbon receptor (AhR) on TAMs. AhR activation leads to the expression of arginase 1 and IL-10 in TAMs and suppresses the expression of IFN-γ in $CD8^+$ T cells. Another metabolite of the gut microbiome, trimethylamine N-oxide (TMAO), is different from indole in its production, which is completely dependent on gut bacteria[121]. Choline is the main source of circulating TMAO. However, unlike the effect of indole, choline-supplemented mice had increased TMAO levels, accompanied by a significant reduction in PDAC burden[122]. Flow cytometry showed that the expression of MHCI and MHCII on TAMs was significantly increased, accompanied by a significant increase in activated $CD8^+$ and $CD4^+$ T cells. Further research found that TMAO directly changed TAMs into a phenotype that could support the T-cell response and reduce the burden of PDAC. However, the role of $CD8^+$ T cells mediated by the microbiome in the gut/tumor seems not limited to the stimulation of gut microbiome metabolites. Riquelme *et al*[12] found that patients with long-term survival had higher intratumor microbiome diversity than those with short-term survival. Moreover, PDAC tumor volume was reduced in mice that were gavaged with feces from long-term survival patients, and this effect could be eliminated by the depletion of $CD8^+$ T cells. Although the causal relationship between the enrichment of microbial communities and tumors is still unclear, it suggests that the construction of microbial communities in the gut/tumors may be more effective than studying the role of a single strain.

The role of IL-33 and ILC2s in pancreatic cancer is highly controversial. KRAS mutant PDAC cells can secrete IL-33 through the KRAS-MEK-ERK pathway[123]. Intratumor fungi and their cell-free extracts can activate dectin-1 on PDAC. The activation of dectin-1 promotes the secretion of IL-33 by PDAC cells through the Src-Syk-CARD9 pathway. This shows the important role of intratumoral fungi in mediating the secretion of PDAC cells. However, the source of IL-33 may not be limited to PDAC cells. Another study showed a different result. Sun *et al*[124] conducted immunohistochemistry on 20 human PDAC tissues and found that pericytes and cancer-associated fibroblasts were the major cell sources of IL-33 production in PDAC tissues and promoted PDAC metastasis through the IL-33-ST2-CXCL3-CXCR2 axis, although both studies found that the expression of IL-33 in PDAC was increased. The increase in IL-33 in the TME of PDAC promotes the infiltration of TH2 cells and ILCs in PDAC through the IL-33/ST2 axis[123]. These immune cells promote the tumorigenic process through their cytokine networks, leading to PDAC progression[125-127]. In addition to IL-33, the role of its downstream ILC2s is also controversial. The role of bipartisan politicians of ILC2s is also reflected in PDAC. ILC2s can also promote the effective infiltration of immune cells. ILC2s can inhibit the progression of PDAC tumors through the ILC2-$CD103^+$ DC-$CD8^+$ T axis[128]. The level of immunity in PDAC appears to affect the effect of ILCs.

THE MICROBIOME AND CANCER THERAPY

Antibiotics

In a retrospective clinical study, increased overall survival (OS) and progression-free survival (PFS) in patients with metastatic PDAC were associated with antibiotic use[129]. Several preclinical studies have found that ablation of the gut and intratumor microbiome with antibiotics in a PDAC in situ mouse model can prevent tumor progression[12,120,130]. In the abnormal esophagus, the use of selective antibiotics or probiotics to reverse the type II microbiome to a type I microbiome in the esophagus can reduce the risk of esophageal carcinogenesis[94]. However, the effect caused by this antibiotic is related to the type of tumor and the type of antibiotics. Treatment of mice carrying colon cancer xenografts with the antibiotic metronidazole was found to reduce cancer cell proliferation and tumor growth[131]. However, treatment with metronidazole in pancreatic cancer significantly increased the tumor load [122]. In pancreatic cancer, quinolone therapy is linked to the improvement of OS. Postoperative quinolone therapy may prolong the survival time of preoperative treatment and resection of pancreatic cancer[132]. The use of antibiotics can inhibit or kill the pathogenic microbiome in the host. However, frequent use of broad-spectrum antibiotics may interfere with the gut microbiome, leading to ecological disorders and even cancer development[133].

Fecal microbiota transplantation

Fecal microbiota transplantation (FMT) is a method that transplants the entire gut microbiota from a healthy donor into the patient's gut to correct gut microbial abnormalities and reconstruct the structure and function of normal gut microbiota[134]. Metagenomic analysis showed that FMT significantly increased the abundance of potentially beneficial species[135]. The microbiome remodeling induced by FMT may be related to an improved tumor immune microenvironment. Riquelme *et al*[12] concluded that compared with short-term PDAC survivors or healthy controls, PDAC tumor-bearing mice transplanted with the fecal microbiome from long-term survivors of PDAC had antitumor immunity. The bacteria found in the tumor transferred from the intestinal tract to the pancreas, affecting the composition of the tumor microbiome and antitumor immunity in the pancreas. Rosshart *et al*[136] reported that FMT enhanced host resistance to mutagen/inflammation-induced colorectal tumorigenesis. The beneficial role of FMT in the treatment of diseases has been confirmed, but it has not been

widely studied in gastrointestinal tumors.

Probiotics

Probiotics can alter the composition of the gut microbiome and have been shown to inhibit tumor development by downregulating the levels of LPS, inflammatory factors, and chemokines[137]. Various studies have found that supplementation with probiotics that produce SCFAs can inhibit the development of tumors[51,52]. For example, both *Lactobacillus coryniformis* MXJ32 and *Lacticaseibacillus rhamnosus* LS8 can reduce intestinal inflammation by downregulating the expression of inflammatory cytokines (*e.g.*, TNF-α, IL-1β, IL-6, IL-γ, and IL-17a) and chemokines (*e.g.*, CXCL1, CXCL2, CXCL3, CXCL5, and CCL7) and effectively improve colitis-associated CRC[138,139]. However, the effects of these two probiotics on the mechanism of regulating the gut microbiome and specific immune response are not clear. In the study of Heydari *et al*[140], which uses an animal colon cancer model, treatment with probiotics suppressed the increase in miRNA expression and decreased the level of oncogenes, and such treatment was considered beneficial for colon cancer treatment. *Lactobacillus brevis* SBL8803-derived polyphosphate leads to apoptosis of CRC cells by activating extracellular signal-regulated kinase signal transduction. Heptelidic acid, a metabolite of the probiotic *Aspergillus oryzae*, passes through the gut mucosa to reach the pancreas and induces apoptosis in pancreatic cancer cells by activating the p38MAPK signaling pathway[141]. Although probiotic supplements may alter the structure of the microbiome and regulate inflammation to prevent cancer[142], probiotics may adversely affect the reconstruction of gut mucosal host-microbiome ecosystems after antibiotic treatment[143]. Therefore, probiotic therapy may be a promising intervention method[138], but many problems urgently require further research.

Immunotherapy

The use of ICIs has made remarkable progress in the treatment of many cancers, among which the most widely used ICIs are monoclonal antibodies targeting programmed cell death protein 1 (PD-1) and its ligand PD-L1[144]. Although immunotherapy based on anti-PD-1 has a limited response in CRC patients, a growing body of research supports the important role of the gut microbiome in the immune system. The gut microbiome seems to influence the expression of PD-1/PD-L1 indirectly through systemic or locally mediated immune function, thus affecting the efficacy of anti-PD-1 and anti-PD-L1 therapy[134]. The mechanisms by which the gut microbiome improves the efficacy of anti-PD-1 are as follows[145-148]: (1) An increase in beneficial bacteria; (2) Enhancement of the function of DCs; (3) An increase in antitumor $CD8^+$ T-cell activity; and (4) Promotion of T-cell tumor infiltration. Several studies have reported that oral combinations of specific symbiotic bacteria and anti-PD-1/PD-L1 antibodies almost eliminated tumor growth[145,149]. In a mouse cancer model, oral live *Lactobacillus rhamnosus* GG enhanced the antitumor activity of anti-PD-1 immunotherapy by increasing tumor-infiltrating DCs and T cells and significantly inhibited tumor growth[146].

Antibiotics and immunotherapy

There is growing evidence that the gut microbiome can influence immunotherapy responses in patients treated with ICIs[61,62,134]. Preclinical experiments in mice showed that the use of antibiotics could decrease the efficacy of ICIs[144]. In a meta-analysis enrolling 2740 cancer patients, antibiotic use significantly reduced OS and PFS in patients treated with ICIs[150]. But, In a study on pancreatic cancer, researchers discovered that by using broad-spectrum antibiotics to eliminate gut microbiota, they could trigger immunogenic reprogramming within the TME. This made treatment with ICIs more effective by increasing the expression of PD-1[120]. Thus, whether the use of antibiotics can improve the efficacy of ICIs is controversial. At present, some meta-analyses suggest that antibiotic administration may be associated with poor prognosis of tumor patients receiving ICIs[151,152]. However, these studies focused on lung cancer, renal cell carcinoma, urothelial carcinoma, and melanoma[151]. Research on gastrointestinal malignancies is still insufficient. When CRC cells were implanted into germ-free or specific pathogen-free mice, broad-spectrum antibiotics reduced their ICI efficacy[153]. In a mouse model, *H. pylori* infection partially blocked the activity of ICIs and reduced the effect of tumor immunotherapy[61]. However, eradication of *H. pylori* infection through antibiotic therapy did not restore the decreased response of *H. pylori*-induced cancer to immunotherapy. Therefore, the administration of antibiotics to cure *H. pylori* infection is not a good choice to improve the efficacy of cancer immunotherapy. Han *et al*[154] recently demonstrated that antibiotic-induced microbiome disorders enhanced the antitumor efficacy of γ-δ T cells during immunotherapy in a mouse model of hepatocellular carcinoma. γ-δ T cells can generate immune responses to a wide range of antigens. They are believed to serve as a bridge between innate and adaptive immune responses[7]. γ-δ T cells can also infiltrate GC, pancreatic cancer, and colon cancer[155-157]. Thus, the effect of antibiotics on ICIs in patients with gastrointestinal malignancies still needs to be further studied.

FMT and immunotherapy

FMT is a potential way to improve the efficacy of anti-PD-1 therapy[158]. Huang *et al*[158] found that compared with colon cancer-bearing mice treated with anti-PD-1 or FMT alone, FMT combined with

anti-PD-1 showed higher survival and tumor control. The enhancement of anti-PD-1 therapy induced by FMT may be mediated by changes in the microbial genome and blood metabolism. Through metagenomic analysis, FMT altered the composition of the gut microbiome. The relative abundance of B *acteroides species* and *Parabacteroides species* increased significantly. Metabonomic analysis of mouse plasma showed that after FMT, several metabolites, including taxic acid and aspirin, may promote the response to anti-PD-1 therapy through their immunomodulatory function. Accordingly, the composition and function of the gut microbiome may be able to influence the ICI response in cancer[7]. However, FMT did not improve the response to immunotherapy in cancer patients infected with *H. pylori*[62]. In the absence of ICIs, modulation of the gut microbiome with bacteria or FMT has a limited impact on the antitumor immune response or tumor growth[134]. Therefore, FMT may serve as an important therapeutic modality to assist patients treated with ICIs to enhance systemic and antitumor immunity in cancer patients.

Microbial metabolites and immunotherapy

Intestinal epithelial cells are closely related to the immune system. Bacterial metabolites, such as SCFAs, occur in the immune response and are strongly associated with innate immunity and antibody production[159]. The results from a cohort study showed that high levels of fecal or plasma SCFAs were associated with PD-1 treatment response and longer PFS[160]. In mice humanized with gut microbiota from patients, butyrate promoted T-cell infiltration in the TME, thus improving the efficacy of anti-PD-1 monoclonal antibodies[147]. T Tryptophan is an essential amino acid for the human body. Indole, a metabolite of tryptophan, is a biologically active compound that plays an important role in tumor and immune regulation[161]. Indole drives AhR on TAMs and suppresses antitumor immunity. Macrophage AhR is the central driver of TAM function in PDAC. In patients with PDAC, high expression of AhR is associated with rapid disease progression and mortality. TMAO, a metabolite of natural microorganisms, suppresses the immunostimulatory phenotype of macrophages, promotes the activity of effector T cells, and enhances antitumor immunity against PDAC[122]. The combination of TMAO and anti-PD1 in a PDAC mouse model significantly reduced the tumor burden and improved the survival rate compared to TMAO or ICIs alone. Therefore, the immunomodulatory mechanism associated with microbial metabolites may become a new direction to improve PD-1 efficacy in cancer patients[160].

CONCLUSION

In recent years, some progress has been made in the study of microorganisms and tumors. Although the role of the IOM axis in GC and EC needs to be further clarified, it plays an important role in the occurrence and development of gastrointestinal malignancies. Macrophages may be a key component in linking the microbiome and immunity, which has been reflected in the variety of tumors mentioned above. The microbiome may influence tumor immune responses through TLRs on macrophages. ILCs also play a vital role in the host microbiome and, together with T cells, regulate the IOM axis. The IOM axis provides a new direction for the treatment of gastrointestinal malignancies. An increasing number of studies have shown the role of the microbiome in immunotherapy. For example, specific antibiotic use may prevent tumor progression, whereas the combination of antibiotics with ICIs may reduce the efficacy of ICIs. In contrast, FMT has been found to improve the efficacy of immunotherapy. However, the effect of the microbiome on immunotherapy is still controversial, and the mechanism of action is still elusive and needs to be widely validated by more preclinical models and clinical trials.

FOOTNOTES

Author contributions: All authors contributed to the original ideas and writing of this paper; Lin Q and Guan SW wrote the paper; Lin Q draw figures; Yu HB made critical revisions of this paper.

Conflict-of-interest statement: All the authors report no relevant conflicts of interest for this article.

Country/Territory of origin: China

ORCID number: Quan Lin 0000-0001-5842-8032; Shi-Wei Guan 0000-0001-6046-8383; Hai-Bo Yu 0000-0001-7616-3891.

S-Editor: Wang JJ

L-Editor: A
P-Editor: Li X

REFERENCES

1 **Siegel RL**, Miller KD, Fuchs HE, Jemal A. Cancer Statistics, 2021. *CA Cancer J Clin* 2021; **71**: 7-33 [PMID: 33433946 DOI: 10.3322/caac.21654]
2 **Bagchi S**, Yuan R, Engleman EG. Immune Checkpoint Inhibitors for the Treatment of Cancer: Clinical Impact and Mechanisms of Response and Resistance. *Annu Rev Pathol* 2021; **16**: 223-249 [PMID: 33197221 DOI: 10.1146/annurev-pathol-042020-042741]
3 **Schmid P**, Adams S, Rugo HS, Schneeweiss A, Barrios CH, Iwata H, Diéras V, Hegg R, Im SA, Shaw Wright G, Henschel V, Molinero L, Chui SY, Funke R, Husain A, Winer EP, Loi S, Emens LA; IMpassion130 Trial Investigators. Atezolizumab and Nab-Paclitaxel in Advanced Triple-Negative Breast Cancer. *N Engl J Med* 2018; **379**: 2108-2121 [PMID: 30345906 DOI: 10.1056/NEJMoa1809615]
4 **Kojima T**, Shah MA, Muro K, Francois E, Adenis A, Hsu CH, Doi T, Moriwaki T, Kim SB, Lee SH, Bennouna J, Kato K, Shen L, Enzinger P, Qin SK, Ferreira P, Chen J, Girotto G, de la Fouchardiere C, Senellart H, Al-Rajabi R, Lordick F, Wang R, Suryawanshi S, Bhagia P, Kang SP, Metges JP; KEYNOTE-181 Investigators. Randomized Phase III KEYNOTE-181 Study of Pembrolizumab Versus Chemotherapy in Advanced Esophageal Cancer. *J Clin Oncol* 2020; **38**: 4138-4148 [PMID: 33026938 DOI: 10.1200/JCO.20.01888]
5 **Reiss KA**, Mick R, Teitelbaum U, O'Hara M, Schneider C, Massa R, Karasic T, Tondon R, Onyiah C, Gosselin MK, Donze A, Domchek SM, Vonderheide RH. Niraparib plus nivolumab or niraparib plus ipilimumab in patients with platinum-sensitive advanced pancreatic cancer: a randomised, phase 1b/2 trial. *Lancet Oncol* 2022; **23**: 1009-1020 [PMID: 35810751 DOI: 10.1016/S1470-2045(22)00369-2]
6 **Lu Y**, Yuan X, Wang M, He Z, Li H, Wang J, Li Q. Gut microbiota influence immunotherapy responses: mechanisms and therapeutic strategies. *J Hematol Oncol* 2022; **15**: 47 [PMID: 35488243 DOI: 10.1186/s13045-022-01273-9]
7 **Jain T**, Sharma P, Are AC, Vickers SM, Dudeja V. New Insights Into the Cancer-Microbiome-Immune Axis: Decrypting a Decade of Discoveries. *Front Immunol* 2021; **12**: 622064 [PMID: 33708214 DOI: 10.3389/fimmu.2021.622064]
8 **Lozupone CA**, Stombaugh JI, Gordon JI, Jansson JK, Knight R. Diversity, stability and resilience of the human gut microbiota. *Nature* 2012; **489**: 220-230 [PMID: 22972295 DOI: 10.1038/nature11550]
9 **Nosho K**, Sukawa Y, Adachi Y, Ito M, Mitsuhashi K, Kurihara H, Kanno S, Yamamoto I, Ishigami K, Igarashi H, Maruyama R, Imai K, Yamamoto H, Shinomura Y. Association of Fusobacterium nucleatum with immunity and molecular alterations in colorectal cancer. *World J Gastroenterol* 2016; **22**: 557-566 [PMID: 26811607 DOI: 10.3748/wjg.v22.i2.557]
10 **Plottel CS**, Blaser MJ. Microbiome and malignancy. *Cell Host Microbe* 2011; **10**: 324-335 [PMID: 22018233 DOI: 10.1016/j.chom.2011.10.003]
11 **Wang J**, Jia H. Metagenome-wide association studies: fine-mining the microbiome. *Nat Rev Microbiol* 2016; **14**: 508-522 [PMID: 27396567 DOI: 10.1038/nrmicro.2016.83]
12 **Riquelme E**, Zhang Y, Zhang L, Montiel M, Zoltan M, Dong W, Quesada P, Sahin I, Chandra V, San Lucas A, Scheet P, Xu H, Hanash SM, Feng L, Burks JK, Do KA, Peterson CB, Nejman D, Tzeng CD, Kim MP, Sears CL, Ajami N, Petrosino J, Wood LD, Maitra A, Straussman R, Katz M, White JR, Jenq R, Wargo J, McAllister F. Tumor Microbiome Diversity and Composition Influence Pancreatic Cancer Outcomes. *Cell* 2019; **178**: 795-806.e12 [PMID: 31398337 DOI: 10.1016/j.cell.2019.07.008]
13 **Schwabe RF**, Jobin C. The microbiome and cancer. *Nat Rev Cancer* 2013; **13**: 800-812 [PMID: 24132111 DOI: 10.1038/nrc3610]
14 **Garrett WS**. Cancer and the microbiota. *Science* 2015; **348**: 80-86 [PMID: 25838377 DOI: 10.1126/science.aaa4972]
15 **Sepich-Poore GD**, Zitvogel L, Straussman R, Hasty J, Wargo JA, Knight R. The microbiome and human cancer. *Science* 2021; **371** [PMID: 33766858 DOI: 10.1126/science.abc4552]
16 **Sepich-Poore GD**, Guccione C, Laplane L, Pradeu T, Curtius K, Knight R. Cancer's second genome: Microbial cancer diagnostics and redefining clonal evolution as a multispecies process: Humans and their tumors are not aseptic, and the multispecies nature of cancer modulates clinical care and clonal evolution: Humans and their tumors are not aseptic, and the multispecies nature of cancer modulates clinical care and clonal evolution. *Bioessays* 2022; **44**: e2100252 [PMID: 35253252 DOI: 10.1002/bies.202100252]
17 **Nejman D**, Livyatan I, Fuks G, Gavert N, Zwang Y, Geller LT, Rotter-Maskowitz A, Weiser R, Mallel G, Gigi E, Meltser A, Douglas GM, Kamer I, Gopalakrishnan V, Dadosh T, Levin-Zaidman S, Avnet S, Atlan T, Cooper ZA, Arora R, Cogdill AP, Khan MAW, Ologun G, Bussi Y, Weinberger A, Lotan-Pompan M, Golani O, Perry G, Rokah M, Bahar-Shany K, Rozeman EA, Blank CU, Ronai A, Shaoul R, Amit A, Dorfman T, Kremer R, Cohen ZR, Harnof S, Siegal T, Yehuda-Shnaidman E, Gal-Yam EN, Shapira H, Baldini N, Langille MGI, Ben-Nun A, Kaufman B, Nissan A, Golan T, Dadiani M, Levanon K, Bar J, Yust-Katz S, Barshack I, Peeper DS, Raz DJ, Segal E, Wargo JA, Sandbank J, Shental N, Straussman R. The human tumor microbiome is composed of tumor type-specific intracellular bacteria. *Science* 2020; **368**: 973-980 [PMID: 32467386 DOI: 10.1126/science.aay9189]
18 **Dekker E**, Tanis PJ, Vleugels JLA, Kasi PM, Wallace MB. Colorectal cancer. *Lancet* 2019; **394**: 1467-1480 [PMID: 31631858 DOI: 10.1016/S0140-6736(19)32319-0]
19 **Wu J**, Li H, Xie H, Wu X, Lan P. The malignant role of exosomes in the communication among colorectal cancer cell, macrophage and microbiome. *Carcinogenesis* 2019; **40**: 601-610 [PMID: 30864655 DOI: 10.1093/carcin/bgy138]
20 **Cremonesi E**, Governa V, Garzon JFG, Mele V, Amicarella F, Muraro MG, Trella E, Galati-Fournier V, Oertli D, Däster SR, Droeser RA, Weixler B, Bolli M, Rosso R, Nitsche U, Khanna N, Egli A, Keck S, Slotta-Huspenina J, Terracciano

LM, Zajac P, Spagnoli GC, Eppenberger-Castori S, Janssen KP, Borsig L, Iezzi G. Gut microbiota modulate T cell trafficking into human colorectal cancer. *Gut* 2018; **67**: 1984-1994 [PMID: 29437871 DOI: 10.1136/gutjnl-2016-313498]

21 **Goc J**, Lv M, Bessman NJ, Flamar AL, Sahota S, Suzuki H, Teng F, Putzel GG; JRI Live Cell Bank, Eberl G, Withers DR, Arthur JC, Shah MA, Sonnenberg GF. Dysregulation of ILC3s unleashes progression and immunotherapy resistance in colon cancer. *Cell* 2021; **184**: 5015-5030.e16 [PMID: 34407392 DOI: 10.1016/j.cell.2021.07.029]

22 **Tosolini M**, Kirilovsky A, Mlecnik B, Fredriksen T, Mauger S, Bindea G, Berger A, Bruneval P, Fridman WH, Pagès F, Galon J. Clinical impact of different classes of infiltrating T cytotoxic and helper cells (Th1, th2, treg, th17) in patients with colorectal cancer. *Cancer Res* 2011; **71**: 1263-1271 [PMID: 21303976 DOI: 10.1158/0008-5472.CAN-10-2907]

23 **Kostic AD**, Chun E, Robertson L, Glickman JN, Gallini CA, Michaud M, Clancy TE, Chung DC, Lochhead P, Hold GL, El-Omar EM, Brenner D, Fuchs CS, Meyerson M, Garrett WS. Fusobacterium nucleatum potentiates intestinal tumorigenesis and modulates the tumor-immune microenvironment. *Cell Host Microbe* 2013; **14**: 207-215 [PMID: 23954159 DOI: 10.1016/j.chom.2013.07.007]

24 **Kostic AD**, Gevers D, Pedamallu CS, Michaud M, Duke F, Earl AM, Ojesina AI, Jung J, Bass AJ, Tabernero J, Baselga J, Liu C, Shivdasani RA, Ogino S, Birren BW, Huttenhower C, Garrett WS, Meyerson M. Genomic analysis identifies association of Fusobacterium with colorectal carcinoma. *Genome Res* 2012; **22**: 292-298 [PMID: 22009990 DOI: 10.1101/gr.126573.111]

25 **Sears CL**, Garrett WS. Microbes, microbiota, and colon cancer. *Cell Host Microbe* 2014; **15**: 317-328 [PMID: 24629338 DOI: 10.1016/j.chom.2014.02.007]

26 **Gur C**, Ibrahim Y, Isaacson B, Yamin R, Abed J, Gamliel M, Enk J, Bar-On Y, Stanietsky-Kaynan N, Coppenhagen-Glazer S, Shussman N, Almogy G, Cuapio A, Hofer E, Mevorach D, Tabib A, Ortenberg R, Markel G, Miklić K, Jonjic S, Brennan CA, Garrett WS, Bachrach G, Mandelboim O. Binding of the Fap2 protein of Fusobacterium nucleatum to human inhibitory receptor TIGIT protects tumors from immune cell attack. *Immunity* 2015; **42**: 344-355 [PMID: 25680274 DOI: 10.1016/j.immuni.2015.01.010]

27 **Shenker BJ**, Datar S. Fusobacterium nucleatum inhibits human T-cell activation by arresting cells in the mid-G1 phase of the cell cycle. *Infect Immun* 1995; **63**: 4830-4836 [PMID: 7591143 DOI: 10.1128/iai.63.12.4830-4836.1995]

28 **Galaski J**, Shhadeh A, Umaña A, Yoo CC, Arpinati L, Isaacson B, Berhani O, Singer BB, Slade DJ, Bachrach G, Mandelboim O. Fusobacterium nucleatum CbpF Mediates Inhibition of T Cell Function Through CEACAM1 Activation. *Front Cell Infect Microbiol* 2021; **11**: 692544 [PMID: 34336716 DOI: 10.3389/fcimb.2021.692544]

29 **Grivennikov SI**, Wang K, Mucida D, Stewart CA, Schnabl B, Jauch D, Taniguchi K, Yu GY, Osterreicher CH, Hung KE, Datz C, Feng Y, Fearon ER, Oukka M, Tessarollo L, Coppola V, Yarovinsky F, Cheroutre H, Eckmann L, Trinchieri G, Karin M. Adenoma-linked barrier defects and microbial products drive IL-23/IL-17-mediated tumour growth. *Nature* 2012; **491**: 254-258 [PMID: 23034650 DOI: 10.1038/nature11465]

30 **Tjalsma H**, Boleij A, Marchesi JR, Dutilh BE. A bacterial driver-passenger model for colorectal cancer: beyond the usual suspects. *Nat Rev Microbiol* 2012; **10**: 575-582 [PMID: 22728587 DOI: 10.1038/nrmicro2819]

31 **Vivier E**, Artis D, Colonna M, Diefenbach A, Di Santo JP, Eberl G, Koyasu S, Locksley RM, McKenzie ANJ, Mebius RE, Powrie F, Spits H. Innate Lymphoid Cells: 10 Years On. *Cell* 2018; **174**: 1054-1066 [PMID: 30142344 DOI: 10.1016/j.cell.2018.07.017]

32 **Hepworth MR**, Monticelli LA, Fung TC, Ziegler CG, Grunberg S, Sinha R, Mantegazza AR, Ma HL, Crawford A, Angelosanto JM, Wherry EJ, Koni PA, Bushman FD, Elson CO, Eberl G, Artis D, Sonnenberg GF. Innate lymphoid cells regulate CD4+ T-cell responses to intestinal commensal bacteria. *Nature* 2013; **498**: 113-117 [PMID: 23698371 DOI: 10.1038/nature12240]

33 **Rankin LC**, Girard-Madoux MJ, Seillet C, Mielke LA, Kerdiles Y, Fenis A, Wieduwild E, Putoczki T, Mondot S, Lantz O, Demon D, Papenfuss AT, Smyth GK, Lamkanfi M, Carotta S, Renauld JC, Shi W, Carpentier S, Soos T, Arendt C, Ugolini S, Huntington ND, Belz GT, Vivier E. Complementarity and redundancy of IL-22-producing innate lymphoid cells. *Nat Immunol* 2016; **17**: 179-186 [PMID: 26595889 DOI: 10.1038/ni.3332]

34 **Zhu Y**, Shi T, Lu X, Xu Z, Qu J, Zhang Z, Shi G, Shen S, Hou Y, Chen Y, Wang T. Fungal-induced glycolysis in macrophages promotes colon cancer by enhancing innate lymphoid cell secretion of IL-22. *EMBO J* 2021; **40**: e105320 [PMID: 33591591 DOI: 10.15252/embj.2020105320]

35 **Guillerey C**. Roles of cytotoxic and helper innate lymphoid cells in cancer. *Mamm Genome* 2018; **29**: 777-789 [PMID: 30178306 DOI: 10.1007/s00335-018-9781-4]

36 **Wu J**, Cheng H, Wang H, Zang G, Qi L, Lv X, Liu C, Zhu S, Zhang M, Cui J, Ueno H, Liu YJ, Suo J, Chen J. Correlation Between Immune Lymphoid Cells and Plasmacytoid Dendritic Cells in Human Colon Cancer. *Front Immunol* 2021; **12**: 601611 [PMID: 33708200 DOI: 10.3389/fimmu.2021.601611]

37 **Wang H**, Tian T, Zhang J. Tumor-Associated Macrophages (TAMs) in Colorectal Cancer (CRC): From Mechanism to Therapy and Prognosis. *Int J Mol Sci* 2021; **22** [PMID: 34445193 DOI: 10.3390/ijms22168470]

38 **Italiani P**, Boraschi D. From Monocytes to M1/M2 Macrophages: Phenotypical vs. Functional Differentiation. *Front Immunol* 2014; **5**: 514 [PMID: 25368618 DOI: 10.3389/fimmu.2014.00514]

39 **Fan L**, Xu C, Ge Q, Lin Y, Wong CC, Qi Y, Ye B, Lian Q, Zhuo W, Si J, Chen S, Wang L. A. Muciniphila Suppresses Colorectal Tumorigenesis by Inducing TLR2/NLRP3-Mediated M1-Like TAMs. *Cancer Immunol Res* 2021; **9**: 1111-1124 [PMID: 34389559 DOI: 10.1158/2326-6066.CIR-20-1019]

40 **Li R**, Zhou R, Wang H, Li W, Pan M, Yao X, Zhan W, Yang S, Xu L, Ding Y, Zhao L. Gut microbiota-stimulated cathepsin K secretion mediates TLR4-dependent M2 macrophage polarization and promotes tumor metastasis in colorectal cancer. *Cell Death Differ* 2019; **26**: 2447-2463 [PMID: 30850734 DOI: 10.1038/s41418-019-0312-y]

41 **Xu C**, Fan L, Lin Y, Shen W, Qi Y, Zhang Y, Chen Z, Wang L, Long Y, Hou T, Si J, Chen S. Fusobacterium nucleatum promotes colorectal cancer metastasis through miR-1322/CCL20 axis and M2 polarization. *Gut Microbes* 2021; **13**: 1980347 [PMID: 34632963 DOI: 10.1080/19490976.2021.1980347]

42 **Abreu MT**. Toll-like receptor signalling in the intestinal epithelium: how bacterial recognition shapes intestinal function. *Nat Rev Immunol* 2010; **10**: 131-144 [PMID: 20098461 DOI: 10.1038/nri2707]

43 **Chen Y**, Liu B, Wei Y, Kuang DM. Influence of gut and intratumoral microbiota on the immune microenvironment and

anti-cancer therapy. *Pharmacol Res* 2021; **174**: 105966 [PMID: 34728366 DOI: 10.1016/j.phrs.2021.105966]
44 **Gasaly N**, de Vos P, Hermoso MA. Impact of Bacterial Metabolites on Gut Barrier Function and Host Immunity: A Focus on Bacterial Metabolism and Its Relevance for Intestinal Inflammation. *Front Immunol* 2021; **12**: 658354 [PMID: 34122415 DOI: 10.3389/fimmu.2021.658354]
45 **Lavelle A**, Sokol H. Gut microbiota-derived metabolites as key actors in inflammatory bowel disease. *Nat Rev Gastroenterol Hepatol* 2020; **17**: 223-237 [PMID: 32076145 DOI: 10.1038/s41575-019-0258-z]
46 **Makki K**, Deehan EC, Walter J, Bäckhed F. The Impact of Dietary Fiber on Gut Microbiota in Host Health and Disease. *Cell Host Microbe* 2018; **23**: 705-715 [PMID: 29902436 DOI: 10.1016/j.chom.2018.05.012]
47 **Sanders ME**, Merenstein DJ, Reid G, Gibson GR, Rastall RA. Probiotics and prebiotics in intestinal health and disease: from biology to the clinic. *Nat Rev Gastroenterol Hepatol* 2019; **16**: 605-616 [PMID: 31296969 DOI: 10.1038/s41575-019-0173-3]
48 **Khan I**, Huang G, Li XA, Liao W, Leong WK, Xia W, Bian X, Wu J, Hsiao WLW. Mushroom polysaccharides and jiaogulan saponins exert cancer preventive effects by shaping the gut microbiota and microenvironment in Apc(Min/+) mice. *Pharmacol Res* 2019; **148**: 104448 [PMID: 31499195 DOI: 10.1016/j.phrs.2019.104448]
49 **Wang T**, Cai G, Qiu Y, Fei N, Zhang M, Pang X, Jia W, Cai S, Zhao L. Structural segregation of gut microbiota between colorectal cancer patients and healthy volunteers. *ISME J* 2012; **6**: 320-329 [PMID: 21850056 DOI: 10.1038/ismej.2011.109]
50 **Flint HJ**, Duncan SH, Scott KP, Louis P. Links between diet, gut microbiota composition and gut metabolism. *Proc Nutr Soc* 2015; **74**: 13-22 [PMID: 25268552 DOI: 10.1017/S0029665114001463]
51 **Hou H**, Chen D, Zhang K, Zhang W, Liu T, Wang S, Dai X, Wang B, Zhong W, Cao H. Gut microbiota-derived short-chain fatty acids and colorectal cancer: Ready for clinical translation? *Cancer Lett* 2022; **526**: 225-235 [PMID: 34843863 DOI: 10.1016/j.canlet.2021.11.027]
52 **Dalile B**, Van Oudenhove L, Vervliet B, Verbeke K. The role of short-chain fatty acids in microbiota-gut-brain communication. *Nat Rev Gastroenterol Hepatol* 2019; **16**: 461-478 [PMID: 31123355 DOI: 10.1038/s41575-019-0157-3]
53 **Bultman SJ**, Jobin C. Microbial-derived butyrate: an oncometabolite or tumor-suppressive metabolite? *Cell Host Microbe* 2014; **16**: 143-145 [PMID: 25121740 DOI: 10.1016/j.chom.2014.07.011]
54 **Belcheva A**, Irrazabal T, Robertson SJ, Streutker C, Maughan H, Rubino S, Moriyama EH, Copeland JK, Surendra A, Kumar S, Green B, Geddes K, Pezo RC, Navarre WW, Milosevic M, Wilson BC, Girardin SE, Wolever TMS, Edelmann W, Guttman DS, Philpott DJ, Martin A. Gut microbial metabolism drives transformation of MSH2-deficient colon epithelial cells. *Cell* 2014; **158**: 288-299 [PMID: 25036629 DOI: 10.1016/j.cell.2014.04.051]
55 **Devillard E**, McIntosh FM, Duncan SH, Wallace RJ. Metabolism of linoleic acid by human gut bacteria: different routes for biosynthesis of conjugated linoleic acid. *J Bacteriol* 2007; **189**: 2566-2570 [PMID: 17209019 DOI: 10.1128/JB.01359-06]
56 **Evans NP**, Misyak SA, Schmelz EM, Guri AJ, Hontecillas R, Bassaganya-Riera J. Conjugated linoleic acid ameliorates inflammation-induced colorectal cancer in mice through activation of PPARgamma. *J Nutr* 2010; **140**: 515-521 [PMID: 20089779 DOI: 10.3945/jn.109.115642]
57 **Bassaganya-Riera J**, Reynolds K, Martino-Catt S, Cui Y, Hennighausen L, Gonzalez F, Rohrer J, Benninghoff AU, Hontecillas R. Activation of PPAR gamma and delta by conjugated linoleic acid mediates protection from experimental inflammatory bowel disease. *Gastroenterology* 2004; **127**: 777-791 [PMID: 15362034 DOI: 10.1053/j.gastro.2004.06.049]
58 **Smyth EC**, Nilsson M, Grabsch HI, van Grieken NC, Lordick F. Gastric cancer. *Lancet* 2020; **396**: 635-648 [PMID: 32861308 DOI: 10.1016/S0140-6736(20)31288-5]
59 **Peng R**, Liu S, You W, Huang Y, Hu C, Gao Y, Jia X, Li G, Xu Z, Chen Y. Gastric Microbiome Alterations Are Associated with Decreased CD8+ Tissue-Resident Memory T Cells in the Tumor Microenvironment of Gastric Cancer. *Cancer Immunol Res* 2022; **10**: 1224-1240 [PMID: 35881964 DOI: 10.1158/2326-6066.CIR-22-0107]
60 **Artola-Borán M**, Fallegger A, Priola M, Jeske R, Waterboer T, Dohlman AB, Shen X, Wild S, He J, Levesque MP, Yousefi S, Simon HU, Cheng PF, Müller A. Mycobacterial infection aggravates Helicobacter pylori-induced gastric preneoplastic pathology by redirection of de novo induced Treg cells. *Cell Rep* 2022; **38**: 110359 [PMID: 35139377 DOI: 10.1016/j.celrep.2022.110359]
61 **Oster P**, Vaillant L, Riva E, McMillan B, Begka C, Truntzer C, Richard C, Leblond MM, Messaoudene M, Machremi E, Limagne E, Ghiringhelli F, Routy B, Verdeil G, Velin D. Helicobacter pylori infection has a detrimental impact on the efficacy of cancer immunotherapies. *Gut* 2022; **71**: 457-466 [PMID: 34253574 DOI: 10.1136/gutjnl-2020-323392]
62 **Oster P**, Vaillant L, McMillan B, Velin D. The Efficacy of Cancer Immunotherapies Is Compromised by Helicobacter pylori Infection. *Front Immunol* 2022; **13**: 899161 [PMID: 35677057 DOI: 10.3389/fimmu.2022.899161]
63 **Kalali B**, Mejías-Luque R, Javaheri A, Gerhard M. H. pylori virulence factors: influence on immune system and pathology. *Mediators Inflamm* 2014; **2014**: 426309 [PMID: 24587595 DOI: 10.1155/2014/426309]
64 **Takeshima E**, Tomimori K, Takamatsu R, Ishikawa C, Kinjo F, Hirayama T, Fujita J, Mori N. Helicobacter pylori VacA activates NF-kappaB in T cells *via* the classical but not alternative pathway. *Helicobacter* 2009; **14**: 271-279 [PMID: 19674131 DOI: 10.1111/j.1523-5378.2009.00683.x]
65 **Schmees C**, Prinz C, Treptau T, Rad R, Hengst L, Voland P, Bauer S, Brenner L, Schmid RM, Gerhard M. Inhibition of T-cell proliferation by Helicobacter pylori gamma-glutamyl transpeptidase. *Gastroenterology* 2007; **132**: 1820-1833 [PMID: 17484877 DOI: 10.1053/j.gastro.2007.02.031]
66 **Hussein NR**, Argent RH, Marx CK, Patel SR, Robinson K, Atherton JC. Helicobacter pylori dupA is polymorphic, and its active form induces proinflammatory cytokine secretion by mononuclear cells. *J Infect Dis* 2010; **202**: 261-269 [PMID: 20533870 DOI: 10.1086/653587]
67 **Liu X**, Shao L, Liu X, Ji F, Mei Y, Cheng Y, Liu F, Yan C, Li L, Ling Z. Alterations of gastric mucosal microbiota across different stomach microhabitats in a cohort of 276 patients with gastric cancer. *EBioMedicine* 2019; **40**: 336-348 [PMID: 30584008 DOI: 10.1016/j.ebiom.2018.12.034]
68 **Lofgren JL**, Whary MT, Ge Z, Muthupalani S, Taylor NS, Mobley M, Potter A, Varro A, Eibach D, Suerbaum S, Wang TC, Fox JG. Lack of commensal flora in Helicobacter pylori-infected INS-GAS mice reduces gastritis and delays

intraepithelial neoplasia. *Gastroenterology* 2011; **140**: 210-220 [PMID: 20950613 DOI: 10.1053/j.gastro.2010.09.048]
69 **Dai D**, Yang Y, Yu J, Dang T, Qin W, Teng L, Ye J, Jiang H. Interactions between gastric microbiota and metabolites in gastric cancer. *Cell Death Dis* 2021; **12**: 1104 [PMID: 34819503 DOI: 10.1038/s41419-021-04396-y]
70 **Zhang N**, Bevan MJ. Transforming growth factor-β signaling controls the formation and maintenance of gut-resident memory T cells by regulating migration and retention. *Immunity* 2013; **39**: 687-696 [PMID: 24076049 DOI: 10.1016/j.immuni.2013.08.019]
71 **Amsen D**, van Gisbergen KPJM, Hombrink P, van Lier RAW. Tissue-resident memory T cells at the center of immunity to solid tumors. *Nat Immunol* 2018; **19**: 538-546 [PMID: 29777219 DOI: 10.1038/s41590-018-0114-2]
72 **Chen Y**, Zhang S, Wang Q, Zhang X. Tumor-recruited M2 macrophages promote gastric and breast cancer metastasis *via* M2 macrophage-secreted CHI3L1 protein. *J Hematol Oncol* 2017; **10**: 36 [PMID: 28143526 DOI: 10.1186/s13045-017-0408-0]
73 **Li Q**, Wu W, Gong D, Shang R, Wang J, Yu H. Propionibacterium acnes overabundance in gastric cancer promote M2 polarization of macrophages *via* a TLR4/PI3K/Akt signaling. *Gastric Cancer* 2021; **24**: 1242-1253 [PMID: 34076786 DOI: 10.1007/s10120-021-01202-8]
74 **Vinasco K**, Mitchell HM, Kaakoush NO, Castaño-Rodríguez N. Microbial carcinogenesis: Lactic acid bacteria in gastric cancer. *Biochim Biophys Acta Rev Cancer* 2019; **1872**: 188309 [PMID: 31394110 DOI: 10.1016/j.bbcan.2019.07.004]
75 **Zhang L**, Li S. Lactic acid promotes macrophage polarization through MCT-HIF1α signaling in gastric cancer. *Exp Cell Res* 2020; **388**: 111846 [PMID: 31945319 DOI: 10.1016/j.yexcr.2020.111846]
76 **Neal-McKinney JM**, Lu X, Duong T, Larson CL, Call DR, Shah DH, Konkel ME. Production of organic acids by probiotic lactobacilli can be used to reduce pathogen load in poultry. *PLoS One* 2012; **7**: e43928 [PMID: 22962594 DOI: 10.1371/journal.pone.0043928]
77 **Yang P**, Zhang X, Xu R, Adeel K, Lu X, Chen M, Shen H, Li Z, Xu Z. Fungal Microbiota Dysbiosis and Ecological Alterations in Gastric Cancer. *Front Microbiol* 2022; **13**: 889694 [PMID: 35572666 DOI: 10.3389/fmicb.2022.889694]
78 **Fortis C**, Foppoli M, Gianotti L, Galli L, Citterio G, Consogno G, Gentilini O, Braga M. Increased interleukin-10 serum levels in patients with solid tumours. *Cancer Lett* 1996; **104**: 1-5 [PMID: 8640735 DOI: 10.1016/0304-3835(96)04213-9]
79 **Ahmad N**, Ammar A, Storr SJ, Green AR, Rakha E, Ellis IO, Martin SG. IL-6 and IL-10 are associated with good prognosis in early stage invasive breast cancer patients. *Cancer Immunol Immunother* 2018; **67**: 537-549 [PMID: 29256156 DOI: 10.1007/s00262-017-2106-8]
80 **Zhang H**, Li R, Cao Y, Gu Y, Lin C, Liu X, Lv K, He X, Fang H, Jin K, Fei Y, Chen Y, Wang J, Liu H, Li H, Zhang H, He H, Zhang W. Poor Clinical Outcomes and Immunoevasive Contexture in Intratumoral IL-10-Producing Macrophages Enriched Gastric Cancer Patients. *Ann Surg* 2022; **275**: e626-e635 [PMID: 32541216 DOI: 10.1097/SLA.0000000000004037]
81 **Zhong M**, Xiong Y, Zhao J, Gao Z, Ma J, Wu Z, Song Y, Hong X. Candida albicans disorder is associated with gastric carcinogenesis. *Theranostics* 2021; **11**: 4945-4956 [PMID: 33754037 DOI: 10.7150/thno.55209]
82 **Ramirez-Garcia A**, Arteta B, Abad-Diaz-de-Cerio A, Pellon A, Antoran A, Marquez J, Rementeria A, Hernando FL. Candida albicans increases tumor cell adhesion to endothelial cells in vitro: intraspecific differences and importance of the mannose receptor. *PLoS One* 2013; **8**: e53584 [PMID: 23301091 DOI: 10.1371/journal.pone.0053584]
83 **Trinchieri G**. Interleukin-12 and the regulation of innate resistance and adaptive immunity. *Nat Rev Immunol* 2003; **3**: 133-146 [PMID: 12563297 DOI: 10.1038/nri1001]
84 **Langowski JL**, Zhang X, Wu L, Mattson JD, Chen T, Smith K, Basham B, McClanahan T, Kastelein RA, Oft M. IL-23 promotes tumour incidence and growth. *Nature* 2006; **442**: 461-465 [PMID: 16688182 DOI: 10.1038/nature04808]
85 **Ramirez-Garcia A**, Rementeria A, Aguirre-Urizar JM, Moragues MD, Antoran A, Pellon A, Abad-Diaz-de-Cerio A, Hernando FL. Candida albicans and cancer: Can this yeast induce cancer development or progression? *Crit Rev Microbiol* 2016; **42**: 181-193 [PMID: 24963692 DOI: 10.3109/1040841X.2014.913004]
86 **Lagergren J**, Smyth E, Cunningham D, Lagergren P. Oesophageal cancer. *Lancet* 2017; **390**: 2383-2396 [PMID: 28648400 DOI: 10.1016/S0140-6736(17)31462-9]
87 **Baba Y**, Iwatsuki M, Yoshida N, Watanabe M, Baba H. Review of the gut microbiome and esophageal cancer: Pathogenesis and potential clinical implications. *Ann Gastroenterol Surg* 2017; **1**: 99-104 [PMID: 29863142 DOI: 10.1002/ags3.12014]
88 **Neto AG**, Whitaker A, Pei Z. Microbiome and potential targets for chemoprevention of esophageal adenocarcinoma. *Semin Oncol* 2016; **43**: 86-96 [PMID: 26970127 DOI: 10.1053/j.seminoncol.2015.09.005]
89 **Yang L**, Lu X, Nossa CW, Francois F, Peek RM, Pei Z. Inflammation and intestinal metaplasia of the distal esophagus are associated with alterations in the microbiome. *Gastroenterology* 2009; **137**: 588-597 [PMID: 19394334 DOI: 10.1053/j.gastro.2009.04.046]
90 **Lopetuso LR**, Severgnini M, Pecere S, Ponziani FR, Boskoski I, Larghi A, Quaranta G, Masucci L, Ianiro G, Camboni T, Gasbarrini A, Costamagna G, Consolandi C, Cammarota G. Esophageal microbiome signature in patients with Barrett's esophagus and esophageal adenocarcinoma. *PLoS One* 2020; **15**: e0231789 [PMID: 32369505 DOI: 10.1371/journal.pone.0231789]
91 **Maret-Ouda J**, Markar SR, Lagergren J. Gastroesophageal Reflux Disease: A Review. *JAMA* 2020; **324**: 2536-2547 [PMID: 33351048 DOI: 10.1001/jama.2020.21360]
92 **Katzka DA**, Kahrilas PJ. Advances in the diagnosis and management of gastroesophageal reflux disease. *BMJ* 2020; **371**: m3786 [PMID: 33229333 DOI: 10.1136/bmj.m3786]
93 **Spechler SJ**, Souza RF. Barrett's esophagus. *N Engl J Med* 2014; **371**: 836-845 [PMID: 25162890 DOI: 10.1056/NEJMra1314704]
94 **Yang L**, Francois F, Pei Z. Molecular pathways: pathogenesis and clinical implications of microbiome alteration in esophagitis and Barrett esophagus. *Clin Cancer Res* 2012; **18**: 2138-2144 [PMID: 22344232 DOI: 10.1158/1078-0432.CCR-11-0934]
95 **Jiang Q**, Akashi S, Miyake K, Petty HR. Lipopolysaccharide induces physical proximity between CD14 and toll-like receptor 4 (TLR4) prior to nuclear translocation of NF-kappa B. *J Immunol* 2000; **165**: 3541-3544 [PMID: 11034352 DOI:

10.4049/jimmunol.165.7.3541]
96 **Macfarlane S**, Furrie E, Macfarlane GT, Dillon JF. Microbial colonization of the upper gastrointestinal tract in patients with Barrett's esophagus. *Clin Infect Dis* 2007; **45**: 29-38 [PMID: 17554697 DOI: 10.1086/518578]
97 **Blackett KL**, Siddhi SS, Cleary S, Steed H, Miller MH, Macfarlane S, Macfarlane GT, Dillon JF. Oesophageal bacterial biofilm changes in gastro-oesophageal reflux disease, Barrett's and oesophageal carcinoma: association or causality? *Aliment Pharmacol Ther* 2013; **37**: 1084-1092 [PMID: 23600758 DOI: 10.1111/apt.12317]
98 **Yasuda K**, Nakanishi K, Tsutsui H. Interleukin-18 in Health and Disease. *Int J Mol Sci* 2019; **20** [PMID: 30717382 DOI: 10.3390/ijms20030649]
99 **Zheng J**, Meng J, Zhao S, Singh R, Song W. Campylobacter-induced interleukin-8 secretion in polarized human intestinal epithelial cells requires Campylobacter-secreted cytolethal distending toxin- and Toll-like receptor-mediated activation of NF-kappaB. *Infect Immun* 2008; **76**: 4498-4508 [PMID: 18644884 DOI: 10.1128/IAI.01317-07]
100 **Man SM**. The clinical importance of emerging Campylobacter species. *Nat Rev Gastroenterol Hepatol* 2011; **8**: 669-685 [PMID: 22025030 DOI: 10.1038/nrgastro.2011.191]
101 **Eribe ERK**, Olsen I. Leptotrichia species in human infections II. *J Oral Microbiol* 2017; **9**: 1368848 [PMID: 29081911 DOI: 10.1080/20002297.2017.1368848]
102 **Morgenstein AA**, Citron DM, Orisek B, Finegold SM. Serious infection with Leptotrichia buccalis. Report of a case and review of the literature. *Am J Med* 1980; **69**: 782-785 [PMID: 7001901 DOI: 10.1016/0002-9343(80)90452-0]
103 **Di Pilato V**, Freschi G, Ringressi MN, Pallecchi L, Rossolini GM, Bechi P. The esophageal microbiota in health and disease. *Ann N Y Acad Sci* 2016; **1381**: 21-33 [PMID: 27415419 DOI: 10.1111/nyas.13127]
104 **Gao S**, Liu Y, Duan X, Liu K, Mohammed M, Gu Z, Ren J, Yakoumatos L, Yuan X, Lu L, Liang S, Li J, Scott DA, Lamont RJ, Zhou F, Wang H. Porphyromonas gingivalis infection exacerbates oesophageal cancer and promotes resistance to neoadjuvant chemotherapy. *Br J Cancer* 2021; **125**: 433-444 [PMID: 33981017 DOI: 10.1038/s41416-021-01419-5]
105 **Gao SG**, Yang JQ, Ma ZK, Yuan X, Zhao C, Wang GC, Wei H, Feng XS, Qi YJ. Preoperative serum immunoglobulin G and A antibodies to Porphyromonas gingivalis are potential serum biomarkers for the diagnosis and prognosis of esophageal squamous cell carcinoma. *BMC Cancer* 2018; **18**: 17 [PMID: 29298684 DOI: 10.1186/s12885-017-3905-1]
106 **Tan Q**, Ma X, Yang B, Liu Y, Xie Y, Wang X, Yuan W, Ma J. Periodontitis pathogen Porphyromonas gingivalis promotes pancreatic tumorigenesis *via* neutrophil elastase from tumor-associated neutrophils. *Gut Microbes* 2022; **14**: 2073785 [PMID: 35549648 DOI: 10.1080/19490976.2022.2073785]
107 **Yamamura K**, Baba Y, Nakagawa S, Mima K, Miyake K, Nakamura K, Sawayama H, Kinoshita K, Ishimoto T, Iwatsuki M, Sakamoto Y, Yamashita Y, Yoshida N, Watanabe M, Baba H. Human Microbiome Fusobacterium Nucleatum in Esophageal Cancer Tissue Is Associated with Prognosis. *Clin Cancer Res* 2016; **22**: 5574-5581 [PMID: 27769987 DOI: 10.1158/1078-0432.CCR-16-1786]
108 **Kadomoto S**, Izumi K, Mizokami A. The CCL20-CCR6 Axis in Cancer Progression. *Int J Mol Sci* 2020; **21** [PMID: 32707869 DOI: 10.3390/ijms21155186]
109 **Yamazaki T**, Yang XO, Chung Y, Fukunaga A, Nurieva R, Pappu B, Martin-Orozco N, Kang HS, Ma L, Panopoulos AD, Craig S, Watowich SS, Jetten AM, Tian Q, Dong C. CCR6 regulates the migration of inflammatory and regulatory T cells. *J Immunol* 2008; **181**: 8391-8401 [PMID: 19050256 DOI: 10.4049/jimmunol.181.12.8391]
110 **Chen KJ**, Lin SZ, Zhou L, Xie HY, Zhou WH, Taki-Eldin A, Zheng SS. Selective recruitment of regulatory T cell through CCR6-CCL20 in hepatocellular carcinoma fosters tumor progression and predicts poor prognosis. *PLoS One* 2011; **6**: e24671 [PMID: 21935436 DOI: 10.1371/journal.pone.0024671]
111 **Hessmann E**, Buchholz SM, Demir IE, Singh SK, Gress TM, Ellenrieder V, Neesse A. Microenvironmental Determinants of Pancreatic Cancer. *Physiol Rev* 2020; **100**: 1707-1751 [PMID: 32297835 DOI: 10.1152/physrev.00042.2019]
112 **Geller LT**, Barzily-Rokni M, Danino T, Jonas OH, Shental N, Nejman D, Gavert N, Zwang Y, Cooper ZA, Shee K, Thaiss CA, Reuben A, Livny J, Avraham R, Frederick DT, Ligorio M, Chatman K, Johnston SE, Mosher CM, Brandis A, Fuks G, Gurbatri C, Gopalakrishnan V, Kim M, Hurd MW, Katz M, Fleming J, Maitra A, Smith DA, Skalak M, Bu J, Michaud M, Trauger SA, Barshack I, Golan T, Sandbank J, Flaherty KT, Mandinova A, Garrett WS, Thayer SP, Ferrone CR, Huttenhower C, Bhatia SN, Gevers D, Wargo JA, Golub TR, Straussman R. Potential role of intratumor bacteria in mediating tumor resistance to the chemotherapeutic drug gemcitabine. *Science* 2017; **357**: 1156-1160 [PMID: 28912244 DOI: 10.1126/science.aah5043]
113 **Thomas RM**, Gharaibeh RZ, Gauthier J, Beveridge M, Pope JL, Guijarro MV, Yu Q, He Z, Ohland C, Newsome R, Trevino J, Hughes SJ, Reinhard M, Winglee K, Fodor AA, Zajac-Kaye M, Jobin C. Intestinal microbiota enhances pancreatic carcinogenesis in preclinical models. *Carcinogenesis* 2018; **39**: 1068-1078 [PMID: 29846515 DOI: 10.1093/carcin/bgy073]
114 **Wang Y**, Yang G, You L, Yang J, Feng M, Qiu J, Zhao F, Liu Y, Cao Z, Zheng L, Zhang T, Zhao Y. Role of the microbiome in occurrence, development and treatment of pancreatic cancer. *Mol Cancer* 2019; **18**: 173 [PMID: 31785619 DOI: 10.1186/s12943-019-1103-2]
115 **Ghaddar B**, Biswas A, Harris C, Omary MB, Carpizo DR, Blaser MJ, De S. Tumor microbiome links cellular programs and immunity in pancreatic cancer. *Cancer Cell* 2022; **40**: 1240-1253.e5 [PMID: 36220074 DOI: 10.1016/j.ccell.2022.09.009]
116 **Schulthess J**, Pandey S, Capitani M, Rue-Albrecht KC, Arnold I, Franchini F, Chomka A, Ilott NE, Johnston DGW, Pires E, McCullagh J, Sansom SN, Arancibia-Cárcamo CV, Uhlig HH, Powrie F. The Short Chain Fatty Acid Butyrate Imprints an Antimicrobial Program in Macrophages. *Immunity* 2019; **50**: 432-445.e7 [PMID: 30683619 DOI: 10.1016/j.immuni.2018.12.018]
117 **Woo SR**, Corrales L, Gajewski TF. Innate immune recognition of cancer. *Annu Rev Immunol* 2015; **33**: 445-474 [PMID: 25622193 DOI: 10.1146/annurev-immunol-032414-112043]
118 **Lankadasari MB**, Mukhopadhyay P, Mohammed S, Harikumar KB. TAMing pancreatic cancer: combat with a double edged sword. *Mol Cancer* 2019; **18**: 48 [PMID: 30925924 DOI: 10.1186/s12943-019-0966-6]
119 **Lecoultre M**, Dutoit V, Walker PR. Phagocytic function of tumor-associated macrophages as a key determinant of tumor progression control: a review. *J Immunother Cancer* 2020; **8** [PMID: 33335026 DOI: 10.1136/jitc-2020-001408]

120 **Pushalkar S**, Hundeyin M, Daley D, Zambirinis CP, Kurz E, Mishra A, Mohan N, Aykut B, Usyk M, Torres LE, Werba G, Zhang K, Guo Y, Li Q, Akkad N, Lall S, Wadowski B, Gutierrez J, Kochen Rossi JA, Herzog JW, Diskin B, Torres-Hernandez A, Leinwand J, Wang W, Taunk PS, Savadkar S, Janal M, Saxena A, Li X, Cohen D, Sartor RB, Saxena D, Miller G. The Pancreatic Cancer Microbiome Promotes Oncogenesis by Induction of Innate and Adaptive Immune Suppression. *Cancer Discov* 2018; **8**: 403-416 [PMID: 29567829 DOI: 10.1158/2159-8290.CD-17-1134]

121 **al-Waiz M**, Mikov M, Mitchell SC, Smith RL. The exogenous origin of trimethylamine in the mouse. *Metabolism* 1992; **41**: 135-136 [PMID: 1736035 DOI: 10.1016/0026-0495(92)90140-6]

122 **Mirji G**, Worth A, Bhat SA, El Sayed M, Kannan T, Goldman AR, Tang HY, Liu Q, Auslander N, Dang CV, Abdel-Mohsen M, Kossenkov A, Stanger BZ, Shinde RS. The microbiome-derived metabolite TMAO drives immune activation and boosts responses to immune checkpoint blockade in pancreatic cancer. *Sci Immunol* 2022; **7**: eabn0704 [PMID: 36083892 DOI: 10.1126/sciimmunol.abn0704]

123 **Alam A**, Levanduski E, Denz P, Villavicencio HS, Bhatta M, Alhorebi L, Zhang Y, Gomez EC, Morreale B, Senchanthisai S, Li J, Turowski SG, Sexton S, Sait SJ, Singh PK, Wang J, Maitra A, Kalinski P, DePinho RA, Wang H, Liao W, Abrams SI, Segal BH, Dey P. Fungal mycobiome drives IL-33 secretion and type 2 immunity in pancreatic cancer. *Cancer Cell* 2022; **40**: 153-167.e11 [PMID: 35120601 DOI: 10.1016/j.ccell.2022.01.003]

124 **Sun X**, He X, Zhang Y, Hosaka K, Andersson P, Wu J, Jing X, Du Q, Hui X, Ding B, Guo Z, Hong A, Liu X, Wang Y, Ji Q, Beyaert R, Yang Y, Li Q, Cao Y. Inflammatory cell-derived CXCL3 promotes pancreatic cancer metastasis through a novel myofibroblast-hijacked cancer escape mechanism. *Gut* 2022; **71**: 129-147 [PMID: 33568427 DOI: 10.1136/gutjnl-2020-322744]

125 **Mahajan UM**, Langhoff E, Goni E, Costello E, Greenhalf W, Halloran C, Ormanns S, Kruger S, Boeck S, Ribback S, Beyer G, Dombroswki F, Weiss FU, Neoptolemos JP, Werner J, D'Haese JG, Bazhin A, Peterhansl J, Pichlmeier S, Büchler MW, Kleeff J, Ganeh P, Sendler M, Palmer DH, Kohlmann T, Rad R, Regel I, Lerch MM, Mayerle J. Immune Cell and Stromal Signature Associated With Progression-Free Survival of Patients With Resected Pancreatic Ductal Adenocarcinoma. *Gastroenterology* 2018; **155**: 1625-1639.e2 [PMID: 30092175 DOI: 10.1053/j.gastro.2018.08.009]

126 **Liu X**, Xu J, Zhang B, Liu J, Liang C, Meng Q, Hua J, Yu X, Shi S. The reciprocal regulation between host tissue and immune cells in pancreatic ductal adenocarcinoma: new insights and therapeutic implications. *Mol Cancer* 2019; **18**: 184 [PMID: 31831007 DOI: 10.1186/s12943-019-1117-9]

127 **Dey P**, Li J, Zhang J, Chaurasiya S, Strom A, Wang H, Liao WT, Cavallaro F, Denz P, Bernard V, Yen EY, Genovese G, Gulhati P, Liu J, Chakravarti D, Deng P, Zhang T, Carbone F, Chang Q, Ying H, Shang X, Spring DJ, Ghosh B, Putluri N, Maitra A, Wang YA, DePinho RA. Oncogenic KRAS-Driven Metabolic Reprogramming in Pancreatic Cancer Cells Utilizes Cytokines from the Tumor Microenvironment. *Cancer Discov* 2020; **10**: 608-625 [PMID: 32046984 DOI: 10.1158/2159-8290.CD-19-0297]

128 **Moral JA**, Leung J, Rojas LA, Ruan J, Zhao J, Sethna Z, Ramnarain A, Gasmi B, Gururajan M, Redmond D, Askan G, Bhanot U, Elyada E, Park Y, Tuveson DA, Gönen M, Leach SD, Wolchok JD, DeMatteo RP, Merghoub T, Balachandran VP. ILC2s amplify PD-1 blockade by activating tissue-specific cancer immunity. *Nature* 2020; **579**: 130-135 [PMID: 32076273 DOI: 10.1038/s41586-020-2015-4]

129 **Mohindroo C**, Hasanov M, Rogers JE, Dong W, Prakash LR, Baydogan S, Mizrahi JD, Overman MJ, Varadhachary GR, Wolff RA, Javle MM, Fogelman DR, Lotze MT, Kim MP, Katz MHG, Pant S, Tzeng CD, McAllister F. Antibiotic use influences outcomes in advanced pancreatic adenocarcinoma patients. *Cancer Med* 2021; **10**: 5041-5050 [PMID: 34250759 DOI: 10.1002/cam4.3870]

130 **Aykut B**, Pushalkar S, Chen R, Li Q, Abengozar R, Kim JI, Shadaloey SA, Wu D, Preiss P, Verma N, Guo Y, Saxena A, Vardhan M, Diskin B, Wang W, Leinwand J, Kurz E, Kochen Rossi JA, Hundeyin M, Zambrinis C, Li X, Saxena D, Miller G. The fungal mycobiome promotes pancreatic oncogenesis *via* activation of MBL. *Nature* 2019; **574**: 264-267 [PMID: 31578522 DOI: 10.1038/s41586-019-1608-2]

131 **Bullman S**, Pedamallu CS, Sicinska E, Clancy TE, Zhang X, Cai D, Neuberg D, Huang K, Guevara F, Nelson T, Chipashvili O, Hagan T, Walker M, Ramachandran A, Diosdado B, Serna G, Mulet N, Landolfi S, Ramon Y Cajal S, Fasani R, Aguirre AJ, Ng K, Élez E, Ogino S, Tabernero J, Fuchs CS, Hahn WC, Nuciforo P, Meyerson M. Analysis of Fusobacterium persistence and antibiotic response in colorectal cancer. *Science* 2017; **358**: 1443-1448 [PMID: 29170280 DOI: 10.1126/science.aal5240]

132 **Weniger M**, Hank T, Qadan M, Ciprani D, Michelakos T, Niess H, Heiliger C, Ilmer M, D'Haese JG, Ferrone CR, Warshaw AL, Lillemoe KD, Werner J, Liss A, Fernández-Del Castillo C. Influence of Klebsiella pneumoniae and quinolone treatment on prognosis in patients with pancreatic cancer. *Br J Surg* 2021; **108**: 709-716 [PMID: 34157083 DOI: 10.1002/bjs.12003]

133 **Xu H**, Cao C, Ren Y, Weng S, Liu L, Guo C, Wang L, Han X, Ren J, Liu Z. Antitumor effects of fecal microbiota transplantation: Implications for microbiome modulation in cancer treatment. *Front Immunol* 2022; **13**: 949490 [PMID: 36177041 DOI: 10.3389/fimmu.2022.949490]

134 **Rezasoltani S**, Yadegar A, Asadzadeh Aghdaei H, Reza Zali M. Modulatory effects of gut microbiome in cancer immunotherapy: A novel paradigm for blockade of immune checkpoint inhibitors. *Cancer Med* 2021; **10**: 1141-1154 [PMID: 33369247 DOI: 10.1002/cam4.3694]

135 **Mao J**, Wang D, Long J, Yang X, Lin J, Song Y, Xie F, Xun Z, Wang Y, Li Y, Sun H, Xue J, Zuo B, Zhang J, Bian J, Zhang T, Zhang L, Sang X, Zhao H. Gut microbiome is associated with the clinical response to anti-PD-1 based immunotherapy in hepatobiliary cancers. *J Immunother Cancer* 2021; **9** [PMID: 34873013 DOI: 10.1136/jitc-2021-003334]

136 **Rosshart SP**, Vassallo BG, Angeletti D, Hutchinson DS, Morgan AP, Takeda K, Hickman HD, McCulloch JA, Badger JH, Ajami NJ, Trinchieri G, Pardo-Manuel de Villena F, Yewdell JW, Rehermann B. Wild Mouse Gut Microbiota Promotes Host Fitness and Improves Disease Resistance. *Cell* 2017; **171**: 1015-1028.e13 [PMID: 29056339 DOI: 10.1016/j.cell.2017.09.016]

137 **Mima K**, Nakagawa S, Sawayama H, Ishimoto T, Imai K, Iwatsuki M, Hashimoto D, Baba Y, Yamashita YI, Yoshida N, Chikamoto A, Baba H. The microbiome and hepatobiliary-pancreatic cancers. *Cancer Lett* 2017; **402**: 9-15 [PMID:

28527946 DOI: 10.1016/j.canlet.2017.05.001]

138 **Wang T**, Zhang L, Wang P, Liu Y, Wang G, Shan Y, Yi Y, Zhou Y, Liu B, Wang X, Lü X. Lactobacillus coryniformis MXJ32 administration ameliorates azoxymethane/dextran sulfate sodium-induced colitis-associated colorectal cancer *via* reshaping intestinal microenvironment and alleviating inflammatory response. *Eur J Nutr* 2022; **61**: 85-99 [PMID: 34185157 DOI: 10.1007/s00394-021-02627-8]

139 **Wang T**, Zheng J, Dong S, Ismael M, Shan Y, Wang X, Lü X. Lacticaseibacillus rhamnosus LS8 Ameliorates Azoxymethane/Dextran Sulfate Sodium-Induced Colitis-Associated Tumorigenesis in Mice *via* Regulating Gut Microbiota and Inhibiting Inflammation. *Probiotics Antimicrob Proteins* 2022; **14**: 947-959 [PMID: 35788907 DOI: 10.1007/s12602-022-09967-9]

140 **Heydari Z**, Rahaie M, Alizadeh AM, Agah S, Khalighfard S, Bahmani S. Effects of Lactobacillus acidophilus and Bifidobacterium bifidum Probiotics on the Expression of MicroRNAs 135b, 26b, 18a and 155, and Their Involving Genes in Mice Colon Cancer. *Probiotics Antimicrob Proteins* 2019; **11**: 1155-1162 [PMID: 30311185 DOI: 10.1007/s12602-018-9478-8]

141 **Konishi H**, Isozaki S, Kashima S, Moriichi K, Ichikawa S, Yamamoto K, Yamamura C, Ando K, Ueno N, Akutsu H, Ogawa N, Fujiya M. Probiotic Aspergillus oryzae produces anti-tumor mediator and exerts anti-tumor effects in pancreatic cancer through the p38 MAPK signaling pathway. *Sci Rep* 2021; **11**: 11070 [PMID: 34040123 DOI: 10.1038/s41598-021-90707-4]

142 **Mendes MCS**, Paulino DS, Brambilla SR, Camargo JA, Persinoti GF, Carvalheira JBC. Microbiota modification by probiotic supplementation reduces colitis associated colon cancer in mice. *World J Gastroenterol* 2018; **24**: 1995-2008 [PMID: 29760543 DOI: 10.3748/wjg.v24.i18.1995]

143 **Suez J**, Zmora N, Zilberman-Schapira G, Mor U, Dori-Bachash M, Bashiardes S, Zur M, Regev-Lehavi D, Ben-Zeev Brik R, Federici S, Horn M, Cohen Y, Moor AE, Zeevi D, Korem T, Kotler E, Harmelin A, Itzkovitz S, Maharshak N, Shibolet O, Pevsner-Fischer M, Shapiro H, Sharon I, Halpern Z, Segal E, Elinav E. Post-Antibiotic Gut Mucosal Microbiome Reconstitution Is Impaired by Probiotics and Improved by Autologous FMT. *Cell* 2018; **174**: 1406-1423.e16 [PMID: 30193113 DOI: 10.1016/j.cell.2018.08.047]

144 **Routy B**, Le Chatelier E, Derosa L, Duong CPM, Alou MT, Daillère R, Fluckiger A, Messaoudene M, Rauber C, Roberti MP, Fidelle M, Flament C, Poirier-Colame V, Opolon P, Klein C, Iribarren K, Mondragón L, Jacquelot N, Qu B, Ferrere G, Clémenson C, Mezquita L, Masip JR, Naltet C, Brosseau S, Kaderbhai C, Richard C, Rizvi H, Levenez F, Galleron N, Quinquis B, Pons N, Ryffel B, Minard-Colin V, Gonin P, Soria JC, Deutsch E, Loriot Y, Ghiringhelli F, Zalcman G, Goldwasser F, Escudier B, Hellmann MD, Eggermont A, Raoult D, Albiges L, Kroemer G, Zitvogel L. Gut microbiome influences efficacy of PD-1-based immunotherapy against epithelial tumors. *Science* 2018; **359**: 91-97 [PMID: 29097494 DOI: 10.1126/science.aan3706]

145 **Sivan A**, Corrales L, Hubert N, Williams JB, Aquino-Michaels K, Earley ZM, Benyamin FW, Lei YM, Jabri B, Alegre ML, Chang EB, Gajewski TF. Commensal Bifidobacterium promotes antitumor immunity and facilitates anti-PD-L1 efficacy. *Science* 2015; **350**: 1084-1089 [PMID: 26541606 DOI: 10.1126/science.aac4255]

146 **Si W**, Liang H, Bugno J, Xu Q, Ding X, Yang K, Fu Y, Weichselbaum RR, Zhao X, Wang L. Lactobacillus rhamnosus GG induces cGAS/STING- dependent type I interferon and improves response to immune checkpoint blockade. *Gut* 2022; **71**: 521-533 [PMID: 33685966 DOI: 10.1136/gutjnl-2020-323426]

147 **Zhang SL**, Mao YQ, Zhang ZY, Li ZM, Kong CY, Chen HL, Cai PR, Han B, Ye T, Wang LS. Pectin supplement significantly enhanced the anti-PD-1 efficacy in tumor-bearing mice humanized with gut microbiota from patients with colorectal cancer. *Theranostics* 2021; **11**: 4155-4170 [PMID: 33754054 DOI: 10.7150/thno.54476]

148 **Zitvogel L**, Ayyoub M, Routy B, Kroemer G. Microbiome and Anticancer Immunosurveillance. *Cell* 2016; **165**: 276-287 [PMID: 27058662 DOI: 10.1016/j.cell.2016.03.001]

149 **Gopalakrishnan V**, Spencer CN, Nezi L, Reuben A, Andrews MC, Karpinets TV, Prieto PA, Vicente D, Hoffman K, Wei SC, Cogdill AP, Zhao L, Hudgens CW, Hutchinson DS, Manzo T, Petaccia de Macedo M, Cotechini T, Kumar T, Chen WS, Reddy SM, Szczepaniak Sloane R, Galloway-Pena J, Jiang H, Chen PL, Shpall EJ, Rezvani K, Alousi AM, Chemaly RF, Shelburne S, Vence LM, Okhuysen PC, Jensen VB, Swennes AG, McAllister F, Marcelo Riquelme Sanchez E, Zhang Y, Le Chatelier E, Zitvogel L, Pons N, Austin-Breneman JL, Haydu LE, Burton EM, Gardner JM, Sirmans E, Hu J, Lazar AJ, Tsujikawa T, Diab A, Tawbi H, Glitza IC, Hwu WJ, Patel SP, Woodman SE, Amaria RN, Davies MA, Gershenwald JE, Hwu P, Lee JE, Zhang J, Coussens LM, Cooper ZA, Futreal PA, Daniel CR, Ajami NJ, Petrosino JF, Tetzlaff MT, Sharma P, Allison JP, Jenq RR, Wargo JA. Gut microbiome modulates response to anti-PD-1 immunotherapy in melanoma patients. *Science* 2018; **359**: 97-103 [PMID: 29097493 DOI: 10.1126/science.aan4236]

150 **Huang XZ**, Gao P, Song YX, Xu Y, Sun JX, Chen XW, Zhao JH, Wang ZN. Antibiotic use and the efficacy of immune checkpoint inhibitors in cancer patients: a pooled analysis of 2740 cancer patients. *Oncoimmunology* 2019; **8**: e1665973 [PMID: 31741763 DOI: 10.1080/2162402X.2019.1665973]

151 **Wilson BE**, Routy B, Nagrial A, Chin VT. The effect of antibiotics on clinical outcomes in immune-checkpoint blockade: a systematic review and meta-analysis of observational studies. *Cancer Immunol Immunother* 2020; **69**: 343-354 [PMID: 31865400 DOI: 10.1007/s00262-019-02453-2]

152 **Wu Q**, Liu J, Wu S, Xie X. The impact of antibiotics on efficacy of immune checkpoint inhibitors in malignancies: A study based on 44 cohorts. *Int Immunopharmacol* 2021; **92**: 107303 [PMID: 33465728 DOI: 10.1016/j.intimp.2020.107303]

153 **Mager LF**, Burkhard R, Pett N, Cooke NCA, Brown K, Ramay H, Paik S, Stagg J, Groves RA, Gallo M, Lewis IA, Geuking MB, McCoy KD. Microbiome-derived inosine modulates response to checkpoint inhibitor immunotherapy. *Science* 2020; **369**: 1481-1489 [PMID: 32792462 DOI: 10.1126/science.abc3421]

154 **Han J**, Zhang S, Xu Y, Pang Y, Zhang X, Hu Y, Chen H, Chen W, Zhang J, He W. Beneficial Effect of Antibiotics and Microbial Metabolites on Expanded Vδ2Vγ9 T Cells in Hepatocellular Carcinoma Immunotherapy. *Front Immunol* 2020; **11**: 1380 [PMID: 32849498 DOI: 10.3389/fimmu.2020.01380]

155 **Zhang L**, Chen C, Chai D, Li C, Guan Y, Liu L, Kuang T, Deng W, Wang W. The association between antibiotic use and outcomes of HCC patients treated with immune checkpoint inhibitors. *Front Immunol* 2022; **13**: 956533 [PMID: 36059512

DOI: 10.3389/fimmu.2022.956533]

156 **Wu P**, Wu D, Ni C, Ye J, Chen W, Hu G, Wang Z, Wang C, Zhang Z, Xia W, Chen Z, Wang K, Zhang T, Xu J, Han Y, Wu X, Wang J, Gong W, Zheng S, Qiu F, Yan J, Huang J. γδT17 cells promote the accumulation and expansion of myeloid-derived suppressor cells in human colorectal cancer. *Immunity* 2014; **40**: 785-800 [PMID: 24816404 DOI: 10.1016/j.immuni.2014.03.013]

157 **Daley D**, Zambirinis CP, Seifert L, Akkad N, Mohan N, Werba G, Barilla R, Torres-Hernandez A, Hundeyin M, Mani VRK, Avanzi A, Tippens D, Narayanan R, Jang JE, Newman E, Pillarisetty VG, Dustin ML, Bar-Sagi D, Hajdu C, Miller G. γδ T Cells Support Pancreatic Oncogenesis by Restraining αβ T Cell Activation. *Cell* 2016; **166**: 1485-1499.e15 [PMID: 27569912 DOI: 10.1016/j.cell.2016.07.046]

158 **Huang J**, Zheng X, Kang W, Hao H, Mao Y, Zhang H, Chen Y, Tan Y, He Y, Zhao W, Yin Y. Metagenomic and metabolomic analyses reveal synergistic effects of fecal microbiota transplantation and anti-PD-1 therapy on treating colorectal cancer. *Front Immunol* 2022; **13**: 874922 [PMID: 35911731 DOI: 10.3389/fimmu.2022.874922]

159 **Koustas E**, Trifylli EM, Sarantis P, Papadopoulos N, Aloizos G, Tsagarakis A, Damaskos C, Garmpis N, Garmpi A, Papavassiliou AG, Karamouzis MV. Implication of gut microbiome in immunotherapy for colorectal cancer. *World J Gastrointest Oncol* 2022; **14**: 1665-1674 [PMID: 36187397 DOI: 10.4251/wjgo.v14.i9.1665]

160 **Nomura M**, Nagatomo R, Doi K, Shimizu J, Baba K, Saito T, Matsumoto S, Inoue K, Muto M. Association of Short-Chain Fatty Acids in the Gut Microbiome With Clinical Response to Treatment With Nivolumab or Pembrolizumab in Patients With Solid Cancer Tumors. *JAMA Netw Open* 2020; **3**: e202895 [PMID: 32297948 DOI: 10.1001/jamanetworkopen.2020.2895]

161 **Zheng Y**, Wang T, Tu X, Huang Y, Zhang H, Tan D, Jiang W, Cai S, Zhao P, Song R, Li P, Qin N, Fang W. Gut microbiome affects the response to anti-PD-1 immunotherapy in patients with hepatocellular carcinoma. *J Immunother Cancer* 2019; **7**: 193 [PMID: 31337439 DOI: 10.1186/s40425-019-0650-9]

World Journal of Gastrointestinal Oncology

Submit a Manuscript: https://www.f6publishing.com

World J Gastrointest Oncol 2023 May 15; 15(5): 776-786

DOI: 10.4251/wjgo.v15.i5.776

ISSN 1948-5204 (online)

MINIREVIEWS

Microbiota regulation in constipation and colorectal cancer

Li-Wei Wang, Hao Ruan, Bang-Mao Wang, Yuan Qin, Wei-Long Zhong

Specialty type: Oncology

Provenance and peer review: Invited article; Externally peer reviewed.

Peer-review model: Single blind

Peer-review report's scientific quality classification

Grade A (Excellent): 0
Grade B (Very good): 0
Grade C (Good): C, C
Grade D (Fair): 0
Grade E (Poor): 0

P-Reviewer: Feng S, China; Wismayer R, Uganda

Received: December 28, 2022
Peer-review started: December 28, 2022
First decision: January 9, 2023
Revised: January 23, 2023
Accepted: April 21, 2023
Article in press: April 21, 2023
Published online: May 15, 2023

Li-Wei Wang, Bang-Mao Wang, Wei-Long Zhong, Department of Gastroenterology and Hepatology, Tianjin Medical University General Hospital, Tianjin 300052, China

Hao Ruan, China Resources Biopharmaceutical Company Limited, Beijing 100029, China

Yuan Qin, College of Life Sciences and Medicine, Zhejiang Sci-Tech University, Hangzhou 310018, Zhejiang Province, China

Corresponding author: Wei-Long Zhong, PhD, Adjunct Associate Professor, Department of Gastroenterology and Hepatology, Tianjin Medical University General Hospital, No. 154 Anshan Road, Heping District, Tianjin 300052, China. zhongweilong@tmu.edu.cn

Abstract

The relevance of constipation to the development and progression of colorectal cancer (CRC) is currently a controversial issue. Studies have shown that changes in the composition of the gut microbiota, a condition known as ecological imbalance, are correlated with an increasing number of common human diseases, including CRC and constipation. CRC is the second leading cause of cancer-related deaths worldwide, and constipation has been receiving widespread attention as a risk factor for CRC. Early colonoscopy screening of constipated patients, with regular follow-ups and timely intervention, can help detect early intestinal lesions and reduce the risks of developing colorectal polyps and CRC. As an important regulator of the intestinal microenvironment, the gut microbiota plays a critical role in the onset and progression of CRC. An increasing amount of evidence supports the thought that gut microbial composition and function are key determinants of CRC development and progression, with alterations inducing changes in the expression of host genes, metabolic regulation, and local and systemic immunological responses. Furthermore, constipation greatly affects the composition of the gut microbiota, which in turn influences the susceptibility to intestinal diseases such as CRC. However, the crosstalk between the gut microbiota, constipation, and CRC is still unclear.

Key Words: Microbiota; Constipation; Colorectal cancer; Intestinal microenvironment; Immunological responses; Metabolic regulation

Core Tip: The changes in the composition of the gut microbiota are correlated with an increasing number of common human diseases, including colorectal cancer (CRC) and constipation. CRC is the second leading cause of cancer-related deaths worldwide, and constipation has been receiving widespread attention as a risk factor for CRC. An increasing amount of evidence supports the thought that gut microbial composition and function are key determinants of CRC development and progression, with alterations inducing changes in the expression of host genes, metabolic regulation, and local and systemic immunological responses.

Citation: Wang LW, Ruan H, Wang BM, Qin Y, Zhong WL. Microbiota regulation in constipation and colorectal cancer. *World J Gastrointest Oncol* 2023; 15(5): 776-786
URL: https://www.wjgnet.com/1948-5204/full/v15/i5/776.htm
DOI: https://dx.doi.org/10.4251/wjgo.v15.i5.776

INTRODUCTION

There are approximately 100 trillion microbial cells in the gut microbiota, including a varied mix of bacteria, fungi, protozoa, and viruses[1]. Most gut bacteria form complex networks that are important mediators of tissue homeostasis, inflammation, and tumor development[2]. Despite regularly being described to as the "forgotten organ," the symbiotic equilibrium of the gut microbiota plays a crucial role in maintaining host health[3]. The gut microbiota is involved in a variety of physiological activities in the host, such as the fermentation of food components, production of short-chain fatty acids (SCFAs), regulation of immune function, regulation of the growth and differentiation of intestinal epithelial cells (IEC), bile salt metabolism, and production of vitamins and other protective substances. It also acts as a biological barrier to prevent the adhesion and invasion of pathogenic and potentially pathogenic bacteria. This intricate ecosystem not only involves a passive colonizer of the gut, but it also facilitates engagement with the host through a variety of interactions that support a number of physiological functions, including nutrition absorption, immunity, metabolism, and tissue development[4,5].

Colorectal cancer (CRC) is the third most prevalent type of cancer, accounting for nearly 2 million new cases each year, and is the second leading cause of cancer-related deaths globally[6]. As with many other diseases, the onset and progression of CRC are due to a combination of hereditary and environmental factors. The microbiota is an essential environmental component that contributes to the development of cancers such as colorectal, liver, biliary tract, and breast cancers[7]. The microbiota in the colorectum interacts with IEC to obtain energy and regulate the body's immune response; consequently, its role in colorectal carcinogenesis is of great interest.

Constipation is a common gastrointestinal disorder and a common symptom in patients with cancer. It is characterized by scanty stools, hardened stools, or difficulty passing stools, and may occur alone or secondary to other diseases[8]. Constipation is a common problem for 16% of individuals overall and 33.5% of seniors (60-101 years)[9]. Disruption of the intestinal microbial community (ecological dysbiosis) can lead to various changes in host pathophysiology, resulting in functional gastrointestinal disorders, particularly constipation[10].

MICROBIOTA-INDUCED REGULATION OF CRC

It is widely accepted that a variety of variables, including heredity, the environment, and chronic inflammation, contribute to the etiology of CRC[11]. Moreover, inflammation is a recognized driver of CRC development[2,12]. The gut microbiota can affect inflammatory processes in the digestive system as part of its interaction with the host immune system. When feces from patients with CRC were instilled into sterile, carcinogen-fed mice, the gut microbiome promoted the synthesis of chemokines, which increased histological inflammation and the expression of inflammatory genetic markers[13]. This is because the gut microbiota stimulates the production of chemokines (*e.g.*, CCL5, CXCL9, CXCL10, CCL17, and CCL20) through tumorigenic cancer cells, thus favoring the recruitment of beneficial T cells into tumor tissue[14]. The microbiome induces multiple cases of inflammation and activates oncogenic pathways, resulting in increased cytokine expression during inflammation.

The intestinal mucosal barrier usually keeps the immune cells and gut microbiota apart. IECs make up the single layer of the intestinal mucosal barrier, which is joined by tight junctions[15]. The intestinal mucosal barrier is extremely permeable in both humans and CRC mouse models[16]. Increased susceptibility to CRC due to dextran sodium sulfate-induced colitis disrupts the function of the intestinal mucosal barrier[17]. The mucosal barrier in rats is compromised by ammonia, a product of the intestinal microbiota, which has also been associated with an increase in colonic adenomas[18]. Sulfides are toxic to colon cells and inhibit butyrate oxidation, which can damage the barrier of the colon cell[19]. Notably,

even some metabolites can enhance the mucosal barrier function of the intestine. SCFAs are essential nutrients for IEC, which encourage the proliferation and differentiation of these cells and maintain the integrity of the intestinal epithelium[20].

Pattern recognition receptors (PRRs) enable communication between the immune system and microbiota by recognizing specific molecular patterns associated with pathogens[21]. In animal models, these PRRs are present among those associated with coliform-associated carcinogenesis, including Toll-like receptors (TLRs)[22], nucleotide-binding oligomerization-like receptors, retinol-induced gene-I-like receptors[23], and melanoma 2-like receptors[24]. When myeloid differentiation factor 88 (MyD88), a crucial bridge protein required for TLR signaling, is activated, invasive commensal bacteria and their components bind to the TLRs on tumor-infiltrating myeloid cells[25]. This in turn triggers the synthesis of downstream pro-inflammatory cytokines, including IL-23, IL-17A, IL-6, IL22, IL-1β, and TNF-α[14,16,25]. These cytokines promote malignant progression by enhancing cell proliferation, aggressiveness, and resistance to apoptosis. Ultimately, they stimulate the signaling pathways for nuclear factor-κB (NF-κB) and activator of transcription 3 (STAT3), which enhances tumor cell growth[26,27]. Additionally, commensal bacteria and their metabolites boost the expression of IL-17C in transformed IECs *via* TLR/MyD88-dependent signaling. IL-17C promotes tumor cell survival and carcinogenesis by inducing the expressions of B-cell lymphoma-2 and B-cell lymphoma-xL in IECs in an autocrine manner[25].

According to previous studies, oncogenesis can be undertaken using a number of bacteria, such as *Fusobacterium nucleatum* (*F. nucleatum*) adhesion and the invasion of colonic epithelial cells, to regulate oncogenic and inflammatory responses through FadA antigen binding to E-calmodulin on IECs to activate β-linked proteins[28]. Through the activation of TLR-4 signaling to NF-κB and the upregulation of miR-21 expression, myeloid cell infiltration is induced in tumors, and cancer cell proliferation and tumor progression are promoted[29].

In addition to the inflammatory immune mechanisms of gut microbes, the gut microbiota is capable of producing proteins, molecules, and secondary metabolites that are especially harmful to DNA. Host DNA can directly interact with and be modified by these products[30]. Bacteria produce two well-defined genotoxins: Cytolethal distending toxin (CDT) and colistin[31]. Several enteric pathogens, including *Salmonella*, *Escherichia* and *Campylobacter* spp. produce CDT, which induces double-stranded DNA breaks through its deoxyribonuclease activity[32,33]. In the form of a deoxyribonuclease I-like protein, CDT exhibits DNA enzyme activity and regulates cell cycle development[34]. This toxin causes eukaryotic cells to stagnate in the G2 /M transition phase of the cell cycle, which stops the division of eukaryotic cells, but the cytoplasm continues to grow and expand. At last, the nucleus was seriously damaged and chromatin was obviously broken or completely disappeared[35]. *Bacteroides fragilis* (*B. fragilis*) toxins can lead to CRC progression by inducing mutations, damaging DNA, and ultimately damaging the epithelial cell genome[36]. Upon IECs exposure, *B. fragilis* toxin binds to specific IEC receptors and rapidly cleaves the extracellular structural domain of E-calmodulin, leading to complete degradation of E-calmodulin[37]. Subsequently, β-linked protein/T-cell factor-dependent transcriptional activation induces transcription and translation of the c-Myc oncogene and sustained cell proliferation[38].Furthermore, both *B. fragilis* toxins and *Enterococcus faecalis* reactive oxygen species have been linked to strand breaks and chromosomal aberrations *in vitro*[39,40]. Because small-molecule inhibitors that target the production of *Escherichia coli* (*E. coli*) toxins have been demonstrated to reduce the tumor burden in mouse models, their binding or inactivation may have therapeutic or preventative effects on CRC[40].

Besides, Clostridium perfringens belongs to the genus Clostridium, which produces bile acid hydrolases that catalyze the production of secondary bile acids (such as deoxycholic acid and lithocholic acid. Increased secondary bile acids levels activate the Wnt/β-linked protein and NF-κB signaling pathways, resulting in oxidative DNA damage, increased mitotic activity, and activation of intrinsic apoptotic pathways such as mitochondrial cytochrome C release and oxidative stress[41,42]. Secondary bile acids also influence CRC by activating the bile acid receptors G protein-coupled bile acid receptor 5 (TGR5) and farnesoid X receptor (FXR)[43,44] (Figure 1).

MICROBIOTA-INDUCED REGULATION OF CONSTIPATION

It is widely accepted that gut dysfunction, such as intestinal fluid transport, intestinal peristalsis, mucus production, and intestinal nerve conduction disorders, is the primary cause of constipation[45]. However, several recent studies have demonstrated that the gut microbiota and its metabolism play a significant role in the physiology and pathology of constipation. They have the capacity to change intestinal secretion and the microenvironment by interacting with the immune system, enteric nervous system (ENS), and central nervous system[46]. Therefore, gut microbiota may cause intestinal motility disorders through complex mechanisms, but the key underlying mechanisms are still under investigation.

In a constipated state, intestinal motility and secretion can become abnormal if the gut microbiota and metabolism are disrupted[47]. Simultaneously, the host modulates the gut microbiota *via* a variety of PRRs. In terms of the regulation of gastrointestinal motility, most TLRs are expressed in gut microbial

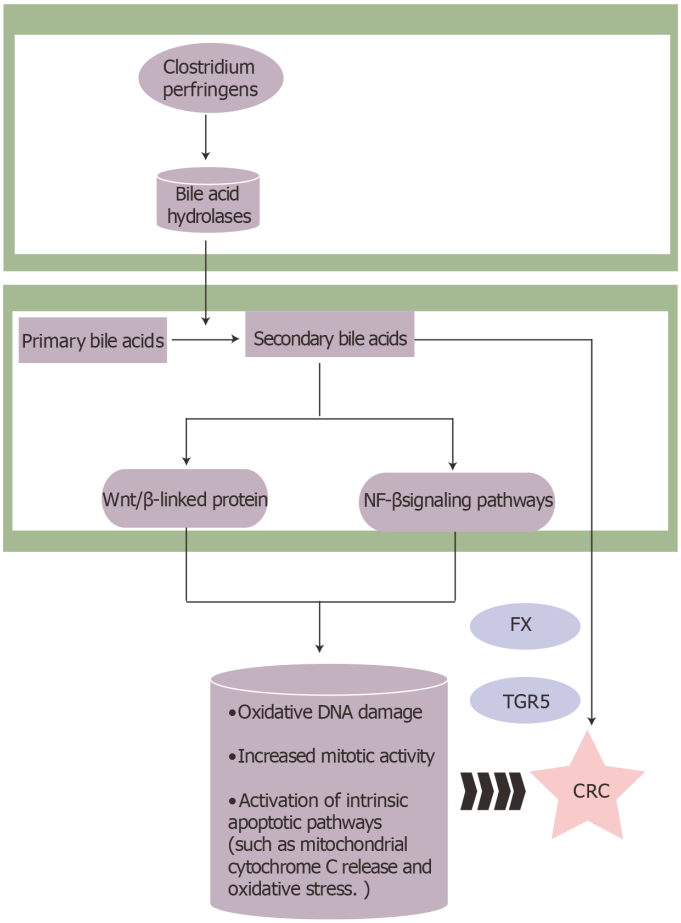

DOI: 10.4251/wjgo.v15.i5.776

Figure 1 A flow diagram of the mechanism of how clostridium perfringens causes DNA damage and hence which mutations leading to colorectal cancer. CRC: Colorectal cancer; FX: Farnesoid X; TGR5: G protein-coupled bile acid receptor 5.

components and gastrointestinal sensory components[48,49]. TLRs can communicate directly with bacterial components to make it easier for gastrointestinal cells and the gut microbiota to work together. For example, there is evidence of the expression of TLR2 in intestinal smooth muscle cells, neurons, glial cells, and interstitial cells of Cajal (ICCs). By binding to TLR2 from the gut microbiota, lipopeptides, peptidoglycan, and lipophilin acid trigger the release of glial cell line-derived neurotrophic factor *via* NF-κB and p38 mitogen-activated protein kinase (MAPK) signaling, maintain ENS and neurogenesis neurons, and exert anti-inflammatory effects to improve gastrointestinal motility in a manner that is not dependent on MyD88[48,50].

Of the receptors previously described, TLR4 is the most suitable for recognizing lipopolysaccharides (LPS) generated from the gut microbiota, along with TLR2. When LPS binds to TLR4 expressed on myeloid macrophages (MM), it induces the production of bone morphogenetic protein 2 (BMP2), which improves gastrointestinal motility. Enteric neurons generate colony-stimulating factor 1 in conjunction with BMP2, which facilitates MM homeostasis and regulates gastrointestinal motility[51]. As a result, the gut microbiota participates in and regulates the crosstalk between the MM and gut neurons, thereby influencing gastrointestinal dynamics. Nevertheless, higher concentrations of LPS expressed on ICCs, cause them to bind to TLR4 and inhibit pacemaker activity in ICC *via* the MAPK and NF-κB signaling pathways, thereby suppressing gastrointestinal motility and leading to reduced fecal production and prolonged defecation[52].

Furthermore, gut microbes can interact with ENS not only through TLRS but also through the intestinal serotonin network to promote the functional maturation of the enteric neural network. This promoted the synthesis and release of serotonin (5-HT) through the action of SCFAs on enterochromaffin cells[53]. 5-HT is a key regulator of gastrointestinal motility and secretion, and consists mainly of 5-HT1, 2, 3, 4, and 7 isoforms, all of which have the ability to act directly on the various receptors on epithelial cells, smooth muscle cells, and enteric neurons, thereby affecting smooth muscle relaxation and contraction[54,55]. Notably, 5-HT is also a major product of tryptophan metabolism. The dysregulation of tryptophan metabolites significantly contributes to the etiology of colonic dysmotility[56,57]. The creation of indole-3-methanol by the microbiota stimulates aryl hydrocarbon receptors in myenteric neurons, allowing them to respond to the microbial environment in the lumen. It also triggers neuron-specific effector mechanisms and the expression of colonic motility[58].

Similarly, the intestinal flora produces gas, which has a significant impact on intestinal motility. Methane, hydrogen, hydrogen sulfide, and carbon dioxide are among the gases generated by gut microorganisms in the digestive tract. In the gastrointestinal system, unabsorbed carbohydrates are fermented by bacteria, producing these byproducts. In fact, the lactulose hydrogen breath test reveals a substantial link between constipation-predominant irritable bowel syndrome and excessive methane levels[59]. The most prevalent methanogenic bacterium in the human gut is *Methanobacterium smegmatis* (*M. smegmatis*)[60]. A clinical study showed that *M. smegmatis* was overgrown in the intestines of constipated patients with elevated methane levels[61]. In addition, nitrate or nitrite from the gut lumen can serve as raw material for the production of NO by gut microbes[62]. It has been established that NO is an inhibitory neurotransmitter that may contribute to reduced gastrointestinal smooth muscle tension and diminished gastrointestinal motility.

Bile acids function as physiological laxatives to modify water and electrolyte transport in the intestinal lumen, as well as to regulate intestinal motility. Bile acids stimulate the TGR5 in enterochromaffin cells and myelinated neurons, releasing 5-HT and calcitonin gene-related peptides[63]. Several studies have shown that ileal bile acid-transport protein inhibitors significantly reduce bowel passage time, and improve constipation symptoms when compared with placebos[64,65]. Gastrointestinal flora modulates the gut microbiota, regulates the synthesis of hepatic bile acids, and promotes the participation of pro-bile acids in various chemical reactions in the body, thereby increasing the diversity of bile acid derivatives[66].

Consequently, the development of functional maturation of the ENS, and the reduction of colonic motility issues, may be aided by microecological management that directly targets specific TLR and 5-HT signaling pathways. At the same time, these findings support the hypothesis that the metabolism of Trp under the control of the gut microbiome is involved in host-microbiota crosstalk and gastrointestinal motility fine-tuning. This suggests that Trp metabolism may be a viable therapeutic target for gastrointestinal motility.

POSSIBLE MECHANISMS WHEREBY CONSTIPATION IS INVOLVED IN THE DEVELOPMENT OF CRC

Because the etiologies of constipation and CRC are similar, it is unknown whether constipation and the emergence of CRC are causally related. Several hypothetical mechanisms may be behind the associations observed in this study. It has been theorized that lower bowel motility, and correspondingly longer transport time, in constipated patients would increase the risk of CRC due to prolonged exposure of the colonic mucosa to fecal carcinogens. Second, it has been suggested that constipation may accelerate the onset of CRC by causing immunological abnormalities and gene mutations or deletions *via* the disruption of intestinal microecology. Furthermore, harmful compounds released by microbial cells are thought to spread to other regions of the body, leading to the development, initiation, or progression of cancer[67,68]. Additionally, any relationship with constipation may be due to inverse causality; in other words, CRC may cause constipation before the clinical manifestation of cancer. Eventually, although CRC is more likely to be detected later than constipation is usually detected, the two conditions may be separate but converging disorders caused by similar underlying risk factors. Therefore, although constipation is not an indication for a colonoscopy, it should be considered in specific individuals (*e.g.*, those over 50 years of age) for colon cancer screening[8].

While associations have been drawn between constipation and CRC in prior studies, the results are contradictory[69,70]. Generally, these studies were often constrained by selection bias, recollection bias, and self-reported data on constipation. The specific relationship between constipation and CRC is not fully understood, and in this context, the gut microbiota may be the key to solving this mystery.

The type and amount of gut microbiota and their metabolites differ between patients with constipation and the healthy population. The abundances of *lactococci*, *rumenococci*, *E. coli*, and *Staphylococcus aureus* in the intestinal flora were considerably higher in the stool of patients with constipation, whereas the abundances of *bifidobacteria* and *lactobacilli* were significantly lower, resulting in severe dysbiosis[71,72]. The abundance of *Bacillus* spp. in the colonic mucosa is significantly higher not only in patients with constipation, but also in those with CRC[73,74]. In addition, when constipation occurs, because dry, hard stools remain in the colon for an extended period of time, they easily consume the mucus of the loose external mucus layer of the intestine. This creates an opportunity for imbalances in the gut microbiota to invade the internal mucus layer, thereby inducing an immune response and causing inflammation, which is a necessary trigger for CRC[47].

The presence of *B. fragilis*, *E. coli*, and *F. nucleatum* in the intestine may also induce the abnormal expression of pro-oncogenes and oncogenes, as well as abnormal mismatch chromosome repair. By doing so, it may trigger cellular heterogeneous hyperplasia and adenomatous polyps, and contribute to the emergence and spread of CRC[75-77]. The increased abundance of *F. nucleatum* and *E. coli* may be involved in colorectal carcinogenesis and development by activating the Wnt and NF-κB signaling pathways, which promote the release of chemokines, adhesion molecules, and pro-inflammatory cytokines. These pathways can even induce chromosomal instability and the abnormal methylation of

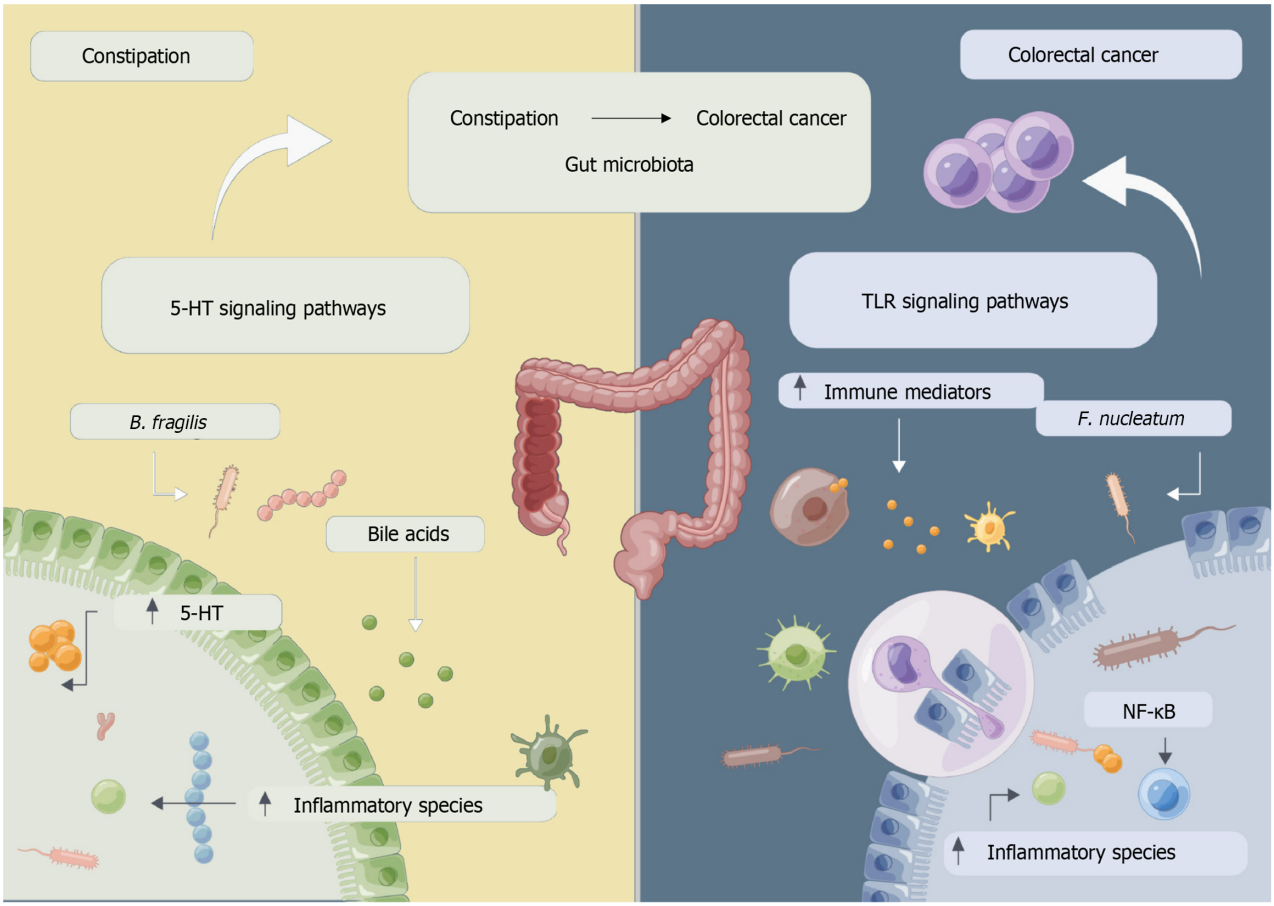

DOI: 10.4251/wjgo.v15.i5.776

Figure 2 Schematic diagram of the role of intestinal bacteria in constipation and bowel cancer. TLR: Toll-like receptor; NF-κB: Nuclear factor-κB; *B. fragilis: Bacteroides fragilis; F. nucleatum: Fusobacterium nucleatum.*

CpG islands to mediate immune cell aggregation, thereby inducing apoptosis and regulating the tumor immune microenvironment. Notably, altered abundance of *E. fragilis* can induce signal transducer and STAT3 activation in colonic epithelial cells, and *Enterococcus faecalis* can induce the formation of reactive oxygen species, related oxidative stress, and DNA damage. This in turn may cause cell proliferation, apoptosis, and abnormal immune responses, leading to colorectal tumor development[78].

Simultaneously, aberrant metabolites of the gut microbiota caused by intestinal microecological dysregulation are also involved in the development and progression of colorectal diseases. In addition to anti-inflammatory and immunomodulatory effects, moderate amounts of butyrate can enhance the defense of the gastrointestinal mucosal barrier. They can also lessen colon cancer cell propagation and migration by increasing the production of mucin-encoding genes; activating the activity of heat shock proteins, trefoil factors, antimicrobial peptides, and glutaminyl transferases; and inhibiting histone deacetylases[79]. However, excessive amounts of butyrate not only inhibit the release of mucin by intestinal cup cells and encourage the absorption of water and electrolytes from the colon, but they also inhibit the contraction of colonic smooth muscle and reduce the movement of the colon. This leads to constipation and may even promote the proliferation of tumor cells or increase the activity of β-catenin, thereby increasing the risk of tumor development[80].

CONCLUSION

Constipation may be involved in the process of CRC development and progression *via* a mechanism that may involve changes in the composition of the flora, and abnormalities in its metabolites caused by dysbiosis of the intestinal flora, leading to intestinal motility dysfunction and/or abnormalities in the immune microenvironment, as shown in Figure 2. The pro-tumorigenic effects of individual cytokines are context-dependent and significantly affected by synergistic effects in a complex cytokine environment.

The crosstalk between the gut microbiota, constipation, and CRC, and their specific mechanisms of action, are still poorly understood. Nevertheless, they also provide a wealth of new ideas and prospective targets for the prevention and treatment of CRC. The direction of relevant gut microbial

research is still dominated by animal studies, and there remain numerous obstacles to be overcome in clinical treatment owing to individual variations, tumor staging, and cross-species translation. To further understand the relationship between the gut microbiota, constipation, and CRC, ongoing preclinical and clinical research is required.

The future study design is as follows: Subjects first need to be pretreated with fecal sample sequencing and macrogenome sequencing, and oral antibiotics to deplete the natural gut microbes. Patients then undergo fecal transplantation and periodic fecal testing with sigmoid biopsy and tumor biopsy at appropriate times to observe the effects of fecal transplantation on constipation and CRC and assess the safety, feasibility, and impact of fecal transplantation on the intestinal microenvironment in patients with constipation and CRC. Future studies should clarify which patients can receive fecal transplants and which donor gut microbes are effective. In addition, the timing of antibiotic pre-treatment all need to be further investigated. Gut microbiota may soon become a potent tool in the battle against CRC.

According to the latest guidelines on constipation, although constipation itself is not an indication of colonoscopy, patients with severe chronic constipation or alarm symptoms should consider colonoscopy to screen for CRC. In addition, CRC screening is not a "one size fits all" concept due to the variable incidence of recognized CRC risk factors. It is now recognized that those people identified as having a greater risk for CRC, such as those with a family history of CRC or CRC-associated genetic illnesses, should be examined at a younger age and using colonoscopy. The guidelines recommend that colonoscopy be started before age 50 or even at age 45 for patients with associated risk factors, or after age 50 if there are no associated risk factors and timely interventions should be made to reduce the risk of developing colorectal polyps and CRC to prevent disease progression.

FOOTNOTES

Author contributions: Wang LW, Qin Y and Zhong WL designed this study; Wang LW, Zhong WL, Wang BM and Ruan H performed the reference analyses; Wang LW and Zhong WL wrote the initial draft of the paper, with contributions from all authors.

Supported by National Natural Science Foundation of China, No. 82000511 and 82170558; Scientific and Technological Projects of Tianjin, No. 21JCQNJC01120; Health Science and Technology Project of Tianjin, No. TJWJ2021QN006; Scientific Research Project of Tianjin Education Commission, No. 2019KJ197; Natural Science Foundation of Zhejiang Province, No. LQ23H050005; and Scientific Research Project of Zhejiang Provincial Education Department, No. Y202250731.

Conflict-of-interest statement: The authors declare that they have no competing interests.

Country/Territory of origin: China

ORCID number: Bang-Mao Wang 0000-0002-4702-9711; Yuan Qin 0000-0002-5651-8293; Wei-Long Zhong 0000-0002-7139-169X.

S-Editor: Zhang H
L-Editor: A
P-Editor: Zhao S

REFERENCES

1 **Qin J**, Li R, Raes J, Arumugam M, Burgdorf KS, Manichanh C, Nielsen T, Pons N, Levenez F, Yamada T, Mende DR, Li J, Xu J, Li S, Li D, Cao J, Wang B, Liang H, Zheng H, Xie Y, Tap J, Lepage P, Bertalan M, Batto JM, Hansen T, Le Paslier D, Linneberg A, Nielsen HB, Pelletier E, Renault P, Sicheritz-Ponten T, Turner K, Zhu H, Yu C, Jian M, Zhou Y, Li Y, Zhang X, Qin N, Yang H, Wang J, Brunak S, Doré J, Guarner F, Kristiansen K, Pedersen O, Parkhill J, Weissenbach J; MetaHIT Consortium, Bork P, Ehrlich SD, Wang J. A human gut microbial gene catalogue established by metagenomic sequencing. *Nature* 2010; **464**: 59-65 [PMID: 20203603 DOI: 10.1038/nature08821]

2 **West NR**, McCuaig S, Franchini F, Powrie F. Emerging cytokine networks in colorectal cancer. *Nat Rev Immunol* 2015; **15**: 615-629 [PMID: 26358393 DOI: 10.1038/nri3896]

3 **O'Hara AM**, Shanahan F. The gut flora as a forgotten organ. *EMBO Rep* 2006; **7**: 688-693 [PMID: 16819463 DOI: 10.1038/sj.embor.7400731]

4 **Bosch TC**, McFall-Ngai MJ. Metaorganisms as the new frontier. *Zoology (Jena)* 2011; **114**: 185-190 [PMID: 21737250 DOI: 10.1016/j.zool.2011.04.001]

5 **Bozkurt HS**, Quigley EM, Kara B. Bifidobacterium animalis subspecies lactis engineered to produce mycosporin-like amino acids in colorectal cancer prevention. *SAGE Open Med* 2019; **7**: 2050312119825784 [PMID: 30719295 DOI: 10.1177/2050312119825784]

6 **Sung H**, Ferlay J, Siegel RL, Laversanne M, Soerjomataram I, Jemal A, Bray F. Global Cancer Statistics 2020: GLOBOCAN Estimates of Incidence and Mortality Worldwide for 36 Cancers in 185 Countries. *CA Cancer J Clin* 2021; **71**: 209-249 [PMID: 33538338 DOI: 10.3322/caac.21660]

7 **Sepich-Poore GD**, Zitvogel L, Straussman R, Hasty J, Wargo JA, Knight R. The microbiome and human cancer. *Science* 2021; **371** [PMID: 33766858 DOI: 10.1126/science.abc4552]

8 **Bharucha AE**, Pemberton JH, Locke GR 3rd. American Gastroenterological Association technical review on constipation. *Gastroenterology* 2013; **144**: 218-238 [PMID: 23261065 DOI: 10.1053/j.gastro.2012.10.028]

9 **Bharucha AE**, Wald A. Chronic Constipation. *Mayo Clin Proc* 2019; **94**: 2340-2357 [PMID: 31054770 DOI: 10.1016/j.mayocp.2019.01.031]

10 **Chassard C**, Dapoigny M, Scott KP, Crouzet L, Del'homme C, Marquet P, Martin JC, Pickering G, Ardid D, Eschalier A, Dubray C, Flint HJ, Bernalier-Donadille A. Functional dysbiosis within the gut microbiota of patients with constipated-irritable bowel syndrome. *Aliment Pharmacol Ther* 2012; **35**: 828-838 [PMID: 22315951 DOI: 10.1111/j.1365-2036.2012.05007.x]

11 **Qing F**, Xie T, Xie L, Guo T, Liu Z. How Gut Microbiota Are Shaped by Pattern Recognition Receptors in Colitis and Colorectal Cancer. *Cancers (Basel)* 2022; **14** [PMID: 35954484 DOI: 10.3390/cancers14153821]

12 **Grivennikov SI**, Greten FR, Karin M. Immunity, inflammation, and cancer. *Cell* 2010; **140**: 883-899 [PMID: 20303878 DOI: 10.1016/j.cell.2010.01.025]

13 **Wong SH**, Zhao L, Zhang X, Nakatsu G, Han J, Xu W, Xiao X, Kwong TNY, Tsoi H, Wu WKK, Zeng B, Chan FKL, Sung JJY, Wei H, Yu J. Gavage of Fecal Samples From Patients With Colorectal Cancer Promotes Intestinal Carcinogenesis in Germ-Free and Conventional Mice. *Gastroenterology* 2017; **153**: 1621-1633.e6 [PMID: 28823860 DOI: 10.1053/j.gastro.2017.08.022]

14 **Cremonesi E**, Governa V, Garzon JFG, Mele V, Amicarella F, Muraro MG, Trella E, Galati-Fournier V, Oertli D, Däster SR, Droeser RA, Weixler B, Bolli M, Rosso R, Nitsche U, Khanna N, Egli A, Keck S, Slotta-Huspenina J, Terracciano LM, Zajac P, Spagnoli GC, Eppenberger-Castori S, Janssen KP, Borsig L, Iezzi G. Gut microbiota modulate T cell trafficking into human colorectal cancer. *Gut* 2018; **67**: 1984-1994 [PMID: 29437871 DOI: 10.1136/gutjnl-2016-313498]

15 **Lee TC**, Huang YC, Lu YZ, Yeh YC, Yu LC. Hypoxia-induced intestinal barrier changes in balloon-assisted enteroscopy. *J Physiol* 2018; **596**: 3411-3424 [PMID: 29178568 DOI: 10.1113/JP275277]

16 **Grivennikov SI**, Wang K, Mucida D, Stewart CA, Schnabl B, Jauch D, Taniguchi K, Yu GY, Osterreicher CH, Hung KE, Datz C, Feng Y, Fearon ER, Oukka M, Tessarollo L, Coppola V, Yarovinsky F, Cheroutre H, Eckmann L, Trinchieri G, Karin M. Adenoma-linked barrier defects and microbial products drive IL-23/IL-17-mediated tumour growth. *Nature* 2012; **491**: 254-258 [PMID: 23034650 DOI: 10.1038/nature11465]

17 **Tanaka T**, Kohno H, Suzuki R, Hata K, Sugie S, Niho N, Sakano K, Takahashi M, Wakabayashi K. Dextran sodium sulfate strongly promotes colorectal carcinogenesis in Apc(Min/+) mice: inflammatory stimuli by dextran sodium sulfate results in development of multiple colonic neoplasms. *Int J Cancer* 2006; **118**: 25-34 [PMID: 16049979 DOI: 10.1002/ijc.21282]

18 **Windey K**, De Preter V, Verbeke K. Relevance of protein fermentation to gut health. *Mol Nutr Food Res* 2012; **56**: 184-196 [PMID: 22121108 DOI: 10.1002/mnfr.201100542]

19 **Nguyen LH**, Ma W, Wang DD, Cao Y, Mallick H, Gerbaba TK, Lloyd-Price J, Abu-Ali G, Hall AB, Sikavi D, Drew DA, Mehta RS, Arze C, Joshi AD, Yan Y, Branck T, DuLong C, Ivey KL, Ogino S, Rimm EB, Song M, Garrett WS, Izard J, Huttenhower C, Chan AT. Association Between Sulfur-Metabolizing Bacterial Communities in Stool and Risk of Distal Colorectal Cancer in Men. *Gastroenterology* 2020; **158**: 1313-1325 [PMID: 31972239 DOI: 10.1053/j.gastro.2019.12.029]

20 **Wang Q**, Xu R. Data-driven multiple-level analysis of gut-microbiome-immune-joint interactions in rheumatoid arthritis. *BMC Genomics* 2019; **20**: 124 [PMID: 30744546 DOI: 10.1186/s12864-019-5510-y]

21 **Rooks MG**, Garrett WS. Gut microbiota, metabolites and host immunity. *Nat Rev Immunol* 2016; **16**: 341-352 [PMID: 27231050 DOI: 10.1038/nri.2016.42]

22 **Kesselring R**, Glaesner J, Hiergeist A, Naschberger E, Neumann H, Brunner SM, Wege AK, Seebauer C, Köhl G, Merkl S, Croner RS, Hackl C, Stürzl M, Neurath MF, Gessner A, Schlitt HJ, Geissler EK, Fichtner-Feigl S. IRAK-M Expression in Tumor Cells Supports Colorectal Cancer Progression through Reduction of Antimicrobial Defense and Stabilization of STAT3. *Cancer Cell* 2016; **29**: 684-696 [PMID: 27150039 DOI: 10.1016/j.ccell.2016.03.014]

23 **Zhu H**, Xu WY, Hu Z, Zhang H, Shen Y, Lu S, Wei C, Wang ZG. RNA virus receptor Rig-I monitors gut microbiota and inhibits colitis-associated colorectal cancer. *J Exp Clin Cancer Res* 2017; **36**: 2 [PMID: 28057020 DOI: 10.1186/s13046-016-0471-3]

24 **Man SM**, Zhu Q, Zhu L, Liu Z, Karki R, Malik A, Sharma D, Li L, Malireddi RK, Gurung P, Neale G, Olsen SR, Carter RA, McGoldrick DJ, Wu G, Finkelstein D, Vogel P, Gilbertson RJ, Kanneganti TD. Critical Role for the DNA Sensor AIM2 in Stem Cell Proliferation and Cancer. *Cell* 2015; **162**: 45-58 [PMID: 26095253 DOI: 10.1016/j.cell.2015.06.001]

25 **Song X**, Gao H, Lin Y, Yao Y, Zhu S, Wang J, Liu Y, Yao X, Meng G, Shen N, Shi Y, Iwakura Y, Qian Y. Alterations in the microbiota drive interleukin-17C production from intestinal epithelial cells to promote tumorigenesis. *Immunity* 2014; **40**: 140-152 [PMID: 24412611 DOI: 10.1016/j.immuni.2013.11.018]

26 **Kortylewski M**, Xin H, Kujawski M, Lee H, Liu Y, Harris T, Drake C, Pardoll D, Yu H. Regulation of the IL-23 and IL-12 balance by Stat3 signaling in the tumor microenvironment. *Cancer Cell* 2009; **15**: 114-123 [PMID: 19185846 DOI: 10.1016/j.ccr.2008.12.018]

27 **Wang K**, Kim MK, Di Caro G, Wong J, Shalapour S, Wan J, Zhang W, Zhong Z, Sanchez-Lopez E, Wu LW, Taniguchi K, Feng Y, Fearon E, Grivennikov SI, Karin M. Interleukin-17 receptor a signaling in transformed enterocytes promotes early colorectal tumorigenesis. *Immunity* 2014; **41**: 1052-1063 [PMID: 25526314 DOI: 10.1016/j.immuni.2014.11.009]

28 **Rubinstein MR**, Wang X, Liu W, Hao Y, Cai G, Han YW. Fusobacterium nucleatum promotes colorectal carcinogenesis by modulating E-cadherin/β-catenin signaling *via* its FadA adhesin. *Cell Host Microbe* 2013; **14**: 195-206 [PMID: 23954158 DOI: 10.1016/j.chom.2013.07.012]

29 **Yang Y**, Weng W, Peng J, Hong L, Yang L, Toiyama Y, Gao R, Liu M, Yin M, Pan C, Li H, Guo B, Zhu Q, Wei Q, Moyer MP, Wang P, Cai S, Goel A, Qin H, Ma Y. Fusobacterium nucleatum Increases Proliferation of Colorectal Cancer Cells and Tumor Development in Mice by Activating Toll-Like Receptor 4 Signaling to Nuclear Factor-κB, and Up-regulating Expression of MicroRNA-21. *Gastroenterology* 2017; **152**: 851-866.e24 [PMID: 27876571 DOI: 10.1053/j.gastro.2016.11.018]

30 **Barrett M**, Hand CK, Shanahan F, Murphy T, O'Toole PW. Mutagenesis by Microbe: the Role of the Microbiota in Shaping the Cancer Genome. *Trends Cancer* 2020; **6**: 277-287 [PMID: 32209443 DOI: 10.1016/j.trecan.2020.01.019]

31 **Fang Y**, Yan C, Zhao Q, Xu J, Liu Z, Gao J, Zhu H, Dai Z, Wang D, Tang D. The roles of microbial products in the development of colorectal cancer: a review. *Bioengineered* 2021; **12**: 720-735 [PMID: 33618627 DOI: 10.1080/21655979.2021.1889109]

32 **Tremblay W**, Mompart F, Lopez E, Quaranta M, Bergoglio V, Hashim S, Bonnet D, Alric L, Mas E, Trouche D, Vignard J, Ferrand A, Mirey G, Fernandez-Vidal A. Cytolethal Distending Toxin Promotes Replicative Stress Leading to Genetic Instability Transmitted to Daughter Cells. *Front Cell Dev Biol* 2021; **9**: 656795 [PMID: 34026755 DOI: 10.3389/fcell.2021.656795]

33 **He Z**, Gharaibeh RZ, Newsome RC, Pope JL, Dougherty MW, Tomkovich S, Pons B, Mirey G, Vignard J, Hendrixson DR, Jobin C. Campylobacter jejuni promotes colorectal tumorigenesis through the action of cytolethal distending toxin. *Gut* 2019; **68**: 289-300 [PMID: 30377189 DOI: 10.1136/gutjnl-2018-317200]

34 **Lara-Tejero M**, Galán JE. A bacterial toxin that controls cell cycle progression as a deoxyribonuclease I-like protein. *Science* 2000; **290**: 354-357 [PMID: 11030657 DOI: 10.1126/science.290.5490.354]

35 **Bezine E**, Vignard J, Mirey G. The cytolethal distending toxin effects on Mammalian cells: a DNA damage perspective. *Cells* 2014; **3**: 592-615 [PMID: 24921185 DOI: 10.3390/cells3020592]

36 **Allen J**, Sears CL. Impact of the gut microbiome on the genome and epigenome of colon epithelial cells: contributions to colorectal cancer development. *Genome Med* 2019; **11**: 11 [PMID: 30803449 DOI: 10.1186/s13073-019-0621-2]

37 **Wu S**, Rhee KJ, Zhang M, Franco A, Sears CL. Bacteroides fragilis toxin stimulates intestinal epithelial cell shedding and gamma-secretase-dependent E-cadherin cleavage. *J Cell Sci* 2007; **120**: 1944-1952 [PMID: 17504810 DOI: 10.1242/jcs.03455]

38 **Wu S**, Morin PJ, Maouyo D, Sears CL. Bacteroides fragilis enterotoxin induces c-Myc expression and cellular proliferation. *Gastroenterology* 2003; **124**: 392-400 [PMID: 12557145 DOI: 10.1053/gast.2003.50047]

39 **Wang X**, Huycke MM. Extracellular superoxide production by Enterococcus faecalis promotes chromosomal instability in mammalian cells. *Gastroenterology* 2007; **132**: 551-561 [PMID: 17258726 DOI: 10.1053/j.gastro.2006.11.040]

40 **Goodwin AC**, Destefano Shields CE, Wu S, Huso DL, Wu X, Murray-Stewart TR, Hacker-Prietz A, Rabizadeh S, Woster PM, Sears CL, Casero RA Jr. Polyamine catabolism contributes to enterotoxigenic Bacteroides fragilis-induced colon tumorigenesis. *Proc Natl Acad Sci U S A* 2011; **108**: 15354-15359 [PMID: 21876161 DOI: 10.1073/pnas.1010203108]

41 **Nusse R**, Clevers H. Wnt/β-Catenin Signaling, Disease, and Emerging Therapeutic Modalities. *Cell* 2017; **169**: 985-999 [PMID: 28575679 DOI: 10.1016/j.cell.2017.05.016]

42 **Jia W**, Xie G, Jia W. Bile acid-microbiota crosstalk in gastrointestinal inflammation and carcinogenesis. *Nat Rev Gastroenterol Hepatol* 2018; **15**: 111-128 [PMID: 29018272 DOI: 10.1038/nrgastro.2017.119]

43 **Gadaleta RM**, Garcia-Irigoyen O, Moschetta A. Bile acids and colon cancer: Is FXR the solution of the conundrum? *Mol Aspects Med* 2017; **56**: 66-74 [PMID: 28400119 DOI: 10.1016/j.mam.2017.04.002]

44 **Sun L**, Cai J, Gonzalez FJ. The role of farnesoid X receptor in metabolic diseases, and gastrointestinal and liver cancer. *Nat Rev Gastroenterol Hepatol* 2021; **18**: 335-347 [PMID: 33568795 DOI: 10.1038/s41575-020-00404-2]

45 **Zhao Q**, Chen YY, Xu DQ, Yue SJ, Fu RJ, Yang J, Xing LM, Tang YP. Action Mode of Gut Motility, Fluid and Electrolyte Transport in Chronic Constipation. *Front Pharmacol* 2021; **12**: 630249 [PMID: 34385914 DOI: 10.3389/fphar.2021.630249]

46 **Pan R**, Wang L, Xu X, Chen Y, Wang H, Wang G, Zhao J, Chen W. Crosstalk between the Gut Microbiome and Colonic Motility in Chronic Constipation: Potential Mechanisms and Microbiota Modulation. *Nutrients* 2022; **14** [PMID: 36145079 DOI: 10.3390/nu14183704]

47 **Yang L**, Wang Y, Zhang Y, Li W, Jiang S, Qian D, Duan J. Gut microbiota: a new avenue to reveal pathological mechanisms of constipation. *Appl Microbiol Biotechnol* 2022; **106**: 6899-6913 [PMID: 36190540 DOI: 10.1007/s00253-022-12197-2]

48 **Brun P**, Giron MC, Qesari M, Porzionato A, Caputi V, Zoppellaro C, Banzato S, Grillo AR, Spagnol L, De Caro R, Pizzuti D, Barbieri V, Rosato A, Sturniolo GC, Martines D, Zaninotto G, Palù G, Castagliuolo I. Toll-like receptor 2 regulates intestinal inflammation by controlling integrity of the enteric nervous system. *Gastroenterology* 2013; **145**: 1323-1333 [PMID: 23994200 DOI: 10.1053/j.gastro.2013.08.047]

49 **Anitha M**, Vijay-Kumar M, Sitaraman SV, Gewirtz AT, Srinivasan S. Gut microbial products regulate murine gastrointestinal motility *via* Toll-like receptor 4 signaling. *Gastroenterology* 2012; **143**: 1006-16.e4 [PMID: 22732731 DOI: 10.1053/j.gastro.2012.06.034]

50 **Yarandi SS**, Kulkarni S, Saha M, Sylvia KE, Sears CL, Pasricha PJ. Intestinal Bacteria Maintain Adult Enteric Nervous System and Nitrergic Neurons *via* Toll-like Receptor 2-induced Neurogenesis in Mice. *Gastroenterology* 2020; **159**: 200-213.e8 [PMID: 32234538 DOI: 10.1053/j.gastro.2020.03.050]

51 **Muller PA**, Koscsó B, Rajani GM, Stevanovic K, Berres ML, Hashimoto D, Mortha A, Leboeuf M, Li XM, Mucida D, Stanley ER, Dahan S, Margolis KG, Gershon MD, Merad M, Bogunovic M. Crosstalk between muscularis macrophages and enteric neurons regulates gastrointestinal motility. *Cell* 2014; **158**: 300-313 [PMID: 25036630 DOI: 10.1016/j.cell.2014.04.050]

52 **Zuo DC**, Choi S, Shahi PK, Kim MY, Park CG, Kim YD, Lee J, Chang IY, So I, Jun JY. Inhibition of pacemaker activity in interstitial cells of Cajal by LPS *via* NF-κB and MAP kinase. *World J Gastroenterol* 2013; **19**: 1210-1218 [PMID:

23482668 DOI: 10.3748/wjg.v19.i8.1210]
53 **Reigstad CS**, Salmonson CE, Rainey JF 3rd, Szurszewski JH, Linden DR, Sonnenburg JL, Farrugia G, Kashyap PC. Gut microbes promote colonic serotonin production through an effect of short-chain fatty acids on enterochromaffin cells. *FASEB J* 2015; **29**: 1395-1403 [PMID: 25550456 DOI: 10.1096/fj.14-259598]
54 **Mawe GM**, Hoffman JM. Serotonin signalling in the gut--functions, dysfunctions and therapeutic targets. *Nat Rev Gastroenterol Hepatol* 2013; **10**: 473-486 [PMID: 23797870 DOI: 10.1038/nrgastro.2013.105]
55 **Sikander A**, Rana SV, Prasad KK. Role of serotonin in gastrointestinal motility and irritable bowel syndrome. *Clin Chim Acta* 2009; **403**: 47-55 [PMID: 19361459 DOI: 10.1016/j.cca.2009.01.028]
56 **Zhang X**, Yang H, Zheng J, Jiang N, Sun G, Bao X, Lin A, Liu H. Chitosan oligosaccharides attenuate loperamide-induced constipation through regulation of gut microbiota in mice. *Carbohydr Polym* 2021; **253**: 117218 [PMID: 33278982 DOI: 10.1016/j.carbpol.2020.117218]
57 **Gao K**, Mu CL, Farzi A, Zhu WY. Tryptophan Metabolism: A Link Between the Gut Microbiota and Brain. *Adv Nutr* 2020; **11**: 709-723 [PMID: 31825083 DOI: 10.1093/advances/nmz127]
58 **Obata Y**, Castaño Á, Boeing S, Bon-Frauches AC, Fung C, Fallesen T, de Agüero MG, Yilmaz B, Lopes R, Huseynova A, Horswell S, Maradana MR, Boesmans W, Vanden Berghe P, Murray AJ, Stockinger B, Macpherson AJ, Pachnis V. Neuronal programming by microbiota regulates intestinal physiology. *Nature* 2020; **578**: 284-289 [PMID: 32025031 DOI: 10.1038/s41586-020-1975-8]
59 **Sahakian AB**, Jee SR, Pimentel M. Methane and the gastrointestinal tract. *Dig Dis Sci* 2010; **55**: 2135-2143 [PMID: 19830557 DOI: 10.1007/s10620-009-1012-0]
60 **Dridi B**, Henry M, El Khéchine A, Raoult D, Drancourt M. High prevalence of Methanobrevibacter smithii and Methanosphaera stadtmanae detected in the human gut using an improved DNA detection protocol. *PLoS One* 2009; **4**: e7063 [PMID: 19759898 DOI: 10.1371/journal.pone.0007063]
61 **Takakura W**, Pimentel M, Rao S, Villanueva-Millan MJ, Chang C, Morales W, Sanchez M, Torosyan J, Rashid M, Hosseini A, Wang J, Leite G, Kowalewski E, Mathur R, Rezaie A. A Single Fasting Exhaled Methane Level Correlates With Fecal Methanogen Load, Clinical Symptoms and Accurately Detects Intestinal Methanogen Overgrowth. *Am J Gastroenterol* 2022; **117**: 470-477 [PMID: 35041624 DOI: 10.14309/ajg.0000000000001607]
62 **Koch CD**, Gladwin MT, Freeman BA, Lundberg JO, Weitzberg E, Morris A. Enterosalivary nitrate metabolism and the microbiome: Intersection of microbial metabolism, nitric oxide and diet in cardiac and pulmonary vascular health. *Free Radic Biol Med* 2017; **105**: 48-67 [PMID: 27989792 DOI: 10.1016/j.freeradbiomed.2016.12.015]
63 **Alemi F**, Poole DP, Chiu J, Schoonjans K, Cattaruzza F, Grider JR, Bunnett NW, Corvera CU. The receptor TGR5 mediates the prokinetic actions of intestinal bile acids and is required for normal defecation in mice. *Gastroenterology* 2013; **144**: 145-154 [PMID: 23041323 DOI: 10.1053/j.gastro.2012.09.055]
64 **Wong BS**, Camilleri M. Elobixibat for the treatment of constipation. *Expert Opin Investig Drugs* 2013; **22**: 277-284 [PMID: 23215781 DOI: 10.1517/13543784.2013.753056]
65 **Nakajima A**, Seki M, Taniguchi S, Ohta A, Gillberg PG, Mattsson JP, Camilleri M. Safety and efficacy of elobixibat for chronic constipation: results from a randomised, double-blind, placebo-controlled, phase 3 trial and an open-label, single-arm, phase 3 trial. *Lancet Gastroenterol Hepatol* 2018; **3**: 537-547 [PMID: 29805116 DOI: 10.1016/S2468-1253(18)30123-7]
66 **Sayin SI**, Wahlström A, Felin J, Jäntti S, Marschall HU, Bamberg K, Angelin B, Hyötyläinen T, Orešič M, Bäckhed F. Gut microbiota regulates bile acid metabolism by reducing the levels of tauro-beta-muricholic acid, a naturally occurring FXR antagonist. *Cell Metab* 2013; **17**: 225-235 [PMID: 23395169 DOI: 10.1016/j.cmet.2013.01.003]
67 **Garrett WS**. Cancer and the microbiota. *Science* 2015; **348**: 80-86 [PMID: 25838377 DOI: 10.1126/science.aaa4972]
68 **Schwabe RF**, Jobin C. The microbiome and cancer. *Nat Rev Cancer* 2013; **13**: 800-812 [PMID: 24132111 DOI: 10.1038/nrc3610]
69 **Staller K**, Olén O, Söderling J, Roelstraete B, Törnblom H, Song M, Ludvigsson JF. Chronic Constipation as a Risk Factor for Colorectal Cancer: Results From a Nationwide, Case-Control Study. *Clin Gastroenterol Hepatol* 2022; **20**: 1867-1876.e2 [PMID: 34687968 DOI: 10.1016/j.cgh.2021.10.024]
70 **Guérin A**, Mody R, Fok B, Lasch KL, Zhou Z, Wu EQ, Zhou W, Talley NJ. Risk of developing colorectal cancer and benign colorectal neoplasm in patients with chronic constipation. *Aliment Pharmacol Ther* 2014; **40**: 83-92 [PMID: 24832002 DOI: 10.1111/apt.12789]
71 **Khalif IL**, Quigley EM, Konovitch EA, Maximova ID. Alterations in the colonic flora and intestinal permeability and evidence of immune activation in chronic constipation. *Dig Liver Dis* 2005; **37**: 838-849 [PMID: 16169298 DOI: 10.1016/j.dld.2005.06.008]
72 **Guo M**, Yao J, Yang F, Liu W, Bai H, Ma J, Ma X, Zhang J, Fang Y, Miao Y, Sun J, Zhang Y, Zhao H. The composition of intestinal microbiota and its association with functional constipation of the elderly patients. *Future Microbiol* 2020; **15**: 163-175 [PMID: 32079430 DOI: 10.2217/fmb-2019-0283]
73 **Parthasarathy G**, Chen J, Chen X, Chia N, O'Connor HM, Wolf PG, Gaskins HR, Bharucha AE. Relationship Between Microbiota of the Colonic Mucosa vs Feces and Symptoms, Colonic Transit, and Methane Production in Female Patients With Chronic Constipation. *Gastroenterology* 2016; **150**: 367-79.e1 [PMID: 26460205 DOI: 10.1053/j.gastro.2015.10.005]
74 **Kostic AD**, Gevers D, Pedamallu CS, Michaud M, Duke F, Earl AM, Ojesina AI, Jung J, Bass AJ, Tabernero J, Baselga J, Liu C, Shivdasani RA, Ogino S, Birren BW, Huttenhower C, Garrett WS, Meyerson M. Genomic analysis identifies association of Fusobacterium with colorectal carcinoma. *Genome Res* 2012; **22**: 292-298 [PMID: 22009990 DOI: 10.1101/gr.126573.111]
75 **Nosho K**, Sukawa Y, Adachi Y, Ito M, Mitsuhashi K, Kurihara H, Kanno S, Yamamoto I, Ishigami K, Igarashi H, Maruyama R, Imai K, Yamamoto H, Shinomura Y. Association of Fusobacterium nucleatum with immunity and molecular alterations in colorectal cancer. *World J Gastroenterol* 2016; **22**: 557-566 [PMID: 26811607 DOI: 10.3748/wjg.v22.i2.557]
76 **Galan-Ros J**, Ramos-Arenas V, Conesa-Zamora P. Predictive values of colon microbiota in the treatment response to

colorectal cancer. *Pharmacogenomics* 2020; **21**: 1045-1059 [PMID: 32896201 DOI: 10.2217/pgs-2020-0044]

77 **Peng C**, Ouyang Y, Lu N, Li N. The NF-κB Signaling Pathway, the Microbiota, and Gastrointestinal Tumorigenesis: Recent Advances. *Front Immunol* 2020; **11**: 1387 [PMID: 32695120 DOI: 10.3389/fimmu.2020.01387]

78 **Hnatyszyn A**, Hryhorowicz S, Kaczmarek-Ryś M, Lis E, Słomski R, Scott RJ, Pławski A. Colorectal carcinoma in the course of inflammatory bowel diseases. *Hered Cancer Clin Pract* 2019; **17**: 18 [PMID: 31338130 DOI: 10.1186/s13053-019-0118-4]

79 **O'Keefe SJ**. Diet, microorganisms and their metabolites, and colon cancer. *Nat Rev Gastroenterol Hepatol* 2016; **13**: 691-706 [PMID: 27848961 DOI: 10.1038/nrgastro.2016.165]

80 **Guo M**, Li Z. Polysaccharides isolated from Nostoc commune Vaucher inhibit colitis-associated colon tumorigenesis in mice and modulate gut microbiota. *Food Funct* 2019; **10**: 6873-6881 [PMID: 31584586 DOI: 10.1039/c9fo00296k]

World Journal of Gastrointestinal Oncology

Submit a Manuscript: https://www.f6publishing.com

World J Gastrointest Oncol 2023 May 15; 15(5): 787-809

DOI: 10.4251/wjgo.v15.i5.787

ISSN 1948-5204 (online)

ORIGINAL ARTICLE

Basic Study

Circ_0003356 suppresses gastric cancer growth through targeting the miR-668-3p/SOCS3 axis

Wei-Dong Li, Hai-Tao Wang, Yue-Ming Huang, Bo-Hao Cheng, Li-Jun Xiang, Xin-Hao Zhou, Qing-Yan Deng, Zhi-Gang Guo, Zhi-Feng Yang, Zhi-Fen Guan, Yao Wang

Specialty type: Oncology

Provenance and peer review: Unsolicited article; Externally peer reviewed.

Peer-review model: Single blind

Peer-review report's scientific quality classification

Grade A (Excellent): 0
Grade B (Very good): B
Grade C (Good): C
Grade D (Fair): 0
Grade E (Poor): 0

P-Reviewer: Shu C, China; Tanabe S, Japan

Received: November 30, 2022
Peer-review started: November 30, 2022
First decision: December 25, 2022
Revised: January 6, 2023
Accepted: April 7, 2023
Article in press: April 7, 2023
Published online: May 15, 2023

Wei-Dong Li, Hai-Tao Wang, Yue-Ming Huang, Bo-Hao Cheng, Li-Jun Xiang, Xin-Hao Zhou, Qing-Yan Deng, Zhi-Gang Guo, Zhi-Feng Yang, Zhi-Fen Guan, Yao Wang, Department of Gastrointestinal Surgery, Zhongshan City People's Hospital, Zhongshan 528403, Guangdong Province, China

Corresponding author: Yao Wang, MD, Professor, Department of Gastrointestinal Surgery, Zhongshan City People's Hospital, No. 2 Sunwen East Road, Zhongshan 528403, Guangdong Province, China. wangyao8065@163.com

Abstract

BACKGROUND

Circular RNAs (circRNAs) have attracted extensive attention as therapeutic targets in gastric cancer (GC). Circ_0003356 is known to be downregulated in GC tissues, but its cellular function and mechanisms remain undefined.

AIM

To investigate the role of circ_0003356 in GC at the molecular and cellular level.

METHODS

Circ_0003356, miR-668-3p, and SOCS3 expression were assessed *via* quantitative real time-polymerase chain reaction (qRT-PCR). Wound healing, EdU, CCK-8, flow cytometry and transwell assays were used to analyze the migration, proliferation, viability, apoptosis and invasion of GC cells. The subcellular localization of circ_0003356 was monitored using fluorescence in situ hybridization. The interaction of circ_0003356 with miR-668-3p was confirmed using RIP-qRT-PCR, RNA pull-down, and dual luciferase reporter assays. We observed protein levels of genes *via* western blot. We injected AGS cells into the upper back of mice and performed immunohistochemistry staining for examining E-cadherin, N-cadherin, Ki67, and SOCS3 expressions. TUNEL staining was performed for the assessment of apoptosis in mouse tumor tissues.

RESULTS

Circ_0003356 and SOCS3 expression was downregulated in GC cells, whilst miR-668-3p was upregulated. Exogenous circ_0003356 expression and miR-668-3p silencing suppressed the migration, viability, proliferation, epithelial to mesenchy-mal transition (EMT) and invasion of GC cells and enhanced apoptosis.

Circ_0003356 overexpression impaired tumor growth in xenograft mice. Targeting of miR-668-3p by circ_0003356 was confirmed through binding assays and SOCS3 was identified as a downstream target of miR-668-3p. The impacts of circ_0003356 on cell proliferation, apoptosis, migration, invasion and EMT were reversed by miR-668-3p up-regulation or SOCS3 down-regulation in GC cells.

CONCLUSION

Circ_0003356 impaired GC development through its interaction with the miR-668-3p/SOCS3 axis.

Key Words: Epithelial-mesenchymal transition; Circ_0003356; Gastric cancer; Invasion; Proliferation; Migration

Core Tip: We observed the low level of circ_0003356 expression in gastric cancer (GC) tissues and cells. Circ_0003356 expression was positively related to GC patient prognosis. Exogenous circ_0003356 overexpression and/or miR-668-3p suppression enhanced apoptosis in GC cells and suppressed GC cell proliferation, migration, invasion, and epithelial to mesenchy-mal transition. The overexpression of circ_0003356 also prevented tumor growth in mice. At the mechansistic level, circ_0003356 was found to interact with the miR-668-3p/SOCS3 axis to impair GC development. Together, we reveal new and important molecular details highlighting circ_0003356 as a novel cancer target.

Citation: Li WD, Wang HT, Huang YM, Cheng BH, Xiang LJ, Zhou XH, Deng QY, Guo ZG, Yang ZF, Guan ZF, Wang Y. Circ_0003356 suppresses gastric cancer growth through targeting the miR-668-3p/SOCS3 axis. *World J Gastrointest Oncol* 2023; 15(5): 787-809
URL: https://www.wjgnet.com/1948-5204/full/v15/i5/787.htm
DOI: https://dx.doi.org/10.4251/wjgo.v15.i5.787

INTRODUCTION

Gastric cancer (GC) encompasses a range of gastrointestinal malignancies[1,2], and ranks as the 2nd main cause of global cancer-associated deaths[3,4]. Chemotherapy, radiotherapy, and surgical resection have progressed GC treatment[5,6], but five-year survival rates remain low[7,8]. Personalized therapy has shown promise for GC treatment[9], but more effective anti-GC targets are required. Circular RNAs (circRNAs) regulate GC occurrence and development. The downregulation of circ_SKA3 inhibits the colony formation, proliferation, migration, and invasion of GC cells *in vitro* and suppresses tumorigenesis *in vivo*[10]. Circ_0005758 up-regulation can inhibit GC cell proliferation, migration and invasion, and suppress tumor growth in xenograft mice[11]. Up-regulation of circ_0021087 impairs proliferation, epithelial to mesenchy-mal transition (EMT), and invasion of GC cells and overpowers tumor development in xenograft mice[12]. CircRNA analysis in GSE184882 indicates that circ_0003356 is lowly expressed in GC tissues, but the molecular effects governing its role in GC suppression have not been investigated at the molecular level.

MicroRNAs (miRNAs) regulate the post-transcriptional expression of a number of genes[13,14] and play a key role in GC progression. The overexpression of miR-548 promotes proliferation, migration and invasion of GC cells *in vitro*[15]. Silencing of miR-762 reduces GC cell viability and facilitates apoptosis [16]. Inhibition of miR-4742-5p suppresses the proliferation, migration and invasion of GC cells[17]. Especially, miR-668-3p is oncogenic in hepatocellular carcinoma (HCC)[18] and colorectal cancer (CRC) cells[19].

SOCS3 is a negative regulator of hormone and cytokine signaling and plays a key role in cancer development[20,21]. Available studies have highlighted the importance of SOCS3 in the manipulation of cancer development. A study from Yu *et al*[22] have revealed that the downregulation of SOCS3 can reverse the suppressive effects of miR-3173-5p inhibitor on colony formation, cell proliferation, migration, invasion and EMT in prostate cancer cells. Another study from Li *et al*[23] have reported that SOCS3 overexpression also suppresses spheroid formation and CRC cell proliferation. In particular, SOCS3 is proven to exert an important role against tumor in GC. For instance, inhibition of miR-340 suppresses cell cycle progression through enhancing the expression of SOCS3 in GC cells[24]. MiR-665 also serves as an oncogene in GC through the downregulation of SOCS3[25]. The regulatory effects of miR-668-3p on SOCS3 in GC cells has not been investigated. Here, we show for the first time that circ_0003356 is downregulated in GC cells and tumor tissues and reveal its association with GC progression.

MATERIALS AND METHODS

Sample collection

GC and normal tissues (n = 80 pairs) were collected from surgical specimens of patients with GC at Zhongshan City People's Hospital. Patients were diagnosed with GC *via* histopathology. No patients had received prior immunotherapy, adjuvant chemotherapy, or radiation therapy before surgery. GC patients were allocated into circ_0003356 low or high-expression groups based on the median expression value in tumor tissues. The Ethics Committee of Zhongshan City People's Hospital provided approval (K2017-182). All participants agreed to the study and provided informed written consent.

Cell culture

AGS and HGC-27 cell lines (human) and GES-1 (non-GC) were cultured in Roswell Park Memorial Institute 1640 medium + 10% fetal bovine serum (FBS) + 1% streptomycin-penicillin. Cells were maintained at 37 °C 5% CO_2.

Quantitative real time-polymerase chain reaction: Cells were lysed in Trizol and total RNA was quantitated on a NanoDrop 2000c spectrophotometer. For circ_0003356 and SOCS3, PrimeScript™ RT reagent kits were used for complementary DNA (cDNA) synthesis. For miR-668-3p, a TaqMan miRNA Assay kit was used for cDNA synthesis. cDNA was amplified using BeyoFast™ SYBR Green qPCR Mix. Primer sequences as shown in Table 1 were bought from TaKaRa. Relative mRNA expression of circ_0003356 and SOCS3 were normalised to GAPDH and calculated using the $2^{-\Delta\Delta Ct}$ method. miR-668-3p was normalised to U6.

Cell transfection

The empty pcDNA3.1 vector, circ_0003356 overexpression vector (pcDNA3.1-circ_0003356), miR-668-3p inhibitor, negative control (NC) inhibitor, miR-668-3p mimic, NC mimic, small interfering RNA (siRNA) against SOCS3 (si-SOCS3) and si-NC were bought from GenePharma (Shanghai, China). Above factors were then transfected into AGS and HGC-27 cells using Lipofectamine 3000 (Invitrogen, Carlsbad, California, United States) for 48 h.

CCK-8 assay: The proliferation of HGC-27 and AGS cells was evaluated *via* a cell counting kit-8 (Dojindo, Osaka, Japan). HGC-27 and AGS cells (1×10^4 cells/well) were plated in 96-well plates for incubating 24 h, 48 h, 72 h and 96 h. After that, each well was treated with CCK-8 reagent (10 μL) for another 1 h. Ultimately, a microplate reader (Bio-Rad, CA, United States) was used for measurement of optical density at 450 nm.

EdU assays: A Cell-Light EdU DNA Cell Proliferation Kit (RiboBio, Guangzhou, China) was used to perform EdU assay. Cells were labeled with 50 μM EdU for 2 h and fixed with 4 % paraformaldehyde (PFA) (4%). Cells were washed in phosphate buffered saline (PBS) containing glycine (2 mg/mL) for 10 min to remove artefacts and permeabilized. Cells were stained with Apollo dye liquor in the dark followed by DAPI. Cells were imaged on a fluorescence microscope.

Flow cytometry analysis: Apoptotic rates were measured by flow cytometry (FACSCalibur, BD, United States). Cells were resuspended in 300 μL binding buffer and incubated with + Annexin V-FITC (5 μL) for 10 min. Cells were labeled with propidium iodide (5 μL) in the dark for 5 min. Apoptotic cells were quantified using FlowJo V10 software.

Wound healing assay: HGC-27 and AGS cells (5×10^4 cells/well) were put to 6-well plates coated with extracellular matrix molecule, which were cultured in RPMI1640 including 10% FBS. When the cell monolayer was formed, a sterile pipette tip was utilized for scratching the monolayer and scratch width was recorded under an inverted microscope (TE2000; Nikon, Tokyo, Japan). After being washed *via* PBS, FBS-free medium was added to culture cells for 24 h, followed by record of scratch wound. At last, the migration rate was calculated according to the following formula: (1 - 24 h scratch width/0 h scratch width) × 100.

Transwell assay: Matrigel-coated transwell chambers (8 μm; BD Biosciences, Franklin Lakes, NJ, United States) were utilized for evaluating invasion of HGC-27 and AGS cells. In detail, 3×10^3 cells were re-suspended in FBS-free RPMI1640 medium (200 μL), which were appended to the upper chamber. In contrast, RPMI1640 medium containing 10% FBS was appended to bottom chambers. Following 24 h of incubation, cells in upper chambers were removed *via* a cotton swab. Cells in bottom chambers were fixed *via* 4% PFA and stained *via* 0.1% crystal violet. At last, the number of these cells was counted through inverted fluorescence microscopy (Leica Microsystems GmbH, Wetzlar, Germany).

Cytoplasmic and nuclear fractions: AGS and HGC-27 cells were lysed on ice in lysis buffer + protease inhibitors and centrifuged for 3 min. The subsequent pellets and supernatants were harvested as nuclear and cytoplasmic fractions. RNA was extracted from each fraction using Buffer SK. Quantitative real-time polymerase chain reaction (qRT-PCR) analysis was performed for the detection of circ_0003356

Table 1 Primer sequences for quantitative real time-polymerase chain reaction analysis used in this study

Genes		Sequences (5'-3')
Circ_0003356	Forward	CCAAGCTTGAAGACGGCAAA
	Reverse	TCATGGGGCTTCACCTTGAC
MiR-668-3p	Forward	TGTCACTCGGCTCGG
	Reverse	TGCGTGTCGTGGAGTC
SOCS3	Forward	CCTGCGCCTCAAGACCTTC
	Reverse	GTCACTGCGCTCCAGTAGAA
U6	Forward	GCTTCGGCAGCACATATACTAAAAT
	Reverse	CAGTGCGTGTCGTGGAGT
GAPDH	Forward	GGAGATTGTTGCCATCAACG
	Reverse	TTGGTGGTGCAGGATGCATT

expression. U6 and 18S rRNA were used as controls of cytoplasmic and nuclear transcripts, respectively.

Fluorescence *in situ* hybridization (FISH): Fluorescence *in situ* hybridization (FISH) was performed using specific probes against circ_0003356 and miR-668-3p. Briefly, cells were fixed in 4% PFA for 15 min and washed with a 70%, 95%, and 100% gradient of ethanol. Cell hybridization was performed at 37 °C in a dark incubator. Cells were blocked in 3% normal goat serum and 1% bovine serum albumin for 1 h. Cells were cultured with HRP-conjugated anti-biotin antibodies at 4 °C for 1 d. Cells were imaged on a fluorescence microscope.

Dual luciferase reporter assay: The online database circinteractome and StarBase v2.0 were used to identify predicted targets of circ_0003356 and miR-668-3p. The interaction of circ_0003356 and miR-668-3p or SOCS3 and miR-668-3p were verified *via* dual luciferase reporter (DLR) assays. Briefly, the 3′-UTR sequences of WT circ_0003356 or SOCS3 comprising the miR-668-3p binding sites were cloned into pRL-CMV. 3′-UTR sequences of circ_0003356 or SOCS3 containing mutant sites for miR-668-3p were also generated. MiR-668-3p mimic or NC mimic were transfected into HGC-27 and AGS cells and luciferase activity was measured 2 d post-transfection.

RNA binding protein immunoprecipitation assay: Cells were lysed in RNA binding protein immunoprecipitation (RIP) buffer and magnetic beads conjugated with anti-Ago2 and anti-immunoglobulin G (IgG) were added to cell lysates. MiR-668-3p and circ_0003356 levels in the beads were analyzed.

RNA pull-down assays: RNA pull-downs were performed using commercial Magnetic RNA-Protein Pull-Down Kits (Pierce). Cells were transfected with 3′-biotinylated miR-668-3p (Bio-miR-668-3p) or Bio-NC mimics. After 2 d, cells were lysed cells and streptavidin-coupled beads added to pull-down biotin-coupled RNA complexes. Circ_0003356 enrichment in the bound fractions was subsequently assayed.

Western blot analysis: Cells were lysed in RIPA buffer and protein content assessed *via* BCA assays. A total of 20 μg of protein was resolved on 10% sodium dodecyl sulphate-polyacrylamide gel electrophoresis (SDS-PAGE) gels and transferred to on polyvinylidene difluoride membranes. Membranes were blocked in non-fat milk for 1 h and probed with anti-N-cadherin (1:6000, ab76011), anti-E-cadherin (1:10000, ab40772), anti-SOCS3 (1:1000, ab280884) and β-actin (1:1000, ab8224) primary antibodies at 4 °C for 24 h. Cells were subsequently labeled with anti-rabbit secondary antibodies (1:2000, ab205718) and proteins were visualized using chemiluminescence.

Establishment of xenograft tumor models: Mice (4-5 wk-old; BALB/c nude; male) were housed at room temperature with 50% humidity and 12 h light/dark cycle. All experiments were approved by the Animal Care and Use Committee of Zhongshan City People's Hospital (K2017-182).

Mice were injected into the upper back with 1×10^7 AGS cells transfected with circ_0003356 or control vector[26]. Mice were assigned into 2 groups (n = 6 mice/group): Thecirc_0003356 group and the vector group. After injection for five weeks, mice were anesthetized with pentobarbital sodium and sacrificed *via* dislocation of cervical vertebrae. Tumors were dissected and tumor volumes calculated (length × width^2)/2.

Immunohistochemistry staining: Mice tumor tissues were fixed in formalin and paraffinized. Tumors were cut into 4 μm sections, dewaxed with xylene, and hydrated in ethanol. Sections were boiled in citrate buffer (10 mmol/L) and cultured using H_2O_2 solution (3%) to inhibit endogenous peroxidase activity. Sections were probed with anti-Ki67 (1:200, ab16667), anti-SOCS3 (1:1000, ab280884), anti-N-

cadherin (1:500, ab76011), and anti-E-cadherin (1:500, ab40772) primary antibodies at 4 °C overnight and labeled with HRP-conjugated secondary antibodies (1:500, ab6112) 30 min. Cells were stained using DAB substrate and counterstained using hematoxylin. Cells were imaged on a light microscope.

TUNEL staining: TUNEL assay was performed using the commercially available *in situ* Cell Death Detection Kit as per the manufactures recommendations.

Statistical analysis

GraphPad Prism 8.0 was used for data analysis. Experiments were performed on a minimum of 3 occasions and are shown as the mean ± SD. Survival curves were plotted using the Kaplan-Meier method. Data were compared using a student's *t*-test.

RESULTS

Circ_0003356 expression is down-regulated in GC tissues

Published GEO and GSE184882 datasets were analyzed[27,28]. Five circRNAs with significant expression differences in GC tissues were identified and selected for heat map analysis (Figure 1A). Then their expression was further determined *via* qRT-PCR. Five circRNAs with low relative expression in tumor tissues compared to normal tissues were identified (n = 20), amongst which circ_0003356 expression (0.2 ± 0.06532) was the lowest (P = 0.0002, Figure 1B). Circ_0003356 was selected for further analysis.

Circ_0003356 expression was validated in GC normal and tumor tissues (n = 80). As expected, circ_0003356 expression was markedly downregulated in tumor tissues (0.4908 ± 0.02457) compared to normal adjacent tissues (0.99 ± 0.0243; P < 0.0001, Figure 1C). Patients with low circ_0003356 expression correlated with a short survival time (P < 0.0001, Figure 1D). Moreover, circ_0003356 displayed lower expression in AGS (0.3833 ± 0.06012) and HGC-27 cells (0.4967 ± 0.06012) than GES-1 cells (P = 0.0004, P = 0.0001, Figure 1E).

Circ_0003356 overexpression promotes cell apoptosis and impairs invasion, proliferation, migration and EMT of AGS and HGC-27 cells

Circ_0003356 was overexpressed in AGS and HGC-27 cells to further explore its influence on GC cell proliferation, apoptosis, migration, invasion, and EMT. Circ_0003356 expression in AGS cells (2.613 ± 0.05207) and HGC-27 cells (2.5 ± 0.05774) was dramatically increased following transfection of pcDNA3.1-circ_0003356 (P < 0.0001, P < 0.0001, Figure 2A). Functional analyses showed that the viability of AGS (1.183 ± 0.06155) and HGC-27 cells (1.247 ± 0.0636) at 96 h were attenuated after circ_0003356 overexpression (P = 0.0002, P = 0.0002, Figure 2B). EdU assays also revealed that the proliferative ability of AGS (22.33 ± 1.764) and HGC-27 cells (20 ± 1.732) was attenuated by circ_0003356 overexpression (P = 0.0025, P = 0.0043, Figure 2C). Apoptotic rates in AGS (22.68 ± 0.2887) and HGC-27 cells' (18.38 ± 0.2887) were increased by circ_0003356 overexpression (P < 0.0001, P < 0.0001, Figure 2D). In terms of the migration and invasion of AGS (24.33 ± 2.728) and HGC-27 cells (20.33 ± 1.764), decreased numbers of invading AGS (168 ± 11.27) and HGC-27 cells (161.7 ± 12.35) were observed in response to circ_0003356 overexpression (P = 0.0001, P = 0.0031, P = 0.0002, P = 0.0016, Figures 2E and F). Circ_0003356 overexpression also attenuated the EMT of AGS (1.07 ± 0.6531, 0.57 ± 0.5168) and HGC-27 (0.93 ± 0.06533, 0.39 ± 0.06137) cells evidenced by reduced N-cadherin expression and the enhanced expression of E-cadherin (P = 0.0006, P = 0.0023, P = 0.0021, P = 0.0007, Figure 2G).

Circ_0003356 directly binds to miR-668-3p

The subvocalization of circ_0003356 in AGS and HGC-27 cells was confirmed through FISH, which showed that circ_0003356 located in AGS and HGC-27 cells' cytoplasm (Figure 3A). The findings were confirmed by qRT-PCR, showing that the circ_0003356 level was in AGS and HGC-27 cells markedly higher in the cytoplasm (85%) than the nuclear (15%) (Figure 3B).

Target predictions were performed using circinteractome, indentifing binding sites between miR-668-3p and circ_0003356 (Figure 3C). We verified this relationship *via* RIP-qRT-PCR, RNA pull-down, and DLR assays. The Ago2 group showed enrichment for circ_0003356 and miR-668-3p in AGS (12.3 ± 0.7024, 15.33 ± 0.3801) and HGC-27 cells (11.3 ± 0.6272, 14.33 ± 0.6912) compared to the IgG group (P = 0.000087, P = 0.0000029, P = 0.00008, P = 0.00004, Figure 3D). The biotinylated miR-668-3p probe enriched more circ_0003356 than the biotinylated NC probe in AGS (0.9033 ± 0.03756) and HGC-27 cells (0.9167 ± 0.0491) (P = 0.0002, P = 0.0004, Figure 3E). Relative luciferase activity in AGS (0.35 ± 0.06532) and HGC-27 (0.31 ± 0.06478) were reduced in cells co-transfected with miR-668-3p mimic and circ_0003356 WT relative to miR-668-3p mimic and circ_0003356 MUT (P = 0.00057, P = 0.00041, Figure 3F). High expression of miR-668-3p was observed in tumor tissues (2.006 ± 0.02872) compared to healthy tissues (0.9984 ± 0.02829) (P < 0.0001, Figure 3G). An inverse relationship between the expression of miR-668-3p and circ_0003356 in tumor tissues was also observed (r = -0.8783, P = 0.0007,

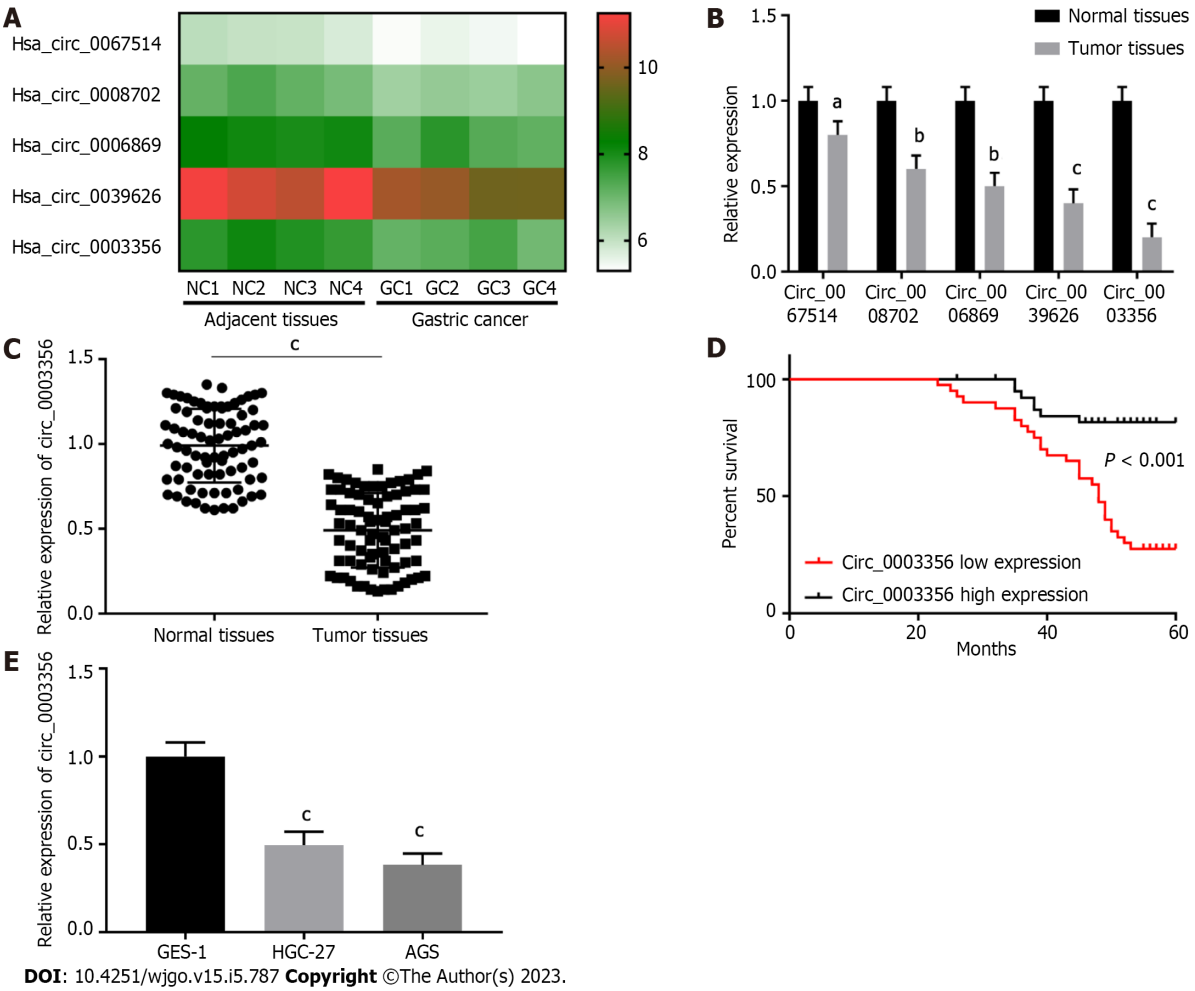

DOI: 10.4251/wjgo.v15.i5.787 **Copyright** ©The Author(s) 2023.

Figure 1 Circ_0003356 is expressed to low levels in gastric cancer tissues. A: CircRNAs in GSE184882 were analyzed and five with the most significant expression differences in gastric cancer (GC) were used for heat map analysis; B: Relative expression of circRNAs in tumor and normal tissues determined by quantitative real-time polymerase chain reaction (qRT-PCR); C: Relative expression of circ_0003356 in tumor and normal tissues determined by qRT-PCR; D: Kaplan-Meier analysis of the correlation between circ_0003356 expression and overall survival of GC patients; E: Relative expression of circ_0003356 in GES-1, HGC-27, and AGS cells determined by qRT-PCR. $^{a}P < 0.05$, $^{b}P < 0.01$, $^{c}P < 0.001$. NC: Negative control; GC: Gastric cancer.

Figure 3H).

Suppression of miR-668-3p promotes apoptosis and reduces proliferation, migration, invasion, and EMT in AGS and HGC-27 cells

Accordingly, the influences of miR-668-3p on cell migration, apoptosis, proliferation, invasion, and EMT were explored. Firstly, miR-668-3p expression in HGC-27 (2.8 ± 0.05508) and AGS (3 ± 0.1155) cells was found to be remarkably higher than GES-1 cells (1.007 ± 0.05207) ($P < 0.0001$, $P < 0.0001$, Figure 4A). When we determined its specific functions, we found that the viability (1.393 ± 0.06128, 1.342 ± 0.0636) and proliferative capacity (12.33 ± 1.453, 14 ± 2.082) of AGS and HGC-27 cells were attenuated by miR-668-3p suppression ($P = 0.00037$, $P = 0.00039$, $P = 0.0033$, $P = 0.0020$, Figures 4B and C). Apototic rates in AGS (21.29 ± 0.8838) and HGC-27 cells' (21.09 ± 0.9074) were raised following miR-668-3p suppression ($P < 0.0001$, $P = 0.0001$, Figure 4D). The migration (25.67 ± 2.603, 41.67 ± 2.906) and invasion (174.7 ± 9.262, 175.7 ± 9.025) of AGS and HGC-27 cells were also repressed following miR-668-3p down-regulation ($P = 0.0001$, $P = 0.0019$, $P = 0.0026$, $P = 0.0023$, Figures 4E and F). The EMT of AGS (1.09 ± 0.06348, 0.4 ± 0.06137) and HGC-27 cells (0.9 ± 0.05627, 0.31 ± 0.06137) was similarly attenuated by miR-668-3p suppression, evidenced by decreased N-cadherin and increased E-cadherin expression ($P = 0.00089$, $P = 0.00051$, $P = 0.00066$, $P = 0.00054$, Figure 4G).

SOCS3 is targeted by miR-668-3p

MiR-668-3p targets were assessed using the starbase2.0 database. SOCS3 contained binding sequences (AGUGAC) of miR-668-3p (Figure 5A). DLR assay was performed to validate this interaction. Relative luciferase activity in AGS (0.37 ± 0.06532) and HGC-27 cells (0.32 ± 0.06532) transfected with SOCS3 WT reporter was reduced in response to transfection of miR-668-3p mimic ($P = 0.00041$, $P = 0.00065$, Figure 5B). The SOCS3 MUT reporter showed no such changes following miR-668-3p mimic addition

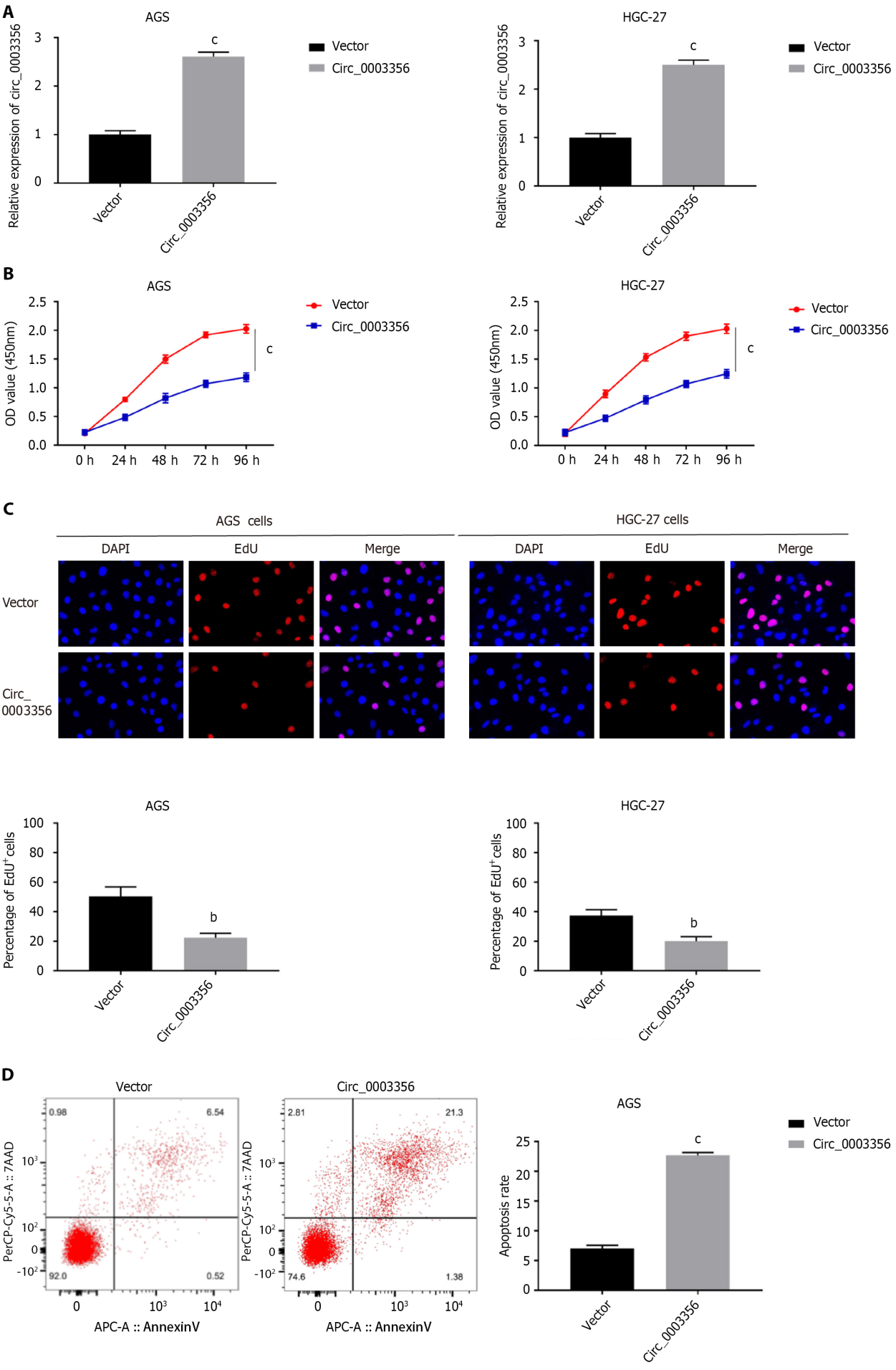
A
AGS
Relative expression of circ_0003356
c
Vector
Circ_0003356
HGC-27
B
OD value (450nm)
0 h
24 h
48 h
72 h
96 h
C
AGS cells
HGC-27 cells
DAPI
EdU
Merge
Vector
Circ_0003356
Percentage of EdU+ cells
b
D
Vector
Circ_0003356
PerCP-Cy5-5-A :: 7AAD
APC-A :: AnnexinV
0.98
6.54
92.0
0.52
2.81
21.3
74.6
1.38
Apoptosis rate

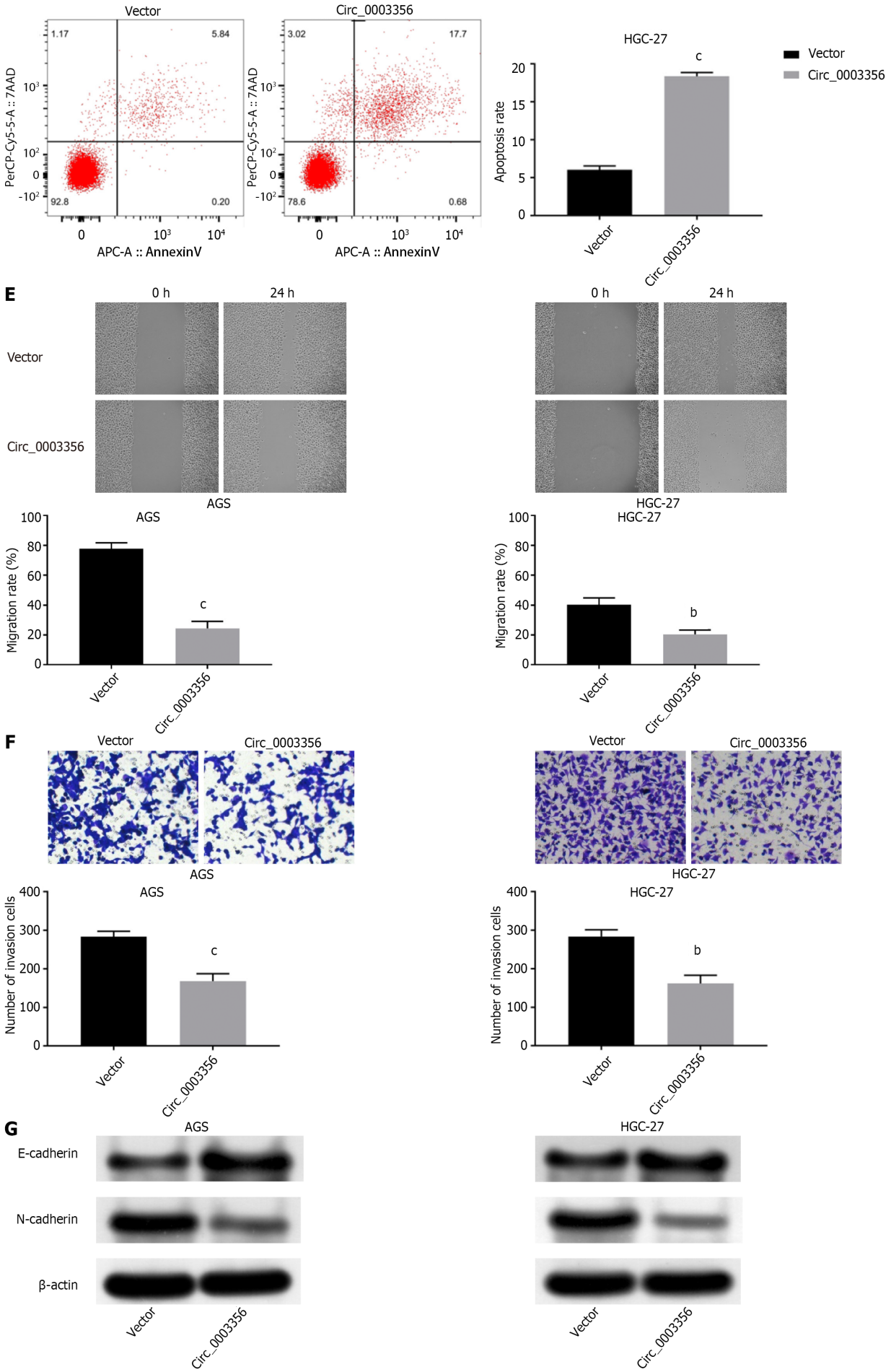
Vector
Circ_0003356
1.17
5.84
92.8
0.20
3.02
17.7
78.6
0.68
PerCP-Cy5-5-A :: 7AAD
APC-A :: AnnexinV
HGC-27
Apoptosis rate
c
Vector
Circ_0003356
E
0 h
24 h
AGS
HGC-27
Migration rate (%)
b
F
Number of invasion cells
G
E-cadherin
N-cadherin
β-actin

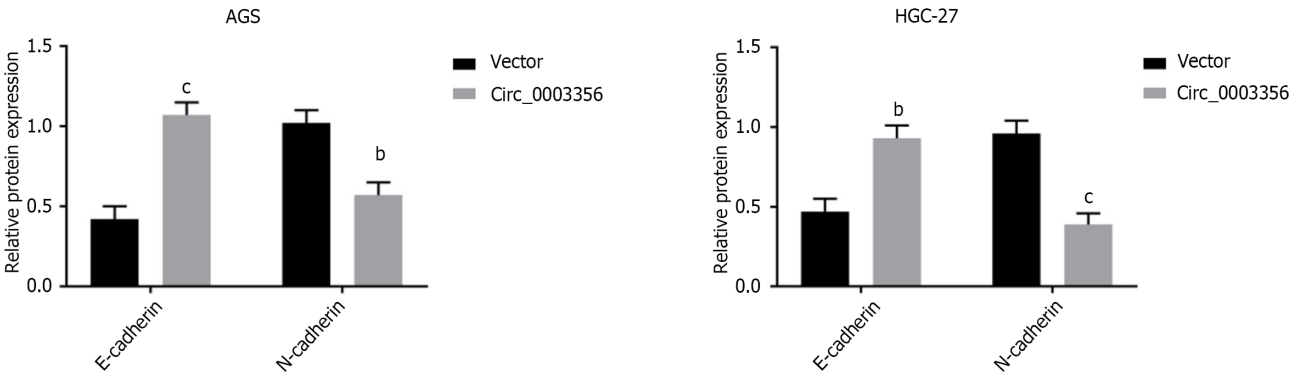

DOI: 10.4251/wjgo.v15.i5.787

Figure 2 Upregulation of circ_0003356 promotes cell apoptosis and suppresses proliferation, migration, invasion, and epithelial-mesenchymal transition of AGS and HGC-27 cells. A: Relative expression of circ_0003356 in AGS and HGC-27 cells detected by quantitative real-time polymerase chain reaction; B: Cell viability in AGS and HGC-27 cells assessed by CCK-8 assay; C: Proliferation of AGS and HGC-27 cells assessed by EdU assays. D: Apoptosis of AGS and HGC-27 cells assessed by flow cytometry; E: Migration of AGS and HGC-27 cells detected by wound healing assays; F: Invasion of AGS and HGC-27 cells detected by transwell assay; G: Levels of epithelial-mesenchymal transition-related proteins (E-cadherin and N-cadherin) in AGS and HGC-27 cells determined using western blotting. $^{b}P < 0.01$, $^{c}P < 0.001$.

(Figure 5B), suggestive of a direct interaction between miR-668-3p and SOCS3. The regulatory relation between miR-668-3p and SOCS3 was assessed through western blotting. SOCS3 expression in AGS and HGC-27 cells was reduced through the addition of miR-668-3p mimic (0.5833 ± 0.03756, 0.6633 ± 0.03528) and boosted by the miR-668-3p inhibitor (1.03 ± 0.04619, 0.92 ± 0.03786), implying an inverse regulatory relationship between miR-668-3p and SOCS3 ($P = 0.0076$, $P = 0.0036$; $P = 0.0038$, $P = 0.0047$, Figures 5C and D). Lower expression of SOCS3 in tumor tissues (0.5001 ± 0.02447) compared to normal tissues (0.9979 ± 0.02526) ($P < 0.0001$, Figure 5E) was also observed. Upon correlation analysis between circ_0003356 and SOCS3 expression ($P < 0.0001$, $r = 0.9364$; Figure 5F), the expression of SOCS3 was negatively associated with miR-668-3p in tumor tissues ($P < 0.0001$, $r = -0.8438$; Figure 5G).

Circ_0003356 inhibits malignant behavior of GC cells via sponging miR-668-3p to target SOCS3

SOCS3 was silenced *via* transfection of si-SOCS3 and its reduced expression confirmed in AGS (0.7267 ± 0.05044) and HGC-27 cells (0.5933 ± 0.05207) ($P = 0.0086$, $P = 0.0065$, Figure 6A). miR-668-3p overexpression (0.6467 ± 0.06394, 0.6633 ± 0.04322) or SOCS3 downregulation (0.6433 ± 0.06394, 0.6267 ± 0.04527) reversed the promoting effect of circ_0003356 on SOCS3 expression level in AGS and HGC-27 cells ($P = 0.0012$, $P = 0.0032$, $P = 0.0030$, $P = 0.0022$, $P = 0.0031$, $P = 0.0031$, Figure 6B). The viability and proliferative capacity of AGS and HGC-27 cells were attenuated by circ_0003356 overexpression, whilst miR-668-3p upregulation or SOCS3 downregulation recovered the circ_0003356-mediated decrease in cell viability and proliferative capacity ($P = 0.00039$, $P = 0.0025$, $P = 0.0037$, $P = 0.00042$, $P = 0.0035$, $P = 0.0051$; $P < 0.0001$, $P = 0.0002$, $P < 0.0001$, $P < 0.0001$, $P = 0.0044$, $P = 0.0012$; Figures 6C and D). The effects of circ_0003356 on the apoptotic rates of AGS and HGC-27 cells were similarly reversed by miR-668-3p upregulation or SOCS3 downregulation ($P < 0.0001$, Figure 6E). When it came to circ_0003356-mediated inhibition of migration, invasion, and EMT, miR-668-3p up-regulation or SOCS3 down-regulation could partially eliminate them ($P < 0.0001$, $P = 0.0017$, $P = 0.0007$, $P < 0.0001$, $P = 0.0039$, $P = 0.0011$; $P < 0.0001$, $P = 0.0009$, $P = 0.0004$, $P < 0.0001$, $P = 0.0006$, $P = 0.0003$; $P = 0.0028$, $P = 0.010$, $P = 0.0164$, $P = 0.0029$, $P = 0.023$, $P = 0.0278$; $P = 0.00314$, $P = 0.0213$, $P = 0.0144$, $P = 0.00285$, $P = 0.0267$, $P = 0.00914$; Figures 6F-H).

Circ_0003356 impedes GC tumorigenesis in vivo

A xenograft mouse model was constructed to confirm the anti-tumor role of circ_0003356 in GC. As depicted in Figures 7A-C, tumor size, volume (110 ± 5.859, $P = 0.0001$), and weight (0.2833 ± 0.03528, $P = 0.0007$) were reduced when circ_0003356 was overexpressed. Decreased expressions of Ki67 (proliferative marker protein) and N-cadherin were observed following circ_0003356 overexpression, while SOCS3 and E-cadherin expression increased, suggestive of inhibitory effects on cell proliferation and EMT (Figure 7D). TUNEL staining indicated that circ_0003356 upregulation increased apoptosis in tumor tissues of mice (Figure 7E). Circ_0003356 expression was found to be boosted (2.423 ± 0.09135) and expression of miR-668-3p (0.5 ± 0.06531) was diminished after circ_0003356 was overexpressed in mouse tumor tissues ($P = 0.000099$, $P = 0.0016$, Figure 7F).

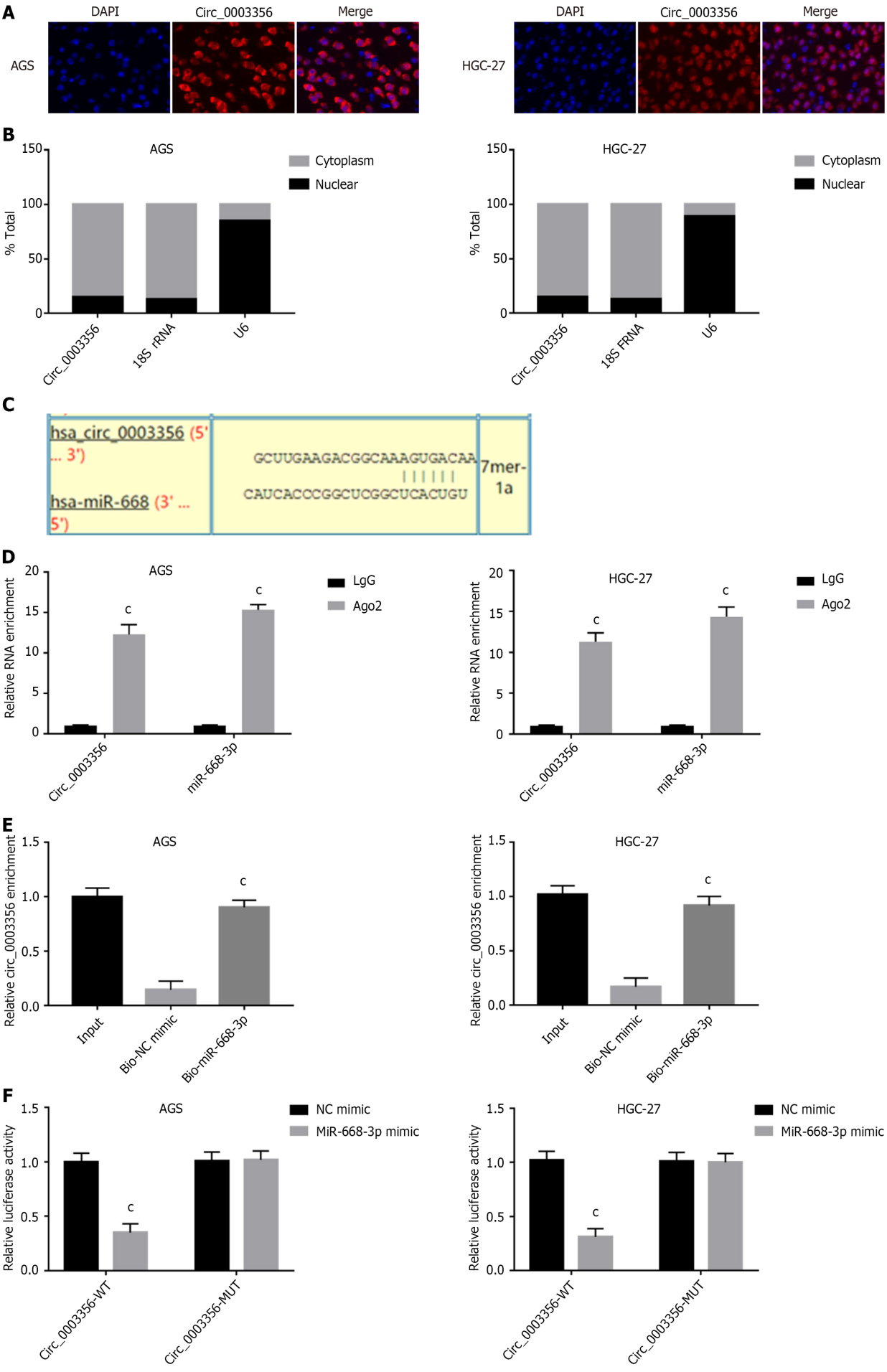
A
DAPI
Circ_0003356
Merge
AGS
HGC-27
B
AGS
HGC-27
Cytoplasm
Nuclear
% Total
Circ_0003356
18S rRNA
18S FRNA
U6
C
hsa_circ_0003356 (5' ... 3')
hsa-miR-668 (3' ... 5')
GCUUGAAGACGGCAAAGUGACAA
CAUCACCCGGCUCGGCUCACUGU
7mer-1a
D
AGS
HGC-27
LgG
Ago2
Relative RNA enrichment
Circ_0003356
miR-668-3p
E
AGS
HGC-27
Relative circ_0003356 enrichment
Input
Bio-NC mimic
Bio-miR-668-3p
F
AGS
HGC-27
NC mimic
MiR-668-3p mimic
Relative luciferase activity
Circ_0003356-WT
Circ_0003356-MUT

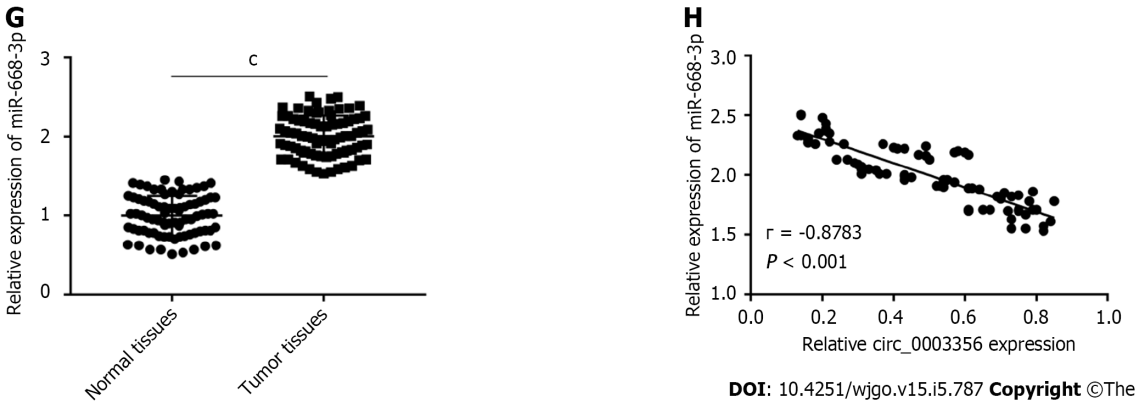

DOI: 10.4251/wjgo.v15.i5.787

Figure 3 Circ_0003356 directly binds to miR-668-3p. A: Fluorescence *in situ* hybridization assays were used to detect the sub-cellular localization of circ_0003356 in AGS and HGC-27 cells; B: Quantitative real-time polymerase chain reaction (qRT-PCR) was used to detect the expression of circ_0003356 in the nucleus and cytoplasm; C: Binding sequences between circ_0003356 and miR-668-3p predicted by circinteractome; D: Interaction between circ_0003356 and miR-668-3p in AGS and HGC-27 cells validated by RIP-qRT-PCR; E: interaction between circ_0003356 and miR-668-3p in AGS and HGC-27 cells validated by RNA pull-down assays; F: Interaction between circ_0003356 and miR-668-3p in AGS and HGC-27 cells validated by dual-luciferase reporter assays; G: Relative expression of miR-668-3p detected by qRT-PCR in tumor tissues and normal tissues; H: Correlation between circ_0003356 and miR-668-3p in gastric cancer tissues analyzed by Pearson's correlation analysis. $^{c}P < 0.001$.

DISCUSSION

Due to a lack of effective treatment strategies and prognostic indicators, GC remains a threat to human health[29,30]. Emerging evidence has implicated circRNAs during GC development[31,32]. Thence, great efforts should be made to comprehensively understand circRNAs. To date, many circRNAs show low expression in GC, such as circ_0021087[12], hsa_circ_0005556[33], and circPSMC3[34]. Here, we observed low expression levels of circ_0003356 in GC cells and tissues. This is the first report to show an association of circ_0003356 with GC. Moreover, increasing findings have indicated that several circRNAs act as prognostic indicators for GC, including hsa_circ_0005556[33] and circ_0000260[35]. Here, based on Kaplan-Meier analysis, patients with low circ_0003356 had poor survival rates.

Accumulating data reveal that circRNAs have an anti-tumor function in GC. For instance, circ_0021087 overexpression suppresses the proliferation, migration, invasion, and EMT of GC cells and impairs tumorigenesis in xenograft mice[12]. CircPSMC3 up-regulation prevents GC cells from migrating, proliferating, and invading, thereby suppressing tumorigenesis in xenograft mice[36]. Similarly, we found that circ_0003356 overexpression repressed proliferation, migration, invasion, and EMT of GC cells and enhanced GC cell apoptosis. *In vivo*, circ_0003356 overexpression suppressed tumorigenesis. These results suggest an anti-tumor role for circ_0003356's in GC, highlighting its potential in the clinical management of GC.

To our knowledge, circRNAs affect gene expression *via* sponging downstream miRNAs in cancer cell [37,38]. Inspired by this, we predicted downstream miRNAs of circ_0003356 using circinteractome. MiR-668-3p was identified as one such target. We performed RIP-qRT-PCR, RNA pull-downs, and DLR assays to verify our prediction. In previous reports, miR-668-3p has shown high expression and carcinogenesis in HCC and CRC[18,19]. Consistent with these studies, we discovered high miR-668-3p expression in GC tissues and cells. The down-regulation of miR-668-3p enhanced cell apoptosis and impaired the proliferation, migration, invasion, and EMT of cells (AGS and HGC-27). These outcomes suggest that miR-668-3p is oncogenic in GC. Several cirRNAs, including circ_0014717 and circTMEM59, target miR-668-3p to suppress tumor development[18,19]. Here, an inverse relationship was observed between miR-668-3p and circ_0003356 expression in tumor tissues of GC patients. MiR-668-3p was negatively regulated by circ_0003356 in mouse tumor tissues. In particular, the inhibitory influence of circ_0003356 on the proliferation, migration, invasion. EMT of GC cells were reversed by miR-3619-5p overexpression. We deduced that circ_0003356 prevents GC malignancy through sponging miR-668-3p.

It is acknowledged that the miRNA-circRNA-mRNA network is closely related to the regulation of GC progression[39]. We therefore predicted target genes of miR-668-3p and found that SOCS3 was targeted by miR-668-3p. SOCS3 has been shown to display low expression in GC tissues and to participate in tumor suppression in GC[24,40]. In this study, we observed that the downregulation of SOCS3 expression in GC tissues was regulated by miR-668-3p. An inverse correlation between SOCS3 and miR-668-3p expression levels in tumor tissues of GC patients was observed. Thus, we deduced that miR-668-3p acts as a tumor promoter, targeting SOCS3 in GC. Additionally, we identified a positive relationship between SOCS3 and circ_0003356 and found that the suppressive effects of circ_0003356 on cell proliferation, migration, invasion, and EMT were reversed by SOCS3 upregulation in GC cells. These findings strongly support the notion that circ_0003356 has an anti-tumor role through sponging miR-668-3p to target SOCS3 in GC.

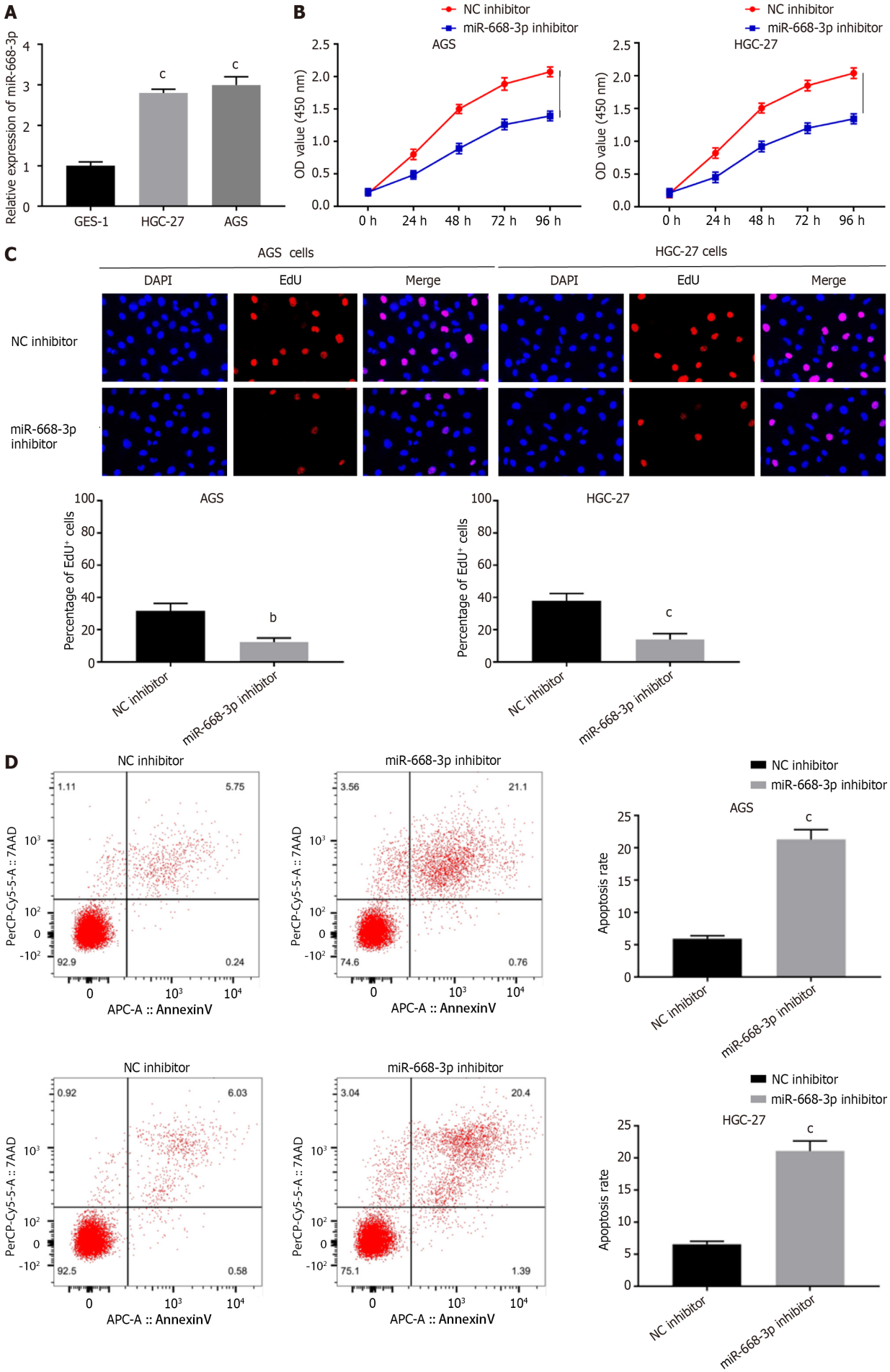
A
Relative expression of miR-668-3p
GES-1
HGC-27
AGS
B
NC inhibitor
miR-668-3p inhibitor
AGS
HGC-27
OD value (450 nm)
0 h
24 h
48 h
72 h
96 h
C
AGS cells
HGC-27 cells
DAPI
EdU
Merge
NC inhibitor
miR-668-3p inhibitor
Percentage of EdU+ cells
D
NC inhibitor
miR-668-3p inhibitor
PerCP-Cy5-5-A :: 7AAD
APC-A :: AnnexinV
Apoptosis rate

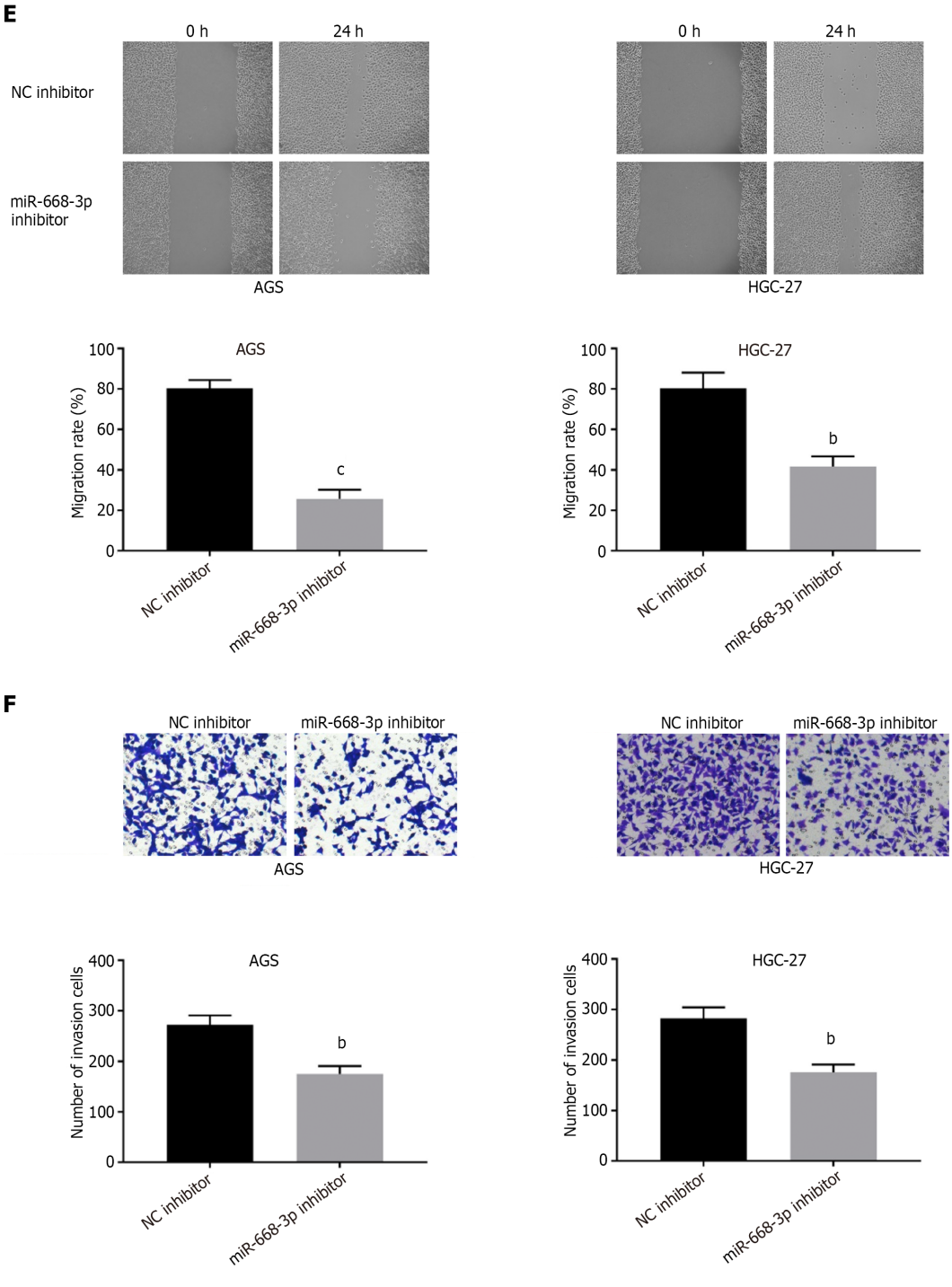
E
0 h
24 h
NC inhibitor
miR-668-3p inhibitor
AGS
HGC-27
Migration rate (%)
c
b
F
Number of invasion cells
G
E-cadherin
N-cadherin
β-actin

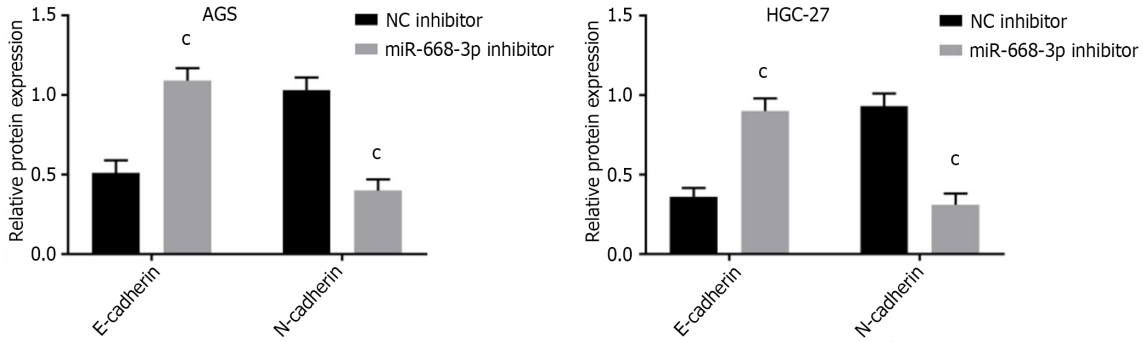

DOI: 10.4251/wjgo.v15.i5.787 **Copyright** ©The Author(s) 2023.

Figure 4 Suppression of miR-668-3p promotes cell apoptosis and impairs the proliferation, migration, invasion, and epithelial-mesenchymal transition of AGS and HGC-27 cells. A: Relative expression of miR-668-3p in GES-1, AGS, and HGC-27 cells detected by quantitative real-time polymerase chain reaction (qRT-PCR); B: Cell viability in AGS and HGC-27 cells assessed by CCK-8 assay; C: Proliferation of AGS and HGC-27 cells assessed by EdU assays; D: Apoptosis of AGS and HGC-27 cells assessed by flow cytometry; E: Relative migration of AGS and HGC-27 cells detected by wound healing assays; F: Invasion of AGS and HGC-27 cells detected by transwell assays; G: Levels of epithelial-mesenchymal transition-related proteins (E-cadherin and N-cadherin) in AGS and HGC-27 cells determined using western blotting. $^{b}P < 0.01$, $^{c}P < 0.001$.

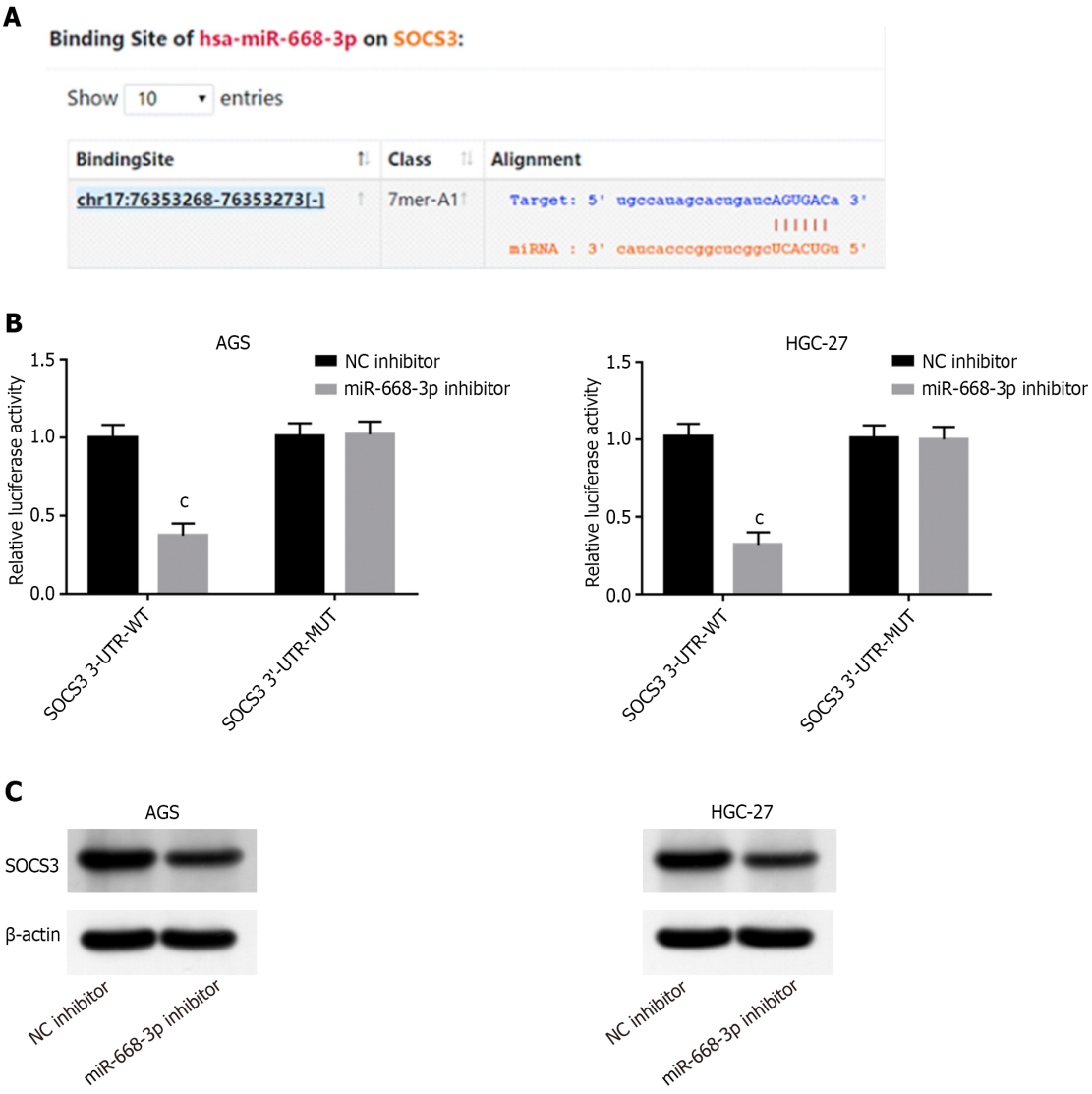

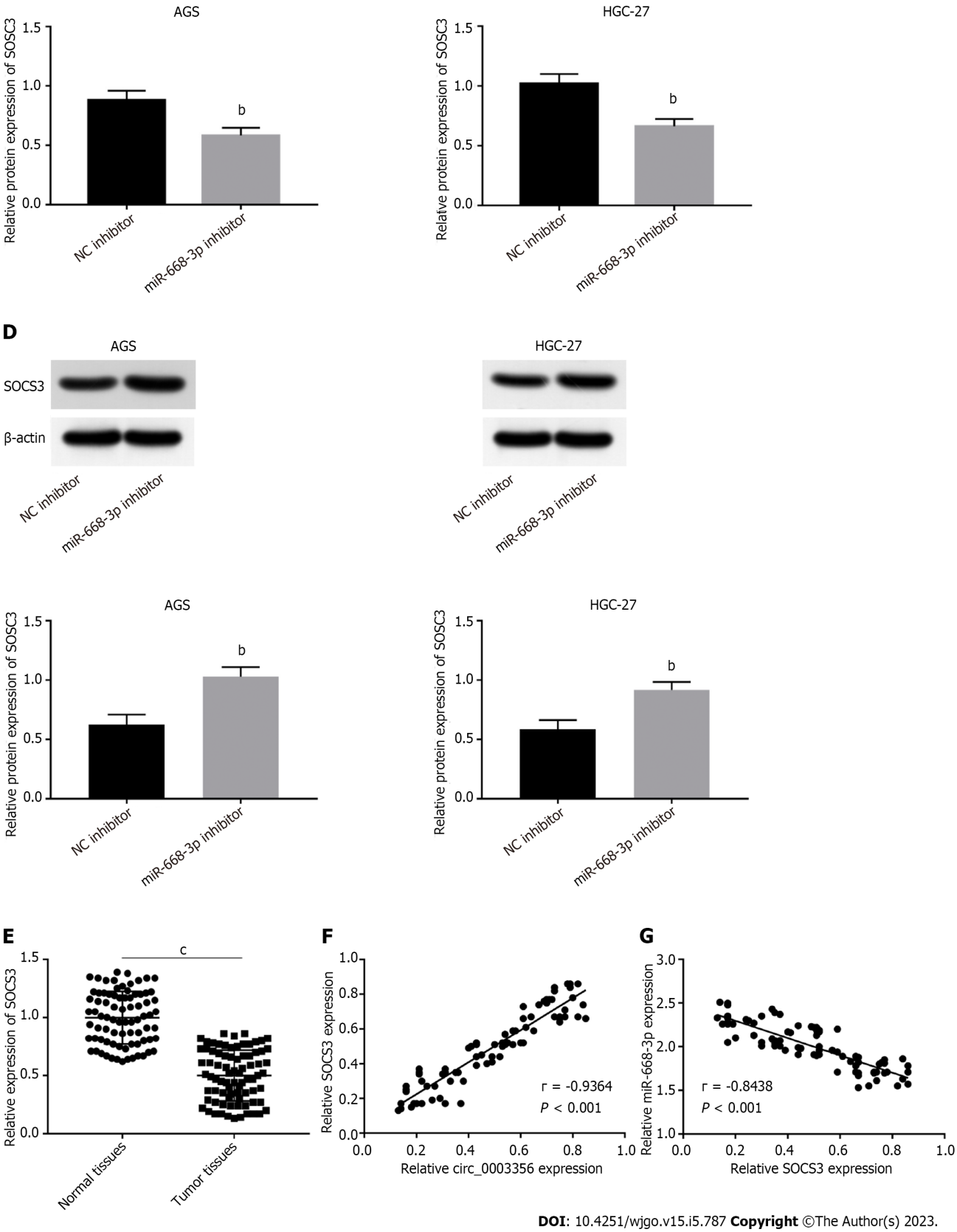

DOI: 10.4251/wjgo.v15.i5.787 **Copyright** ©The Author(s) 2023.

Figure 5 SOCS3 is targeted by miR-668-3p. A: Binding sites between SOCS3 and miR-668-3p were predicted by Starbase v2.0 software; B: Dual-luciferase reporter assays were used to confirm the targeting relationship between SOCS3 and miR-668-3p in AGS and HGC-27 cells; C: Relative expression of SOCS3 in AGS and HGC-27 cells detected by western blotting following miR-668-3p overexpression; D: Relative protein expression of SOCS3 in AGS and HGC-27 cells detected by western blotting after miR-668-3p inhibition; E: Relative mRNA expression of SOCS3 was detected by quantitative real-time polymerase chain reaction in tumor tissues and normal tissues; F: Correlation between circ_0003356 and SOCS3 in gastric cancer (GC) tissues analyzed by Pearson's correlation analysis; G: Correlation between miR-668-3p and SOCS3 in GC tissues analyzed by Pearson's correlation analysis. $^{b}P < 0.01$, $^{c}P < 0.001$.

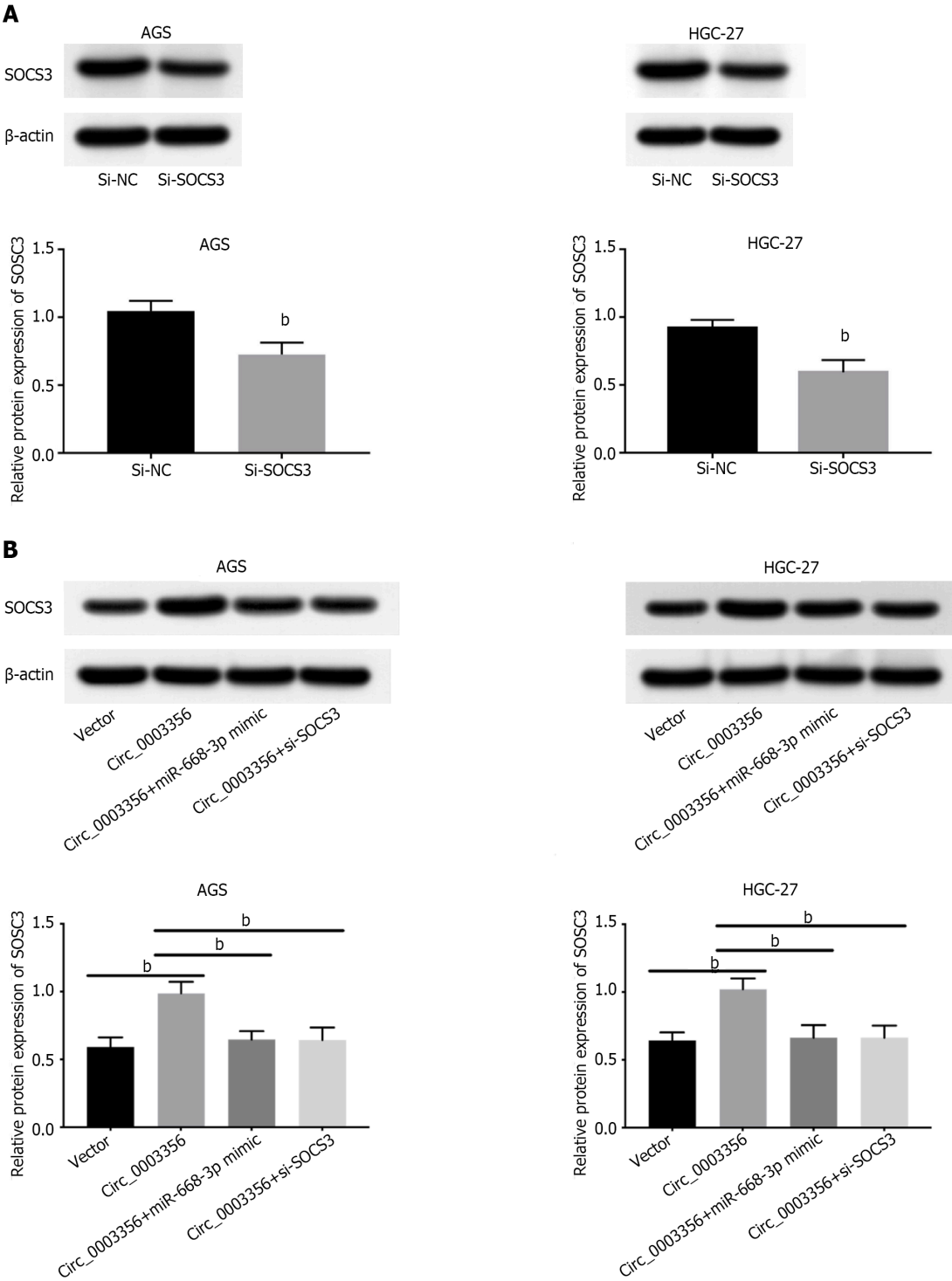
A
AGS
SOCS3
β-actin
Si-NC
Si-SOCS3
HGC-27
Relative protein expression of SOSC3
b
B
Vector
Circ_0003356
Circ_0003356+miR-668-3p mimic
Circ_0003356+si-SOCS3
C
OD value (450 nm)
0 h
24 h
48 h
72 h
96 h
c

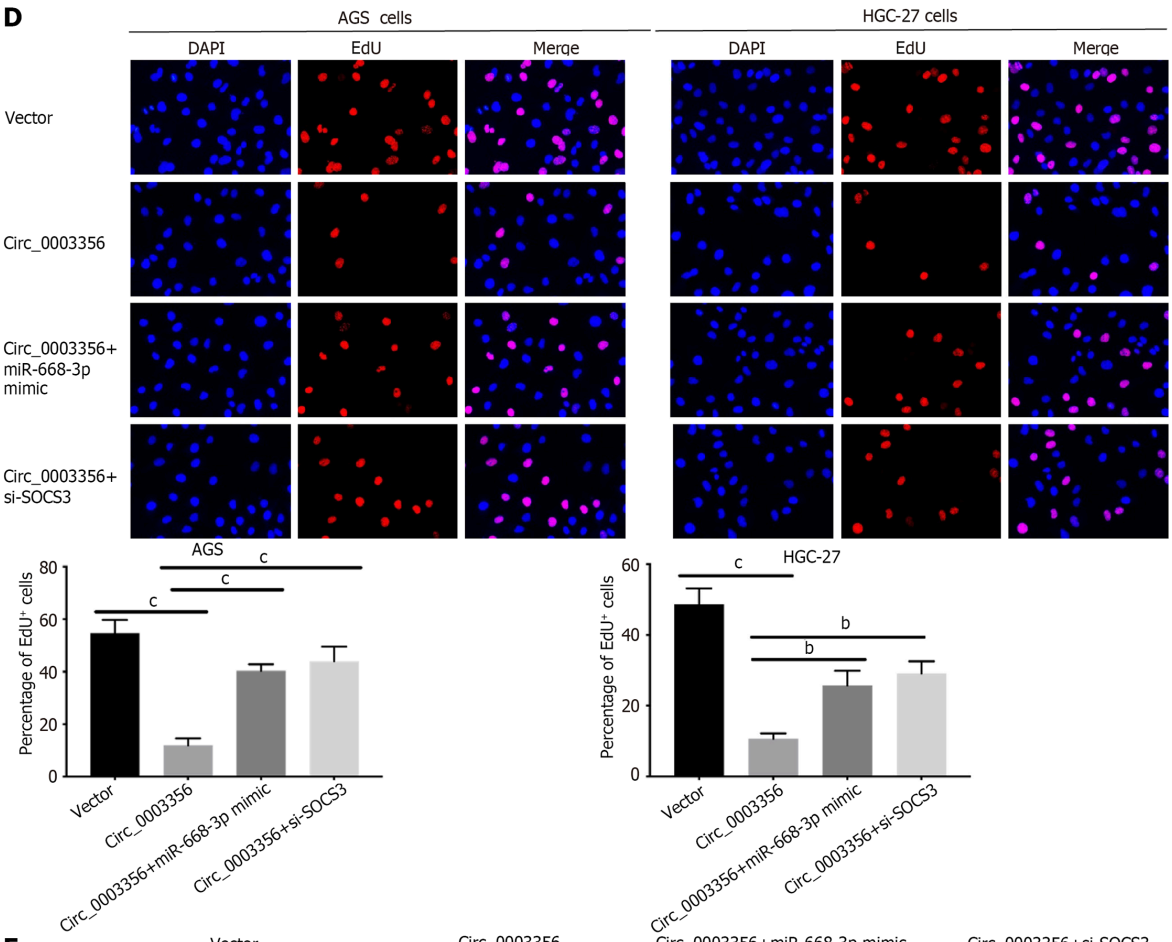
D
AGS cells
HGC-27 cells
DAPI
EdU
Merge
Vector
Circ_0003356
Circ_0003356+ miR-668-3p mimic
Circ_0003356+ si-SOCS3
AGS
HGC-27
Percentage of EdU+ cells
Vector
Circ_0003356
Circ_0003356+miR-668-3p mimic
Circ_0003356+si-SOCS3

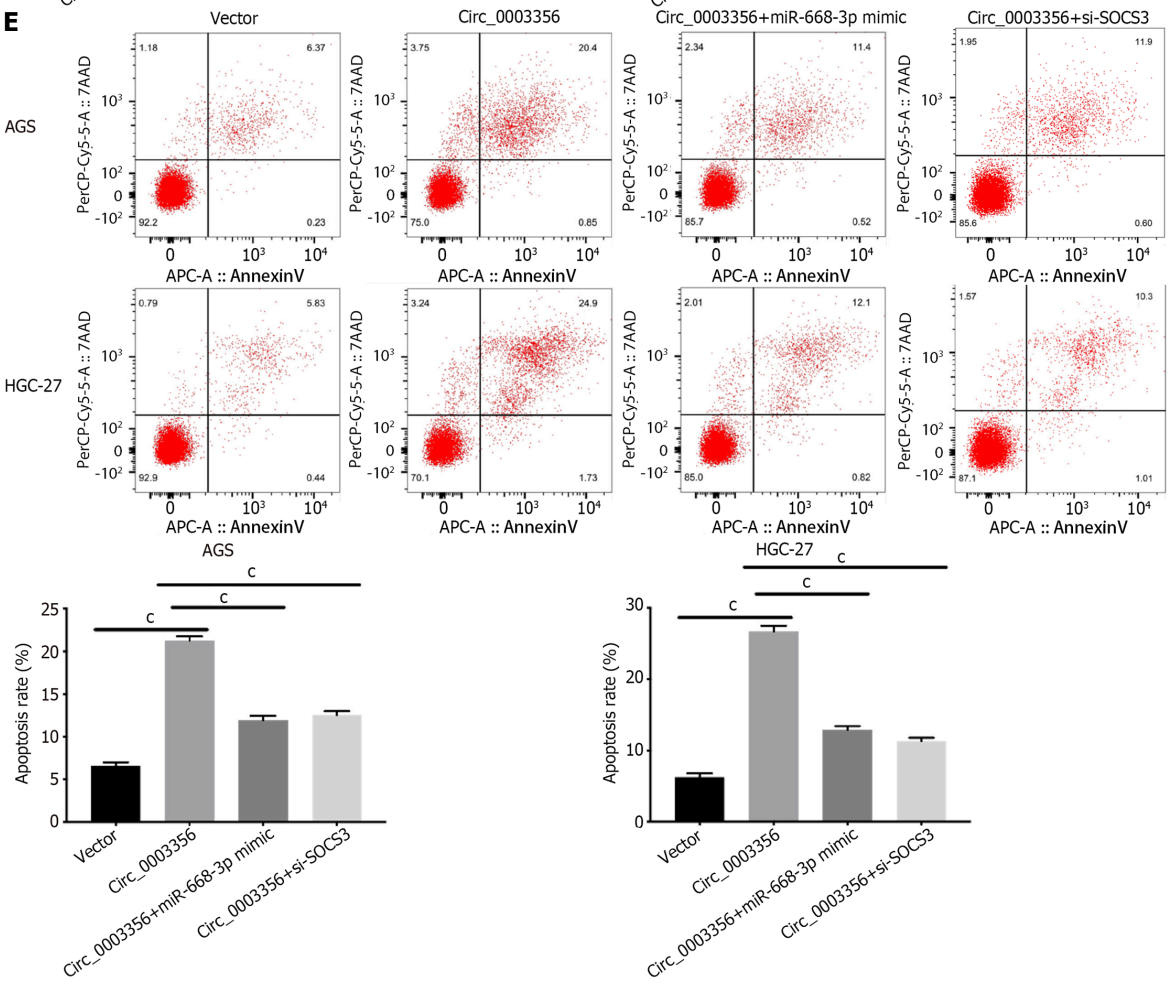
E
Vector
Circ_0003356
Circ_0003356+miR-668-3p mimic
Circ_0003356+si-SOCS3
AGS
HGC-27
PerCP-Cy5-5-A :: 7AAD
APC-A :: AnnexinV
Apoptosis rate (%)

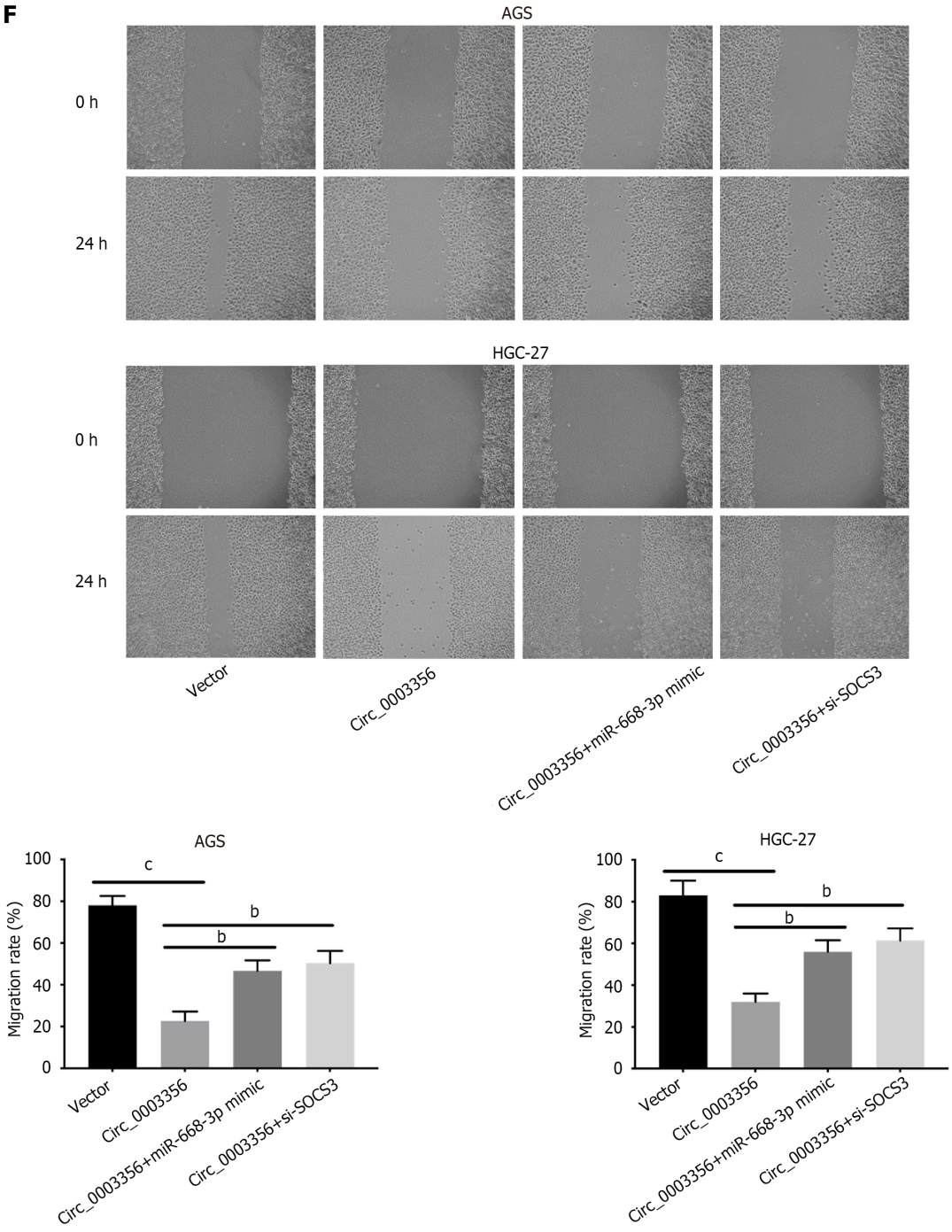
F
AGS
0 h
24 h
HGC-27
0 h
24 h
Vector
Circ_0003356
Circ_0003356+miR-668-3p mimic
Circ_0003356+si-SOCS3
AGS
Migration rate (%)
100
80
60
40
20
0
c
b
b
Vector
Circ_0003356
Circ_0003356+miR-668-3p mimic
Circ_0003356+si-SOCS3
HGC-27
Migration rate (%)
100
80
60
40
20
0
c
b
b
Vector
Circ_0003356
Circ_0003356+miR-668-3p mimic
Circ_0003356+si-SOCS3

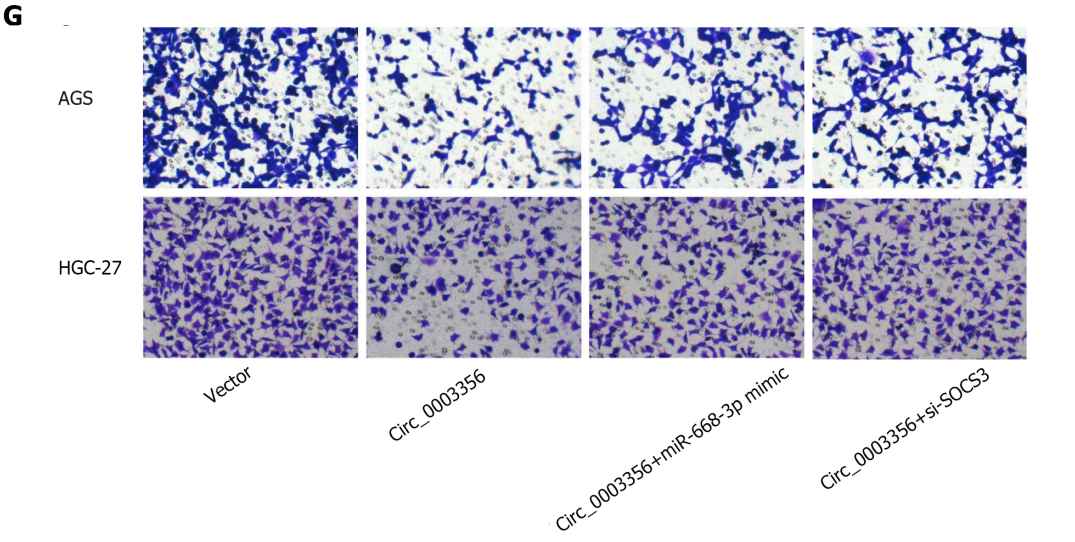
G
AGS
HGC-27
Vector
Circ_0003356
Circ_0003356+miR-668-3p mimic
Circ_0003356+si-SOCS3

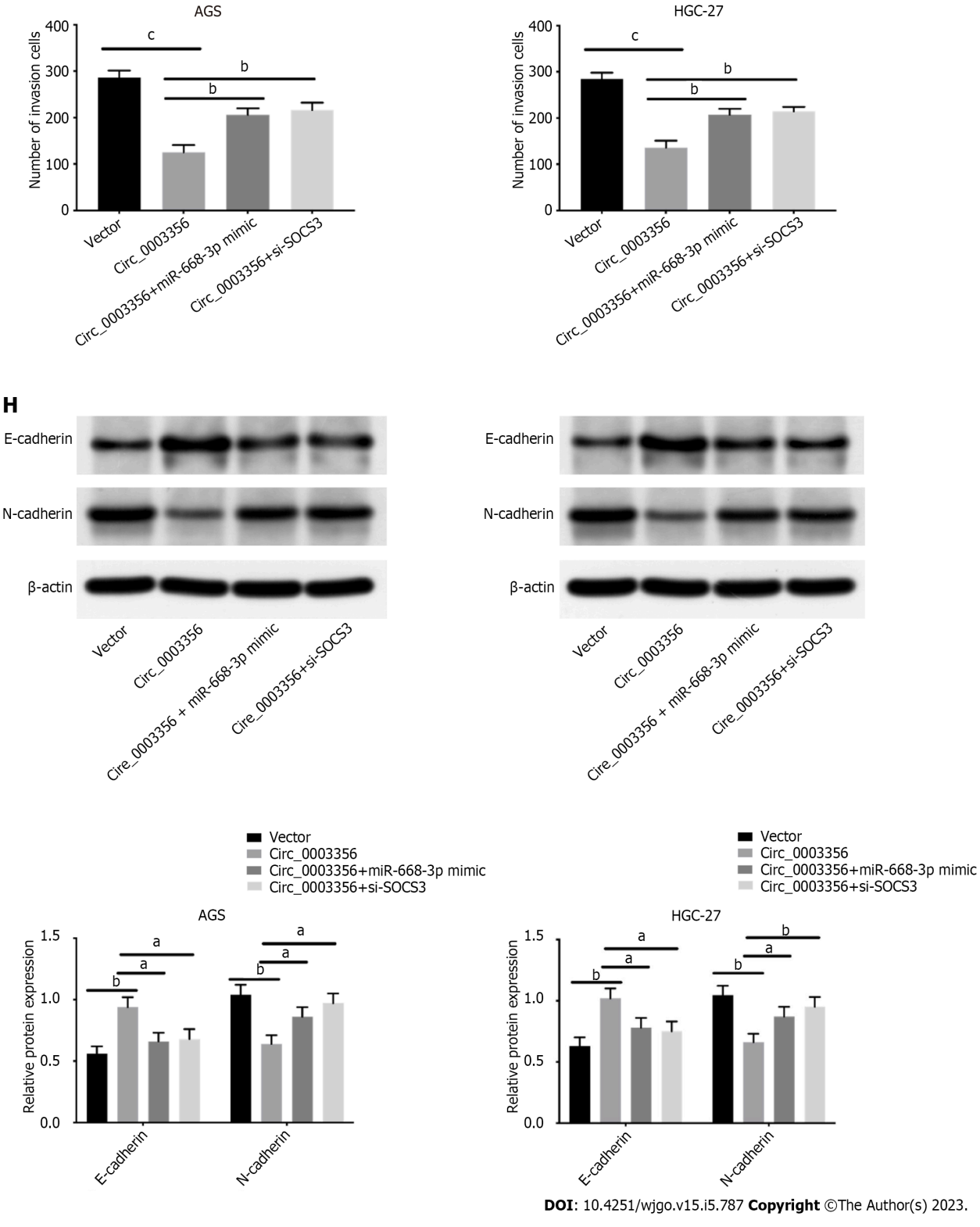

DOI: 10.4251/wjgo.v15.i5.787

Figure 6 Circ_0003356 overexpression suppresses the malignant behavior of gastric cancer cells *via* sponging miR-668-3p to target SOCS3. A and B: Protein expression of SOCS3 in AGS and HGC-27 cells detected by western blot; C: Cell viability in AGS and HGC-27 cells detected by CCK-8 assay; D: Proliferation of AGS and HGC-27 cells assessed by EdU assay; E: Apoptosis of AGS and HGC-27 cells assessed by flow cytometry; F: Relative migration of AGS and HGC-27 cells detected by wound healing assay; G: Relative invasion of AGS and HGC-27 cells detected by transwell assay; H: Levels of epithelial-mesenchymal transition-related proteins (E-cadherin and N-cadherin) in AGS and HGC-27 cells determined by western blotting. $^{a}P < 0.05$, $^{b}P < 0.01$, $^{c}P < 0.001$.

CONCLUSION

In summary, we show that circ_0003356 expression is low in GC tissues and cells and positively related to GC patient prognosis. Circ_0003356 up-regulation or miR-668-3p inhibition facilitated cell apoptosis and suppressed proliferation, migration, invasion and EMT in cells (AGS and HGC-27). Circ_0003356

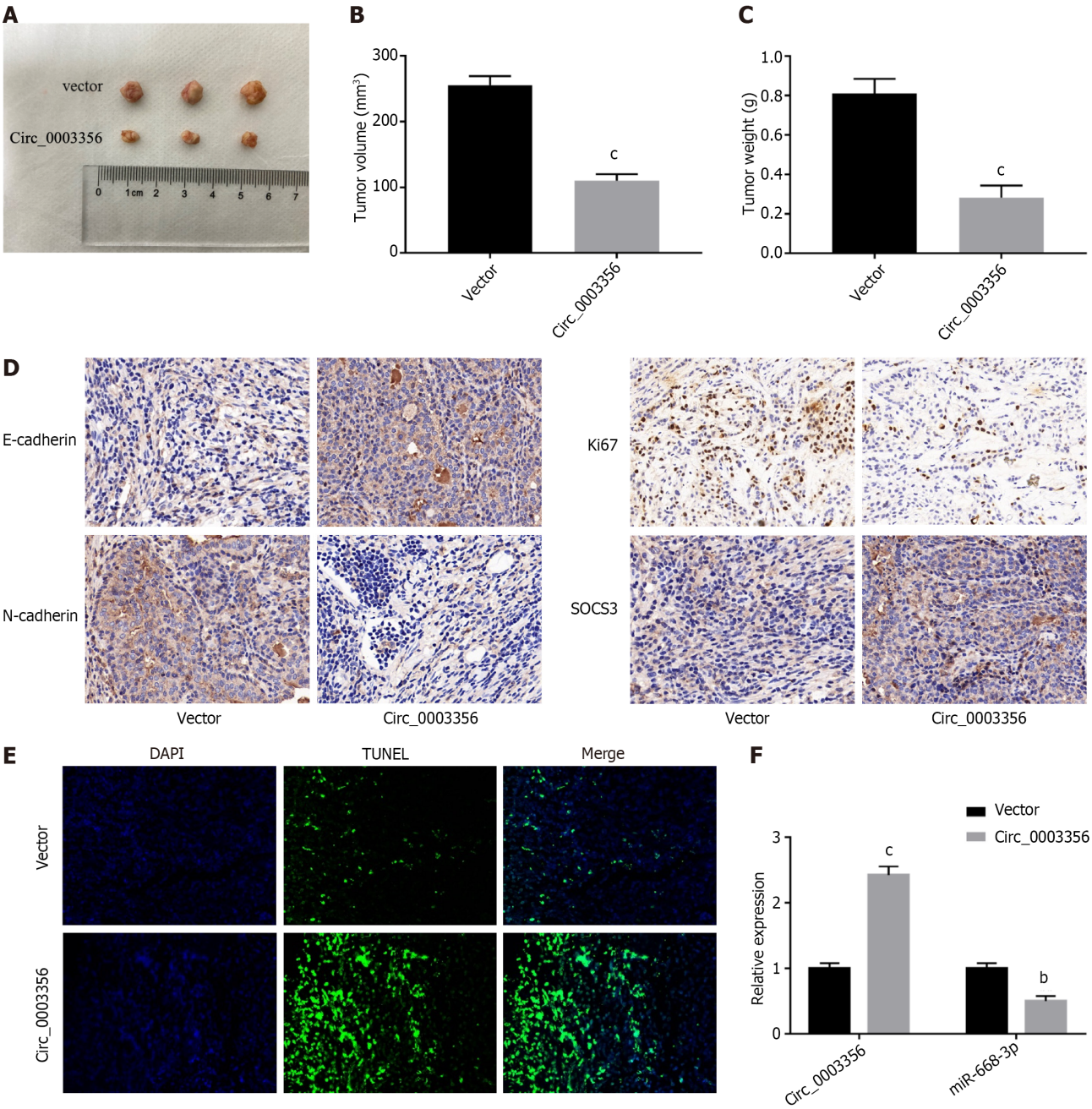

DOI: 10.4251/wjgo.v15.i5.787 **Copyright** ©The Author(s) 2023.

Figure 7 Circ_0003356 upregulation impedes gastric cancer tumorigenesis *in vivo*. A: Representative images of tumor in xenograft mice; B: Average volumes of xenograft mice; C: Average tumor weights of xenograft mice; D: Expression of E-cadherin, N-cadherin, Ki67, and SOCS3 in tumor tissues of xenograft mice determined by immunohistochemical staining; E: TUNEL staining to detect cell apoptosis in tumor tissues of mice; F: Expression of circ_0003356 and miR-668-3p determined by quantitative real-time polymerase chain reaction in tumor tissues of mice. $^{b}P < 0.01$, $^{c}P < 0.001$.

overexpression also prevented tumor growth in mice. Mechanistically, circ_0003356 was found to interact with the miR-668-3p/SOCS3 axis to impair GC development. Overall, this investigation provides a new perspective on the therapeutic targets of GC.

ARTICLE HIGHLIGHTS

Research background

Gastric cancer (GC) is a common malignant tumor with high prevalence and mortality. Circular RNA (circRNA) analysis in GSE184882 has indicated that circ_0003356 shows abnormal expression in GC tissues, but the function of circ_0003356 remains unclear in GC.

Research motivation
To seek the prognostic biomarker and therapeutic target for GC.

Research objectives
In order to explore the function and mechanism of circ_0003356 in GC.

Research methods
Quantitative real-time polymerase chain reaction was used to detect expression of circ_0003356. The clinical value of circ_0003356 for GC prognosis was evaluated. The role of circ_0003356 in GC was assessed *via in vitro* and *in vivo* experiments. The molecular mechanism of circ_0003356 on miR-668-3p/SOCS3 axis was validated.

Research results
Circ_0003356 expression was markedly decreased in GC tissues and cells, and it was positively associated with survival time of GC patients. Moreover, functional analyses showed that circ_0003356 overexpression inhibited malignant behaviors of GC cells *via* targeting the miR-668-3p/SOCS3 axis.

Research conclusions
Circ_0003356 is lowly expressed in GC tissues and cells, displaying potential as a prognostic biomarker for GC. Circ_0003356 up-regulation represses the malignancy of GC *via* targeting the miR-668-3p/SOCS3 axis.

Research perspectives
Other mechanisms of circ_0003356 in GC may be probed in future researches, and its application in treatment of GC will be extended.

FOOTNOTES

Author contributions: Li WD, Wang HT, and Wang Y designed the study; Huang YM, Cheng BH, Xiang LJ, and Zhou XH collected the data; Deng QY, Guo ZG, Yang ZF, Guan ZF, and Wang Y analyzed the data; Li WD and Wang HT wrote the manuscript; and all authors approved the final manuscript.

Supported by Zhongshan Social Public Welfare and Basic Research Project, No. 200421093453685.

Institutional review board statement: The Ethics Committee of Zhongshan City People's Hospital gave the approval (K2017-182).

Institutional animal care and use committee statement: All experiments were approved by the Animal Care and Use Committee of Zhongshan City People's Hospital (K2017-182).

Informed consent statement: All participants have also agreed to this investigation by offering their written consent.

Conflict-of-interest statement: All the authors report no relevant conflicts of interest for this article.

Data sharing statement: All the data used to support the findings of this study are included within the article.

ARRIVE guidelines statement: The authors have read the ARRIVE guidelines, and the manuscript was prepared and revised according to the ARRIVE guidelines.

Country/Territory of origin: China

ORCID number: Wei-Dong Li 0000-0001-5924-7989; Yao Wang 0000-0003-2777-0796.

S-Editor: Wang JJ
L-Editor: A
P-Editor: Zhang XD

REFERENCES

1 **Curea FG**, Hebbar M, Ilie SM, Bacinschi XE, Trifanescu OG, Botnariuc I, Anghel RM. Current Targeted Therapies in HER2-Positive Gastric Adenocarcinoma. *Cancer Biother Radiopharm* 2017; **32**: 351-363 [PMID: 29265917 DOI: 10.1089/cbr.2017.2249]

2 **Smyth EC**, Nilsson M, Grabsch HI, van Grieken NC, Lordick F. Gastric cancer. *Lancet* 2020; **396**: 635-648 [PMID: 32861308 DOI: 10.1016/S0140-6736(20)31288-5]

3 **Amiri M**, Janssen F, Kunst AE. The decline in stomach cancer mortality: exploration of future trends in seven European countries. *Eur J Epidemiol* 2011; **26**: 23-28 [PMID: 21086022 DOI: 10.1007/s10654-010-9522-9]

4 **Ruiz EF**, Torres-Roman JS, Servan SA, Martinez-Herrera JF, Arce-Huamani MA, Carioli G, La Vecchia C. Trends and geographic pattern of stomach cancer mortality in Peru. *Cancer Epidemiol* 2019; **58**: 193-198 [PMID: 30522779 DOI: 10.1016/j.canep.2018.10.018]

5 **Sexton RE**, Al Hallak MN, Diab M, Azmi AS. Gastric cancer: a comprehensive review of current and future treatment strategies. *Cancer Metastasis Rev* 2020; **39**: 1179-1203 [PMID: 32894370 DOI: 10.1007/s10555-020-09925-3]

6 **Hoshi H**. Management of Gastric Adenocarcinoma for General Surgeons. *Surg Clin North Am* 2020; **100**: 523-534 [PMID: 32402298 DOI: 10.1016/j.suc.2020.02.004]

7 **Allemani C**, Weir HK, Carreira H, Harewood R, Spika D, Wang XS, Bannon F, Ahn JV, Johnson CJ, Bonaventure A, Marcos-Gragera R, Stiller C, Azevedo e Silva G, Chen WQ, Ogunbiyi OJ, Rachet B, Soeberg MJ, You H, Matsuda T, Bielska-Lasota M, Storm H, Tucker TC, Coleman MP; CONCORD Working Group. Global surveillance of cancer survival 1995-2009: analysis of individual data for 25,676,887 patients from 279 population-based registries in 67 countries (CONCORD-2). *Lancet* 2015; **385**: 977-1010 [PMID: 25467588 DOI: 10.1016/S0140-6736(14)62038-9]

8 **Ang TL**, Fock KM. Clinical epidemiology of gastric cancer. *Singapore Med J* 2014; **55**: 621-628 [PMID: 25630323 DOI: 10.11622/smedj.2014174]

9 **Fontana E**, Smyth EC. Novel targets in the treatment of advanced gastric cancer: a perspective review. *Ther Adv Med Oncol* 2016; **8**: 113-125 [PMID: 26929787 DOI: 10.1177/1758834015616935]

10 **Wang C**, Jiang H, Peng J, Weng D, Zhang Y, Zhou Y, Zhang Q. Circular RNA circ_SKA3 enhances gastric cancer development by targeting miR-520h. *Histol Histopathol* 2023; **38**: 317-328 [PMID: 36134741 DOI: 10.14670/HH-18-521]

11 **Li P**, Xiao W. Circ_0005758 impedes gastric cancer progression through miR-1229-3p/GCNT4 feedback loop. *Toxicol In Vitro* 2022; **85**: 105454 [PMID: 35970245 DOI: 10.1016/j.tiv.2022.105454]

12 **Yu Y**, Li H, Wu C, Li J. Circ_0021087 acts as a miR-184 sponge and represses gastric cancer progression by adsorbing miR-184 and elevating FOSB expression. *Eur J Clin Invest* 2021; **51**: e13605 [PMID: 34076278 DOI: 10.1111/eci.13605]

13 **Saliminejad K**, Khorram Khorshid HR, Soleymani Fard S, Ghaffari SH. An overview of microRNAs: Biology, functions, therapeutics, and analysis methods. *J Cell Physiol* 2019; **234**: 5451-5465 [PMID: 30471116 DOI: 10.1002/jcp.27486]

14 **Bartel DP**. Metazoan MicroRNAs. *Cell* 2018; **173**: 20-51 [PMID: 29570994 DOI: 10.1016/j.cell.2018.03.006]

15 **Chen G**, Shang J, Li M, Zhang H, Xu H. miR-548 predicts clinical prognosis and functions as a tumor promoter in gastric cancer. *Clin Exp Med* 2022 [PMID: 35976514 DOI: 10.1007/s10238-022-00870-9]

16 **Yu K**, Zhu H. MiR-762 regulates the activation of PI3K/AKT and Hippo pathways involved in the development of gastric cancer by targeting LZTS1. *Am J Transl Res* 2022; **14**: 5050-5058 [PMID: 35958482]

17 **Bae WJ**, Woo KJ, Ahn JM, Yang CM, Kim YS, Kim S, Lee D. miR-4742-5p promotes invasiveness of gastric cancer *via* targeting Rab43: An in vitro study. *Biochem Biophys Res Commun* 2022; **613**: 180-186 [PMID: 35597125 DOI: 10.1016/j.bbrc.2022.05.044]

18 **Ma H**, Huang C, Huang Q, Li G, Li J, Huang B, Zhong Q, Cao C. Circular RNA circ_0014717 Suppresses Hepatocellular Carcinoma Tumorigenesis Through Regulating miR-668-3p/BTG2 Axis. *Front Oncol* 2020; **10**: 592884 [PMID: 33598424 DOI: 10.3389/fonc.2020.592884]

19 **Feng Y**, Wang X, Huang C, Zhang D, Liu T, Zhang C, Zhang Y, Ji D, Tang J, Sun Y. Upregulated circTMEM59 Inhibits Cell Growth and Metastasis by miR-668-3p/ID4 Axis in Colorectal Cancer. *Oxid Med Cell Longev* 2022; **2022**: 7242124 [PMID: 35656024 DOI: 10.1155/2022/7242124]

20 **Gao Y**, Zhao H, Wang P, Wang J, Zou L. The roles of SOCS3 and STAT3 in bacterial infection and inflammatory diseases. *Scand J Immunol* 2018; **88**: e12727 [PMID: 30341772 DOI: 10.1111/sji.12727]

21 **Qin H**, Holdbrooks AT, Liu Y, Reynolds SL, Yanagisawa LL, Benveniste EN. SOCS3 deficiency promotes M1 macrophage polarization and inflammation. *J Immunol* 2012; **189**: 3439-3448 [PMID: 22925925 DOI: 10.4049/jimmunol.1201168]

22 **Yu C**, Fan Y, Zhang Y, Liu L, Guo G. LINC00893 inhibits the progression of prostate cancer through miR-3173-5p/SOCS3/JAK2/STAT3 pathway. *Cancer Cell Int* 2022; **22**: 228 [PMID: 35818076 DOI: 10.1186/s12935-022-02637-4]

23 **Li L**, Zhang J, Peng H, Jiang X, Liu Z, Tian H, Hou S, Xie X, Peng Q, Zhou T. Knockdown of miR-92a suppresses the stemness of colorectal cancer cells *via* mediating SOCS3. *Bioengineered* 2022; **13**: 5613-5624 [PMID: 35184640 DOI: 10.1080/21655979.2021.2022267]

24 **Xiao C**, Hong H, Yu H, Yuan J, Guo C, Cao H, Li W. MiR-340 affects gastric cancer cell proliferation, cycle, and apoptosis through regulating SOCS3/JAK-STAT signaling pathway. *Immunopharmacol Immunotoxicol* 2018; **40**: 278-283 [PMID: 29658372 DOI: 10.1080/08923973.2018.1455208]

25 **Tang H**, Long Q, Zhuang K, Yan Y, Han K, Guo H, Lu X. miR-665 promotes the progression of gastric adenocarcinoma *via* elevating FAK activation through targeting SOCS3 and is negatively regulated by lncRNA MEG3. *J Cell Physiol* 2020; **235**: 4709-4719 [PMID: 31650535 DOI: 10.1002/jcp.29349]

26 **Luo Z**, Rong Z, Zhang J, Zhu Z, Yu Z, Li T, Fu Z, Qiu Z, Huang C. Circular RNA circCCDC9 acts as a miR-6792-3p sponge to suppress the progression of gastric cancer through regulating CAV1 expression. *Mol Cancer* 2020; **19**: 86 [PMID: 32386516 DOI: 10.1186/s12943-020-01203-8]

27 **Barrett T**, Wilhite SE, Ledoux P, Evangelista C, Kim IF, Tomashevsky M, Marshall KA, Phillippy KH, Sherman PM, Holko M, Yefanov A, Lee H, Zhang N, Robertson CL, Serova N, Davis S, Soboleva A. NCBI GEO: archive for functional

genomics data sets--update. *Nucleic Acids Res* 2013; **41**: D991-D995 [PMID: 23193258 DOI: 10.1093/nar/gks1193]

28 **Song J**, Yu S, Zhong D, Yang W, Jia Z, Yuan G, Li P, Zhang R, Li Y, Zhong G, Chen Z. The circular RNA hsa_circ_000780 as a potential molecular diagnostic target for gastric cancer. *BMC Med Genomics* 2021; **14**: 282 [PMID: 34838011 DOI: 10.1186/s12920-021-01096-6]

29 **Karimi P**, Islami F, Anandasabapathy S, Freedman ND, Kamangar F. Gastric cancer: descriptive epidemiology, risk factors, screening, and prevention. *Cancer Epidemiol Biomarkers Prev* 2014; **23**: 700-713 [PMID: 24618998 DOI: 10.1158/1055-9965.EPI-13-1057]

30 **Johnston FM**, Beckman M. Updates on Management of Gastric Cancer. *Curr Oncol Rep* 2019; **21**: 67 [PMID: 31236716 DOI: 10.1007/s11912-019-0820-4]

31 **Li R**, Jiang J, Shi H, Qian H, Zhang X, Xu W. CircRNA: a rising star in gastric cancer. *Cell Mol Life Sci* 2020; **77**: 1661-1680 [PMID: 31659415 DOI: 10.1007/s00018-019-03345-5]

32 **Wei L**, Sun J, Zhang N, Zheng Y, Wang X, Lv L, Liu J, Xu Y, Shen Y, Yang M. Noncoding RNAs in gastric cancer: implications for drug resistance. *Mol Cancer* 2020; **19**: 62 [PMID: 32192494 DOI: 10.1186/s12943-020-01185-7]

33 **Yang L**, Yu Y, Yu X, Zhou J, Zhang Z, Ying S, Guo J, Yan Z. Downregulated Expression of hsa_circ_0005556 in Gastric Cancer and Its Clinical Significance. *Dis Markers* 2019; **2019**: 2624586 [PMID: 31827632 DOI: 10.1155/2019/2624586]

34 **Rong D**, Lu C, Zhang B, Fu K, Zhao S, Tang W, Cao H. CircPSMC3 suppresses the proliferation and metastasis of gastric cancer by acting as a competitive endogenous RNA through sponging miR-296-5p. *Mol Cancer* 2019; **18**: 25 [PMID: 30777076 DOI: 10.1186/s12943-019-0958-6]

35 **Liu S**, Wu M, Peng M. Circ_0000260 Regulates the Development and Deterioration of Gastric Adenocarcinoma with Cisplatin Resistance by Upregulating MMP11 *via* Targeting MiR-129-5p. *Cancer Manag Res* 2020; **12**: 10505-10519 [PMID: 33122949 DOI: 10.2147/CMAR.S272324]

36 **Rong D**, Lu C, Zhang B, Fu K, Zhao S, Tang W, Cao H. Correction to: CircPSMC3 suppresses the proliferation and metastasis of gastric cancer by acting as a competitive endogenous RNA through sponging miR-296-5p. *Mol Cancer* 2020; **19**: 140 [PMID: 32907590 DOI: 10.1186/s12943-020-01252-z]

37 **Li J**, Sun D, Pu W, Wang J, Peng Y. Circular RNAs in Cancer: Biogenesis, Function, and Clinical Significance. *Trends Cancer* 2020; **6**: 319-336 [PMID: 32209446 DOI: 10.1016/j.trecan.2020.01.012]

38 **Wang KW**, Dong M. Role of circular RNAs in gastric cancer: Recent advances and prospects. *World J Gastrointest Oncol* 2019; **11**: 459-469 [PMID: 31236197 DOI: 10.4251/wjgo.v11.i6.459]

39 **Cheng J**, Zhuo H, Xu M, Wang L, Xu H, Peng J, Hou J, Lin L, Cai J. Regulatory network of circRNA-miRNA-mRNA contributes to the histological classification and disease progression in gastric cancer. *J Transl Med* 2018; **16**: 216 [PMID: 30068360 DOI: 10.1186/s12967-018-1582-8]

40 **Shi Y**, Zheng C, Jin Y, Bao B, Wang D, Hou K, Feng J, Tang S, Qu X, Liu Y, Che X, Teng Y. Reduced Expression of METTL3 Promotes Metastasis of Triple-Negative Breast Cancer by m6A Methylation-Mediated COL3A1 Up-Regulation. *Front Oncol* 2020; **10**: 1126 [PMID: 32766145 DOI: 10.3389/fonc.2020.01126]

World Journal of Gastrointestinal Oncology

Submit a Manuscript: https://www.f6publishing.com

World J Gastrointest Oncol 2023 May 15; 15(5): 810-827

DOI: 10.4251/wjgo.v15.i5.810

ISSN 1948-5204 (online)

ORIGINAL ARTICLE

Basic Study

BZD9L1 benzimidazole analogue hampers colorectal tumor progression by impeding angiogenesis

Chern Ein Oon, Ayappa V Subramaniam, Lik Yang Ooi, Ashwaq Hamid Salem Yehya, Yeuan Ting Lee, Gurjeet Kaur, Sreenivasan Sasidharan, Beiying Qiu, Xiaomeng Wang

Specialty type: Oncology

Provenance and peer review: Invited article; Externally peer reviewed.

Peer-review model: Single blind

Peer-review report's scientific quality classification

Grade A (Excellent): 0
Grade B (Very good): B, B
Grade C (Good): 0
Grade D (Fair): 0
Grade E (Poor): 0

P-Reviewer: Wang YG, China; Zhang X, China

Received: January 3, 2023
Peer-review started: January 3, 2023
First decision: February 13, 2023
Revised: February 17, 2023
Accepted: April 21, 2023
Article in press: April 21, 2023
Published online: May 15, 2023

Chern Ein Oon, Ayappa V Subramaniam, Lik Yang Ooi, Yeuan Ting Lee, Gurjeet Kaur, Sreenivasan Sasidharan, Institute for Research in Molecular Medicine, Universiti Sains Malaysia, Penang 11800, Malaysia

Ashwaq Hamid Salem Yehya, Cancer Research, Eman Biodiscoveries, Kedah 08000, Malaysia

Ashwaq Hamid Salem Yehya, Vatche and Tamar Division of Digestive Diseases, Department of Medicine, David Geffen School of Medicine at University of California Los Angeles, Los Angeles, CA 90095, United States

Beiying Qiu, Xiaomeng Wang, Academic Clinical Program, Duke-NUS Medical School, National University of Singapore, Singapore 169857, Singapore

Beiying Qiu, Singapore National Eye Centre, Singapore Eye Research Institute, Singapore 168751, Singapore

Xiaomeng Wang, Singapore National Eye Centre, Singapore Eye Research Institute, Singapore 169857, Singapore

Corresponding author: Chern Ein Oon, DPhil, PhD, Associate Professor, Institute for Research in Molecular Medicine, Universiti Sains Malaysia, Gelugor, Penang 11800, Malaysia.
chern.oon@usm.my

Abstract

BACKGROUND

The development of new vasculatures (angiogenesis) is indispensable in supplying oxygen and nutrients to fuel tumor growth. Epigenetic dysregulation in the tumor vasculature is critical to colorectal cancer (CRC) progression. Sirtuin (SIRT) enzymes are highly expressed in blood vessels. BZD9L1 benzimidazole analogue is a SIRT 1 and 2 inhibitor with reported anticancer activities in CRC. However, its role has yet to be explored in CRC tumor angiogenesis.

AIM

To investigate the anti-angiogenic potential of BZD9L1 on endothelial cells (EC) *in vitro*, *ex vivo* and in HCT116 CRC xenograft *in vivo* models.

METHODS

EA.hy926 EC were treated with half inhibitory concentration (IC_{50}) (2.5 μM), IC_{50} (5.0 μM), and double IC_{50} (10.0 μM) of BZD9L1 and assessed for cell proliferation, adhesion and SIRT 1 and 2 protein expression. Next, 2.5 μM and 5.0 μM of BZD9L1 were employed in downstream *in vitro* assays, including cell cycle, cell death and sprouting in EC. The effect of BZD9L1 on cell adhesion molecules and SIRT 1 and 2 were assessed *via* real-time quantitative polymerase chain reaction (qPCR). The growth factors secreted by EC post-treatment were evaluated using the Quantibody Human Angiogenesis Array. Indirect co-culture with HCT116 CRC cells was performed to investigate the impact of growth factors modulated by BZD9L1-treated EC on CRC. The effect of BZD9L1 on sprouting impediment and vessel regression was determined using mouse choroids. HCT116 cells were also injected subcutaneously into nude mice and analyzed for the outcome of BZD9L1 on tumor necrosis, Ki67 protein expression indicative of proliferation, cluster of differentiation 31 (CD31) and CD34 EC markers, and SIRT 1 and 2 genes *via* hematoxylin and eosin, immunohistochemistry and qPCR, respectively.

RESULTS

BZD9L1 impeded EC proliferation, adhesion, and spheroid sprouting through the downregulation of intercellular adhesion molecule 1, vascular endothelial cadherin, integrin-alpha V, SIRT1 and SIRT2 genes. The compound also arrested the cells at G1 phase and induced apoptosis in the EC. In mouse choroids, BZD9L1 inhibited sprouting and regressed sprouting vessels compared to the negative control. Compared to the negative control, the compound also reduced the protein levels of angiogenin, basic fibroblast growth factor, platelet-derived growth factor and placental growth factor, which then inhibited HCT116 CRC spheroid invasion in co-culture. In addition, a significant reduction in CRC tumor growth was noted alongside the downregulation of human SIRT1 (hSIRT1), hSIRT2, CD31, and CD34 EC markers and murine SIRT2 gene, while the murine SIRT1 gene remained unaffected, compared to vehicle control. Histology analyses revealed that BZD9L1 at low (50 mg/kg) and high (250 mg/kg) doses reduced Ki-67 protein expression, while BZD9L1 at the high dose diminished tumor necrosis compared to vehicle control.

CONCLUSION

These results highlighted the anti-angiogenic potential of BZD9L1 to reduce CRC tumor progression. Furthermore, together with previous anticancer findings, this study provides valuable insights into the potential of BZD9L1 to co-target CRC tumor vasculatures and cancer cells *via* SIRT1 and/or SIRT2 down-regulation to improve the therapeutic outcome.

Key Words: Colorectal cancer; BZD9L1; Sirtuin; Benzimidazole; Angiogenesis

Core Tip: BZD9L1 hampered EA.hy926 endothelial cell functions through cell cycle arrest and induction of apoptosis. BZD9L1 also reduced the cell adhesion, sirtuin 1 (SIRT1) and SIRT2 gene expression in endothelial cells (EC) compared to the negative control. The compound down-regulated angiogenin, basic fibroblast growth factor, platelet-derived growth factor, and placental growth factor proteins in EC and impeded HCT116 colorectal cancer (CRC) invasion compared to the negative control group. BZD9L1 negatively impacted choroidal sprouting and CRC tumor angiogenesis *in vivo* compared to the vehicle control group. BZD9L1 reduced tumor necrosis, Ki-67 proliferation marker, hSIRT1, hSIRT2, murine cluster of differentiation 31 (mCD31), mCD34 and murine SIRT2 (mSIRT2) gene expression compared to vehicle control. Findings from this study may provide insights for the BZD9L1 benzimidazole analogue to be further explored as a potential anti-angiogenic agent in CRC.

Citation: Oon CE, Subramaniam AV, Ooi LY, Yehya AHS, Lee YT, Kaur G, Sasidharan S, Qiu B, Wang X. BZD9L1 benzimidazole analogue hampers colorectal tumor progression by impeding angiogenesis. *World J Gastrointest Oncol* 2023; 15(5): 810-827

URL: https://www.wjgnet.com/1948-5204/full/v15/i5/810.htm

DOI: https://dx.doi.org/10.4251/wjgo.v15.i5.810

INTRODUCTION

Cancer may arise from genetic or epigenetic dysregulations. Many conventional therapies focus on removing and disrupting malignant cells but fail to target the tumor microenvironment, which could

fuel tumor growth through pathway crosstalks and the secretion of cytokines. Epigenetic dysregulation has been shown to stimulate oncogenic transformation in many cancer types, including colorectal cancer (CRC). Furthermore, research has highlighted the importance of epigenetic regulation in angiogenesis, which is key to CRC growth and metastasis. Advancements in therapeutic care for CRC patients have identified various angiogenesis inhibitors targeting the tyrosine kinases and vascular endothelial growth factor (VEGF) proteins used in clinics. However, some patients are resilient or have become less susceptible to these anti-angiogenic drugs[1], possibly due to dynamic host response factors or mutations within tumors that render drug insensitivity. Therefore, there is a need to uncover alternative targeted therapies. Sirtuins (SIRT 1-7) are nicotinamide adenine dinucleotide (NAD+) -dependent class III histone deacetylases. Their potential roles through epigenetic modulation in cancer have stimulated investigation to seek potent and selective SIRT inhibitors, potentially leading to new therapeutic breakthroughs.

Benzimidazole derivatives have been widely used in other areas, such as antiviral[2] and anti-mycobacterial[3] agents; hence their pharmacokinetics are well understood. The discovery of indole analogues as potent sirtuin inhibitors[4] and the high similarities between the indole and benzimidazole core structures have led to the discovery of BZD9L1[5] and its reported anticancer activities as a single agent[6] or in combination with 5-fluorouracil in CRC[7]. However, to our knowledge, no known sirtuin inhibitors have been studied concerning their application to modulate angiogenesis. Hence, this study opens a new avenue for developing a prospective anti-angiogenic agent (BZD9L1) through sirtuin inhibition in CRC.

MATERIALS AND METHODS

Cells and cell culture

The Ea. hy926 endothelial cells (EC) and the HCT-116 CRC cell line were purchased from American Type Culture Collection (ATCC®). The cells were maintained in Dulbecco's Modified Eagle Medium (DMEM) and Roswell Park Memorial Institute (RPMI), respectively (Thermo Scientific, United States), supplemented with 5% fetal bovine serum (Biowest, United States), 1% penicillin-streptomycin (Nacalai Tesque, United States). Cells were kept at 37°C in a humidified incubator with 5% CO_2 atmosphere.

Treatments

BZD9L1 was synthesized as previously described[5]. BZD9L1 was prepared and dissolved in dimethyl sulfoxide (DMSO) (Nacalai Tesque, United States) for *in vitro* and *ex vivo* evaluations. Different concentrations of BZD9L1 and anti-angiogenic agents Sunitinib (AdooQ Bioscience, CA, United States)[8] or activin A receptor like type 1 (ALK1) inhibitor (Axon MedChem)[9] positive controls were used to treat the cells according to assay requirements. For animal administration, BZD9L1 was prepared in 0.5% sodium carboxymethyl cellulose (CMC) solution as previously reported[10] and administered to the rodents *via* intraperitoneal injection, in which 0.5% CMC was also employed as the vehicle control *in vivo*.

Animals for in vivo study

The animal study was approved and conducted in strict accordance with Universiti Sains Malaysia Animal Ethical Committee [No. USM/IACUC/2017/(105)(872)]. Male and female athymic nude mice were procured from EMAN Biodiscoveries Sdn. Bhd. The mice were maintained in filter-top cages under controlled atmospheric conditions at Natureceuticals Sdn Bhd, Kawasan Perindustrian Sungai Petani, Sungai Petani, Kedah. The mice were 4-6 wk of age with a body weight of 18-20 g. The mice were provided with autoclaved food and water. The bedding was refreshed every 48 h.

Animals for ex vivo study

Male and female C57BL/6J mice were sourced from Invivos (Singapore) and retained on a 12 h light-dark cycle. The mice were fed a standard rodent chow (NCD, 18% kcal from fat, Harlan). The *ex vivo* assays, which require the choroids from the mice, were performed in compliance with the National University of Singapore Institutional Animal Care and Use Committee guidelines (IACUC) (No. 2020/SHS/1597).

Cell viability assay

The 3-(4,5-dimethylthiazol-2-yl)-2,5 diphenyl tetrazolium bromide (MTT) cell viability assay was performed to determine half inhibitory concentration (IC_{50}) and suitable dosage of BZD9L1. MTT reagent diluted with phosphate-buffered saline (PBS) at 5 mg/mL was used for the MTT assay. Cells (2.5×10^3) were seeded in 96-well plates with 100 µL of compatible media per well and incubated in 5% CO_2 at 37 °C for 24 h. Different doses of BZD9L1 (0 µM, 1.560 µM, 3.125 µM, 6.250 µM, 12.500 µM, 25.000 µM, 50.000 µM, and 100.000 µM) were tested on Ea.hy926 cells to select the best cytotoxic concentrations and then incubated in 5% CO_2 at 37 °C. After 72 h, 20 µL of MTT reagent per well was added and then

incubated in 5% CO_2 at 37 ℃ for 4. Next, the supernatant was carefully aspirated and 200 µL of DMSO added. After gently shaking the plate, the mixture's optical density (OD) was measured using a microplate reader (TECAN, Switzerland) at 570 nm primary and 620 nm reference wavelength. The percentage of viable cells at each treatment concentration was calculated using the following equation: Cell viability (%) = (absorbance of samples/absorbance of vehicle control) × 100%.

xCELLigence cell adhesion assay

The effect of BZD9L1 towards cell adhesion was determined using the xCELLigence Real-Time Cell Analysis (RTCA) instrument (Agilent Technologies, United States) according to the standard manufacturer's protocol. Briefly, the cells were resuspended in treatment media conditions: Vehicle control, 2.5 µM, 5.0 µM, and 10.0 µM of BZD9L1. Then, the cells and treatment media were seeded into the E96 xCELLigence plate at 1 × 10^4 cells per well. The E-96 xCELLigence plate was incubated for 30 min at room temperature and placed on the xCELLigence station in the cell culture incubator. The cellular impedance was continuously monitored every 30 min for 5 h. Impedance recordings from each well in the E96 xCELLigence plate were automatically converted to cell index (CI) values by the xCELLigence RTCA software.

xCELLigence cell proliferation assay

Real-time analysis of EA.hy926 cell proliferation was evaluated using the xCELLigence RTCA instrument (Agilent Technologies, United States). Firstly, 100 µL of growth media was added to each well of an E96 xCELLigence plate. The plate was then inserted into the xCELLigence station. Next, baseline impedance measurement was performed to obtain background readings. EA.hy926 cells were harvested and adjusted to 1 × 10^4 cells per well. The cells were resuspended in 100 µL of media and seeded into the E96 xCELLigence plate. E-96 xCELLigence plate containing cells was incubated for 30 min at room temperature and placed on the xCELLigence station in the cell culture incubator. After 24 h, treatment comprising of vehicle control, BZD9L1 at 2.5 µM, 5.0 µM, and 10.0 µM were introduced to the cells in the plate, then returned to the xCELLigence station in an incubator for continuous impedance recording. Cell proliferation was monitored every 30 min for 72 h. Measured impedance recordings from cells in each well on the E96 xCELLigence plate were automatically converted to Cell Index (CI) values by the xCELLigence RTCA software.

Cell cycle analysis

The cell cycle analysis was performed to differentiate different cell cycle phases that were arrested after the treatments above. On day 0, Ea.hy926 cells were seeded in a T25 culture flask at a concentration of 5 × 10^5 per flask. Each treatment group was assigned a flask. The cells were incubated at 37 ℃ in a humidified atmosphere of 5% (v/v) CO_2 to promote cell attachment. The next day, the medium was meticulously removed and replaced with fresh medium containing treatments and then incubated for 72 h at 37 ℃ in a humidified atmosphere of 5% (v/v) CO_2. After 72 h, the cells were collected, centrifuged, and fixed with 70% ethanol (molecular grade) at 4 ℃. Finally, the fixed cells were stained with 500 µL of warm propidium iodide (PI) solution plus 50 µL of RNase A stock solution (1 mg/mL). The cells were incubated in the dark for 30 min. The stained cells were kept on ice until the scheduled flow cytometry analysis using BD FACSCalibur (BD Biosciences, United States).

Apoptosis detection

Apoptotic cells were detected by flow cytometry using Annexin V-fluorescein isothiocyanate (FITC) Apoptosis Detection Kit (Elabscience, China). On day 0, Ea. hy926 cells were seeded in a T25 culture flask at a concentration of 5 × 10^5 per flask. Each treatment group was assigned a flask. The cells were incubated at 37 ℃ in a humidified atmosphere of 5% (v/v) CO_2 to promote cell attachment. The next day, the medium was meticulously removed and replaced with fresh medium containing treatments before incubation for 72 h at 37 ℃ in a humidified atmosphere of 5% (v/v) CO_2. After 72 h, the cells were harvested and centrifuged, and the cell concentration was adjusted to 1 × 10^6 for each tube. The Annexin V-FITC Apoptosis Detection Kit was used to stain the cells, and cell apoptosis was determined by flow cytometry, according to the manufacturer's instruction. The tubes were incubated at room temperature for 15 min in the dark, after which the cells were subjected to flow cytometry analysis immediately using BD FACSCalibur (BD Biosciences, United States) using 488 nm excitation and 525 nm emission for FITC and 655-730 nm emission for PI.

Hanging drop spheroid formation and sprouting assay

The 3-dimensional spheroid sprouting assay mimics the *in vivo* microenvironment of tissue or tumors. Hanging drop spheroid formation and sprouting assay was conducted to provide a three-dimensional aspect to both architecture and share the limited drug penetration properties since drugs are primarily confined to the outer cell layers. Culturing cells in three dimensions is much more representative of the *in vivo* environment than traditional two-dimensional cultures. In this present study, Ea.hy 926 was used to generate micro-spheroids. After trypsinization of cultured cells, the cells were harvested and resuspended in DMEM medium containing 0.25% methylcellulose. Drops (20 µL) of medium containing

2×10^3 cells were seeded onto the lids of 100 mm petri dishes, and the dishes were supplied with 5 mL of PBS to maintain humidity. The drops were incubated for 72 h to encourage the occurrence formation of spheroids. Treatments were prepared at different concentrations of BZD9L1 (2.5 μM and 5.0 μM) and sunitinib (18 μM) as a positive control in media and then added to each well. The resulting aggregate cells (spheroids) were harvested carefully using 200 μL pipettes and then introduced into a 96-well plate precoated with 50 μL matrigel per well. The plate was left to incubate in the incubator at 37 ℃, and pictures were taken using a phase contrast microscope (Zeiss, Germany) on days 0 and 3. The length of the sprouts was measured and analyzed as previously described[11] using Image J (Fiji).

Angiogenesis array

The Quantibody Human Angiogenesis Array (RayBiotech, Inc, Norcross, GA) was used to determine the concentration of ten proangiogenic cytokines [angiogenin, angiopoietin-2, epidermal growth factor (EGF), basic fibroblast growth factor (bFGF), heparin-binding EGF, hepatocyte growth factor, leptin, platelet-derived growth factor (PDGF-BB), placental growth factor (PIGF), and VEGF-A)] secreted by the EC. Each cytokine was arrayed in quadruplicate, together with positive and negative controls. In addition, one standard glass slide was divided into 16 wells of identical cytokine antibody array. Approximately 2.5×10^3 of Ea. hy926 cells were seeded in 96-well plates with 100 μL of compatible media per well and incubated in 5% CO_2 at 37 ℃ for 24 h. The next day, vehicle control, 2.5 μM, and 5.0 μM of BZD9L1 treatment were prepared using 1% serum media and introduced to the cells. After 48 h, the media was discarded, and the cells were washed with 1 × PBS twice before reintroducing serum-free media. After another 48 h, the conditioned media was collected. The conditioned media was used on the angiogenesis antibody array kit (Quantibody Human Angiogenesis Array 1) as per manufacturer's instructions. The slides were mailed to RayBiotech testing services (Singapore) for laser scanning analysis. Data were extracted and analyzed using the RayBio Q Analyzer software (RayBiotech, Inc).

RNA extraction

Total cellular RNA was extracted from EA.hy926 cells treated with vehicle control (DMSO) or different concentrations of BZD9L1 at 4 h time point, or HCT116 xenograft tumors post-treatment, using GENEZOL (Geneaid, New Taipei City, Taiwan) according to the manufacturer's instructions. Firstly, the spent medium was discharged from each well and the cells were rinsed with 1 × PBS twice. Next, 1 mL of GENEZOL reagent solution was added to each well. The cells were lysed *via* repeated pipetting and followed by 10 min of incubation at room temperature for sample homogenization. The lysed cells were then transferred into 2 mL microcentrifuge tubes. An accurate amount of 200 μL chloroform was added to each tube. Each tube was mixed thoroughly by vortexing for 15 s. The lysates were then centrifuged at 16000 g for 15 min at 4 ℃. The colourless upper aqueous phase was carefully transferred into a new 1.5 mL microcentrifuge tube without drawing any of the interphase or organic phase layer that appears white and red in the three-layers mixture respectively. Next, 1 to 1 volume of ice-cold isopropanol was added to the aqueous phase. The 1.5 mL tubes were inverted several times for proper mixing, followed by 10 min of incubation at room temperature. The tubes were centrifuged at 16000 × g for 10 min at 4 ℃ to form a tight RNA pellet. The supernatant was removed completely, and the pellet was resuspended with 1 mL 75% ethanol. The mixture was vortexed briefly and centrifuged again at 16000 g at 4 ℃ for 5 min to remove all traces of ethanol. The supernatant was carefully removed by using a pipette tip, and the pellet was allowed to air dry for 15 min. After 15 min of air drying, the pellet was resuspended with 20 μL DEPC-treated water and incubated at 60 ℃ for 15 min to dissolve the RNA pellet. RNA was then converted to cDNA or immediately stored at -80 ℃ freezer until further use. The purity and concentration of the isolated RNA were determined by measuring the optical density at 260 nm and 260/280 nm ratio using a NanoDrop 2000 spectrophotometer (Thermo Scientific, Pennsylvania, United States). A preset of 40 ng/μL per OD was used with a baseline correction of 340 nm.

Quantitative polymerase chain reaction

The RNA was reverse transcribed into cDNA using Tetro cDNA Synthesis Kit (Bioline, United States) according to the manufacturer's protocol. Real-time quantitative polymerase chain reaction (qPCR) was performed using the KAPA SYBR FAST qPCR Kit Master Mix (2 ×) Universal (Biosystems, United States) with the following conditions: denaturation, 95 ℃ for 20 s; annealing, 58 ℃, 20 s and extension, 68 ℃, 30 s. All samples were tested in triplicate PCR reactions, and the mean of the reactions was used for calculating the expression levels. All the data were collected from the linear range of each amplification. Two housekeeping genes (HKGs) were used to normalize the expression of genes of interest (GOIs). Expression levels of GOIs were normalized to glyceraldehyde 3-phosphate dehydrogenase (GAPDH) and human 18S ribosomal RNA (18S rRNA) gene for human targets, and mouse 18S ribosomal RNA (m18S rRNA) and mouse Peptidylprolyl isomerase A (mPpia) genes for mouse targets. The data were analyzed using the comparative CT (ΔΔCT) method, where the expression value of the GOI was normalized to the respective HKG. The change of gene expression was determined by setting the expression value of vehicle control sample to 1, and expression values of GOI were compared where values < 1 represented downregulation and values > 1 represented upregulation of that particular GOI. The final results were reported as mean ± SEM to reflect the triplicate measurements. The list of primers

used for qPCR analysis is listed in Table 1.

Ex vivo mouse choroid microvascular assay

Organotypic cultures are *in vitro* growth of 3D biological tissues that closely emulate part of their natural function and physiology. Choroid sprouting assay was performed as described[12]. C57BL/6J mice were killed by cervical dislocation. The choroid explants from post-natal day 3 C57BL/6J mice were isolated through a very tedious process under a stereo microscope. Briefly, the cornea and lens were removed from the anterior of the eye, followed by the separation of the peripheral choroid-sclera complex from the retina. The choroid was then cut into 1mm × 1mm segments. The choroid explants were then incubated in reduced growth factor Matrigel (BD Biosciences). Vascular outgrowth, including cells from the microenvironment from the choroidal tissues treated with DMSO vehicle control, BZD9L1 at 10 μM and 20 μM or ALK1 inhibitor (Axon MedChem) at 100 nM. After 96 h, the effect of BZD9L1 on the morphological changes of vessel sprouts was noted. The regression study performed as previously reported[13], in which treatment media containing either DMSO (negative control), BZD9L1 at concentrations of 10 μM and 20 μM or ALK1 inhibitor at 50 nM were added to the explants on day 2 when the embedded choroids had sprouted. Media were changed every other day. Images were taken 24 h post-treatment. Imaging and quantifying the sprouting area were performed under the Eclipse Ti-E Inverted Research Microscope (Nikon, Tokyo, Japan). and TRI2 software (version: 3.0.1.2, TRI2, Oxford, United Kingdom).

Indirect co-culture assay

The co-culture assay was conducted to study the interaction between ECs and cancer cells. The application of a co-culture model promotes a better understanding of the dynamic tumor-EC relationship that occurs *in vivo* in an inexpensive and *in vitro* laboratory setting. In this study, the co-culture was conducted indirectly. Ea. hy926 and HCT116 cell lines were used in this experiment. Steps to collect conditioned media were repeated as per described for the angiogenesis array. The conditioned media can be used fresh or stored in a -80 ℃ freezer for later use. Treatments were prepared at different concentrations of BZD9L1 (2.5 μM and 5.0 μM) and sunitinib (18 μM) as a positive control. HCT 116 spheroids were prepared and introduced into the rat tail collagen mixed to a concentration of 1.6 mg/mL before mixing it with spheroid suspension, a spreviously described[7]. The mixture was dispensed at 400 uL in each well in a 24-well plate. The plate was incubated for 30 min before 500 μL of the conditioned media was introduced. The plate was left in the incubator at 37 ℃, and pictures were taken using a phase contrast microscope (Zeiss, Germany) on days 0 and 3.

Tumor xenograft model

Xenograft models are based on the implantation of human tumor cells into genetically modified mice models that are immunocompromised to avoid graft *vs* host reaction of the mouse against the human tumor tissue. Male/female athymic nude mice (procured from EMAN Biodiscoveries Sdn. Bhd.) were maintained in filter-top cages under controlled atmospheric conditions. The mice were 4-6 wk of age with a body weight of 18-20 g. Mice were provided autoclaved food and water, and the bedding was changed every 48 h. HCT-116 cells at 90% confluency were harvested and injected subcutaneously onto the right dorsal flank of the animal at a density of 1×10^6 cells per 200 μL of media mixed with matrigel at a ratio of 1:1. The mice were then randomly divided into four groups (n = 6) and given different treatments, consisting of vehicle control, BZD9L1 at 50 mg/kg or 250 mg/kg and sunitinib at 40 mg/kg as the positive control[14], when at least three tumors reached 100 mm^3. The treatments were diluted in 0.5% carboxymethylcellulose (CMC) solution. The control group was treated with 0.5% CMC only. The treatments were injected intraperitoneally at a maximum volume of 250 μL once every three days, alongside the measurement of weight and tumor size using the standard formula: Volume of tumor = π/6 × (length × width × height), as previously reported[7].

The animals were euthanized when the tumor reached the maximum size of 1000 mm^3. The tumors were harvested and fixed in a 10% buffered formaldehyde solution and then processed by an automated tissue processing machine for histological examination. The HCT116 xenograft tumor samples were cut into small pieces using a sterile surgical blade for gene expression analyses. GENEZOL reagent was added to the tumor tissue sample and placed on ice. The tissue was then homogenized using a handheld homogenizer. The mixture was centrifuged at 13000 × g for 15 min at 4 ℃ to separate the phases. The upper aqueous phase was transferred to a new 2.0 mL microcentrifuge tube, followed by the RNA extraction protocol described above.

Hematoxylin & Eosin staining

The impact of BZD9L1 treatment on tumor necrosis affecting tumor growth was determined by establishing a necrotic score. First, the slides were deparaffinized by heating the slides in the oven at 60 ℃ for 10 min. The slides were then immersed in the following order: Xylene (twice), absolute ethanol (twice), 95% ethanol (twice), 70% ethanol (once) and lastly, in distilled water, for 5 min each. Next, the slides were stained with hematoxylin for 5 min and then washed with distilled water for another 5 min. The slides were later counterstained with eosin for 15 s. Finally, the slides were washed for 5 min and

Table 1 List of primers

Genes	Primer sequences	
	Forward sequences (5' to 3')	Reverse sequences (3' to 5')
mPpia	GAGCTGTTTGCAGACAAAGTTC	CCCTGGCACATGAATCCTGG
m18SrRNA	GGACCAGAGCGAAAGCATTTGCC	TCAATCTCGGGTGGCTGAACGC
18S rRNA	CGGCTACCACATCCAAGGAA	GCTGGAATTACCGCGGCT
mCD31	CCAAAGCCAGTAGCATCATGGTC	GGATGGTGAAGTTGGCTACAGG
mCD34	CTTCCCCAACTGGCATACTGC	TCCAGAGCATTTGATTTCTCCC
GAPDH	TGAACGGGAAGCTCACTGG	TCCACCACCCTGTTGCTGTA
ICAM	CGACTGGACGAGAGGGATTG	TTATGACTGCGGCTGCTACC
VE-cadherin	CCCTTCTTCACCCAGACCAA	CCGGTCAAACTGCCCATACT
ITGA5	CGGGCCCCTGCACCAACAAG	CAGCTGTGGCCACCTGACGC
mSIRT 1	CGGCTACCGAGGTCCATATAC	CAGCTCAGGTGGAGGAATTGT
mSIRT 2	GAGCCGGACCGATTCAGAC	AGACGCTCCTTTTGGGAACC
SIRT 1	TCTAACTGGAGCTGGGGTGT	TGGGAAGTCTACAGCAAGGC
SIRT 2	GCCCTTTACCAACATGGCTG	TTCGTACAACACCCAGAGCG

ITGA5: Integrin-alpha V; GAPDH: Glyceraldehyde 3-phosphate dehydrogenase; SIRT: Sirtuin; ICAM: Intercellular adhesion molecule; VE-cadherin: Vascular endothelial cadherin; CD31: Cluster of differentiation 31.

air-dried before being mounted.

Immunohistochemistry

The effect of BZD9L1 on proliferation was ascertained through Ki67 protein expression analysis on the xenograft tumor sections. The formalin fixed paraffin embedded slides were deparaffinized by heating the slides in an oven at 60 ℃ for 10 min. The slides were then immersed in the following order: absolute ethanol (twice), 95% ethanol (twice), 70% ethanol (once), followed lastly in distilled water for 5 min each. This procedure was carried out using the Dako Envision FLEX Kit. The sections were incubated in High pH antigen retrieval buffer (Dako) for 30 min. Next, the slides were washed with the wash buffer three times, for 5 min each. A few drops of Envision FLEX Peroxidase solution were introduced to the tissue for 10 min. The sections were then incubated with primary antibody Ki67 (Dako, Clone MIB-1, Cat#M7240, mouse monoclonal) and incubated at 4 ℃ overnight at 1:50 dilution. On the next day, the sections were rinsed in TBST and incubated with goat anti-mouse IgG secondary antibody for 1 h at 1:500 dilution, rinsed three times in TBST and followed by incubation with Dako® DAB solution. The slides were counterstained with hematoxylin for 5 min and then rinsed off before being mounted with glycerol (Sigma) and examined under a light microscope (CX41, Olympus). The Ki-67 score was established as the percentage of tumor cells positive for brown nuclear staining over the total number of nuclei from five random fields per tumor section.

Statistical analysis

GraphPad Prism 9.4.0 (GraphPad, United States) and Microsoft Excel (Microsoft, United States) were used for statistical analysis. The analysis of variance (One-way ANOVA) test was employed to compare mean values among three or more data sets, and Bonferroni post-test was employed to compare any two data sets among the three or more sets. Statistical significance was indicated in the figures, where $^{a}P < 0.05$, $^{b}P < 0.01$, and $^{c}P < 0.001$, compared to the negative control or vehicle control. The non-regression curve was used to track the change in the tumor size and mouse body weight over time. Error bars represent the SEM.

RESULTS

BZDL1 reduced the viability and adhesion of Ea.HY926 cells

The effects of BZD9L1 on cell viability were assessed with MTT assay at 72 h. The half- IC_{50} of BZD9L1 in Ea HY926 was established to be at 5.2 μm (Figure 1A). BZD9L1 at 10 μM reduced the ability of the EC in suspension to adhere to the microtiter plates (E-Plates®) at 5 h (Figure 1B). BZD9L1 at 2.5 μM and 5.0

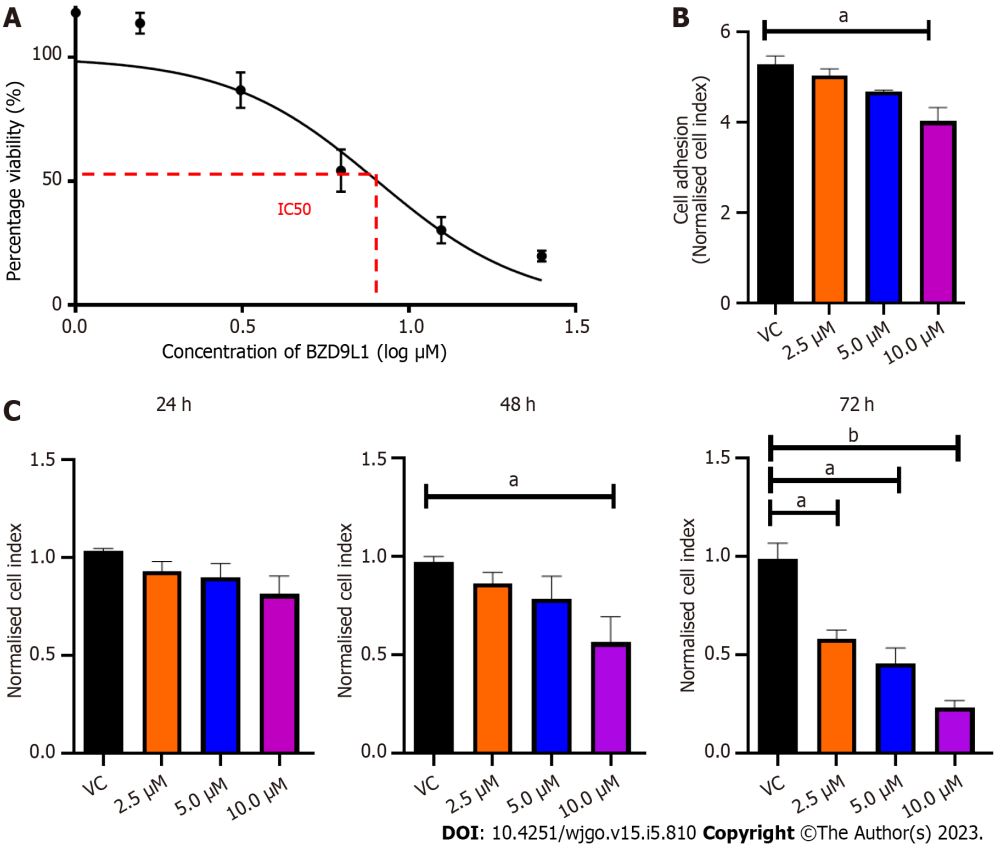

DOI: 10.4251/wjgo.v15.i5.810

Figure 1 Cell viability and adhesion analyses of Ea.HY926 endothelial cells treated with different concentrations of BZD9L1. A: Cell viability was determined using the MTT assay. The inhibitory concentration of BZD9L1 in Ea HY926 is 5.20 μm ± 0.38 μm (n = 3) at 72 h; B: Real-time xCELLigence impedance analysis of the area under the curve of BZD9L1-treated Ea.HY926 cells in suspension over 5 h. BZD9L1 at 10 μM reduced the ability of the endothelial cells to adhere to the microtiter plates (E-Plates®); C: Real-time xCELLigence impedance analysis of normalized cell index of BZD9L1-treated Ea.HY926 cells over 72 h. BZD9L1 at 2.5 μM and 5.0 μM had no significant impact on cell proliferation at 24 h and 48 h. Statistical analysis ($^aP < 0.05$; $^bP < 0.01$), one-way ANOVA with Bonferroni posthoc test, n = 3 independent experiments using GraphPad Prism 9.4.0. Error bars represent SEM. VC: Vehicle control.

μM had no significant impact on cell proliferation at 24 h and 48 h (Figure 1C). Hence the aforementioned IC_{50} value (5.0 μm) and half its IC_{50} (2.5 μm) were selected for downstream experiments.

BZD9L1 reduced SIRT1, SIRT2, intercellular adhesion molecule 1, integrin-alpha V and vascular endothelial cadherin genes in Ea.HY926 cells

As BZD9L1 is a small molecule inhibitor with SIRT1 and 2 inhibitory activities, Ea.HY926 cells were treated with non-killing doses of BZD9L1 at 2.5 μM and 5.0 μM to investigate its repressive effects on SIRT 1 and SIRT 2. SIRT 1 and 2 gene expression were significantly reduced in cells treated with BZD9L1 at 2.5 μM and 5.0 μM, compared to the negative control (Figure 2A). BZD9L1 also significantly down-regulated intercellular adhesion molecule 1 (ICAM-1), integrin-alpha V (ITGA5) and vascular endothelial cadherin (VE-cadherin) cell adhesion molecules (Figure 2B) compared to the negative control.

BZD9L1 induced apoptotic cell death and arrested Ea HY926 cells at the G1 phase

The live, necrotic, early apoptotic, and late apoptotic fractions and cell cycle distribution of cells were detected by Annexin V and PI staining at 72 h post-treatment. Cells treated with BZD91 at 2.5 μM and 5.0 μM showed a significant increase in early and late apoptosis compared to the negative control (Figure 3A). BZD9L1 at 2.5 μM and 5.0 μM induced cell cycle arrest at the G1 phase compared to the negative control group (Figure 3B).

BZD9L1 hampered Ea.HY926 EC spheroid and mouse choroid sprouting

BZD9L1 at 2.5 μM and 5.0 μM significantly reduced Ea.HY926 EC spheroid sprouting compared to negative control 72 h post-treatment (Figure 3C). Considering the native tissue and microenvironmental factor, BZD9L1 employed at higher concentrations of 10 μM, and 20 μM decreased the sprouting area in mouse choroids compared to the negative control 96 h post-treatment (Figure 4A). Interestingly, BZD9L1 at both concentrations also regressed sproutings of mouse choroids 24 h post-treatment of sprouted choroids (Figure 4B). ALK1 inhibited both the sprouting and regression processes in mouse

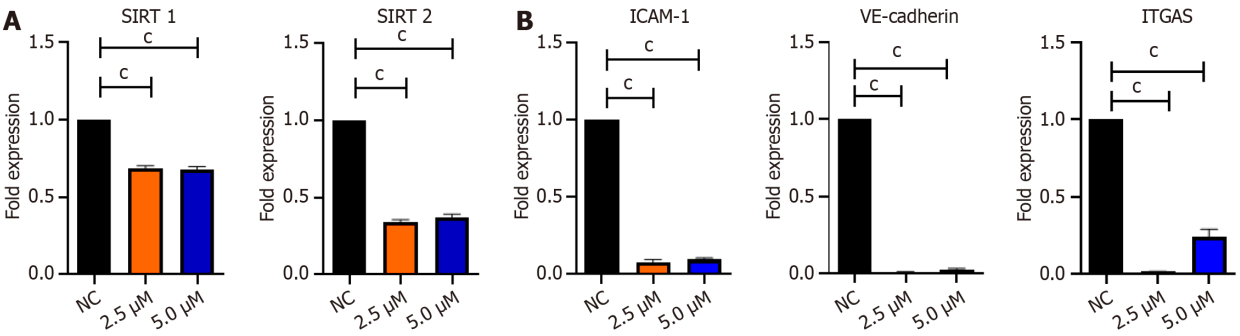

DOI: 10.4251/wjgo.v15.i5.810 **Copyright** ©The Author(s) 2023.

Figure 2 Quantitative polymerase chain reaction analysis of Ea.HY926 cells treated with BZD9L1 for 4 h. A: BZD9L1 reduced the gene expression levels of sirtuin 1 (SIRT1) and SIRT 2; B: Intercellular adhesion molecule 1 (ICAM-1), vascular endothelial cadherin (VE-cadherin) and integrin-alpha V (ITGA5) cell adhesion markers including ICAM-1, VE-cadherin and ITGA5, compared to the negative control (NC). Statistical analysis ($^cP < 0.001$), one-way ANOVA with Bonferroni posthoc test, $n = 3$ independent experiments using GraphPad Prism 9.4.0. Error bars represent SEM. SIRT: Sirtuin; ICAM-1: Intercellular adhesion molecule 1; NC: Negative control; VE-cadherin: Vascular endothelial cadherin; ITGA5: Integrin-alpha V.

choroids.

Conditioned media from BZD9L1-treated ECs reduced CRC spheroid invasion

Co-culture models are widely utilized to examine how physical contact between cells and autocrine and/or paracrine interactions affect cell activity. An indirect co-culture was performed to determine the effects of BZD9L1 on EC and CRC spheroids. The 48-h post-treatment conditioned media from Ea.HY926 cells were used to treat CRC spheroids to study the tumor-EC relationship. Analysis of the EC-conditioned media revealed that BZD9L1 at 5 μM diminished Angiogenin (A), bFGF (B), PDGF-BB (C), and PIGF (D) levels compared to the negative control group (Figure 5A). The other six cytokines were either not expressed at basal levels or below the detection limit. The conditioned media from all treatment groups significantly reduced the invasion of the CRC spheroids relative to the negative control group (Figure 5B).

BZD9L1 inhibited colorectal tumor growth and angiogenesis in the xenograft model

Sunitinib at 40 mg/kg and BZD9L1 inhibited tumor growth in low- (50 mg/kg) and high- (250 mg/kg) dose groups compared to the vehicle group (Figure 6A). Notably, the tumor growth in high-dose-treated mice was significantly impeded compared to the low-dose-treated mice group. The 250 mg/kg BZD9L1-treated xenograft tumor growth was equally inhibited to the same level as the 40 mg/kg Sunitinib positive control-treated mice. The weight of the tumor also decreased with the increasing doses of BZD9L1 (Figure 6B). There was no change in the body weight in all treatment groups compared to the vehicle control group except for the Sunitinib-treated group (Figure 6C). BZD9L1 (50 mg/kg) did not significantly reduce tumor necrosis compared to vehicle control Figure 6D. However, only BZD9L1 (250 mg/kg) and Sunitinib positive control significantly inhibited tumor necrosis compared to the vehicle control group. In addition, BZD9L1 at low and high doses significantly reduced Ki67 protein expression in tumor tissue compared to vehicle control Figure 6E. qPCR analyses of the xenograft tumors revealed no significant change in murine SIRT1 (mSIRT1) but a down-regulation of mSIRT2 in BZD9L1-treated groups at both 50 mg/kg and 250 mg/kg, compared to the vehicle control group (Figure 7A). In addition, BZD9L1 at 250 mg/kg reduced hSIRT1 and hSIRT2 gene expression in mice, compared to the vehicle control group. Although BZD9L1 at the low dose did not significantly reduce cluster of differentiation 31 (CD31) gene expression compared to the vehicle control, BZD9L1 at high doses decreased both CD31 and CD34 gene expression compared to the vehicle control (Figure 7B).

DISCUSSION

The fundamental stages of sprouting angiogenesis comprise enzymatic degradation of the EC basement membrane, followed by EC proliferation, migration, tube formation in response to growth factors gradient and finally, mural cell stabilization. Despite the emergence of novel targeted therapies targeting cancer cells or the tumor vasculature, the development of small molecule inhibitors to treat CRC to arrest the two main features of CRC, namely uncontrollable malignant cell proliferation and angiogenesis simultaneously, remain a potential avenue to be explored. The anticancer and SIRT 1 and 2 inhibitory activities of BZD9L1 have previously been established[5]. The human EC line Ea.HY926 was chosen for this study because it is continuous, exhibits various characteristics common to vascular ECs, and is frequently employed as an *in vitro* model for angiogenesis[15,16]. Despite the reduction of EC

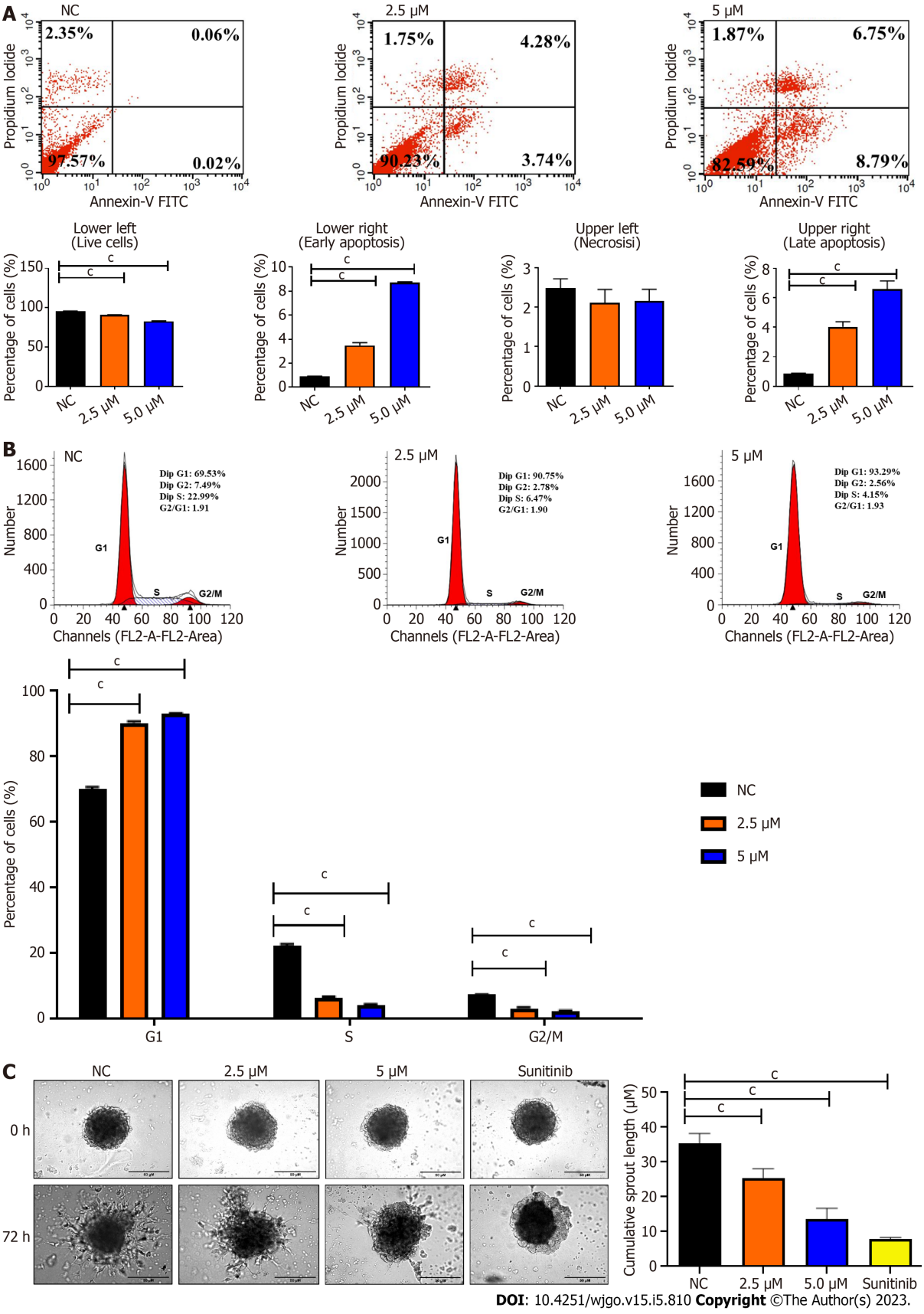

DOI: 10.4251/wjgo.v15.i5.810 **Copyright** ©The Author(s) 2023.

Figure 3 Representative cytograms and endothelial cells sprouting spheroids depict the negative impact of BZD9L1 on endothelial cell functions. A: BZD9L1 at 2.5 μM and 5.0 μM induced apoptosis; B: Cell cycle arrest at G1 phase; C: But reduced Ea.Hy 926 spheroid sprouting compared to the negative control at 72 h. Sunitinib anti-angiogenic agent was used as the positive control. Statistical analysis ($^cP < 0.001$), one-way ANOVA with Bonferroni posthoc test, $n = 3$ independent experiments using GraphPad Prism 9.4.0. Error bars represent SEM. NC: Negative control.

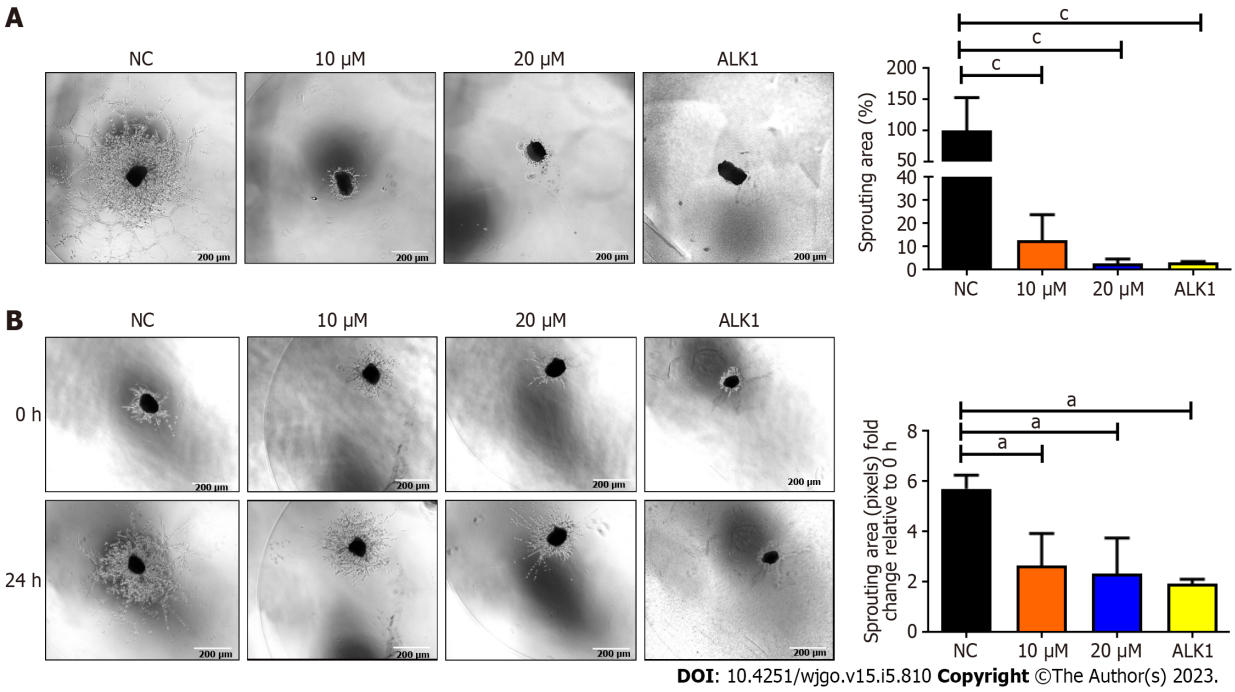

DOI: 10.4251/wjgo.v15.i5.810 **Copyright** ©The Author(s) 2023.

Figure 4 Analyses of mouse choroidal endothelial sprouts in sprouting and regression models. A: BZD9L1 impeded mouse choroidal endothelial sprouting 96 h post-treatment; B: Regressed choroid sprouting 24 h post-treatment compared to the negative control. A receptor like type 1 anti-angiogenic agent was used as the positive control regression and sprouting assays. Statistical analysis ($^{a}P < 0.05$; $^{c}P < 0.001$), one-way ANOVA with Bonferroni posthoc test, $n = 2$ independent experiments using GraphPad Prism 9.4.0. Error bars represent SEM. ALK1: A receptor like type 1; NC: Negative control.

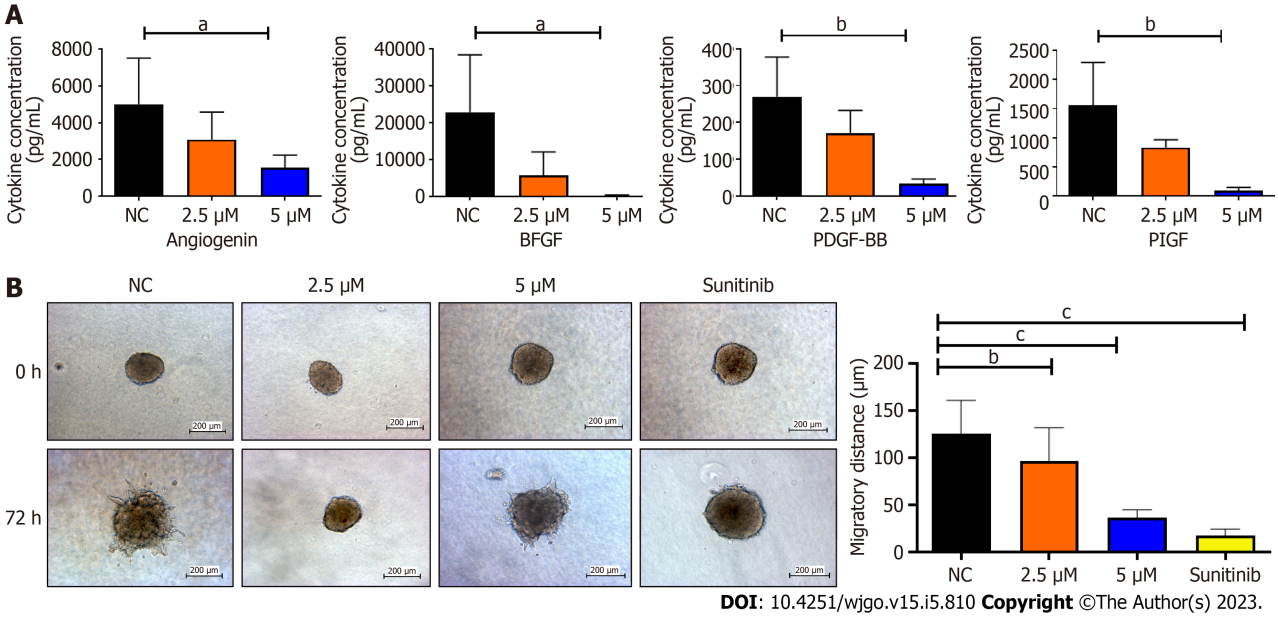

DOI: 10.4251/wjgo.v15.i5.810 **Copyright** ©The Author(s) 2023.

Figure 5 Refreshed conditioned media from Ea.Hy 926 endothelial cells 48 h post-treatment with Sunitinib positive control, BZD9L1 at 2.5 μM, 5.0 μM, or negative control for 48 h prior, were subjected to Quantibody Human Angiogenesis array and indirect co-culture with HCT116 colorectal cancer spheroids. A: BZD9L1 at 5 μM down-regulated angiogenin, fibroblast growth factor, platelet-derived growth factor and placental growth factor cytokine concentrations in Ea.Hy 926 conditioned media; B: The endothelial conditioned media from BZD9L1 or sunitinib positive control-treated groups impeded HCT116 tumor invasion at 72 h. Statistical analysis ($^{a}P < 0.05$; $^{b}P < 0.01$; $^{c}P < 0.001$), one-way ANOVA with Bonferroni posthoc test, $n = 2$ independent experiments for protein array analysis and $n = 3$ independent replicates for co-culture analysis using GraphPad Prism 9.4.0. Error bars represent SEM. NC: Negative control. bFGF: Fibroblast growth factor; PDGF-BB: Platelet-derived growth factor; PIGF: Placental growth factor; NC: Negative control.

adhesive capability at double the IC_{50} of BZD9L1 (10 μM) compared to the negative control at 5 h (Figure 1B), the implicated dose was non-toxic, as revealed by the mean cell index of the EC at early point (Figure 1C). The downregulation of ICAM-1, VE-cadherin and ITGA5 cell adhesion molecules post BZD9L1 treatment in Ea HY926 highlights its potential to inhibit the early steps of angiogenesis.

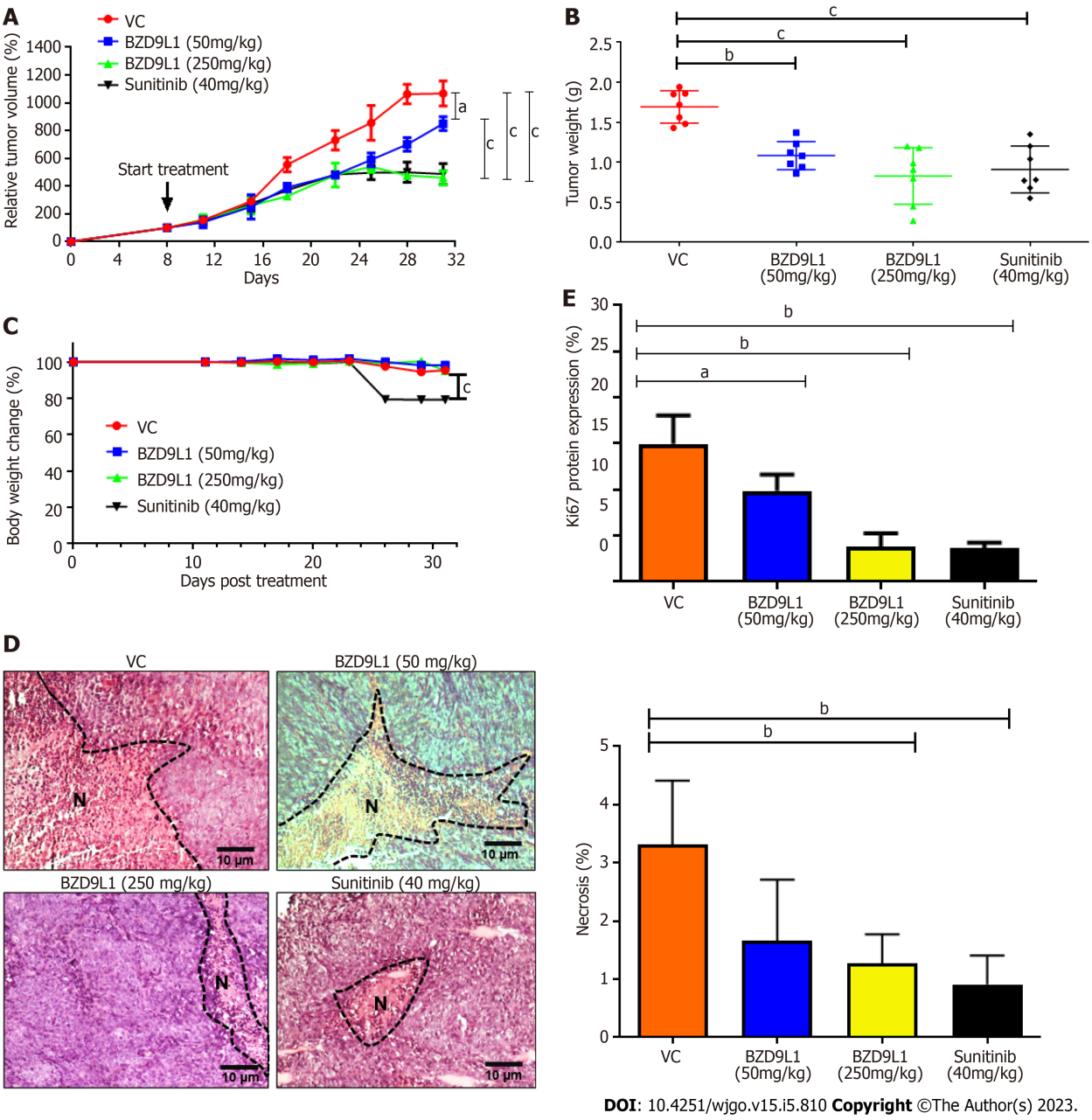

DOI: 10.4251/wjgo.v15.i5.810 **Copyright** ©The Author(s) 2023.

Figure 6 Tumor growth analyses of HCT116 tumor xenograft in nude mice. Treatments were administered when the tumors reached 100 mm^3. A: Relative tumor volume; B: Tumor weight and; C: Percentage body weight change in mice treated with vehicle control (0.5% carboxymethylcellulose), BZD9L1 (50 mg/kg per 3 d, BZD9L1 (250 mg/kg per 3 d) and sunitinib (40 mg/kg per 3 d) as the positive control; D: Tumor necrosis percentage in sections stained with haematoxylin and eosin. N indicates necrotic tissues; E: Ki67 proliferation protein expression in treated and vehicle control groups. Statistical analysis ($^aP < 0.05$; $^bP < 0.01$; $^cP < 0.001$). The non-linear fit was used to track the tumor size and body weight change over time, one-way ANOVA with Bonferroni posthoc test for tumor weight, $n = 6$ animals per group) using GraphPad Prism 9.4.0. Error bars represent SEM. VC: Vehicle control.

The effect of BZD9L1 on a panel of cell adhesion molecules and their post-translational modifications may be crucial to determine the specific mechanisms that may impact EC adhesion stability and function, thus warrants further investigations.

Cell viability is influenced by cell proliferation and cell death. During angiogenesis, ECs exhibit an increased proliferation rate. Cell proliferation is important in the elongation and maturation of new blood vessels. BZD9L1 at all doses reduced the mean cell index (indicative of cell viability or proliferation) of EC at 72 h when compared to the negative control. Nevertheless, a significant decrease in cell index was only noted in EC treated with 10 μM BZD9L1 at 48 h, which served as the basis for proceeding with downstream molecular assays using half the IC_{50} (2.5 μM) and IC_{50} (5.0 μM) BZD9L1. BZD9L1 at the tested doses significantly induced apoptosis and arrested EC at the G1 phase (Figure 3A and B), which suggests that BZD9L1 reduced EC viability by triggering apoptotic cell death and inhibiting cell cycle progression. The G1 phase is where cells prepare to divide. If cells cannot carry out DNA repair at G1 cell cycle arrest, they will enter the apoptosis stage. Cells commit suicide during the

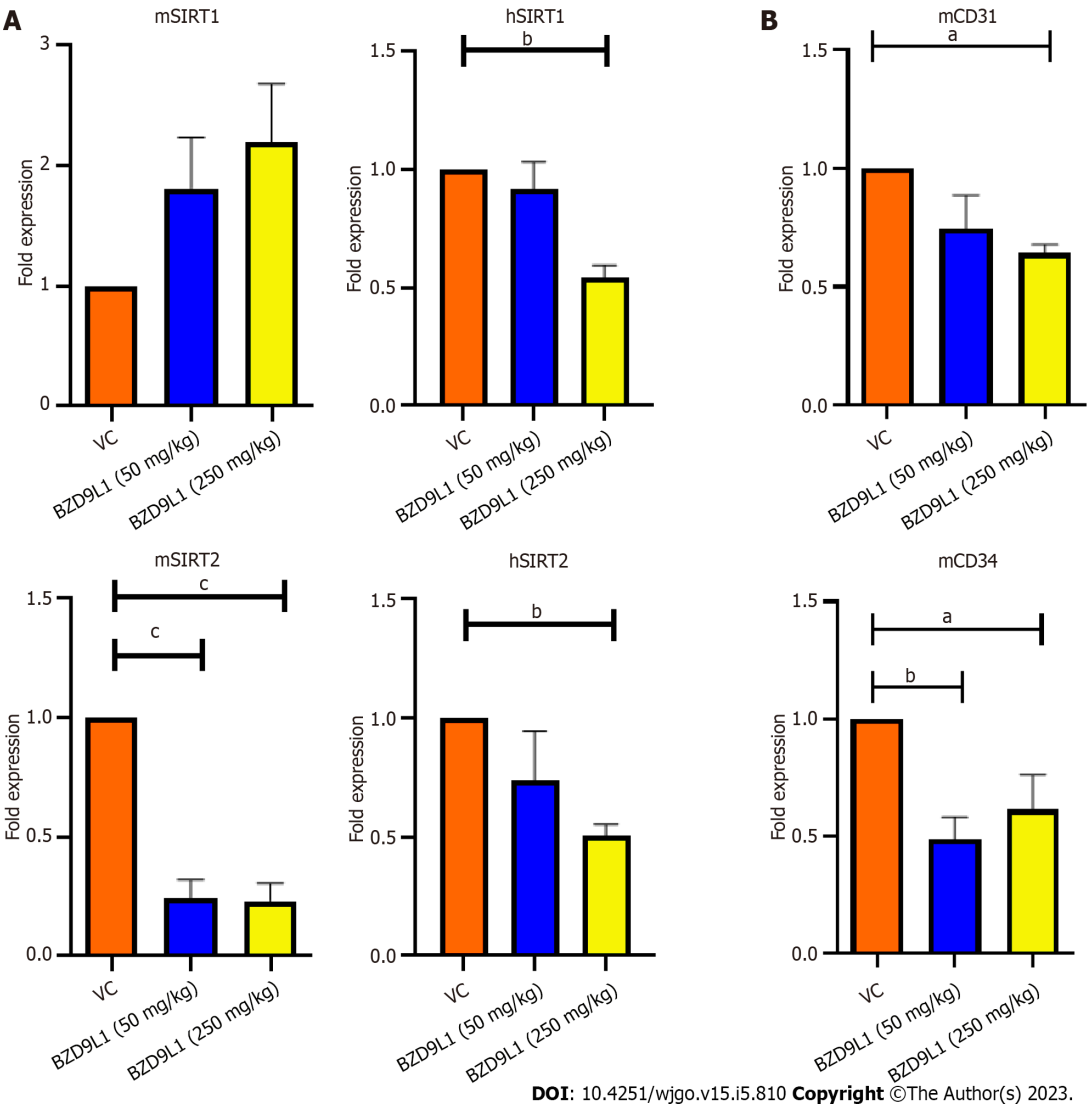

DOI: 10.4251/wjgo.v15.i5.810

Figure 7 Quantitative polymerase chain reaction analyses of murine SIRT1, mSIRT2 and endothelial cell markers in HCT116 tumor xenograft in nude mice. A: BZD9L1 did not significantly affect murine SIRT1 (mSIRT1) gene expression in the colorectal cancer xenograft tumors but downregulated mSIRT2 at low (50 mg/kg) and high (250 mg/kg) doses and reduced human SIRT1 (hSIRT1) and hSIRT2 gene expression at 250 mg/kg, compared to vehicle control; B: BZD9L1 at the high dose significantly reduced cluster of differentiation 31 (CD31) gene expression. Both low and high doses of BZD9L1 decreased mCD34 gene expression compared to vehicle control. Statistical analysis $^{a}P < 0.05$; $^{b}P < 0.01$; $^{c}P < 0.001$), one-way ANOVA with Bonferroni posthoc test, $n = 6$ animals per group) using GraphPad Prism 9.4.0. Error bars represent SEM. VC: Vehicle control.

process of cell apoptosis as a result of signals that start programmed cell death. Apoptosis is crucial for blood vessel regression during angiogenesis[17,18]. Correspondingly, BZD9L1 increased the percentage of apoptotic EC compared with the negative control group, which is corroborated by our previous report in CRC[6].

In a meta-analysis, elevated expression of SIRT1 in CRC is correlated with vascular invasion and inferior outcomes[19]. Meanwhile, increased SIRT2 expression was associated with poor prognosis in CRC patients and the inhibition of SIRT2 Limited CRC tumor angiogenesis *via* inactivation of the STAT3/VEGFA signaling pathway[20]. BZD9L1 downregulated the gene expression of SIRT1 and 2 in Ea.HY926 cells *in vitro* (Figure 2A). Endothelial cell proliferation, migration, and the assembling of vascular networks were reduced when SIRT1 and SIRT2 activities were blocked *in vitro*[20-22]. BZD9L1 at 250 mg/kg reduced the expression of hSIRT1 and hSIRT2 genes, highlighting the ability of BZD9L1 to modulate human SIRTs in HCT116 xenograft tumours which collectively led to the inhibition of tumor growth. However, mSIRT2 but not mSIRT1 was significantly downregulated by BZD9L1 *in vivo* (Figure 7A). BZD9L1 was previously reported to display a higher affinity for SIRT2 than SIRT1[5], which may explain this observation. Furthermore, the tumor microenvironment may play a role in therapeutic response. SIRT1 and SIRT2 are also expressed in other stromal cells, and their interplay may regulate tumor immune responses that impact CRC progression[23,24].

SIRT 1 and SIRT 2 inhibition have been shown to suppress EC proliferation, migration and angiogenesis[25,26]. In human retinal microvascular ECs, SIRT1 downregulation prevented EC

migration and tube formation, whereas SIRT1 overexpression had the opposite effects[26]. The SIRT2 inhibitor, AK-1, dramatically reduced the ability of human umbilical vein ECs (HUVECs) to form tubes [27]. EC spheroid (Figure 3C) and choroidal sprouting (Figure 4A) were shown to be negatively affected by BZD9L1 in an increasing dose. In addition, the compound also regressed sprouting choroids compared to the negative control (Figure 4B). A recent study proved that when sprouting angiogenesis occurs, the vascular endothelium expresses SIRT1 in high levels, and inhibiting SIRT1 function prevents the development and migration of endothelial sprouts as well as the *in vitro* construction of a primitive vascular network[21]. Furthermore, a study on primary murine lung ECs exhibited that when the chemotactic response was muted, tube development was attenuated, and the length of the EC spheroid sprout was shorter in cells lacking SIRT1[28]. Furthermore, SIRT2 knockdown in HUVECs diminished its angiogenic potential, while overexpression of SIRT2 Led to contrasting outcomes[29]. Altogether, these findings highlighted that BZD9L1 negatively regulated SIRT 1 and SIRT 2 to reduce EC viability, adhesion and sprouting.

The EC-conditioned media treated with BZD9L1 at 5 μM portrayed angiogenin, bFGF, PDGF-BB, and PIGF to be significantly reduced compared to the negative control (Figure 5A). Several studies have previously reported angiogenin being essential in EC proliferation that can promote the development of new blood vessels[30,31]. Angiogenin was also shown to stimulate progenitor cell proliferation and protect the stemness of primitive hematopoietic stem/progenitor cells, which suggests that its downregulation may negatively regulate angiogenesis *via* BZD9L1 inhibitory effects. bFGF can impact the upregulation of VEGF directly and promote EC proliferation[32]. The ECs secrete PDGF-BB that binds to PDGFR-β on the mural cells, which then affects the formation and maturation of new capillaries. PlGF also positively regulates angiogenesis; thus, its inhibition reduces EC growth, migration, and survival [33]. Therefore, the downregulation of these cytokines in BZD9L1-treated EC at 5 μM may collectively impede the steps of angiogenesis and HCT116 CRC invasion through paracrine signalling in the co-culture model, while at 2.5 μM, BZD9L1 may potentially reduce CRC invasion through the regulation of other growth factors that were not captured by the protein array (Figure 5B).

BZD9L1 was previously reported to have anti-tumor effects in CRC xenograft models when used in adjunct with 5-Fluorouracil[7]. BZD9L1 did not lead to any acute or repeated dose toxicity symptoms, and neither were there any cellular or molecular changes that would be considered significantly and biologically toxic[10]. In this study, BZD9L1 significantly inhibited the progression of CRC tumor xenograft models. Although the body weight of mice treated with BZD9L1 remained unaffected compared to the vehicle control group, the weight of the mice treated with sunitinib declined treatment, as also confirmed by other studies supporting the weight loss potential of sunitinib in mice by targeting fat cells, leading to appetite loss[34,35]. The mechanisms of weight loss due to sunitinib treatment are poorly understood.

Tumor necrosis is linked to poor prognosis and overall survival of CRC patients[36]. Therefore, the reduction of tumor necrosis in mice treated with 250 mg/kg BZD9L1 further underlines the therapeutic potential of this benzimidazole analogue. On the other hand, Ki67 protein expression was significantly reduced in all treatment groups compared to the vehicle control group, indicating the possibility of BZD9L1 to reduce tumor growth to be *via* the impediment of tumor proliferation. In this study, the amount of vessels left post-treatment were determined *via* gene expression analyses of mCD31 and mCD34, due to the high necrotic nature of the tumors which limited the accurate interpretation of immunohistochemical staining (Figure 7B). BZD9L1 at a high dose significantly reduced mCD31 gene expression compared to the vehicle control group, while both low and high doses of the compound decreased mCD34 gene levels. This may be due to the expression profile of CD31 and CD34, which are not limited strictly to just EC but also a subset of leukocytes and/or hematopoietic progenitor cells that express the CD31 and CD34 antigens, respectively. In addition, gene expression may not positively correlate to protein expression levels due to the turnover rate and possible post-translational modification. Despite this, anti-CD31 and CD34 antibodies are often employed as a diagnostic for vascular malignancies and are highly sensitive indicators of EC differentiation[37,38].

Pathophysiological angiogenesis is mediated by the VEGR which correlates with increased microvessels density and metastatic spread in CRC[39]. Clinical studies showed that resistance developed against angiogenesis inhibitor in single-agent anti-angiogenic therapy. Research has demonstrated the blockage of the VEGF pathway to normalise the tumour-associated vessels. As tumour vasculature matures, angiogenesis inhibitor temporarily reduces tumour hypoxia by improving targeted therapy's efficacy to ensure delivery of oxygen or cytotoxic or cytostatic drugs to the tumour sites[40]. However, the normalisation of tumour vascular usually occurs only transiently at the initial time of anti-angiogenic therapy. Hypoxia increases with prolonged VEGF inhibition due to vessel pruning, which consecutively induces systemic secretion of other pro-angiogenic cytokines[41].

The failure of anti-angiogenic monotherapy may be attributed to the induction of VEGF-independent compensatory mechanisms. The activation of other angiogenic signaling pathways may also induce the expression of other pro-angiogenic cytokines instead of VEGF[42]. Therefore, the development of new inhibitors that target other molecules that are involved in the angiogenesis signaling pathway may be essential. In our study, BZD9L1 did not significantly affect VEGF expression. Hence the compound may be a potential candidate to be employed as an adjunct to VEGF inhibitors or chemotherapy in CRC, as previously reported[7]. Besides, anti-angiogenic therapy combined with chemotherapy or immune

checkpoint inhibitors has demonstrated promising therapeutic effects with enhanced clinical benefits for cancer patients[43]. As such, small molecule inhibitors with anti-angiogenic and anti-cancer capabilities, such as that portrayed by BZD9L1, could be a promising new strategy for cancer therapy by targeting the two distinct features of CRC.

CONCLUSION

BZD9L1 hindered the processes of angiogenesis in EC through the down-regulation of cell adhesion molecules, SIRT1 and SIRT2 genes. Similarly, the angiogenesis array displayed a depletion of angiogenesis cytokines angiogenin, bFGF, PDGF-BB and PIGF in BZD9L1-treated ECs. Furthermore, BZD9L1 arrested the cells at the G1 phase and induced apoptosis in EC. These results suggest that BZD9L1 displayed cytotoxic and cytostatic properties to negatively regulate the formation of new blood vessels. The sprouting potential and the sprout regression were also noted in mouse choroid tissues post-treatment. Moreover, the indirect co-culture assay demonstrated that BZD9L1 could reduce CRC spheroid invasion compared to the negative control. This result potentially suggests that suppression of angiogenesis may obstruct cancer cell progression, as further confirmed *in vivo*. In mice, BZD9L1 had the ability to retard HCT116 colorectal xenograft tumor growth. In relation to this, the tumor necrosis and Ki67 protein expression percentage in the tumor sections were reduced in the BZD9L1-treated groups compared to vehicle control. CD31 and CD34 protein expressions were not evaluated due to the limitation posed by necrosis in the tumor sections. However, gene analyses revealed a decline in these well-reported EC markers in BZD9L1-treated mice.

Overall, this project has provided insights into the potential of BZD9L1 to reduce EC growth and progression *in vitro* and hinder CRC tumor growth *in vivo*. It is noteworthy that this study should be recapitulated using at least one other primary ECs or ECs derived from CRC to confirm the findings. Moreover, BZD9L1 may regulate other angiogenesis players and cancer pathways to impact cancer progression, as suggested in a recent study where 58 other BZD9L1-regulated targets were identified [44]. *In vivo* study in an orthotopic model where the tumor cells will be engrafted into the organ, which matches the cancer cell type may also provide a more realistic model to study the mechanism of action of BZD9L1 and its impact on the tumor microenvironment. Additionally, real-time vessel perfusion imaging may be performed to more accurately assess the efficacy of BZD9L1 treatment[45]. This study provides valuable insights into BZD9L1 as a potential anti-angiogenic agent in CRC.

ARTICLE HIGHLIGHTS

Research background

The growth and spread of colorectal cancer (CRC) are highly dependent on angiogenesis. Epigenetic regulation of the genes in endothelial cells (ECs) in the vicinity of tumor cells plays a vital role in tumor angiogenesis. Sirtuins are class III histone deacetylase enzymes that are implicated in angiogenesis. Their potential roles in cancer have stimulated investigation to seek potent and selective sirtuin (SIRT) inhibitors, potentially leading to new therapeutic breakthroughs. BZD9L1 is a reported small molecule inhibitor with anticancer activities. However, its potential as an anti-angiogenic agent has not been explored.

Research motivation

A patient's prognosis and survival rate remain heterogenous for which tumor attributes, dynamic host response factors, and treatment quality may be accountable. Some CRC patients become resilient to these anti-angiogenic drugs and standard therapies such as chemotherapy and radiation. Hence, this work opens a new avenue for the establishment of a potential novel anti-angiogenic agent through sirtuin inhibition in tumor angiogenesis.

Research objectives

To determine the anti-angiogenic activity of BZD9L1 benzimidazole analogue in CRC.

Research methods

The *in vitro* experiments comprise cell viability, adhesion. spheroid sprouting, quantitative polymerase chain reaction (qPCR), angiogenesis protein array, cell cycle and apoptosis analyses *via* flow cytometry and indirect co-culture. Mouse choroids were employed to assess the negative impact of BZD9L1 on sprouting and vessel regression. HCT116 CRC cells were injected subcutaneously into athymic nude mice and treated with vehicle control or BZD9L1 at 50 mg/kg and 250 mg/kg. Hematoxylin and eosin staining was performed to determine the percentage of necrosis in the tumor section. Finally, immunohistochemistry and qPCR were conducted to investigate the expression of Ki67 protein and murine

CD34/ CD31 as well as SIRT1 and SIRT2, respectively.

Research results

Findings from this study highlighted the ability of BZD9L1 to inhibit EC functions in *in vitro*, *ex vivo* and co-culture models. Additionally, BZD9L1 retarded tumor growth *in vivo* compared to the vehicle control group. Overall, the findings underscore the potential of BZD9L1 to treat CRC.

Research conclusions

BZD9L1 impeded angiogenesis in ECs, mouse choroid tissues and the CRC xenograft model. This study provides valuable insights into BZD9L1 as a potential anti-angiogenic agent in CRC.

Research perspectives

Findings from this study may provide the basis for BZD9L1 benzimidazole analogue as a targeted therapy for the treatment of CRC.

ACKNOWLEDGEMENTS

We acknowledge the Union for International Cancer Control (UICC) for the International Cancer Technology Transfer Fellowship (ICRETT) awarded to Associate Professor Dr Chern Ein Oon which enabled networking and collaboration with Associate Professor Dr Xiaomeng Wang. We thank Mr. David Chung Tze Yang from Genomax Technologies Sdn. Bhd. for technical support on the xCELLigence RTCA instrument (Agilent Technologies).

FOOTNOTES

Author contributions: Oon CE and Subramaniam AV remain to have equal contributions as co-first authors; Oon CE, Subramaniam AV, Ooi LY, and Qiu B carried out the experiments; Lee YT synthesized the BZD9L1 compound; Oon CE drafted and reviewed the manuscript; Subramaniam AV and Ooi LY provided scientific input for "Discussion"; Oon CE, Subramaniam AV, Ooi LY, Qiu B, and Kaur G analyzed the data; Sasidharan S provided scientific input for *in vivo* study; Wang X derived the *ex vivo* angiogenesis models; Oon CE conceived and designed the experiments, and supervised the project; and all the authors have read and approved the final manuscript.

Supported by the Ministry of Higher Education Malaysia for the Fundamental Research Grant Scheme, No. FRGS/1/2021/SKK06/USM/02/7.

Institutional animal care and use committee statement: All procedures involving animals were reviewed and approved by the National University of Singapore Institutional Animal Care and Use Committee guidelines (approval No. 2020/SHS/1597) and Universiti Sains Malaysia Animal Ethical Committee [approval No. USM/IACUC/2017/(105)(872)].

Conflict-of-interest statement: The authors declare that they have no conflict of interest.

Data sharing statement: No additional data are available.

ARRIVE guidelines statement: The authors have read the ARRIVE Guidelines, and the manuscript was prepared and revised according to the ARRIVE Guidelines.

Country/Territory of origin: Malaysia

ORCID number: Chern Ein Oon 0000-0002-4685-6408; Gurjeet Kaur 0000-0002-6232-5703.

Corresponding Author's Membership in Professional Societies: Global Young Academy.

S-Editor: Chen YL
L-Editor: A
P-Editor: Zhao S

REFERENCES

1 **Saif MW**, Elfiky A, Salem RR. Gastrointestinal perforation due to bevacizumab in colorectal cancer. *Ann Surg Oncol* 2007; **14**: 1860-1869 [PMID: 17356952 DOI: 10.1245/s10434-006-9337-9]

2 **Komazin G**, Ptak RG, Emmer BT, Townsend LB, Drach JC. Resistance of human cytomegalovirus to D- and L-ribosyl benzimidazoles as a tool to identify potential targets for antiviral drugs. *Nucleosides Nucleotides Nucleic Acids* 2003; **22**: 1725-1727 [PMID: 14565505 DOI: 10.1081/NCN-120023123]

3 **Pieroni M**, Tipparaju SK, Lun S, Song Y, Sturm AW, Bishai WR, Kozikowski AP. Pyrido[1,2-a]benzimidazole-based agents active against tuberculosis (TB), multidrug-resistant (MDR) TB and extensively drug-resistant (XDR) TB. *ChemMedChem* 2011; **6**: 334-342 [PMID: 21259445 DOI: 10.1002/cmdc.201000490]

4 **Napper AD**, Hixon J, McDonagh T, Keavey K, Pons JF, Barker J, Yau WT, Amouzegh P, Flegg A, Hamelin E, Thomas RJ, Kates M, Jones S, Navia MA, Saunders JO, DiStefano PS, Curtis R. Discovery of indoles as potent and selective inhibitors of the deacetylase SIRT1. *J Med Chem* 2005; **48**: 8045-8054 [PMID: 16335928 DOI: 10.1021/jm050522v]

5 **Yoon Y**, Ali M, Wei A, Choon T, Oon C, Shirazi A, Parang K. Correction: discovery of a potent and highly fluorescent sirtuin inhibitor. *Medchemcomm* 2015; **6**: 2235 [DOI: 10.1039/C5MD90057C]

6 **Tan YJ**, Lee YT, Yeong KY, Petersen SH, Kono K, Tan SC, Oon CE. Anticancer activities of a benzimidazole compound through sirtuin inhibition in colorectal cancer. *Future Med Chem* 2018; **10**: 2039-2057 [PMID: 30066578 DOI: 10.4155/fmc-2018-0052]

7 **Tan YJ**, Lee YT, Petersen SH, Kaur G, Kono K, Tan SC, Majid AMSA, Oon CE. BZD9L1 sirtuin inhibitor as a potential adjuvant for sensitization of colorectal cancer cells to 5-fluorouracil. *Ther Adv Med Oncol* 2019; **11**: 1758835919878977 [PMID: 31632470 DOI: 10.1177/1758835919878977]

8 **Cabebe E**, Wakelee H. Sunitinib: a newly approved small-molecule inhibitor of angiogenesis. *Drugs Today (Barc)* 2006; **42**: 387-398 [PMID: 16845442 DOI: 10.1358/dot.2006.42.6.985633]

9 **Cunha SI**, Pietras K. ALK1 as an emerging target for antiangiogenic therapy of cancer. *Blood* 2011; **117**: 6999-7006 [PMID: 21467543 DOI: 10.1182/blood-2011-01-330142]

10 **Lee YT**, Tan YJ, Mok PY, Kaur G, Sreenivasan S, Falasca M, Oon CE. Sex-divergent expression of cytochrome P450 and SIRTUIN 1-7 proteins in toxicity evaluation of a benzimidazole-derived epigenetic modulator in mice. *Toxicol Appl Pharmacol* 2022; **445**: 116039 [PMID: 35489524 DOI: 10.1016/j.taap.2022.116039]

11 **Oon CE**, Bridges E, Sheldon H, Sainson RCA, Jubb A, Turley H, Leek R, Buffa F, Harris AL, Li JL. Role of Delta-like 4 in Jagged1-induced tumour angiogenesis and tumour growth. *Oncotarget* 2017; **8**: 40115-40131 [PMID: 28445154 DOI: 10.18632/oncotarget.16969]

12 **Shao Z**, Friedlander M, Hurst CG, Cui Z, Pei DT, Evans LP, Juan AM, Tahiri H, Duhamel F, Chen J, Sapieha P, Chemtob S, Joyal JS, Smith LE. Choroid sprouting assay: an ex vivo model of microvascular angiogenesis. *PLoS One* 2013; **8**: e69552 [PMID: 23922736 DOI: 10.1371/journal.pone.0069552]

13 **Qiu B**, Tan A, Tan YZ, Chen QY, Luesch H, Wang X. Largazole Inhibits Ocular Angiogenesis by Modulating the Expression of VEGFR2 and p21. *Mar Drugs* 2021; **19** [PMID: 34436310 DOI: 10.3390/md19080471]

14 **Voce P**, D'Agostino M, Moretti S, Sponziello M, Rhoden K, Calcinaro F, Tamburrano G, Tallini G, Puxeddu E, Filetti S, Russo D, Durante C. Sunitinib inhibits tumor vascularity and growth but does not affect Akt and ERK phosphorylation in xenograft tumors. *Oncol Rep* 2011; **26**: 1075-1080 [PMID: 21850379 DOI: 10.3892/or.2011.1422]

15 **Edgell CJ**, McDonald CC, Graham JB. Permanent cell line expressing human factor VIII-related antigen established by hybridization. *Proc Natl Acad Sci U S A* 1983; **80**: 3734-3737 [PMID: 6407019 DOI: 10.1073/pnas.80.12.3734]

16 **Bauer J**, Margolis M, Schreiner C, Edgell CJ, Azizkhan J, Lazarowski E, Juliano RL. In vitro model of angiogenesis using a human endothelium-derived permanent cell line: contributions of induced gene expression, G-proteins, and integrins. *J Cell Physiol* 1992; **153**: 437-449 [PMID: 1280276 DOI: 10.1002/jcp.1041530302]

17 **Dimmeler S**, Zeiher AM. Endothelial cell apoptosis in angiogenesis and vessel regression. *Circ Res* 2000; **87**: 434-439 [PMID: 10988233 DOI: 10.1161/01.res.87.6.434]

18 **Chavakis E**, Dimmeler S. Regulation of endothelial cell survival and apoptosis during angiogenesis. *Arterioscler Thromb Vasc Biol* 2002; **22**: 887-893 [PMID: 12067894 DOI: 10.1161/01.atv.0000017728.55907.a9]

19 **Hong WG**, Pyo JS. The clinicopathological significance of SIRT1 expression in colon cancer: An immunohistochemical study and meta-analysis. *Pathol Res Pract* 2018; **214**: 1550-1555 [PMID: 30082156 DOI: 10.1016/j.prp.2018.07.022]

20 **Hu F**, Sun X, Li G, Wu Q, Chen Y, Yang X, Luo X, Hu J, Wang G. Inhibition of SIRT2 limits tumour angiogenesis *via* inactivation of the STAT3/VEGFA signalling pathway. *Cell Death Dis* 2018; **10**: 9 [PMID: 30584257 DOI: 10.1038/s41419-018-1260-z]

21 **Potente M**, Ghaeni L, Baldessari D, Mostoslavsky R, Rossig L, Dequiedt F, Haendeler J, Mione M, Dejana E, Alt FW, Zeiher AM, Dimmeler S. SIRT1 controls endothelial angiogenic functions during vascular growth. *Genes Dev* 2007; **21**: 2644-2658 [PMID: 17938244 DOI: 10.1101/gad.435107]

22 **Edatt L**, Poyyakkara A, Raji GR, Ramachandran V, Shankar SS, Kumar VBS. Role of Sirtuins in Tumor Angiogenesis. *Front Oncol* 2019; **9**: 1516 [PMID: 32010617 DOI: 10.3389/fonc.2019.01516]

23 **Fang H**, Huang Y, Luo Y, Tang J, Yu M, Zhang Y, Zhong M. SIRT1 induces the accumulation of TAMs at colorectal cancer tumor sites *via* the CXCR4/CXCL12 axis. *Cell Immunol* 2022; **371**: 104458 [PMID: 34847407 DOI: 10.1016/j.cellimm.2021.104458]

24 **Jiang C**, Liu J, Guo M, Gao X, Wu X, Bai N, Guo W, Li N, Yi F, Cheng R, Xu H, Zhou T, Jiang B, Sun T, Wei S, Cao L. The NAD-dependent deacetylase SIRT2 regulates T cell differentiation involved in tumor immune response. *Int J Biol Sci* 2020; **16**: 3075-3084 [PMID: 33061819 DOI: 10.7150/ijbs.49735]

25 **Gao Z**, Wang H, Xiao FJ, Shi XF, Zhang YK, Xu QQ, Zhang XY, Ha XQ, Wang LS. SIRT1 mediates Sphk1/S1P-induced proliferation and migration of endothelial cells. *Int J Biochem Cell Biol* 2016; **74**: 152-160 [PMID: 26923291 DOI: 10.1016/j.biocel.2016.02.018]

26 **Lin Y**, Li L, Liu J, Zhao X, Ye J, Reinach PS, Qu J, Yan D. SIRT1 Deletion Impairs Retinal Endothelial Cell Migration Through Downregulation of VEGF-A/VEGFR-2 and MMP14. *Invest Ophthalmol Vis Sci* 2018; **59**: 5431-5440 [PMID:

30452596 DOI: 10.1167/iovs.17-23558]

27 **Jung SY**, Kim CM, Kim DY, Lee DH, Lee KS, Kwon S-M. The Role of Sirtuin-2 in Tubular Forming Activity of Human Umbilical Vein Endothelial Cells. *J Life Sci* 2013; **23**: 131-136 [DOI: 10.5352/JLS.2013.23.1.131]

28 **Das A**, Huang GX, Bonkowski MS, Longchamp A, Li C, Schultz MB, Kim LJ, Osborne B, Joshi S, Lu Y, Treviño-Villarreal JH, Kang MJ, Hung TT, Lee B, Williams EO, Igarashi M, Mitchell JR, Wu LE, Turner N, Arany Z, Guarente L, Sinclair DA. Impairment of an Endothelial NAD(+)-H(2)S Signaling Network Is a Reversible Cause of Vascular Aging. *Cell* 2018; **173**: 74-89.e20 [PMID: 29570999 DOI: 10.1016/j.cell.2018.02.008]

29 **Tang Y**, Jin G, Zhang B, Chen K. SIRT2 is down-regulated in myocardial infarction mice and regulates reparative angiogenesis *via* targeting AKT signaling pathway. *Int J Cli Exp Med* 2017; **10**: 11820-11827

30 **Hu G**, Riordan JF, Vallee BL. Angiogenin promotes invasiveness of cultured endothelial cells by stimulation of cell-associated proteolytic activities. *Proc Natl Acad Sci U S A* 1994; **91**: 12096-12100 [PMID: 7991590 DOI: 10.1073/pnas.91.25.12096]

31 **Kim BS**, Kim JS, Yang SS, Kim HW, Lim HJ, Lee J. Angiogenin-loaded fibrin/bone powder composite scaffold for vascularized bone regeneration. *Biomater Res* 2015; **19**: 18 [PMID: 26331087 DOI: 10.1186/s40824-015-0040-4]

32 **Stavri GT**, Zachary IC, Baskerville PA, Martin JF, Erusalimsky JD. Basic fibroblast growth factor upregulates the expression of vascular endothelial growth factor in vascular smooth muscle cells. Synergistic interaction with hypoxia. *Circulation* 1995; **92**: 11-14 [PMID: 7788904 DOI: 10.1161/01.CIR.92.1.11]

33 **Xiang L**, Varshney R, Rashdan NA, Shaw JH, Lloyd PG. Placenta growth factor and vascular endothelial growth factor a have differential, cell-type specific patterns of expression in vascular cells. *Microcirculation* 2014; **21**: 368-379 [PMID: 24410720 DOI: 10.1111/micc.12113]

34 **Kumar RM**, Arlt MJ, Kuzmanov A, Born W, Fuchs B. Sunitinib malate (SU-11248) reduces tumour burden and lung metastasis in an intratibial human xenograft osteosarcoma mouse model. *Am J Cancer Res* 2015; **5**: 2156-2168 [PMID: 26328246]

35 **Tanaka Y**, Shibata MA, Morimoto J, Otsuki Y. Sunitinib suppresses tumor growth and metastases in a highly metastatic mouse mammary cancer model. *Anticancer Res* 2011; **31**: 1225-1234 [PMID: 21508369]

36 **Väyrynen SA**, Väyrynen JP, Klintrup K, Mäkelä J, Karttunen TJ, Tuomisto A, Mäkinen MJ. Clinical impact and network of determinants of tumour necrosis in colorectal cancer. *Br J Cancer* 2016; **114**: 1334-1342 [PMID: 27195424 DOI: 10.1038/bjc.2016.128]

37 **Vieira SC**, Silva BB, Pinto GA, Vassallo J, Moraes NG, Santana JO, Santos LG, Carvasan GA, Zeferino LC. CD34 as a marker for evaluating angiogenesis in cervical cancer. *Pathol Res Pract* 2005; **201**: 313-318 [PMID: 15991838 DOI: 10.1016/j.prp.2005.01.010]

38 **Baumann CI**, Bailey AS, Li W, Ferkowicz MJ, Yoder MC, Fleming WH. PECAM-1 is expressed on hematopoietic stem cells throughout ontogeny and identifies a population of erythroid progenitors. *Blood* 2004; **104**: 1010-1016 [PMID: 15126319 DOI: 10.1182/blood-2004-03-0989]

39 **Lopes-Coelho F**, Martins F, Pereira SA, Serpa J. Anti-Angiogenic Therapy: Current Challenges and Future Perspectives. *Int J Mol Sci* 2021; **22** [PMID: 33916438 DOI: 10.3390/ijms22073765]

40 **Jain RK**. Normalizing tumor vasculature with anti-angiogenic therapy: a new paradigm for combination therapy. *Nat Med* 2001; **7**: 987-989 [PMID: 11533692 DOI: 10.1038/nm0901-987]

41 **Ribatti D**, Annese T, Ruggieri S, Tamma R, Crivellato E. Limitations of Anti-Angiogenic Treatment of Tumors. *Transl Oncol* 2019; **12**: 981-986 [PMID: 31121490 DOI: 10.1016/j.tranon.2019.04.022]

42 **Gacche RN**. Compensatory angiogenesis and tumor refractoriness. *Oncogenesis* 2015; **4**: e153 [PMID: 26029827 DOI: 10.1038/oncsis.2015.14]

43 **Song Y**, Fu Y, Xie Q, Zhu B, Wang J, Zhang B. Anti-angiogenic Agents in Combination With Immune Checkpoint Inhibitors: A Promising Strategy for Cancer Treatment. *Front Immunol* 2020; **11**: 1956 [PMID: 32983126 DOI: 10.3389/fimmu.2020.01956]

44 **Tan YJ**, Lee YT, Mancera RL, Oon CE. BZD9L1 sirtuin inhibitor: Identification of key molecular targets and their biological functions in HCT 116 colorectal cancer cells. *Life Sci* 2021; **284**: 119747 [PMID: 34171380 DOI: 10.1016/j.lfs.2021.119747]

45 **Porter TR**, Xie F, Silver M, Kricsfeld D, Oleary E. Real-time perfusion imaging with low mechanical index pulse inversion Doppler imaging. *J Am Coll Cardiol* 2001; **37**: 748-753 [PMID: 11693747 DOI: 10.1016/s0735-1097(00)01204-3]

World Journal of Gastrointestinal Oncology

Submit a Manuscript: https://www.f6publishing.com

World J Gastrointest Oncol 2023 May 15; 15(5): 828-842

DOI: 10.4251/wjgo.v15.i5.828

ISSN 1948-5204 (online)

ORIGINAL ARTICLE

Retrospective Cohort Study

LipoCol Forte capsules reduce the risk of liver cancer: A propensity score-matched, nationwide, population-based cohort study

Hsiang-Chun Lai, Hung-Jen Lin, Ying-Hsiu Shih, Jen-Wei Chou, Kuan-Wen Lin, Long-Bin Jeng, Sheng-Teng Huang

Specialty type: Gastroenterology and hepatology

Provenance and peer review: Unsolicited article; Externally peer reviewed.

Peer-review model: Single blind

Peer-review report's scientific quality classification

Grade A (Excellent): 0
Grade B (Very good): B
Grade C (Good): 0
Grade D (Fair): D
Grade E (Poor): 0

P-Reviewer: Deng Y, China; Gupta L, Indonesia

Received: January 25, 2023
Peer-review started: January 25, 2023
First decision: February 28, 2023
Revised: March 3, 2023
Accepted: April 19, 2023
Article in press: April 19, 2023
Published online: May 15, 2023

Hsiang-Chun Lai, Graduate Institute of Chinese Medicine, School of Chinese Medicine, College of Chinese Medicine, China Medical University, Taichung 40447, Taiwan

Hung-Jen Lin, School of Post-Baccalaureate Chinese Medicine, College of Chinese Medicine, China Medical University, Taichung 40402, Taiwan

Ying-Hsiu Shih, Management Office for Health Data, China Medical University Hospital, Taichung 40447, Taiwan

Jen-Wei Chou, Department of Internal Medicine, China Medical University Hospital, Taichung 40447, Taiwan

Kuan-Wen Lin, Department of Surgery, China Medical University Hospital, Taichung 40447, Taiwan

Long-Bin Jeng, Organ Transplantation Center, China Medical University Hospital, Taichung 40447, Taiwan

Sheng-Teng Huang, Department of Chinese Medicine, China Medical University Hospital, Taichung 40447, Taiwan

Sheng-Teng Huang, Cancer Research Center for Traditional Chinese Medicine, Department of Medical Research, China Medical University Hospital, Taichung 40447, Taiwan

Sheng-Teng Huang, An-Nan Hospital, China Medical University, Tainan 709204, Taiwan

Sheng-Teng Huang, School of Chinese Medicine, China Medical University, Taichung 40447, Taiwan

Corresponding author: Sheng-Teng Huang, MD, PhD, Doctor, Department of Chinese Medicine, China Medical University Hospital, No. 2 Yude Road, North District, Taichung 40447, Taiwan. sheng.teng@yahoo.com

Abstract

BACKGROUND

Liver cancer is among the top five most common cancers globally. Lipid-lowering drugs such as statins can lower the risk of liver cancer, but may also cause liver damage. LipoCol Forte capsules (LFC), a red yeast rice product, have de-

monstrated significant antihypercholesterolemic effects and a good safety profile in clinical studies.

AIM
To evaluate whether LFC lowers the risk of liver cancer in adults in this propensity score-matched, nationwide, population-based cohort study.

METHODS
We used data from Taiwan's National Health Insurance Research Database, which includes electronic medical records for up to 99.99% of Taiwan's population. LFC users and LFC non-users were matched 1:1 by propensity scores between January 2010 and December 2017. All had follow-up data for at least 1 year. Statistical analyses compared demographic distributions including sex, age, comorbidities, and prescribed medications. Cox regression analyses estimated adjusted hazard ratios (aHRs) after adjusting for potential confounders.

RESULTS
We enrolled 33231 LFC users and 33231 non-LFC users (controls). No significant differences between the study cohorts were identified regarding comorbidities and medications [standardized mean difference (SMD) < 0.05]. At follow-up, the overall incidence of liver cancer was significantly lower in the LFC cohort compared with controls [aHR 0.91; 95% confidence interval (CI): 0.86-0.95; $P < 0.001$]. The risk of liver cancer was significantly reduced in both females (aHR 0.87; 95%CI: 0.8-0.94; $P < 0.001$) and males (aHR 0.93; 95%CI: 0.87-0.98; $P < 0.01$) in the LFC cohort compared with their counterparts in the non-LFC cohort. The antitumor protective effects applied to patients with comorbidities (including hypertension, ischemic stroke, diabetes mellitus, hyperlipidemia, hepatitis B infection and hepatitis C infection). Those using LFC for more than 84 drug days had a 0.64-fold lower risk of liver cancer compared with controls ($P < 0.001$). Compared with controls, the risk of developing liver cancer in the LFC cohort progressively decreased over time; the lowest incidence of liver cancer occurred in LFC users followed-up for more than 6 years (27.44 *vs* 31.49 per 1,000 person-years; aHR 0.75; 95%CI: 0.68-0.82; $P < 0.001$).

CONCLUSION
This retrospective cohort study indicates that LFC has a significantly protective effect on lowering the risk of liver cancer, in a dose-dependent and time-dependent manner.

Key Words: LipoCol Forte capsules; Hyperlipidemia; Liver cancer; Hepatocellular carcinoma; Retrospective cohort study; Taiwan National Health Insurance Research Database

Core Tip: LipoCol Forte capsules (LFC), a red yeast rice product, have lipid-lowering effects and good safety reports. Lipid-lowering therapies such as statins can lower the risk of liver cancer, but may also cause liver damage. We evaluated whether LFC lowers the risk of liver cancer in adults in this propensity score-matched, nationwide, population-based cohort study. The LFC cohort had a 9% lower incidence of liver cancer compared with controls; this lower risk was dose-dependent and time-dependent, with a 0.64-fold lower risk found in those using LFC for more than 84 drug days. The lowest incidence of liver cancer occurred in LFC users followed-up for more than 6 years.

Citation: Lai HC, Lin HJ, Shih YH, Chou JW, Lin KW, Jeng LB, Huang ST. LipoCol Forte capsules reduce the risk of liver cancer: A propensity score-matched, nationwide, population-based cohort study. *World J Gastrointest Oncol* 2023; 15(5): 828-842
URL: https://www.wjgnet.com/1948-5204/full/v15/i5/828.htm
DOI: https://dx.doi.org/10.4251/wjgo.v15.i5.828

INTRODUCTION

LipoCol Forte capsules (LFC) are a product of red yeast rice, which is made by fermenting rice with yeasts, mainly *Monascus purpureus*[1]. Asian countries and territories, including China, Japan and Taiwan, have traditionally used red yeast to make rice wine, increase the intensity of food flavoring and as a food coloring. Traditional Chinese medicine uses red yeast rice as a digestive aid, to promote blood

circulation and alleviate dampness. This fermented rice contains several types of monacolins, gamma-aminobutyric acid, flavonoids, pigments (*e.g.*, rubropunctamine and monascorubramine), polyketides, and dimerumic acid[2,3]. Monacolins are known for their lipid-lowering qualities. In particular, monacolin K lowers cholesterol levels by inhibiting hydroxymethyl glutaryl coenzyme A reductase (HMG-CoA), the rate-controlling enzyme of the cholesterol synthesis pathway[1]. The renowned lipid-lowering drug, lovastatin, is mainly monacolin K. LFC has received approval from the Taiwan Food and Drug Administration for the indication of antihyperlipidemia[4]. Each 600 mg capsule of LFC contains the equivalent of 5.76 mg of lovastatin and the recommended oral dose is twice daily[4]. In a Taiwanese study involving 79 patients with hyperlipidemia, twice-daily dosing with *Monascus purpureus* Went rice therapy (600 mg) LFC significantly reduced levels of low-density lipoprotein (LDL) cholesterol, total cholesterol, triglycerides and apolipoprotein B levels after 4 and 8 weeks compared with placebo therapy, without any major side effects[5]. In another study involving 1530 elderly patients with hypertension and a history of myocardial infarction enrolled in the Chinese Coronary Secondary Prevention Study, a partial extract of red yeast rice reduced the incidence of cardiovascular events and all-cause mortality by lowering LDL and total cholesterol[6].

The Global Burden of Diseases, Injuries, and Risk Factors Study 2019 reported that liver cancer was among the leading five cancers globally by disability-adjusted life years[7]. Risk factors for liver cancer include viral hepatitis (*e.g.*, hepatitis B and hepatitis C), parasitic infestation, alcohol, toxins (*e.g.*, aflatoxin, pesticides) and insulin resistance[8]. In East Asia, hepatitis B and C infections are major contributors to the development of liver cancer[8]. Nonalcoholic fatty liver disease (NAFLD) has been reported by several studies to be an important risk factor for liver cancer[9]. Metabolic dysfunction related to oxidative stress and lipotoxicity promote the development of chronic liver inflammation and fibrosis, and consequently increase the risk of NAFLD-related hepatocellular carcinoma (HCC)[9]. Recently, lipid-lowering therapies such as statins have been linked to a lower risk for HCC[10]. However, these drugs are associated with unwanted side effects such as elevated liver enzymes, myalgia and diabetogenic effects[11]. The risk of adverse drug reactions can increase when statins are co-administered with cytochrome P450 3A4 inhibitors, so some patients discontinue statins in order to decrease the risk of myopathy and other drug-related toxicities[11].

Similar lipid-lowering effects have been reported with red yeast rice products, with a safety advantage[12]. Up until now, no research has reported the preventive effects of red yeast rice on the risk for liver cancer. We are the first to propose that LFC, a red yeast rice extract, decreases the incidence of liver cancer *via* lipid-lowering benefits. In view of the time-consuming nature of cancer development, we decided to conduct a population-based retrospective cohort study using data from the Taiwan National Health Insurance Research Database (NHIRD) for this investigation into the association between LFC use and liver cancer occurrence.

MATERIALS AND METHODS

Data source and ethics approval

The data analyzed in this study were extracted from Taiwan's NHIRD, which was established in 1995 and now includes up to 99.99% of Taiwan's population with their electronic medical records. The database includes demographic data, comprehensive inpatient and outpatient health care information, diagnostic codes, and prescription details for each beneficiary. Prior to 2016, diagnoses in the NHIRD used the International Classification of Diseases, Ninth Edition, Clinical Modification (ICD-9-CM); since 2016, the Tenth Edition (ICD-10) has been used. This study was approved by the Central Regional Research Ethics Committee of China Medical University, Taichung, Taiwan [CMUH109-REC2-031(CR-2)]. The encrypted nature of all individual information contained in the NHIRD meant that informed patient consent could be waived.

Study population

The case cohort consisted of the LFC users (ATC: A047152) during the period from January 2010 through December 2017. For the case cohort, the index date was defined as the first date with a prescription of LFC, whereas for the LFC non-users the index date was a random date within the study period. Patients aged less than 20 years, who had been diagnosed with liver cancer or any other cancer before the index date, or diagnosed with liver cancer within 1 year of LFC use and withdrew from the insurance program before the index date were excluded. Each patient in the case cohort was frequency-matched with the controls (randomly selected from all NHI beneficiaries aged 20 years and more) at a 1:1 ratio by sex, age (every 5 years span), baseline comorbidities, medicine and the index year (Figure 1).

Main outcome and relevant variables

The main outcome of this cohort study was liver cancer (ICD-9-CM codes 155.0, 155.1, 155.2; ICD-10-CM codes C220, C221, C228, C229). The end date of this study was the date when the patients were diagnosed with liver cancer, were lost to follow-up due to withdrawal from the NHIRD or death, or until December 31, 2017. All disease codes including main outcomes and baseline comorbidities were

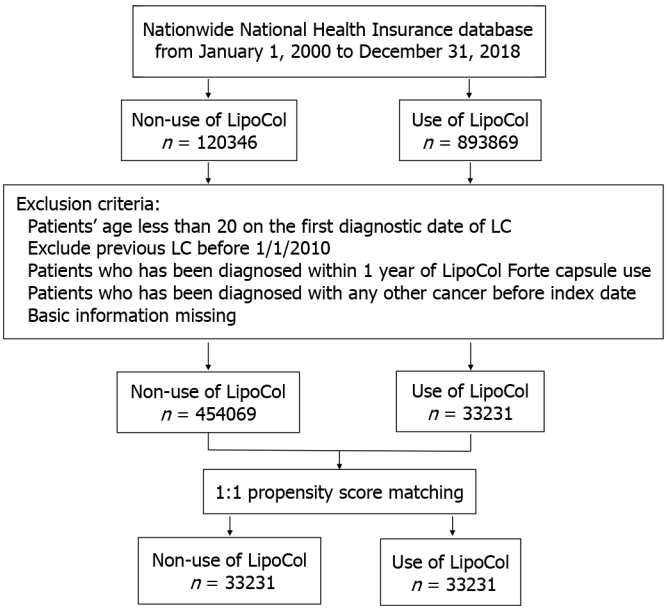

Figure 1 Flow chart of the enrollment of study subjects. LC: Liver cancer.

defined as at least 2 clinic visits or 1 inpatient admission. Comorbidities included hypertension (ICD-9-CM codes 401-405; ICD-10-CM codes I10, I11.0, I11.9, I12.0, I12.9, I13.0, I13.10, I13.11, I15.0, I15.1, I15.8, I15.9), coronary heart disease (ICD-9-CM codes 410-414; ICD-10-CM codes I20.0, I20.1, I20.8, I20.9, I21. I22, I24.1, I24.8, I24.9, I25.1, I25.2), ischemic stroke (ICD-9-CM codes 433, 434, 436, 437; ICD-10-CM codes I63, I65, I66, I67, I68, G46.3-G46.8), hemorrhagic stroke (ICD-9-CM codes 430, 431, 432; ICD-10-CM codes I60-I62), diabetes mellitus (ICD-9-CM code 250; ICD-10-CM codes E08-E13), hyperlipidemia (ICD-9-CM code 272; ICD-10-CM code E78), renal insufficiency (ICD-9-CM codes 585, 586, 588.8, 588.9; ICD-10-CM codes N18, N19, N25.8, N25.9), cirrhosis (ICD-9-CM codes 571.2, 571.5, 571.6; ICD-10-CM codes K70.2, K70.30, K70.31, K74.0, K74.1, K74.2, K74.3, K74.4, K74.5, K74.60, K74.69), alcoholic liver damage (ICD-9-CM codes 571.0, 571.1, 571.3; ICD-10-CM codes K70.0, K70.10, K70.11, K70.40, K70.41, K70.0), NAFLD (ICD-9-CM code 571.8; ICD-10-CM codes K74.4, K75.81, K76.0, K76.89), hepatitis B virus (HBV) infection (ICD-9-CM codes V02.61, 070.20, 070.22, 070.30, 070.32; ICD-10-CM codes Z22.51, B16.2, B16.9, B18.1, B19.10, B19.11) and hepatitis C virus (HCV) infection (ICD-9-CM codes V02.62, 070.41, 070.44, 070.51, 070.54; ICD-10-CM codes Z22.52, B17.10, B17.11, B18.2, B19.20, B19.21) were matched. We also compared medication use between the study groups for statins (simvastatin, lovastatin, fluvastatin, atorvastatin, pravastatin, and rosuvastatin), non-statin lipid-lowering drugs (cholestyramine, colestipol, colesevelam, nicolar, lipo-nicin, acipimox, probucol, gemfibrozil, bezafibrate, etofibrate, fenofibrate, and ezetimibe), aspirin, HBV treatments (lamivudine, adefovir, entecavir, telbivudine, tenofovir and peg-interferon α-2a) and HCV treatments (Harvoni, Sovaldi, Zepatier, Maviret, Epclusa, Viekirax plus Exviera, Daklinza, Daklinza plus Sunvepra and Interferon plus Ribavirin), metformin and thiazolidinedione (TZD) (Pioglitazone and Rosiglitazone).

Statistical analysis

We used the Chi-square test to compare baseline demographic characteristics, comorbidities and medication status between the LFC and non-LFC cohorts. Categorical variables are listed as counts and percentages; the differences in continuous variables are presented as the means and standard deviations, and were evaluated using the unpaired Student's *t*-test. The standardized mean difference (SMD) was calculated to assess the difference of each variable between the LFC users and non-LFC users. An SMD value of less than 0.05 indicated a negligible difference between the two cohorts. In this study, we calculated the hazard ratios (HRs) and 95% confidence intervals (CIs) in univariate and multivariate Cox proportional hazard regression models. Multivariate analysis adjusted for the variables of age, sex, comorbidities and medications. The Kaplan–Meier method was used to estimate the cumulative incidence of liver cancer; the cumulative incidence curve was plotted by R software. SAS statistical software version 9.4 (SAS Institute Inc., Cary, NC, United States) was used for all statistical analyses. Statistical significance was set as a *P* value of less than 0.05.

RESULTS

Baseline demographics and comorbidities of the study population are shown in Table 1. We enrolled

Table 1 Demographic characteristics and comorbidities for non-LipoCol Forte capsules users and LipoCol Forte capsules user populations in Taiwan between 2010 and 2017

Variables	Non-LFC users (*n* = 33231)		LFC users (*n* = 33231)		SMD
	n	%	*n*	%	
Sex					
Female	15869	47.75	15798	47.54	0.004
Male	17362	52.25	17433	52.46	0.004
Age (yr)					
20-29	300	0.90	319	0.96	0.006
30-39	1434	4.32	1545	4.65	0.016
40-49	3677	11.07	3816	11.48	0.013
> 50	27820	83.72	27551	82.91	0.022
mean (SD)	63.22	13.60	62.75	13.62	0.035
Comorbidities					
Hypertension	21195	63.78	20825	62.67	0.023
Coronary heart disease	11255	33.87	10972	33.02	0.018
Ischemic stroke	6902	20.77	6784	20.41	0.009
Hemorrhagic stroke	816	2.46	939	2.83	0.023
Diabetes mellitus	12348	37.16	12172	36.63	0.011
Hyperlipidemia	16793	50.53	16196	48.74	0.036
Renal insufficiency	4028	12.12	4007	12.06	0.002
Cirrhosis	2585	7.78	2643	7.95	0.007
Alcoholic liver damage	2554	7.69	2606	7.84	0.006
Nonalcoholic fatty liver disease	1648	4.96	1825	5.49	0.024
HBV infection	3239	9.75	3342	10.06	0.010
HCV infection	2061	6.20	2196	6.61	0.017
Medications					
Statin	12008	36.13	11666	35.11	0.022
Non-statin lipid-lowering drug	6339	19.08	6161	18.54	0.014
Aspirin	15564	46.84	15330	46.13	0.014
HBV treatment	1531	4.61	1572	4.73	0.006
HCV treatment	7	0.02	10	0.03	0.006
Metformin	8674	26.10	8469	25.49	0.014
Thiazolidinediones	2533	7.62	2483	7.47	0.006

Student's *t*-test. LFC: LipoCol Forte capsules; SMD: Standardized mean difference (a standardized mean difference of 0.05 or less indicates a negligible difference); SD: Standard deviation; HBV: Hepatitis B virus; HCV: Hepatitis C virus.

33231 patients in the LFC cohort and 33231 controls in the non-LFC cohort. Similar proportions in the LFC cohort and non-LFC cohort were male (52.46% and 52.25%, respectively); corresponding mean ages were 62.75 ± 13.62 years and 63.22 ± 13.60 years, respectively. The study subjects were predominantly aged 50 years and over. No significant differences between the study cohorts were observed for the distributions of comorbidities and medications (SMD < 0.05).

Analyses stratified for demographic characteristics, comorbidities and medications in the patients with liver cancer are shown in Table 2. In analyses adjusting for age, sex, comorbidities and medications, the overall incidence of liver cancer was significantly lower in the LFC cohort than in the non-LFC cohort (19.26 *vs* 20.62 per 1000 person-years; aHR 0.91; 95%CI: 0.86-0.95; $P < 0.001$). The risk of liver cancer was significantly reduced in both females (aHR 0.87; 95%CI: 0.8-0.94; $P < 0.001$) and males

Table 2 Incidence rates, hazard ratios and 95% confidence intervals of liver cancer, stratified by sex, age, comorbidities and medications, comparing LipoCol Forte capsules users with non-LipoCol Forte capsules users

	Non-LFC users			LFC users			Crude			Adjusted		
Variable	Event	Person-years	IR	Event	Person-years	IR	cHR	95%CI	*P* value	aHR[1]	95%CI	*P* value
Overall	3848	186604	20.62	3700	192122	19.26	0.89	(0.85, 0.94)[c]	< 0.001	0.91	(0.86, 0.95)[c]	< 0.001
Sex												
Female	1416	91487	15.48	1267	94190	13.45	0.83	(0.77, 0.9)[c]	< 0.001	0.87	(0.8, 0.94)[c]	< 0.001
Male	2432	95117	25.57	2433	97932	24.84	0.93	(0.88, 0.99)[a]	0.014	0.93	(0.87, 0.98)[b]	0.008
Age (yr)												
20-29	11	1884	5.84	9	2054	4.38	0.67	(0.27, 1.68)	0.396	0.61	(0.24, 1.59)	0.313
30-39	68	8881	7.66	77	9854	7.81	0.96	(0.69, 1.34)	0.827	0.79	(0.56, 1.11)	0.178
40-49	285	22392	12.73	290	23617	12.28	0.95	(0.8, 1.12)	0.508	0.91	(0.77, 1.07)	0.249
> 50	3484	153447	22.71	3324	156597	21.23	0.89	(0.85, 0.94)[c]	< 0.001	0.91	(0.87, 0.95)[c]	< 0.001
Comorbidities												
Hypertension												
No	1169	69398	16.85	1281	73107	17.52	1	(0.92, 1.08)	0.910	0.93	(0.86, 1.01)	0.090
Yes	2679	117206	22.86	2419	119015	20.33	0.85	(0.81, 0.9)[c]	< 0.001	0.89	(0.84, 0.94)[c]	< 0.001
Coronary heart disease												
No	2455	124923	19.65	2413	130037	18.56	0.9	(0.85, 0.95)[c]	< 0.001	0.88	(0.84, 0.94)[c]	< 0.001
Yes	1393	61681	22.58	1287	62085	20.73	0.89	(0.83, 0.96)[b]	0.004	0.94	(0.87, 1.02)	0.143
Ischemic stroke												
No	3002	149577	20.07	2983	154633	19.29	0.92	(0.87, 0.97)[b]	0.001	0.91	(0.86, 0.96)[c]	< 0.001
Yes	846	37027	22.85	717	37489	19.13	0.8	(0.73, 0.89)[c]	< 0.001	0.9	(0.81, 0.99)[a]	0.033
Hemorrhagic stroke												
No	3738	182382	20.50	3586	187046	19.17	0.89	(0.85, 0.94)[c]	< 0.001	0.9	(0.86, 0.95)[c]	< 0.001
Yes	110	4222	26.05	114	5076	22.46	0.86	(0.66, 1.12)	0.265	1	(0.76, 1.32)	0.992
Diabetes mellitus												
No	2023	119363	16.95	1972	124172	15.88	0.9	(0.84, 0.96)[c]	< 0.001	0.89	(0.84, 0.95)[c]	< 0.001

Yes	1825	67241	27.14	1728	67950	25.43	0.9	(0.84, 0.96)[b]	0.001	0.92	(0.86, 0.98)[a]	0.010
Hyperlipidemia												
No	1986	92314	21.51	1980	98628	20.08	0.9	(0.84, 0.96)[c]	< 0.001	0.89	(0.83, 0.94)[c]	< 0.001
Yes	1862	94290	19.75	1720	93494	18.40	0.89	(0.83, 0.95)[c]	< 0.001	0.93	(0.87, 1)[a]	0.040
Renal insufficiency												
No	3319	165852	20.01	3221	170964	18.84	0.9	(0.86, 0.95)[c]	< 0.001	0.9	(0.85, 0.94)[c]	< 0.001
Yes	529	20752	25.49	479	21158	22.64	0.86	(0.76, 0.97)[a]	0.016	0.96	(0.85, 1.1)	0.580
Cirrhosis												
No	2514	174893	14.38	2314	180074	12.85	0.84	(0.8, 0.89)[c]	< 0.001	0.83	(0.79, 0.88)[c]	< 0.001
Yes	1334	11711	113.91	1386	12048	115.04	0.98	(0.91, 1.06)	0.606	1	(0.93, 1.08)	0.921
Alcoholic liver damage												
No	3297	173575	19.00	3164	178842	17.69	0.89	(0.84, 0.93)[c]	< 0.001	0.88	(0.84, 0.93)[c]	< 0.001
Yes	551	13029	42.29	536	13281	40.36	0.95	(0.85, 1.07)	0.432	1	(0.88, 1.13)	0.970
Nonalcoholic fatty liver disease												
No	3553	177753	19.99	3404	182155	18.69	0.89	(0.85, 0.94)[c]	< 0.001	0.9	(0.86, 0.94)[c]	< 0.001
Yes	295	8851	33.33	296	9967	29.70	0.86	(0.73, 1.01)	0.06	0.92	(0.78, 1.09)	0.322
HBV infection												
No	2604	170246	15.30	2501	175001	14.29	0.89	(0.84, 0.94)[c]	< 0.001	0.88	(0.83, 0.93)[c]	< 0.001
Yes	1244	16359	76.05	1199	17121	70.03	0.89	(0.82, 0.96)[b]	0.003	0.91	(0.84, 0.99)[a]	0.025
HCV infection												
No	2784	176772	15.75	2658	181323	14.66	0.89	(0.84, 0.94)[c]	< 0.001	0.88	(0.83, 0.93)[c]	< 0.001
Yes	1064	9832	108.22	1042	10799	96.49	0.85	(0.78, 0.92)[c]	< 0.001	0.9	(0.82, 0.98)[a]	0.016
Medication												
Statins												
No	2693	120440	22.36	2681	125954	21.29	0.91	(0.87, 0.97)[b]	0.001	0.91	(0.86, 0.96)[c]	< 0.001
Yes	1155	66164	17.46	1019	66168	15.40	0.84	(0.77, 0.92)[c]	< 0.001	0.92	(0.84, 1)	0.058
Non-statin lipid-lowering drugs												
No	3203	151343	21.16	3080	157120	19.60	0.89	(0.85, 0.93)[c]	< 0.001	0.9	(0.86, 0.95)[c]	< 0.001

Yes	645	35261	18.29	620	35003	17.71	0.92	(0.82, 1.03)	0.135	0.94	(0.84, 1.05)	0.295
Aspirin												
No	1947	101738	19.14	1935	105708	18.31	0.91	(0.86, 0.97)[b]	0.004	0.88	(0.83, 0.94)[c]	< 0.001
Yes	1901	84866	22.40	1765	86414	20.43	0.88	(0.82, 0.94)[c]	< 0.001	0.93	(0.87, 1)[a]	0.043
HBV treatment												
No	2971	179610	16.54	2788	184920	15.08	0.87	(0.82, 0.91)[c]	< 0.001	0.83	(0.79, 0.88)[c]	< 0.001
Yes	877	6994	125.40	912	7203	126.62	0.97	(0.89, 1.07)	0.592	0.99	(0.9, 1.09)	0.807
HCV treatment												
No	3843	186594	20.60	3697	192084	19.25	0.89	(0.86, 0.94)[c]	< 0.001	0.91	(0.87, 0.95)[c]	< 0.001
Yes	5	10	487.00	3	39	77.83	0.21	(0.04, 1.07)	0.060	NA	NA	1
Metformin												
No	2471	140106	17.64	2413	145474	16.59	0.9	(0.85, 0.96)[c]	< 0.001	0.9	(0.85, 0.95)[c]	< 0.001
Yes	1377	46498	29.61	1287	46648	27.59	0.89	(0.82, 0.96)[b]	0.002	0.92	(0.85, 0.99)[a]	0.033
Thiazolidinediones												
No	3453	173105	19.95	3331	178541	18.66	0.89	(0.85, 0.94)[c]	< 0.001	0.91	(0.87, 0.95)[c]	< 0.001
Yes	395	13499	29.26	369	13581	27.17	0.9	(0.78, 1.04)	0.141	0.89	(0.77, 1.03)	0.110

[1]Adjusted in multivariate analysis by sex, age, comorbidities and medications.
[a]$P < 0.05$.
[b]$P < 0.01$.
[c]$P < 0.001$.
LFC: LipoCol Forte capsules; IR: Incidence rate per 1000 person-years; cHR: Crude hazard ratio; aHR: Adjusted hazard ratio; HBV: Hepatitis B virus; HCV: Hepatitis C virus; NA: Not available.

(aHR 0.93; 95%CI: 0.87-0.98; $P < 0.01$) in the LFC cohort compared with their counterparts in the non-LFC cohort. In the subgroup aged over 50 years, LFC users had a significantly lower risk of liver cancer compared with LFC non-users (aHR 0.91; 95%CI: 0.87-0.95; $P < 0.001$). In comorbidity-specific analysis, LFC users with hypertension (aHR 0.89; 95%CI: 0.84-0.94; $P < 0.001$), ischemic stroke (aHR 0.9; 95%CI: 0.81-0.99; $P < 0.05$), diabetes mellitus (aHR 0.92; 95%CI: 0.86-0.98; $P = 0.01$), hyperlipidemia (aHR 0.93; 95%CI: 0.87-1; $P < 0.05$), HBV infection (aHR 0.91; 95%CI: 0.84-0.99; $P < 0.05$), or HCV infection (aHR 0.9; 95%CI: 0.82-0.98; $P < 0.05$) were significantly less likely to develop liver cancer compared with their counterparts in the non-LFC cohort. Among patients with LFC using other medications, those on aspirin (aHR 0.93; 95%CI: 0.87-1; $P < 0.05$) or metformin (aHR 0.92; 95%CI: 0.85-0.99; $P < 0.05$) had a significantly reduced risk of liver cancer compared with patients on aspirin or metformin in the non-LFC cohort.

As shown in Table 3, when analyses assessed the risk of developing liver cancer stratified by days of LFC use and adjusted for demographic factors, comorbidities and medications, the risk of liver cancer was 0.94-fold lower among patients using LFC for fewer than 28 drug days; 0.79-fold lower among those using LFC for any time between 28 and 84 drug days and 0.64-fold lower among those using LFC for more than 84 drug days with medication consumption. After adjusting for age, sex, all comorbidities and medications listed, stratified with each dose of LFC treatment, we found that a higher cumulative dosage of LFC and longer duration had the most protective effects against the development of liver cancer (aHR 0.46; 95%CI: 0.39-0.55) (Table 4). When we further stratified the patients by duration of follow-up into three groups including 2-3 years, 4-6 years and beyond 6 years (Table 5), the risk of developing liver cancer in the LFC cohort progressively decreased over time compared with the risk in the non-LFC cohort; the lowest incidence of liver cancer occurred in LFC users followed-up for more than 6 years (27.44 *vs* 31.49 per 1000 person-years; aHR 0.75; 95%CI: 0.68-0.82; $P < 0.001$). Figure 2 shows the significantly lower cumulative incidence of liver cancer in the LFC cohort compared with the non-LFC cohort after 8 years of follow-up ($P < 0.001$).

DISCUSSION

Although previous studies have shown a benefit with statins in reducing the risk of HCC, this is the first study using a population-based database to show that LFC use significantly decreased the risk of liver cancer by 9% (aHR 0.91) in analyses adjusted for sex, age, comorbidities and medication use. Furthermore, the protective effect of LFC use was dose-dependent, with a progressively lower risk of liver cancer seen with prolonged LFC use.

LFC is a product of red yeast rice. Red yeast rice is a traditional Chinese food that is created by fermenting a red yeast strain (most commonly *Monascus purpureus*) with rice. The major active component in red yeast rice is monacolin K (lovastatin), which has demonstrated good oral bioavailability in red yeast rice products, including LFC[13], and has proven efficacy in the management of dyslipidemia and prevention of steatohepatitis[14,15]. The ability of LFC to prevent metabolic dysfunction suggests that this product may reduce oxidative stress, chronic inflammation and lipid toxicities, and thus prevent liver cancer development[9]. Other research has also suggested that red yeast rice helps to prevent coronary heart disease, diabetes mellitus and cancer[16]. Rice fermented with *Monascus purpureus* reportedly inhibits prostate cancer by decreasing gene expression of androgen-synthesizing enzymes and inducing autophagy[17,18]. Other research also claims beneficial effects of red yeast rice in colon cancer, breast cancer and liver cancers[19-21]. In another study, ankaflavin extracted from *Monascus*-fermented red rice inhibited the growth of human cancer cell lines Hep G2 and A549 by cell cycle arrest and appeared to induce apoptosis[21]. *Monascus purpureus* CWT715 fermented extract has demonstrated antioxidation activity in the BNL cell line (mouse liver cancer) and antimigratory, antiinvasive activities in SK-Hep-1 human hepatocarcinoma cells by inducing nm^{2}3-H1 (non-metastasis protein 23-H1) protein expression[22,23]. Rubropunctamine and monascorubramine, the red *Monascus* pigments, reportedly induce antimitotic effects on immortalized human kidney epithelial cells[24]. Interestingly, azaphilone compounds extracted from rice fermented with *Monascus purpureus* have shown selective cytotoxicity in human cancer cells and not in normal cells at equivalent concentrations[25,26]. Dysbiosis is correlated to liver carcinogenesis. A higher Firmicutes/Bacteroidetes ratio might be associated with a higher liver cancer risk and lower response rate to nivolumab treatment [27]. Red yeast rice can modulate gut microbiota by decreasing *Firmicutes*, *Bacteroidetes*, and *Clostridium* species and increasing *Lactobacillus* and *Ruminococcacea*[28-31]. This amelioration of gut microbiota composition shows that red yeast rice has the potential to prevent liver cancer occurrence. Thus, we hypothesized that LFC can prevent liver cancer not only by lowering cholesterol levels, but also *via* direct antitumor effects with possible mechanisms including cell cycle arrest, antimitotic and gut microbiota modulation.

In subgroup analysis, the benefit of LFC use was significant in both males and females, although LFC appeared to be more protective in females (aHR 0.87) than in males (aHR 0.93). This might be due to sex differences in liver cancer, as for instance is the case with inflammation-driven HCC, which occurs more often in males than in females[32]. Moreover, gender differences exist in the association between metabolic factors and HCC risk[33]. However, we observed significant benefits with LFC treatment only in the over-50-year-old age group, reflected by the larger numbers of cases diagnosed with liver cancers in older-aged patients. Our analyses adjusted for important confounding factors including all lipid-lowering drugs, aspirin, metformin and TZD. Statins have been shown in previous studies to reduce the occurrence of liver cancer, with HRs ranging from 0.4 to 0.72[10,34-36]. A 2013 population-based, case-control study conducted in Taiwan using NHIRD data revealed that statin use reduced the likelihood of HCC by 28% (aHR 0.72)[36]. The same study also identified that the individual statins lovastatin, simvastatin and atorvastatin all significantly lowered the risk of HCC[36]. In our study, the fact that LFC shares a similar pharmacological pathway to that of statins meant that LFC use protected against the development of liver cancer in patients with comorbidities including hypertension, coronary heart disease, ischemic stroke, hemorrhagic stroke, diabetes mellitus, HBV and HCV infection. In patients

Table 3 Incidence and hazard ratios of liver cancer, stratified by the duration of LipoCol Forte capsules use

Variable	*n*	PY	IR	cHR	95%CI	*P* value	aHR[1]	95%CI	*P* value
Non-use of LipoCol Forte capsules as reference	3848	186604	20.621	1.00	Reference		1.00	Reference	
LipoCol Forte capsules									
< 28 d	3115	161794	19.253	0.9	(0.86, 0.94)[c]	< 0.001	0.94	(0.89, 0.98)[b]	0.006
28-84 d	533	27871	19.124	0.87	(0.79, 0.95)[b]	0.002	0.79	(0.72, 0.87)[c]	< 0.001
> 84 d	52	2457	21.165	0.99	(0.75, 1.3)	0.925	0.64	(0.48, 0.84)[b]	0.001

[1]Adjusted in multivariate analysis by sex, age, comorbidities and medications.
[a]*P* < 0.05.
[b]*P* < 0.01.
[c]*P* < 0.001.
PY: Person-years; IR: Incidence rate per 1000 person-years; cHR: Crude hazard ratio; aHR: Adjusted hazard ratio.

Table 4 Cox proportional hazard model estimated hazard ratio among cumulative dose of LipoCol Forte capsules

Variable	*n*	PY	IR	cHR	95%CI	*P* value	aHR[1]	95%CI	*P* value
Non-use of LFC as reference	3848	186604.2	20.6212	1.00	(Reference)	-	1.00	(Reference)	-
LFC dose (g)									
< 91	3182	158379	20.09	0.94	(0.9, 0.98)[b]	0.0089	0.98	(0.94, 1.03)	0.4435
91-179	366	21568	16.97	0.77	(0.69, 0.86)[c]	<0.001	0.69	(0.62, 0.77)[c]	< 0.001
> 179	152	12175	12.48	0.55	(0.47, 0.65)[c]	<0.001	0.46	(0.39, 0.55)[c]	< 0.001

[1]Adjusted in multivariate analysis by sex, age, comorbidities and medications.
[a]*P* < 0.05.
[b]*P* < 0.01.
[c]*P* < 0.001.
LFC: LipoCol Forte capsules; PY: Person-years; IR: Incidence rate per 1000 person-years; cHR: Crude hazard ratio; aHR: Adjusted hazard ratio.

Table 5 The risk of liver cancer by stratified follow-up years

Follow-up time	Non-LFC users			LFC users			cHR	95%CI	aHR[1]	95%CI
	n	PY	IR	*n*	PY	IR				
2-3 yr	1367	93294	14.65	1332	92819	14.35	0.98	(0.91, 1.06)	1.01	(0.93, 1.09)
4-6 yr	1554	63868	24.33	1401	64063	21.87	0.9	(0.84, 0.97)[b]	0.92	(0.86, 0.99)[a]
> 6 yr	927	29442	31.49	967	35241	27.44	0.77	(0.7, 0.84)[c]	0.75	(0.68, 0.82)[c]

[1]Adjusted in multivariate analysis by sex, age, comorbidities and medications.
[a]*P* < 0.05.
[b]*P* < 0.01.
[c]*P* < 0.001.
LFC: LipoCol Forte capsules; PY: Person-years; IR: Incidence rate per 1000 person-years; cHR: Crude hazard ratio; aHR: Adjusted hazard ratio.

without major liver cancer risks such as cirrhosis, alcoholic liver damage, NAFLD, HBV or HCV infection, LFC showed protective effects against liver cancer (aHRs 0.83-0.9). Our results suggest that LFC use is also appropriate for patients who are considered to be at "low risk" of liver cancer. LFC use was beneficial in users of both statin and non-statin lipid-lowering drugs. However, statistical significance was achieved only by the non-users (aHR 0.91 in the statin cohort and aHR 0.9 in the non-statin lipid-lowering drug cohort), due to limited case numbers or fewer synergistic effects because of similar mechanisms between the different classes of lipid-lowering agents. Aspirin has previously been reported to reduce the risk of HCC with increasing dose and duration[37], which is similar to what we observed, with aHRs ranging from 0.61 to 0.73. Notably, patients not receiving HBV or HCV treatment still derived significant benefit from LFC use (aHR 0.83 in the HBV non-treatment cohort and aHR 0.91

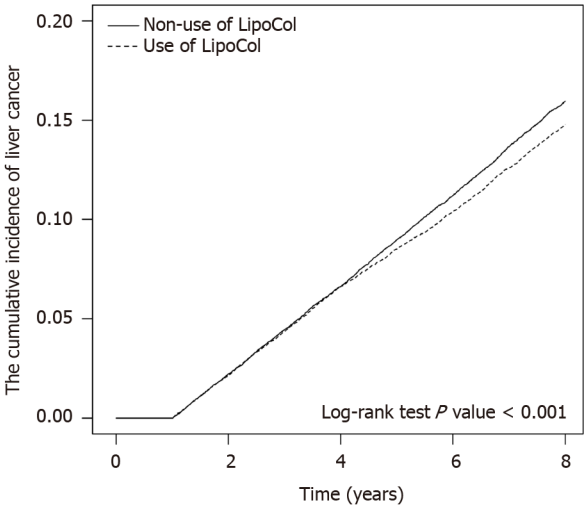

Figure 2 Kaplan-Meier analysis shows the cumulative incidence of liver cancer for patients using LipoCol Forte capsules in comparison with non-users during follow-up lasting more than 8 years.

in the HCV non-treatment cohort). However, the HBV and HCV treatment groups did not reach statistical significance, which is likely due to the treatment of HBV and HCV reducing the progression of liver cancer and potentially masking the LFC-induced protective effect. Moreover, Taiwan's NHIRD did not cover direct-acting antiviral agents in HCV treatment until 2016. Consequently, we only enrolled 8 cases in our cohort study and are therefore unable to formulate any meaningful conclusion. Studies have reported that metformin and TZD lower the risk of HCC, with aHRs ranging from 0.49 to 0.72[38-41]. Thus, we included these drugs in our analyses of confounding factors, to exclude the possibility of an interaction. We observed a significant dose-dependent association between LFC use and the incidence of liver cancer, with aHRs of 0.94, 0.79 and 0.64, respectively, for patients who used LFC for up to 28 d, 28-84 d, or more than 84 d. Our result is similar to reports from other drug-HCC prevention investigations[36,38]. We also report progressively lower cumulative incidence values of liver cancer among LFC users compared with non-LFC users in the 4-6-year subgroup (aHR 0.92; $P < 0.05$) and in the over 6 years subgroup (aHR 0.75; $P < 0.001$). These findings indicate that LFC use reduces the risk of liver cancer development in the long-term.

Taiwan's NHI is a universal healthcare system that covers nearly all of the country's population. The large database enhances the possibility of producing conclusive patient data, with adjustment for sex, age, comorbidities and medication use. However, several limitations must be noted with this study. First, we used the ICD-9-CM (from 2010 to 2015) and the ICD-10-CM (from 2016 to 2017) algorithms to define diseases diagnosed by clinical physicians. We included only patients with correct ICD-9-CM or ICD-10-CM coding after a single inpatient admission, or after two outpatient clinical visits, to increase the validity and accuracy of comorbidity diagnoses. The major outcome of liver cancer diagnosis was double-checked using the Registry for Catastrophic Illness Patient Database. Second, the NHIRD data lack important information on potential confounding factors, including body mass index, cirrhosis severity, hepatitis viral load, alcohol consumption, environmental/chemical exposure, and family history. Furthermore, biochemical data, abdominal ultrasound reports, computed tomography reports, grading and staging of liver cancer, cannot be defined in Taiwan's NHI database studies. The demographic characteristics of our patients, the proportions with cirrhosis, alcoholic liver damage or HBV/HCV infection, were not significantly different between the groups. Thus, the background risk of liver cancer occurrence was likely similar for each group. However, by highlighting potential confounding factors, especially the aspect of drug interactions, our analysis is more advanced than previous NHIRD studies. Third, although we took all potential confounding factors into account, a causal relationship between LFC and liver cancer risk could not be directly inferred owing to the observational nature of this study. Thus, we excluded liver cancers diagnosed within 1 year of study commencement. We also considered potential mechanisms in the management of dyslipidemia, direct antitumor effects and microbiota theories as explanations of our findings, as mentioned earlier. Longer-term, prospective clinical studies are needed to confirm our findings.

CONCLUSION

This is the first study to show that LFC use significantly decreases the risk of liver cancer by 9% in analyses adjusted for sex, age, comorbidities, and medication use. The protective effect of LFC was dose-dependent. Thus, our results of this cohort study suggest that LFC therapy may be associated with

reducing risk of liver cancer over an 8-year follow-up. However, long-term studies are needed to confirm our findings. Since LFC is a cheap and commonly used product, prospective clinical trials are feasible and necessary to confirm its beneficial effects on the prevention of liver cancer.

ARTICLE HIGHLIGHTS

Research background

Liver cancer is among the top five most common cancers globally. Anti-lipid therapies such as statins lowered risk of liver cancer. Lipid-lowering drugs such as statins can lower the risk of liver cancer, but may also cause liver damage. LipoCol Forte capsules (LFC), a red yeast rice product, have demonstrated significant antihypercholesterolemic effects and a good safety profile in clinical studies.

Research motivation

We evaluated whether using LFC lowers the risk of liver cancer.

Research objectives

The objective of this study was to evaluate whether LFC lowers the risk of liver cancer in adults, by analyzing data from Taiwan's National Health Insurance Research Database (NHIRD) in a propensity score-matched, nationwide, population-based cohort study.

Research methods

Patients using LFC and those not using LFC (controls) between January 2010 and December 2017 were selected from Taiwan's NHIRD and matched 1:1 by propensity scores. Statistical analyses assessed between-group demographic differences by sex, age, comorbidities, and prescribed medications.

Research results

We enrolled 33231 patients in the LFC cohort and 33231 controls. The overall incidence of liver cancer was significantly lower in the LFC cohort compared with controls (aHR 0.91; $P < 0.001$). The risk of liver cancer was significantly reduced in both females and males in the LFC cohort compared with their counterparts in the non-LFC cohort. There was a 0.64-fold lower liver cancer risk among those using LFC for more than 84 drug days. The risk of developing liver cancer in the LFC cohort progressively decreased over time; the lowest incidence of liver cancer occurred in LFC users followed-up for more than 6 years.

Research conclusions

This retrospective cohort study indicates that LFC has a significantly protective effect against the development of liver cancer, in a dose-dependent and time-dependent manner.

Research perspectives

Since LFC is a cheap and commonly used product, prospective clinical trials are feasible and necessary to confirm its beneficial effects in the prevention of liver cancer.

ACKNOWLEDGEMENTS

The authors would like to thank MacDonald IJ (China Medical University) for the critical reading and revision of our manuscript.

FOOTNOTES

Author contributions: Lai HC contributed to the conceptualization, methodology, and writing-original draft; Lin HJ contributed to the resources, investigation, validation, and editing; Shih YH contributed to the software, formal analysis, visualization; Chou JW, Lin KW, and Jeng LB contributed to the resources and supervision; Huang ST contributed to the methodology, writing-reviewing and editing, project administration, and funding acquisition.

Supported by the Ministry of Science and Technology of Taiwan, No. NSTC111-2320-B-039-025; and China Medical University Hospital, No. DMR-111-013 and No. DMR-111-195.

Institutional review board statement: The study was approved by the Research Ethics Committee of China Medical University Hospital [CMUH109-REC2-031(CR-2)] and was in compliance with the Declaration of Helsinki.

Informed consent statement: Patients were not required to give informed consent to the study because the analysis used anonymous clinical data that were obtained after each patient agreed to treatment by written consent.

Conflict-of-interest statement: The authors declare that they have no conflict of interest.

Data sharing statement: The datasets generated for this study are available on request to the corresponding author.

STROBE statement: The authors have read the STROBE Statement-checklist of items, and the manuscript was prepared and revised according to the STROBE Statement-checklist of items.

Country/Territory of origin: Taiwan

ORCID number: Hsiang-Chun Lai 0000-0001-7885-619X; Hung-Jen Lin 0000-0002-5258-2490; Ying-Hsiu Shih 0000-0002-3967-784X; Jen-Wei Chou 0000-0002-4674-6487; Kuan-Wen Lin 0000-0002-5983-2480; Long-Bin Jeng 0000-0002-2928-4698; Sheng-Teng Huang 0000-0002-7495-6115.

S-Editor: Yan JP
L-Editor: A
P-Editor: Wu RR

REFERENCES

1 **Cicero AFG**, Fogacci F, Banach M. Red Yeast Rice for Hypercholesterolemia. *Methodist Debakey Cardiovasc J* 2019; **15**: 192-199 [PMID: 31687098 DOI: 10.14797/mdcj-15-3-192]

2 **Wang TJ**, Lien AS, Chen JL, Lin CH, Yang YS, Yang SH. A Randomized Clinical Efficacy Trial of Red Yeast Rice (Monascus pilosus) Against Hyperlipidemia. *Am J Chin Med* 2019; **47**: 323-335 [PMID: 30871361 DOI: 10.1142/S0192415X19500150]

3 **Liu BY**, Xu F, Bai J, Yan DJ, Zhang L, Zhang D, Hu YC. Six new monacolin analogs from red yeast rice. *Chin J Nat Med* 2019; **17**: 394-400 [PMID: 31171275 DOI: 10.1016/S1875-5364(19)30046-9]

4 **Chen TL**, Yeh CC, Lin CS, Shih CC, Liao CC. Effects of red yeast rice prescription (LipoCol Forte) on adverse outcomes of surgery. *QJM* 2019; **112**: 253-259 [PMID: 30496589 DOI: 10.1093/qjmed/hcy278]

5 **Lin CC**, Li TC, Lai MM. Efficacy and safety of Monascus purpureus Went rice in subjects with hyperlipidemia. *Eur J Endocrinol* 2005; **153**: 679-686 [PMID: 16260426 DOI: 10.1530/eje.1.02012]

6 **Li JJ**, Lu ZL, Kou WR, Chen Z, Wu YF, Yu XH, Zhao YC; Chinese Coronary Secondary Prevention Study Group. Beneficial impact of Xuezhikang on cardiovascular events and mortality in elderly hypertensive patients with previous myocardial infarction from the China Coronary Secondary Prevention Study (CCSPS). *J Clin Pharmacol* 2009; **49**: 947-956 [PMID: 19602720 DOI: 10.1177/0091270009337509]

7 **Global Burden of Disease 2019 Cancer Collaboration**, Kocarnik JM, Compton K, Dean FE, Fu W, Gaw BL, Harvey JD, Henrikson HJ, Lu D, Pennini A, Xu R, Ababneh E, Abbasi-Kangevari M, Abbastabar H, Abd-Elsalam SM, Abdoli A, Abedi A, Abidi H, Abolhassani H, Adedeji IA, Adnani QES, Advani SM, Afzal MS, Aghaali M, Ahinkorah BO, Ahmad S, Ahmad T, Ahmadi A, Ahmadi S, Ahmed Rashid T, Ahmed Salih Y, Akalu GT, Aklilu A, Akram T, Akunna CJ, Al Hamad H, Alahdab F, Al-Aly Z, Ali S, Alimohamadi Y, Alipour V, Aljunid SM, Alkhayyat M, Almasi-Hashiani A, Almasri NA, Al-Maweri SAA, Almustanyir S, Alonso N, Alvis-Guzman N, Amu H, Anbesu EW, Ancuceanu R, Ansari F, Ansari-Moghaddam A, Antwi MH, Anvari D, Anyasodor AE, Aqeel M, Arabloo J, Arab-Zozani M, Aremu O, Ariffin H, Aripov T, Arshad M, Artaman A, Arulappan J, Asemi Z, Asghari Jafarabadi M, Ashraf T, Atorkey P, Aujayeb A, Ausloos M, Awedew AF, Ayala Quintanilla BP, Ayenew T, Azab MA, Azadnajafabad S, Azari Jafari A, Azarian G, Azzam AY, Badiye AD, Bahadory S, Baig AA, Baker JL, Balakrishnan S, Banach M, Bärnighausen TW, Barone-Adesi F, Barra F, Barrow A, Behzadifar M, Belgaumi UI, Bezabhe WMM, Bezabih YM, Bhagat DS, Bhagavathula AS, Bhardwaj N, Bhardwaj P, Bhaskar S, Bhattacharyya K, Bhojaraja VS, Bibi S, Bijani A, Biondi A, Bisignano C, Bjørge T, Bleyer A, Blyuss O, Bolarinwa OA, Bolla SR, Braithwaite D, Brar A, Brenner H, Bustamante-Teixeira MT, Butt NS, Butt ZA, Caetano Dos Santos FL, Cao Y, Carreras G, Catalá-López F, Cembranel F, Cerin E, Cernigliaro A, Chakinala RC, Chattu SK, Chattu VK, Chaturvedi P, Chimed-Ochir O, Cho DY, Christopher DJ, Chu DT, Chung MT, Conde J, Cortés S, Cortesi PA, Costa VM, Cunha AR, Dadras O, Dagnew AB, Dahlawi SMA, Dai X, Dandona L, Dandona R, Darwesh AM, das Neves J, De la Hoz FP, Demis AB, Denova-Gutiérrez E, Dhamnetiya D, Dhimal ML, Dhimal M, Dianatinasab M, Diaz D, Djalalinia S, Do HP, Doaei S, Dorostkar F, Dos Santos Figueiredo FW, Driscoll TR, Ebrahimi H, Eftekharzadeh S, El Tantawi M, El-Abid H, Elbarazi I, Elhabashy HR, Elhadi M, El-Jaafary SI, Eshrati B, Eskandarieh S, Esmaeilzadeh F, Etemadi A, Ezzikouri S, Faisaluddin M, Faraon EJA, Fares J, Farzadfar F, Feroze AH, Ferrero S, Ferro Desideri L, Filip I, Fischer F, Fisher JL, Foroutan M, Fukumoto T, Gaal PA, Gad MM, Gadanya MA, Gallus S, Gaspar Fonseca M, Getachew Obsa A, Ghafourifard M, Ghashghaee A, Ghith N, Gholamalizadeh M, Gilani SA, Ginindza TG, Gizaw ATT, Glasbey JC, Golechha M, Goleij P, Gomez RS, Gopalani SV, Gorini G, Goudarzi H, Grosso G, Gubari MIM, Guerra MR, Guha A,

Gunasekera DS, Gupta B, Gupta VB, Gupta VK, Gutiérrez RA, Hafezi-Nejad N, Haider MR, Haj-Mirzaian A, Halwani R, Hamadeh RR, Hameed S, Hamidi S, Hanif A, Haque S, Harlianto NI, Haro JM, Hasaballah AI, Hassanipour S, Hay RJ, Hay SI, Hayat K, Heidari G, Heidari M, Herrera-Serna BY, Herteliu C, Hezam K, Holla R, Hossain MM, Hossain MBH, Hosseini MS, Hosseini M, Hosseinzadeh M, Hostiuc M, Hostiuc S, Househ M, Hsairi M, Huang J, Hugo FN, Hussain R, Hussein NR, Hwang BF, Iavicoli I, Ibitoye SE, Ida F, Ikuta KS, Ilesanmi OS, Ilic IM, Ilic MD, Irham LM, Islam JY, Islam RM, Islam SMS, Ismail NE, Isola G, Iwagami M, Jacob L, Jain V, Jakovljevic MB, Javaheri T, Jayaram S, Jazayeri SB, Jha RP, Jonas JB, Joo T, Joseph N, Joukar F, Jürisson M, Kabir A, Kahrizi D, Kalankesh LR, Kalhor R, Kaliyadan F, Kalkonde Y, Kamath A, Kameran Al-Salihi N, Kandel H, Kapoor N, Karch A, Kasa AS, Katikireddi SV, Kauppila JH, Kavetskyy T, Kebede SA, Keshavarz P, Keykhaei M, Khader YS, Khalilov R, Khan G, Khan M, Khan MN, Khan MAB, Khang YH, Khater AM, Khayamzadeh M, Kim GR, Kim YJ, Kisa A, Kisa S, Kissimova-Skarbek K, Kopec JA, Koteeswaran R, Koul PA, Koulmane Laxminarayana SL, Koyanagi A, Kucuk Bicer B, Kugbey N, Kumar GA, Kumar N, Kurmi OP, Kutluk T, La Vecchia C, Lami FH, Landires I, Lauriola P, Lee SW, Lee SWH, Lee WC, Lee YH, Leigh J, Leong E, Li J, Li MC, Liu X, Loureiro JA, Lunevicius R, Magdy Abd El Razek M, Majeed A, Makki A, Male S, Malik AA, Mansournia MA, Martini S, Masoumi SZ, Mathur P, McKee M, Mehrotra R, Mendoza W, Menezes RG, Mengesha EW, Mesregah MK, Mestrovic T, Miao Jonasson J, Miazgowski B, Miazgowski T, Michalek IM, Miller TR, Mirzaei H, Mirzaei HR, Misra S, Mithra P, Moghadaszadeh M, Mohammad KA, Mohammad Y, Mohammadi M, Mohammadi SM, Mohammadian-Hafshejani A, Mohammed S, Moka N, Mokdad AH, Molokhia M, Monasta L, Moni MA, Moosavi MA, Moradi Y, Moraga P, Morgado-da-Costa J, Morrison SD, Mosapour A, Mubarik S, Mwanri L, Nagarajan AJ, Nagaraju SP, Nagata C, Naimzada MD, Nangia V, Naqvi AA, Narasimha Swamy S, Ndejjo R, Nduaguba SO, Negoi I, Negru SM, Neupane Kandel S, Nguyen CT, Nguyen HLT, Niazi RK, Nnaji CA, Noor NM, Nuñez-Samudio V, Nzoputam CI, Oancea B, Ochir C, Odukoya OO, Ogbo FA, Olagunju AT, Olakunde BO, Omar E, Omar Bali A, Omonisi AEE, Ong S, Onwujekwe OE, Orru H, Ortega-Altamirano DV, Otstavnov N, Otstavnov SS, Owolabi MO, P A M, Padubidri JR, Pakshir K, Pana A, Panagiotakos D, Panda-Jonas S, Pardhan S, Park EC, Park EK, Pashazadeh Kan F, Patel HK, Patel JR, Pati S, Pattanshetty SM, Paudel U, Pereira DM, Pereira RB, Perianayagam A, Pillay JD, Pirouzpanah S, Pishgar F, Podder I, Postma MJ, Pourjafar H, Prashant A, Preotescu L, Rabiee M, Rabiee N, Radfar A, Radhakrishnan RA, Radhakrishnan V, Rafiee A, Rahim F, Rahimzadeh S, Rahman M, Rahman MA, Rahmani AM, Rajai N, Rajesh A, Rakovac I, Ram P, Ramezanzadeh K, Ranabhat K, Ranasinghe P, Rao CR, Rao SJ, Rawassizadeh R, Razeghinia MS, Renzaho AMN, Rezaei N, Rezapour A, Roberts TJ, Rodriguez JAB, Rohloff P, Romoli M, Ronfani L, Roshandel G, Rwegerera GM, S M, Sabour S, Saddik B, Saeed U, Sahebkar A, Sahoo H, Salehi S, Salem MR, Salimzadeh H, Samaei M, Samy AM, Sanabria J, Sankararaman S, Santric-Milicevic MM, Sardiwalla Y, Sarveazad A, Sathian B, Sawhney M, Saylan M, Schneider IJC, Sekerija M, Seylani A, Shafaat O, Shaghaghi Z, Shaikh MA, Shamsoddin E, Shannawaz M, Sharma R, Sheikh A, Sheikhbahaei S, Shetty A, Shetty JK, Shetty PH, Shibuya K, Shirkoohi R, Shivakumar KM, Shivarov V, Siabani S, Siddappa Malleshappa SK, Silva DAS, Singh JA, Sintayehu Y, Skryabin VY, Skryabina AA, Soeberg MJ, Sofi-Mahmudi A, Sotoudeh H, Steiropoulos P, Straif K, Subedi R, Sufiyan MB, Sultan I, Sultana S, Sur D, Szerencsés V, Szócska M, Tabarés-Seisdedos R, Tabuchi T, Tadbiri H, Taherkhani A, Takahashi K, Talaat IM, Tan KK, Tat VY, Tedla BAA, Tefera YG, Tehrani-Banihashemi A, Temsah MH, Tesfay FH, Tessema GA, Thapar R, Thavamani A, Thoguluva Chandrasekar V, Thomas N, Tohidinik HR, Touvier M, Tovani-Palone MR, Traini E, Tran BX, Tran KB, Tran MTN, Tripathy JP, Tusa BS, Ullah I, Ullah S, Umapathi KK, Unnikrishnan B, Upadhyay E, Vacante M, Vaezi M, Valadan Tahbaz S, Velazquez DZ, Veroux M, Violante FS, Vlassov V, Vo B, Volovici V, Vu GT, Waheed Y, Wamai RG, Ward P, Wen YF, Westerman R, Winkler AS, Yadav L, Yahyazadeh Jabbari SH, Yang L, Yaya S, Yazie TSY, Yeshaw Y, Yonemoto N, Younis MZ, Yousefi Z, Yu C, Yuce D, Yunusa I, Zadnik V, Zare F, Zastrozhin MS, Zastrozhina A, Zhang J, Zhong C, Zhou L, Zhu C, Ziapour A, Zimmermann IR, Fitzmaurice C, Murray CJL, Force LM. Cancer Incidence, Mortality, Years of Life Lost, Years Lived With Disability, and Disability-Adjusted Life Years for 29 Cancer Groups From 2010 to 2019: A Systematic Analysis for the Global Burden of Disease Study 2019. *JAMA Oncol* 2022; **8**: 420-444 [PMID: 34967848 DOI: 10.1001/jamaoncol.2021.6987]

8 **Gomaa AI**, Khan SA, Toledano MB, Waked I, Taylor-Robinson SD. Hepatocellular carcinoma: epidemiology, risk factors and pathogenesis. *World J Gastroenterol* 2008; **14**: 4300-4308 [PMID: 18666317 DOI: 10.3748/wjg.14.4300]

9 **Huang DQ**, El-Serag HB, Loomba R. Global epidemiology of NAFLD-related HCC: trends, predictions, risk factors and prevention. *Nat Rev Gastroenterol Hepatol* 2021; **18**: 223-238 [PMID: 33349658 DOI: 10.1038/s41575-020-00381-6]

10 **Wong YJ**, Qiu TY, Ng GK, Zheng Q, Teo EK. Efficacy and Safety of Statin for Hepatocellular Carcinoma Prevention Among Chronic Liver Disease Patients: A Systematic Review and Meta-analysis. *J Clin Gastroenterol* 2021; **55**: 615-623 [PMID: 33606427 DOI: 10.1097/MCG.0000000000001478]

11 **Ramkumar S**, Raghunath A, Raghunath S. Statin Therapy: Review of Safety and Potential Side Effects. *Acta Cardiol Sin* 2016; **32**: 631-639 [PMID: 27899849 DOI: 10.6515/acs20160611a]

12 **Ong YC**, Aziz Z. Systematic review of red yeast rice compared with simvastatin in dyslipidaemia. *J Clin Pharm Ther* 2016; **41**: 170-179 [PMID: 26956355 DOI: 10.1111/jcpt.12374]

13 **Chen CH**, Yang JC, Uang YS, Lin CJ. Improved dissolution rate and oral bioavailability of lovastatin in red yeast rice products. *Int J Pharm* 2013; **444**: 18-24 [PMID: 23352857 DOI: 10.1016/j.ijpharm.2013.01.028]

14 **Lee HS**, Lee YJ, Chung YH, Nam Y, Kim ST, Park ES, Hong SM, Yang YK, Kim HC, Jeong JH. Beneficial Effects of Red Yeast Rice on High-Fat Diet-Induced Obesity, Hyperlipidemia, and Fatty Liver in Mice. *J Med Food* 2015; **18**: 1095-1102 [PMID: 26133037 DOI: 10.1089/jmf.2014.3259]

15 **Fujimoto M**, Tsuneyama K, Chen SY, Nishida T, Chen JL, Chen YC, Fujimoto T, Imura J, Shimada Y. Study of the effects of monacolin k and other constituents of red yeast rice on obesity, insulin-resistance, hyperlipidemia, and nonalcoholic steatohepatitis using a mouse model of metabolic syndrome. *Evid Based Complement Alternat Med* 2012; **2012**: 892697 [PMID: 23320041 DOI: 10.1155/2012/892697]

16 **Yang CW**, Mousa SA. The effect of red yeast rice (Monascus purpureus) in dyslipidemia and other disorders. *Complement Ther Med* 2012; **20**: 466-474 [PMID: 23131380 DOI: 10.1016/j.ctim.2012.07.004]

17 **Hong MY**, Henning S, Moro A, Seeram NP, Zhang Y, Heber D. Chinese red yeast rice inhibition of prostate tumor growth in SCID mice. *Cancer Prev Res (Phila)* 2011; **4**: 608-615 [PMID: 21278313 DOI: 10.1158/1940-6207.CAPR-10-0219]

18 **Chiu HW**, Fang WH, Chen YL, Wu MD, Yuan GF, Ho SY, Wang YJ. Monascuspiloin enhances the radiation sensitivity of human prostate cancer cells by stimulating endoplasmic reticulum stress and inducing autophagy. *PLoS One* 2012; **7**: e40462 [PMID: 22802963 DOI: 10.1371/journal.pone.0040462]

19 **Mahmoud AM**, Aboul-Soud MA, Han J, Al-Sheikh YA, Al-Abd AM, El-Shemy HA. Transcriptional profiling of breast cancer cells in response to mevinolin: Evidence of cell cycle arrest, DNA degradation and apoptosis. *Int J Oncol* 2016; **48**: 1886-1894 [PMID: 26983896 DOI: 10.3892/ijo.2016.3418]

20 **Hong MY**, Seeram NP, Zhang Y, Heber D. Anticancer effects of Chinese red yeast rice *versus* monacolin K alone on colon cancer cells. *J Nutr Biochem* 2008; **19**: 448-458 [PMID: 17869085 DOI: 10.1016/j.jnutbio.2007.05.012]

21 **Su NW**, Lin YL, Lee MH, Ho CY. Ankaflavin from Monascus-fermented red rice exhibits selective cytotoxic effect and induces cell death on Hep G2 cells. *J Agric Food Chem* 2005; **53**: 1949-1954 [PMID: 15769119 DOI: 10.1021/jf048310e]

22 **Chang WT**, Chuang CH, Lee WJ, Huang CS. Extract of Monascus purpureus CWT715 Fermented from Sorghum Liquor Biowaste Inhibits Migration and Invasion of SK-Hep-1 Human Hepatocarcinoma Cells. *Molecules* 2016; **21** [PMID: 27941649 DOI: 10.3390/molecules21121691]

23 **Huang CS**, Hu HH, Tsai YM, Chang WT. In vitro effects of Monascus purpureus on antioxidation activity during fermentation of Kinmen sorghum liquor waste. *J Biosci Bioeng* 2013; **115**: 418-423 [PMID: 23266115 DOI: 10.1016/j.jbiosc.2012.11.003]

24 **Knecht A**, Humpf HU. Cytotoxic and antimitotic effects of N-containing Monascus metabolites studied using immortalized human kidney epithelial cells. *Mol Nutr Food Res* 2006; **50**: 406-412 [PMID: 16598808 DOI: 10.1002/mnfr.200500238]

25 **Li JJ**, Shang XY, Li LL, Liu MT, Zheng JQ, Jin ZL. New cytotoxic azaphilones from Monascus purpureus-fermented rice (red yeast rice). *Molecules* 2010; **15**: 1958-1966 [PMID: 20336024 DOI: 10.3390/molecules15031958]

26 **Zhu L**, Yau LF, Lu JG, Zhu GY, Wang JR, Han QB, Hsiao WL, Jiang ZH. Cytotoxic dehydromonacolins from red yeast rice. *J Agric Food Chem* 2012; **60**: 934-939 [PMID: 22224625 DOI: 10.1021/jf203579f]

27 **Chung MW**, Kim MJ, Won EJ, Lee YJ, Yun YW, Cho SB, Joo YE, Hwang JE, Bae WK, Chung IJ, Shin MG, Shin JH. Gut microbiome composition can predict the response to nivolumab in advanced hepatocellular carcinoma patients. *World J Gastroenterol* 2021; **27**: 7340-7349 [PMID: 34876793 DOI: 10.3748/wjg.v27.i42.7340]

28 **Zhou W**, Guo R, Guo W, Hong J, Li L, Ni L, Sun J, Liu B, Rao P, Lv X. Monascus yellow, red and orange pigments from red yeast rice ameliorate lipid metabolic disorders and gut microbiota dysbiosis in Wistar rats fed on a high-fat diet. *Food Funct* 2019; **10**: 1073-1084 [PMID: 30720827 DOI: 10.1039/c8fo02192a]

29 **Dong Y**, Cheng H, Liu Y, Xue M, Liang H. Red yeast rice ameliorates high-fat diet-induced atherosclerosis in Apoe(-/-) mice in association with improved inflammation and altered gut microbiota composition. *Food Funct* 2019; **10**: 3880-3889 [PMID: 31187839 DOI: 10.1039/c9fo00583h]

30 **Huang YP**, Li P, Du T, Du XJ, Wang S. Protective effect and mechanism of Monascus-fermented red yeast rice against colitis caused by Salmonella enterica serotype Typhimurium ATCC 14028. *Food Funct* 2020; **11**: 6363-6375 [PMID: 32609139 DOI: 10.1039/d0fo01017k]

31 **Huang ZR**, Chen M, Guo WL, Li TT, Liu B, Bai WD, Ai LZ, Rao PF, Ni L, Lv XC. Monascus purpureus-fermented common buckwheat protects against dyslipidemia and non-alcoholic fatty liver disease through the regulation of liver metabolome and intestinal microbiome. *Food Res Int* 2020; **136**: 109511 [PMID: 32846589 DOI: 10.1016/j.foodres.2020.109511]

32 **Zheng B**, Zhu YJ, Wang HY, Chen L. Gender disparity in hepatocellular carcinoma (HCC): multiple underlying mechanisms. *Sci China Life Sci* 2017; **60**: 575-584 [PMID: 28547581 DOI: 10.1007/s11427-016-9043-9]

33 **Chen CL**, Kuo MJ, Yen AM, Yang WS, Kao JH, Chen PJ, Chen HH. Gender Difference in the Association Between Metabolic Factors and Hepatocellular Carcinoma. *JNCI Cancer Spectr* 2020; **4**: pkaa036 [PMID: 33134821 DOI: 10.1093/jncics/pkaa036]

34 **Vahedian-Azimi A**, Shojaie S, Banach M, Heidari F, Cicero AFG, Khoshfetrat M, Jamialahmadi T, Sahebkar A. Statin therapy in chronic viral hepatitis: a systematic review and meta-analysis of nine studies with 195,602 participants. *Ann Med* 2021; **53**: 1227-1242 [PMID: 34296976 DOI: 10.1080/07853890.2021.1956686]

35 **Yang SY**, Wang CC, Chen KD, Liu YW, Lin CC, Chuang CH, Tsai YC, Yao CC, Yen YH, Hsiao CC, Hu TH, Tsai MC. Statin use is associated with a lower risk of recurrence after curative resection in BCLC stage 0-A hepatocellular carcinoma. *BMC Cancer* 2021; **21**: 70 [PMID: 33446127 DOI: 10.1186/s12885-021-07796-7]

36 **Lai SW**, Liao KF, Lai HC, Muo CH, Sung FC, Chen PC. Statin use and risk of hepatocellular carcinoma. *Eur J Epidemiol* 2013; **28**: 485-492 [PMID: 23681775 DOI: 10.1007/s10654-013-9806-y]

37 **Memel ZN**, Arvind A, Moninuola O, Philpotts L, Chung RT, Corey KE, Simon TG. Aspirin Use Is Associated with a Reduced Incidence of Hepatocellular Carcinoma: A Systematic Review and Meta-analysis. *Hepatol Commun* 2021; **5**: 133-143 [PMID: 33437907 DOI: 10.1002/hep4.1640]

38 **Tseng CH**. Metformin and risk of hepatocellular carcinoma in patients with type 2 diabetes. *Liver Int* 2018; **38**: 2018-2027 [PMID: 29956875 DOI: 10.1111/liv.13872]

39 **Antwi SO**, Li Z, Mody K, Roberts LR, Patel T. Independent and Joint Use of Statins and Metformin by Elderly Patients With Diabetes and Overall Survival Following HCC Diagnosis. *J Clin Gastroenterol* 2020; **54**: 468-476 [PMID: 32271517 DOI: 10.1097/MCG.0000000000001182]

40 **Yip TC**, Wong VW, Chan HL, Tse YK, Hui VW, Liang LY, Lee HW, Lui GC, Kong AP, Wong GL. Thiazolidinediones reduce the risk of hepatocellular carcinoma and hepatic events in diabetic patients with chronic hepatitis B. *J Viral Hepat* 2020; **27**: 904-914 [PMID: 32340077 DOI: 10.1111/jvh.13307]

41 **Huang MY**, Chung CH, Chang WK, Lin CS, Chen KW, Hsieh TY, Chien WC, Lin HH. The role of thiazolidinediones in hepatocellular carcinoma risk reduction: a population-based cohort study in Taiwan. *Am J Cancer Res* 2017; **7**: 1606-1616 [PMID: 28744408]

World Journal of Gastrointestinal Oncology

Submit a Manuscript: https://www.f6publishing.com

World J Gastrointest Oncol 2023 May 15; 15(5): 843-858

DOI: 10.4251/wjgo.v15.i5.843

ISSN 1948-5204 (online)

ORIGINAL ARTICLE

Retrospective Study

Epidemiology and outcome of individuals with intraductal papillary neoplasms of the bile duct

Rong-Shou Wu, Wen-Jun Liao, Jing-Sheng Ma, Jia-Kun Wang, Lin-Quan Wu, Ping Hou

Specialty type: Gastroenterology and hepatology

Provenance and peer review: Unsolicited article; Externally peer reviewed.

Peer-review model: Single blind

Peer-review report's scientific quality classification

Grade A (Excellent): A, A
Grade B (Very good): 0
Grade C (Good): C
Grade D (Fair): D
Grade E (Poor): 0

P-Reviewer: Kitamura K, Japan; Šarenac TM, Serbia; Tuysuz U, Turkey; Zamani M, Iran

Received: November 5, 2022
Peer-review started: November 5, 2022
First decision: February 2, 2023
Revised: February 16, 2023
Accepted: March 15, 2023
Article in press: March 15, 2023
Published online: May 15, 2023

Rong-Shou Wu, Wen-Jun Liao, Jia-Kun Wang, Lin-Quan Wu, Ping Hou, Department of Hepatobiliary and Pancreatic Surgery, The Second Affiliated Hospital of Nanchang University, Nanchang 330000, Jiangxi Province, China

Jing-Sheng Ma, Department of Organ Transplantation, The Second Affiliated Hospital of Nanchang University, Nanchang 330000, Jiangxi Province, China

Ping Hou, Department of General Surgery, The First Affiliated Hospital of Gannan Medical College, No. 23 Qingnian Road, Zhanggong District, Ganzhou 341000, Jiangxi Province, China

Corresponding author: Ping Hou, PhD, Surgeon, Surgical Oncologist, Department of General Surgery Department, The First Affiliated Hospital of Gannan Medical College, No. 23 Qingnian Road, Zhanggong District, Ganzhou 341000, Jiangxi Province, China.
houping1986@126.com

Abstract

BACKGROUND

Intraductal papillary neoplasm of the bile duct (IPNB) is a rare distinct subtype of precursor lesions of biliary carcinoma. IPNB is considered to originate from luminal biliary epithelial cells, typically displays mucin-hypersecretion or a papillary growth pattern, and results in cystic dilatation[1]. IPNB develops anywhere in the intrahepatic and extrahepatic biliary tracts, and can occur in various pathological stages from low-grade dysplasia to invasive carcinoma. IPNBs have similar phenotypic changes in the occurrence and development of all subtypes, and the prognosis is significantly better than that of traditional (non-papillary) cholangiocarcinoma.

AIM

To evaluate the clinicopathological features of IPNB to provide evidence-based guidance for treatment.

METHODS

Invasive IPNB, invasive intraductal papillary mucinous neoplasm of the pancreas (IPMN), and traditional cholangiocarcinoma data for affected individuals from 1975 to 2016 were obtained from the Surveillance, Epidemiology, and End Results (SEER) database. Annual percentage changes (APCs) in the incidence and incidence-based (IB) mortality were calculated. We identified the independent predictors of overall survival (OS) and cancer-specific survival (CSS) in indivi-

duals with invasive IPNB.

RESULTS

The incidence and IB mortality of invasive IPNB showed sustained decreases, with an APC of -4.5% (95%CI: -5.1% to -3.8%) and -3.3% (95%CI: -4.1% to -2.6%) ($P < 0.001$), respectively. Similar decreases in incidence and IB mortality were seen for invasive IPMN but not for traditional cholangiocarcinoma. Both OS and CSS for invasive IPNB were better than for invasive IPMN and traditional cholangiocarcinoma. A total of 1635 individuals with invasive IPNB were included in our prognosis analysis. The most common tumor sites were the pancreaticobiliary ampulla (47.9%) and perihilar tract (36.7%), but the mucin-related subtype of invasive IPNB was the main type, intrahepatically (approximately 90%). In the univariate and multivariate Cox regression analysis, age, tumor site, grade and stage, subtype, surgery, and chemotherapy were associated with OS and CSS ($P < 0.05$).

CONCLUSION

Incidence and IB mortality of invasive IPNB trended steadily downward. The heterogeneity of IPNB comprises site and the tumor's mucin-producing status.

Key Words: Surveillance, Epidemiology, and End Results database; Intraductal papillary neoplasms of the bile duct; Subtype; Annual percentage changes; Prognosis

Core Tip: Intraductal papillary neoplasms of the bile duct (IPNB) is a rare subtype of biliary cholangiocarcinoma, and also considered as a counterpart of intraductal papillary mucinous neoplasm of the pancreas (IPMN). Current management decisions are based on anecdotal evidence and small case series. There have been no large-sample multicenter studies of IPNB. This manuscript aimed to evaluate the clinicopathological features of IPNB to provide evidence-based guidance for treatment.

Citation: Wu RS, Liao WJ, Ma JS, Wang JK, Wu LQ, Hou P. Epidemiology and outcome of individuals with intraductal papillary neoplasms of the bile duct. *World J Gastrointest Oncol* 2023; 15(5): 843-858
URL: https://www.wjgnet.com/1948-5204/full/v15/i5/843.htm
DOI: https://dx.doi.org/10.4251/wjgo.v15.i5.843

INTRODUCTION

Intraductal papillary neoplasm of the bile duct (IPNB) is a rare distinct subtype of precursor lesions of biliary carcinoma. IPNB is considered to originate from luminal biliary epithelial cells, typically displays mucin-hypersecretion or a papillary growth pattern, and results in cystic dilatation[1]. IPNB develops anywhere in the intrahepatic and extrahepatic biliary tracts, and can occur in various pathological stages from low-grade dysplasia to invasive carcinoma. IPNBs have similar phenotypic changes in the occurrence and development of all subtypes, and the prognosis is significantly better than that of traditional (non-papillary) cholangiocarcinoma[2]. Based on these characteristics, IPNBs have been called mucinous cholangiocarcinoma, biliary papillomatosis, biliary intraductal papillary neoplasm, mucin-hypersecreting intrahepatic biliary neoplasm, and intraductal papillary neoplasm of the liver[3,4].

According to the 2010 World Health Organization (WHO) classification of tumors in the digestive system, IPNB is defined as the biliary counterpart of intraductal papillary mucinous neoplasm of the pancreas (IPMN) and has identical histopathologic pancreaticobiliary, gastric, intestinal, and oncocytic features[5,6]. Because of the anatomical proximity of the pancreas and the bile duct, the simultaneous development of the foregut endoderm, the peribiliary gland containing multipotent stem cells in biliary tract can differentiate into cholangiocytes as well as hepatocytes or pancreatocytes[7]. However, several important differences between IPMN and IPNB exist, such as the incidence and prognosis of invasive cancer, frequency of each tumor subtype, frequency of mucin production, and the presence of known high risk factors, such as choledocholithiasis and parasitic infection, and gene mutation, such as CTNNB1, TP53, SMAD4 and PIK3CA[8-10].Compared with traditional cholangiocarcinoma, IPNB has also been described anecdotally as a tumor type with limited invasive potential, typically involving only cellular atypia and at most, carcinoma in situ[5].

Unlike invasive IPMN and traditional cholangiocarcinoma in the biliary tract, very little is known about the clinicopathological features and prognostic variables of invasive IPNB. Previous studies were based solely on single-center case series, for example, Wu *et al*[11] reported that IPNB occured mainly in patients of advanced age. In addition, a multicenter study indicated that IPNB shown a better long-term prognosis than traditional cholangiocarcinoma, and were relatively invasive features in extrahepatic lesions[12]. Therefore, the epidemiology, tumor characteristics, treatment strategy, and long-term results of invasive IPNB are limited because of the relatively low case numbers. We conducted a Surveillance, Epidemiology, and End Results (SEER) database evaluation of invasive IPNB to address these shortcomings, and to further elucidate the epidemiological and clinical trends to guide treatment decision-making and to identify further clinical and scientific research areas.

MATERIALS AND METHODS

Data source

The SEER database is an authoritative source of information about cancer incidence and survival rates in the United States. SEER currently collects and publishes data on cancer incidence and survival from population-based cancer registries covering approximately 28% of the United States population, and the database is maintained by the National Cancer Institute (NCI). The SEER Program is the only comprehensive population-based source of information in the United States for cancer stage during diagnosis, incidence, and survival data. Mortality data reported by SEER are provided by the National Center for Health Statistics. Population data used to calculate cancer incidence have passed appropriate standards before abstraction.

Study population

This was a retrospective cohort study using data from SEER databases submitted up to November 2018. Data from 1975 to 2016 are available from 18 SEER registries (with additional and treatment fields): Alaska Natives, Atlanta, California (excluding San Francisco/San José Monterey/Los Angeles), Connecticut, Detroit (metropolitan), Greater Georgia, Hawaii, Iowa, Kentucky, Los Angeles, Louisiana, New Jersey, New Mexico, Rural Georgia, San Francisco-Oakland standard metropolitan statistical area, San José Monterey, Seattle, and Utah. The data are adjusted for areas affected by hurricanes Katrina and Rita.

The database was queried by selecting biliary tract [including other biliary (C240–C249), intrahepatic bile duct (C221), and liver (C220) and pancreas (C250-C259)] as the disease sites [sites recoded according to the international classification of disease (ICD) O–3/WHO 2008)] and using the following codes from the ICD for oncology (ICD-O) 3rd edition: 8050/3, 8260/3, 8450/3, 8453/3, 8471/3, 8480/3, 8481/3, and 8503/3 for invasive IPNB and invasive IPMN[13-16] and 8140/3 and 8160/3 for data on individuals with traditional adenocarcinoma and cholangiocarcinoma of the biliary tract, for comparison[17]. We included 34972 patients with pathological evidence of traditional adenocarcinoma or cholangiocarcinoma of the biliary tract and 9527 patients with invasive IPMN. Invasive IPNBs were categorized as the mucinous subtype of invasive IPNBs (ICD-O-3rd: 8453/3, 8471/3, 8480/3, 8481/3) and the non-mucinous subtype of invasive IPNBs (ICD-O-3rd: 8050/3 8260/3 8450/3, 8503/3). All individuals in our study cohort had pathologically-confirmed diagnoses. In addition, because the smallest unit of survival was months rather than days, the data for individuals who died within 1 mo after diagnosis were excluded to avoid analyzing the situation where the survival time was zero. If individuals did not have complete demographic or clinical pathology and follow-up information, they were excluded (Figure 1).

We recorded the following demographic and clinicopathological variables: sex, age at diagnosis, year of diagnosis, race, detailed tumor site according to the tumor, node and metastasis (TNM) 7 and cancer staging schema, version 0204, histological subtype, SEER historic stage, grade, surgery, radiotherapy, chemotherapy, survival (in months), vital status recode, and cause-specific death. The SEER stage classification provides consistent time rather than the American Joint Committee on Cancer stage classification, which may have changed during the study period. Field descriptions of the TNM7/CSv0204 + schema information was collected under the specifications of a particular schema according to site and histology, such as site recode: 003 am pull avatar bile (defined pancreaticobiliary ampulla); 006 bile ducts distal; 007 bile ducts intrahepatic; 008 bile ducts perihilar; 009 biliary other; and 062 liver. The SEER historic stages are divided into four stages: localized stage (confined to the primary site), regional stage (spread to regional lymph nodes), distant stage (cancer had metastasized), and unstaged or unknown. The types of surgical treatment include defined radical surgery, non-defined radical surgery, and palliative surgery. The defined radical surgery includes: radical surgery (partial/total removal of primary site plus partial or total removal of other organs); radical surgery; partial/simple removal of primary site with dissection of lymph nodes; wedge resection, nitric oxide synthase (NOS) segmental resection, lobectomy; extended lobectomy: resection of a single lobe plus a segment of another lobe. The undefined radical surgery includes surgery, NOS; partial/simple removal of primary site without dissection of lymph nodes; surgery of regional and/or distant site(s)/node(s) only. Palliative surgery included: excisional biopsy; polypectomy; excision of lesion and photodynamic therapy. The primary

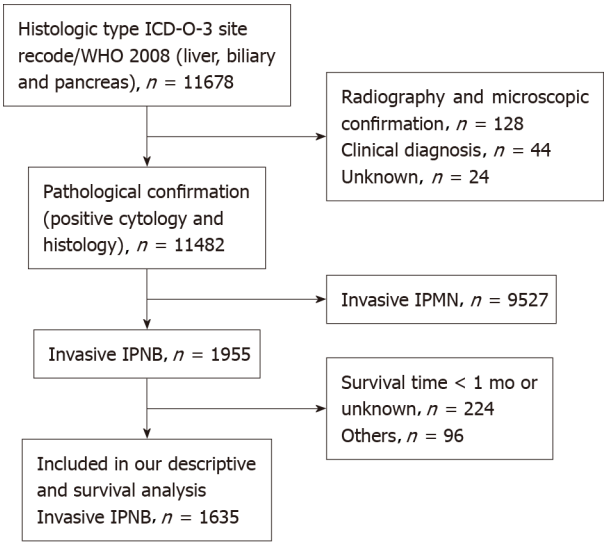

DOI: 10.4251/wjgo.v15.i5.843

Figure 1 Flow diagram of individual selection from the 11678 individuals identified to have invasive intraductal papillary neoplasm of the bile duct within the Surveillance, Epidemiology, and End Results database from 1975-2016 to identify those who were included in our descriptive (excluding incidence trends) and survival analyses. IPNB: Intraductal papillary neoplasm of the bile duct.

outcomes of our cohort study were the overall survival (OS) rate and the cancer-specific survival (CSS) rate. OS was calculated as the time from diagnosis to death (from any cause), and CSS was calculated as the time from diagnosis to death (attributable to the cancer).

Statistical analyses

The incidence rates of invasive IPNB, invasive IPMN, and cholangiocarcinoma were calculated per 1000000 persons, and results were age-adjusted to the 2000 United States standard population using SEER*Stat (version 8.3.8). Annual percentage changes (APCs) of incidence and incidence-based (IB) mortality were calculated using the NCI joinpoint regression analysis program (version 4.8.0.1). APC is a method of describing incidence or mortality trends over time by showing slope gradients or directions for each straight segment. Therefore, tumor incidence or mortality rate is considered to change by a constant percentage from the previous year. We used linear-by-linear association tests to evaluate the trends in the ordinal data, which provides a meaningful measure of ordinal variables; the SEER*Stat software calculates 95%CIs. The Kaplan- Meier method and the log-rank test were used to calculate the cumulative survival rate and survival curves. We used a Cox proportional hazard regression model in the multivariable analysis using IBM SPSS Statistics software (version 26; IBM Corp., Armonk, NY). The multi-variables analysed included patient age, site, tumour grade, stage, mucin classification and treatment. *P* values were two-sided, and *P* values < 0.05 were considered statistically significant.

RESULTS

Characteristics of the included individuals and the tumors

A total of 11678 individuals were diagnosed with invasive IPNB and invasive IPMN in the pancreaticobiliary duct system from 1975 to 2016. Of these individuals, 1635 individuals met our study criteria (Figure 1). The percentages of the mucin-related subtype and non-mucin subtype of invasive IPNBs were 56.6% (*n* = 926) and 43.4% (*n* = 709), respectively. The mean age and standard deviation in the total cohort was 69 ± 12.2 years, and the median age of the overall cohort was 68 years (range: 27-97 years). Individuals aged ≥ 68 and < 68 years accounted for 51.3% and 48.7% of the individuals, respectively. The proportions of men and women in the total cohort were 54.8% (*n* = 896) and 45.2% (*n* = 739), respectively. The vast majority of invasive IPNB patients were white (*n* = 1278, 78.2%). The tumor sites differed significantly and were most commonly the pancreaticobiliary ampulla (*n* = 783, 47.9%) and the perihilar tract (*n* = 600, 36.7%), followed by the liver (*n* = 100, 6.1%), intrahepatic biliary tract (*n* = 99, 6.1%), and distal tract (*n* = 53, 3.2%). The mucin-related subtype of invasive IPNB was the main type in the intrahepatic biliary duct system. The percentages of the locations of the mucin-related subtype were both nearly 90% (liver: 90/100, intrahepatic bile duct: 87/99). Most individuals had SEER historic stage regional tumors (*n* = 814, 49.8%), followed by the localized stage (*n* = 401, 24.5%), distant stage (*n* = 317, 19.4%), and unstaged or unknown (*n* = 103, 6.3%). Tumors were categorized by pathological grade as follows: well-differentiated, grade I (*n* = 373, 22.8%); moderately-differentiated, grade II (*n* = 532, 32.5%);

poorly-differentiated, grade III (n = 227, 13.9%); and undifferentiated grade (n = 22, 1.3%) and unknown grade (n = 481, 29.4%). In the total cohort, 60.1% (n = 982) of individuals with invasive IPNB underwent surgery, and 35.4% (n = 579) received defined radical surgery, 22.9% (n = 375) received undefined radical surgery, 1.8% (n = 28) received palliative surgery, while only 17.5% (n = 286) received radiotherapy, and 28.0% (n = 458) received chemotherapy (Table 1). Approximately 11.5% (n = 188) of the individuals underwent combined radiotherapy, and chemotherapy, while 15.0% (n = 245) of the individuals underwent combined surgery and chemotherapy; 11.4% (n = 187) underwent combined surgery and radiotherapy. Only 8.1% (n = 133) of the individuals received triple therapy (chemotherapy, radiotherapy, and surgery).

Overall incidence and mortality trends

During the study period, the incidence of invasive IPNB decreased steadily (Figure 2A), as with invasive IPMN; however, the incidence of traditional cholangiocarcinoma increased steadily (Figure 2B and C). The incidence of invasive IPNB was 2.2 cases per 1000000 individuals in 1975 and 0.3 cases per 1000000 individuals in 2016. The APC over this period was -4.5% (95%CI: -5.1% to -3.8%; P < 0.05). While the slope of the decrease increased near 1999, the APC (*i.e.*, the extent of the decrease) for the incidence of invasive IPNB from 1999 to 2016 was -6.6% per year (95%CI: -8.8% to -4.4%; P < 0.05), whereas from 1975 to 1999, the change was -3.2% per year (Supplementary Figure 1A). Similarly, the incidence of invasive IPMN also showed a sustained decrease (Figure 2B). The incidence of invasive IPMN was 6.8 cases per 1000000 individuals in 1975 and 3.1 cases per 1000000 individuals in 2016. The APC of invasive IPMN over this period was -1.9% (95%CI: -2.3% to -1.5%; P < 0.05). Conversely, the incidence of traditional cholangiocarcinoma in the biliary tract increased steadily. The incidence of traditional cholangiocarcinoma was 11.4 cases per 1000000 individuals in 1975 and 28.3 cases per 1000000 individuals in 2016, and the APC was 2.18% (95%CI: 2.0%-2.3%; P < 0.05) (Figure 2C).

The IB mortality of invasive IPNB also showed a steady decrease over the study period (Figure 2D), with an APC of -3.3% (95%CI: -4.1% to -2.6%; P < 0.05), and a decrease from 2.1 cases per 1000000 individuals in 1975 to 0.5 cases per 1000000 individuals in 2016 (Figure 2D). While the slope of the decrease increased near 1999, the APC for the IB mortality of invasive IPNB from 1999 to 2016 was -5.7% per year (95%CI: -7.9% to -3.3%; P < 0.05), whereas from 1977 to 1999, the change was -2.5% per year (95%CI: -4.2% to -0.8%; P < 0.05) (Supplementary Figure 1B). The changes were similar for IPMN, which also showed decreased IB mortality over the study period, with an APC of -1.83% (95%CI: -2.2% to -0.8%; P < 0.05) (Figure 2E). Conversely, the IB mortality for traditional cholangiocarcinoma increased during the study period, from 6.6 cases per 1000000 individuals in 1975 to 24.9 cases per 1000000 individuals in 2016; the APC was 2.36% (95%CI: 2.1%-2.6%; P < 0.05) (Figure 2F).

Trends by sex

Regarding the incidence by sex, we found a steady decreasing trend in invasive IPNB incidence in males from 1975 to 2016; the APC was -4.8 % (95%CI: -5.7 to -3.8; P < 0.01). The incidence in males was 3.6 per 1000000 individuals in 1975 and 0.5 per 1000000 individuals in 2016 (Supplementary Figure 2A). The incidence of invasive IPNB in females followed a similar pattern. The APC was -4.5% (95%CI: -5.4 to -3.7; P < 0.01), and 2.2 per 1000000 individuals in 1975 and 0.3 per 1000000 individuals in 2016 (Supplementary Figure 2B). In both males and females, the IB mortality rate of invasive IPNB also decreased during 1975-2016. The APCs were -3.39% (95%CI: -4.4 to -2.4; P < 0.01) and -3.43% (95%CI: -4.2 to -2.7; P < 0.01), respectively (Supplementary Figure 2C and D).

OS and CSS in invasive IPNB, invasive IPMN, and traditional cholangiocarcinoma

Both OS and CSS for invasive IPNB improved (Supplementary Figure 3A and B) during 1975-1985, 1986-1995, 1996-2005, and 2005-2016. The Kaplan-Meier OS and CSS analyses showed that invasive IPNB had better survival than invasive IPMN and traditional cholangiocarcinoma (Figure 3A and B; log-rank P < 0.001). The median OS and CSS of individuals with invasive IPNB in this cohort was 17 mo (95%CI: 15-18 mo) and 27 mo (95%CI: 24-29 mo), respectively, and the 1-, 3-, and 5-year OS and CSS rates were 58.2% and 68.6%, 31.5% and 43.5%, and 23.2% and 36.4%, respectively. However, the median OS and CSS of individuals with invasive IPMN was the worst at only 6 mo (95%CI: 5.8-6.2 mo) and 9 mo (95%CI: 8.6-9.4 mo), respectively, and the 1-, 3-, and 5-year OS and CSS rates were 30.3% and 39.5%, 11.5% and 18.8%, and 8.4% and 15%, respectively. The median OS and CSS of individuals with traditional cholangiocarcinoma was 10 mo (95%CI: 9.7-10.2 mo) and 15 mo (95%CI: 14.6-15 mo), respectively; and 1-, 3- and 5-year OS rates were 43.9% and 54.1%, 18.3% and 28.6%, and 12.4% and 22.2%, respectively.

The OS and CSS for invasive IPNB differed for different tumor locations and subtypes. Kaplan-Meier and long-rank analyses showed that the non-mucin subtype had better OS and CSS than for the mucin subtype, and invasive IPNB located in the distal tract and at the ampulla had the best prognosis (Figure 3C-F; log-rank P < 0.001). Interestingly, both the OS and CSS of the mucin and non-mucin subtypes of invasive IPMN were also statistically significant (Supplementary Figure 3C and D; log-rank P < 0.001). The median OS and CSS of individuals with the non-mucin subtype of invasive IPNB were 27 mo (95%CI: 24-30 mo) and 42 mo (95%CI: 32-52 mo), respectively, and the 1-, 3-, and 5-year OS and

Table 1 Demographics and clinicopathologic characteristics of patients with invasive intraductal papillary neoplasm of the bile duct, *n* (%)

Variable	Total (*n* = 1635)	Subtype 1 (mucin)	Subtype 2 (non-mucin)
Age at diagnosis, yr		*n* = 926	*n* = 709
< 68	796 (48.7)	464 (50.1)	332 (46.8)
≥ 68	839 (51.3)	462 (49.9)	377 (53.2)
Sex			
Male	896 (54.8)	504 (56.3)	392 (55.3)
Female	739 (45.2)	422 (45.6)	317 (44.7)
Race			
White	1278 (78.2)	741 (80.0)	537 (75.7)
Black	116 (7.1)	67 (7.2)	49 (7.1)
Others	241 (14.7)	118 (12.7)	123 (17.3)
THM 7/CSv0204+ schema			
Liver	100 (6.1)	90 (9.7)	10 (1.4)
Intrahepatic bile	99 (6.1)	87 (9.4)	12 (1.7)
Perihilar bile	600 (36.6)	304 (32.8)	296 (41.7)
Distal bile	53 (3.2)	27 (2.9)	26 (3.7)
Pancreaticobiliaryampulla	783 (47.9)	418 (45.1)	365 (51.5)
SEER historic stage			
Localized	401 (24.5)	130 (14)	271 (38.2)
Regional	814 (49.8)	482 (52.1)	332 (46.8)
Distant	317 (19.4)	259 (28)	58 (8.2)
Unstaged	103 (6.3)	55 (5.9)	48 (6.8)
Grade			
Well (I)	373 (22.8)	119 (12.9)	254 (35.8)
Moderately (II)	532 (32.5)	310 (33.5)	222 (31.3)
Poorly (III)	227 (13.8)	176 (19.0)	51 (7.2)
Undifferentiated (IV)	22 (1.3)	11 (1.2)	11 (1.6)
Unknown	481 (29.4)	310 (33.5)	171 (24.1)
Surgery			
Performed	982 (60.1)	483 (52.2)	489 (70.4)
Defined radical surgery	579 (35.4)	336 (36.3)	243 (35.0)
Undefined radical surgery	375 (22.9)	130 (14.1)	235 (33.4)
Palliative surgery	28 (1.8)	17 (1.8)	11 (2.0)
Non	653 (39.9)	443 (47.8)	210 (29.6)
Radiatherapy			
Performed	286 (17.5)	173 (18.7)	113 (15.9)
Non	1349 (82.5)	753 (81.3)	596 (84.1)
Chemotherapy			
Performed	458 (28.0)	339 (36.6)	119 (16.8)
Non	1177 (72.0)	587 (63.4)	590 (83.2)

SEER: Surveillance, Epidemiology, and End Results database.

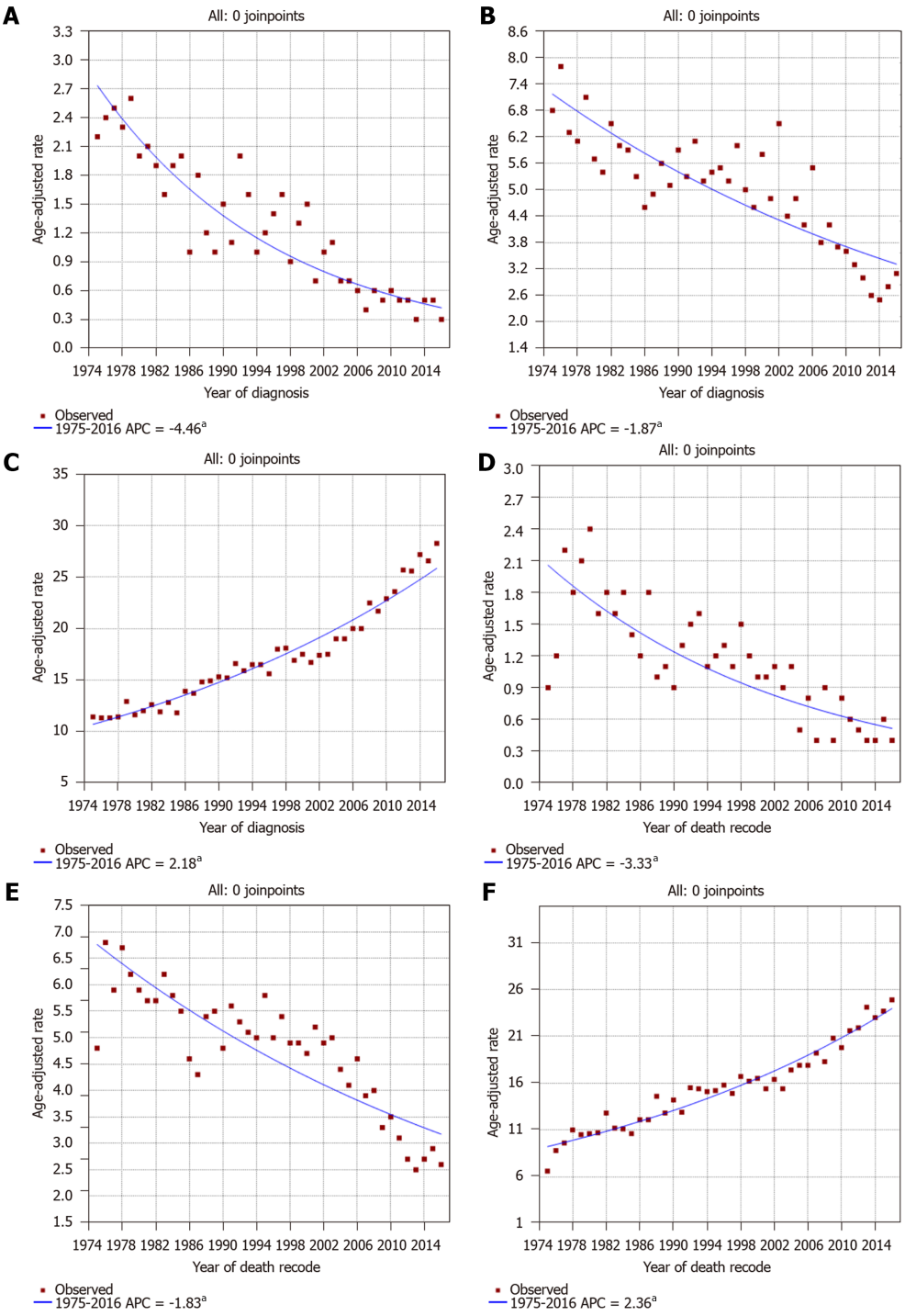

DOI: 10.4251/wjgo.v15.i5.843

Figure 2 Incidence and incidence-based mortality trends for invasive intraductal papillary neoplasm of the bile duct, invasive intraductal papillary mucinous neoplasm of the pancreas, and traditional cholangiocarcinoma in Surveillance, Epidemiology, and End Results 9 regs research data, Nov 2018 Sub (1975-2016). [a]*P* < 0.05. A: Incidence trends in invasive intraductal papillary neoplasm of the bile duct (IPNB); B: Incidence trends in invasive intraductal papillary mucinous neoplasm of the pancreas (IPMN); C: Incidence trends in traditional cholangiocarcinoma; D: Incidence-based (IB) mortality trends in invasive IPNB; E: IB mortality trends in invasive IPMN; F: IB mortality trends in traditional cholangiocarcinoma.

CSS rates were 69.4% and 77.8%, 41.7% and 53.1%, and 31.4% and 43.9%, respectively. The median OS and CSS of individuals with the mucin subtype of invasive IPNB were 12 mo (95%CI: 10-13 mo) and 19 mo (95%CI: 16-21 mo), respectively, and the 1-, 3-, and 5-year OS and CSS rates were 49.2% and 61.2%, 23.7% and 36.9%, and 17.1% and 31.2%, respectively. The median OS and CSS of individuals with

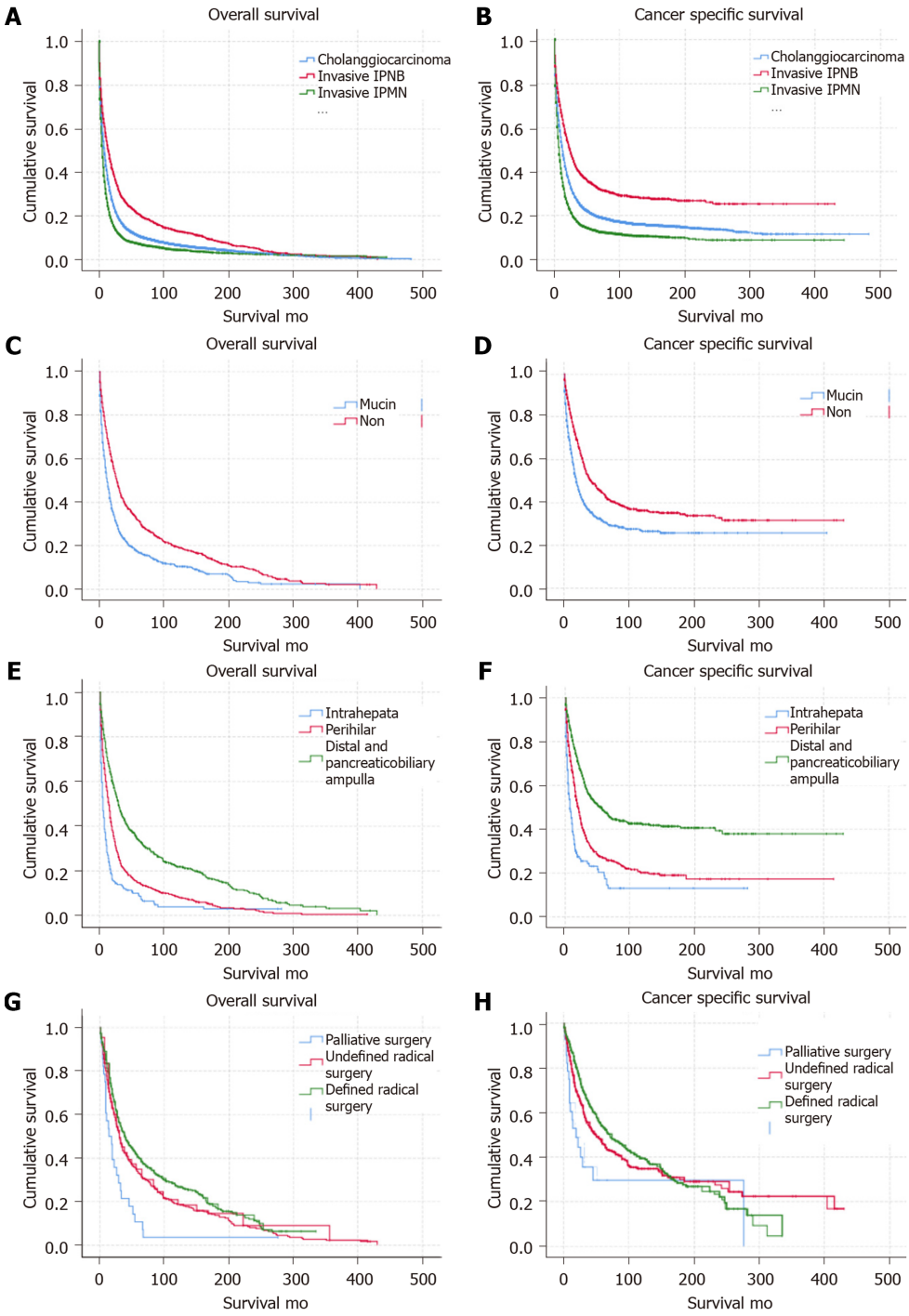

DOI: 10.4251/wjgo.v15.i5.843

Figure 3 Long-term overall survival and cancer-specific survival outcomes using Kaplan-Meier analysis. A and B: Overall survival (OS) and cancer-specific survival (CSS) were better for invasive intraductal papillary neoplasm of the bile duct (IPNB) and worse for invasive intraductal papillary mucinous neoplasm of the pancreas (IPMN) compared with traditional cholangiocarcinoma ($P < 0.001$); C and D: OS and CSS in individuals with the non-mucin subtype of invasive IPNB was better than for the mucin subtype ($P < 0.05$); E and F: OS and CSS in individuals with invasive IPNB at distal sites and at the pancreaticobiliary ampulla was better than at other sites ($P < 0.001$); G and H: OS and CSS in individuals with invasive IPNB with defined radical surgery was better than other type of surgical treatment ($P < 0.001$).

invasive IPNB in the distal tract and the pancreaticobiliary ampulla were 29 mo (95%CI: 26-33 mo) and 54 mo (95%CI: 42-66 mo), and the 1-, 3-, and 5-year OS and CSS rates were 69.1% and 78.9%, 43.9% and 56%, and 33.7% and 48.3%, respectively. In intrahepatic locations, namely the liver and intrahepatic biliary tract, the median OS and CSS were 5 mo (95%CI: 4-6 mo) and 7 mo (95%CI: 4-10 mo), and the 1-, 3-, and 5-year OS and CSS rates were 27.1% and 37.4%, 12.5% and 23.0%, and 9.2% and 18.8%, respectively. In the perihilar location, the median OS and CSS were 14 mo (95%CI: 12-16 mo) and 20 mo (95%CI: 17-23 mo), and the 1-, 3-, and 5-year OS and CSS rates were 52.9% and 63.8%, 21.2% and 33.6%, and 33.7% and 48.30%, respectively.

In addition to tumor location and subtype, univariable Kaplan-Meier analysis and the log rank test for OS and CSS in individuals with invasive IPNBs also depended on age, tumor grade, SEER historic stage, and treatment. Kaplan–Meier and log-rank analysis of variance indicated that age ≥ 68 years, tumor grade (moderately-differentiated, poorly-differentiated, and undifferentiated or unknown grade), SEER historic stage (regional, distant, and unknown stage), and not undergoing surgery and chemotherapy were associated with higher mortality ($P < 0.05$) (Table 2).

OS and CSS for invasive IPNB and subtypes in surgical group

The median OS and CSS for the total cohort with invasive IPNB in the surgical group was 34 mo (95%CI: 30-37 mo) and 64 mo (95%CI: 48-80 mo), respectively, and the 1-, 3-, and 5-year survival rates were 77.0% and 84.3%, 48.2% and 59.6%, and 36.9% and 50.8%, respectively. In both the surgical group and non-surgical group, individuals with the non-mucin subtype of invasive IPNB had better OS and CSS compared with the mucin subtype ($P = 0.000$) (Supplementary Figure 4A-D). The median OS and CSS of patients with the mucin subtype of invasive IPNB was 27 mo (95%CI: 23-31 mo) and 52 mo (95%CI: 36-68 mo), respectively, compared with 43 mo (95%CI: 35-51 mo) and 72 mo (95%CI: 45-97 mo), respectively. For the mucin subtype of invasive IPNB, the 1-, 3-, and 5-year OS and CSS rates were 74.0% and 83.1%, 41.6% and 54.3%, and 31.3% and 47.6%, respectively. For the non-mucin subtype of invasive IPNB, the 1-, 3-, and 5-year OS and CSS rates were 79.9% and 85.5%, 54.3% and 63.3%, and 42%and 53.8%, respectively. Meanwhile, the OS and CSS of individuals with resected invasive IPNB in the distal tract and the pancreaticobiliary ampulla had the best prognosis compared with individuals with tumors in other sites. The median OS and CSS of patients with invasive IPNB in the distal tract and the pancreaticobiliary ampulla was 44 mo (95%CI: 36-52 mo) and 72 mo (95%CI: 55-88 mo), respectively, and the 1-, 3-, and 5-year survival rates were 80.9% and 86.9%, 55.2% and 64.7%, and 43.3% and 56.7%, respectively. In particular, the 3-, 5-, and 10-year OS and CSS rates of patients with radical resected invasive IPNB in the distal tract and the pancreaticobiliary ampulla were 93.9% and 95.4%, 89.2% and 91.6%, and 73.4% and 81.5%, respectively (Figures 3G, H and 4).

Multivariable Cox regression

According to the multivariable Cox regression analysis of OS and CSS adjusted for the results of the univariable analysis ($P < 0.05$), both OS and CSS were statistically significantly different when comparing surgery and chemotherapy, as follows: surgery not performed *vs* performed [hazard ratio (HR) = 2.99; 95%CI: 2.59-3.45; $P < 0.001$) and (HR = 3.04, 95%CI: 2.55-3.61; $P < 0.001$), respectively; chemotherapy not performed *vs* performed (HR = 1.23, 95%CI: 1.09-1.40; $P < 0.001$) and (HR = 1.21, 95%CI: 1.04-1.14; $P < 0.02$), respectively. Tumor subtype was another important factor related to OS and CSS. For the non-mucin subtype of invasive IPNB *vs* the mucin subtype, OS HR = 0.78; 95%CI: 0.67-0.88; $P < 0.001$ and CSS HR = 0.86; 95%CI: 0.73-0.99; $P < 0.04$. Individuals aged ≥ 68 years (HR = 1.36, 95%CI: 1.21-1.52; $P < 0.001$) had unfavorable OS compared with individuals aged < 68 years. Tumors in the perihilar location (OS: HR = 1.63; 95%CI: 1.36-1.96; $P < 0.001$) and tumors located in the distal tract and at the pancreaticobiliary ampulla (OS HR = 1.41; 95%CI: 1.25-1.60; $P < 0.001$) had better OS *vs* tumor in the intrahepatic location. Likewise, a relatively favorable OS was observed in individuals with well-differentiated grade and localized stage lymph node metastasis compared with moderately- or poorly-differentiated grades and regional and distant lymph node metastasis ($P < 0.01$). The related OS values were as follows: SEER historic regional stage HR = 1.33, 95%CI: 1.16-1.53, $P < 0.001$ and distant stage OS HR = 2.09, 95%CI: 1.75-2.50, $P < 0.001$ *vs* the localized stage; moderately-differentiated tumors (grade II) HR = 1.20, 95%CI: 1.03-1.40, $P < 0.02$ and poorly-differentiated tumors (grade III and IV) HR = 1.26, 95%CI: 1.03-1.52, $P < 0.02$) *vs* well-differentiated (grade I) (Figure 5).

DISCUSSION

To our knowledge, our study is the first to use SEER data to identify the rare incidence of invasive IPNB occurring throughout the biliary tract. We evaluated the incidence and IB mortality associated with invasive IPMN of the pancreas, which may represent a carcinogenic pathway different from the traditional carcinogenic pathway of cholangiocarcinoma caused by flat atypical hyperplasia[18]. The incidence and IB mortality of invasive IPNB and invasive IPMN showed steady decreases in the United States population over the study period, but an increasing trend for traditional cholangiocarcinoma in the biliary tract. The continued decline in the APC of invasive IPNB and IPMN over the study period may be associated with the fact that preventive measures have improved greatly according to the etiology, treatment, and management in recent years. Conversely, treatment for traditional cholangiocarcinoma may still have severe challenges. Hence, more resources should be devoted to traditional cholangiocarcinoma, and efforts should be made to develop improved prevention and treatment strategies.

The prognoses of individuals with invasive IPNB were better than for individuals with invasive IPMN and traditional cholangiocarcinoma. The median OS and CSS in individuals with invasive IPNBs was higher than that of individuals with invasive IPMN and traditional cholangiocarcinoma in the

Table 2 Univariable analysis of factors associated with overall survival and cancer-specific survival

Variable	Univariate (*P* value)	
	Overall survival	Cancer specific survival
Age at diagnosis, yr	0.000	0.030
< 68		
≥ 68		
Sex	0.785	0.355
Male		
Female		
Race	0.062	0.689
White		
Black		
Others		
TNM7/CSv0204+ schema	0.000	0.000
Intrahepata and liver		
Perihilar		
Distal and pancreaticobiliary ampulla		
SEER historic stage	0.000	0.000
Localized		
Regional		
Distant		
Unstaged		
Grade	0.000	0.000
Well		
Moderate		
Poor and undifferentiated		
Unknown		
Classification	0.000	0.000
Mucin		
Non		
Surgery	0.000	0.000
Defined radical surgery		
Undefined radical surgery		
Palliative surgery		
Non		
Radiatheray	0.909	0.222
Performed		
Non		
Chemotherapy	0.075	0.040
Performed		
Non		

SEER: Surveillance, Epidemiology, and End Results database.

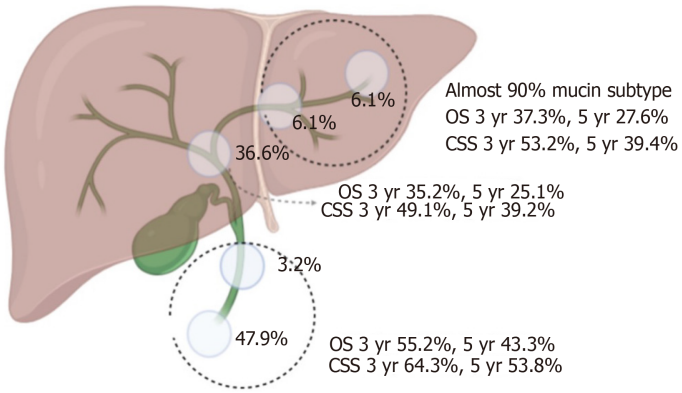

DOI: 10.4251/wjgo.v15.i5.843

Figure 4 Percentage incidence at different sites, overall survival, and cancer-specific survival of invasive intraductal papillary neoplasm of the bile duct in the surgical group. OS: Overall survival; CCS: Cancer-specific survival.

biliary tract. As reported previously, the prognosis of invasive IPNB is much better than that of traditional cholangiocarcinoma in the biliary tract[19]. It is not clear whether this is because of inherent biological characteristics of these tumors or the growth pattern of IPNB, which grows mainly in the intra-bile ducts, and which may contribute to the early diagnosis of biliary obstruction before it invades the surrounding tissue. However, previous studies consistently indicated that invasive IPNB had a higher degree of malignancy and a worse prognosis compared with invasive IPMN[20]. We found that ampullary invasive IPNB accounted for 47.9% of the individuals in our study cohort, and the prognosis for ampullary tumors was much better than that of individuals with tumors in other pancreaticobiliary ducts.

Our analysis also identified several important clinicopathological features and prognosis findings related to invasive IPNB. Outcomes after surgery for IPNB were generally not well-reported and were hampered by the fact that verifying outcome measurements were used. Gordon-Weeks *et al*[21] reported a 5-year OS rate of 65%, with a range of 24%-84% across seven studies. Our study indicated that HRs for both OS and CSS for invasive IPNB in individuals who did not undergo surgery were three times higher than for individuals who underwent surgery, and the 5-year OS and CSS rates for individuals with invasive IPNB treated with surgery were 36.9% and 50.8%, respectively. These results appear to be more persuasive because, in our cohort, we ruled out benign IPNB and carcinoma in situ, and evaluated only invasive IPNB (ICD-O, 3rd/3). Furthermore, for the first time, to our knowledge, we provided clear evidence that adjuvant chemotherapy can improve OS and CSS rates in individuals with invasive IPNB. In individuals with resected invasive IPMNs, the counterpart to invasive IPNB, adjuvant chemotherapy and radiotherapy were associated with significantly improved OS in the presence of nodal metastases [22-24]. Conversely, radiotherapy had no statistically significant effect on OS and CSS in individuals with invasive IPNB.

In addition to therapeutic factors, our study also indicated that age, tumor grade, SEER lymph node metastasis, tumor site, and mucin-related subtypes also affected the prognosis of individuals with invasive IPNB. In fact, IPNB is a heterogeneous disease, and invasive IPNB belongs to mainly pancreaticobiliary and intestinal type tumors, with invasive colloid carcinoma[25-27]. In our study, most of the mucin-related subtypes belonged to the colloid intestinal-type IPNB, which was always associated with *KRAS*, *GNAS*, and *RNF43* mutations[9]. Our published study have shown that mucus production is also associated with GNAS mutation in highly malignancy hepatic mucoepidermoid carcinoma[28]. Individuals with the mucin subtype of invasive IPNB suffered a much worse prognosis following resection compared with individuals with the non-mucin subtype, which was inconsistent with the results of the study by Kim *et al*[27] mainly because the study included mild and carcinoma in situ intestinal types. Meanwhile, the prognosis of invasive IPNB located in the distal bile duct and ampulla was significantly better than that of intrahepatic and perihilar invasive IPNB. On the one hand, intrahepatic invasive IPNB constituted more than 90% mucin-related subtype, which indicated worse prognosis. On the other hand, in individuals with invasive IPNB located in the distal bile duct or ampulla, the clinical symptoms often appeared earlier. Pancreaticoduodenectomy is the main choice of surgical methods for tumors in these sites, which can maximize the chance of radical cure. In addition, the majority of the individuals in this study cohort were white (78.2%), and there is no significant statistic comparing other races for OS and CSS. Because the high-risk factors for IPNB are related to endemic clonorchiasis infections and hepatolithiasis in Asian races compared with the risk factors in Western countries[20].

This study has limitations. First, studies using the SEER database involve a retrospective design, and the registries contain data for individuals from different institutions and time periods. According to 2019 WHO proposal, intraductal papillary neoplasm of ampulla are not included in IPNB[29]. In fact,

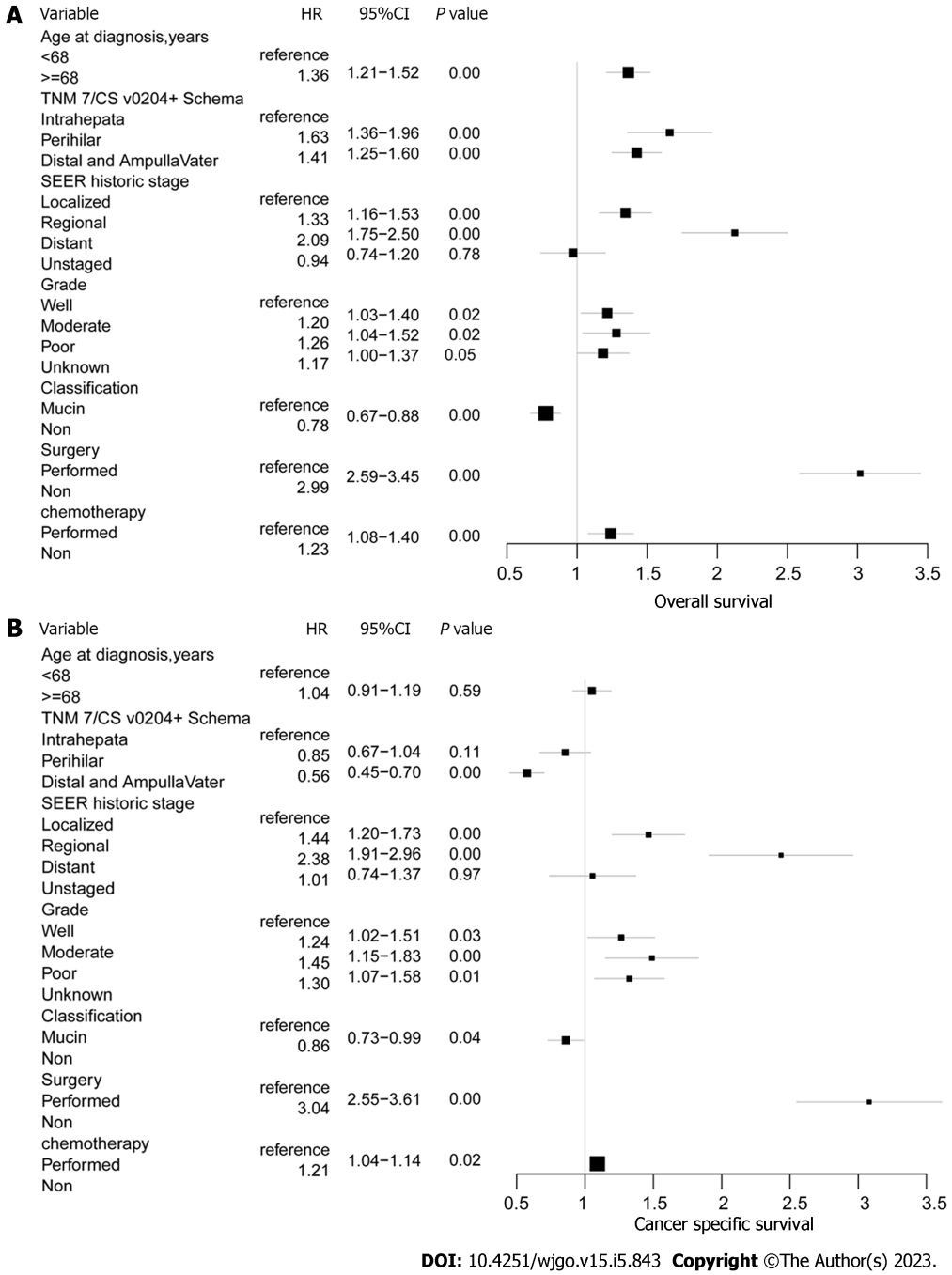

DOI: 10.4251/wjgo.v15.i5.843

Figure 5 Cox proportional hazard regression analysis of overall survival, and cancer-specific survival for total invasive intraductal papillary neoplasm of the bile duct. A: Overall survival; B: Cancer-specific survival.

the peribiliary glands are attracted attention as a potential origin of IPNB, and predominantly occur at branching points of the biliary tree and are most numerous at the hepatopancreatic ampulla[30,31]. Additionally, the database lacks central reviews by professional pathologists. Second, the study cohort lacked detailed information regarding tumor recurrence, and palliative surgical methods and chemotherapy regimens, which have considerable OS and CSS impact. Furthermore, we used the ICD-O code for IPMN as the reference for IPNB. A group of pathologists in Japan and South Korea suggested that IPNB should be divided into two types; type 1 is the histological counterpart of IPMN, and type 2 has a more complex histological structure[32]. Despite these limitations, some interesting observations were identified. First, in our study cohort, the prognosis between mucin and non-mucin subtypes differed significantly, which also indicated that the expression of mucin is related to the subtypes of IPMN and IPNB[9]. Mucus secretion was mainly immunohistochemically positive for MUC1, which was always associated with the invasive phenotype and individuals' prognosis, similar to previous published reports[21]. Importantly, we also detected correlations between tumor type and location. The minority of invasive IPNBs (6.1%) occurred in the liver, and the majority occurred in the perihilar region

(36.6%) and the pancreaticobiliary ampulla (49.7%). This is because IPNB may originate from biliary stem/progenitor cells, which are located mainly in the peribiliary gland of the perihilum and the hepatopancreatic ampulla; however, biliary stem/progenitor cells also can originate from the canals of Hering and large intrahepatic biliary ducts[30,33-35].

CONCLUSION

In conclusion, the current population-based study revealed a gradual decrease in the incidence and IB mortality rates of invasive IPNB in the United States population during 1975-2016, which was similar to findings for invasive IPMN, but in contrast to the rates for traditional cholangiocarcinoma in the biliary tract. The majority of invasive IPNBs occurred in the perihilum and pancreaticobiliary ampulla. The prognosis of invasive IPNB was not only regarding tumor grade and SEER historic stage, but also for different sites and tumor subtypes. Surgery and chemotherapy are associated with improved invasive IPNB outcomes; individuals who do not undergo surgery have the highest risk of death.

ARTICLE HIGHLIGHTS

Research background

Intraductal papillary neoplasm of the bile duct (IPNB) is a rare distinct subtype of precursor lesions of biliary carcinoma. IPNB is considered to originate from luminal biliary epithelial cells, typically displays mucin-hypersecretion or a papillary growth pattern, and results in cystic dilatation. According to the 2010 World Health Organization classification of tumors in the digestive system, IPNB is defined as the biliary counterpart of intraductal papillary mucinous neoplasm of the pancreas (IPMN) and has identical histopathologic pancreaticobiliary, gastric, intestinal, and oncocytic features. There are still several important differences between IPMN and IPNB exist, unlike invasive IPMN and traditional cholangiocarcinoma in the biliary tract, very little is known about the clinicopathological features and prognostic variables of invasive IPNB.

Research motivation

The epidemiology, tumor characteristics, treatment strategy, and long-term results of invasive IPNB are limited because of the relatively low case numbers.

Research objectives

We conducted a Surveillance, Epidemiology, and End Results (SEER) database evaluation of invasive IPNB to address these shortcomings, and to further elucidate the epidemiological and clinical trends to guide treatment decision-making and to identify further clinical and scientific research areas.

Research methods

Invasive IPNB, IPMN, and traditional cholangiocarcinoma data for affected individuals from 1975 to 2016 were obtained from the SEER database. Annual percentage changes in the incidence and incidence-based (IB) mortality were calculated.

Research results

The incidence and IB mortality of invasive IPNB showed sustained decreases. Similar decreases in incidence and IB mortality were seen for invasive IPMN but not for traditional cholangiocarcinoma. Both overall survival (OS) and cancer-specific survival (CSS) for invasive IPNB were better than for invasive IPMN and traditional cholangiocarcinoma. The most common tumor sites were the pancreaticobiliary ampulla (47.9%) and perihilar tract (36.7%), but the mucin-related subtype of invasive IPNB was the main type, intrahepatically (approximately 90%). In the univariate and multivariate Cox regression analysis, age, tumor site, grade and stage, subtype, surgery, and chemotherapy were associated with OS and CSS ($P < 0.05$).

Research conclusions

Current population-based study revealed a gradual decrease in the incidence and IB mortality rates of invasive IPNB in the United States population during 1975-2016. The prognosis of invasive IPNB was not only regarding tumor grade and SEER historic stage, but also for different sites and tumor subtypes. Surgery and chemotherapy are associated with improved invasive IPNB outcomes; individuals who do not undergo surgery have the highest risk of death.

Research perspectives

The inspiration of this article is that we found a rare case of hepatic mucoidepidermoid carcinoma

(HMEC) in our cancer research center, and found that the malignancy mucinous carcinoma in liver including IPNB, mucinous cystadenocarcinoma and adenosquamous carcinoma. So in our future research direction, we will analyze IPNB cases' tissues from our center by the next generation sequencing, combined with our published article to analyze the relationship between IPNB and HMEC.

ACKNOWLEDGEMENTS

We thank Peng Huang, PhD, from the center for Evidence-Base Medicine, School of Public Health, Nanchang University for professional knowledge guidance in statistics.

FOOTNOTES

Author contributions: Wu RS and Liao WJ contributed equally to this work, Wu RS and Hou P contributed to the conceptualization, formal analysis, software, and writing-original draft; Liao WJ and Wu LQ contributed to the conceptualization, writing-review and editing, project administration; Ma JS and Wang JK contributed to the data curation and methodology. All authors had access to the study data and reviewed and approved the final article. All authors read and approved the final manuscript

Supported by the National Natural Science Foundation of China, No. 81860431 and 82060447; and the Jiangxi Natural Science Foundation, No. 20181BBG70025.

Institutional review board statement: The Surveillance, Epidemiology, and End Results Program of the National Cancer Institute belong to public databases. The patients involved in the database have obtained ethical approval.

Conflict-of-interest statement: The authors declare no conflict of interests.

Data sharing statement: Technical appendix, statistical code, and dataset available from the corresponding author at houping1986@16.com.

Country/Territory of origin: China

ORCID number: Rong-Shou Wu 0000-0003-2695-1907; Ping Hou 0000-0003-4436-1871.

S-Editor: Zhang H
L-Editor: A
P-Editor: Zhang H

REFERENCES

1 **Chen TC**, Nakanuma Y, Zen Y, Chen MF, Jan YY, Yeh TS, Chiu CT, Kuo TT, Kamiya J, Oda K, Hamaguchi M, Ohno Y, Hsieh LL, Nimura Y. Intraductal papillary neoplasia of the liver associated with hepatolithiasis. *Hepatology* 2001; **34**: 651-658 [PMID: 11584359 DOI: 10.1053/jhep.2001.28199]

2 **Zen Y**, Fujii T, Itatsu K, Nakamura K, Minato H, Kasashima S, Kurumaya H, Katayanagi K, Kawashima A, Masuda S, Niwa H, Mitsui T, Asada Y, Miura S, Ohta T, Nakanuma Y. Biliary papillary tumors share pathological features with intraductal papillary mucinous neoplasm of the pancreas. *Hepatology* 2006; **44**: 1333-1343 [PMID: 17058219 DOI: 10.1002/hep.21387]

3 **Lee SS**, Kim MH, Lee SK, Jang SJ, Song MH, Kim KP, Kim HJ, Seo DW, Song DE, Yu E, Lee SG, Min YI. Clinicopathologic review of 58 patients with biliary papillomatosis. *Cancer* 2004; **100**: 783-793 [PMID: 14770435 DOI: 10.1002/cncr.20031]

4 **Shibahara H**, Tamada S, Goto M, Oda K, Nagino M, Nagasaka T, Batra SK, Hollingsworth MA, Imai K, Nimura Y, Yonezawa S. Pathologic features of mucin-producing bile duct tumors: two histopathologic categories as counterparts of pancreatic intraductal papillary-mucinous neoplasms. *Am J Surg Pathol* 2004; **28**: 327-338 [PMID: 15104295 DOI: 10.1097/00000478-200403000-00005]

5 **Nakanuma Y**, Miyata T, Uchida T. Latest advances in the pathological understanding of cholangiocarcinomas. *Expert Rev Gastroenterol Hepatol* 2016; **10**: 113-127 [PMID: 26492529 DOI: 10.1586/17474124.2016.1104246]

6 **Bosman FT**, Carneiro F, Hruban RH, Theise ND. WHO classification of tumours of the digestive system. 4th ed. Lyon, France: IARC, 2010

7 **Eberhard D**, Tosh D, Slack JM. Origin of pancreatic endocrine cells from biliary duct epithelium. *Cell Mol Life Sci* 2008; **65**: 3467-3480 [PMID: 18810318 DOI: 10.1007/s00018-008-8427-1]

8 **Fukumura Y**, Nakanuma Y, Kakuda Y, Takase M, Yao T. Clinicopathological features of intraductal papillary neoplasms of the bile duct: a comparison with intraductal papillary mucinous neoplasm of the pancreas with reference to subtypes. *Virchows Arch* 2017; **471**: 65-76 [PMID: 28550497 DOI: 10.1007/s00428-017-2144-9]

9 **Ohtsuka M**, Kimura F, Shimizu H, Yoshidome H, Kato A, Yoshitomi H, Furukawa K, Takeuchi D, Takayashiki T, Suda K, Takano S, Kondo Y, Miyazaki M. Similarities and differences between intraductal papillary tumors of the bile duct with and without macroscopically visible mucin secretion. *Am J Surg Pathol* 2011; **35**: 512-521 [PMID: 21412069 DOI: 10.1097/PAS.0b013e3182103f36]

10 **Nakanuma Y**, Uesaka K, Kakuda Y, Sugino T, Kubota K, Furukawa T, Fukumura Y, Isayama H, Terada T. Intraductal Papillary Neoplasm of Bile Duct: Updated Clinicopathological Characteristics and Molecular and Genetic Alterations. *J Clin Med* 2020; **9** [PMID: 33317146 DOI: 10.3390/jcm9123991]

11 **Wu X**, Li B, Zheng C, Chang X, Zhang T, He X, Zhao Y. Intraductal papillary neoplasm of the bile duct: a single-center retrospective study. *J Int Med Res* 2018; **46**: 4258-4268 [PMID: 30111208 DOI: 10.1177/0300060518792800]

12 **Kim JR**, Jang KT, Jang JY, Lee K, Kim JH, Kim H, Kim SW, Kwon W, Choi DW, Heo J, Han IW, Hwang S, Kim WJ, Hong SM, Kim DS, Yu YD, Kim JY, Nah YW, Park HW, Choi HJ, Han HS, Yoon YS, Park SJ, Hong EK, Seo HI, Park DY, Kang KJ, Kang YN, Yu HC, Moon WS, Lim CS, Bae JM, Jo S, Lee W, Roh YH, Jeong JS, Jeong CY, Lee JS, Song IS, Kim KH, Kim HG, Cho CH, Joo SH, Won KY, Kim HJ, Choi JH, Chu CW, Lee JH, Park IY, Lee H, Lee SE, Kim HS, Lee HK, Cho MS, Han KM. Clinicopathologic analysis of intraductal papillary neoplasm of bile duct: Korean multicenter cohort study. *HPB (Oxford)* 2020; **22**: 1139-1148 [PMID: 31837945 DOI: 10.1016/j.hpb.2019.11.007]

13 **Gaitanidis A**, Alevizakos M, Tsaroucha A, Tsalikidis C, Simopoulos C, Pitiakoudis M. Conditional survival analysis for patients with intraductal papillary mucinous neoplasms (IPMNs) undergoing curative resection. *Eur J Surg Oncol* 2018; **44**: 693-699 [PMID: 29426780 DOI: 10.1016/j.ejso.2018.01.011]

14 **Worni M**, Akushevich I, Gloor B, Scarborough J, Chino JP, Jacobs DO, Hahn SM, Clary BM, Pietrobon R, Shah A. Adjuvant radiotherapy in the treatment of invasive intraductal papillary mucinous neoplasm of the pancreas: an analysis of the surveillance, epidemiology, and end results registry. *Ann Surg Oncol* 2012; **19**: 1316-1323 [PMID: 22002799 DOI: 10.1245/s10434-011-2088-2]

15 **Kargozaran H**, Vu V, Ray P, Bagaria S, Steen S, Ye X, Gagandeep S. Invasive IPMN and MCN: same organ, different outcomes? *Ann Surg Oncol* 2011; **18**: 345-351 [PMID: 20809175 DOI: 10.1245/s10434-010-1309-4]

16 **Wasif N**, Bentrem DJ, Farrell JJ, Ko CY, Hines OJ, Reber HA, Tomlinson JS. Invasive intraductal papillary mucinous neoplasm versus sporadic pancreatic adenocarcinoma: a stage-matched comparison of outcomes. *Cancer* 2010; **116**: 3369-3377 [PMID: 20564064 DOI: 10.1002/cncr.25070]

17 **Khan SA**, Emadossadaty S, Ladep NG, Thomas HC, Elliott P, Taylor-Robinson SD, Toledano MB. Rising trends in cholangiocarcinoma: is the ICD classification system misleading us? *J Hepatol* 2012; **56**: 848-854 [PMID: 22173164 DOI: 10.1016/j.jhep.2011.11.015]

18 **Rocha FG**, Lee H, Katabi N, DeMatteo RP, Fong Y, D'Angelica MI, Allen PJ, Klimstra DS, Jarnagin WR. Intraductal papillary neoplasm of the bile duct: a biliary equivalent to intraductal papillary mucinous neoplasm of the pancreas? *Hepatology* 2012; **56**: 1352-1360 [PMID: 22504729 DOI: 10.1002/hep.25786]

19 **Fujikura K**, Fukumoto T, Ajiki T, Otani K, Kanzawa M, Akita M, Kido M, Ku Y, Itoh T, Zen Y. Comparative clinicopathological study of biliary intraductal papillary neoplasms and papillary cholangiocarcinomas. *Histopathology* 2016; **69**: 950-961 [PMID: 27410028 DOI: 10.1111/his.13037]

20 **Zen Y**, Jang KT, Ahn S, Kim DH, Choi DW, Choi SH, Heo JS, Yeh MM. Intraductal papillary neoplasms and mucinous cystic neoplasms of the hepatobiliary system: demographic differences between Asian and Western populations, and comparison with pancreatic counterparts. *Histopathology* 2014; **65**: 164-173 [PMID: 24456415 DOI: 10.1111/his.12378]

21 **Gordon-Weeks AN**, Jones K, Harriss E, Smith A, Silva M. Systematic Review and Meta-analysis of Current Experience in Treating IPNB: Clinical and Pathological Correlates. *Ann Surg* 2016; **263**: 656-663 [PMID: 26501712 DOI: 10.1097/SLA.0000000000001426]

22 **Mungo B**, Croce C, Oba A, Ahrendt S, Gleisner A, Friedman C, Schulick RD, Del Chiaro M. Controversial Role of Adjuvant Therapy in Node-Negative Invasive Intraductal Papillary Mucinous Neoplasm. *Ann Surg Oncol* 2021; **28**: 1533-1542 [PMID: 32743713 DOI: 10.1245/s10434-020-08916-6]

23 **Wu JY**, Wang YF, Ma H, Li SS, Miao HL. Nomograms predicting long-term survival in patients with invasive intraductal papillary mucinous neoplasms of the pancreas: A population-based study. *World J Gastroenterol* 2020; **26**: 535-549 [PMID: 32089629 DOI: 10.3748/wjg.v26.i5.535]

24 **Aronsson L**, Marinko S, Ansari D, Andersson R. Adjuvant therapy in invasive intraductal papillary mucinous neoplasm (IPMN) of the pancreas: a systematic review. *Ann Transl Med* 2019; **7**: 689 [PMID: 31930090 DOI: 10.21037/atm.2019.10.37]

25 **Aoki Y**, Mizuma M, Hata T, Aoki T, Omori Y, Ono Y, Mizukami Y, Unno M, Furukawa T. Intraductal papillary neoplasms of the bile duct consist of two distinct types specifically associated with clinicopathological features and molecular phenotypes. *J Pathol* 2020; **251**: 38-48 [PMID: 32100878 DOI: 10.1002/path.5398]

26 **Choi SC**, Lee JK, Jung JH, Lee JS, Lee KH, Lee KT, Rhee JC, Jang KT, Choi SH, Heo JS, Choi DW, Lim JH. The clinicopathological features of biliary intraductal papillary neoplasms according to the location of tumors. *J Gastroenterol Hepatol* 2010; **25**: 725-730 [PMID: 20492329 DOI: 10.1111/j.1440-1746.2009.06104.x]

27 **Kim KM**, Lee JK, Shin JU, Lee KH, Lee KT, Sung JY, Jang KT, Heo JS, Choi SH, Choi DW, Lim JH. Clinicopathologic features of intraductal papillary neoplasm of the bile duct according to histologic subtype. *Am J Gastroenterol* 2012; **107**: 118-125 [PMID: 21946282 DOI: 10.1038/ajg.2011.316]

28 **Hou P**, Su X, Cao W, Xu L, Zhang R, Huang Z, Wang J, Li L, Wu L, Liao W. Whole-exome sequencing reveals the etiology of the rare primary hepatic mucoepidermoid carcinoma. *Diagn Pathol* 2021; **16**: 29 [PMID: 33832503 DOI: 10.1186/s13000-021-01086-3]

29 **Nagtegaal ID**, Odze RD, Klimstra D, Paradis V, Rugge M, Schirmacher P, Washington KM, Carneiro F, Cree IA; WHO

Classification of Tumours Editorial Board. The 2019 WHO classification of tumours of the digestive system. *Histopathology* 2020; **76**: 182-188 [PMID: 31433515 DOI: 10.1111/his.13975]

30 **Cardinale V**, Wang Y, Carpino G, Reid LM, Gaudio E, Alvaro D. Mucin-producing cholangiocarcinoma might derive from biliary tree stem/progenitor cells located in peribiliary glands. *Hepatology* 2012; **55**: 2041-2042 [PMID: 22262236 DOI: 10.1002/hep.25587]

31 **Nakagawa H**, Hayata Y, Yamada T, Kawamura S, Suzuki N, Koike K. Peribiliary Glands as the Cellular Origin of Biliary Tract Cancer. *Int J Mol Sci* 2018; **19** [PMID: 29895797 DOI: 10.3390/ijms19061745]

32 **Nakanuma Y**, Jang KT, Fukushima N, Furukawa T, Hong SM, Kim H, Lee KB, Zen Y, Jang JY, Kubota K. A statement by the Japan-Korea expert pathologists for future clinicopathological and molecular analyses toward consensus building of intraductal papillary neoplasm of the bile duct through several opinions at the present stage. *J Hepatobiliary Pancreat Sci* 2018; **25**: 181-187 [PMID: 29272078 DOI: 10.1002/jhbp.532]

33 **Carpino G**, Cardinale V, Onori P, Franchitto A, Berloco PB, Rossi M, Wang Y, Semeraro R, Anceschi M, Brunelli R, Alvaro D, Reid LM, Gaudio E. Biliary tree stem/progenitor cells in glands of extrahepatic and intraheptic bile ducts: an anatomical in situ study yielding evidence of maturational lineages. *J Anat* 2012; **220**: 186-199 [PMID: 22136171 DOI: 10.1111/j.1469-7580.2011.01462.x]

34 **Nakanuma Y**, Kurumaya H, Ohta G. Multiple cysts in the hepatic hilum and their pathogenesis. A suggestion of periductal gland origin. *Virchows Arch A Pathol Anat Histopathol* 1984; **404**: 341-350 [PMID: 6093347 DOI: 10.1007/BF00695218]

35 **Turner R**, Lozoya O, Wang Y, Cardinale V, Gaudio E, Alpini G, Mendel G, Wauthier E, Barbier C, Alvaro D, Reid LM. Human hepatic stem cell and maturational liver lineage biology. *Hepatology* 2011; **53**: 1035-1045 [PMID: 21374667 DOI: 10.1002/hep.24157]

World Journal of Gastrointestinal Oncology

Submit a Manuscript: https://www.f6publishing.com

World J Gastrointest Oncol 2023 May 15; 15(5): 859-877

DOI: 10.4251/wjgo.v15.i5.859

ISSN 1948-5204 (online)

ORIGINAL ARTICLE

Retrospective Study

Real-world 10-year retrospective study of the guidelines for diagnosis and treatment of primary liver cancer in China

Yun-Wei Yan, Xin-Kui Liu, Shun-Xiang Zhang, Qing-Feng Tian

Specialty type: Oncology

Provenance and peer review: Unsolicited article; Externally peer reviewed.

Peer-review model: Single blind

Peer-review report's scientific quality classification

Grade A (Excellent): A
Grade B (Very good): B
Grade C (Good): C, C
Grade D (Fair): 0
Grade E (Poor): 0

P-Reviewer: De Raffele E, Italy; El-Shishtawy MM, Egypt; Masuda S, Japan

Received: December 5, 2022
Peer-review started: December 5, 2022
First decision: February 21, 2023
Revised: March 6, 2023
Accepted: April 4, 2023
Article in press: April 4, 2023
Published online: May 15, 2023

Yun-Wei Yan, Qing-Feng Tian, Department of Epidemiology and Health Statistics, College of Public Health, Zhengzhou University, Zhengzhou 450001, Henan Province, China

Xin-Kui Liu, Department of Medical Records Management, The First Affiliated Hospital of Zhengzhou University, Zhengzhou 450001, Henan Province, China

Shun-Xiang Zhang, Department of Epidemiology and Health Statistics and Henan Key Laboratory for Tumour Epidemiology, College of Public Health, Zhengzhou University, Zhengzhou 450001, Henan Province, China

Corresponding author: Qing-Feng Tian, PhD, Professor, Department of Epidemiology and Health Statistics, College of Public Health, Zhengzhou University, No. 100 Kexue Avenue, Zhengzhou 450001, Henan Province, China. tianqf@zzu.edu.cn

Abstract

BACKGROUND

Hepatocellular carcinoma (HCC) is a common malignant tumor worldwide. Many regions across the world have issued various HCC diagnosis and treatment protocols to improve the diagnosis and targeted treatment of patients with HCC. However, real-world studies analysing the practice, application value, and existing problems of the China Liver Cancer (CNLC) staging system are scarce.

AIM

To analyze the current situation and problems associated with the Guidelines for Diagnosis and Treatment of Primary Liver Cancer in China.

METHODS

We collected the medical records of all patients with HCC admitted to the First Affiliated Hospital of Zhengzhou University from January 1, 2011 to December 31, 2019, and recorded the hospitalization information of those patients until December 31, 2020. All information on the diagnosis and treatment of the target patients was recorded, and their demographic and sociological characteristics, CNLC stages, screening situations, and treatment methods and effects were analyzed. The survival status of the patients was obtained from follow-up data.

RESULTS

This study included the medical records of 3022 patients with HCC. Among these cases, 304 patients were screened before HCC diagnosis; their early-stage

diagnosis rate was 69.08%, which was significantly higher than that of patients with HCC who were diagnosed without screening and early detection (33.74%). Herein, patients with no clinical outcome at discharge were followed up, and the survival information of 1128 patients was obtained. A Cox model was used to analyse independent risk factors affecting overall survival, which were revealed as age > 50 years, no screening, alpha-fetoprotein > 400 ng/mL, Child–Pugh grade B, and middle and late CNLC stages. Based on the Cox model survival analysis, in our study, patients with HCC identified *via* screening had significant advantages in overall and tumor-free survival after hepatectomy.

CONCLUSION

Early diagnosis and treatment can be achieved by screening groups at high risk for HCC based on the guidelines; however, real-world compliance is poor.

Key Words: China liver cancer; Compliance; Guideline; Hepatocellular carcinoma; Real-world study

Core Tip: This retrospective study evaluated the current situation and problems associated with the Guidelines for Diagnosis and Treatment of Primary Liver Cancer in China. The findings revealed that 70% of hepatocellular carcinoma (HCC) treatments at the First Affiliated Hospital of Zhengzhou University were performed according to the guidelines. Patients who underwent liver resection in accordance with the guidelines had a significant survival advantage. Furthermore, screening for HCC high-risk groups according to the guidelines can achieve early diagnosis and treatment; however, real-world compliance is poor.

Citation: Yan YW, Liu XK, Zhang SX, Tian QF. Real-world 10-year retrospective study of the guidelines for diagnosis and treatment of primary liver cancer in China. *World J Gastrointest Oncol* 2023; 15(5): 859-877
URL: https://www.wjgnet.com/1948-5204/full/v15/i5/859.htm
DOI: https://dx.doi.org/10.4251/wjgo.v15.i5.859

INTRODUCTION

Hepatocellular carcinoma (HCC) is a common malignant tumor worldwide. According to 2020 data from the GLOBOCAN database, the global incidence of liver cancer ranked sixth among all malignant tumors, and its mortality ranked third[1]. In a recent study, the 1-, 3-, 5-, and 10-year survival rates of HCC in Asian countries were 34.8%, 19%, 18.1%, and 4.1%, respectively[2]. Many regions worldwide have issued HCC diagnosis and treatment protocols, such as the Barcelona Clinic Liver Cancer (BCLC) and Hong Kong Liver Cancer (HKLC) staging systems and guidelines from the European Association for the Study of the Liver (EASL), the Asian–Pacific Association for the Study of the Liver (APASL), and the Japan Society of Hepatology (JSH), to improve the diagnosis and targeted treatment of patients with HCC[3-7]. However, no unified, widely recognized staging scheme applies to all populations worldwide.

Liver cancer is the fourth most common malignancy and the second leading cause of cancer-related deaths in China[8]. Therefore, based on the current situation of HCC diagnosis, multidisciplinary comprehensive treatment, and research in China, the National Health Commission issued Guidelines for Diagnosis and Treatment of Primary Liver Cancer in China in 2017[9] (referred to as 'the guidelines' hereafter) and updated them in 2019 and 2022[10]. Based on the liver function status, the tumor size, number, and invasion; and the general conditions of patients with HCC, a China Liver Cancer (CNLC) staging system was proposed for the Chinese population, including CNLC stages Ia, Ib, IIa, IIb, IIIa, IIIb, and IV[9,10]. The method of CNLC staging was first published in 2017[9]. Due to the short period since its publication, currently, there are no real-world studies on diagnosing and treating patients based on CNLC staging. Only a few studies have been performed on specific treatment methods in different CNLC stages[11-13]. The screening of high-risk HCC groups and the diagnosis and treatment of patients with HCC are also recommended by the guidelines. Some studies have analysed the situations of patients with HCC undergoing liver resection (LR) or interventional therapy based on CNLC staging [11-13]. In a comparative study, Vitale *et al*[14] found that CNLC staging was superior to BCLC staging as a prognostic staging system. However, these studies were traditional randomized controlled trials or comparative studies in literature reviews, and they only included patients who underwent LR or interventional therapy. There are some real-world studies on BCLC staging in clinical practice, but none exist on the practice of CNLC staging in real clinical settings in China[15-17]. Therefore, real-world

studies analysing the practice, application value, and existing problems of CNLC staging in China's real clinical environment are lacking[18,19]. Hence, we aimed to analyze the current situation and problems associated with Guidelines for Diagnosis and Treatment of Primary Liver Cancer in China.

In this study, inpatients with liver cancer from the First Affiliated Hospital of Zhengzhou University, the largest hospital in China, were selected as the study group. The hospital is also home to the National Regional Liver Cancer Diagnosis and Treatment Centre and the National Liver Transplant Centre. We collected the complete medical records of all patients with HCC who were diagnosed and treated in the hospital from January 1, 2011, to December 31, 2019, and the hospitalization information of these patients was recorded until December 31, 2020. The data collected from the large sample of patients with HCC were classified into CNLC stages to evaluate the compliance between CNLC staging and real-life clinical diagnosis and treatment in China. These data were also used to systematically review and analyze the diagnosis and treatment of Chinese patients with HCC in the real world and identify the current situation and problems associated with the guidelines for HCC diagnosis and treatment in China to provide a reference to further optimize the screening, diagnosis, clinical staging, and treatment of HCC.

MATERIALS AND METHODS

The statistical methods of this study were reviewed by Cheng Cheng from the Department of Epidemiology and Health Statistics at Zhengzhou University.

Primary and secondary outcomes

The main research results of this paper show that compliance in the clinical application of the Chinese guidelines for HCC diagnosis and treatment is good, screening compliance is poor,- and following the guidelines for screening and treatment can help patients to obtain certain survival benefits. This study also found that patients who underwent hepatectomy according to the guidelines had a significant advantage in tumor-free survival compared with those whose treatment did not follow the guidelines.

Study design and target population

This was a real-world retrospective study based on the medical records system of the First Affiliated Hospital of Zhengzhou University.

The inclusion criteria involved patients: (1) With a final diagnosis of HCC; (2) aged ≥ 18 years at HCC diagnosis; (3) who had not received a related treatment in other hospitals before being diagnosed with HCC; (4) without complications with other serious immune system diseases, such as human immunodeficiency virus, syphilis, and leukemia; (5) without other malignant tumors; and (6) with complete clinical data.

The exclusion criteria included patients: (1) Without a final diagnosis of HCC; (2) with a diagnosis of intrahepatic cholangiocarcinoma (ICC) or HCC–ICC; (3) aged < 18 years; (4) with HCC diagnosed and treated in other hospitals; (5) with HCC diagnosed before January 1, 2011; (6) with other severe immune system diseases; (7) with other malignant tumors; and (8) with missing clinical data that could not be staged.

The guidelines define HCC as a malignant tumor of liver cells, while ICC refers to cancer of the intrahepatic bile duct branch lined with complex epithelial cells. The most common malignancies of ICC are adenocarcinomas. As this was a retrospective study, the patients included those who had been definitively clinically diagnosed with HCC and excluded those clinically diagnosed with ICC and HCC–ICC.

This study was approved (ZZUIRB2022-151) by Zhengzhou University. In accordance with national legislative and institutional requirements, participation in the study did not require written informed consent. The general guarantor of the study ensured the protection and confidentiality of the original data and examined the data analysis. This study was performed in accordance with the moral principles of the Declaration of Helsinki.

Data collection

The main data collected included patients' demographic characteristics, imaging and serological reports, treatment plans, and prognoses that could be traced back.

The following demographic and sociological characteristics were collected: (1) Hospitalization number; (2) sex; (3) age; (4) dates of admission and discharge; (5) clinical status at discharge; (6) presence of chronic diseases (*e.g.*, hypertension, diabetes, and stroke); (7) presence of a family history of cancer; (8) presence of chronic viral hepatitis; (9) presence of cirrhosis; and (10) whether the patient was screened for HCC.

The patients' imaging diagnostic reports included computed tomography and magnetic resonance imaging findings, liver biopsy records, and intraoperative images when diagnosed with HCC. The data collected included: (1) Number of tumors; (2) maximum diameter of a single tumor; (3) presence of extrahepatic or lymph node metastasis; (4) degree of tumor differentiation; (5) presence of ascites and its

severity; and (6) presence of portal hypertension.

The serological reports of the patients included: (1) Alpha-fetoprotein (AFP); (2) total bilirubin; (3) albumin levels; and (4) prothrombin time. The AFP level in CNLC staging recommended by the guidelines is divided into three[9,10]: AFP ≤ 20, 20–400, and > 400 (ng/mL); according to the guidelines, an AFP level > 400 ng/mL is considered significantly increased.

The treatment information collected included: (1) Whether the patients accepted surgical treatment and the method, which included LR, radiofrequency ablation (RFA), liver transplantation (LT), and transcatheter arterial chemoembolization (TACE); and (2) whether the patients used oral anti-tumor drugs and the dosage regimen.

Patient survival: For patients with no clinical outcome in the hospital, we followed up with their families *via* telephone to determine the survival status of the patients. The main contents of the follow-up included: (1) Whether the patients survived until December 31, 2020; and (2) if the patient died, the cause and time of death were noted.

Data analysis

CNLC staging: We performed CNLC staging according to the guidelines, as follows: (1) CNLC Ia stage: performance status (PS): 0–2, Child–Pugh A/B liver function, single tumor, diameter ≤ 5 cm, with no vascular tumor thrombus and extrahepatic metastasis on imaging; (2) CNLC stage Ib: PS 0–2, Child–Pugh A/B liver function, single tumor, diameter > 5 cm, or two to three tumors, maximum diameter ≤ 3 cm, with no vascular tumor thrombus and extrahepatic metastasis; (3) CNLC stage IIa: PS 0–2, Child–Pugh A/B liver function, two to three tumors, maximum diameter > 3 cm, with no vascular tumor thrombus and extrahepatic metastasis; (4) CNLC stage IIb: PS 0–2, Child–Pugh A/B liver function, tumor number ≥ 4, status regardless of tumor diameter, with no vascular tumor thrombus and extrahepatic metastasis; (5) CNLC stage IIIa: PS 0–2, Child–Pugh A/B liver function, tumor status regardless of vascular tumor thrombus and no extrahepatic metastasis; (6) CNLC stage IIIb: PS 0–2, Child–Pugh A/B liver function, regardless of tumor status, whether there was vascular tumor thrombus on imaging, and extrahepatic metastasis; and (7) CNLC stage IV: PS 3–4 or Child–Pugh C liver function, regardless of tumor status, with presence or absence of vascular tumor thrombus on imaging and presence or absence of extrahepatic metastasis[9,10]. Patients with CNLC stages Ia, Ib, and IIa are generally considered to have early-stage HCC; those with CNLC stages IIb and IIIa are considered to have middle-stage HCC, and those with CNLC stages IIIb and IV are considered to have late-stage HCC.

Screening analysis

The guidelines recommend that early screening for HCC includes liver ultrasound imaging and serum AFP level determination[9,10]. Furthermore, the guidelines identify high-risk groups for HCC as those with hepatitis B virus (HBV) and/or hepatitis C virus (HCV) infection, excessive alcohol consumption, non-alcoholic steatohepatitis, cirrhosis caused by other causes, and a family history of liver cancer, especially in males older than 40 years[9,10].

In this study, patients with HCC who were diagnosed by screening were (1): Those who reported that they might have a high risk for HCC and those diagnosed with HCC *via* regular re-examination; and (2) those diagnosed with HCC during a routine physical examination without any symptoms.

Diagnosis and treatment analysis

The diagnosis and treatment of these patients in the real world and their compliance with the treatment recommended by the guidelines were analyzed. As this study was retrospective, information on the treatment methods received by the patients was collected from the hospital's electronic medical records system and confirmed by attending clinicians.

Treatment effect analysis

The therapeutic effects of the patients in this study were reflected mainly in two aspects: (1) The survival analysis of 1128 patients traced back to the clinical outcomes based on different CNLC staging, whether it complied with the guidelines, and the main risk factors affecting the patients' survival; and (2) the analysis of tumor-free survival and risk factors for postoperative tumor recurrence in patients with HCC who received LR.

Statistical analysis

The baseline characteristics and treatment modalities of the study population based on CNLC staging were summarized as frequencies (percentages), means (standard deviations), or medians (ranges). Categorical variables were summarized as numbers and percentages, and continuous variables were presented as medians, ranges, and 95%CI. Categorical data were compared using Chi-squared or Fisher's exact tests, and continuous variables were compared using Mann–Whitney's *U* test. The primary outcome was overall survival time and the secondary outcome was tumor-free survival time. The overall survival time since HCC diagnosis and the median tumor-free survival time after LR in each CNLC stage were determined using Kaplan–Meier estimations. Comparisons of overall survival

probability rates between groups were illustrated using Kaplan–Meier survival curves, and the survival differences between groups were estimated using log–rank tests. Statistical significance was set at $P < 0.05$. Finally, we used Cox models to analyze independent factors affecting overall survival time and tumor-free survival in patients who received LR.

RESULTS

General characteristics of patients with HCC

Between 2011 and 2019, 4579 patients were diagnosed with HCC and hospitalized in the First Affiliated Hospital of Zhengzhou University, with 3022 patients screened for inclusion in this study (Figure 1). Among the patients included, 2487 (82.3%) males and 535 (17.7%) females were diagnosed with HCC for the first time between the ages of 18 and 84 years, with an average age of 59.57 years. The proportions of patients with HCC with a history of smoking and drinking were 38.32% and 31.40%, respectively. Among the eligible patients, chronic liver disease was as follows: 2793 had HBV, 187 had HCV, 106 had non-alcoholic fatty liver disease (NAFLD), and 24 developed alcoholic liver disease (ALD). The following complications were noted: A total of 533 had hypertension, 360 had diabetes, and 95 had coronary heart disease. At initial diagnosis, 36.2% of the patients had normal AFP values (< 20 ng/mL), and 38.7% had significantly elevated AFP levels (> 400 ng/mL). The highest proportion of patients with significantly increased AFP was found in those with CNLC stage IV, reaching 59.5% (Table 1). The total number of patient hospitalizations was 14441, with an average hospitalization number and duration of 4.78 times and 9.59 d, respectively.

Diagnosis and CNLC staging of patients with HCC

Chinese Liver Cancer staging was performed for all patients with HCC, including 620 with CNLC stage Ia, 447 with CNLC stage Ib, 60 with CNLC stage IIa, 887 with CNLC stage IIb, 552 with CNLC stage IIIa, 362 with CNLC stage IIIb, and 94 with CNLC stage IV. The final diagnosis methods of patients with different CNLC stages also differed. The diagnosis methods of patients with CNLC stage Ia, Ib, and IIa were mainly pathology based, accounting for 70.3%, 60.4%, and 63.3%, respectively. The diagnosis methods of patients with CNLC stage IIb, IIIa, IIIb, and IV were mainly based on imaging examinations and clinical features (Table 1), accounting for 67.3%, 58.6%, 69.3%, and 81.9%, respectively. The liver function grades of the patients were as follows: There were 2191 patients with Child–Pugh grade A, 737 with Child–Pugh grade B, and 94 with Child–Pugh grade C (Table 2).

Compliance and effect of HCC screening

Of the 3022 patients with HCC, 304 (10.06%) were diagnosed during screening (Table 3), 69.08% were in the early stage, 28.29% were in the middle stage, and 2.63% were in the late stage. Among 2718 patients with HCC who were not diagnosed during screening, only 33.74% were in the early stage, which was a significantly lower level than in those who were screened ($P < 0.01$). Among the patients who were screened, 90.79% had Child–Pugh grade-A liver function, while only 70.46% of the patients who were not screened had Child–Pugh grade-A liver function, and the difference was statistically significant ($P < 0.01$) (Table 3). These results suggest that screening can detect early CNLC HCC stages and that these patients had better liver function. Additionally, patients with HCC who were screened had a greater probability of receiving curative treatment methods, such as LR and LT.

Treatment of patients with HCC at different CNLC stages

Among 3022 patients, 2648 (87.62%) received active anti-tumor therapy, 803 received LR, 203 received RFA, 92 received LT, 1052 received TACE, 185 received TACE + RFA, 89 received TACE + LR, and 224 received systemic anti-tumor therapy in their first treatment. The remaining 374 received only palliative therapy or had their treatment discontinued, and the patient was discharged. Overall, 2212 patients received the treatment recommended by the guidelines, accounting for 73.20% (2212/3022) of all patients, and 83.76% (2212/2641) received active anti-tumor therapy. Among these patients, 74.3%, 88.8%, 86.6%, 69.3%, 74.8%, 60.4%, and 58.5% of those in stages Ia, Ib, IIa, IIb, IIIa, IIIb, and IV received the treatments recommended by the guidelines, respectively (Table 2). The results indicated that the treatment recommended by the guidelines was in good agreement with the clinical treatment of HCC in China during the last 10 years. Patients in the early and middle stages were more likely to accept the treatment recommended by the guidelines. Table 4 shows that 76.27% of the patients receiving guideline-recommended treatment had Child–Pugh grade-A liver function, while only 62.22% of the patients not receiving the treatment recommended by the guidelines had Child–Pugh grade-A liver function ($P < 0.001$). This suggests that the liver function status of the patients was an important factor affecting their treatment choice. Table 4 also shows the CNLC staging characteristics of 810 patients who did not receive the treatment recommended by the guidelines: Of these, 26.79% were in the early stage of HCC, 50.74% were in the middle stage, and 22.47% were in the late stage, indicating that most of the patients who did not receive the treatment recommended by the guidelines were in the middle stage of

Table 1 Baseline characteristics of patients with different China Liver Cancer staging levels, *n* (%)

Variables	CNLC staging							
	Total	Ia	Ib	IIa	IIb	IIIa	IIIb	IV
Sex								
Male	2487 (82.3)	492 (79.3)	365 (81.7)	47 (78.3)	742 (83.7)	468 (84.7)	295 (81.4)	78 (82.9)
Female	535 (17.7)	128 (20.7)	82 (18.3)	13 (21.7)	145 (16.3)	84 (16.3)	67 (18.6)	16 (17.1)
Age								
≤ 50	884 (29.2)	185 (29.8)	116 (25.9)	16 (26.7)	245 (27.7)	175 (31.7)	112 (30.9)	35 (37.3)
> 50	2138 (70.8)	435 (70.2)	331 (74.1)	44 (73.3)	642 (72.3)	377 (68.3)	250 (69.1)	59 (62.7)
Chronic hepatitis								
HBV	2793 (90.6)	558 (90.0)	398 (89.0)	52 (86.6)	808 (91.0)	513 (92.9)	323 (89.2)	87 (92.5)
HCV	187 (6.1)	48 (7.7)	22 (4.9)	6 (10.0)	54 (6.0)	32 (5.7)	19 (5.2)	6 (6.3)
NAFLD	106 (3.5)	34 (32.0)	27 (25.4)	0 (0.0)	23 (21.6)	12 (11.3)	8 (7.5)	2 (1.8)
ALD	24 (0.7)	4 (16.6)	3 (12.5)	1 (4.1)	7 (29.1)	6 (25.0)	2 (8.3)	1 (4.1)
Complications								
Hypertension	533 (17.6)	125 (20.1)	87 (19.4)	9 (15.0)	158 (17.8)	82 (14.8)	60 (16.5)	12 (12.7)
Diabetes	360 (11.9)	75 (12.0)	42 (9.3)	12 (20.0)	112 (12.6)	68 (12.3)	39 (10.7)	12 (12.7)
Coronary heart disease	95 (3.1)	22 (3.5)	15 (3.3)	1 (1.6)	30 (3.3)	13 (2.3)	12 (3.3)	2 (2.1)
Smoking history	1158 (38.32)	215 (34.96)	170 (39.63)	25 (35.71)	340 (38.16)	223 (39.89)	152 (41.76)	33 (35.11)
Drinking history	949 (31.40)	182 (29.59)	136 (31.70)	18 (25.71)	277 (31.09)	176 (31.48)	128 (35.16)	32 (34.04)
AFP (ng/mL)								
≤ 20	1094 (36.2)	345 (55.7)	187 (41.8)	42 (70.0)	318 (35.9)	115 (20.8)	90 (24.8)	16 (17.0)
20–400	757 (25.1)	170 (27.4)	101 (22.6)	18 (30.0)	223 (26.2)	132 (23.9)	80 (22.1)	22 (23.5)
> 400	1171 (38.7)	105 (16.9)	159 (35.6)	0 (0.0)	336 (37.9)	305 (55.2)	192 (53.1)	56 (59.5)

HBV: Hepatitis B virus; HCV: Hepatitis C virus; CNLC: China Liver Cancer staging; AFP: Alpha-fetoprotein; NAFLD: Non-alcoholic fatty liver disease; ALD: Alcoholic liver disease.

HCC.

Real-world data showed that among the 2648 patients receiving active anti-tumor therapy, the treatment choice was not the same in each CNLC stage (Figure 2). LR and RFA accounted for 53.64% and 17.22%, respectively, inpatients with CNLC stage Ia HCC, while in patients with CNLC stage Ib HCC, LR (44.03%) and TACE (33.96%) were mainly selected. In patients with CNLC stage IIa, treatment was mainly with LR (48.28%) and TACE (22.41%), while those with CNLC stage IIb were treated mainly with TACE (54.95%) and LR (13.28%). In CNLC stage IIIa, TACE (45.75%) and LR (27.45%) were mostly selected, while patients in CNLC stage IIIb received mainly TACE (52.03%) and systemic anti-tumor therapy (23.25%). Among 94 patients with CNLC stage IV HCC, 61 received anti-tumor therapy, with most receiving TACE (45.90%) and LT (21.31%). These results suggest that patients in the early stage of HCC were more likely to receive LR, while those in the middle and late stages were more likely to receive TACE.

Patient prognosis

Overall survival analysis: In this study, patients who did not have a clinical outcome during hospitalization were followed up to December 31, 2020. We collected the clinical outcomes of 1128 patients. Among the general clinical characteristics of these patients, 922 (81.74%) were male, and 798 (70.74%) were over the age of 50. There were 992 (87.94%) patients with HBV, 56 (4.96%) with HCV, 62 (5.50%) with NAFLD, and 18 (1.60%) with ALD. There were 226 (20.04%) patients with hypertension, 159 (14.10%) with diabetes, and 33 (2.93%) with coronary heart disease. Of the patient population, 408 (36.17%) and 337 (29.88%) had a history of smoking and drinking, respectively. There were 870 (77.13%) cases of Child–Pugh grade A, 228 (20.21%) cases of Child–Pugh Grade B, and 30 (2.66%) cases of Child–Pugh grade C (Table 5). In terms of overall survival, 407 deaths and 721 survivals were observed, with a median survival of 54.0 mo (95%CI: 50.0–61.0). Statistically significant differences were observed

Table 2 Diagnosis and treatment of patients with different China Liver Cancer staging levels, *n* (%)

	CNLC staging							
	Total (*n* = 3022)	Ia (*n* = 620)	Ib (*n* = 447)	IIa (*n* = 60)	IIb (*n* = 887)	IIIa (*n* = 552)	IIIb (*n* = 362)	IV (*n* = 94)
HCC diagnosis								
Pathology	1390 (45.9)	436 (70.3)	270 (60.4)	38 (63.3)	290 (32.6)	228 (41.3)	111 (30.6)	17 (18.1)
Imaging	1632 (54.1)	184 (29.6)	117 (39.5)	22 (36.6)	597 (67.3)	324 (58.6)	251 (69.3)	77 (81.9)
Child–Pugh grade								
A	2191 (72.5)	537 (86.6)	378 (84.5)	48 (80.0)	625 (70.4)	369 (66.8)	234 (64.6)	0 (0.0)
B	737 (24.3)	83 (13.4)	69 (15.4)	12 (20.0)	262 (29.5)	183 (33.1)	128 (35.4)	0 (0.0)
C	94 (3.1)	0 (0.0)	0 (0.0)	0 (0.0)	0 (0.0)	0 (0.0)	0 (0.0)	94 (100.0)
Treatments								
LR	803 (26.5)	324 (52.2)[1]	188 (42.0)[1]	28 (46.6)[1]	102 (11.4)[1]	126 (22.8)[1]	35 (9.6)	0 (0.0)
RFA	203 (6.7)	104 (16.7)[1]	27 (6.0)[1]	5 (8.3)	48 (5.5)	10 (1.8)	6 (1.6)	3 (3.1)
LT	92 (3.0)	10 (1.6)[1]	4 (0.8)[1]	0 (0.0)	38 (4.2)	25 (4.5)	6 (1.6)	9 (9.5)[1]
TACE	1052 (34.8)	93 (15.0)	145 (32.4)[1]	13 (21.6)[1]	422 (47.5)[1]	210 (38.0)[1]	141 (38.9)[1]	28 (29.7)
TACE + RFA	185 (6.1)	46 (7.4)	33 (7.3)[1]	7 (11.6)[1]	67 (7.5)	11 (1.9)	15 (4.1)[1]	6 (6.3)
LR + RFA	89 (2.9)	23 (3.7)[1]	19 (4.2)	4 (6.6)[1]	17 (1.8)[1]	19 (3.4)[1]	5 (1.3)	2 (2.1)
Systemic anti-tumor therapy	224 (7.4)	4 (0.6)	12 (2.6)	1 (1.6)	74 (8.3)[1]	58 (10.5)[1]	63 (17.4)[1]	13 (13.8)[1]
BSC	374 (12.3)	16 (2.5)	20 (4.4)	2 (3.3)	119 (13.4)	93 (16.8)	91 (25.1)	33 (35.1)[1]
Adherence[1]	2212 (73.2)	461 (74.3)	397 (88.8)	52 (86.6)	615 (69.3)	413 (74.8)	219 (60.4)	55 (58.5)

[1]Treatment modalities recommended by the Guidelines for Diagnosis and Treatment of Primary Liver Cancer in China.
HCC: Hepatocellular carcinoma; CNLC: China Liver Cancer staging; LR: Liver resection; RFA: Radiofrequency ablation; LT: Liver transplantation; TACE: Transcatheter arterial chemoembolization; BSC: Best supportive care.

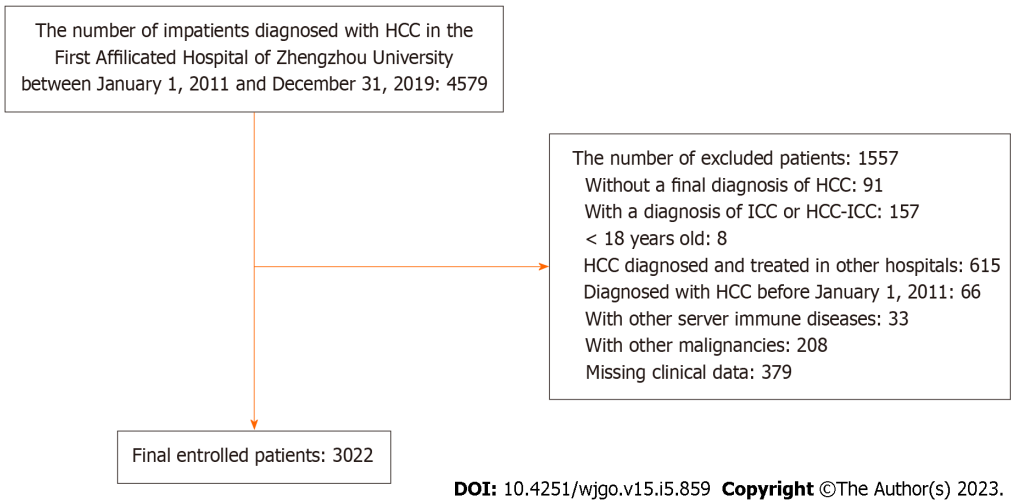

DOI: 10.4251/wjgo.v15.i5.859

Figure 1 Flowchart of selection of study participants. HCC: Hepatocellular carcinoma; ICC: Intrahepatic cholangiocarcinoma.

in overall survival among patients with different CNLC staging ($P < 0.001$), with a median survival of 73 mo (95%CI: 63.0–99.0) in the early stage, 39 mo (95%CI: 33.0–47.0) in the middle stage, and 21 mo (95%CI: 15.0–29.0) in the late stage (Figure 3A). No statistically significant differences were observed in terms of overall survival between patients who complied with the treatment recommended by the guidelines and those who did not ($P = 0.344$). The median survival was 54 mo (95%CI: 47.0–58.0) and 51 mo (95%CI: 41.0–64.0), respectively (Figure 3B).

Table 3 Compliance with and effect of hepatocellular carcinoma screening, *n* (%)

Variable	Total (*n* = 3022)	Whether to undergo screening		χ^2	P value
		Yes, *n* = 304 (10.06%)	No, *n* = 2718 (89.94%)		
Sex				0.254	0.614
Male	2487 (82.30)	247 (81.25)	2240 (82.41)		
Female	535 (17.70)	57 (18.75)	478 (17.59)		
Age				0.621	0.431
< 50	884 (29.25)	83 (27.30)	801 (29.47)		
≥ 50	2138 (70.75)	221 (72.70)	1917 (70.53)		
Chronic hepatitis				1.891	0.595
HBV	2694 (89.15)	266 (87.50)	2428 (89.33)		
HCV	142 (4.70)	19 (6.25)	123 (4.53)		
Mix	45 (1.49)	5 (1.64)	40 (1.47)		
None	141 (4.66)	14 (4.61)	127 (4.67)		
Smoking				0.652	0.419
Yes	1158 (38.32)	110 (36.18)	1048 (38.56)		
No	1864 (61.68)	194 (63.82)	1670 (61.44)		
Alcohol				1.217	0.270
Yes	949 (31.40)	87 (28.62)	862 (31.71)		
No	2073 (68.60)	217 (71.38)	1856 (68.29)		
Hypertension				2.714	0.099
Yes	533 (17.64)	64 (21.05)	469 (17.26)		
No	2489 (82.36)	240 (78.95)	2249 (82.74)		
Diabetes				0.002	0.968
Yes	360 (11.91)	36 (11.84)	324 (11.92)		
No	2662 (88.09)	268 (88.16)	2394 (88.08)		
Coronary heart disease				3.559	0.059
Yes	95 (3.14)	15 (4.93)	80 (2.94)		
No	2927 (96.86)	289 (95.07)	2638 (97.06)		
Family history of tumors				0.009	0.923
Yes	473 (15.65)	47 (15.46)	426 (15.67)		
No	2549 (84.35)	257 (84.54)	2292 (84.33)		
AFP (ng/mL)				41.808	0.000[a]
≤ 20	1094 (36.20)	145 (47.70)	949 (34.92)		
20-400	757 (25.05)	93 (30.59)	664 (24.43)		
> 400	1171 (38.75)	66 (21.71)	1105 (40.65)		
Child-Pugh Grade				58.031	0.000[a]
A	2191 (72.50)	276 (90.79)	1915 (70.46)		
B	737 (24.39)	28 (9.21)	709 (26.09)		
C	94 (3.11)	0 (0.00)	94 (3.45)		
CNLC				183.202	0.000[a]
Ia	620 (20.52)	141 (46.38)	479 (17.62)		
Ib	447 (14.79)	57 (18.75)	390 (14.35)		

IIa	60 (1.99)	12 (3.95)	48 (1.77)
IIb	887 (29.35)	59 (19.41)	828 (30.46)
IIIa	552 (18.27)	27 (8.88)	525 (19.32)
IIIb	362 (11.98)	8 (2.63)	354 (13.02)
IV	94 (3.10)	0 (0.00)	94 (3.46)

[a]$P < 0.01$.
HBV: Hepatitis B virus; HCV: Hepatitis C virus; Mix: HBV complicated with HCV; CNLC: China Liver Cancer staging; AFP: Alpha-fetoprotein.

Table 4 Analysis of treatment compliance among patients with hepatocellular carcinoma according to the Guidelines for Diagnosis and Treatment of Primary Liver Cancer in China, *n* (%)

Variable	Total (*n* = 3022)	Compliance with guideline-recommended treatment		χ^2	P value
		Yes, *n* = 2212 (73.20%)	No, *n* = 810 (26.80%)		
Sex				3.191	0.074
Male	2487 (82.30)	1837 (83.05)	650 (80.25)		
Female	535 (17.70)	375 (16.95)	160 (19.75)		
Age				0.652	0.419
< 50	884 (29.25)	656 (29.66)	228 (28.15)		
≥ 50	2138 (70.75)	1556 (70.34)	582 (71.85)		
Chronic hepatitis				2.046	0.309
HBV	2694 (89.15)	1979 (89.47)	715 (88.27)		
HCV	142 (4.70)	96 (4.34)	46 (5.68)		
Mixed	45 (1.49)	36 (1.63)	9 (1.11)		
None	141 (4.66)	101 (4.56)	40 (4.94)		
AFP (ng/mL)				1.859	0.395
≤ 20	1094 (36.20)	786 (35.53)	308 (38.02)		
20–400	757 (25.05)	555 (25.09)	202 (24.94)		
> 400	1171 (38.75)	871 (39.38)	300 (37.04)		
Child–Pugh grade				59.828	0.000[a]
A	2191 (72.50)	1687 (76.27)	504 (62.22)		
B	737 (24.39)	470 (21.25)	267 (32.96)		
C	94 (3.11)	55 (2.49)	39 (4.81)		
CNLC				74.941	0.000[a]
Early stage (Ia, Ib, and IIa)	1127 (37.29)	910 (41.14)	217 (26.79)		
Middle stage (IIb and IIIa)	1439 (47.62)	1028 (46.47)	411 (50.74)		
Late stage (IIIb and IV)	456 (15.09)	274 (12.39)	182 (22.47)		

[a]$P < 0.01$.
HBV: Hepatitis B virus; HCV: Hepatitis C virus; Mix: HBV complicated with HCV; CNLC: China Liver Cancer staging; AFP: Alpha-fetoprotein.

Subsequently, we used the Cox model to analyse the risk factors affecting patients' survival. The univariate results showed that age, screening, Child–Pugh grade, AFP level, and CNLC staging were risk factors affecting the survival time of patients with HCC ($P < 0.05$). A multivariate analysis used to verify these results revealed that the following independent risk factors affected overall survival: Age > 50 years [hazard ratio (HR): 1.359, 95%CI: 1.081–1.709], no screening (HR: 2.181, 95%CI: 1.435–3.313), AFP > 400 ng/mL (HR: 1.576, 95%CI: 1.256–1.977), Child–Pugh grade B (HR: 1.813, 95%CI: 1.480–2.252), middle-stage HCC (HR: 2.610, 95%CI: 2.056–3.312), and late-stage HCC (HR: 3.967, 95%CI: 2.827–5.591)

Table 5 Basic characteristics of followed-up patients with hepatocellular carcinoma (*n* = 1128), *n* (%)

Variables	CNLC staging							
	Total	Ia	Ib	IIa	IIb	IIIa	IIIb	IV
Sex								
Male	922 (81.74)	261 (80.56)	152 (79.58)	21 (75.00)	252 (84.00)	151 (84.36)	60 (78.95)	25 (83.33)
Female	206 (18.26)	63 (19.44)	39 (20.42)	7 (25.00)	48 (16.00)	28 (15.64)	16 (21.05)	5 (16.67)
Age								
≤ 50	330 (29.26)	105 (32.41)	51 (26.70)	8 (28.57)	74 (24.67)	54 (30.17)	23 (30.26)	15 (50.00)
> 50	798 (70.74)	219 (67.59)	140 (73.30)	20 (71.43)	226 (75.33)	125 (69.83)	53 (69.74)	15 (50.00)
Chronic hepatitis								
HBV	992 (87.94)	284 (87.65)	167 (87.43)	21 (75.00)	266 (88.67)	161 (89.94)	68 (89.47)	25 (83.33)
HCV	56 (4.96)	21 (6.48)	8 (4.19)	3 (10.71)	12 (4.00)	8 (4.47)	2 (2.63)	2 (6.67)
NAFLD	62 (5.50)	14 (4.32)	14 (7.33)	3 (10.71)	17 (5.67)	6 (3.35)	6 (7.89)	2 (6.67)
ALD	18 (1.60)	5 (1.54)	2 (1.05)	1 (3.57)	5 (1.67)	4 (2.23)	0 (0.00)	1 (3.33)
Complications								
Hypertension	226 (20.04)	70 (21.60)	38 (19.90)	5 (17.86)	65 (21.67)	28 (15.64)	17 (22.37)	3 (10.00)
Diabetes	159 (14.10)	2 (12.96)	21 (10.99)	6 (21.43)	49 (16.33)	24 (13.41)	11 (14.47)	6 (20.00)
Coronary heart disease	33 (2.93)	7 (2.16)	8 (4.19)	1 (3.57)	10 (3.33)	2 (1.12)	4 (5.26)	1 (3.33)
Smoking	408 (36.17)	121 (37.35)	68 (35.60)	8 (28.57)	101 (33.67)	67 (37.43)	30 (39.47)	13 (43.33)
Drinking	337 (29.88)	98 (30.25)	53 (27.75)	7 (25.00)	88 (29.33)	50 (27.93)	29 (38.16)	12 (40.00)
AFP (ng/mL)								
≤ 20	491 (43.53)	184 (56.79)	90 (47.12)	11 (39.29)	129 (43.00)	46 (25.70)	24 (31.58)	7 (23.33)
20–400	289 (25.62)	92 (28.40)	43 (22.51)	8 (28.57)	75 (25.00)	47 (26.26)	16 (21.05)	8 (26.67)
> 400	348 (30.85)	48 (14.81)	58 (30.37)	9 (32.14)	96 (32.00)	86 (48.04)	36 (47.37)	15 (50.00)
Child–Pugh grade								
A	870 (77.13)	284 (87.65)	168 (87.96)	23 (82.14)	213 (71.00)	132 (73.74)	50 (65.79)	0 (0.00)
B	228 (20.21)	40 (12.35)	23 (12.04)	5 (17.86)	87 (29.00)	47 (26.26)	26 (34.21)	0 (0.00)
C	30 (2.66)	0 (0.00)	0 (0.00)	0 (0.00)	0 (0.00)	0 (0.00)	0 (0.00)	30 (100.00)

CNLC: China Liver Cancer staging; HBV: Hepatitis B virus; HCV: Hepatitis C virus; NAFLD: Non-alcoholic fatty liver disease; ALD: Alcoholic liver disease; AFP: Alpha-fetoprotein.

(Table 6).

Tumor-free survival in patients with HCC treated with LR: Overall, 803 patients underwent LR, including 768 who received LR as recommended by the guidelines and 35 who did not receive LR as recommended by the guidelines. Statistically significant differences were observed in terms of tumor-free survival between patients who received guideline-recommended LR treatment and those who received non-guideline-recommended LR treatment ($P < 0.001$), with median tumor-free survival of 18 mo (95%CI: 14.0–21.0) and 2 mo (95%CI: 1.0-4.0), respectively (Figure 4A). Among the 803 patients receiving LR at different CNLC stages, 540 patients had early-stage HCC; of these, 200 experienced a recurrence during the study period, with a maximum of 87 mo and a median of 24 mo of tumor-free survival (95%CI: 20.0–30.0). A total of 228 patients had middle-stage HCC, 130 of whom experienced a recurrence during the study, with a maximum tumor-free survival of 59 mo and a median of 5 mo (95%CI: 4.0–7.0). Finally, 35 patients had late-stage HCC, 22 of whom experienced a recurrence during the study, with a maximum tumor-free survival of 54 mo and a median of 2 mo (95%CI: 1.0–4.0). The results showed a statistically significant difference in tumor-free survival between patients who received LR in the early stage of HCC and those who received LR in the middle and late stages of the disease ($P < 0.001$). No statistically significant differences were observed in tumor-free survival between patients who received LR in the middle and late stages of HCC ($P = 0.099$) (Figure 4B).

Table 6 Analysis of overall survival in patients with hepatocellular carcinoma

Variables	Univariate analysis	Multivariate analysis	
	P value	P value	Hazard ratio (95%CI)
Sex	0.5736	–	
Age (> 50)	0.0074[a]	0.0087[b]	1.359 (1.081–1.709)
Screening	< 0.001[b]	0.0003[b]	2.181 (1.435–3.313)
HBV	0.0703	–	
HCV	0.0354	–	
Child-Pugh grade	< 0.001[b]		
A			1 reference
B		< 0.001[b]	1.813 (1.480–2.252)
C		0.3798	1.274 (0.742–2.190)
CNLC staging	< 0.001[b]		
Early			1 reference
Middle		< 0.001[b]	2.610 (2.056–3.312)
Late		< 0.001[b]	3.967 (2.827–5.591)
AFP (ng/mL)	< 0.001[b]		
≤ 20			1 reference
20–400		0.615	1.070 (0.822–1.392)
> 400		< 0.001[b]	1.576 (1.256–1.977)

[a]$P < 0.05$.
[b]$P < 0.01$.
CI: Confidence interval; HCC: Hepatocellular carcinoma; HBV: Hepatitis B virus; HCV: Hepatitis C virus; CNLC: China Liver Cancer staging, AFP: Alpha-fetoprotein.

The Cox model was used to analyze the risk factors for postoperative recurrence in patients undergoing LR. The univariate results showed that sex, Child–Pugh grade, AFP level, and CNLC staging were independent factors for tumor recurrence ($P < 0.05$). These results were verified using a multivariate analysis, revealing that AFP > 400 ng/mL (HR: 1.612, 95%CI: 1.256–2.070), Child–Pugh grade B (HR: 1.771, 95%CI: 1.243–2.524), middle-stage HCC (HR: 2.556, 95%CI: 2.032–3.215), and late-stage HCC (HR: 3.312, 95%CI: 2.113–5.192) were independent factors affecting the postoperative recurrence of HCC (Table 7).

DISCUSSION

Liver cancer staging is important for selecting treatment options and evaluating prognosis. Many staging systems exist, such as the BCLC, EASL, APASL, JSH, and HKLC systems[3-7]. Among them, the most widely used is the BCLC staging system. The CNLC staging system was established specifically for Chinese people by the National Health Commission in combination with China's specific national conditions and practice accumulation[9,10]. As China has the highest number of liver cancer cases of all countries[1], evaluating the use of China's guidelines for HCC diagnosis and treatment in a real-world setting can provide a broad clinical reference for global liver cancer prevention and treatment.

The strength of this study is that we collected real-world data from a large sample of patients with HCC and conducted CNLC staging for those patients to evaluate the compliance between CNLC staging and real clinical diagnosis and treatment in China. We also performed a systematic review and an analysis of the diagnosis and treatment choices of Chinese patients with HCC in the real world.

The guidelines recommend that imaging and pathological diagnosis are used in HCC diagnosis. In this study, the diagnosis methods of patients in CNLC stages Ia, Ib, and IIa were mainly pathology based, with frequencies of 70.3%, 60.4%, and 63.3%, respectively. The diagnosis methods of patients in CNLC stages IIb, IIIa, IIIb, and IV were based mainly on imaging examinations and clinical features, with frequencies of 67.3%, 58.6%, 69.3%, and 81.9%, respectively.

Table 7 Analysis of factors influencing postoperative recurrence in patients with hepatocellular carcinoma

Variables	Univariate analysis	Multivariate analysis	
	P value	P value	Hazard ratio (95%CI)
Sex	0.0455[a]	0.0164[a]	0.694 (0.515–0.935)
Age (> 50)	0.9711	–	
Screening	0.0678	–	
HBV	0.7773	–	
HCV	0.3531	–	
Child-Pugh grade	0.0012[b]	0.0016[b]	1.771 (1.243–2.524)
CNLC staging	< 0.001[b]		
Early			1 reference
Middle		< 0.001[b]	2.556 (2.032–3.215)
Late		< 0.001[b]	3.312 (2.113-5.192)
AFP (ng/mL)	< 0.001[b]		
≤ 20			1 reference
20–400		0.338	1.139 (0.873–1.487)
> 400		< 0.001[b]	1.612 (1.256–2.070)

[a]$P < 0.05$.
[b]$P < 0.01$.
CI: Confidence interval; HCC: Hepatocellular carcinoma; HBV: Hepatitis B virus; HCV: Hepatitis C virus; CNLC: China Liver Cancer staging; AFP: Alpha-fetoprotein.

In this study, 304 patients were screened before HCC diagnosis. No statistical differences were observed in demographic characteristics between screened and unscreened patients; however, significant differences were observed in terms of liver function grade, AFP levels, and CNLC staging. Among those patients diagnosed *via* screening, 90.79% had Child–Pugh grade-A liver function, while only 70.46% of unscreened patients had the same. The AFP levels of screened patients were low when they were diagnosed with HCC, and only 21.71% of the patients had significantly increased AFP levels (> 400 ng/mL). The proportion of patients who were not screened with significantly increased AFP levels was 40.56%.

Regarding different HCC stages, 69.08%, 28.29%, and 2.63% of patients with early-, middle-, and late-stage HCC were detected *via* screening, while 33.74%, 49.78%, and 16.48% of patients were detected without screening, respectively. The guidelines recommend the regular screening of groups at high risk for HCC to detect more patients with early-stage HCC. Thus, screening can detect more patients with early-stage HCC and encourage patients to undergo curative treatments, thus extending their survival time.

The guidelines recommend screening for groups at high risk for HCC; however, cluster sampling screening is only available in pilot cities, and a planned and regular national screening program is lacking[20]. Currently, some Asian countries and regions, for example, Korea and Japan, have unified national screening programs, and stratified and phased screening programs have been implemented in Taiwan for groups at high risk for HCC. Because of these programs, screening has detected more patients with early-stage HCC, leading to more effective treatment, longer survival, and better quality of life[21-24]. In Europe and the United States, numerous studies have demonstrated the efficacy and cost-effectiveness of HCC screening[25-27]. For example, in a prospective study conducted in France, HCC screening was cost-effective while prolonging patients' survival, even after adjusting for lead-time bias [28]. In a study by Da Fonseca *et al*[29], improved compliance and targeting were key factors in HCC screening. The present study discovered that only 10.06% of patients in the real medical environment received screening or regular physical examinations before HCC diagnosis, indicating that in the real world, Chinese patients with HCC have poor screening compliance.

Studies on compliance with the guidelines in clinical practice in China are limited, with only a few studies on the effectiveness of specific treatment methods based on CNLC staging[11-13] and a systematic review comparing the advantages and disadvantages of CNLC staging with those of other staging methods[14]. In China and other regions, several related studies have been conducted on compliance with BCLC guidelines in clinical practice. For example, in a retrospective study conducted by Zhong *et al*[30] in China, treatment in BCLC staging was compared with that in CNLC staging in

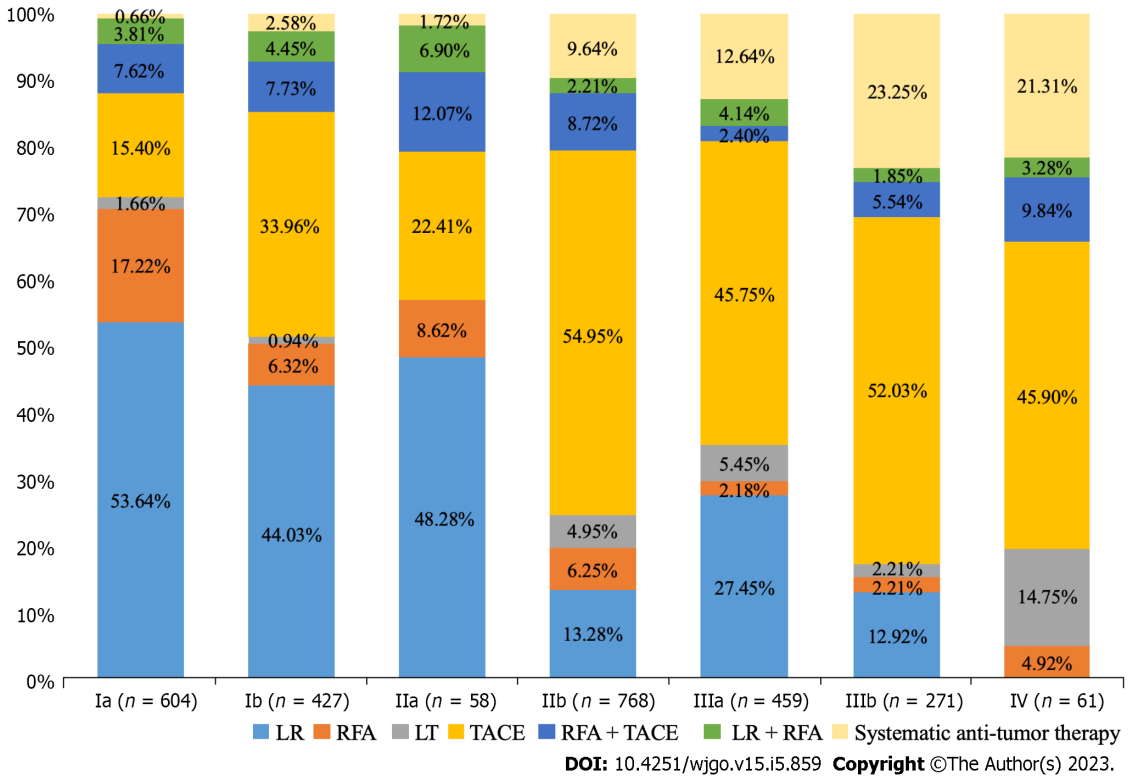

DOI: 10.4251/wjgo.v15.i5.859

Figure 2 Subsequent therapies for patients with hepatocellular carcinoma with different levels of China Liver Cancer staging. LR: Liver resection; RFA: Radiofrequency ablation; LT: Liver transplantation; TACE: Transcatheter arterial chemoembolization.

clinical practice. However, that study did not analyse the screening, diagnosis, and prognosis of patients, which are limitations. In a prospective study based on 160 patients in Korea, Kim *et al*[15] found that only 66% of patients adhered to the treatment regimen recommended by the BCLC guidelines. The main reasons for not using the recommended treatment included refusing surgery, uncertain malignant nodules, lack of a suitable donor, and financial problems. In a study conducted at a general hospital in Italy, Borzio *et al*[16] found that overall adherence to the BCLC guidelines reached 70%, with better adherence by patients in the early and late stages than by those in the middle stage, possibly due to greater heterogeneity in patients in the middle stage. In a multi-center study in Argentina, overall adherence to the BCLC guidelines among patients with HCC was only 50%, which may have been related to the lack of flexibility in BCLC staging and to clinical decision-making by physicians[17].

In this study, we discovered that 73.20% of the treatment methods used in the clinical diagnosis and treatment of patients with HCC in China were consistent with those recommended by the guidelines. Among patients in different HCC stages, 80.75%, 71.39%, and 60.01% of those with early-, middle-, and late-stage HCC received treatments compliant with the guidelines, respectively, which may have been related to the fact that patients in the early stage have more treatment options and are more likely to accept radical treatments[31]. Due to the large individual heterogeneity among patients with middle-stage HCC, selecting appropriate clinical treatment methods is challenging for physicians. Therefore, patients may choose treatment methods over or under those recommended in the clinical diagnosis and treatment guidelines, that are closely related to their liver function and general activity status[32]. In all patients receiving treatment, more than 50% of those with early-stage HCC received LR therapy for the first time, while more than 50% of patients with middle- and late-stage HCC received TACE.

Since most patients were hospitalized in the study hospital after HCC diagnosis, we were able to analyze tumor-free survival in those who underwent LR. This study's results showed a significant difference in tumor-free survival between patients with early-stage HCC and those with middle- and late-stage HCC who received LR, while no statistical differences were observed between patients in the middle and late stages. Statistically significant ($P < 0.001$) differences were observed in tumor-free survival between patients who complied with the guidelines while receiving LR and those who did not. In the analysis of influencing factors for recurrence after hepatectomy, patients with Child–Pugh grade-A liver function were considered as a reference because no patient with Child–Pugh grade-C liver function received hepatectomy. Patients with Child–Pugh grade-B liver function experienced more recurrence after hepatectomy ($P < 0.01$), indicating that the status of patients' liver function was an important risk factor for recurrence after LR[33].

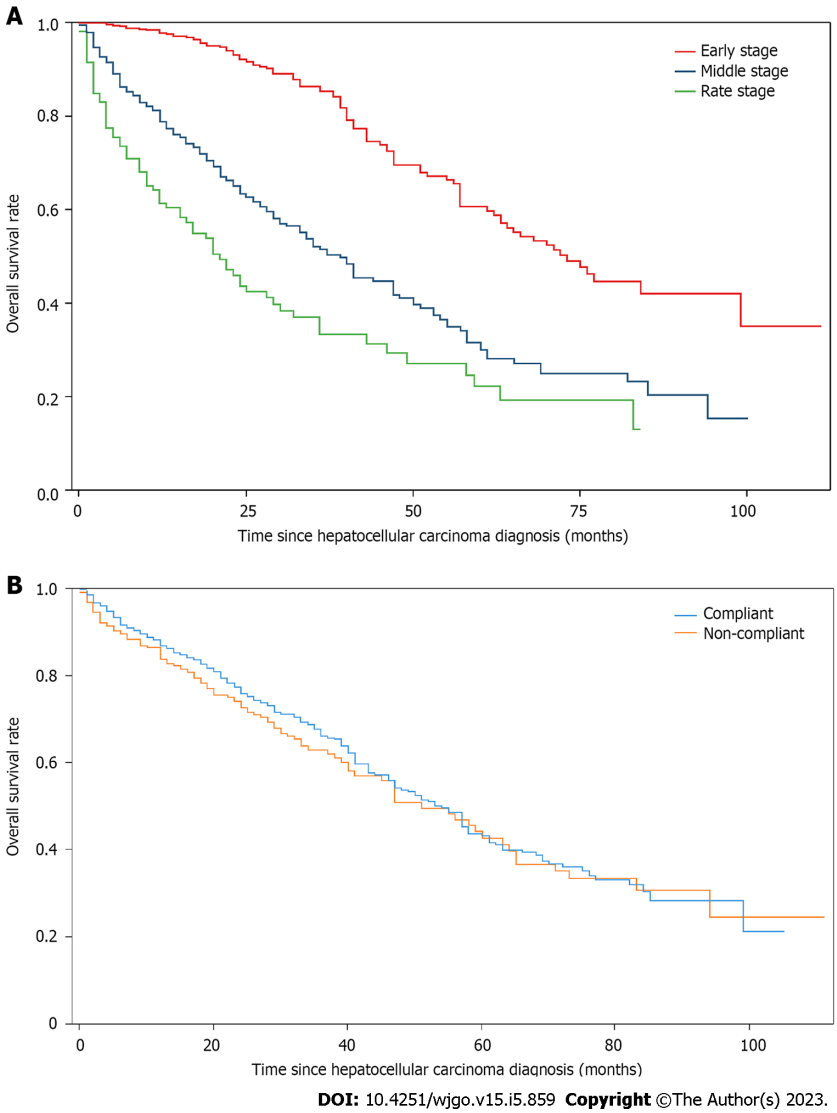

DOI: 10.4251/wjgo.v15.i5.859

Figure 3 Overall survival rate. A: Overall survival rate in patients with different levels of China Liver Cancer staging ($P < 0.001$); B: Patients who did and did not receive treatment recommended by the Guidelines for Diagnosis and Treatment of Primary Liver Cancer in China ($P = 0.344$).

In a cohort study by Liao *et al*[11], two nomograms were constructed to compare the reliability of tumor node metastasis (TNM), BCLC, and CNLC staging in predicting the prognosis of Chinese patients with HCC undergoing LR therapy. The results showed that AFP levels and CNLC staging were the main factors affecting the tumor-free survival of patients. Similarly, CNLC staging predicted the prognosis of patients better than TNM and BCLC staging. However, a cohort study by Li *et al*[13] that examined the prognosis of patients who underwent LR at different stages showed that age, AFP level, tumor size, and tumor number were the main factors affecting early postoperative recurrence.

LR remains the best treatment for HCC. Patients with different stages have shown survival advantages after LR, especially those with early HCC[13]. Similarly, the guidelines recommend that LR be used for eligible patients with late-stage HCC as it has advantages over other treatment methods[13]. In a meta-analysis, survival rates were significantly higher in an LR group than in a TACE group among patients with HCC at BCLC stages B and C[34]. Our study's results also revealed a significant difference in tumor-free survival between patients with early-stage HCC and those with middle- and late-stage HCC after LR, with those at the early stage demonstrating a significant survival advantage after LR. The guidelines recommend LR for eligible patients with middle-stage HCC after screening; however, compared with those in the late stage, LR-treated patients with middle-stage HCC have an advantage in terms of tumor-free survival, but it is limited. More studies are required to demonstrate the survival benefits and cost-effectiveness of LR compared with those of other treatments for patients with middle- and late-stage HCC.

This study's results showed that patients who were treated in accordance with the guidelines had a survival advantage over those who were not, but the advantage was limited (54 *vs* 51 mo), with no statistical difference. This result may be related to the fact that the treatment recommended by the guidelines is relatively fixed. Depending on the actual situation, patients may receive more positive or

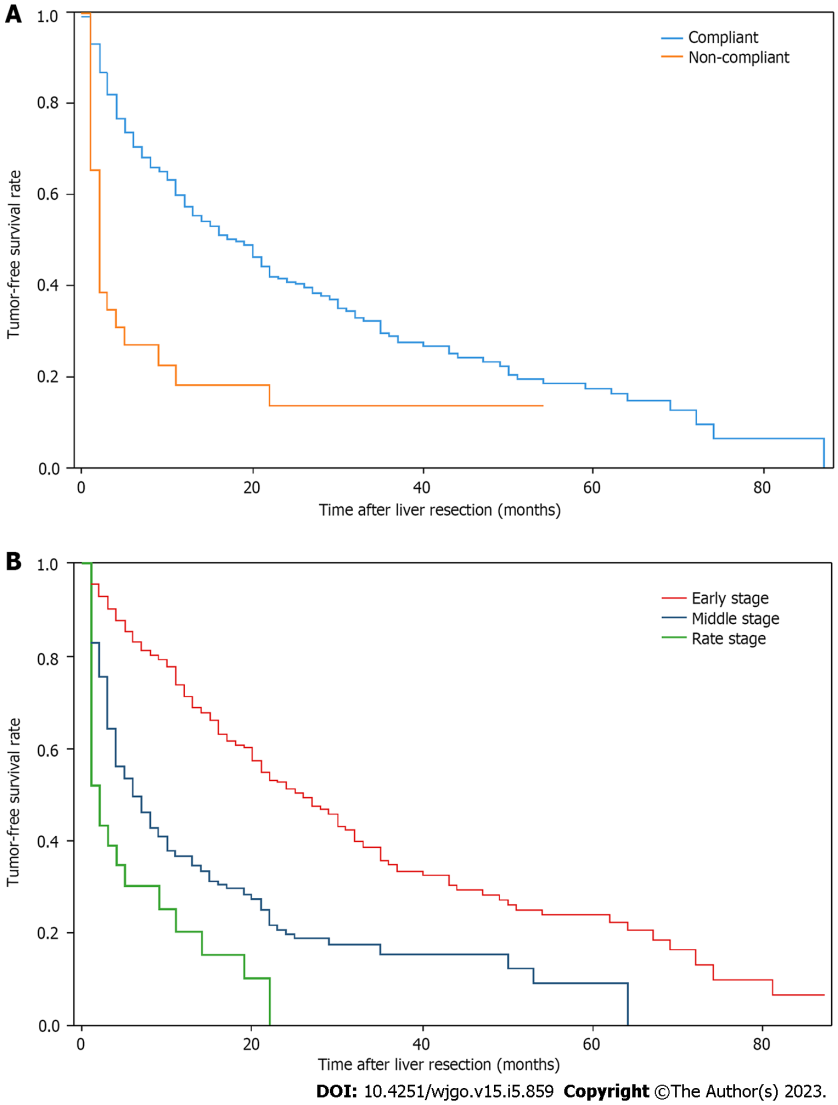

DOI: 10.4251/wjgo.v15.i5.859

Figure 4 Tumor-free survival rate. A: Tumor-free survival rate after liver resection in patients with hepatocellular carcinoma with and without guideline compliance ($P < 0.001$); B: Tumor-free survival rate after liver resection among patients with different China Liver Cancer staging levels. Early stage *vs* middle stage, $P < 0.001$; early stage *vs* late stage, $P < 0.001$; middle stage *vs* late stage, $P = 0.099$.

negative treatment since various factors affect patients' treatment plans. This result is also reflected in a study by Yen *et al*[31] that showed that in patients with stage-B and -C BCLC, the choice of treatment over the guidelines had survival advantages for these patients. In contrast, in patients with BCLC at stages 0 and C, treatment options under the recommended treatment guidelines did not affect overall survival. Moreover, a study conducted in Italy by Guarino *et al*[35] revealed that receiving BCLC-recommended treatment had no significant impact on patients' overall survival.

However, some studies on patients with specific treatment modalities and specific HCC stages have revealed that receiving the treatment methods recommended in the guidelines provides survival benefits for patients[36-39]. Our study's results also revealed that patients who received LR treatment based on the guidelines had a significant advantage in terms of tumor-free survival compared with those who did not. We discovered significant differences in the survival time of patients with different stages of HCC. We discovered that the main risk factors affecting the survival of patients with HCC were age > 50 years, no screening, AFP > 400 ng/mL, Child–Pugh grade B, and middle and late CNLC stages. A retrospective study conducted in China by Wang and Li[40] showed that hepatitis B surface antigen, AFP levels, Child–Pugh grade, BCLC stage, antiviral therapy, and treatment methods were important prognostic factors for HCC, and BCLC stage and tumor size were independent prognostic factors, which were similar results to those obtained in our study. Hence, Child–Pugh grade, AFP level, and clinical HCC stage are risk factors affecting the survival of patients with HCC.

This study has some limitations. The data used in this study were obtained from the inpatient information of a single regional medical center, and they should be verified by future multi-center studies. Some patients who were diagnosed with HCC in our study hospital were discharged and treated in other medical institutions. Consequently, the treatment information of these patients could

not be obtained, which might have led to the underestimation of the treatment level received. Some patients with ICC may have been included in the study while some with HCC may have been excluded because pathological examinations were not performed in all cases. The attending physician followed the guidelines used to distinguish HCC and ICC; however, it is impossible to rule out ICC or HCC-ICC absolutely because the guidelines are not 100% accurate. The studied patients were followed up; however, only 1128 patients were traced in this retrospective study due to the long study period and the loss of samples, which might have affected the HCC survival rate analysis to some extent. Prospective studies are required to further understand patient survival.

This study's results suggest that screening enables the early diagnosis of HCC. However, due to the retrospective nature of the study, data on patients' willingness to undergo screening as well as influencing factors, such as wealth or area of residence, could not be collected. Finally, large-sample multi-center studies are required to provide high-quality evidence for the screening, diagnosis, and treatment guidelines of HCC in China.

CONCLUSION

The findings revealed that 70% of HCC treatments at the First Affiliated Hospital of Zhengzhou University were performed according to the guidelines. The most frequently used treatment for patients at all stages of HCC was that recommended in the guidelines. No benefit was demonstrated in patients with HCC as a whole who received guideline-recommended treatment; however, those who underwent LR in accordance with the guidelines had a significant survival advantage. We also demonstrated that although screening groups at high risk for HCC according to the guidelines can achieve early diagnosis and treatment, real-world compliance is poor.

ARTICLE HIGHLIGHTS

Research background

Hepatocellular carcinoma (HCC) is a common malignant tumor worldwide; however, no staging scheme that would apply across populations is currently described in the extant literature. Although a China Liver Cancer (CNLC) staging system was proposed for the Chinese population, there is no study regarding the practice of CNLC staging in real clinical settings in China, which the current study addresses.

Research motivation

Although HCC patients detected through screening in the current study had a significant survival advantage compared with those who were not screened, the screening compliance in patients remained was poor. Therefore, improving patients' screening compliance would be the key to achieving early HCC diagnosis and treatment, which we have identified as the direction of future research.

Research objectives

Most importantly, the study highlighted that although no benefit was demonstrated in HCC patients for receiving the treatment recommended by the guidelines, the patients who underwent liver resection in accordance with the guidelines had a significant survival advantage.

Research methods

The results of the current study demonstrated that patients who were treated according to the CNLC guidelines had a survival advantage over those who were not treated per the guidelines. However, this advantage was limited *i.e.*, 54 *vs* 51 mo, and no statistical difference was observed. This result also corroborated with a study, which demonstrated survival advantage for Barcelona Clinic Liver Cancer stages B and C with the choice of treatment over the guidelines. Prospective studies are required to further understand the survival of patients.

Research results

The hospitalisation information of patients with HCC admitted to the First Affiliated Hospital of Zhengzhou University was obtained, which included demographic characteristics, imaging and serological reports, treatment, and patients' prognosis. Thereafter, the CNLC staging was done according to the guidelines. Each stage was characterised by the performance status, tumor number and diameter, liver function status using Child-Pugh A/B, and infringements such as vascular tumor thrombus and extrahepatic metastasis on imaging.

Research conclusions

The study aimed to investigate the present situation and problems of HCC diagnosis and treatment guidelines in China, since real-world studies for the existing problems of CNLC staging in China's clinical practice are lacking.

Research perspectives

The method of CNLC staging includes CNLC stages Ia, Ib, IIa, IIb, IIIa, IIIb, and IV, and it is based on the liver function status, tumor size, number, and invasion, and the general conditions of patients with HCC. However, given that the first method of CNLC staging was published as recently as 2017, only a few studies have addressed specific treatment methods in different CNLC staging. Since this study highlights significant difference in the tumor-free survival time between patients undergoing hepatectomy according to the guideline and those undergoing hepatectomy without the guideline, these findings will aid in future research to improve clinical decision making for HCC treatment.

ACKNOWLEDGEMENTS

We thank the hepatobiliary surgeons of the First Affiliated Hospital of Zhengzhou University who provided clinical advice for analysing the case data. We are also grateful to our colleagues for their assistance in checking the data.

FOOTNOTES

Author contributions: Yan YW, Zhang SX and Tian QF designed the study; Yan YW and Liu XK performed the data collection and conducted the data analysis; Yan YW wrote the manuscript; Zhang SX and Tian QF revised the manuscript; all authors approved the final version of the manuscript.

Supported by The Major Project of Science and Technology in Henan Province, No. 161100311400.

Institutional review board statement: The study was approved by the Institutional review board of Zhengzhou University, No. ZZUIRB2022-151.

Informed consent statement: Patients were not required to give informed consent to the study because the analysis used anonymous data that were obtained after each patient agreed to treatment by written consent.

Conflict-of-interest statement: All the authors report no relevant conflicts of interest for this article.

Data sharing statement: No additional data are available.

Country/Territory of origin: China

ORCID number: Yun-Wei Yan 0000-0002-0590-600X; Xin-Kui Liu 0000-0003-0880-5850; Shun-Xiang Zhang 0000-0003-3127-5675; Qing-Feng Tian 0000-0002-0020-6389.

S-Editor: Fan JR
L-Editor: A
P-Editor: Zhang XD

REFERENCES

1 **Sung H**, Ferlay J, Siegel RL, Laversanne M, Soerjomataram I, Jemal A, Bray F. Global Cancer Statistics 2020: GLOBOCAN Estimates of Incidence and Mortality Worldwide for 36 Cancers in 185 Countries. *CA Cancer J Clin* 2021; **71**: 209-249 [PMID: 33538338 DOI: 10.3322/caac.21660]

2 **Hassanipour S**, Vali M, Gaffari-Fam S, Nikbakht HA, Abdzadeh E, Joukar F, Pourshams A, Shafaghi A, Malakoutikhah M, Arab-Zozani M, Salehiniya H, Mansour-Ghanaei F. The survival rate of hepatocellular carcinoma in Asian countries: a systematic review and meta-analysis. *EXCLI J* 2020; **19**: 108-130 [PMID: 32038120 DOI: 10.17179/excli2019-1842]

3 **Llovet JM**, Brú C, Bruix J. Prognosis of hepatocellular carcinoma: the BCLC staging classification. *Semin Liver Dis* 1999;

19: 329-338 [PMID: 10518312 DOI: 10.1055/s-2007-1007122]

4 **European Association for the Study of the Liver**. EASL Clinical Practice Guidelines: Management of hepatocellular carcinoma. *J Hepatol* 2018; **69**: 182-236 [PMID: 29628281 DOI: 10.1016/j.jhep.2018.03.019]

5 **Omata M**, Cheng AL, Kokudo N, Kudo M, Lee JM, Jia J, Tateishi R, Han KH, Chawla YK, Shiina S, Jafri W, Payawal DA, Ohki T, Ogasawara S, Chen PJ, Lesmana CRA, Lesmana LA, Gani RA, Obi S, Dokmeci AK, Sarin SK. Asia-Pacific clinical practice guidelines on the management of hepatocellular carcinoma: a 2017 update. *Hepatol Int* 2017; **11**: 317-370 [PMID: 28620797 DOI: 10.1007/s12072-017-9799-9]

6 **Kudo M**, Chung H, Osaki Y. Prognostic staging system for hepatocellular carcinoma (CLIP score): its value and limitations, and a proposal for a new staging system, the Japan Integrated Staging Score (JIS score). *J Gastroenterol* 2003; **38**: 207-215 [PMID: 12673442 DOI: 10.1007/s005350300038]

7 **Yau T**, Tang VY, Yao TJ, Fan ST, Lo CM, Poon RT. Development of Hong Kong Liver Cancer staging system with treatment stratification for patients with hepatocellular carcinoma. *Gastroenterology* 2014; **146**: 1691-700.e3 [PMID: 24583061 DOI: 10.1053/j.gastro.2014.02.032]

8 **Zhou M**, Wang H, Zeng X, Yin P, Zhu J, Chen W, Li X, Wang L, Liu Y, Liu J, Zhang M, Qi J, Yu S, Afshin A, Gakidou E, Glenn S, Krish VS, Miller-Petrie MK, Mountjoy-Venning WC, Mullany EC, Redford SB, Liu H, Naghavi M, Hay SI, Murray CJL, Liang X. Mortality, morbidity, and risk factors in China and its provinces, 1990-2017: a systematic analysis for the Global Burden of Disease Study 2017. *Lancet* 2019; **394**: 1145-1158 [PMID: 31248666 DOI: 10.1016/S0140-6736(19)30427-1]

9 **Zhou J**, Sun HC, Wang Z, Cong WM, Wang JH, Zeng MS, Yang JM, Bie P, Liu LX, Wen TF, Han GH, Wang MQ, Liu RB, Lu LG, Ren ZG, Chen MS, Zeng ZC, Liang P, Liang CH, Chen M, Yan FH, Wang WP, Ji Y, Cheng WW, Dai CL, Jia WD, Li YM, Li YX, Liang J, Liu TS, Lv GY, Mao YL, Ren WX, Shi HC, Wang WT, Wang XY, Xing BC, Xu JM, Yang JY, Yang YF, Ye SL, Yin ZY, Zhang BH, Zhang SJ, Zhou WP, Zhu JY, Liu R, Shi YH, Xiao YS, Dai Z, Teng GJ, Cai JQ, Wang WL, Dong JH, Li Q, Shen F, Qin SK, Fan J. Guidelines for Diagnosis and Treatment of Primary Liver Cancer in China (2017 Edition). *Liver Cancer* 2018; **7**: 235-260 [PMID: 30319983 DOI: 10.1159/000488035]

10 **Zhou J**, Sun H, Wang Z, Cong W, Wang J, Zeng M, Zhou W, Bie P, Liu L, Wen T, Han G, Wang M, Liu R, Lu L, Ren Z, Chen M, Zeng Z, Liang P, Liang C, Yan F, Wang W, Ji Y, Yun J, Cai D, Chen Y, Cheng W, Cheng S, Dai C, Guo W, Hua B, Huang X, Jia W, Li Y, Liang J, Liu T, Lv G, Mao Y, Peng T, Ren W, Shi H, Shi G, Tao K, Wang X, Xiang B, Xing B, Xu J, Yang J, Yang Y, Ye S, Yin Z, Zhang B, Zhang L, Zhang S, Zhang T, Zhao Y, Zheng H, Zhu J, Zhu K, Shi Y, Xiao Y, Dai Z, Teng G, Cai J, Cai X, Li Q, Shen F, Qin S, Dong J, Fan J. Guidelines for the Diagnosis and Treatment of Hepatocellular Carcinoma (2019 Edition). *Liver Cancer* 2020; **9**: 682-720 [PMID: 33442540 DOI: 10.1159/000509424]

11 **Liao R**, Wei XF, Che P, Yin KL, Liu L. Nomograms Incorporating the CNLC Staging System Predict the Outcome of Hepatocellular Carcinoma After Curative Resection. *Front Oncol* 2021; **11**: 755920 [PMID: 35127471 DOI: 10.3389/fonc.2021.755920]

12 **Qin J**, Huang Y, Zhou H, Yi S. Efficacy of Sorafenib Combined With Immunotherapy Following Transarterial Chemoembolization for Advanced Hepatocellular Carcinoma: A Propensity Score Analysis. *Front Oncol* 2022; **12**: 807102 [PMID: 35463356 DOI: 10.3389/fonc.2022.807102]

13 **Li C**, Wang H, Chen R, Zhang H, Xu Y, Zhang B, Li Y, Zhang C, Yang Y, Wang X, Li X. Outcomes and recurrence patterns following curative hepatectomy for hepatocellular carcinoma patients with different China liver cancer staging. *Am J Cancer Res* 2022; **12**: 907-921 [PMID: 35261811]

14 **Vitale A**, Farinati F, Finotti M, Di Renzo C, Brancaccio G, Piscaglia F, Cabibbo G, Caturelli E, Missale G, Marra F, Sacco R, Giannini EG, Trevisani F, Cillo U; Associazione Italiana Per Lo Studio Del Fegato Aisf Hcc Special Interest Group; Italian Liver Cancer Ita Li Ca Study Group. Overview of Prognostic Systems for Hepatocellular Carcinoma and ITA.LI.CA External Validation of MESH and CNLC Classifications. *Cancers (Basel)* 2021; **13** [PMID: 33918125 DOI: 10.3390/cancers13071673]

15 **Kim SE**, Lee HC, Kim KM, Lim YS, Chung YH, Lee YS, Suh DJ. Applicability of the BCLC staging system to patients with hepatocellular carcinoma in Korea: analysis at a single center with a liver transplant center. *Korean J Hepatol* 2011; **17**: 113-119 [PMID: 21757982 DOI: 10.3350/kjhep.2011.17.2.113]

16 **Borzio M**, Fornari F, De Sio I, Andriulli A, Terracciano F, Parisi G, Francica G, Salvagnini M, Marignani M, Salmi A, Farinati F, Carella A, Pedicino C, Dionigi E, Fanigliulo L, Cazzaniga M, Ginanni B, Sacco R; EpaHCC Group. Adherence to American Association for the Study of Liver Diseases guidelines for the management of hepatocellular carcinoma: results of an Italian field practice multicenter study. *Future Oncol* 2013; **9**: 283-294 [PMID: 23414477 DOI: 10.2217/fon.12.183]

17 **Piñero F**, Marciano S, Fernández N, Silva J, Zambelo Y, Cobos M, Zerega A, Ridruejo E, Miguez C, Ameigeiras B, D'Amico C, Gaite L, Coronel M, Bermúdez C, Rosales C, Romero G, McCormack L, Reggiardo V, Colombato L, Gadano A, Rubinstein F, Silva M; Argentinean Association for the Study of Liver Diseases (A. A.E.E.H). Adherence to Barcelona Clinic Liver Cancer therapeutic algorithm for hepatocellular carcinoma in the daily practice: a multicenter cohort study from Argentina. *Eur J Gastroenterol Hepatol* 2018; **30**: 376-383 [PMID: 29509603 DOI: 10.1097/MEG.0000000000001049]

18 **Sun X**, Tan J, Tang L, Guo JJ, Li X. Real world evidence: experience and lessons from China. *BMJ* 2018; **360**: j5262 [PMID: 29437644 DOI: 10.1136/bmj.j5262]

19 **Mospan AR**, Morris HL, Fried MW. Real-world evidence in hepatocellular carcinoma. *Liver Int* 2021; **41** Suppl 1: 61-67 [PMID: 34155788 DOI: 10.1111/liv.14864]

20 **Dai M**, Mao AY, Shi JF. [Sustainability of cancer screening program in urban China: a multicenter assessment from service supplier's and demander's perspectives]. *Zhonghua Liu Xing Bing Xue Za Zhi* 2018; **39**: 139-141 [PMID: 29495195 DOI: 10.3760/cma.j.issn.0254-6450.2018.02.002]

21 **Kuo MJ**, Chen HH, Chen CL, Fann JC, Chen SL, Chiu SY, Lin YM, Liao CS, Chang HC, Lin YS, Yen AM. Cost-effectiveness analysis of population-based screening of hepatocellular carcinoma: Comparing ultrasonography with two-stage screening. *World J Gastroenterol* 2016; **22**: 3460-3470 [PMID: 27022228 DOI: 10.3748/wjg.v22.i12.3460]

22 **Kim HL**, An J, Park JA, Park SH, Lim YS, Lee EK. Magnetic Resonance Imaging Is Cost-Effective for Hepatocellular

Carcinoma Surveillance in High-Risk Patients With Cirrhosis. *Hepatology* 2019; **69**: 1599-1613 [PMID: 30365164 DOI: 10.1002/hep.30330]

23 **Kwon JW**, Tchoe HJ, Lee J, Suh JK, Lee JH, Shin S. The Impact of National Surveillance for Liver Cancer: Results from Real-World Setting in Korea. *Gut Liver* 2020; **14**: 108-116 [PMID: 30974929 DOI: 10.5009/gnl18522]

24 **Tanaka H**, Iijima H, Nouso K, Aoki N, Iwai T, Takashima T, Sakai Y, Aizawa N, Iwata K, Ikeda N, Iwata Y, Enomoto H, Saito M, Imanishi H, Nishiguchi S. Cost-effectiveness analysis on the surveillance for hepatocellular carcinoma in liver cirrhosis patients using contrast-enhanced ultrasonography. *Hepatol Res* 2012; **42**: 376-384 [PMID: 22221694 DOI: 10.1111/j.1872-034X.2011.00936.x]

25 **Lima PH**, Fan B, Bérubé J, Cerny M, Olivié D, Giard JM, Beauchemin C, Tang A. Cost-Utility Analysis of Imaging for Surveillance and Diagnosis of Hepatocellular Carcinoma. *AJR Am J Roentgenol* 2019; **213**: 17-25 [PMID: 30995098 DOI: 10.2214/AJR.18.20341]

26 **Cucchetti A**, Trevisani F, Cescon M, Ercolani G, Farinati F, Poggio PD, Rapaccini G, Nolfo MAD, Benvegnù L, Zoli M, Borzio F, Giannini EG, Caturelli E, Chiaramonte M, Pinna AD; Italian Liver Cancer (ITA. LI.CA) Group. Cost-effectiveness of semi-annual surveillance for hepatocellular carcinoma in cirrhotic patients of the Italian Liver Cancer population. *J Hepatol* 2012; **56**: 1089-1096 [PMID: 22245900 DOI: 10.1016/j.jhep.2011.11.022]

27 **Eltabbakh M**, Zaghla H, Abdel-Razek W, Elshinnawy H, Ezzat S, Gomaa A, Waked I. Utility and cost-effectiveness of screening for hepatocellular carcinoma in a resource-limited setting. *Med Oncol* 2015; **32**: 432 [PMID: 25502085 DOI: 10.1007/s12032-014-0432-7]

28 **Costentin CE**, Layese R, Bourcier V, Cagnot C, Marcellin P, Guyader D, Pol S, Larrey D, De Lédinghen V, Ouzan D, Zoulim F, Roulot D, Tran A, Bronowicki JP, Zarski JP, Riachi G, Calès P, Péron JM, Alric L, Bourlière M, Mathurin P, Blanc JF, Abergel A, Serfaty L, Mallat A, Grangé JD, Attali P, Bacq Y, Wartelle C, Dao T, Thabut D, Pilette C, Silvain C, Christidis C, Nguyen-Khac E, Bernard-Chabert B, Zucman D, Di Martino V, Sutton A, Letouzé E, Imbeaud S, Zucman-Rossi J, Audureau E, Roudot-Thoraval F, Nahon P; ANRS CO12 CirVir Group. Compliance With Hepatocellular Carcinoma Surveillance Guidelines Associated With Increased Lead-Time Adjusted Survival of Patients With Compensated Viral Cirrhosis: A Multi-Center Cohort Study. *Gastroenterology* 2018; **155**: 431-442.e10 [PMID: 29729258 DOI: 10.1053/j.gastro.2018.04.027]

29 **Da Fonseca LG**, Forner A. Adherence and quality are key for a beneficial HCC surveillance. *Liver Int* 2020; **40**: 751-753 [PMID: 32255572 DOI: 10.1111/liv.14421]

30 **Zhong JH**, Peng NF, You XM, Ma L, Xiang X, Wang YY, Gong WF, Wu FX, Xiang BD, Li LQ. Tumor stage and primary treatment of hepatocellular carcinoma at a large tertiary hospital in China: A real-world study. *Oncotarget* 2017; **8**: 18296-18302 [PMID: 28407686 DOI: 10.18632/oncotarget.15433]

31 **Yen YH**, Cheng YF, Wang JH, Lin CC, Chen CH, Wang CC. Adherence to the modified Barcelona Clinic Liver Cancer guidelines: Results from a high-volume liver surgery center in East Asias. *PLoS One* 2021; **16**: e0249194 [PMID: 33765059 DOI: 10.1371/journal.pone.0249194]

32 **Li JW**, Goh BG, Chang PE, Tan CK. Barcelona Clinic Liver Cancer outperforms Hong Kong Liver Cancer staging of hepatocellular carcinoma in multiethnic Asians: Real-world perspective. *World J Gastroenterol* 2017; **23**: 4054-4063 [PMID: 28652658 DOI: 10.3748/wjg.v23.i22.4054]

33 **Wang YY**, Zhong JH, Su ZY, Huang JF, Lu SD, Xiang BD, Ma L, Qi LN, Ou BN, Li LQ. Albumin-bilirubin versus Child-Pugh score as a predictor of outcome after liver resection for hepatocellular carcinoma. *Br J Surg* 2016; **103**: 725-734 [PMID: 27005482 DOI: 10.1002/bjs.10095]

34 **Hyun MH**, Lee YS, Kim JH, Lee CU, Jung YK, Seo YS, Yim HJ, Yeon JE, Byun KS. Hepatic resection compared to chemoembolization in intermediate- to advanced-stage hepatocellular carcinoma: A meta-analysis of high-quality studies. *Hepatology* 2018; **68**: 977-993 [PMID: 29543988 DOI: 10.1002/hep.29883]

35 **Guarino M**, Tortora R, de Stefano G, Coppola C, Morisco F, Salomone Megna A, Izzo F, Nardone G, Piai G, Adinolfi LE, D'Adamo G, Gaeta GB, Messina V, Francica G, De Girolamo V, Coppola N, Persico M, Di Costanzo GG; Progetto Epatocarcinoma Campania Group. Adherence to Barcelona Clinic Liver Cancer guidelines in field practice: Results of Progetto Epatocarcinoma Campania. *J Gastroenterol Hepatol* 2018; **33**: 1123-1130 [PMID: 28994145 DOI: 10.1111/jgh.14013]

36 **Farinati F**, Vanin V, Giacomin A, Pozzan C, Cillo U, Vitale A, Di Nolfo AM, Del Poggio P, Benvegnu' L, Rapaccini G, Zoli M, Borzio F, Giannini EG, Caturelli E, Trevisani F; Italian Liver Cancer (ITA. LI.CA) group. BCLC stage B hepatocellular carcinoma and transcatheter arterial chemoembolization: a 20-year survey by the Italian Liver Cancer group. *Liver Int* 2015; **35**: 223-231 [PMID: 25074434 DOI: 10.1111/liv.12649]

37 **Pecorelli A**, Lenzi B, Gramenzi A, Garuti F, Farinati F, Giannini EG, Ciccarese F, Piscaglia F, Rapaccini GL, Di Marco M, Caturelli E, Zoli M, Borzio F, Sacco R, Cabibbo G, Felder M, Morisco F, Gasbarrini A, Baroni GS, Foschi FG, Biasini E, Masotto A, Virdone R, Bernardi M, Trevisani F; Italian LiverCancer (ITA. LI.CA) group. Curative therapies are superior to standard of care (transarterial chemoembolization) for intermediate stage hepatocellular carcinoma. *Liver Int* 2017; **37**: 423-433 [PMID: 27566596 DOI: 10.1111/liv.13242]

38 **Torzilli G**, Belghiti J, Kokudo N, Takayama T, Capussotti L, Nuzzo G, Vauthey JN, Choti MA, De Santibanes E, Donadon M, Morenghi E, Makuuchi M. A snapshot of the effective indications and results of surgery for hepatocellular carcinoma in tertiary referral centers: is it adherent to the EASL/AASLD recommendations? *Ann Surg* 2013; **257**: 929-937 [PMID: 23426336 DOI: 10.1097/SLA.0b013e31828329b8]

39 **Radu P**, Groza I, Iancu C, Al Hajjar N, Andreica V, Sparchez Z. Treatment of hepatocellular carcinoma in a tertiary Romanian center. Deviations from BCLC recommendations and influence on survival rate. *J Gastrointestin Liver Dis* 2013; **22**: 291-297 [PMID: 24078986]

40 **Wang CY**, Li S. Clinical characteristics and prognosis of 2887 patients with hepatocellular carcinoma: A single center 14 years experience from China. *Medicine (Baltimore)* 2019; **98**: e14070 [PMID: 30681563 DOI: 10.1097/MD.0000000000014070]

World Journal of Gastrointestinal Oncology

Submit a Manuscript: https://www.f6publishing.com

World J Gastrointest Oncol 2023 May 15; 15(5): 878-891

DOI: 10.4251/wjgo.v15.i5.878

ISSN 1948-5204 (online)

ORIGINAL ARTICLE

Randomized Controlled Trial

Efficacy of image-enhanced endoscopy for colorectal adenoma detection: A multicenter, randomized trial

Zhi-Peng Qi, En-Pan Xu, Dong-Li He, Yan Wang, Bai-Sheng Chen, Xue-Si Dong, Qiang Shi, Shi-Lun Cai, Qi Guo, Ni Li, Xing Li, Hai-Yan Huang, Bing Li, Di Sun, Jian-Guang Xu, Zhang-Han Chen, Ayimukedisi Yalikong, Jin-Yi Liu, Zhen-Tao Lv, Jian-Min Xu, Ping-Hong Zhou, Yun-Shi Zhong

Specialty type: Gastroenterology and hepatology

Provenance and peer review: Unsolicited article; Externally peer reviewed.

Peer-review model: Single blind

Peer-review report's scientific quality classification

Grade A (Excellent): A, A
Grade B (Very good): 0
Grade C (Good): 0
Grade D (Fair): 0
Grade E (Poor): 0

P-Reviewer: Toskas A, United Kingdom; Trna J, Czech Republic

Received: December 5, 2022
Peer-review started: December 5, 2022
First decision: January 9, 2023
Revised: January 24, 2023
Accepted: April 12, 2023
Article in press: April 12, 2023
Published online: May 15, 2023

Zhi-Peng Qi, En-Pan Xu, Qiang Shi, Shi-Lun Cai, Bing Li, Di Sun, Zhang-Han Chen, Ayimukedisi Yalikong, Jin-Yi Liu, Zhen-Tao Lv, Ping-Hong Zhou, Yun-Shi Zhong, Endoscopy Center, Zhongshan Hospital of Fudan University, Shanghai 200030, China

Dong-Li He, Qi Guo, Endoscopy Center, Shanghai Xuhui Central Hospital, Shanghai 200030, China

Yan Wang, Endoscopy Center, Traditional Chinese Medical Hospital, Rongcheng 264300, Shandong Province, China

Bai-Sheng Chen, Department of Endoscopy Center, Xiamen Branch of Affiliated Zhongshan Hospital of Fudan University, Xiamen 361000, Fujian Province, China

Xue-Si Dong, Ni Li, Office of Cancer Screening, National Cancer Center/National Clinical Research Center for Cancer/Cancer Hospital, Chinese Academy of Medical Sciences and Peking Union Medical College, Beijing 100000, China

Xing Li, Department of Gastroenterology, Pingxiang People's Hospital, Pingxiang 337000, Jiangxi Province, China

Hai-Yan Huang, Department of Clinical Medicine, Xiaogang Hospital, Ningbo 315000, Zhejiang Province, China

Jian-Guang Xu, Endoscopy Center, Quzhou People's Hospital, Quzhou 324000, Zhejiang Province, China

Jian-Min Xu, Department of General Surgery, Zhongshan Hospital of Fudan University, Shanghai 200030, China

Corresponding author: Yun-Shi Zhong, MD, PhD, Doctor, Surgeon, Endoscopy Center, Zhongshan Hospital of Fudan University, No. 180 Fenglin Road, Shanghai 200030, China. zhong.yunshi@zs-hospital.sh.cn

Abstract

BACKGROUND

Improved adenoma detection at colonoscopy has decreased the risk of developing

colorectal cancer. However, whether image-enhanced endoscopy (IEE) further improves the adenoma detection rate (ADR) is controversial.

AIM

To compare IEE with white-light imaging (WLI) endoscopy for the detection and identification of colorectal adenoma.

METHODS

This was a multicenter, randomized, controlled trial. Participants were enrolled between September 2019 to April 2021 from 4 hospital in China. Patients were randomly assigned to an IEE group with WLI on entry and IEE on withdrawal (n = 2113) or a WLI group with WLI on both entry and withdrawal (n = 2098). The primary outcome was the ADR. The secondary endpoints were the polyp detection rate (PDR), adenomas per colonoscopy, adenomas per positive colonoscopy, and factors related to adenoma detection.

RESULTS

A total of 4211 patients (966 adenomas) were included in the analysis (mean age, 56.7 years, 47.1% male). There were 2113 patients (508 adenomas) in the IEE group and 2098 patients (458 adenomas) in the WLI group. The ADR in two group were not significantly different [24.0% *vs* 21.8%, 1.10, 95% confidence interval (CI): 0.99-1.23, P = 0.09]. The PDR was higher with IEE group (41.7%) than with WLI group (36.1%, 1.16, 95%CI: 1.07-1.25, P = 0.01). Differences in mean withdrawal time (7.90 ± 3.42 min *vs* 7.85 ± 3.47 min, P = 0.30) and adenomas per colonoscopy (0.33 ± 0.68 *vs* 0.28 ± 0.62, P = 0.06) were not significant. Subgroup analysis found that with narrow-band imaging (NBI), between-group differences in the ADR, were not significant (23.7% *vs* 21.8%, 1.09, 95%CI: 0.97-1.22, P = 0.15), but were greater with linked color imaging (30.9% *vs* 21.8%, 1.42, 95%CI: 1.04-1.93, P = 0.04). the second-generation NBI (2G-NBI) had an advantage of ADR than both WLI and the first-generation NBI (27.0% *vs* 21.8%, P = 0.01; 27.0% *vs* 21.2.0%, P = 0.01).

CONCLUSION

This prospective study confirmed that, among Chinese, IEE didn't increase the ADR compared with WLI, but 2G-NBI increase the ADR.

Key Words: Endoscopy; Image-enhanced endoscopy; Adenoma detection rate; White-light imaging; Narrow-band imaging

Core Tip: This study is the biggest randomized controlled trial comparing image-enhanced endoscopy (IEE) with white-light imaging (WLI) over the world, providing the solid evidence. This study provides strong evidence that IEE do not increase adenoma detection rate (ADR) compared with WLI, but second-generation-narrow-band imaging increase the ADR. IEE improved the polyp detection rate without additional withdrawal time.

Citation: Qi ZP, Xu EP, He DL, Wang Y, Chen BS, Dong XS, Shi Q, Cai SL, Guo Q, Li N, Li X, Huang HY, Li B, Sun D, Xu JG, Chen ZH, Yalikong A, Liu JY, Lv ZT, Xu JM, Zhou PH, Zhong YS. Efficacy of image-enhanced endoscopy for colorectal adenoma detection: A multicenter, randomized trial. *World J Gastrointest Oncol* 2023; 15(5): 878-891

URL: https://www.wjgnet.com/1948-5204/full/v15/i5/878.htm

DOI: https://dx.doi.org/10.4251/wjgo.v15.i5.878

INTRODUCTION

Colorectal cancer is relatively common worldwide, with over 1 million new cases and an estimated 550000 deaths reported in 2018[1]. The 5-year survival rate of advanced colorectal cancer is less than 40%, but detection at an early stage greatly improves the prognosis. Increasing the adenoma detection rate (ADR) by 1.0% can reduce the risk of colorectal cancer by 3.0%[2]. Colonoscopy is an ideal strategy for decreasing the prevalence of colorectal cancer by early detection and endoscopic resection of precancerous lesions. The current standard practice for detecting polyps and adenomas is endoscopy with white-light imaging (WLI), and it has a reported polyp/adenoma miss rate of 26%[3,4]. Given the need

for improved detection, image-enhanced endoscopy (IEE) was developed to overcome the limitations of conventional colonoscopy.

IEE includes narrow-band imaging (NBI), flexible spectral imaging color enhancement, linked color imaging (LCI), and i-Scan, which are continually evolving. IEE improves the visualization of mucosal microstructure and microvasculature and the identification of lesions compared with WLI[5]. In a multicenter, randomized, crossover trial comparing LCI and WLI in polyp detection, Min *et al*[6] reported that the polyp detection rate (PDR) of LCI was 8% higher than that of WLI. A meta-analysis found that the ADR of NBI was significantly higher than that of WLI in patients with the best bowel preparations[7]. However, some studies have reported that NBI did not increase ADR or PDR[8-10]. As the additional benefit of IEE is still controversial, we conducted a prospective, multicenter, randomized, controlled study named the Image-Enhanced Endoscopy in Colonoscopy Screening trail in 4 hospitals in China to compare the ADR of IEE and WLI during colonoscopies. The primary objective was to determine whether IEE detected significantly more adenomas than WLI in patients with elective screening, surveillance, or diagnostic colonoscopy.

MATERIALS AND METHODS

Methods

Trail design: This prospective, multicenter, randomized, controlled trial was conducted at 4 hospitals in China in following the ethical principles of Declaration of Helsinki (B2019-131R). The study was prepared following the Consolidated Standards of Reporting Trials statement for reporting randomized controlled trials (RCTs)[11], and was registered on the Chinese Clinical Trial Registry (ChiCTR19000-26026). This was a nonprofit study, and no funding was received or solicited from endoscopy equipment manufacturers. All authors had access to the study data and have reviewed and approved the final manuscript. The full trial protocol see supplement.

Trial participants: Consecutive eligible patients who were 18-80 years of age and scheduled to undergo colonoscopy were considered eligible for this trial. Patients without bowel preparation or poor bowel preparation indicated by a Boston Bowel Preparation Scale (BBPS) score < 6, or with untreated adenoma in previous examinations, familial polyposis, severe emphysema, interstitial pneumonia, or ischemic heart disease; and those who could not tolerate anesthesia and examination, and patients or their family members who could not understand the conditions and goals of this study were excluded. Eligible patients were informed by the endoscopists about the study aims, procedures, and potential risks. Written informed consent was obtained from all patients.

Randomization: Before colonoscopy withdrawal, eligible patients were randomly assigned 1:1 to the IEE group with WLI on entry and IEE on withdrawal or the WLI group with WLI on both entry and withdrawal. Patients were stratified by age to groups < 50 and ≥ 50 years of age. The investigators used a central customized system (https://uapkd.bioknow.net/#/) to generate random numbers for the group assignments for the eligible patients at each center. Then, the investigators will allocate the patients to different groups based on the results of the customized random system and each center will compete for entry.

Endoscopists and endoscopy equipment: The participating endoscopist at each study center had at least 5 years of work experience in colonoscopy and had rigorous IEE diagnostic training. The endoscopy systems used in this study included CV-260, CV-290 (Olympus) or ELUXEO 7000 (Fujifilm) devices, and high definition colonoscopes was used for all procedures without any mucosal exposure devices.

Endoscopic procedures and histopathology: All patients performed bowel preparations following the local hospital protocol, and conscious sedation was administered according to the judgment of the anesthetist. The endoscope was advanced to the cecum under WLI. Cecal intubation was confirmed by identification of the appendiceal orifice and ileocecal valve or by intubation of the ileum, and the bowel preparation was assessed by the BBPS score obtained during advancement of the endoscope to the cecum. Once cecal intubation was confirmed, the colonoscope was withdrawn to the anus by the assigned method, either IEE or WLI. Detected lesions were evaluated by the Paris morphological classification criteria and removed by the endoscopist[12]. The size and location of lesions were recorded. Withdrawal time were defined as the time from cecal intubation to extraction through the anus and were measured with a stopwatch, excluding the time used for washing of the colonic mucosa, suctioning of fluid, or performance of polypectomy, biopsy, or any other therapeutic maneuvers[13]. The data were recorded on standardized case report forms before being transferred to online electronic report forms (https://wa.zs-hospital.sh.cn/).

Histological samples were fixed in paraffin, processed by standard procedures, and examined by experienced pathologists who were blinded to the study procedures. Histological results were reported following the Vienna classification of gastrointestinal neoplasia[14]. Advanced adenoma was defined as

an adenoma ≥ 10 mm in diameter with any villous histology, high-grade dysplasia, or invasive carcinoma[15].

Outcomes: The primary endpoint was ADR, defined as the proportion of patients with at least one detected adenoma of any size[15]. The secondary endpoints were PDR, diminutive ADR, adenomas per colonoscopy, and factors related to adenoma detection. PDR was defined as the proportion of patients with at least one detected polyp. The diminutive ADR included detection of at least one adenoma that was < 5 mm. Screening colonoscopies included those for which there was no diagnostic or surveillance indication. Surveillance colonoscopies included those for which there was no diagnostic indication and were performed in a patient who had a colonoscopy within the previous 10 years or who had a history of polyps or colorectal cancer. Diagnostic colonoscopies were those performed in patients who had one or more symptoms before the procedure[16].

Sample size calculation

The sample size estimate was based on an ADR of 13.4% by WLI in Chinese populations in previous studies[16]. In our experience, the ADR was around 10% when WLI was used. An increase in the ADR of 3% with IEE was considered clinically significant. Participants were allocated to the experimental and control groups in equal numbers. The Power and Sample Size Calculation program (PASS 2008; NCSS, LLC; https://www.ncss.com), estimated a sample size of 2012 per group using chi-square or Mann-Whitney *U* tests for comparison, assuming a type I error rate of 5% with 80% power, and a single-sided $P < 0.05$ for statistical significance. We planned to include 4200 subjects. The sample size was calculated by Dr. Li and Dr. Dong.

Statistical analysis

Intention-to-treat (see Supplementary Tables 1-7) and per protocol analyses were both conducted. Differences were expressed as relative risk (RR) with 95% confidence intervals (CIs). Continuous variables were tested for normal distribution and reported as means and standard deviation. Normally distributed variables were compared with student's *t*-test and non-normally distributed variables were compared with the Mann-Whitney *U* test. Categorical variables were reported as frequencies and percentages (%), and compared with the χ^2 test or Fisher's exact test when applicable. The χ^2 test was used for the analysis of the primary outcome (ADR). RR and 95%CIs were calculated for dichotomous outcomes and for the ADR in the IEE group relative to the WLI group. Secondary dichotomous outcomes and subgroup outcomes were analyzed in the way as the primary outcome. For the safety analysis, the frequency of adverse events and adverse reactions were calculated and analyzed using χ^2 or Fisher exact tests. Details of adverse events and adverse reactions were recorded for deep analysis. The analysis was performed with SPSS v.18.0. (IBM Corp. Armonk, NY, United States). All reported *P*-values were two-sided, and those ≤ 0.05 were considered significant.

RESULTS

Study population

Figure 1 was a flow chart of the trial design and procedures. Between September 2019 and April 2021, 4372 consecutive patients were considered for inclusion, and 91 were excluded because they were < 18 or > 80 years of age or had previously unresected colorectal polyps (Figure 1). The remaining 4281 patients were randomized to the IEE (n = 2140) or WLI (n = 2141) groups. 70 patients failed cecal intubation because of poor bowel preparation, technical difficulties, or intolerance. A total of 4211 patients were included in the analysis, with 2113 in the IEE group and 2098 in the WLI group. No adverse events related to endoscopy occurred. The baseline characteristics of the patients in the two groups were similar (Table 1). The mean age, number of men, colorectal surgery history, and colonoscopy history of IEE and WLI were 56.7 ± 12.9 years and 56.8 ± 13.0 years, 1002 (47.7%) and 982 (46.8%), 149 (7.1%) and 134 (6.4%), 892 (42.2%) and 879 (41.9%), respectively. Between-group differences were not significant (all $P > 0.05$). The most common colonoscopy indication in both groups was diagnostic, 880(41.6%) patients in the IEE group and 876 (41.8%) in the WLI group ($P > 0.05$).

Primary outcome

The primary outcome results are shown in Table 2 and Figure 2. A total of 966 adenomas were detected in 4211 patients. 508 adenomas were found in 2113 IEE patients and 458 were found in 2098 WLI patients. The ADR were 24.0% in the IEE patients and 21.8% in the WLI patients (RR = 1.10, 95%CI: 0.99-1.23, $P > 0.05$). The mean withdrawal time were 7.90 ± 3.42 min in the IEE group and 7.85 ± 3.47 min in the WLI group ($P > 0.05$). Differences in advanced ADR and diminutive ADR in the two groups were not significant (all $P > 0.05$). Regardless of age (< 50 or ≥ 50 years of age), sex, and colonoscopy indication, differences in the ADR were not significant (all $P > 0.05$).

Table 1 Baseline characteristics

	IEE group (*n* = 2113)	WLI group (*n* = 2098)
Age (yr)	56.7 ± 12.9	56.8 ± 13.0
Male gender	1002 (47.7)	982 (46.8)
BMI (kg/m^2)	23.4 ± 3.2	23.5 ± 3.2
Comorbidities		
ASA1	1468 (69.5)	1510 (72.0)
ASA2	640 (30.3)	580 (27.6)
ASA3	5 (0.2)	8 (0.4)
Colorectal surgery history	149 (7.1)	134 (6.4)
Colonoscopy indication		
Diagnostic	880 (41.6)	876 (41.8)
Surveillance	613 (29.0)	601 (28.6)
Screening	620 (29.3)	621 (29.6)
Colonoscopy history	892 (42.2)	879 (41.9)

Dates are *n* or *n* (%). IEE: Image-enhanced endoscopy; WLI: White-light imaging endoscopy; BMI: Body mass index.

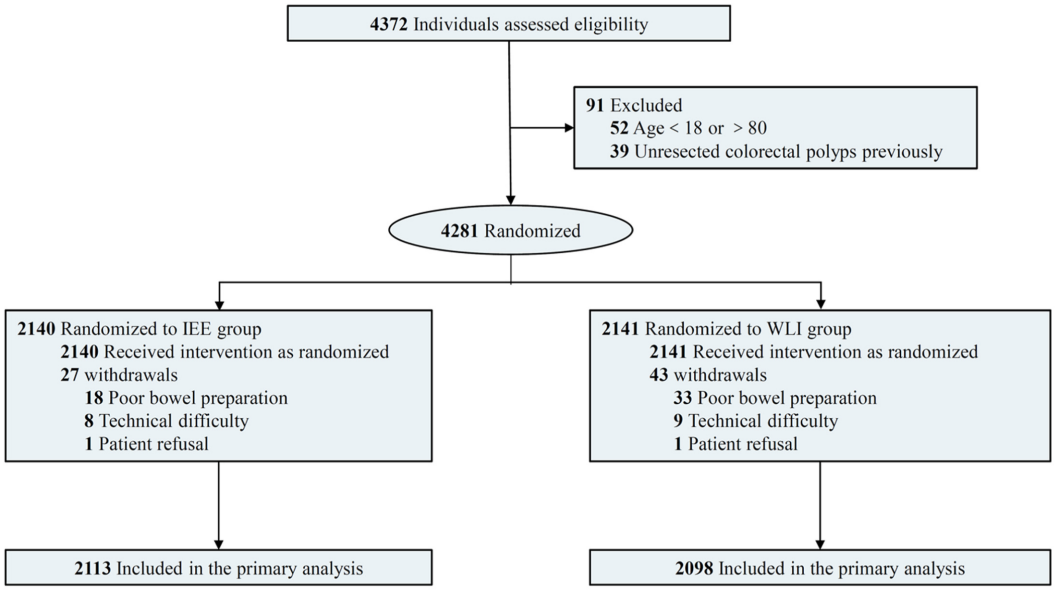

DOI: 10.4251/wjgo.v15.i5.878

Figure 1 Flow chart. IEE: Image-enhanced endoscopy; WLI: White-light imaging endoscopy.

Secondary outcomes

The secondary outcomes are shown in Table 3 and Figure 2. A total of 2907 polyps were detected in 4211 patients, including 1588 polyps in 2113 IEE patients and 1319 polyps in 2098 WLI patients. The PDR in the IEE group was significantly greater than that in the WLI group (41.7% *vs* 36.1%, RR = 1.16, 95%CI: 1.07-1.25, $P = 0.01$). Pathological evaluation found that adenomas were the most common polyps in both the IEE (43.5%) and WLI (44.7%) groups, and that the difference was not significant (RR = 0.97, 95%CI: 0.90-1.06, $P > 0.05$). Adenomas per colonoscopy were 0.33 ± 0.68 and 0.28 ± 0.62, respectively in the IEE and WLI groups ($P > 0.05$). There were also no significant differences in the size, morphology, pathology, or site of the adenoma polyps detected in both groups (all $P > 0.05$).

Subgroup analysis

The outcomes of the NBI and WLI groups are shown in Tables 4 and 5, Supplementary Table 8 and 9, and Figure 2. The ADR of the two groups were similar (23.7% *vs* 21.8%, RR = 1.09, 95%CI: 0.97-1.22, P =

Table 2 Overall adenoma detection rate in patients of the two group

	IEE group (*n* = 2113)	WLI group (*n* = 2098)	*P* value	Relative risk (95%CI)
ADR	508/2113 (24.0)	458/2098 (21.8)	0.09	1.10 (0.99-1.23)
Advanced ADR	127/2113 (6.0)	116/2098 (5.5)	0.50	1.09 (0.85-1.39)
Diminutive ADR	323/2113 (15.3)	286/2098 (13.6)	0.13	1.12 (0.97-1.30)
ADR in different ages				
< 50 yr	67/586 (11.4)	54/557 (9.7)	0.34	1.18 (0.84-1.66)
≥ 50 yr	441/1527 (28.9)	404/1541 (26.2)	0.10	1.10 (0.98-1.24)
ADR in different gender				
Male	288/1002 (28.7)	254/982 (25.9)	0.15	1.11 (0.96-1.28)
Female	220/1111 (19.8)	204/1116 (18.3)	0.36	1.08 (0.91-1.29)
ADR with different indications				
Diagnostic				
< 50 yr	26/270 (9.6)	23/256 (9.0)	0.80	1.07 (0.63-1.83)
≥ 50 yr	179/610 (29.3)	166/620 (26.8)	0.32	1.10 (0.92-1.31)
Surveillance				
< 50 yr	9/104 (8.7)	7/93 (7.5)	0.77	1.15 (0.45-2.97)
≥ 50 yr	138/509 (27.1)	126/508 (24.8)	0.40	1.09 (0.89-1.5)
Screening				
< 50 yr	32/212 (15.1)	24/208 (11.5)	0.28	1.31 (0.80-2.14)
≥ 50 yr	124/408 (30.4)	112/413 (27.1)	0.30	1.12 (0.90-1.39)
Withdrawal time	7.90 ± 3.42	7.85 ± 3.47	0.30	

Dates are *n* or *n* (%). ADR: Adenoma detection rate; IEE: Image-enhanced endoscopy; WLI: White light imaging; CI: Confidence interval.

0.15). The mean withdrawal time of the two groups were 7.90 ± 3.46 min and 7.85 ± 3.47 min ($P > 0.05$), and between-group differences in the values of other variables related to ADR were not significant. However, the second-generation NBI (2G-NBI) had an advantage of ADR than both WLI and first-generation NBI (1G-NBI) [27.0% *vs* 21.8%, RR = 1.24, 95%CI: 1.08-1.42, $P = 0.01$; 21.2% *vs* 27.0% (2G), RR = 0.78, 95%CI: 0.67-0.92, $P = 0.01$]. The mean withdrawal time of them was similar ($P > 0.05$). And the 2G-NBI was more suitable for small adenoma than WLI and 1G-NBI [17.1% *vs* 13.6%, RR = 1.26, 95%CI: 1.05-1.51, $P = 0.01$; 13.5% *vs* 17.1% (2G), RR = 0.79, 95%CI: 0.64-0.97, $P = 0.02$]. The PDR in the NBI group was significantly greater than that in the WLI group (41.6% *vs* 36.1%, RR = 1.15, 95%CI: 1.07-1.25, $P < 0.01$). There were no significant differences in the size, morphology, pathology, or site of the adenomas detected in the two groups (all $P > 0.05$). The PDR in the 2G-NBI group was significantly greater than that in both the WLI group (50.7% *vs* 36.1%, RR = 1.41, 95%CI: 1.29-1.53, $P = 0.01$), and the 1G-NBI group [34.7% *vs* 50.7% (2G), RR = 0.68, 95%CI: 0.62-0.76, $P = 0.01$].

As shown in Tables 4 and 5. The ADR was higher in the LCI than in the WLI group (30.9% *vs* 21.8%, RR = 1.42, 95%CI: 1.04-1.93, $P = 0.04$) and in the LCI *vs* the WLI group in screening patients < 50 years of age (47.1% *vs* 11.5%, RR = 4.08, 95%CI: 2.17-7.65, $P = 0.01$). The PDR were also not significantly different (44.3% *vs* 36.1%, RR = 1.23, 95%CI: 0.98-1.55, $P = 0.10$). In all treatment groups, the proportions of adenomas, hyperplastic polyps, and cancers was higher with LCI than with WLI (all $P < 0.05$), but the proportions of inflammatory polyps and chronic mucosal inflammation was higher in WLI group (both $P < 0.05$). The number of adenomas per colonoscopy in the LCI group was more than that of WLI (0.44 ± 0.87 *vs* 0.28 ± 0.62, $P = 0.03$) and there were no significant differences in the size, morphology, pathology, or site (all $P > 0.05$).

The outcomes of the NBI and LCI groups are shown in Tables 4 and 5. The ADR in each group were not significantly different (23.7% *vs* 30.9%, RR = 0.77, 95%CI: 0.56-1.04, $P = 0.10$), but the ADR in patient < 50 years of age was lower in the NBI group than in the LCI group (10.2% *vs* 25.0%, RR = 0.41, 95%CI: 0.24-0.71, $P = 0.01$). The PDR were also not significantly different (41.6% *vs* 44.3%, RR = 0.94, 95%CI: 0.75-1.18, $P = 0.60$). The proportions of adenomatous and hyperplastic polyps, and cancer were higher in with LCI compared with NBI (all $P < 0.05$), but differences in the proportions of inflammatory polyps and chronic mucosal inflammation were at the contrary (both $P < 0.05$). There were no significant

Table 3 All polyps analysis of both group

	IEE group (*n* = 2113)	WLI group (*n* = 2098)	*P* value	Relative risk (95%CI)
PDR	882/2113 (41.7)	757/2098 (36.1)	0.01	1.16 (1.07-1.25)
All polyps	1588	1319		
Inflammatory polyp	426 (26.8)	341 (25.9)	0.55	1.04 (0.92-1.17)
Hyperplastic polyp	179 (11.3)	150 (11.4)	0.93	0.99 (0.81-1.22)
Adenoma polyp	690 (43.5)	590 (44.7)	0.49	0.97 (0.90-1.06)
Sessile serrated adenoma	10 (0.6)	11 (0.8)	0.52	0.76 (0.32-1.77)
Chronic inflammation	262 (16.5)	211 (16.0)	0.71	1.03 (0.87-1.22)
Cancer	16 (1.0)	13 (1.0)	0.95	1.02 (0.49-2.12)
Others	5 (0.3)	3 (0.2)	0.74[1]	1.38 (0.33-5.78)
Adenoma per colonoscopy	0.33 ± 0.68	0.28 ± 0.62	0.06	
Adenoma polyp	690	590		
Size			0.44	
≤ 5 mm	338 (49.0)	294 (49.8)		0.98 (0.88-1.10)
6-9 mm	211 (30.6)	163 (27.6)		1.11 (0.93-1.32)
≥ 10 mm	141 (20.4)	133 (22.5)		0.91 (0.74-1.12)
Shape			0.39	
Pedunculated	72 (10.4)	76 (12.9)		0.81 (0.60-1.10)
Subpedunculated	186 (27.0)	154 (26.1)		1.03 (0.86-1.24)
Flat	432 (62.6)	360 (61.0)		1.03 (0.94-1.12)
Pathology			0.80	
Tubular adenoma	670 (97.1)	569 (96.4)		1.01 (0.99-1.03)
Tubulovillous adenoma	18 (2.6)	19 (3.2)		0.81 (0.43-1.53)
Villous adenoma	2 (0.3)	2 (0.3)		0.86 (0.12-6.05)
Site			0.50	
Left	258 (37.4)	236 (40.0)		0.94 (0.81-1.07)
Right	357 (51.7)	299 (50.7)		1.02 (0.92-1.14)
Rectum	75 (10.9)	55 (9.3)		1.17 (0.84-1.62)

[1]Using fisher exact test.

Others in image-enhanced endoscopy group: Dermatofibroma × 1, fibroepithelial polyp × 1, neuroendocrine tumor × 1, soft fibroma × 1, gland hyperplasia × 1. Others in white light imaging group: Neuroendocrine tumor × 1, lymphoid polyps × 1, inflammatory granulation tissue × 1. Dates are *n* or *n* (%). PDR: Polyp detection rate; IEE: Image-enhanced endoscopy; WLI: White light imaging; CI: Confidence interval.

differences in the size, morphology, pathology, or site of polyps detected by NBI and LCI (all $P > 0.05$).

DISCUSSION

IEE was developed to meet the need improve the ADR, but the superiority of IEE is controversial. This randomized trial compared the ADR achieved with IEE and WLI in a large population, which, to the best of our knowledge, largest endoscopy study in China even over the world.

In this study, IEE had a higher ADR than WLI, but the difference was not statistically significant (24.0% *vs* 21.8%, $P = 0.09$). The lack of difference may have resulted from the 54.3 percentage of adenomas detected by the 1G-NBI modality, which, in the subgroup analysis had an ADR similar to that of WLI (21.2% *vs* 21.8%, $P = 0.67$). The NBI generally required better bowel preparation, as residual debris severely impaired visualization of the colonic mucosa and dim light reduced the recognizability of adenoma, weakening its effect. It was consistent with previous literature reports. One meta-analysis

Table 4 Overall adenoma detection rate in patients of the subgroup

	NBI group (*n* = 2016)	LCI group (*n* = 97)	WLI group (*n* = 2098)	*P* value[1]	RR (95%CI)	*P* value[2]	RR (95%CI)	*P* value[3]	RR (95%CI)
ADR	478/2016 (23.7)	30/97 (30.9)	458/2098 (21.8)	0.15	1.09 (0.97-1.22)	0.04	1.42 (1.04-1.93)	0.10	0.77 (0.56-1.04)
Advanced ADR	122/2016 (6.1)	5/97 (5.2)	116/2098 (5.5)	0.47	1.10 (0.86-1.40)	0.87	0.93 (0.39-2.23)	0.72	1.17 (0.49-2.80)
Diminutive ADR	304/2016 (15.1)	19/97 (19.6)	286/2098 (13.6)	0.19	1.11 (0.95-1.28)	0.10	1.44 (0.95-2.18)	0.23	0.77 (0.51-1.17)
ADR in different ages									
< 50 yr	55/538 (10.2)	12/48 (25.0)	54/557 (9.7)	0.77	1.05 (0.74-1.51)	0.01	2.58 (1.49-4.48)	0.01	0.41 (0.24-0.71)
≥ 50 yr	423/1478 (28.6)	18/49 (36.7)	404/1541 (26.2)	0.14	1.09 (0.97-1.23)	0.10	1.40 (0.96-2.04)	0.22	0.78 (0.54-1.14)
ADR in different gender									
Male	270/953 (28.3)	18/49 (36.7)	254/982 (25.9)	0.22	1.10 (0.95-1.27)	0.09	1.42 (0.97-2.08)	0.21	0.77 (0.53-1.13)
Female	208/1063 (19.6)	12/48 (25.0)	204/1116 (18.3)	0.44	1.07 (0.90-1.27)	0.24	1.37 (0.83-2.27)	0.36	0.78 (0.47-1.30)
ADR with different indications									
Diagnostic									
< 50 yr	23/247 (9.3)	3/23 (13.0)	23/256 (9.0)	0.90	1.04 (0.60-1.80)	0.46[4]	1.45 (0.47-4.47)	0.47[4]	0.71 (0.23-2.20)
≥ 50 yr	171/590 (29.0)	8/20 (40.0)	166/620 (26.8)	0.39	1.08 (0.90-1.30)	0.19	1.49 (0.86-2.60)	0.29	0.73 (0.42-1.26)
Surveillance									
< 50 yr	8/96 (8.3)	1/8 (12.5)	7/93 (7.5)	0.84	1.11 (0.42-2.93)	0.50[4]	1.66 (0.23-11.87)	0.53[4]	0.67 (0.10-4.69)
≥ 50 yr	134/496 (27.0)	4/13 (30.8)	126/508 (24.8)	0.42	1.09 (0.88-1.34)	0.75[4]	1.24 (0.54-2.84)	0.76[4]	0.88 (0.38-2.01)
Screening									
< 50 yr	24/195 (12.3)	8/17 (47.1)	24/208 (11.5)	0.81	1.07 (0.63-1.81)	0.01	4.08 (2.17-7.65)	0.01[4]	0.26 (0.14-0.49)
≥ 50 yr	118/392 (30.1)	6/16 (37.5)	112/413 (27.1)	0.35	1.11 (0.89-1.38)	0.40	1.38 (0.72-2.65)	0.58	0.80 (0.42-1.54)
Withdrawal time	7.90 ± 3.46	7.82 ± 2.67	7.85 ± 3.47	0.47		0.02		0.05	

[1]The *P* value between narrow band imaging group and white light imaging group.
[2]The *P* value between linked color imaging group and white light imaging group.
[3]The *P* value between narrow band imaging group and linked color imaging group.
[4]Using fisher exact test.
Dates are *n* or *n* (%). ADR: Adenoma detection rate; RR: Relative risk; NBI: Narrow band imaging; WLI: White light imaging; LCI: Linked color imaging; CI: Confidence interval.

with nine RCTs and 2936 subjects comparing the ADR between 1G-NBI and WLE showed that ADR was similar on both group (36% *vs* 34%; *P* = 0.413)[17]; Another meta-analysis also show that 1G-NBI failed to express a better ADR compared with HD-WLE [odds ratio (OR) = 1.01, 95%CI: 0.74- 1.37][8]. However, 2G-NBI having been changed to obtain brighter images than 1G-NBI, even brighter than WLE, to improve ADR. In our subgroup analysis, 2G-NBI depicted a better ADR than WLE as previously reported. An RCT comparing 2G-NBI with WLE showed that the 2G-NBI could detect more adenomas per patient compared with WLE (2.0 *vs* 1.51, *P* = 0.031)[18]. One meta-analysis enrolling 11 RCTs, including 3 RCTs using 2G-NBI, showed 2G-NBI had a better ADR than WLE (OR = 1.28; 95%CI: 1.05-1.56, *P* = 0.02)[7]. The great number of 1G-NBI covered the advantage of 2G-NBI, leading to IEE failed to improve ADR. However, 2G-NBI had a better ADR showed by our subgroup analysis, and it can help improve the quality of colonoscopy.

Table 5 Subgroup analysis of all polyps

	NBI group (*n* = 2016)	LCI group (*n* = 97)	WLI group (*n* = 2098)	*P* value[1]	RR (95%CI)	*P* value[2]	RR (95%CI)	*P* value[3]	RR (95%CI)
PDR	839/2016 (41.6)	43/97 (44.3)	757/2098 (36.1)	0.01	1.15 (1.07-1.25)	0.10	1.23 (0.98-1.55)	0.60	0.94 (0.75-1.18)
All polyps	1519	69	1319						
Inflammatory polyp	421 (27.7)	5 (7.2)	341 (25.9)	0.26	1.07 (0.95-1.21)	0.01	0.28 (0.12-0.66)	0.01	3.83 (1.64-8.93)
Hyperplastic polyp	164 (10.8)	15 (21.7)	150 (11.4)	0.63	0.95 (0.77-1.17)	0.01	1.91 (1.19-3.07)	0.01	0.50 (0.31-0.80)
Adenoma polyp	647 (42.6)	43 (62.3)	590 (44.7)	0.25	0.95 (0.88-1.04)	0.01	1.39 (1.15-1.69)	0.01	0.68 (0.56-0.83)
Sessile serrated adenoma	10 (0.7)	0 (0)	11 (0.8)	0.59	0.79 (0.34-1.85)	1.00[4]		1.00[4]	
Chronic inflammation	259 (17.1)	3 (4.3)	211 (16.0)	0.45	1.07 (0.90-1.26)	0.01	0.27 (0.09-0.83)	0.01	3.92 (1.29-11.93)
Cancer	13 (0.9)	3 (4.3)	13 (1.0)	0.72	0.87 (0.40-1.87)	0.04[4]	4.41 (1.29-15.12)	0.03[4]	0.20 (0.06-0.68)
Others	5 (0.3)	0 (0)	3 (0.2)	0.73[4]	1.45 (0.35-6.04)	1.00[4]		1.00[4]	
Adenoma per colonoscopy	0.32 ± 0.67	0.44 ± 0.87	0.28 ± 0.62	0.11		0.03		0.10	
Adenoma polyp	647	43	590						
Size				0.56		0.22		0.33	
≤ 5 mm	315 (48.7)	23 (53.5)	294 (49.8)		0.98 (0.87-1.09)		1.07 (0.80-1.44)		0.91 (0.68-1.22)
6-9 mm	196 (30.3)	15 (34.9)	163 (27.6)		1.10 (0.92-1.31)		1.26 (0.82-1.94)		0.87 (0.57-1.33)
≥ 10 mm	136 (21.0)	5 (11.6)	133 (22.5)		0.93 (0.76-1.15)		0.52 (0.22-1.19)		1.81 (0.78-4.18)
Shape				0.43		0.79		1.00[4]	
Pedunculated	68 (10.5)	4 (9.3)	76 (12.9)		0.82 (0.60-1.11)		0.72 (0.28-1.88)		1.13 (0.43-2.95)
Subpedunculated	174 (26.9)	12 (27.9)	154 (26.1)		1.03 (0.86-1.24)		1.07 (0.65-1.76)		0.96 (0.59-1.58)
Flat	405 (62.6)	27 (62.8)	360 (61.0)		1.03 (0.94-1.12)		1.03 (0.81-1.31)		1.00 (0.79-1.26)
Pathology				0.90		0.68[4]		0.67	
Tubular adenoma	627 (96.9)	43 (100)	569 (96.4)		1.01 (0.98-1.03)				
Tubulovillous adenoma	18 (2.8)	0 (0)	19 (3.2)		0.86 (0.46-1.63)				
Villous adenoma	2 (0.3)	0 (0)	2 (0.3)		0.91 (0.13-6.45)				
Site				0.57		0.29[4]		0.31	
Left	246 (38.0)	12 (27.9)	236 (40.0)		0.95 (0.83-1.09)		0.70 (0.43-1.14		1.36 (0.83-2.23)
Right	330 (51.0)	27 (62.8)	299 (50.7)		1.01 (0.90-1.12)		1.24 (0.97-1.58)		0.81 (0.64-1.04)
Rectum	71 (11.0)	4 (9.3)	55 (9.3)		1.18 (0.84-1.64)		1.00 (0.38-2.62)		1.18 (0.45-3.08)

[1]The *P* value between narrow band imaging group and white light imaging group.

[2]The *P* value between linked color imaging group and white light imaging group.
[3]The *P* value between narrow band imaging group and linked color imaging group.
[4]Using fisher exact test.
Dates are *n* or *n* (%). Others in narrow band imaging group: Dermatofibroma × 1, fibroepithelial polyp × 1, neuroendocrine tumor × 1, soft fibroma × 1, gland hyperplasia × 1. Others in white light imaging group: Neuroendocrine tumor × 1, lymphoid polyps × 1, inflammatory granulation tissue × 1. PDR: Polyp detection rate; RR: Relative risk; NBI: Narrow band imaging; WLI: White light imaging; LCI: Linked color imaging; CI: Confidence interval.

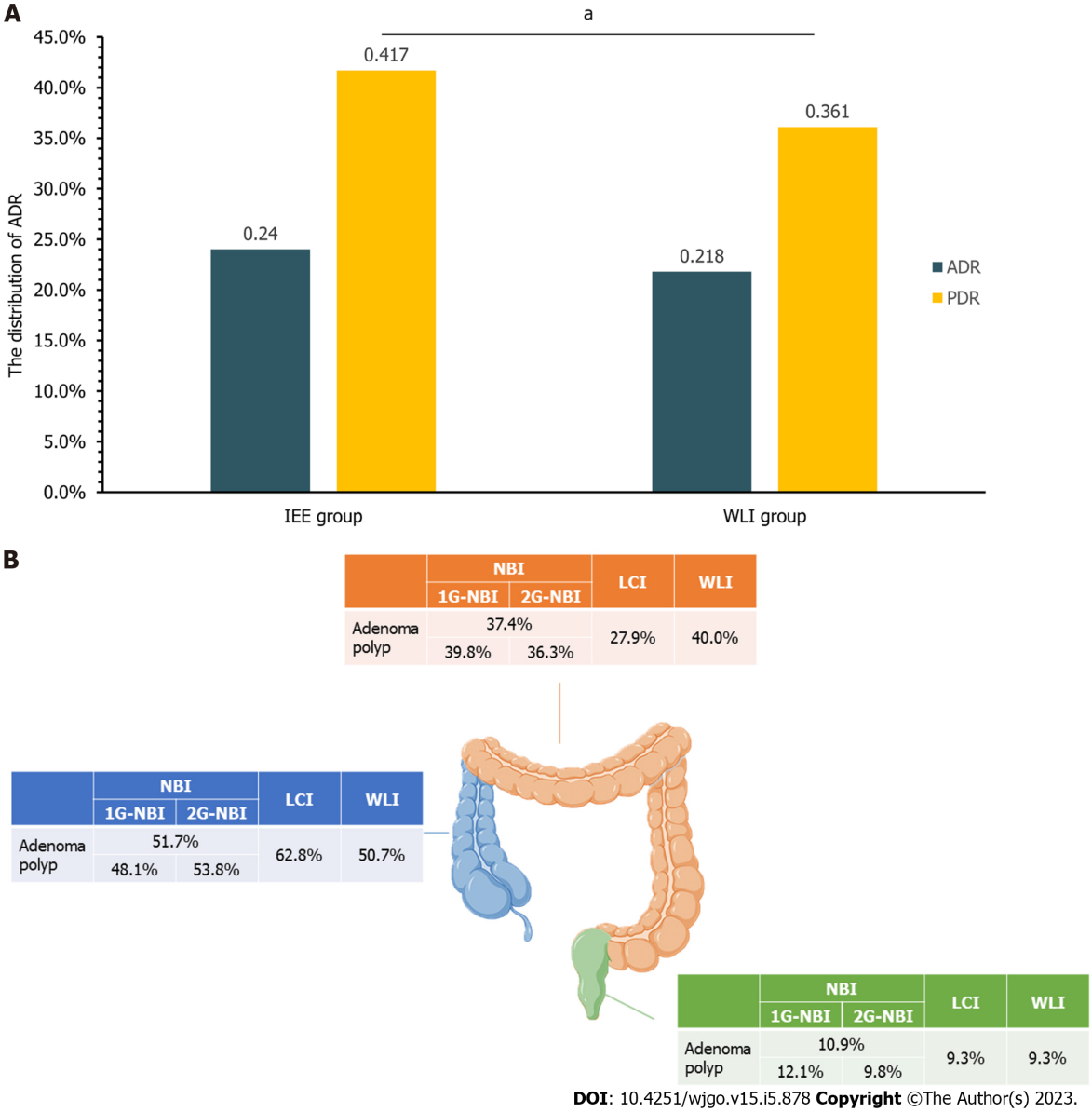

DOI: 10.4251/wjgo.v15.i5.878 **Copyright** ©The Author(s) 2023.

Figure 2 The distribution of adenoma detection rate and adenoma. A: The adenoma detection rate and polyp detection rate of image-enhanced endoscopy and white-light imaging endoscopy group; B: The distribution of adenomas in the colorectum. [a]*P* < 0.05. IEE: Image-enhanced endoscopy; WLI: White-light imaging endoscopy; ADR: Adenoma detection rate; PDR: Polyp detection rate; NBI: Narrow-band imaging; LCI: Linked color imaging; 1G-NBI: First-generation narrow-band imaging.

The experience of endoscopists is known to affect the ADR[5]. Munroe *et al*[4] showed that the adenoma miss rate of trainees decreased as their experience increased and competency improved during tandem colonoscopy training. In another retrospective study involving 24943 procedures and 14 endoscopists, the number of procedures was independently associated with ADR. Endoscopists with > 1000 procedures had a higher ADR than those with < 200 procedures (OR = 1.51, 95%CI: 1.33-1.71, *P* = 0.001)[19]. All endoscopists in our study had at least 5 years of colonoscopy experience, and had a higher ADR (21.8%) than the 20% aspirational target recommended by the working group in the United Kingdom and Ireland[20], and most Asian endoscopists (ADR: 8%-20.3%)[16,21,22]. Operator experience might narrow the difference between WLI and IEE. Endoscopist performance may also be affected by the Hawthorne effect. Several studies reported that endoscopists paid more attention during

the procedure than usual when they knew they were being monitored[23,24]. The high ADR of our endoscopists might explain the smaller than expected differences between the ADR achieved with WLI and IEE.

Although the difference between the ADR observed with IEE and WLI was similar, the PDR of IEE was higher than that of WLI (41.7% *vs* 36.1%, $P = 0.01$), which meant that IEE had a higher sensitivity of polyp detection than WLI. The result is consistent with previous reports that IEE (NBI, i-SCAN, and autofluorescence) benefited polyp detection[25-27]. However, most small non-neoplastic lesions of < 5 mm diameter are benign and need not be removed. Therefore, it is important to distinguish neoplastic from non-neoplastic polyps before endoscopic biopsy to avoid additional treatment-related complications and costs. We were unable to accurately assess the specificity of IEE because of incomplete NBI and LCI classification records, but many studies have previously confirmed that IEE was better than WLI for the differentiation of neoplastic from non-neoplastic polyps[28-30]. A randomized study showed that NBI with magnification had a sensitivity of 90.5% and a specificity of 89.2% for the differentiation of neoplastic and non-neoplastic lesions, which was comparable to magnifying chromoendoscopy. Therefore, IEE detected more polyps and more accurately differentiated neoplastic from non-neoplastic polyps. We recommend that trainees use IEE to reduce messed diagnoses. Although NBI reduced brightness, it significantly improved the visual characterization of polyps. Therefore, senior, expert endoscopy experts can choose white light or IEE mode according to their preference, but for trainees, NBI or LCI mode are recommended to improve the ADR whenever it is difficult to identify lesions in the white light mode.

Subgroup analysis showed 2G-NBI not only had advantage of ADR, but detecting the small adenoma or polyp. Our result revealed that 2G-NBI depicted more small adenomas than WLI and 1G-NBI ($P < 0.05$). What's more, the proportion of inflammatory polyps, usually having a small size, was higher in 2G-NBI than others (all $P < 0.05$). Rex *et al*[31] recorded that 2G-NBI could demonstrate a better ADR with 5-10 mm than WLI ($P = 0.032$). Another RCT in 2015 also showed that 2G-NBI might have priority to adenoma with < 5 mm than WLI ($P = 0.039$)[18]. Combining our data, we recommend 2G-NBI as the major IEE modality.

Subgroup analysis also found a significant difference in the ADR achieved with LCI and WLI (30.9% *vs* 21.8%, $P = 0.04$) and the mean number of adenomas per colonoscopy (0.44 ± 0.87 *vs* 0.28 ± 0.62, $P = 0.03$). ADR and the mean number of adenomas per colonoscopy are both critical indicators reflecting the quality of colonoscopy[32], and improved performance might be clinically relevant because a highly quality colonoscopy has been associated with an increased ADR[15]. LCI, using an appropriate balance of combined narrow-band short-wavelength light and white light, achieves a bright, clear image, making up for the shortcomings of NBI[33]. Therefore, in clinical practice, when NBI or WLI is too dim to identify a polyp, LCI can be of assistance. Although our results are similar to those of previous studies[6,15], the limit of insufficient sample size in the LCI group could cause bias, which required a larger sample size to provide statistical significance for the ADR. The detection rate for sessile serrated lesions was low, reflecting a different prevalence in Chinese patients[16], and the detailed results was attached in Supplementary Table 10.

When we calculated the sample size, we assumed that the ADR was around 10% when WLI was used. That was far lower than the final result, but it does not impair the reliability of the study, and may even make it more reliable. If the ADR used to calculate the sample size was, then fewer than 4200 subjects were needed. Consequently, the result based on the protocol was reasonable and reliable.

This study strengths included its large sample (4211) which was the largest endoscopic study in China even over the word. In additional, it was the first large, multicenter endoscopic RCT in China, which provided strong evidence with Asian population for guideline development and provided reference for other populations. What's more, multi-center involved hospitals of different regions and levels in China making the data become more popularize. Furthermore, IEE and WLI procedures had similar withdrawal time, which improving the comparability of ADR between the two groups. Finally, we included two IEE modalities, NBI and LCI, providing a reference for follow-up studies.

The study limitations included a lack of double blinding because of the obvious image characteristics of IEE. Furthermore, the proficiency of different operators in different enhancement modes may have introduced selection bias[34]. Moreover, most patient re-examinations were performed after the study had ended, and the results were not included in the analysis. It was thus difficult to verify the missed diagnosis and misdiagnosis rates of IEE and WLI. In addition, there were objective differences in population distribution and medical conditions in various regions of our country, resulting in different sample sizes of groups enrolled in each center.

CONCLUSION

In summary, in this RCT performed in an expert setting, IEE did not increase the proportion of patients with at least one detected adenoma compared with WLI. However, the 2G-NBI depicted a better ADR than WLI.

ARTICLE HIGHLIGHTS

Research background

Adenoma detection rate (ADR) as main outcome quality parameter of colonoscopy is under controversial with the use of the image-enhanced endoscopy (IEE). Although there have some randomized controlled trials (RCTs) to compare different IEE with white-light imaging (WLI), the sample is limited and there is still lacking the RCT of IEE with Asian population.

Research motivation

To compare IEE with WLI for the detection and identification of colorectal adenoma and provide the solid outcomes.

Research objectives

To compare IEE with WLI endoscopy for the detection and identification of colorectal adenoma.

Research methods

We designed a prospective, multicenter, randomized, controlled trial to compere the ADR between the IEE group and WLI group.

Research results

The ADR in two group were not significantly different [24.0% *vs* 21.8%,1.10, 95% confidence interval (CI): 0.99-1.23, P = 0.09]. The polyp detection rate was higher with IEE group (41.7%) than with WLI group (36.1%, 1.16, 95%CI: 1.07-1.25, P = 0.01). Differences in mean withdrawal time (7.90 ± 3.42 min *vs* 7.85 ± 3.47 min, P = 0.30) and adenomas per colonoscopy (0.33 ± 0.68 *vs* 0.28 ± 0.62, P = 0.06) were not significant. Subgroup analysis found that with narrow-band imaging (NBI), between-group differences in the ADR, were not significant (23.7% *vs* 21.8%, 1.09, 95%CI: 0.97-1.22, P = 0.15), but were greater with linked color imaging (30.9% *vs* 21.8%, 1.42, 95%CI: 1.04-1.93, P = 0.04). The second-generation NBI (2G-NBI) had an advantage of ADR than both WLI and 1G-NBI (27.0% *vs* 21.8%, P = 0.01; 27.0% *vs* 21.2.0%, P = 0.01).

Research conclusions

This prospective study confirmed that, among Chinese, IEE didn't increase the ADR compared with WLI, but 2G-NBI increase the ADR. Colonoscopists with low ADR might consider using 2G-NBI for performance.

Research perspectives

The efficacy of various modes of IEE still needs to be verified by clinical research.

FOOTNOTES

Author contributions: Qi ZP, Xu EP and He DL contributed equally. Li N, Xu JM, Zhou PH, and Zhong YS contributed to the concept and design of the study and critical revision of the manuscript for important intellectual content; Qi ZP and Xu EP drafted the manuscript; Dong XS and Li N contributed to the statistical analysis; Zhang YS obtained funding; He DL, Xu JM, Zhou PH, and Zhong YS involved in the administrative, technical, or material support; Wang Y, Chen BS, Guo Q, and Li X contributed to the supervision of this manuscript; and all authors involved in the acquisition, analysis, or interpretation of data.

Supported by the National Key R&D Program of China, No. 2018YFC1315005; National Natural Science Foundation of China, No. 82002515; Shanghai Sailing Program, No. 20YF1407200; and China Postdoctoral Science Foundation, No. 2020M681177.

Institutional review board statement: This study was approved by the Ethics Committee of Zhongshan Hospital Fudan University (B2019-131R).

Clinical trial registration statement: This study was registered on the Chinese Clinical Trial Registry (ChiCTR1900026026).

Informed consent statement: Written informed consent was obtained from all patients.

Conflict-of-interest statement: All the authors report no relevant conflicts of interest for this article.

Data sharing statement: Technical appendix, statistical code, and dataset available from the corresponding author at zhong.yunshi@zs-hospital.sh.cn.

CONSORT 2010 statement: The authors have read the CONSORT 2010 Statement, and the manuscript was prepared and revised according to the CONSORT 2010 Statement.

Country/Territory of origin: China

ORCID number: Zhi-Peng Qi 0000-0003-0489-4163; En-Pan Xu 0000-0001-7341-3437; Dong-Li He 0000-0002-1825-9307; Shi-Lun Cai 0000-0002-5000-9658; Ni Li 0000-0003-1742-3803; Bing Li 0000-0002-8727-3591; Di Sun 0000-0003-1823-5759; Ayimukedisi Yalikong 0000-0002-7328-8354; Zhen-Tao Lv 0000-0003-4460-0166; Ping-Hong Zhou 0000-0002-5434-0540; Yun-Shi Zhong 0000-0001-8382-3747.

S-Editor: Wang JJ
L-Editor: A
P-Editor: Zhang YL

REFERENCES

1 **Bray F**, Ferlay J, Soerjomataram I, Siegel RL, Torre LA, Jemal A. Global cancer statistics 2018: GLOBOCAN estimates of incidence and mortality worldwide for 36 cancers in 185 countries. *CA Cancer J Clin* 2018; **68**: 394-424 [PMID: 30207593 DOI: 10.3322/caac.21492]

2 **Corley DA**, Jensen CD, Marks AR, Zhao WK, Lee JK, Doubeni CA, Zauber AG, de Boer J, Fireman BH, Schottinger JE, Quinn VP, Ghai NR, Levin TR, Quesenberry CP. Adenoma detection rate and risk of colorectal cancer and death. *N Engl J Med* 2014; **370**: 1298-1306 [PMID: 24693890 DOI: 10.1056/NEJMoa1309086]

3 **van Rijn JC**, Reitsma JB, Stoker J, Bossuyt PM, van Deventer SJ, Dekker E. Polyp miss rate determined by tandem colonoscopy: a systematic review. *Am J Gastroenterol* 2006; **101**: 343-350 [PMID: 16454841 DOI: 10.1111/j.1572-0241.2006.00390.x]

4 **Munroe CA**, Lee P, Copland A, Wu KK, Kaltenbach T, Soetikno RM, Friedland S. A tandem colonoscopy study of adenoma miss rates during endoscopic training: a venture into uncharted territory. *Gastrointest Endosc* 2012; **75**: 561-567 [PMID: 22341103 DOI: 10.1016/j.gie.2011.11.037]

5 **McCarty TR**, Aihara H. Role of image-enhanced endoscopy: how to improve colorectal polyp detection rates in the coming decade. *Gastrointest Endosc* 2020; **91**: 113-114 [PMID: 31865985 DOI: 10.1016/j.gie.2019.07.025]

6 **Min M**, Deng P, Zhang W, Sun X, Liu Y, Nong B. Comparison of linked color imaging and white-light colonoscopy for detection of colorectal polyps: a multicenter, randomized, crossover trial. *Gastrointest Endosc* 2017; **86**: 724-730 [PMID: 28286095 DOI: 10.1016/j.gie.2017.02.035]

7 **Atkinson NSS**, Ket S, Bassett P, Aponte D, De Aguiar S, Gupta N, Horimatsu T, Ikematsu H, Inoue T, Kaltenbach T, Leung WK, Matsuda T, Paggi S, Radaelli F, Rastogi A, Rex DK, Sabbagh LC, Saito Y, Sano Y, Saracco GM, Saunders BP, Senore C, Soetikno R, Vemulapalli KC, Jairath V, East JE. Narrow-Band Imaging for Detection of Neoplasia at Colonoscopy: A Meta-analysis of Data From Individual Patients in Randomized Controlled Trials. *Gastroenterology* 2019; **157**: 462-471 [PMID: 30998991 DOI: 10.1053/j.gastro.2019.04.014]

8 **Pasha SF**, Leighton JA, Das A, Harrison ME, Gurudu SR, Ramirez FC, Fleischer DE, Sharma VK. Comparison of the yield and miss rate of narrow band imaging and white light endoscopy in patients undergoing screening or surveillance colonoscopy: a meta-analysis. *Am J Gastroenterol* 2012; **107**: 363-70; quiz 371 [PMID: 22186978 DOI: 10.1038/ajg.2011.436]

9 **Hazewinkel Y**, Tytgat KM, van Leerdam ME, Koornstra JJ, Bastiaansen BA, van Eeden S, Fockens P, Dekker E. Narrow-band imaging for the detection of polyps in patients with serrated polyposis syndrome: a multicenter, randomized, back-to-back trial. *Gastrointest Endosc* 2015; **81**: 531-538 [PMID: 25088921 DOI: 10.1016/j.gie.2014.06.043]

10 **Sabbagh LC**, Reveiz L, Aponte D, de Aguiar S. Narrow-band imaging does not improve detection of colorectal polyps when compared to conventional colonoscopy: a randomized controlled trial and meta-analysis of published studies. *BMC Gastroenterol* 2011; **11**: 100 [PMID: 21943365 DOI: 10.1186/1471-230X-11-100]

11 **Schulz KF**, Altman DG, Moher D; CONSORT Group. CONSORT 2010 statement: updated guidelines for reporting parallel group randomised trials. *BMJ* 2010; **340**: c332 [PMID: 20332509 DOI: 10.1136/bmj.c332]

12 The Paris endoscopic classification of superficial neoplastic lesions: esophagus, stomach, and colon: November 30 to December 1, 2002. *Gastrointest Endosc* 2003; **58**: S3-43 [PMID: 14652541 DOI: 10.1016/s0016-5107(03)02159-x]

13 **Repici A**, Badalamenti M, Maselli R, Correale L, Radaelli F, Rondonotti E, Ferrara E, Spadaccini M, Alkandari A, Fugazza A, Anderloni A, Galtieri PA, Pellegatta G, Carrara S, Di Leo M, Craviotto V, Lamonaca L, Lorenzetti R, Andrealli A, Antonelli G, Wallace M, Sharma P, Rosch T, Hassan C. Efficacy of Real-Time Computer-Aided Detection of Colorectal Neoplasia in a Randomized Trial. *Gastroenterology* 2020; **159**: 512-520.e7 [PMID: 32371116 DOI: 10.1053/j.gastro.2020.04.062]

14 **Schlemper RJ**, Riddell RH, Kato Y, Borchard F, Cooper HS, Dawsey SM, Dixon MF, Fenoglio-Preiser CM, Fléjou JF, Geboes K, Hattori T, Hirota T, Itabashi M, Iwafuchi M, Iwashita A, Kim YI, Kirchner T, Klimpfinger M, Koike M,

Lauwers GY, Lewin KJ, Oberhuber G, Offner F, Price AB, Rubio CA, Shimizu M, Shimoda T, Sipponen P, Solcia E, Stolte M, Watanabe H, Yamabe H. The Vienna classification of gastrointestinal epithelial neoplasia. *Gut* 2000; **47**: 251-255 [PMID: 10896917 DOI: 10.1136/gut.47.2.251]

15 **Houwen BBSL**, Hazewinkel Y, Pellisé M, Rivero-Sánchez L, Balaguer F, Bisschops R, Tejpar S, Repici A, Ramsoekh D, Jacobs MAJM, Schreuder RM, Kaminski MF, Rupinska M, Bhandari P, van Oijen MGH, Koens L, Bastiaansen BAJ, Tytgat KM, Fockens P, Vleugels JLA, Dekker E. Linked Colour imaging for the detection of polyps in patients with Lynch syndrome: a multicentre, parallel randomised controlled trial. *Gut* 2022; **71**: 553-560 [PMID: 34086597 DOI: 10.1136/gutjnl-2020-323132]

16 **Jia H**, Pan Y, Guo X, Zhao L, Wang X, Zhang L, Dong T, Luo H, Ge Z, Liu J, Hao J, Yao P, Zhang Y, Ren H, Zhou W, Guo Y, Zhang W, Chen X, Sun D, Yang X, Kang X, Liu N, Liu Z, Leung F, Wu K, Fan D. Water Exchange Method Significantly Improves Adenoma Detection Rate: A Multicenter, Randomized Controlled Trial. *Am J Gastroenterol* 2017; **112**: 568-576 [PMID: 27922025 DOI: 10.1038/ajg.2016.501]

17 **Dinesen L**, Chua TJ, Kaffes AJ. Meta-analysis of narrow-band imaging versus conventional colonoscopy for adenoma detection. *Gastrointest Endosc* 2012; **75**: 604-611 [PMID: 22341105 DOI: 10.1016/j.gie.2011.10.017]

18 **Horimatsu T**, Sano Y, Tanaka S, Kawamura T, Saito S, Iwatate M, Oka S, Uno K, Yoshimura K, Ishikawa H, Muto M, Tajiri H. Next-generation narrow band imaging system for colonic polyp detection: a prospective multicenter randomized trial. *Int J Colorectal Dis* 2015; **30**: 947-954 [PMID: 25925690 DOI: 10.1007/s00384-015-2230-x]

19 **Dong Z**, Sun H, Li B, Zhang Q, Sun K, Wang Z, Qian X, Wang J, Zhan T, Jiang Y, Chen Y, Xu S. Comprehensive evaluation of the learning curve to achieve satisfactory adenoma detection rate. *J Gastroenterol Hepatol* 2021; **36**: 1649-1655 [PMID: 33105040 DOI: 10.1111/jgh.15314]

20 **Rees CJ**, Thomas Gibson S, Rutter MD, Baragwanath P, Pullan R, Feeney M, Haslam N; British Society of Gastroenterology, the Joint Advisory Group on GI Endoscopy, the Association of Coloproctology of Great Britain and Ireland. UK key performance indicators and quality assurance standards for colonoscopy. *Gut* 2016; **65**: 1923-1929 [PMID: 27531829 DOI: 10.1136/gutjnl-2016-312044]

21 **Gong D**, Wu L, Zhang J, Mu G, Shen L, Liu J, Wang Z, Zhou W, An P, Huang X, Jiang X, Li Y, Wan X, Hu S, Chen Y, Hu X, Xu Y, Zhu X, Li S, Yao L, He X, Chen D, Huang L, Wei X, Wang X, Yu H. Detection of colorectal adenomas with a real-time computer-aided system (ENDOANGEL): a randomised controlled study. *Lancet Gastroenterol Hepatol* 2020; **5**: 352-361 [PMID: 31981518 DOI: 10.1016/S2468-1253(19)30413-3]

22 **Wang P**, Berzin TM, Glissen Brown JR, Bharadwaj S, Becq A, Xiao X, Liu P, Li L, Song Y, Zhang D, Li Y, Xu G, Tu M, Liu X. Real-time automatic detection system increases colonoscopic polyp and adenoma detection rates: a prospective randomised controlled study. *Gut* 2019; **68**: 1813-1819 [PMID: 30814121 DOI: 10.1136/gutjnl-2018-317500]

23 **Buchner AM**, Shahid MW, Heckman MG, Diehl NN, McNeil RB, Cleveland P, Gill KR, Schore A, Ghabril M, Raimondo M, Gross SA, Wallace MB. Trainee participation is associated with increased small adenoma detection. *Gastrointest Endosc* 2011; **73**: 1223-1231 [PMID: 21481861 DOI: 10.1016/j.gie.2011.01.060]

24 **Rogart JN**, Siddiqui UD, Jamidar PA, Aslanian HR. Fellow involvement may increase adenoma detection rates during colonoscopy. *Am J Gastroenterol* 2008; **103**: 2841-2846 [PMID: 18759826 DOI: 10.1111/j.1572-0241.2008.02085.x]

25 **Bisschops R**, Tejpar S, Willekens H, De Hertogh G, Van Cutsem E. Virtual chromoendoscopy (I-SCAN) detects more polyps in patients with Lynch syndrome: a randomized controlled crossover trial. *Endoscopy* 2017; **49**: 342-350 [PMID: 28107763 DOI: 10.1055/s-0042-121005]

26 **East JE**, Suzuki N, Stavrinidis M, Guenther T, Thomas HJ, Saunders BP. Narrow band imaging for colonoscopic surveillance in hereditary non-polyposis colorectal cancer. *Gut* 2008; **57**: 65-70 [PMID: 17682000 DOI: 10.1136/gut.2007.128926]

27 **Ramsoekh D**, Haringsma J, Poley JW, van Putten P, van Dekken H, Steyerberg EW, van Leerdam ME, Kuipers EJ. A back-to-back comparison of white light video endoscopy with autofluorescence endoscopy for adenoma detection in high-risk subjects. *Gut* 2010; **59**: 785-793 [PMID: 20551463 DOI: 10.1136/gut.2008.151589]

28 **Chang CC**, Hsieh CR, Lou HY, Fang CL, Tiong C, Wang JJ, Wei IV, Wu SC, Chen JN, Wang YH. Comparative study of conventional colonoscopy, magnifying chromoendoscopy, and magnifying narrow-band imaging systems in the differential diagnosis of small colonic polyps between trainee and experienced endoscopist. *Int J Colorectal Dis* 2009; **24**: 1413-1419 [PMID: 19603174 DOI: 10.1007/s00384-009-0760-9]

29 **Guo TJ**, Chen W, Chen Y, Wu JC, Wang YP, Yang JL. Diagnostic performance of magnifying endoscopy with narrow-band imaging in differentiating neoplastic colorectal polyps from non-neoplastic colorectal polyps: a meta-analysis. *J Gastroenterol* 2018; **53**: 701-711 [PMID: 29383442 DOI: 10.1007/s00535-018-1436-4]

30 **Tischendorf JJ**, Wasmuth HE, Koch A, Hecker H, Trautwein C, Winograd R. Value of magnifying chromoendoscopy and narrow band imaging (NBI) in classifying colorectal polyps: a prospective controlled study. *Endoscopy* 2007; **39**: 1092-1096 [PMID: 18072061 DOI: 10.1055/s-2007-966781]

31 **Rex DK**, Clodfelter R, Rahmani F, Fatima H, James-Stevenson TN, Tang JC, Kim HN, McHenry L, Kahi CJ, Rogers NA, Helper DJ, Sagi SV, Kessler WR, Wo JM, Fischer M, Kwo PY. Narrow-band imaging versus white light for the detection of proximal colon serrated lesions: a randomized, controlled trial. *Gastrointest Endosc* 2016; **83**: 166-171 [PMID: 25952085 DOI: 10.1016/j.gie.2015.03.1915]

32 **Park SK**, Kim HY, Lee CK, Cha JM, Eun CS, Han DS, Lee BI, Shin JE, Park DI. Comparison of adenoma detection rate and adenoma per colonoscopy as a quality indicator of colonoscopy. *Scand J Gastroenterol* 2016; **51**: 886-890 [PMID: 27001284 DOI: 10.3109/00365521.2016.1157892]

33 **Okada M**, Sakamoto H, Takezawa T, Hayashi Y, Sunada K, Lefor AK, Yamamoto H. Laterally Spreading Tumor of the Rectum Delineated with Linked Color Imaging Technology. *Clin Endosc* 2016; **49**: 207-208 [PMID: 26867550 DOI: 10.5946/ce.2015.077]

34 **Leung WK**, Guo CG, Ko MKL, To EWP, Mak LY, Tong TSM, Chen LJ, But DYK, Wong SY, Liu KSH, Tsui V, Lam FYF, Lui TKL, Cheung KS, Lo SH, Hung IFN. Linked color imaging versus narrow-band imaging for colorectal polyp detection: a prospective randomized tandem colonoscopy study. *Gastrointest Endosc* 2020; **91**: 104-112.e5 [PMID: 31276672 DOI: 10.1016/j.gie.2019.06.031]

World Journal of Gastrointestinal Oncology

Submit a Manuscript: https://www.f6publishing.com

World J Gastrointest Oncol 2023 May 15; 15(5): 892-901

DOI: 10.4251/wjgo.v15.i5.892

ISSN 1948-5204 (online)

CASE REPORT

Acute respiratory distress syndrome and severe pneumonitis after atezolizumab plus bevacizumab for hepatocellular carcinoma treatment: A case report

Su Hyeon Cho, Ga Ram You, Chan Park, Sang-Geon Cho, Jong Eun Lee, Sung Kyu Choi, Sung Bum Cho, Jae Hyun Yoon

Specialty type: Gastroenterology and hepatology

Provenance and peer review: Unsolicited article; Externally peer reviewed.

Peer-review model: Single blind

Peer-review report's scientific quality classification

Grade A (Excellent): 0
Grade B (Very good): B
Grade C (Good): C
Grade D (Fair): 0
Grade E (Poor): 0

P-Reviewer: Lin J, China; Martin M, France

Received: January 13, 2023
Peer-review started: January 13, 2023
First decision: January 21, 2023
Revised: February 1, 2023
Accepted: April 7, 2023
Article in press: April 7, 2023
Published online: May 15, 2023

Su Hyeon Cho, Sung Kyu Choi, Jae Hyun Yoon, Department of Gastroenterology and Hepatology, Chonnam National University Hospital and Medical School, Gwangju 61469, South Korea

Ga Ram You, Sung Bum Cho, Department of Gastroenterology and Hepatology, Hwasun Chonnam National University Hospital and Medical School, Hwasun 58128, South Korea

Chan Park, Jong Eun Lee, Department of Radiology, Chonnam National University Hospital and Medical School, Gwangju 61469, South Korea

Sang-Geon Cho, Department of Nuclear Medicine, Chonnam National University Hospital, Hwasun 58128, South Korea

Corresponding author: Jae Hyun Yoon, MD, Associate Professor, Department of Gastroenterology and Hepatology, Chonnam National University Hospital and Medical School, Je-bong ro 42, Dong Gu, Gwangju 61469, South Korea. zenmake14@gmail.com

Abstract

BACKGROUND

Hepatocellular carcinoma (HCC) is one of the most common cancers worldwide and has a high mortality. However, the treatment options for advanced HCC are limited to tyrosine kinase inhibitors, such as sorafenib and lenvatinib. Since previous regimens have an insufficient efficacy, the combination therapy of atezolizumab and bevacizumab (Ate/Bev) has been investigated, which showed an improvement in progression-free and overall survival. However, the adverse events of this combination therapy in advanced HCC have not been established. Herein, we report a novel case of an unresectable HCC and acute respiratory distress syndrome (ARDS) after a combination therapy of Ate/Bev.

CASE SUMMARY

An 82-year-old male visited our outpatient clinic for an incidentally detected liver mass. Liver magnetic resonance imaging and enhanced chest computed tomography (CT) were performed, which showed arterial hyperenhancement with washout in delayed phase suggesting HCC, and a well-defined metastatic solid nodule, respectively. F-18 fluorodeoxyglucose positron emission tomography (PET)-CT exhibited multiple hypermetabolic lesions in the iliac bone,

lumbar vertebrae, and femur. Because of the high burden of the intrahepatic tumor, transarterial radioembolization was initially performed; after 37 d, a combination therapy of Ate/Bev was administered. The patient visited the emergency department three days after Ate/Bev treatment complaining of dyspnea. He was diagnosed with severe pneumonitis based on CT. Despite administering oxygen *via* a high-flow nasal cannula, the P/F ratio was only 74; therefore, the patient was diagnosed with ARDS based on the overall examination results. Low tidal volume with high positive end-expiratory pressure, sedative agents combined with a neuromuscular blocker, and a systemic steroid were promptly applied to manage the ARDS. However, the patient did not recover from the hypoxia and expired 31 h after being admitted.

CONCLUSION

Clinicians should be aware of severe pneumonitis due to the immune-related adverse events of this combination therapy, and patients should be closely monitored after therapy.

Key Words: Hepatocellular carcinoma; Systemic therapy; Adverse events; Pneumonitis; Atezolizumab; Acute respiratory distress syndrome

Core Tip: Nowadays, the combination therapy of atezolizumab and bevacizumab is recommended as the first-line systemic treatment for advanced hepatocellular carcinomas. A global phase III study and recent real-world studies demonstrated rare life-threatening adverse events of atezolizumab and bevacizumab. However, our patient underwent acute respiratory distress syndrome and finally died three days after treatment. To the best of our knowledge, this is the first case of severe respiratory failure resulting in death with a very short interval from atezolizumab and bevacizumab administration. Therefore, we suggest close monitoring of lung toxicity after therapy.

Citation: Cho SH, You GR, Park C, Cho SG, Lee JE, Choi SK, Cho SB, Yoon JH. Acute respiratory distress syndrome and severe pneumonitis after atezolizumab plus bevacizumab for hepatocellular carcinoma treatment: A case report. *World J Gastrointest Oncol* 2023; 15(5): 892-901
URL: https://www.wjgnet.com/1948-5204/full/v15/i5/892.htm
DOI: https://dx.doi.org/10.4251/wjgo.v15.i5.892

INTRODUCTION

Hepatocellular carcinoma (HCC) is the sixth most common cancer and the third leading cause of cancer-related mortality globally[1]. HCC can be treated with various options depending on the tumor stage, remaining liver function, performance status score, and tumor burden[2]. Early-stage HCC has curative treatment options, such as surgical resection, radiofrequency ablation, or liver transplantation. However, only 10%–20% of patients are candidates for curative therapies, and 80% of patients have unresectable HCCs that can only be treated with locoregional therapies, such as transarterial chemoembolization, transarterial radioembolization (TARE), radiotherapy, or palliative management, including systemic therapy[3]. Despite the various locoregional therapies, many patients eventually progress to advanced stages of HCC. Therefore, systemic therapy for managing advanced HCC is clinically significant.

Since 2008, sorafenib, an oral multi-kinase inhibitor, has been used as a first-line systemic chemotherapy based on the SHARP trial, which demonstrated the increased overall survival of patients with advanced HCC compared with placebo-treated advanced HCC patients[4]. In 2018, lenvatinib, another oral multi-kinase inhibitor, was approved as a first-line therapy for advanced HCC according to the REFLECT trial, which demonstrated its non-inferiority over sorafenib in terms of overall survival [5]. However, in large-scale real-world GIDEON study, which comprised of 3202 HCC patients, the presented median overall survival was 13.6 mo in Child-Pugh A group and 5.2 mo in the Child-Pugh B group. The ELEVATOR study, which investigated the real-world efficacy of lenvatinib, showed that the median overall survival was 10.7 mo in the Child-Pugh A group and 5.3 mo in the Child-Pugh B group. Efforts have been devoted to improve the clinical outcomes of patients with advanced HCC undergoing systemic chemotherapy.

With the introduction of various immune checkpoint inhibitors (ICIs), several clinical trials had attempted to verify their treatment efficacy. The CheckMate 459 trial compared the overall survival between nivolumab and sorafenib, of which nivolumab treatment did not significantly improve overall

survival[6]. Also, the KEYNOTE-240 trial compared the overall survival and progression free survival between pembrolizumab and placebo in advanced HCC patients who were previously treated with sorafenib, and failed to reach statistical significance[7]. The IMbrave150 trial investigated the efficacy of the combination therapy of atezolizumab, an anti-PD-L1 antibody, and bevacizumab, a vascular endothelial growth factor (VEGF) -targeting antibody, for treating advanced HCC. The progression-free and overall survival were longer in the combination therapy group than in the sorafenib treatment group, with no differences in grade 3 or 4 adverse events[8,9]. Based on these results, many clinical guidelines have been updated to include atezolizumab and bevacizumab as a first-line systemic treatment for advanced HCC[2]. However, regarding the safety of atezolizumab and bevacizumab, few reports have described the adverse events, especially drug-related pneumonitis.

Herein, we present the novel case of a patient who had an unresectable HCC and experienced acute respiratory distress syndrome (ARDS) due to severe pneumonitis three days after being treated with atezolizumab and bevacizumab.

CASE PRESENTATION

Chief complaints

An 82-year-old male visited our outpatient clinic for an incidentally detected liver mass discovered on abdominal ultrasonography.

History of present illness

He denied fever, night sweats, weight loss, and abdominal pain.

History of past illness

The patient was on medication for hypertension and diabetes mellitus for 20 and 10 years, respectively. He also had underlying liver cirrhosis of an unknown cause, which was diagnosed 13 years ago.

Personal and family history

The patient had no family history.

Physical examination

There were no abnormal findings on physical examination.

Laboratory examinations

The laboratory workup showed the following: platelet count, 510 × 10^9/L (reference range, 130–450 × 10^9/L); total bilirubin, 0.63 mg/dL (reference range, 0.22–1.3 mg/dL); aspartate aminotransferase level, 37 U/L (reference range, 10–37 U/L); alanine aminotransferase level, 46 U/L (reference range, 10–37 U/L); albumin level, 4.0 g/dL (reference range, 3.5–5.2 g/dL); and prothrombin time, 0.97 international normalized ratio (INR; reference range, 0.8–1.2 INR). In the serum laboratory examinations for viral hepatitis, the hepatitis B surface antigen and hepatitis C antibody were negative, whereas the hepatitis B core antibody and hepatitis B surface antibody were positive, implying a prior hepatitis B viral infection. The alpha-fetoprotein level was 84.97 IU/mL, and the protein level induced by vitamin K absence-II (PIVKA-II) was 60232 mAU/mL.

Imaging examinations

Abdominal CT revealed a 16 cm × 11 cm × 10 cm mass with early arterial enhancement and early washout in the delayed phase. Several daughter nodules were found around the main mass. Ascites was not detected (Figure 1). Liver magnetic resonance imaging with Gadoxetate disodium (Primovist®) and enhanced chest CT were performed as the staging workup for the HCC, which showed showed arterial hyperenhancement with washout assessed in the portal venous phase in the enhanced T1-weighted images, and a 7-mm well-defined solid nodule suspected to be a metastatic nodule in the right middle lobe with interstitial lung abnormality (ILA) findings, such as bilateral subpleural reticulation and non-emphysematous cysts with traction bronchiectasis, respectively (Figure 1). Although the patient did not have respiratory symptoms such as dyspnea, pulmonary function tests were performed for ILA evaluation. His forced vital capacity (FVC) and 1-second forced expiratory volume (FEV1) were 1.87 L (52.4% of predicted value) and 1.39 L (63.2% of predicted value), respectively. The FEV1/FVC ratio was 109.7% of predicted value that showed restrictive patterns of lung disease. Because of the suspicious malignant metastatic pulmonary lesions, F-18 fluorodeoxyglucose (FDG) positron emission tomography (PET)-CT was performed to thoroughly evaluate the extrahepatic metastasis, which showed multiple hypermetabolic lesions in both iliac bones, lumbar vertebrae, and the right femur (Figure 2). A solid nodule in the right middle lobe also had mild focal hypermetabolic activity compared to the surrounding lung parenchyma with a maximum standardized uptake value of 1.0.

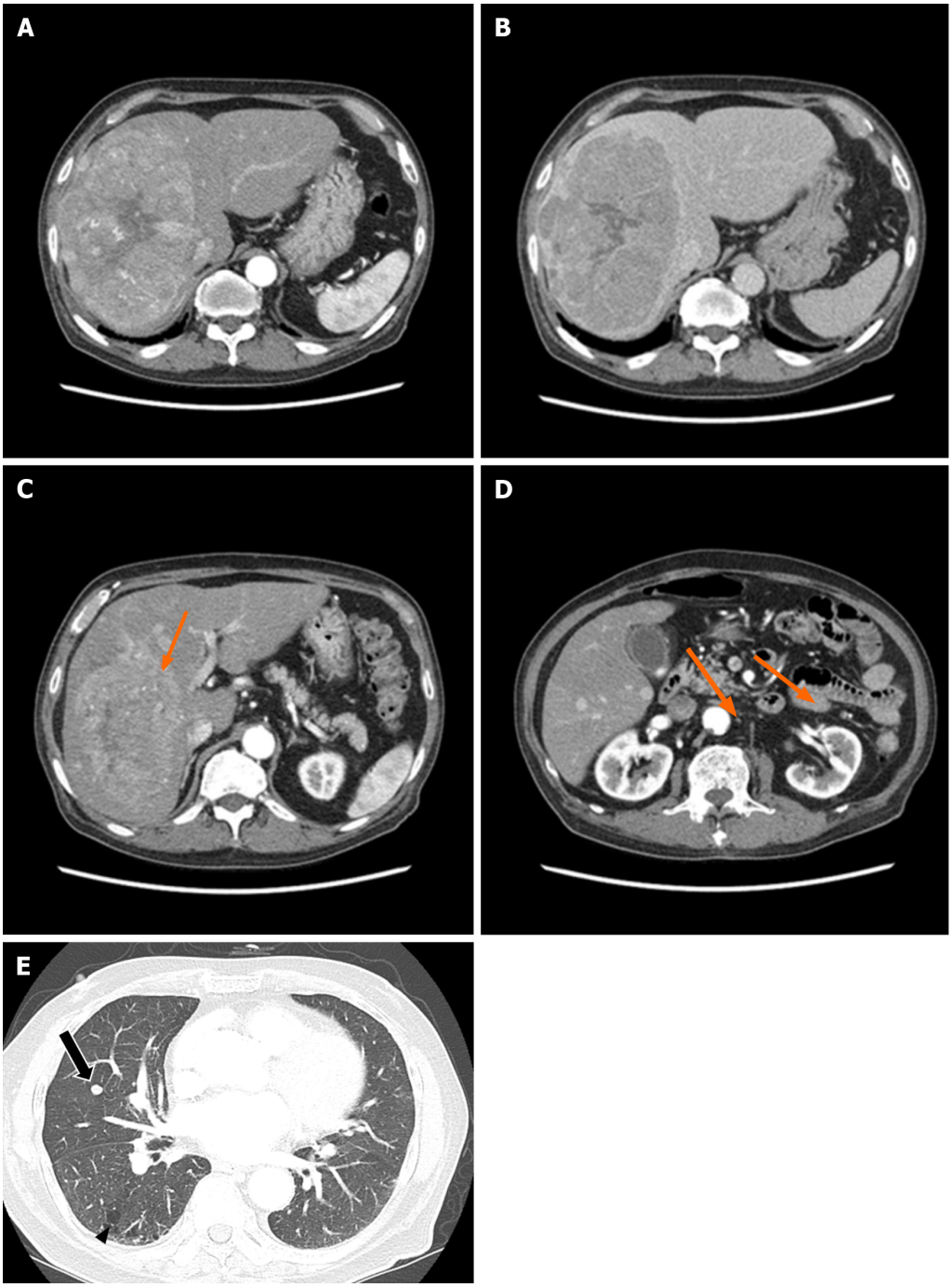

DOI: 10.4251/wjgo.v15.i5.892

Figure 1 The patient's abdominal dynamic computed tomography (CT) at the initial diagnosis. (A, C, D; arterial phase, B; delayed phase). A and B: An oval mass with a size of 16 cm × 11 cm × 10 cm was located in the right hepatic lobe with early enhancement and delayed washout features; C and D: Several satellite nodules were examined in the liver (orange arrows); E: The lung window of the transverse CT scan obtained at the level of the inferior pulmonary veins shows a well-defined round nodule, suspected to be a metastatic nodule, in the right middle lobe (arrow), as well as subpleural reticulation and non-emphysematous cysts (arrowhead).

FINAL DIAGNOSIS

The patient was diagnosed with compensated liver cirrhosis, Child-Pugh A (score, 5) and HCC with multiple extrahepatic metastases [modified Union for International Cancer Control Stage (mUICC) IVB, Barcelona Clinic Liver Cancer (BCLC) C]. His performance status score was 0. He was willing to receive anticancer treatment. Although the patient demonstrated an extrahepatic metastasis, TARE of the primary intrahepatic HCC in the right lobe was planned to address the high tumor burden of the mass and to debulk it. Systemic therapy was administered for the remaining lesions.

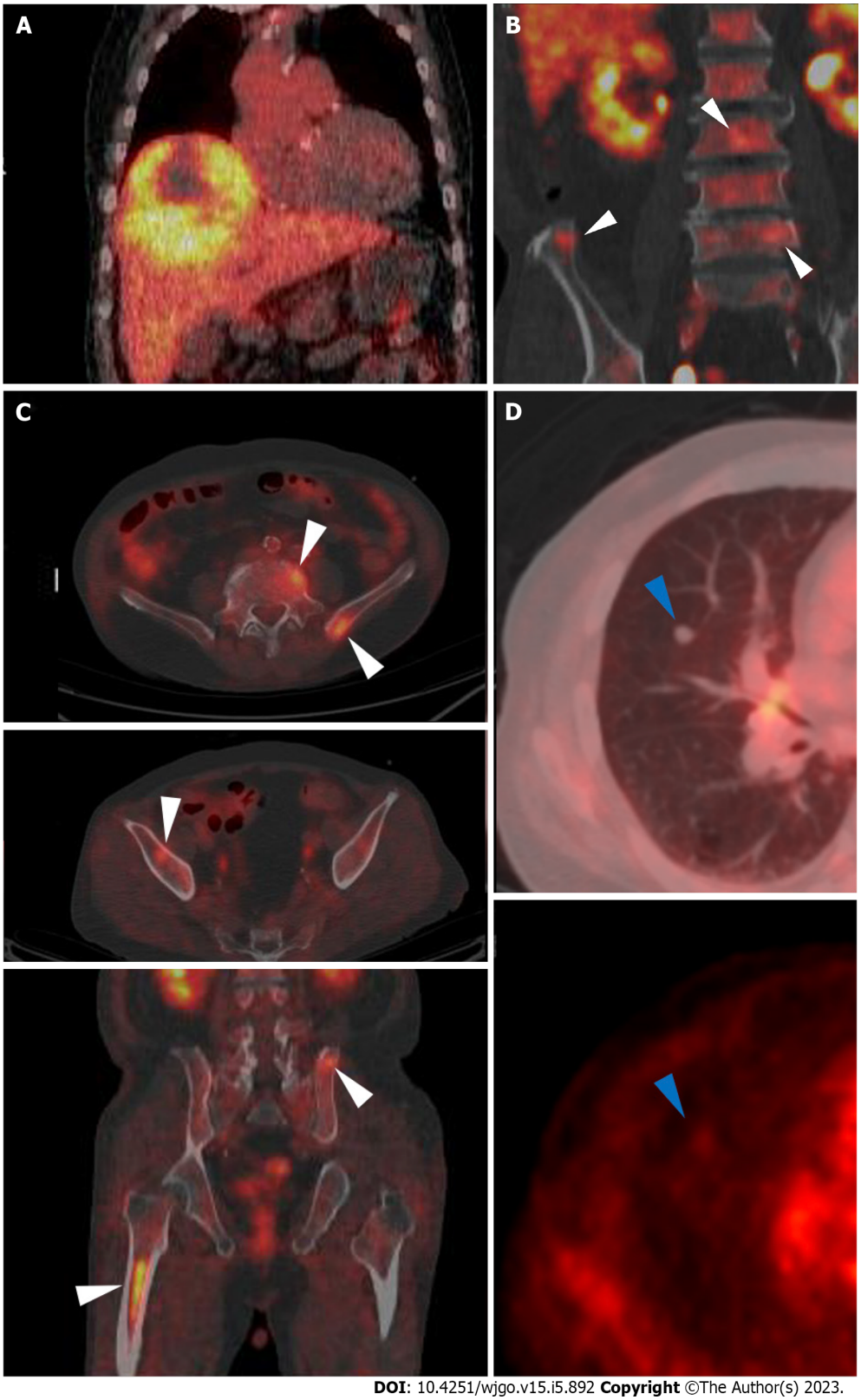

DOI: 10.4251/wjgo.v15.i5.892

Figure 2 F-18 fluorodeoxyglucose positron emission tomography/computed tomography images. A: A large hypermetabolic tumor was noted in the right hepatic lobe [maximum standardized uptake value (SUVmax) 5.1]; B and C: Multiple hypermetabolic lesions (SUVmax 4.8) are seen in both iliac bones, lumbar vertebrae, and the right femur (white arrowheads); D: A solid nodule with mild hypermetabolic activity was noted in the right middle lobe (blue arrowheads).

TREATMENT

Prior to the TARE, a Technetium-99m macro aggregated albumin (99mTc-MAA) perfusion lung scan was performed to assess the hepatopulmonary shunt. The calculated lung shunt fraction was only 8.44%, and the TARE was conducted as scheduled. A hypervascular mass (about 15 cm) with several

daughter nodules in the right hepatic lobe fed by branches of the right hepatic, left hepatic, and left inferior phrenic arteries was examined *via* angiography. An Yttrium-90 (Y90) infusion was performed by feeding the branches of the right hepatic artery, and the mean dose volumes were 108.419 Gy on the tumor, 85.543 Gy on the liver, and 0.873 Gy on both lungs (0.714 and 0.159 Gy on the right and left lungs, respectively). Additionally, chemoembolization using a doxorubicin-lipiodol mixture was performed through the branches of the right hepatic artery, while bland embolization of the left inferior phrenic artery was simultaneously conducted (Figure 3).

Postoperatively, the patient's general condition was tolerable without abdominal pain, and no complications, such as liver failure or post-embolization syndrome, were observed. The patient was discharged after two days. A restaging baseline CT was performed 34 d after the initial TARE and before the systemic therapy. Abdominal CT showed more necrotic changes in the known primary HCC lesion, with some sparse lipiodol uptake in several daughter nodules. Chest CT showed no remarkable changes in the 7-mm metastatic nodule. Since the patient's general condition was tolerable, systemic therapy using the combination of atezolizumab and bevacizumab was administered the day after the CT scan. For the systemic therapy, 1200 mg of atezolizumab and 870 mg (15 mg/kg body weight) of bevacizumab were infused for 60 and 90 min, respectively. No acute side effects occurred during the injections, and the patient returned home in the same day.

OUTCOME AND FOLLOW-UP

However, three days after the combination therapy of atezolizumab and bevacizumab, the patient visited the emergency room for severe dyspnea (Modified Medical Research Council Dyspnea Grade 4). The serum laboratory workup showed that the total bilirubin was 0.49 mg/dL (reference range, 0.22–1.3 mg/dL), aspartate aminotransferase level was 59 U/L (reference range, 10–37 U/L), and alanine aminotransferase level was 36 U/L (reference range, 10–37 U/L). The arterial blood gas test showed hypoxemia [partial pressure of oxygen (pO_2), 84 mmHg] under 0.9 of the fraction of inspired oxygen (FiO_2) level. Chest CT revealed newly detected diffused ground-glass opacities with bilateral septal thickening and consolidations (Figure 4). Infectious pneumonia was ruled out due to lack of related symptoms, such as fever or purulent sputum, and negative microbiological test (*e.g.*, sputum culture and respiratory virus exam) results. Although oxygen was administered *via* a high-flow nasal cannula, the P/F ratio was only 74; therefore, the patient was diagnosed with ARDS based on the overall examination results. The patient was immediately admitted to the intensive care unit after tracheal intubation. Low tidal volume with high positive end-expiratory pressure, sedative agents combined with a neuromuscular blocker, and a systemic steroid (125 mg of methylprednisolone per day) were promptly applied to manage the ARDS. However, the patient's P/F ratio worsened, and he did not recover from the hypoxia. Unfortunately, he expired 31 h after being admitted.

DISCUSSION

The paradigm in the systemic treatment of HCC has shifted from conventional tyrosine kinase inhibitors (TKI) to a combination of an ICI with a TKI or another ICI[10]. According to the IMBrave150 trial, a pivotal study on the use of atezolizumab and bevacizumab for unresectable HCCs, the progression-free survival of this combination treatment was better than that of sorafenib[8]. Follow-up results demonstrated a meaningful survival benefit of the combination therapy of atezolizumab and bevacizumab[9]. Therefore, the HCC treatment guidelines have been updated, including the combination therapy of atezolizumab and bevacizumab as a first-line therapy for advanced HCCs[2,11]. Conventional TKI agents, such as sorafenib, lenvatinib, and cabozantinib, are considered second-line treatments or alternatives to the first-line treatment for ineligible patients for the combination therapy of atezolizumab and bevacizumab.

In addition to treatment efficacy, the safety profile of drug administration is an essential concern. Conventional TKI agents have various treatment-related adverse events, such as diarrhea, hypertension, proteinuria, and skin toxicities, such as rash, desquamation, and hand-foot skin reactions[12]. The IMBrave 150 trial showed a better safety profile for atezolizumab and bevacizumab compared with that of sorafenib. The most common grade 3 or grade 4 adverse events with an incidence of more than 10% in the IMBrave150 trial were hypertension (15.2%), increased aspartate aminotransferase levels (7.0%), and increased alanine aminotransferase levels (3.6%), which were mostly consistent with the follow-up study. Although 1.2% of the patients experienced grade 1–2 pneumonitis, no patients with severe grade toxicity were found. This finding was consistent with the follow-up study (2.0% of patients had grade 1–2 pneumonitis).

Considering the timeline of the combination therapy of atezolizumab and bevacizumab into clinical practice, few real-world studies regarding the treatment efficacy and safety profile have been completed, reporting conflicting results. D'Alessio *et al*[13] conducted a multi-national, retrospective study on 202 patients with HCC treated with the combination of atezolizumab and bevacizumab. They

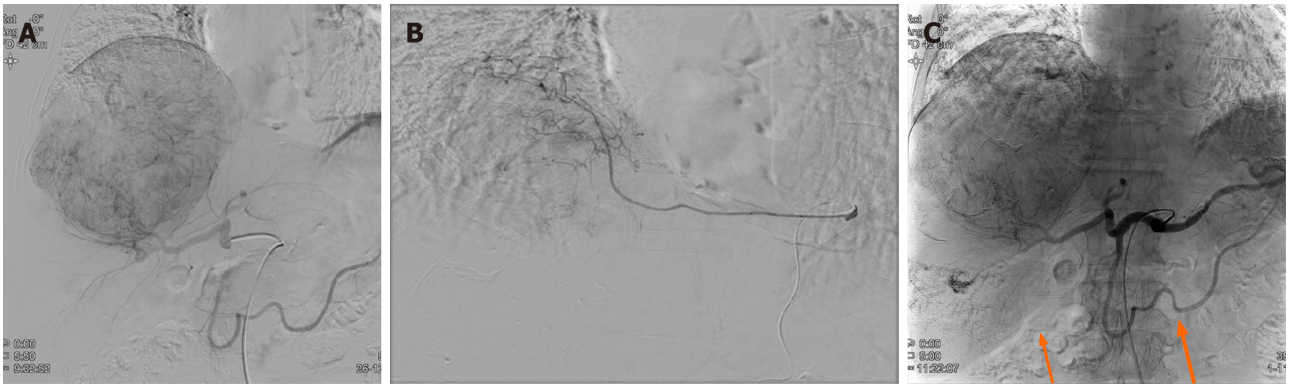

DOI: 10.4251/wjgo.v15.i5.892 **Copyright** ©The Author(s) 2023.

Figure 3 Digital subtraction angiography and completion angiography after transarterial radioembolization and chemoembolization. A: The common hepatic artery angiogram shows a large hypervascular staining of the main mass. The satellite nodules of the right inferior lobe are not identified in this image. No tumor staining is found at the cranial portion of the tumor; B: The left inferior phrenic artery angiogram shows a hypervascular staining of the cranial portion of the tumor. This branch was embolized with tris-acryl gelatin microspheres and gelatin sponge particles; C: The completion angiogram shows the decreased staining of the main mass and lipiodol-laden tumors (orange arrows) in the right hepatic lobe.

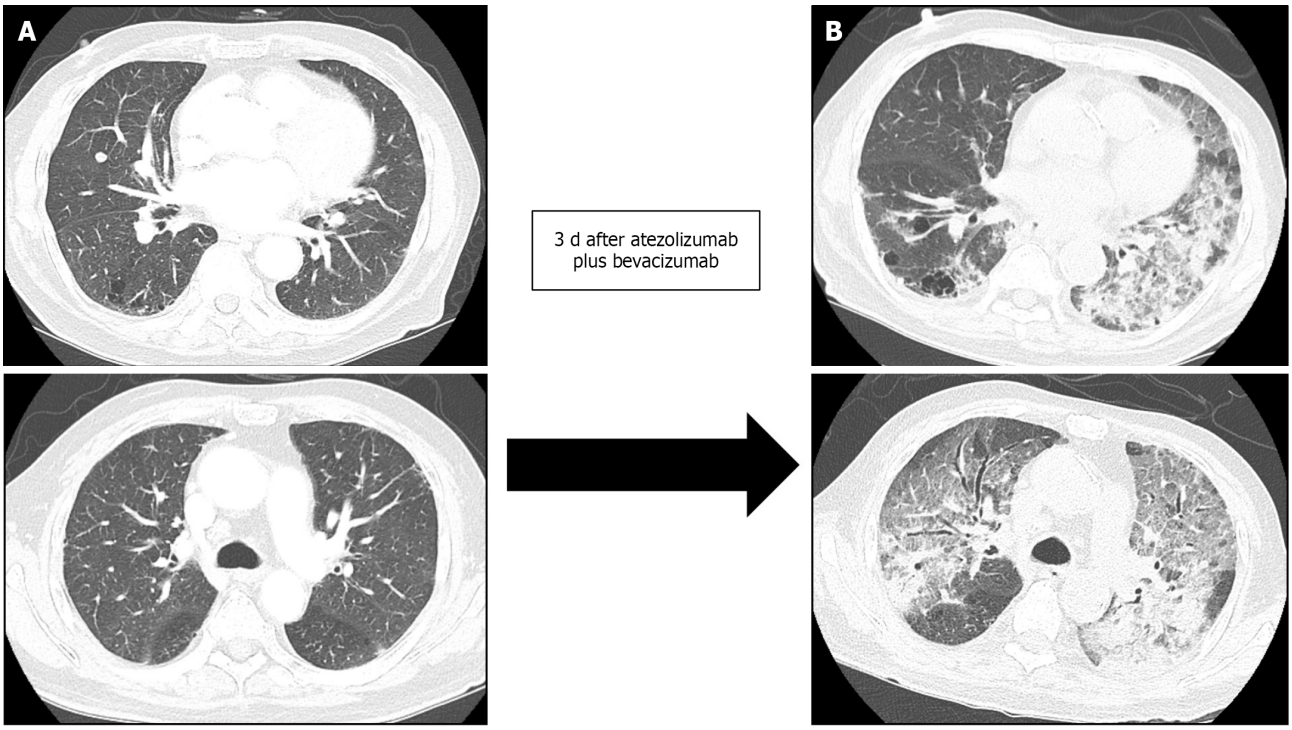

DOI: 10.4251/wjgo.v15.i5.892 **Copyright** ©The Author(s) 2023.

Figure 4 Development of acute respiratory distress syndrome three days after the combination therapy of atezolizumab and bevacizumab. The lung window of the transverse computed tomography (CT) scan obtained at the level of the left main pulmonary and main pulmonary trunk arteries shows the mixed areas of ground-glass opacity and bilateral consolidation with the anteroposterior gradient (B), compared to baseline CT which was scanned 3 and 4 d prior to atezolizumab and bevacizumab therapy and acute respiratory distress syndrome, respectively, (A) which demonstrated no inflammatory changes and minimal pulmonary fibrosis.

observed that 1.0% of the patients experienced treatment-related pneumonitis of more than grade 3. Tada *et al*[14] compared the results of the combination of atezolizumab and bevacizumab in elderly (≥ 75 years old) and nonelderly (< 75 years old) HCC patients, and revealed that the treatment efficacy and safety did not differ between the groups, and reported no drug-related pneumonitis. However, Ng *et al* [15] performed a study on the immune-related adverse events (irAEs) associated with the use of ICIs, including atezolizumab, in advanced HCCs, and found that pneumonitis occurred in 3.0%–10.0% of the patients (2.4% of which had pneumonitis of grade 3 or higher) and the pneumonitis was lethal in 0.2%–2.0% of the patients. Additionally, Endo *et al*[16] recently reported two fatal cases after applying atezolizumab plus bevacizumab on patients with pre-existing lung diseases. One patient showed

honeycomb lungs before treatment and died 5 d after treatment. Another patient previously underwent right lower lobectomy due to lung adenocarcinoma. She died after 11 courses of treatment.

Pneumonitis is an uncommon but possible adverse event closely related to the use of various ICIs in HCC patients. The KEYNOTE-240 trial studied the use of pembrolizumab, an anti-PD-1 monoclonal antibody, in HCC patients, and reported an occurrence of pneumonitis of any grade in 18.3% of the patients, and grade 3 or 4 pneumonitis in 7.2% of the patients[17]. Lung-related irAEs due to ICIs have been investigated in other malignancies, such as lung cancer, renal cell cancer, and melanoma[18]. Lung-related irAEs should be managed based on the grade of pneumonitis. In patients with grade 3 or grade 4 pneumonitis with severe symptoms and life-threatening respiratory compromise, ICI use must be permanently discontinued, and glucocorticoids and empirical antibiotics must be administered[19]. Discontinuing ICI therapy and initiating systemic steroids are highly effective treatments for ICI-related pneumonitis. However, ICI-induced pneumonitis accounts for 35.0% of PD-1/PD-L1 inhibitor-related deaths and may have a similar fatal clinical course to that of our case[20].

Although the associated factors for predicting the development of pneumonitis have been investigated, limited data are available. Decreased pulmonary function and a history of smoking likely increase the risk of pneumonitis[21]. Concurrent radiation therapy, combination immunotherapy, and previous high-dose chemotherapy have also been proposed as potential risk factors[22]. Furthermore, the presence of ILAs is associated with the risk of complications from medical interventions, such as chemotherapy and surgery[23]. Chest CT done on our patient before atezolizumab and bevacizumab therapy showed ILA findings, which may have influenced the rapid onset of ARDS. Although our patient underwent combination therapy of ICI and TKI a meta-analysis by Nishino *et al*[24] reported significantly higher incidences of all-grade pneumonitis (6.6% *vs* 1.6%; $P < 0.001$) and grade 3 or higher pneumonitis (1.5% *vs* 0.2%; $P = 0.001$) in the ICI-combination therapy group than in the monotherapy group. Despite varying reported onset times of pneumonitis after treatment initiation (range, 9 d–19 mo)[21], the median time to onset is reported to be shorter when a combination therapy of ICIs is used[25,26]. The presenting symptoms of ICI-induced pneumonitis are nonspecific, including dyspnea (53.0%), cough (35.0%), and fever (12.0%)[17], and the incidence level for these risk factors in clinical practice in terms of atezolizumab and bevacizumab combination therapy is not yet established. Therefore, clinicians must be aware of the possibilities and characteristics of immune-related pneumonitis associated with these treatments.

This study has some limitations. First, thorough post-treatment pulmonary pathological and laboratory examinations may have clarified the patient's diagnosis; however, a biopsy was not eligible because of the rapid course of the ARDS, and the family did not want an autopsy. Additionally, several serum biomarkers, such as Krebs von den Lungen-6 (KL-6), were related to the diagnosis of interstitial lung disease. If the results of the biomarkers were available, an acute exacerbation of interstitial lung disease could have been ruled out; unfortunately, these laboratory tests were not performed. Second, radiation pneumonitis due to the initial TARE likely occurred. However, the calculated radiation dose to both lungs was 0.873 Gy (left lung, 0.159 Gy; right lung, 0.714 Gy), which was lower than the recommended dose for preventing pneumonitis[27]. Considering that the CT results were from three days before the combination therapy of atezolizumab and bevacizumab, the possibility of radiation pneumonitis due to the TARE was substantially low. However, although respiratory symptoms such as cough, dyspnea and immune-associated pneumonia are well-known ICI-related adverse events, fatal ARDS with an extremely short duration from therapy, as was in our case, has not been reported; therefore, our case report may be of value.

CONCLUSION

Our case implies that the combination therapy of atezolizumab and bevacizumab to treat HCCs might cause fatal pneumonitis leading to ARDS; however, the benefit of this treatment could outweigh the irAEs in terms of survival. Additionally, the severe adverse events of the newly introduced atezolizumab and bevacizumab therapy are uncommon. However, clinicians should be aware of the possible lung toxicity caused by this treatment, especially in newly developed respiratory symptoms of patients. Once the diagnosis is made, management based on the severity of pneumonitis is highly required. Furthermore, future studies should verify the risk factors of developing pneumonitis to identify high-risk patient groups.

FOOTNOTES

Author contributions: Cho SH, You GR, and Yoon JH contributed to analysis and interpretation of the data and drafting of the article; Park C, Lee JE, and Cho SG contributed to technical and material support; Choi SK and Cho SB contributed to critical revision and final approval of this article; Cho SH and You GR contributed equally to this work as co-first author.

Supported by National Research Foundation of Korea, No. NRF-2021R1F1A1061719.

Informed consent statement: Written informed consent was obtained from the patient's wife for the publication of this case report and any accompanying images.

Conflict-of-interest statement: All the authors report no relevant conflicts of interest for this article.

CARE Checklist (2016) statement: The authors have read the CARE Checklist (2016), and the manuscript was prepared and revised according to the checklist.

Country/Territory of origin: South Korea

ORCID number: Su Hyeon Cho 0000-0002-5911-1114; Ga Ram You 0000-0002-7001-7372; Chan Park 0000-0002-9838-8757; Sang-Geon Cho 0000-0002-1373-1887; Jong Eun Lee 0000-0002-8754-6801; Sung Kyu Choi 0000-0002-6878-3385; Sung Bum Cho 0000-0001-9816-3446; Jae Hyun Yoon 0000-0002-4993-2496.

S-Editor: Liu JH
L-Editor: A
P-Editor: Zhang XD

REFERENCES

1 **Sung H**, Ferlay J, Siegel RL, Laversanne M, Soerjomataram I, Jemal A, Bray F. Global Cancer Statistics 2020: GLOBOCAN Estimates of Incidence and Mortality Worldwide for 36 Cancers in 185 Countries. *CA Cancer J Clin* 2021; **71**: 209-249 [PMID: 33538338 DOI: 10.3322/caac.21660]
2 **Reig M**, Forner A, Rimola J, Ferrer-Fàbrega J, Burrel M, Garcia-Criado Á, Kelley RK, Galle PR, Mazzaferro V, Salem R, Sangro B, Singal AG, Vogel A, Fuster J, Ayuso C, Bruix J. BCLC strategy for prognosis prediction and treatment recommendation: The 2022 update. *J Hepatol* 2022; **76**: 681-693 [PMID: 34801630 DOI: 10.1016/j.jhep.2021.11.018]
3 **Belghiti J**, Kianmanesh R. Surgical treatment of hepatocellular carcinoma. *HPB (Oxford)* 2005; **7**: 42-49 [PMID: 18333160 DOI: 10.1080/13651820410024067]
4 **Llovet JM**, Ricci S, Mazzaferro V, Hilgard P, Gane E, Blanc JF, de Oliveira AC, Santoro A, Raoul JL, Forner A, Schwartz M, Porta C, Zeuzem S, Bolondi L, Greten TF, Galle PR, Seitz JF, Borbath I, Häussinger D, Giannaris T, Shan M, Moscovici M, Voliotis D, Bruix J; SHARP Investigators Study Group. Sorafenib in advanced hepatocellular carcinoma. *N Engl J Med* 2008; **359**: 378-390 [PMID: 18650514 DOI: 10.1056/NEJMoa0708857]
5 **Kudo M**, Finn RS, Qin S, Han KH, Ikeda K, Piscaglia F, Baron A, Park JW, Han G, Jassem J, Blanc JF, Vogel A, Komov D, Evans TRJ, Lopez C, Dutcus C, Guo M, Saito K, Kraljevic S, Tamai T, Ren M, Cheng AL. Lenvatinib *vs* sorafenib in first-line treatment of patients with unresectable hepatocellular carcinoma: a randomised phase 3 non-inferiority trial. *Lancet* 2018; **391**: 1163-1173 [PMID: 29433850 DOI: 10.1016/S0140-6736(18)30207-1]
6 **Yau T**, Park JW, Finn RS, Cheng AL, Mathurin P, Edeline J, Kudo M, Harding JJ, Merle P, Rosmorduc O, Wyrwicz L, Schott E, Choo SP, Kelley RK, Sieghart W, Assenat E, Zaucha R, Furuse J, Abou-Alfa GK, El-Khoueiry AB, Melero I, Begic D, Chen G, Neely J, Wisniewski T, Tschaika M, Sangro B. Nivolumab *vs* sorafenib in advanced hepatocellular carcinoma (CheckMate 459): a randomised, multicentre, open-label, phase 3 trial. *Lancet Oncol* 2022; **23**: 77-90 [PMID: 34914889 DOI: 10.1016/S1470-2045(21)00604-5]
7 **Finn RS**, Ryoo BY, Merle P, Kudo M, Bouattour M, Lim HY, Breder V, Edeline J, Chao Y, Ogasawara S, Yau T, Garrido M, Chan SL, Knox J, Daniele B, Ebbinghaus SW, Chen E, Siegel AB, Zhu AX, Cheng AL; KEYNOTE-240 investigators. Pembrolizumab As Second-Line Therapy in Patients With Advanced Hepatocellular Carcinoma in KEYNOTE-240: A Randomized, Double-Blind, Phase III Trial. *J Clin Oncol* 2020; **38**: 193-202 [PMID: 31790344 DOI: 10.1200/JCO.19.01307]
8 **Finn RS**, Qin S, Ikeda M, Galle PR, Ducreux M, Kim TY, Kudo M, Breder V, Merle P, Kaseb AO, Li D, Verret W, Xu DZ, Hernandez S, Liu J, Huang C, Mulla S, Wang Y, Lim HY, Zhu AX, Cheng AL; IMbrave150 Investigators. Atezolizumab plus Bevacizumab in Unresectable Hepatocellular Carcinoma. *N Engl J Med* 2020; **382**: 1894-1905 [PMID: 32402160 DOI: 10.1056/NEJMoa1915745]
9 **Cheng AL**, Qin S, Ikeda M, Galle PR, Ducreux M, Kim TY, Lim HY, Kudo M, Breder V, Merle P, Kaseb AO, Li D, Verret W, Ma N, Nicholas A, Wang Y, Li L, Zhu AX, Finn RS. Updated efficacy and safety data from IMbrave150: Atezolizumab plus bevacizumab vs. sorafenib for unresectable hepatocellular carcinoma. *J Hepatol* 2022; **76**: 862-873 [PMID: 34902530 DOI: 10.1016/j.jhep.2021.11.030]
10 **Su TH**, Hsu SJ, Kao JH. Paradigm shift in the treatment options of hepatocellular carcinoma. *Liver Int* 2022; **42**: 2067-2079 [PMID: 34515412 DOI: 10.1111/liv.15052]
11 **Kudo M**, Kawamura Y, Hasegawa K, Tateishi R, Kariyama K, Shiina S, Toyoda H, Imai Y, Hiraoka A, Ikeda M, Izumi N,

Moriguchi M, Ogasawara S, Minami Y, Ueshima K, Murakami T, Miyayama S, Nakashima O, Yano H, Sakamoto M, Hatano E, Shimada M, Kokudo N, Mochida S, Takehara T. Management of Hepatocellular Carcinoma in Japan: JSH Consensus Statements and Recommendations 2021 Update. *Liver Cancer* 2021; **10**: 181-223 [PMID: 34239808 DOI: 10.1159/000514174]

12 **Bellmunt J**, Eisen T, Fishman M, Quinn D. Experience with sorafenib and adverse event management. *Crit Rev Oncol Hematol* 2011; **78**: 24-32 [PMID: 20399677 DOI: 10.1016/j.critrevonc.2010.03.006]

13 **D'Alessio A**, Fulgenzi CAM, Nishida N, Schönlein M, von Felden J, Schulze K, Wege H, Gaillard VE, Saeed A, Wietharn B, Hildebrand H, Wu L, Ang C, Marron TU, Weinmann A, Galle PR, Bettinger D, Bengsch B, Vogel A, Balcar L, Scheiner B, Lee PC, Huang YH, Amara S, Muzaffar M, Naqash AR, Cammarota A, Personeni N, Pressiani T, Sharma R, Pinter M, Cortellini A, Kudo M, Rimassa L, Pinato DJ. Preliminary evidence of safety and tolerability of atezolizumab plus bevacizumab in patients with hepatocellular carcinoma and Child-Pugh A and B cirrhosis: A real-world study. *Hepatology* 2022; **76**: 1000-1012 [PMID: 35313048 DOI: 10.1002/hep.32468]

14 **Tada T**, Kumada T, Hiraoka A, Hirooka M, Kariyama K, Tani J, Atsukawa M, Takaguchi K, Itobayashi E, Fukunishi S, Tsuji K, Ishikawa T, Tajiri K, Ochi H, Yasuda S, Toyoda H, Ogawa C, Nishimura T, Hatanaka T, Kakizaki S, Shimada N, Kawata K, Tanaka T, Ohama H, Nouso K, Morishita A, Tsutsui A, Nagano T, Itokawa N, Okubo T, Arai T, Imai M, Naganuma A, Koizumi Y, Nakamura S, Joko K, Iijima H, Hiasa Y; Real-life Practice Experts for HCC (RELPEC) Study Group and the Hepatocellular Carcinoma Experts from 48 clinics in Japan (HCC 48) Group. Safety and efficacy of atezolizumab plus bevacizumab in elderly patients with hepatocellular carcinoma: A multicenter analysis. *Cancer Med* 2022; **11**: 3796-3808 [PMID: 35441477 DOI: 10.1002/cam4.4763]

15 **Ng KYY**, Tan SH, Tan JJE, Tay DSH, Lee AWX, Ang AJS, Wong LWJ, Choo SP, Tai DW, Lee JJX. Impact of Immune-Related Adverse Events on Efficacy of Immune Checkpoint Inhibitors in Patients with Advanced Hepatocellular Carcinoma. *Liver Cancer* 2022; **11**: 9-21 [PMID: 35222504 DOI: 10.1159/000518619]

16 **Endo K**, Kuroda H, Oikawa T, Ito Y, Abe T, Kooka Y, Kakisaka K, Miyasaka A, Sugai T, Matsumoto T. Immune Checkpoint Inhibitor-Related Pneumonia in Unresectable Hepatocellular Carcinoma: Two Fatal Cases under Atezolizumab plus Bevacizumab. *Liver Cancer* 2022; **11**: 572-575 [PMID: 36589724 DOI: 10.1159/000526388]

17 **Hsu C**, Rimassa L, Sun HC, Vogel A, Kaseb AO. Immunotherapy in hepatocellular carcinoma: evaluation and management of adverse events associated with atezolizumab plus bevacizumab. *Ther Adv Med Oncol* 2021; **13**: 17588359211031141 [PMID: 34377156 DOI: 10.1177/17588359211031141]

18 **Das S**, Johnson DB. Immune-related adverse events and anti-tumor efficacy of immune checkpoint inhibitors. *J Immunother Cancer* 2019; **7**: 306 [PMID: 31730012 DOI: 10.1186/s40425-019-0805-8]

19 **Brahmer JR**, Lacchetti C, Schneider BJ, Atkins MB, Brassil KJ, Caterino JM, Chau I, Ernstoff MS, Gardner JM, Ginex P, Hallmeyer S, Holter Chakrabarty J, Leighl NB, Mammen JS, McDermott DF, Naing A, Nastoupil LJ, Phillips T, Porter LD, Puzanov I, Reichner CA, Santomasso BD, Seigel C, Spira A, Suarez-Almazor ME, Wang Y, Weber JS, Wolchok JD, Thompson JA; National Comprehensive Cancer Network. Management of Immune-Related Adverse Events in Patients Treated With Immune Checkpoint Inhibitor Therapy: American Society of Clinical Oncology Clinical Practice Guideline. *J Clin Oncol* 2018; **36**: 1714-1768 [PMID: 29442540 DOI: 10.1200/JCO.2017.77.6385]

20 **Wang DY**, Salem JE, Cohen JV, Chandra S, Menzer C, Ye F, Zhao S, Das S, Beckermann KE, Ha L, Rathmell WK, Ancell KK, Balko JM, Bowman C, Davis EJ, Chism DD, Horn L, Long GV, Carlino MS, Lebrun-Vignes B, Eroglu Z, Hassel JC, Menzies AM, Sosman JA, Sullivan RJ, Moslehi JJ, Johnson DB. Fatal Toxic Effects Associated With Immune Checkpoint Inhibitors: A Systematic Review and Meta-analysis. *JAMA Oncol* 2018; **4**: 1721-1728 [PMID: 30242316 DOI: 10.1001/jamaoncol.2018.3923]

21 **Kalisz KR**, Ramaiya NH, Laukamp KR, Gupta A. Immune Checkpoint Inhibitor Therapy-related Pneumonitis: Patterns and Management. *Radiographics* 2019; **39**: 1923-1937 [PMID: 31584861 DOI: 10.1148/rg.2019190036]

22 **Nishino M**, Ramaiya NH, Hatabu H, Hodi FS, Armand PF. PD-1 inhibitor-related pneumonitis in lymphoma patients treated with single-agent pembrolizumab therapy. *Br J Haematol* 2018; **180**: 752-755 [PMID: 27861725 DOI: 10.1111/bjh.14441]

23 **Hatabu H**, Hunninghake GM, Richeldi L, Brown KK, Wells AU, Remy-Jardin M, Verschakelen J, Nicholson AG, Beasley MB, Christiani DC, San José Estépar R, Seo JB, Johkoh T, Sverzellati N, Ryerson CJ, Graham Barr R, Goo JM, Austin JHM, Powell CA, Lee KS, Inoue Y, Lynch DA. Interstitial lung abnormalities detected incidentally on CT: a Position Paper from the Fleischner Society. *Lancet Respir Med* 2020; **8**: 726-737 [PMID: 32649920 DOI: 10.1016/S2213-2600(20)30168-5]

24 **Nishino M**, Giobbie-Hurder A, Hatabu H, Ramaiya NH, Hodi FS. Incidence of Programmed Cell Death 1 Inhibitor-Related Pneumonitis in Patients With Advanced Cancer: A Systematic Review and Meta-analysis. *JAMA Oncol* 2016; **2**: 1607-1616 [PMID: 27540850 DOI: 10.1001/jamaoncol.2016.2453]

25 **Gosangi B**, McIntosh L, Keraliya A, Irugu DVK, Baheti A, Khandelwal A, Thomas R, Braschi-Amirfarzan M. Imaging features of toxicities associated with immune checkpoint inhibitors. *Eur J Radiol Open* 2022; **9**: 100434 [PMID: 35967881 DOI: 10.1016/j.ejro.2022.100434]

26 **Delaunay M**, Cadranel J, Lusque A, Meyer N, Gounant V, Moro-Sibilot D, Michot JM, Raimbourg J, Girard N, Guisier F, Planchard D, Metivier AC, Tomasini P, Dansin E, Pérol M, Campana M, Gautschi O, Früh M, Fumet JD, Audigier-Valette C, Couraud S, Dalle S, Leccia MT, Jaffro M, Collot S, Prévot G, Milia J, Mazieres J. Immune-checkpoint inhibitors associated with interstitial lung disease in cancer patients. *Eur Respir J* 2017; **50** [PMID: 28798088 DOI: 10.1183/13993003.00050-2017]

27 **Weber M**, Lam M, Chiesa C, Konijnenberg M, Cremonesi M, Flamen P, Gnesin S, Bodei L, Kracmerova T, Luster M, Garin E, Herrmann K. EANM procedure guideline for the treatment of liver cancer and liver metastases with intra-arterial radioactive compounds. *Eur J Nucl Med Mol Imaging* 2022; **49**: 1682-1699 [PMID: 35146577 DOI: 10.1007/s00259-021-05600-z]

World Journal of Gastrointestinal Oncology

Submit a Manuscript: https://www.f6publishing.com

World J Gastrointest Oncol 2023 May 15; 15(5): 902-910

DOI: 10.4251/wjgo.v15.i5.902

ISSN 1948-5204 (online)

CASE REPORT

Oral fruquintinib combined with tegafur-gimeracil-oteracil potassium for advanced colorectal cancer to obtain longer progression-free survival: A case report

Fan-Jie Qu, Shuang Wu, Yan Kong

Specialty type: Oncology

Provenance and peer review: Unsolicited article; Externally peer reviewed.

Peer-review model: Single blind

Peer-review report's scientific quality classification

Grade A (Excellent): 0
Grade B (Very good): B, B
Grade C (Good): 0
Grade D (Fair): 0
Grade E (Poor): 0

P-Reviewer: Atanasova EG, Bulgaria; Bordonaro M, United States

Received: January 26, 2023
Peer-review started: January 26, 2023
First decision: March 8, 2023
Revised: March 13, 2023
Accepted: April 7, 2023
Article in press: April 7, 2023
Published online: May 15, 2023

Fan-Jie Qu, Shuang Wu, Yan Kong, Department of Oncology, Affiliated Dalian Third People's Hospital of Dalian Medical University, Dalian 116033, Liaoning Province, China

Corresponding author: Yan Kong, MD, Professor, Department of Oncology, Affiliated Dalian Third People's Hospital of Dalian Medical University, No. 40 Qianshan Road, Dalian 116033, Liaoning Province, China. kongkongyan2022@163.com

Abstract

BACKGROUND

After the failure of second-line standard therapy, effective treatment options for metastatic colorectal cancer are limited, and the duration of remission cannot meet clinical needs. In addition, associated drug toxicity may lead to treatment interruption that may affect patient outcomes. Therefore, more safe, effective and convenient treatments are urgently needed.

CASE SUMMARY

Here, we describe a patient with advanced colorectal cancer with multiple metastases in both lungs. Oxaliplatin combined with 5-fluorouracil or capecitabine was given as the first-line treatment, and bevacizumab combined with irinotecan was given as the second-line treatment after disease progression. However, treatment was interrupted due to recurrent grade 2 nausea and grade 1 diarrhea. He received targeted therapy with fruquintinib starting on August 26, 2020 and responded well for 12 mo. After slow progression of the lung metastases, progression-free survival was again achieved over 13.5 mo by continued treatment of fruquintinib in combination with tegafur-gimeracil-oteracil potassium chemotherapy. Overall treatment duration was more than 25.5 mo. The treatments delayed tumor progression, reduced drug side effects, maintained a good quality of life, and further extended overall survival.

CONCLUSION

This case report detailed preliminary evidence showing that the combination of fruquintinib with tegafur-gimeracil-oteracil potassium chemotherapy double oral therapy may result in longer progression-free survival in patients with advanced colorectal cancer.

Key Words: Fruquintinib; Tegafur-gimeracil-oteracil potassium (S-1); Advanced colorectal

cancer; Progression-free survival; Case report

Core Tip: After the failure of second-line standard therapy, effective treatment options for metastatic colorectal cancer (CRC) are limited. Here, we describe a patient with CRC with multiple lung metastases. Disease progression occurred after oxaliplatin + 5-fluorouracil or capecitabine as first-line treatment and bevacizumab + irinotecan as second-line treatment. The patient received targeted therapy with fruquintinib and responded well for 12 mo. Progression-free survival was again achieved over 13.5 mo by continuing fruquintinib in combination with tegafur-gimeracil-oteracil potassium chemotherapy. This case detailed preliminary evidence showing that the combination of fruquintinib with tegafur-gimeracil-oteracil potassium resulted in longer progression-free survival in patients with CRC.

Citation: Qu FJ, Wu S, Kong Y. Oral fruquintinib combined with tegafur-gimeracil-oteracil potassium for advanced colorectal cancer to obtain longer progression-free survival: A case report. *World J Gastrointest Oncol* 2023; 15(5): 902-910
URL: https://www.wjgnet.com/1948-5204/full/v15/i5/902.htm
DOI: https://dx.doi.org/10.4251/wjgo.v15.i5.902

INTRODUCTION

Colorectal cancer (CRC) is one of the most common cancers worldwide and the second most common cause of cancer-related deaths worldwide[1,2]. The most common cause of death in patients with CRC is distant metastasis, with approximately 25%-40% of patients with CRC already having metastases at the time of initial diagnosis[3,4].

Treatment recommendations for metastatic CRC (mCRC) include single or combination chemotherapy [5-fluorouracil (5-FU), capecitabine, oxaliplatin, and irinotecan] with or without targeted therapy (bevacizumab and cetuximab)[5]. These regimens are generally used for first-line and second-line treatments. The median overall survival for advanced CRC has now reached 30 mo by rational drug distribution[6]. For patients who do not respond to first-line and second-line standard therapies, the drugs approved for third-line treatment of mCRC in China currently include regorafenib, fruquintinib and garcia-carbonero (TAS-102), but the efficacy of these three regiments is limited[7,8,10].

5-FU combined with anti-vascular therapy showed synergistic efficacy and increased antitumor activity in refractory mCRC. The toxicity of the combined regimen was considered tolerable[11]. However, the use of bevacizumab needs to be carried out in the hospital. If the combination of two oral drugs is selected, it may reduce the inconvenience of repeated visits to the hospital and improve patient compliance and quality of life.

CASE PRESENTATION

Chief complaints

A 58-year-old male presented for treatment in March 2018 due to continuous increased frequency of defecation. Colonoscopy and biopsy revealed sigmoid adenocarcinoma, while chest computed tomography (CT) during the same period indicated multiple pulmonary nodules, which was considered metastasis.

History of present illness

He underwent laparoscopic radical resection of the left half colon on March 28, 2020. The postoperative pathological examination showed: (Sigmoid lesion) moderately differentiated adenocarcinoma; tumor size: 6.5 cm × 4.5 cm; invasion of the whole layer; and 19 lymph nodes around the intestine were negative for cancer metastasis. Immunohistochemistry examinations revealed the following: MSH2 (+), MLH1 (+), PMS2 (+), MSH6 (+), and suggestive pMMR. Genetic testing revealed *KRAS*, *NRAS*, *BRAF* wildtype, microsatellite stable, and *UGT1A1* GG type.

History of past illness

He had a history of hypertension and paroxysmal atrial fibrillation for 3 years.

Imaging examinations

In April 2018, reexamination by chest CT 1 mo after surgery revealed that the pulmonary nodules were larger than before, and abdomen CT showed no active findings.

FINAL DIAGNOSIS

The patient was diagnosed with stage IV sigmoid adenocarcinoma with multiple lung metastases.

TREATMENT

The patient refused to use bevacizumab and cetuximab because of concerns about adverse events such as hypertension and rash associated with targeted drug therapy. Instead starting in April 2018, the patient received six cycles of first-line treatment with mFOLFOX6 regimen (oxaliplatin 165 mg IV on day 1 + leucovorin 0.6 g IV on day 1 + 5-FU 0.75 g IV on day 1 + 5-FU 4.5 g CIV 46 h q2w), during which the intrapulmonary metastases were stable. In August 2018, the patient voluntarily stopped taking the mFOLFOX6 regimen due to personal reasons and did not receive maintenance treatment. Follow-up CT examination during drug withdrawal indicated slow progression of lung lesions.

In February 2019, the patient began the XELOX protocol (oxaliplatin 200 mg IV on day 1 +capecitabine 1.5 g PO bid on days 1–14 q3w) for five cycles of intermittent treatment. After the lung lesions were stable for a period of time, the patient stopped treatment again in July 2019. CT reexamination in October 2019 indicated that the lesions in the lung were enlarged. We judged the efficacy as progressive disease, and the progression-free survival (PFS) time of first-line treatment was 19 mo.

The major adverse events during treatment were grade 2 nausea and vomiting after chemotherapy, myelosuppression (grade 1 leukopenia and neutropenia and grade 2 thrombocytopenia), grade 1 liver dysfunction, and grade 1 numbness of the hands and feet. These adverse reactions and the inconvenience of repeated visits to the hospital were the main reasons the patient decided to stop treatment many times. The patient had no coughing and wheezing during treatment and maintained an Eastern Cooperative Oncology Group performance score of 0.

The patient was still unable to receive cetuximab due to anxiety about the rash. Second-line bevacizumab combined with irinotecan was initiated in November 2019 for a total of eight cycles. Bevacizumab (500 mg) and irinotecan (350 mg) were given every 3 wk. During second-line treatment, the patient's treatment was interrupted for 2 mo due to the coronavirus disease 2019 pandemic. The treatment evaluation was stable disease. However, grade 2 nausea and vomiting and grade 1 diarrhea occurred repeatedly during the treatment, and the patient could not tolerate these adverse events. Second-line treatment continued until July 2020. Due to no signs of disease progression (Figure 1A-C), the patient again requested that the treatment be discontinued and replaced with oral medication.

Therefore, treatment with oral fruquintinib [5 mg once a day (qd) on days 1–21 every 4 wk] was administrated as a third-line treatment starting on August 26, 2020. CT reexamination after 3 mo of treatment showed no significant change in the size of the metastatic lesions in both lungs, but the cavity in the lesions increased (Figure 1D-F). Subsequent follow-up and CT examination of the lung lesions remained stable (Figure 1G-I), while the main toxicity experienced by the patient during this period was hypertension, which could be well managed.

After 12 mo, some lesions in the lung slowly enlarged again (Figure 1J-L). After communication with the patient, the patient refused to receive intravenous therapy. Considering the slow growth of the lesions and no new metastatic lesions after comprehensive evaluation, our treatment group suggested that the patient should continue fruquintinib in combination with another oral chemotherapy drug: tegafur-gimeracil-oteracil potassium capsules (S-1). After repeated consultations with the patient and the signing of informed consent, the regimen of fruquintinib + S-1 was initiated as fourth-line treatment in September 2021. Fruquintinib (5 mg) was given once daily, 2 wk on and 1 wk off; S-1 (60 mg) was given twice daily, 2 wk on and 1 wk off.

During administration, the patient experienced grade 2 leukocyte decline and grade 1 diarrhea. Considering the patient's high quality of life requirements, we decided to adjust the dose of S-1 based on toxicity 9graded according to National Cancer Institute CTCAE V.4.0) and possible benefits. S-1 was adjusted from 60 mg twice daily to 40 mg in the morning and 60 mg in the evening. At the same time, nifedipine sustained release tablets and skin moisturizing care were given regularly to monitor the adverse reactions (grade I hypertension, grade I hand-foot syndrome). Follow-up during medication was regular, and chest CT examination showed stable lung metastases until August 2022 (Figure 2). The patient maintained good quality of life, and the Eastern Cooperative Oncology Group score was 0.

Unfortunately, another chest CT examination in October 2022 revealed the enlargement of pulmonary metastases and the appearance of multiple new lesions (Figure 2), which was judged to be disease progression. In addition, abdomen CT still showed no active findings. PFS of 13.5 mo was achieved by fruquintinib S-1.

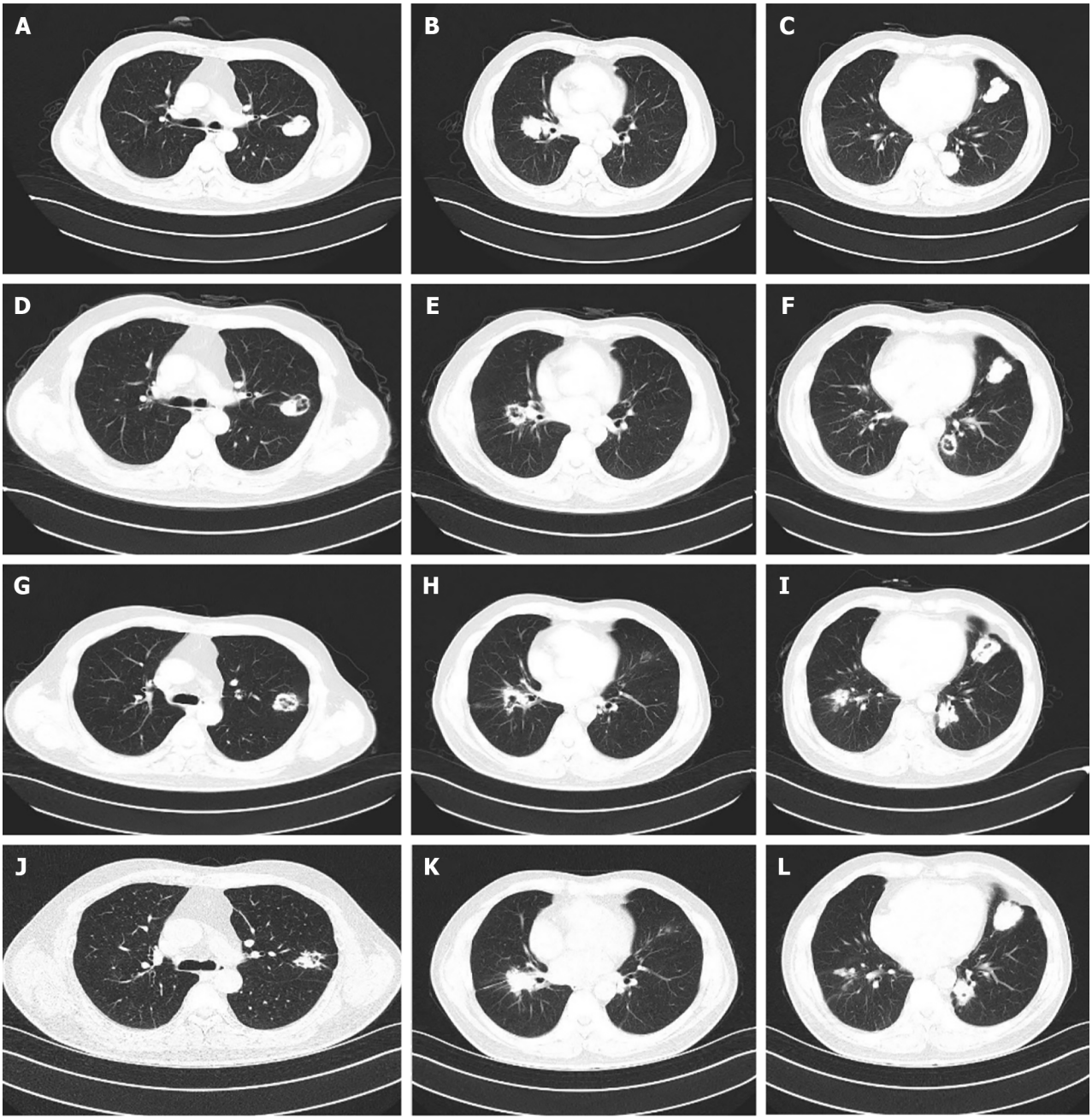

DOI: 10.4251/wjgo.v15.i5.902

Figure 1 Chest computed tomography before and after treatment with fruquintinib showed multiple metastases in both lungs. A-C: A baseline chest computed tomography (CT) scan before fruquintinib treatment on August 24, 2020; D-F: CT after fruquintinib treatment was given for 3 mo (November 30, 2020); G-I: CT after fruquintinib treatment was given for 8 mo (May 31, 2021); J-L: CT after fruquintinib treatment was given for 12 mo (August 31, 2021).

OUTCOME AND FOLLOW-UP

The patient achieved a continuous survival benefit from continued treatment with fruquintinib monotherapy after diagnosis of mCRC and subsequent combination therapy with S-1, including at least 25.5 mo of PFS and 30 mo of overall survival (Figure 3).

Considering that the second-line treatment of irinotecan had not shown resistance combined with the genetic test results of the patient, we started the cetuximab plus irinotecan regimen as the fifth-line treatment starting in October 2022. The efficacy of this regimen was not available by the submission date.

In this case report, informed consent was obtained before each treatment. The therapeutic effect was evaluated by the Response Evaluation Criteria in Solid Tumors criteria. The nature and severity of adverse events were evaluated according to the National Cancer Institute CTCAE 4.0.

Informed consent for treatment was signed by the patient before each treatment, and written informed consent was obtained from the patient in order to publish relevant clinical and imaging data. These situations are in line with the ethical standards to be implemented in research involving human

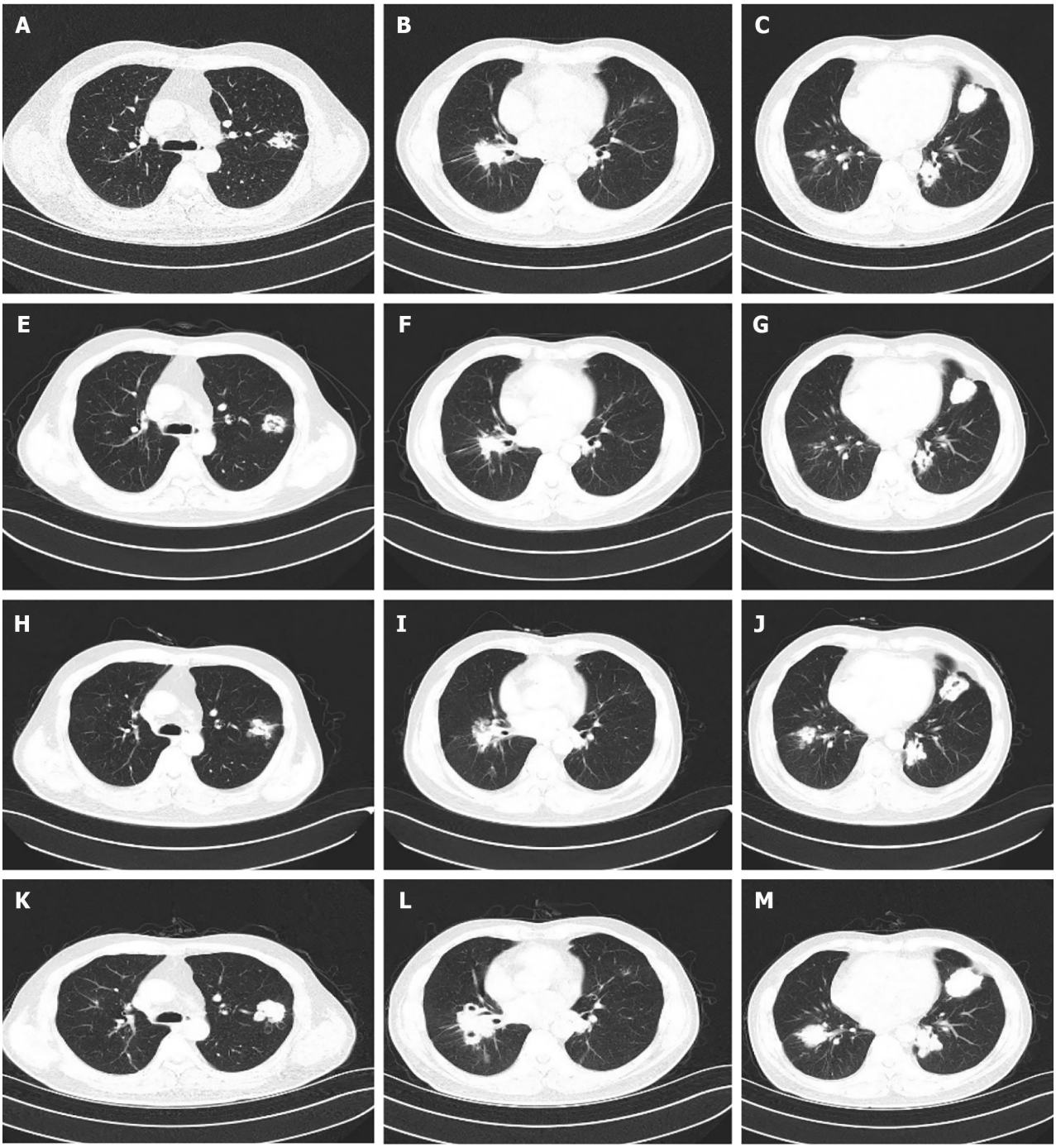

DOI: 10.4251/wjgo.v15.i5.902

Figure 2 Chest computed tomography before and after treatment with fruquintinib plus tegafur-gimeracil-oteracil potassium showed multiple metastases in both lungs. A-C: Computed tomography (CT) before fruquintinib plus tegafur-gimeracil-oteracil potassium (S-1) treatment (August 31, 2021); D-F: CT after fruquintinib plus S-1 treatment was given for 2 mo (November 1, 2021); G-I: CT after fruquintinib plus S-1 treatment was given for 10 mo (June 13, 2022); J-L: CT after fruquintinib plus S-1 treatment was given for 13.5 mo (October 12, 2022).

participants by institutions and/or national research councils as well as the Declaration of Helsinki (2013 revision).

DISCUSSION

Angiogenesis plays a critical role in the neoplastic growth, progression, and metastasis of CRC[12]. It was reported that vascular endothelial growth factor (VEGF) secreted by tumor cells can stimulate endothelial cell survival and proliferation, causing changes in vascular permeability and promoting neo-angiogenesis[12]. Anti-angiogenetic therapy is an important strategy for mCRC treatment. Anti-

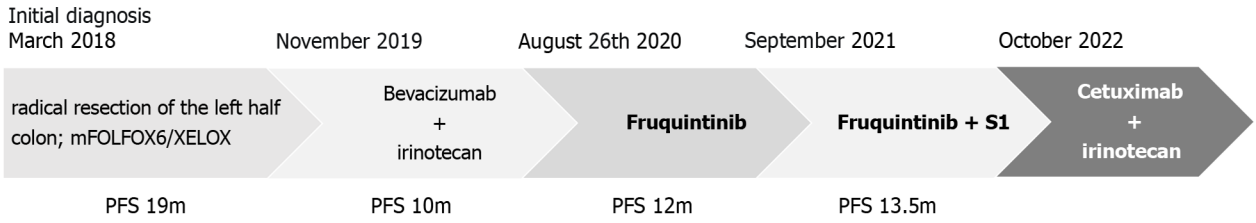

DOI: 10.4251/wjgo.v15.i5.902 **Copyright** ©The Author(s) 2023.

Figure 3 Treatment timeline of the patient. mFOLFOX6: Oxaliplatin, leucovorin, and 5-FU; PFS: Progression-free survival; S1: Tegafur-gimeracil-oteracil potassium; XELOX: Oxaliplatin and capecitabine.

angiogenic agents include the small molecule inhibitors that block the activity of VEGF receptor kinases and the neutralization antibody of VEGF (monoclonal antibodies), which inhibit angiogenesis, cause vascular degeneration, and normalize tumor blood vessels[14]. Bevacizumab is the most successful antibody for neutralizing VEGF, and it has been authorized for mCRC first-line and second-line treatment combined with chemotherapy[5,15,16]. Nonetheless, there are some disadvantages associated with the use of bevacizumab as a monoclonal antibody, including immunogenicity and intravenous administration.

Fruquintinib is a highly selective and potent small-molecule inhibitor against VEGF receptor 1, 2, and 3[17]. It originated and was developed by Hutchison MediPharma and was authorized for third-line treatment in mCRC in China. Fruquintinib is a highly selective inhibitor of the VEGF signaling pathway, which can decrease cell proliferation of human umbilical vein endothelial cells and human lymphatic endothelial cells. It also decreases tumor angiogenesis and lymphangiogenesis, effectively reduces blood vessel density, inhibits tumor proliferation and migration, and has strong antitumor activity[17].

In clinical studies, fruquintinib has shown a survival benefit in mCRC patients. In the phase III FRESCO trial, the fruquintinib group had significantly prolonged median overall survival compared with the placebo group [9.3 mo; 95% confidence interval (CI): 8.2-10.5 *vs* 6.6 mo; 95%CI: 5.9-8.1]. The median PFS of fruquintinib was also significantly increased (3.7 mo; 95%CI: 3.7-4.6 *vs* 1.8 mo; 95%CI: 1.8-1.8)[8]. Fruquintinib also showed an acceptable safety and tolerability profile[8,9].

Our patient chose fruquintinib after drug resistance and intolerance of first-line and second-line treatments. He achieved 12 mo of PFS with monotherapy while maintaining a good quality of life. However, fruquintinib also faced the challenge of drug resistance.

In addition to molecular targeted therapy drugs, chemotherapy is still the main treatment for patients with advanced CRC, among which 5-FU based chemotherapy combined with oxaliplatin or irinotecan is the preferred standard treatment for patients with advanced or recurrent CRC[18]. However, if a patient does not respond to chemotherapy or has a toxic reaction, there are few remaining options.

In 2017, another oral drug, trifluridine-tipiracil (TAS-102), was approved by the United States Food and Drug Administration, which finally offered another potential option for patients with mCRC[19]. TAS-102 has shown a significant overall survival benefit compared with placebo in patients with chemorefractory mCRC in the phase III RECOURSE trial, with a longer median overall survival (7.1 mo *vs* 5.3 mo) and a longer median PFS (2.0 mo *vs* 1.7 mo) in the TAS-102 group[10]. Unfortunately, neither fruquintinib nor TAS-102 gave patients with refractory mCRC a satisfactory PFS[8,10].

Considering that targeted anti-angiogenic drugs combined with chemotherapy play a synergistic antitumor role by inhibiting neovascularization, inducing vascular normalization, and enhancing cytotoxic drug delivery, anti-angiogenic therapy combined with chemotherapy drugs have been explored for refractory CRC. Pfeiffer *et al*[11] conducted a phase II clinical study after previous studies achieved good results and continued to explore the safety and effectiveness of the combination of bevacizumab and TAS-102. The median PFS was 2.6 mo in the TAS-102 group and 4.6 mo in the TAS-102 + bevacizumab group. TAS-102 combined with bevacizumab showed significant clinically relevant improvement in PFS with tolerable toxicity compared to TAS-102 monotherapy.

Based on these results, continuous anti-vascular targeted therapy combined with cytotoxic drugs may have clinical significance in patients with refractory advanced CRC. This combination therapy may change practice in the future, but we do not yet understand the characteristics of patients most suitable for second-line post-combination therapy. At present, the price of TAS-102 is relatively high in China, and it is not covered by medical insurance. Meanwhile, bevacizumab requires intravenous infusion. Therefore, a safe, effective, and more convenient and economical treatment plan is urgently needed in clinic.

S-1, a novel oral 5-FU derivative developed by Taiho Pharmaceuticals Company (Japan), has been widely used in the treatment of gastrointestinal malignancies[20]. S-1 monotherapy has an effectiveness rate of 19%-39% in the treatment of advanced CRC[21,22] and has been shown to be as effective as 5-FU and capecitabine[23,24]. In these studies, the toxicity of S-1 treatment was primarily hematological, while hand-foot syndrome was more common in the capecitabine group. However, there was no statistically significant difference between the two groups. Therefore, S-1 is also an option for the treatment of

advanced CRC[22,23,24].

Based on the above information, it is reasonable to conclude that fruquintinib combined with S-1 may be superior to fruquintinib or S-1 alone in some patients with refractory CRC who do not respond to standard therapy. The therapeutic mechanism of this combination regimen may be associated with the synergistic antitumor action in addition to the respective antitumor effects of fruquintinib and S-1.

In this case, some lung metastases slowly enlarged after 12 mo of monotherapy with fruquintinib. Combined with the results of the above related studies and after repeated communication with the patient and signing the informed consent, the patient began treatment with the combination of fruquintinib and cytotoxic drug S-1. The patient gained 13.5 mo of PFS, and the lung metastases were again well controlled. Only grade 2 leukopenia, grade 1 diarrhea, grade 1 hypertension, and grade 1 hand-foot syndrome were observed during the treatment period.

In the phase III CORRECT, FRESCO, and RECOURSE trials, the median PFS of patients in the regorafenib group, fruquintinib group, and TAS-102 group were 1.9 mo, 3.7 mo, and 2.0 mo, respectively[7,8,10]. Considering that the absolute PFS benefit time of third-line treatment was shorter in previous clinical trials, we hypothesize that the combination of fruquintinib and S-1 caused the longer survival benefit. At the same time, the combination of the two oral drugs reduced the inconvenience of repeated visits to the hospital and improved the patient's quality of life. This treatment combination may have potential clinical significance in future salvage treatment of advanced CRC. Since China is still a developing country, we also need to consider the factors of pharmacoeconomics to reduce the economic burden of patients as much as possible[25]. The strategy of using oral drugs also reduced the risk of exposure to coronavirus disease 2019 during the pandemic. To our knowledge, this is the first time that fruquintinib combined with S-1 in the treatment of advanced CRC has been reported with a good efficacy.

CONCLUSION

In conclusion, the prognosis of CRC after advanced multiline therapy is extremely poor, and survival after existing third-line and post-third-line therapies is limited. Therefore, it is very important to explore suitable therapies for patients with refractory advanced CRC to prolong the overall survival time of patients and enhance the quality of life of patients as much as possible.

Although fruquintinib combined with S1 is not currently the standard treatment for mCRC, this case provides evidence for its antitumor activity and safety. Given that only 1 patient was observed in this report and the clinical data is very limited, further investigation and accumulation of more experience are needed. Further clinical studies can be conducted to demonstrate the efficacy and safety of this combination regimen.

FOOTNOTES

Author contributions: Qu FJ, Wu S, and Kong Y were responsible for collecting data, analyzing data, and writing the article; Kong Y was responsible for guiding the writing and participating in the revision of the article; All authors read and approved the final manuscript.

Informed consent statement: The patient provided informed written consent prior to study enrollment.

Conflict-of-interest statement: The authors declare that there are no conflicts of interest regarding the publication of this paper.

CARE Checklist (2016) statement: The authors have read the CARE Checklist (2016), and the manuscript was prepared and revised according to the CARE Checklist (2016).

Country/Territory of origin: China

ORCID number: Yan Kong 0000-0001-9191-0365.

S-Editor: Ma YJ
L-Editor: Filipodia A
P-Editor: Wu RR

REFERENCES

1 **Siegel RL**, Miller KD, Fuchs HE, Jemal A. Cancer Statistics, 2021. *CA Cancer J Clin* 2021; **71**: 7-33 [PMID: 33433946 DOI: 10.3322/caac.21654]

2 **Sung H**, Ferlay J, Siegel RL, Laversanne M, Soerjomataram I, Jemal A, Bray F. Global Cancer Statistics 2020: GLOBOCAN Estimates of Incidence and Mortality Worldwide for 36 Cancers in 185 Countries. *CA Cancer J Clin* 2021; **71**: 209-249 [PMID: 33538338 DOI: 10.3322/caac.21660]

3 **Shah MA**, Renfro LA, Allegra CJ, André T, de Gramont A, Schmoll HJ, Haller DG, Alberts SR, Yothers G, Sargent DJ. Impact of Patient Factors on Recurrence Risk and Time Dependency of Oxaliplatin Benefit in Patients With Colon Cancer: Analysis From Modern-Era Adjuvant Studies in the Adjuvant Colon Cancer End Points (ACCENT) Database. *J Clin Oncol* 2016; **34**: 843-853 [PMID: 26811529 DOI: 10.1200/JCO.2015.63.0558]

4 **Xu R**, Wang W, Zhu B, Lin X, Ma D, Zhu L, Zhao Q, Nie Y, Cai X, Li Q, Fang W, Li H, Wang N, Chen Y, Peng C, Fang H, Shen L. Disease characteristics and treatment patterns of Chinese patients with metastatic colorectal cancer: a retrospective study using medical records from China. *BMC Cancer* 2020; **20**: 131 [PMID: 32070312 DOI: 10.1186/s12885-020-6557-5]

5 **Cao R**, Zhang S, Ma D, Hu L. A multi-center randomized phase II clinical study of bevacizumab plus irinotecan, 5-fluorouracil, and leucovorin (FOLFIRI) compared with FOLFIRI alone as second-line treatment for Chinese patients with metastatic colorectal cancer. *Med Oncol* 2015; **32**: 325 [PMID: 25481673 DOI: 10.1007/s12032-014-0325-9]

6 **Heinemann V**, von Weikersthal LF, Decker T, Kiani A, Vehling-Kaiser U, Al-Batran SE, Heintges T, Lerchenmüller C, Kahl C, Seipelt G, Kullmann F, Stauch M, Scheithauer W, Hielscher J, Scholz M, Müller S, Link H, Niederle N, Rost A, Höffkes HG, Moehler M, Lindig RU, Modest DP, Rossius L, Kirchner T, Jung A, Stintzing S. FOLFIRI plus cetuximab versus FOLFIRI plus bevacizumab as first-line treatment for patients with metastatic colorectal cancer (FIRE-3): a andomized, open-label, phase 3 trial. *Lancet Oncol* 2014; **15**: 1065-1075 [PMID: 25088940 DOI: 10.1016/S1470-2045(14)70330-4]

7 **Grothey A**, Van Cutsem E, Sobrero A, Siena S, Falcone A, Ychou M, Humblet Y, Bouché O, Mineur L, Barone C, Adenis A, Tabernero J, Yoshino T, Lenz HJ, Goldberg RM, Sargent DJ, Cihon F, Cupit L, Wagner A, Laurent D; CORRECT Study Group. Regorafenib monotherapy for previously treated metastatic colorectal cancer (CORRECT): an international, multicentre, andomized, placebo-controlled, phase 3 trial. *Lancet* 2013; **381**: 303-312 [PMID: 23177514 DOI: 10.1016/S0140-6736(12)61900-X]

8 **Li J**, Qin S, Xu RH, Shen L, Xu J, Bai Y, Yang L, Deng Y, Chen ZD, Zhong H, Pan H, Guo W, Shu Y, Yuan Y, Zhou J, Xu N, Liu T, Ma D, Wu C, Cheng Y, Chen D, Li W, Sun S, Yu Z, Cao P, Chen H, Wang J, Wang S, Wang H, Fan S, Hua Y, Su W. Effect of Fruquintinib vs Placebo on Overall Survival in Patients With Previously Treated Metastatic Colorectal Cancer: The FRESCO Randomized Clinical Trial. *JAMA* 2018; **319**: 2486-2496 [PMID: 29946728 DOI: 10.1001/jama.2018.7855]

9 **Li J**, Guo W, Bai Y, Deng Y, Yang L, Chen Z, Zhong H, Xu R, Pan H, Shu Y, Yuan Y, Zhou J, Xu N, Liu T, Ma D, Wu C, Cheng Y, Xu J, Chen D, Li W, Sun S, Yu Z, Cao P, Shen L, Chen H, Wang S, Wang H, Fan S, Guo X, Wang N, Han R, Zhang B, Qin S. Safety Profile and Adverse Events of Special Interest for Fruquintinib in Chinese Patients with Previously Treated Metastatic Colorectal Cancer: Analysis of the Phase 3 FRESCO Trial. *Adv Ther* 2020; **37**: 4585-4598 [PMID: 32901330 DOI: 10.1007/s12325-020-01477-w]

10 **Mayer RJ**, Van Cutsem E, Falcone A, Yoshino T, Garcia-Carbonero R, Mizunuma N, Yamazaki K, Shimada Y, Tabernero J, Komatsu Y, Sobrero A, Boucher E, Peeters M, Tran B, Lenz HJ, Zaniboni A, Hochster H, Cleary JM, Prenen H, Benedetti F, Mizuguchi H, Makris L, Ito M, Ohtsu A; RECOURSE Study Group. Randomized trial of TAS-102 for refractory metastatic colorectal cancer. *N Engl J Med* 2015; **372**: 1909-1919 [PMID: 25970050 DOI: 10.1056/NEJMoa1414325]

11 **Pfeiffer P**, Yilmaz M, Möller S, Zitnjak D, Krogh M, Petersen LN, Poulsen LØ, Winther SB, Thomsen KG, Qvortrup C. TAS-102 with or without bevacizumab in patients with chemorefractory metastatic colorectal cancer: an investigator-initiated, open-label, andomized, phase 2 trial. *Lancet Oncol* 2020; **21**: 412-420 [PMID: 31999946 DOI: 10.1016/S1470-2045(19)30827-7]

12 **Kerbel RS**. Tumor angiogenesis. *N Engl J Med* 2008; **358**: 2039-2049 [PMID: 18463380 DOI: 10.1056/NEJMra0706596]

13 **Dvorak HF**. Vascular permeability factor/vascular endothelial growth factor: a critical cytokine in tumor angiogenesis and a potential target for diagnosis and therapy. *J Clin Oncol* 2002; **20**: 4368-4380 [PMID: 12409337 DOI: 10.1200/JCO.2002.10.088]

14 **Tampellini M**, Sonetto C, Scagliotti GV. Novel anti-angiogenic therapeutic strategies in colorectal cancer. *Expert Opin Investig Drugs* 2016; **25**: 507-520 [PMID: 26938715 DOI: 10.1517/13543784.2016.1161754]

15 **Venook AP**, Niedzwiecki D, Lenz HJ, Innocenti F, Fruth B, Meyerhardt JA, Schrag D, Greene C, O'Neil BH, Atkins JN, Berry S, Polite BN, O'Reilly EM, Goldberg RM, Hochster HS, Schilsky RL, Bertagnolli MM, El-Khoueiry AB, Watson P, Benson AB 3rd, Mulkerin DL, Mayer RJ, Blanke C. Effect of First-Line Chemotherapy Combined With Cetuximab or Bevacizumab on Overall Survival in Patients With KRAS Wild-Type Advanced or Metastatic Colorectal Cancer: A Randomized Clinical Trial. *JAMA* 2017; **317**: 2392-2401 [PMID: 28632865 DOI: 10.1001/jama.2017.7105]

16 **Moehler M**, Sprinzl MF, Abdelfattah M, Schimanski CC, Adami B, Godderz W, Majer K, Flieger D, Teufel A, Siebler J, Hoehler T, Galle PR, Kanzler S. Capecitabine and irinotecan with and without bevacizumab for advanced colorectal cancer patients. *World J Gastroenterol* 2009; **15**: 449-456 [PMID: 19152449 DOI: 10.3748/wjg.15.449]

17 **Sun Q**, Zhou J, Zhang Z, Guo M, Liang J, Zhou F, Long J, Zhang W, Yin F, Cai H, Yang H, Gu Y, Ni L, Sai Y, Cui Y, Zhang M, Hong M, Sun J, Yang Z, Qing W, Su W, Ren Y. Discovery of fruquintinib, a potent and highly selective small molecule inhibitor of VEGFR 1, 2, 3 tyrosine kinases for cancer therapy. *Cancer Biol Ther* 2014; **15**: 1635-1645 [PMID: 25482937 DOI: 10.4161/15384047.2014.964087]

18 **Schmoll HJ**, Van Cutsem E, Stein A, Valentini V, Glimelius B, Haustermans K, Nordlinger B, van de Velde CJ, Balmana J, Regula J, Nagtegaal ID, Beets-Tan RG, Arnold D, Ciardiello F, Hoff P, Kerr D, Köhne CH, Labianca R, Price T, Scheithauer W, Sobrero A, Tabernero J, Aderka D, Barroso S, Bodoky G, Douillard JY, El Ghazaly H, Gallardo J, Garin

A, Glynne-Jones R, Jordan K, Meshcheryakov A, Papamichail D, Pfeiffer P, Souglakos I, Turhal S, Cervantes A. ESMO Consensus Guidelines for management of patients with colon and rectal cancer. a personalized approach to clinical decision making. *Ann Oncol* 2012; **23**: 2479-2516 [PMID: 23012255 DOI: 10.1093/annonc/mds236]

19 **Marcus L**, Lemery SJ, Khasar S, Wearne E, Helms WS, Yuan W, He K, Cao X, Yu J, Zhao H, Wang Y, Stephens O, Englund E, Agarwal R, Keegan P, Pazdur R. FDA Approval Summary: TAS-102. *Clin Cancer Res* 2017; **23**: 2924-2927 [PMID: 28213365 DOI: 10.1158/1078-0432.CCR-16-2157]

20 **Shirasaka T**, Nakano K, Takechi T, Satake H, Uchida J, Fujioka A, Saito H, Okabe H, Oyama K, Takeda S, Unemi N, Fukushima M. Antitumor activity of 1 M tegafur-0.4 M 5-chloro-2,4-dihydroxypyridine-1 M potassium oxonate (S-1) against human colon carcinoma orthotopically implanted into nude rats. *Cancer Res* 1996; **56**: 2602-2606 [PMID: 8653704]

21 **Shin SJ**, Jeong JH, Park YS, Lee KH, Shim BY, Kim TW, Oh DY, Lee MA, Kim YT, Kim YH, Zang DY, Roh JK, Ahn JB. Phase II trial of S-1 monotherapy in elderly or frail patients with metastatic colorectal cancer. *Invest New Drugs* 2011; **29**: 1073-1080 [PMID: 20306116 DOI: 10.1007/s10637-010-9418-2]

22 **Shirao K**, Ohtsu A, Takada H, Mitachi Y, Hirakawa K, Horikoshi N, Okamura T, Hirata K, Saitoh S, Isomoto H, Satoh A. Phase II study of oral S-1 for treatment of metastatic colorectal carcinoma. *Cancer* 2004; **100**: 2355-2361 [PMID: 15160338 DOI: 10.1002/cncr.20277]

23 **Hong YS**, Park YS, Lim HY, Lee J, Kim TW, Kim KP, Kim SY, Baek JY, Kim JH, Lee KW, Chung IJ, Cho SH, Lee KH, Shin SJ, Kang HJ, Shin DB, Jo SJ, Lee JW. S-1 plus oxaliplatin versus capecitabine plus oxaliplatin for first-line treatment of patients with metastatic colorectal cancer: a andomized, non-inferiority phase 3 trial. *Lancet Oncol* 2012; **13**: 1125-1132 [PMID: 23062232 DOI: 10.1016/S1470-2045(12)70363-7]

24 **Liu H**, Wang Y, Li G, Song W, Wang R. Clinical study of tegafur-gimeracil-oteracil potassium capsule (s-1) and oxaliplatin combination chemotherapy in advanced colorectal cancer. *J Cancer Res Ther* 2015; **11**: 331-335 [PMID: 26148595 DOI: 10.4103/0973-1482.157339]

25 **Guan X**, Li H, Xiong X, Peng C, Wang N, Ma X, Ma A. Cost-effectiveness analysis of fruquintinib versus regorafenib as the third-line therapy for metastatic colorectal cancer in China. *J Med Econ* 2021; **24**: 339-344 [PMID: 33571036 DOI: 10.1080/13696998.2021.1888743]

Published by **Baishideng Publishing Group Inc**
7041 Koll Center Parkway, Suite 160, Pleasanton, CA 94566, USA
Telephone: +1-925-3991568
E-mail: bpgoffice@wjgnet.com
Help Desk: https://www.f6publishing.com/helpdesk
https://www.wjgnet.com